UNIVERSITY OF CALIFORNIA, SAN DIEGO

Elucidating the Functions and Signaling Mechanisms of the Chemokine CXCL12 and Its Receptors CXCR4 and CXCR7 in Cancer

A dissertation submitted in partial satisfaction of the
requirements for the degree of Doctor of Philosophy

in

Biomedical Sciences

by

Morgan L. O'Hayre

Committee in charge:

Professor Tracy Handel, Chair
Professor Anthony Hunter
Professor Elizabeth Komives
Professor Alexandra Newton
Professor Jing Yang

2011

This dissertation of Morgan L. O'Hayre is approved, and it is acceptable in quality and form for publication on microfilm and electronically:

_____

_____

_____

_____

_____
Chair

University of California, San Diego

2011

DEDICATION

I dedicate this dissertation to my Grandma Lucy, who continues to be an inspiration and encouragement for me even though she is no longer with us.

EPIGRAPH

A system maintains a certain fluid stability that can be destroyed by a misstep in just one niche

Frank Herbert

TABLE OF CONTENTS

LIST OF ABBREVIATIONS

ACN..... Acetonitrile

AMD3100 ..... 1,1′-[1,4-Phenylenebis(methylene)]bis [1,4,8,11-tetraazacyclotetradecane]

APC..... Allophycocyanin

CLL..... Chronic lymphocytic leukemia

Cys..... Cysteine

$DiOC_6$ ..... 3,3′-dihexyloxacarbocyanine iodide

DMSO ..... Dimethyl sulfoxide

DTT ..... Dithiothreitol

ECM ..... Extracellular Matrix

EDTA..... Ethylenediaminetetraacetic acid

ESI ..... Electrospray Ionization

EtOH ..... Ethanol

ERK..... Extracellular signal regulated kinase

FBS ..... Fetal bovine serum

FDR..... False discovery rate

GAG ..... Glycosaminoglycan

GAPDH..... Glyceraldehyde 3 phosphate dehydrogenase

GFP..... Green Fluorescent Protein

GPCR..... G Protein Coupled Receptor

HEK293..... Human Embryonic Kidney cells

HIV ..... Human Immunodeficiency Virus

HPLC..... High Performance Liquid Chromatography

IMAC ..... Immobilized Metal Affinity Chromatography

LN ..... Lymph node

LN_2 ..... Liquid Nitrogen

LTQ ..... Linear Ion Trap

MDM2 ..... Murine double minute 2

MMP ..... Matrix metalloprotease

MS ..... Mass spectrometry

NaCl ..... Sodium Chloride

NLC ..... Nurse-like cell

PBMC ..... Peripheral blood mononuclear cell

PBS ..... Phosphate Buffered Saline

PCR ..... Polymerase Chain Reaction

PDCD4 ..... Programmed Cell Death Factor 4

PE ..... Phycoerythrin

PHLPP ..... PH domain and leucine rich repeat protein phosphatatases

PI ..... Propidium iodide

PKC ..... Protein kinase C

Ptx ..... Pertussis toxin

RT ..... Room temperature

SCID ..... Severe combined immunodeficiency

SDF-1 ..... Stromal cell derived factor 1 (CXCL12)

Ser ..... Serine

Thr ..... Threonine

WT ..... Wild Type

ZAP-70 ..... Zeta-chain-associated protein 70 kD

LIST OF FIGURES

LIST OF TABLES

ACKNOWLEDGEMENTS

I would like to thank Dr. Tracy Handel for her support and advice and most of all, for allowing me to pursue my research interests. Her trust, encouragement and the freedom she has provided me have allowed me to develop and grow as a scientist. I would also like to thank my committee members for their guidance over the years: Dr. Tony Hunter, Dr. Elizabeth Komives, Dr. Alexandra Newton and Dr. Jing Yang. Thank you, Dr. Elizabeth Komives, for insightful discussions regarding the phosphoproteomics work. Additionally, many thanks to Dr. Jing Yang and her lab for contributing invaluable resources including numerous protocols, helpful guidance, hands-on instruction on mouse procedures, and use of their equipment for the breast cancer work, I cannot thank them enough.

I have been lucky to have a number of great collaborators and so countless thanks go to Dr. Davorka Messmer and her lab- Ila and Jessie in particular, for their wonderful collaboration on the CLL work. Thanks to Dr. Thomas Kipps and Laura Rassenti for the access to CLL patient cells, which has made this work possible. Along these lines, I would also like to recognize the CLL patients who volunteered their cells for research; it is because of their openness and willingness to participate that we are able to address interesting research questions and hopefully eventually find better treatments for the disease. Dr. Alexandra Newton and her lab, in particular Matt, have provided insights and helpful suggestions for the PHLPP1 project. I would also like to acknowledge Dr. Pieter Dorrestein and his lab for providing training, helpful discussions and the use of his mass spectrometer. This dissertation work was also made possible through many core resources and expertise including Dr. Kersi Pestonjamasp at the

UCSD microscopy core and Dr. Majid Ghassemian at the Mass Spectrometry facility. Dr. Larry Gross and Dr. Steve Bark have also provided their time, resources and instruction on operating the mass spectrometers. Thank you to Erin Foley and Chris Gregg for dealing with all the flow cytometer issues over the years as well.

Many thanks to the past and present members of the Handel lab for all the good memories and fun times, and for helping get through the bad since research can be full of disappointments. In particular, I would like to thank Ariane for her encouragement and Rina as my partner in “crime”. Rina has been an amazing colleague at the bench and a great friend outside of the lab. By working together, we were able to accomplish much more than we could have individually, allowing us to explore many new avenues of research in the lab and have fun while doing so.

I would like to extend acknowledgements to my family- Mom, Dad, Ryan and Lisa, for their continuous support throughout my graduate school career. Even though they may not always understand my research, I thank them for understanding how important it is to me. My friends have also provided invaluable support over the years to help relieve stress and enjoy life outside of lab. Thank you Linda, Mandy, Emi, Emilie, Molly and Audrey for all the fun hiking trips and get-togethers. Also thanks to Robert, Laura, John and Nisha for joining in on several camping trips (even if they were Robert-style luxury) and ski trips. Thanks to Team UnderPhunDed- Katie, Janine, Leona, Tim, Tony, Rebecca, and Amy in particular, for the stress-relieving running sessions, I am looking forward to future relay races. Nisha- thank you for 6 years of putting up with me as a roommate and for your great friendship, it has meant a great deal to always have a friend to come home to. I would like to extend a special thanks to Jahn for believing in me, encouraging me, and making me smile over the years. Finally, to my friends who

live a distance away but continue to provide their support- Eva, Julia, Scott, Simona, Jes, and Becca, thank you!

Lastly, none of this research is possible without the funding sources. I received funding through the NIH Molecular pharmacology training grant (GM007752) and a California Breast Cancer Research Program Dissertation Award (14GB-0147). This work was also supported through the Lymphoma Research Foundation awarded to Tracy M Handel, Davorka Messmer and Thomas J Kipps and the Department of Defense Breast Cancer Research Program to Tracy M Handel.

Chapter 1 figures and text in part, were published in the following review articles, for which the dissertation author was a major contributing author. All authors contributed to the ideas, written text and figures for the articles:

Morgan O'Hayre, Catherina L Salanga, Tracy M Handel, Samantha J Allen. Chemokines and cancer: migration, intracellular signaling, and intercellular communication in the microenvironment. (2008) *Biochemical Journal* 409: 635-649.

Morgan O'Hayre, Catherina L Salanga, Tracy M Handel, Damon Hamel. Emerging Concepts and Approaches for Chemokine-Receptor Drug Discovery. (2010) *Expert Opinion on Drug Discovery* 5(11): 1109-1122.

Catherina L Salanga, Morgan O'Hayre, and Tracy M Handel. Modulation of chemokine receptor activity through dimerization and crosstalk. (2009) *Cell Mol Life Sci*. 66:1370-86.

Chapter 3 in full is a reprint of the material as it is published in *Blood*: Davorka Messmer*, Jessie-F Fecteau*, Morgan O'Hayre*, Ila S Bharati, Tracy M Handel, Thomas J Kipps. Chronic Lymphocytic Leukemia Cells Receive Raf-Dependent Survival Signals in Response to CXCL12 that Are Sensitive to Inhibition by Sorafenib. (2011) *Blood*

117(3): 882-9. **Authors contributed equally.* The dissertation author was a major contributing author for this article, along with Davorka Messmer and Jessie-F Fecteau. Ila S Bharati also performed experiments for this work.

Chapter 4 is currently being prepared for the submission of publication of the material. The following are the contributing authors: Morgan O'Hayre, Matthew Niederst, Jessie-F Fecteau, Thomas J Kipps, Davorka Messmer, Alexandra C Newton, Tracy M Handel. This dissertation author is the primary investigator and author on this work. Matthew Niederst also performed experiments contributing to this work.

Chapter 5 in full is a reprint of the material as it appears in *Methods in Enzymology*: Morgan O'Hayre, Catherina L Salanga, Pieter C Dorrestein, Tracy M Handel. Phosphoproteomic analysis of chemokine signaling networks. (2009) *Methods Enzymol* 460:331-46. The dissertation author was a major contributing author for this article and Catherina Salanga provided equal contribution.

Chapter 6 in full is a reprint of the material as published in *PLoS One***:** Morgan O'Hayre, Catherina L Salanga, Thomas J Kipps, Davorka Messmer, Pieter C Dorrestein, Tracy M Handel. Elucidating the CXCL12/CXCR4 Signaling Network in Chronic Lymphocytic Leukemia through Phosphoproteomics Analysis. (2010) *PLoS One* 5(7): e11716. This dissertation author is the primary investigator and author on this work. Catherina L Salanga also performed experiments for this publication.

CURRICULUM VITAE

EDUCATION

PhD, Biomedical Sciences Graduate Program

University of California, San Diego (UCSD) *La Jolla, CA* *2005-2011*

Thesis Advisor: Dr. Tracy Handel

Dissertation: Elucidating the Functions and Signaling Mechanisms of the Chemokine CXCL12 and Its Receptors CXCR4 and CXCR7 in Cancer

Bachelor of Science, Biochemistry, *Summa Cum Laude*

Colorado State University (CSU) *Fort Collins, CO* *2001-2005*

Minor in chemistry, University Honors Program

Honors Thesis: Effect of Dominant Negative and Constitutively Active Forms of MKK3 and MKK6 on the pH-responsive Induction of Phosphoenolpyruvate Carboxykinase (PEPCK) mRNA in LLC-PK1-FBPase+ cells (*Curthoys laboratory)*

PUBLICATIONS

Fecteau JF, Bharati I, **O'Hayre M**, Handel TM, Kipps TJ, Messmer D. Sorafenib-Induced Apoptosis of Chronic Lymphocytic Leukemia Cells is Associated with Downregulation of Mcl-1, STAT3, and CREB. Submitted to *Molecular Medicine.*

Messmer D*, Fecteau JF*, **O'Hayre M*,** Bharati IS, Handel TM, Kipps TJ. Chronic Lymphocytic Leukemia Cells Receive Raf-dependent Survival Signals in Response to CXCL12 that Are Sensitive to Inhibition by Sorafenib. (2011) *Blood* 117(3): 882-9*. *Authors contributed equally.*

O'Hayre M, Salanga CL, Handel TM, Hamel D. Emerging Concepts and Approaches for Chemokine-Receptor Drug Discovery. (2010) *Expert Opinion on Drug Discovery* 5(11): 1109-1122. Review.

O'Hayre M, Salanga CL, Kipps TJ, Messmer D, Dorrestein PC, Handel TM. Elucidating the CXCL12/CXCR4 Signaling Network in Chronic Lymphocytic Leukemia through Phosphoproteomics Analysis. (2010) *PLoS One* 5(7): e11716.

O'Hayre M, Salanga CL, Dorrestein PC, and Handel TM. Phosphoproteomic analysis of chemokine signaling networks. (2009) *Methods Enzymol* 460:331-46.

Salanga CL, **O'Hayre M**, and Handel TM. Modulation of chemokine receptor activity through dimerization and crosstalk. (2009) *Cell Mol Life Sci*. 66:1370-86. Review.

O'Hayre M, Salanga CL, Handel TM, Allen SJ. Chemokines and cancer: migration, intracellular signaling, and intercellular communication in the microenvironment. (2008) *Biochemical Journal* 409: 635-649. Review.

Andratsch M, Feifel E, Taylor L, **O'Hayre M**, Schramek H, Curthoys NP, Gstraunthaler G. TGF-beta signaling and its effect on glutaminase expression in LLC-PK1-FBPase+ cells. (2007) *Am J Physiol Renal Physiol* 293(3): F847-53.

O'Hayre M, Taylor L, Andratsch M, Feifel E, Gstraunthaler G, Curthoys NP. Effects of constitutively active and dominant negative MKK3 and MKK6 on the pH-responsive increase in phosphoenolpyruvate carboxykinase mRNA. (2006) *Journal of Biological Chemistry* 281(5): 2982-8.

RESEARCH EXPERIENCE

Graduate Student

UCSD School of Pharmacy, Handel Laboratory *San Diego, CA 2006 - 2011*

- CXCL12/CXCR4 in survival of Chronic Lymphocytic Leukemia (CLL) cells
    - Phosphoproteomics analysis of CXCL12-induced signaling networks
    - Characterization of CXCL12 signaling through cell biology and pharmacology-based approaches
    - Survival analysis of CLL cells in presence of CXCL12 and other chemokines in response to irradiation/DNA damage and treatment with drugs/inhibitors
    - Characterization of crosstalk in the microenvironment: Nurselike cell-CLL communication
    - Investigation of loss of PHLPP1 expression in CLL through adenoviral expression and bisulfite sequencing methylation analysis
- Effects of differential CXCR4 and CXCR7 expression on breast cancer progression
    - *In vivo* mouse tumor growth and metastasis model of human breast cancer cells expressing differential levels of CXCR4 and CXCR7
    - Quantitative RT-PCR characterization of gene expression changes from CXCL12
    - Immunofluorescence imaging of receptor localization
    - Characterization of growth and survival properties of breast cancer cells in culture

Lab Research Assistant

CSU Department of Biochemisty, Curthoys Laboratory *Fort Collins, CO 2003-2005*

- Characterizing the signaling response of a porcine renal proximal tubule cell line (LLC-PK1-FBPase+ cells) to acidosis (growth in acidic media, pH 6.9)
    - Investigate p38-MAPK involvement in regulation of PEPCK expression
    - Use of dominant negative and constitutively active MKK isoforms

NSF Research Experience for Undergraduates (REU) International Internship

Universität Innsbruck, Gstraunthaler Laboratory *Innsbruck, Austria Spring 2004*

- Characterizing the signaling response of LLC-PK1-FBPase+ cells to acidosis and TGF-β
    - Signaling analysis of p38-MAPK and ERK1/2 in regulating of PEPCK and glutaminase gene expression

---

SKILLS

- Cell culture and transfection, transduction: cell lines and primary PBMCs and leukemia cells, ficoll isolation of PBMCs

- Flow cytometry
- Signal transduction analysis: western blot, stimulations and inhibitor studies
- Cell survival, calcium flux, transwell migration and proliferation assays
- Proteomics and phosphoproteomics sample preparation: IMAC phosphopeptide enrichment, pulling and packing capillary LC columns
- Mouse work: mammary fat pad implants (survival surgery), necropsies, IP and subcutaneous injections, blood/serum collection, tissue preparation for histology
- Mass spectrometry: MALDI, LC-MS/MS (LTQ, orbitrap and API4000)
- Mass spectrometry analysis: InsPecT, ProteinPilot, DAVID functional annotation
- 2D gel electrophoresis
- Molecular biology (cloning, mutagenesis)
- Protein expression and purification
- DNA methylation analysis by bisulfite sequencing
- Immunofluorescence, deconvolution microscopy

HONORS AND FELLOWSHIPS

- California Breast Cancer Research Program Dissertation Award Fellowship *2008-2010*
- NIH Cellular and Molecular Pharmacology Training Grant *2005- 2008*
- Best Performance in First Year Classes Award, UCSD BMS Program *2006*
- NSF Graduate Research Fellowship Honorable Mention *2006*
- Chancellor's Fellowship, UCSD *2005-2008*
- Summa Cum Laude from the College of Natural Sciences, CSU *2005*
- Frank X. Gassner Award for Excellence in Undergraduate Research, CSU *2005*
- Highest Honors at the Undergraduate Research and Creativity Symposium, CSU *2005*
- Outstanding Science Student of the Year, CSU Students as Leaders in Science *2005*
- Achievement Rewards for College Scientists (ARCS) scholarship *2004-2005*
- Colorado State University Honors Program *2001-2005*

TEACHING AND LEADERSHIP

- Teaching Assistant for Metabolic Biochemistry with Dr. Yunde Zhao *winter 2007*
- Lectures for 1st year graduate seminar classes *2007-2009*
- San Diego Science Festival Volunteer *April 2009*
- Biomedical Sciences Admissions and Recruitment Student Representative *2007-2008*
- REU alumni panel discussion at Colorado State University *August 2004 and 2008*
- Science at the Daycare volunteer, Early Childhood Education Center *2005-2007*

ABSTRACT OF THE DISSERTATION

Elucidating the Functions and Signaling Mechanisms of the Chemokine CXCL12 and Its Receptors CXCR4 and CXCR7 in Cancer

by

Morgan L. O'Hayre

Doctor of Philosophy

University of California, San Diego, 2011

Tracy Handel, Chair

Chemokines have elicited interest in the field of immunology for many years due to their role in directing the migration of immune cells. Approximately a decade ago, chemokines and their receptors became a major focus area in cancer biology due to their role in directing the "migration", or metastasis, of cancer cells from tissues of origin to distant sites. A renewed interest in the role of chemokines in cancer has come with the expanding field of the tumor microenvironment, in particular, with a drive towards understanding the contributions of non-cancerous stromal cells, immune cells, and extracellular matrix components to the survival, growth, proliferation and invasive properties of cancer cells. These constituents of the microenvironment are known to

release a variety of molecules including cytokines, growth factors, proteases and chemokines that modulate the growth and development of tumors.

My dissertation work has focused on understanding the role of chemokines and their receptors in the cell survival, proliferation, and metastasis of cancer cells. Specifically, I have examined the functions and signaling pathways induced by the chemokine CXCL12 and its receptors, CXCR4 and CXCR7, in two types of cancer: Chronic Lymphocytic Leukemia (CLL) and breast cancer. To this end, a variety of traditional cellular biology, molecular biology and pharmacological approaches as well as more global phosphoproteomics methods were employed. Overall, this work demonstrates the importance of CXCL12 to the survival and malignancy of CLL and unveils numerous potential molecular targets for therapeutic intervention, including the proposed use of a multi-kinase inhibitor, sorafenib, for treatment of CLL. Additionally, investigation of the individual and combined contributions of CXCR4 and CXCR7 to breast cancer progression has provided insight into some important signaling differences and cross-modulation of these receptors. Using a mouse model for metastasis, we have demonstrated that although high CXCR4 expression promotes breast cancer metastasis, co-expression with high levels of CXCR7 dramatically reduces metastasis without reducing primary tumor growth. Mechanisms by which CXCR7 may modulate CXCR4 function are also explored. A better understanding of how chemokines function in the context of health and disease may provide promising leads for future drug discovery.

CHAPTER 1

Introduction to Chemokines

1.1 General Introduction to Chemokines and Chemokine Receptors

Chemokines comprise a family of small secreted proteins (70-130 amino acid, 8-14 kDa) that bind to the chemokine receptor subfamily of class A G-protein coupled receptors (GPCRs) [*1*]. Traditionally, chemokines and their receptors have been divided into four families based on the pattern of cysteine residues in the ligands (CXC, CC, C, and CX3C). They have also been functionally classified, based on their pivotal role in directing the migration of immune cells, as being "homeostatic" or "inflammatory", although some chemokines exhibit hallmarks of both categories [*2-3*]. Homeostatic chemokines are constitutively expressed and control leukocyte navigation during immune surveillance. Inflammatory chemokines, which constitute the vast majority, are inducible and control cell recruitment to sites of infection and inflammation [*2-3*].

The general mechanism by which chemokines direct the migration of cells involves the establishment of a chemokine gradient from an originating tissue that attracts receptor-bearing cells to that tissue. The receptor-bearing cells rolling along the endothelial cell lining of blood vessels can then come into contact with chemokines tethered to cell surface glucosaminoglycans (GAGs), thereby activating the chemokine receptors and triggering adhesion molecules and integrins that facilitate the extravasation of the cell into the tissue (Figure 1.1) [*2-4*]. In addition to their well-known function as leukocyte migration cues, chemokines have also been shown to play important roles in development, angiogenesis, lymphopoiesis, hematopoiesis and tissue remodeling/wound healing [*5-6*].

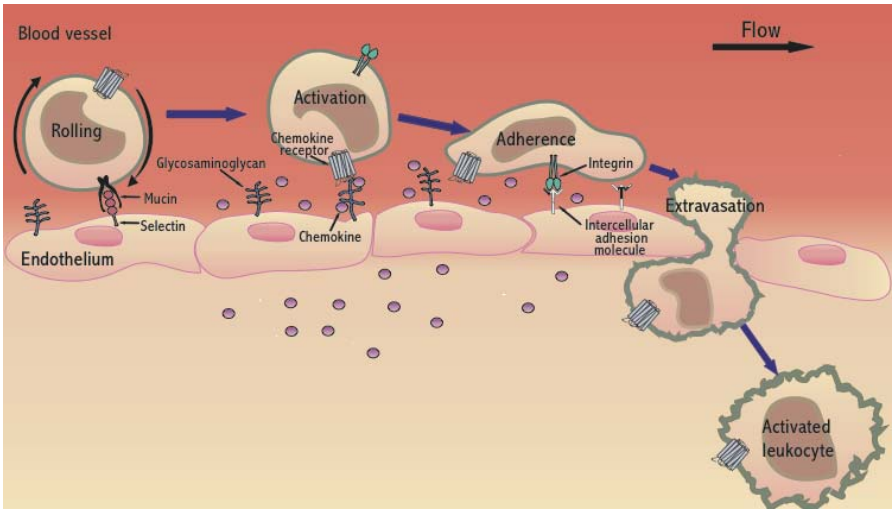

Figure 1.1 Leukocyte chemotaxis towards a chemokine gradient. Illustration depicts chemotaxis of a leukocyte towards a chemokine gradient and extravasation through an endothelial cell layer.

There are approximately 50 known chemokines and despite their variable levels of sequence homology, they adopt a characteristic fold that consists of an N-terminal unstructured domain that is critical for signaling, a three stranded β-sheet connected by loops and turns, and a C-terminal helix (Figure 1.2) [*7*]. These chemokine ligands bind to 19 known chemokine receptors (Figure 1.3) as well as 2 decoy chemokine receptors, DARC and D6, and several virally-encoded chemokine binding proteins (e.g. US28 and vGPCR) [*1, 8*]. As many chemokines will often bind more than one receptor and receptors will often bind more than one chemokine, there is a high degree of complexity that serves in some cases as functional redundancy and yet also helps in the fine-tuning of chemokine/receptor signaling and function, discussed in more detail in the next section of this chapter.

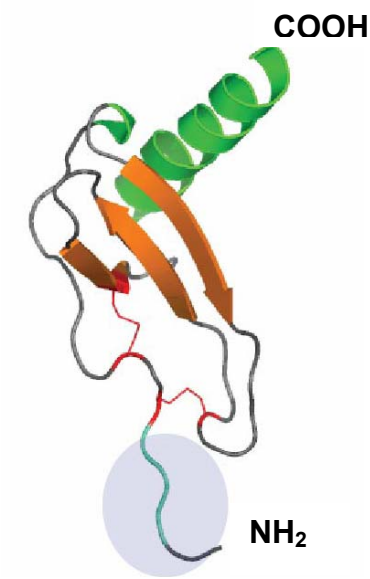

Figure 1.2 Structure of the IL-8 monomer (PDB ID 1IL8) [*9*]. The N-terminal signaling domain is highlighted; this region is postulated to insert into the helical bundle of the receptor to trigger receptor activation. Reprinted from O'Hayre et al. (2008) *Biochem Journal* [*10*].

In addition to binding their receptors, many chemokines dimerize or form higher order oligomers that appear to be important for localization to glycosaminoglycans (GAGs) on cell surfaces and the extracellular matrix (ECM) [*4*]. Although they are believed to bind their receptors as monomers in the context of signaling cell migration, oligomerization is possibly important for signaling related to other processes and is critical for *in vivo* cell migration and function [*11-12*]. The significance of oligomerization to *in vivo* cell migration has largely been attributed to facilitating chemokine binding to cell surface GAGs, thereby providing an anchor for their accumulation under the strong shear flow conditions in the blood vessels [*4*]. The ability of chemokines to bind to GAGs is also thought to be important for the transcytosis, presentation and accumulation of chemokines to these localized areas that then allows them to function as directional cues [*13*]. In support of this theory, it has been shown that oligomerization deficient and

GAG-binding deficient chemokine variants result in impaired leukocyte migration *in vivo* [*4*].

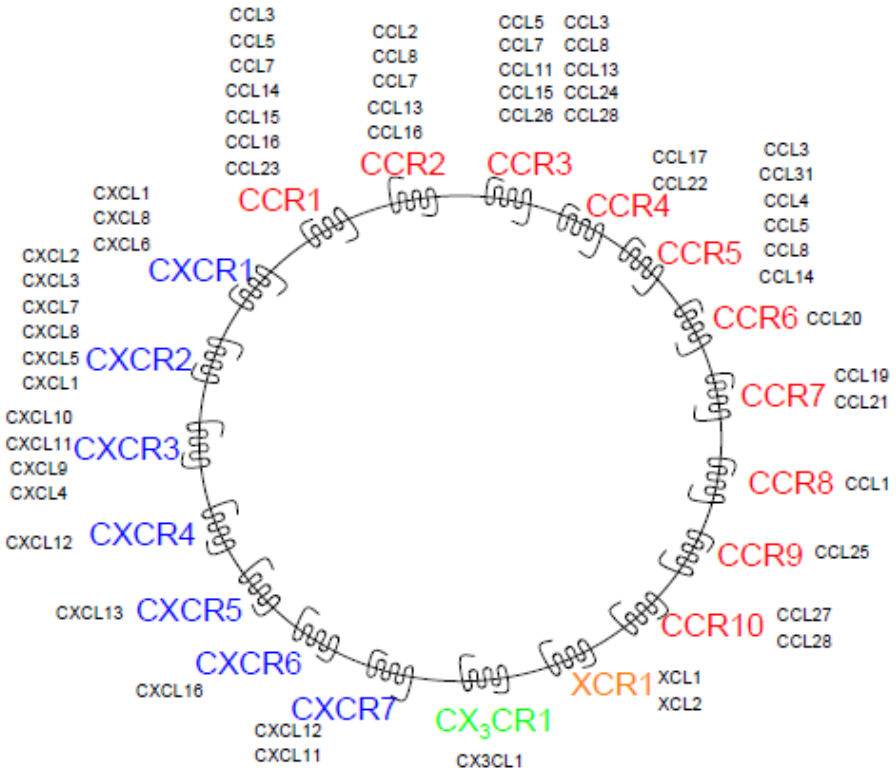

Figure 1.3 Diagram of chemokine:chemokine receptor interactions. The known chemokine receptors are shown in the circle and their respective chemokine ligands are listed next to the receptor names. Adapted from Johnson et al. (2004) *Biochem Soc*.[*14*]

1.2 Diversity and Signaling Complexity in the Chemokine Network

Chemokines induce a number of intracellular signaling pathways by activating second messengers (e.g. calcium mobilization) and phosphorylation cascades in order to mediate a myriad of functions including cell migration, survival and proliferation [*10*]. The chemokine receptors are seven transmembrane GPCRs. As such, they have been best characterized with respect to signaling through heterotrimeric G proteins, primarily involving Gi (Figure 1.4) [*15*].

When a chemokine agonist binds to the extracellular side of its receptor, it stabilizes the receptor into a conformation that activates heterotrimeric G proteins inside the cell by exposing important motifs such as the DRY box [*16*]. The G proteins have 3 subunits: α, β and γ. The Gα subunit interacts directly with the GPCR C-terminal domain, intracellular loops two and three, and with the G-protein β subunit, which forms a tight complex with the γ subunit**.** In the inactive state, the Gα subunit binds GDP. Upon ligand binding and activation of the GPCR, GDP dissociates from Gα. GDP is then replaced by GTP, Gα-GTP dissociates from the receptor and from G$\beta\gamma$, and both of these complexes subsequently activate a variety of downstream effectors that ultimately lead to a physiological response (Figure 1.4). Refraction to continued stimuli involves receptor desensitization and internalization by agonist-dependent phosphorylation of the C-terminal tail of the GPCR by G-protein receptor kinases (GRKs) [*17*]. Receptor phosphorylation subsequently promotes binding of arrestins, which sterically block further interaction with G proteins and mediate receptor internalization through clathrin coated pits [*18*]. Endocytosis of a GPCR can lead to either lysosomal degradation or recycling back to the cell surface and resensitization. In addition to their involvement in internalization, β-arrestins can function as signal transducers by activating pathways such as Akt, PI3K, MAPK, and NF-κB, which lead to a variety of cellular responses (Figures 1.4 and 1.5) [*19*].

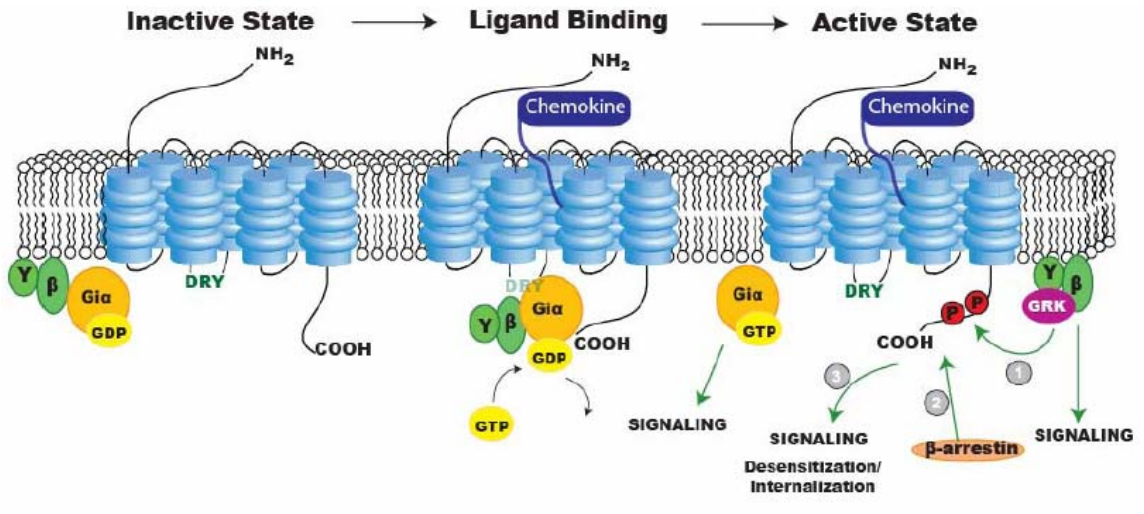

Figure 1.4 Chemokine receptor activation and signaling. Chemokine binding induces a conformational change in the receptor that allows for G-protein binding and nucleotide exchange as well as subsequent activation of signaling pathways, desensitization and internalization. Reprinted from O'Hayre et al. (2008) *Biochem Journal* [*10*]. Animated figure is available online from *Biochem Journal* website.

Additionally, there is ample evidence indicating that chemokine receptors can also signal through other G protein subtypes (other than Gi) or even through non-G-protein mediated pathways [*20-23*]. Furthermore, although the α subunit of G proteins has traditionally been regarded as the major signaling subunit, the βγ subunits are crucial for activation of many chemokine-induced pathways. Two of the major pathways activated by Gβγ are Phosphoinositide 3-Kinase gamma (PI3Kγ) and Phospholipase C (PLC), while Gαi proteins mainly inhibit adenylyl cyclase and transduce signals through tyrosine kinases such as Src [*15*]. Figure 1.5 summarizes the major signaling cascades and functional outcomes of chemokine-receptor activation. However, not all chemokines necessarily activate all pathways depicted and specific subsets or combinations of these pathways may be employed to induce the various functional responses. Factors such as cell type, receptor expression levels, G protein availability, and disease state will also influence the signaling response from chemokine-induced receptor activation.

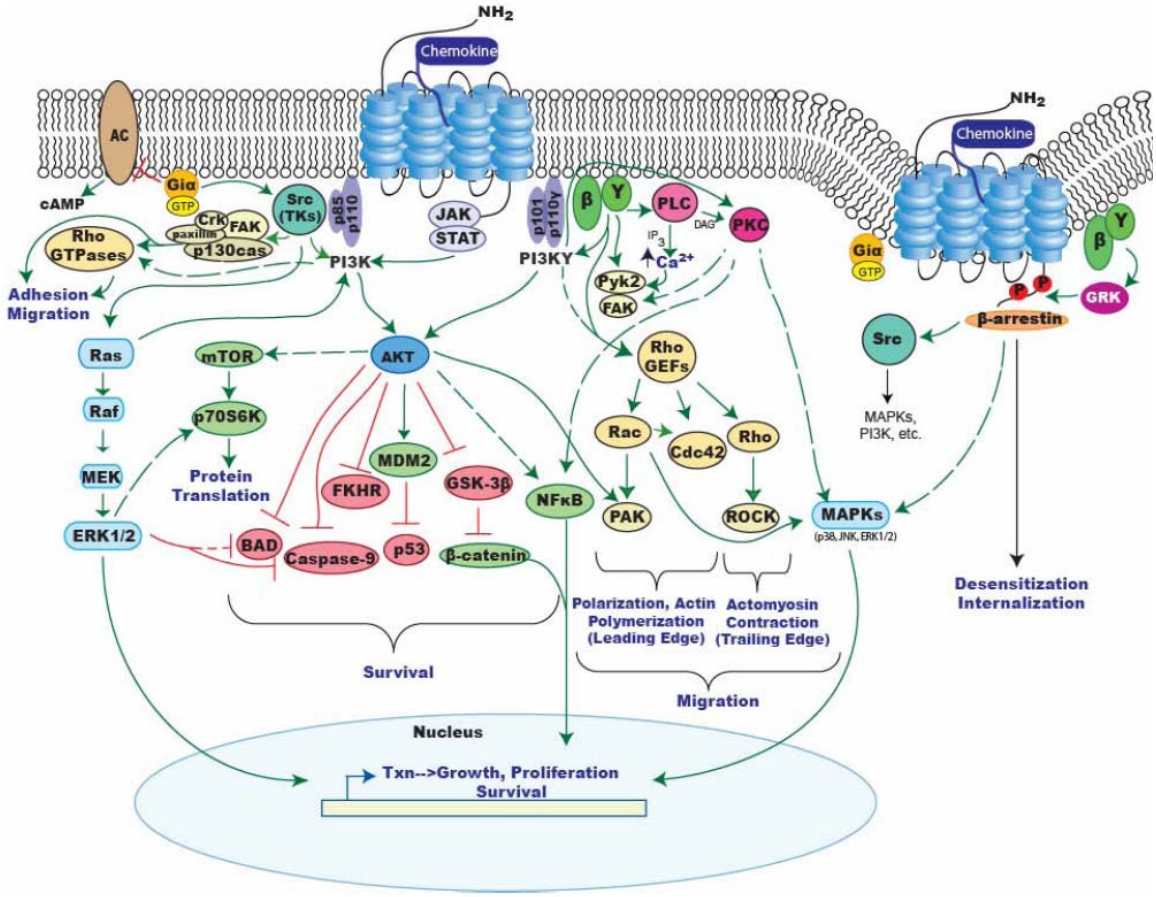

Figure 1.5 Chemokine receptor signaling in migration and survival/proliferation. Green arrows indicate activation of molecules while red bars indicate inhibition. Dashed lines represent indirect effects on target molecule. Reprinted from O'Hayre et al. (2008) *Biochem Journal* [*10*].

Functional Selectivity/Ligand Bias of Chemokines and Implications on Design of Therapeutic Agents

Due to their structural homology and common chemoattractant-related functions, the diversity of chemokine signaling may be greatly underappreciated. The sheer number of chemokines and receptors, along with the fact that many chemokines bind the same receptor and many receptors engage multiple chemokines offers the possibility of many outputs (Figure 1.3). While such promiscuous partnering gives the appearance of redundancy, emerging evidence suggests that cross-reactivity amongst ligands and

receptors can result in quantitative and qualitative differences in the cellular response [*24-25*]. For example, it is clear that ligands of the same receptor can elicit different responses, even when their binding affinities are not too dissimilar. Ultimately, this must be due to differences in the ligand induced conformational states and dynamics of the receptors and how they couple into downstream pathways. In an elegant comparative study of CCL17 and CCL22, D'Ambrosio and coworkers showed quantitative differences in CCR4-mediated signaling [*26*]. CCL22 was much more effective than CCL17 in the induction of integrin dependent T-cell adhesion, receptor desensitization and internalization. Furthermore, the authors showed that although CCL22 is the higher affinity ligand (but only by 2-3 fold), it dissociates more rapidly than CCL17, and they proposed the intriguing hypothesis that the frequency of association/dissociation may be a critical parameter in the activation of certain intracellular signaling pathways.

These concepts lead into an aspect of GPCR signaling that has recently become an area of intense interest, particularly for drug discovery- biased agonism/antagonism, also known as functional selectivity. Here, the "bias" or "selectivity" refers to the ability of different ligands that bind the same receptor to elicit differential signaling responses. With respect to drug development targeting chemokine receptors, critics have argued that the apparent redundancy in the network may be therapeutically problematic in that blocking a single receptor may never produce clinical efficacy due to the presence of overlapping functions of multiple receptors. However, there is mounting evidence that in at least some cases, different ligands for the same receptor elicit different signaling response to fine-tune the biological readout (Figure 1.6). The idea then with respect to drug discovery is that it may be possible to selectively inhibit certain signaling pathways while sparing others, thereby avoiding unwanted effects. While most examples illustrating differential signaling of receptors are in response to endogenous or modified

chemokine ligands, in principle, similar control of receptor signaling could be commandeered by small molecules as has been demonstrated for other GPCRs [*27*].

As previously described, chemokine receptors transduce many different types of signals including those for calcium mobilization, inhibition of adenylyl cyclase and activation of kinase cascades (e.g. Raf/MEK/ERK1/2). These signaling responses and their regulation through receptor desensitization, internalization, and recycling or degradation are modulated by interactions of specific proteins with the intracellular loops and C-termini of the receptors. The key modulators include G proteins, G protein-coupled receptor kinases (GRKs), and β-arrestins [*28*]. Thus despite the redundancy within the chemokine network with respect to ligand-receptor binding, there are numerous mechanisms in place for unique signaling properties, or ligand bias (Figure 1.6). While the structural basis for such ligand bias is largely unknown, it is likely that slight differences in receptor conformation accommodate or block interactions with certain intracellular modulators [*29-33*].

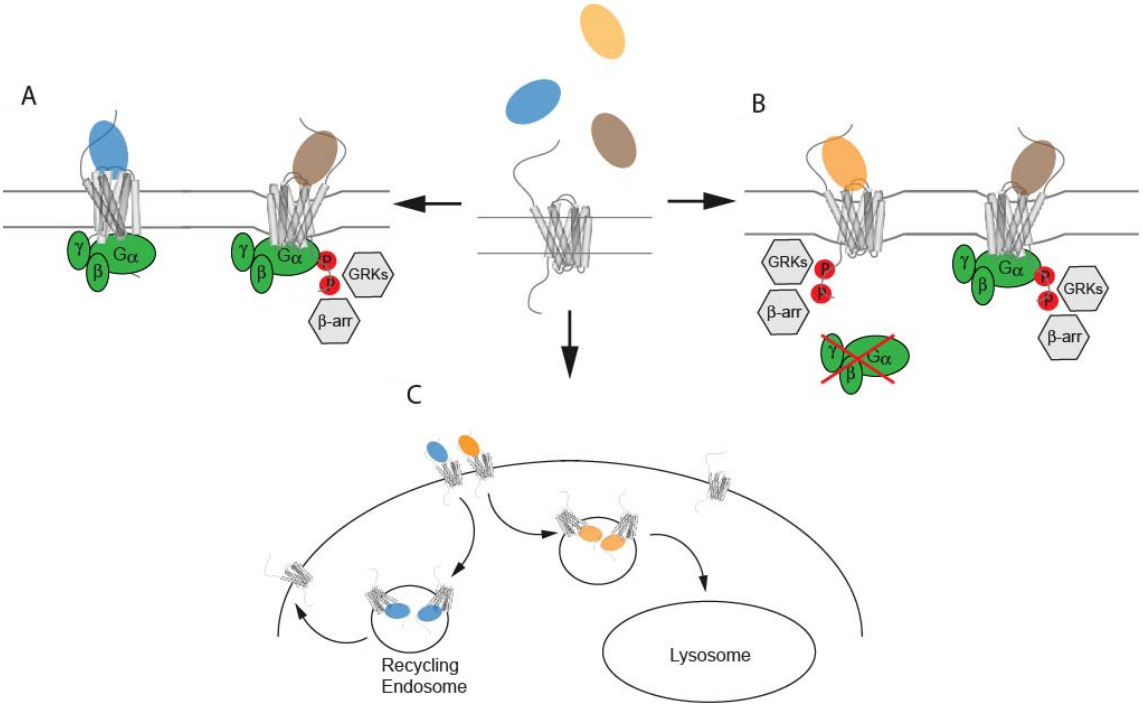

Figure 1.6 Potential scenarios of functional selectivity of chemokine receptor signaling. A) Depiction of a scenario for ligand bias in which one ligand (brown) may induce typical G-protein activation and β-arrestin recruitment leading to receptor desensitization and internalization while another ligand (blue) for the same receptor solely activates G-proteins. B) Alternative scenario in which another ligand (orange) for the receptor could activate β -arrestins, GRKs and receptor internalization but not G-protein signaling. C) It is also possible that two different ligands may similarly activate G-protein and β-arrestin pathways, but then the trafficking of the receptor could differ; for example, the receptor could be targeted to the lysosome for degradation or recycled to the cell surface through recycling endosomes. Internalization is depicted as a slight indentation of the membrane, and the three panels are meant to be independent scenarios. Reprinted from O'Hayre et al. (2010) *Expert Opin Drug Discov [34]*.

Some well established evidence for ligand bias within the chemokine network involves the CCR7 ligands, CCL19 and CCL21. Both CCL19 and CCL21 bind CCR7 with similar affinities, induce signaling through Gi, and have similar efficacies in terms of inducing calcium mobilization and cell migration [*35*]. However, CCL19 but not CCL21 effectively internalizes CCR7 and induces strong phosphorylation of the C-terminus of the receptor (similar to Figure 1.6 A) [*35-37*]. The potency and intensity of CCL19-

mediated ERK1/2 activation was also higher than that of CCL21-mediated activation [*35*]. Recently, it was shown that CCL19 was unique in engaging GRK3, which could possibly account for some of the differences in the receptor responses to these two ligands [*37*]. The role of β-arrestin2 in regulating CCL19 but not CCL21 endocytosis and migration has also been proposed, suggesting the possibility for distinct interactions with intracellular modulators depending on the ligand [*38*]. As CCL19 and CCL21 are endogenous ligands that can compete with one another for CCR7 binding [*39*], these results suggest that functional selectivity can be achieved through orthosteric modulation of receptor conformation, not just allosteric modulation.

Another example of functional selectivity within the chemokine network involves the decoy receptor D6, which is believed to be important for dampening the immune response by scavenging a variety of inflammatory chemokines. D6 binds multiple chemokines, one of which is CCL14. CCL14 can be proteolyzed to forms that are either active (9-74) or inactive (1-74 and 11-74) for CCR1/CCR3/CCR5 signaling. Interestingly, D6 has the ability to bind all forms of CCL14, but selectively traffics only the 9-74 active form into intracellular degradation pathways [*40*]. Additionally, extreme examples of orthosteric chemokines with biased signaling are single point mutants of MCP-1/CCL2, which have variable effects on inhibition of adenylyl cyclase, calcium mobilization and chemotaxis [*41*] and the CCL5/RANTES analogues discussed below.

The ability to bias signaling responses is clearly attractive for the development of therapeutic targets, whereby one could selectively target signaling events that may be contributing to disease while preserving other functions, and thereby reduce some of the negative off-target effects of therapeutics. One of the early discoveries in the chemokine field demonstrating this potential is aminooxypentane (AOP)-RANTES, a chemically modified form of CCL5/RANTES that functions as a CCR5 biased agonist/HIV inhibitor

[*42-43*]. Unlike classic receptor antagonists that compete for endogenous chemokine binding without promoting receptor activation, AOP-RANTES was found to maintain many agonist functions including calcium mobilization, chemotaxis and receptor internalization. However, upon internalization, it inhibited recycling of the receptor to the cell surface in contrast to wild type (WT) RANTES. Thus the potent anti-HIV activity of AOP-RANTES (for R5 tropic HIV strains) has been largely attributed to its internalization and recycling properties which promote overall low CCR5 surface expression [*43*]. This effect is consistent with the observations that high levels of endogenous CCR5 chemokines can suppress HIV infection and that elevated gene copy number of CCL3L1 correlates with lower susceptibility to HIV [*44-45*]. Interestingly, like CCL5/RANTES which binds CCR1, CCR3 and CCR5, AOP-RANTES can bind and elicit chemotaxis and calcium flux responses through these other receptors as well [*46*]. However, unlike the effects of AOP-RANTES on inhibiting CCR5 recycling in eosinophils, it actually promotes CCR1 recycling and does not alter CCR3 down-modulation or recycling, suggesting that functional targeting for different receptors can also be achieved [*47*].

Taking the AOP-RANTES concept one step further, Hartley and coworkers attempted to engineer a RANTES analogue that had antagonist activity rather than agonist activity, while retaining high affinity for CCR5 and the ability to internalize the receptor [*48*]. The underlying premise was that for entry inhibitors, it may be preferable to have a chemokine analogue that does not promote cell migration and other Gi-linked activation processes in order to avoid local inflammation. Using phage display, they successfully produced the recombinant variant, 5P14-RANTES, which showed no detectable G protein activation upon binding, but had a strong propensity to internalize, indicating that it is indeed possible to identify molecules with this fairly unique combination of biased properties.

The prevalence of biased agonism emphasizes the limitations of identifying antagonists simply based on binding properties. To gain a more complete understanding of agonist and antagonist functions, it is important to perform a range of assays to examine the effects on G protein and β-arrestin dependent pathways as well as potential alterations in receptor trafficking and processing (recycling/degradation) (Figure 1.6). As mentioned above with the AOP-RANTES HIV inhibitor, antagonists that cross react with multiple receptors may still provide selectivity for the receptor of interest in terms of function, again underscoring the importance of functional assays to complement binding studies. Additionally, as chemokines can often bind to multiple receptors, the concept of biased receptors, in addition to biased ligands, should be mentioned. Biased receptors refer to a situation in which the same ligand binding to different receptors elicits different responses [*49*]. This idea of receptor bias may be an important consideration, particularly in the context of cross regulation and receptor heterodimerization, as discussed in the next section.

Furthermore, chemokines can be agonists of some receptors and antagonists of others, so what then is their true function? As an example of this concept the ligands CXCL11, CXCL9, and CXCL10 (IP-10) are agonists of CXCR3, but antagonists of CCR3 [*50*] while CXCR3 may act as a decoy receptor of CCL11 [*50*]. N-terminal proteolytic processing may also activate or deactivate chemokines or change their specificity. As already discussed, signaling downstream of chemokine-receptor activation is also complex and many factors can influence the functional outcome. Thus, although there is some degree of overlap in chemokine receptor-mediated pathway activation, current research indicates specificity in many receptor-ligand interactions not only due to the ability of different ligands to induce different signals from a given receptor (termed functional selectivity) [*10, 51*] but also correlating with their spatial and temporal control

[*52*]. While complexity contributes to fine-tuning of normal chemokine functions, it may also facilitate the ability of cells in pathological states to adapt various pathways for purposes not normally used in a particular cell type. Thus, the signaling and physiological response downstream of receptor activation can also vary depending on chemokine-receptor combination, cell type and pathophysiological state [*53-54*].

1.3 Chemokine Receptor Oligomerization and Crosstalk

Chemokines and their receptors are not isolated entities, but instead function in complex networks involving homo- and heteromer formation as well as crosstalk with other signaling complexes. Direct physical associations with other receptors and indirect crosstalk with orthogonal signaling pathways can have functional consequences on chemokine receptor activity. Modulation of chemokine receptor activity through these mechanisms has significant implications in physiological and pathological processes, as well as drug discovery and drug efficacy. However, there are many challenges in studying the occurrence and effects of chemokine receptor dimerization/oligomerization and crosstalk, and thus there is a limited understanding of these variations on the classic paradigm of GPCR activation involving one ligand, one receptor and one G protein per activation event. One major hurdle in studying GPCR oligomerization is the inherent difficulty of recapitulating native cell conditions that are physiologically relevant. Although current biochemical and biophysical techniques allow the study of GPCR oligomer formation in cells, it is challenging because of the potential for missing pertinent GPCR interactions, or alternatively, identifying artificial GPCR interactions because of overexpression.

Nevertheless, dimer and higher order oligomerization of GPCRs is now recognized as a prevalent and important event in the activation and function of many

GPCRs [*55-56*]. While the relevance of chemokine receptor homo- and hetero- oligomer formation is still under investigation [*57*], it could affect ligand-receptor specificity, the activation of downstream signaling pathways, and the duration of the signal in normal or malignant cells. Of the ~ 20 chemokine receptors currently known, nearly half have been reported to physically associate with another chemokine receptor, either through homo- or heterodimerization (Table 1.1). In some instances high sequence homology between receptors is thought to be a good indicator of the capacity for heterodimer formation. However, heterodimers can also form between chemokine receptors with lower sequence identify, and across the CC and CXC subclasses, so the propensity for such interactions is unclear.

Table 1.1 Summary of Established Chemokine Receptor Dimers. As published in Salanga et al. (2009) *Cell Mol Life Sci*. [*58*].

Homodimers	**Constitutive or Inducible**
CCR2	Constitutive [*59*], Inducible [*60*]
CCR5	Constitutive [*61*], Inducible [*62*]
CXCR1	Constitutive [*63*]
CXCR2	Constitutive [*63-65*]
CXCR4	Constitutive [*66-68*], Inducible [*69*]
DARC	Constitutive [*70*]

Heterodimers	**Constitutive or Inducible**	**Functional Effect**
CCR2/CCR5	Constitutive [*59*], Inducible [*60*]	Transinhibition of ligand binding [*59*], altered signaling [*71*]
CXCR1/CXCR2	Constitutive [*63*]	None
CXCR4/CCR2	Constitutive [*68, 72*]	Transinhibition of chemotaxis and calcium response [*68*]
CXCR4/CXCR7	Constitutive [*73*]	Delayed ERK activation, enhanced calcium response [*73*]
CXCR4/CCR5	Constitutive [*74*]	T cell co-stimulation and alternative signaling[*74*]
DARC/CCR5	Constitutive [*70*]	Transinhibition of chemotaxis and calcium response [*70*]

Strong evidence for the existence and functional relevance of chemokine receptor dimerization has been demonstrated in the context of disease states. The importance of CCR5 for HIV-1 entry into cells has been clearly demonstrated by a small population of individuals possessing the allelic truncation variant, CCR5Δ32, which is retained in the ER and confers resistance to HIV-1 infection [*75*-*76*]. The mechanism for protection of homozygous individuals is clear, since the receptor never makes it to the cell surface. However, in heterozygous individuals, the CCR5 truncation mutant oligomerizes with intracellular wild-type (WT) CCR5, thereby causing retention of WT CCR5 in the ER, and thus resistance to HIV.

Another body of evidence for functional relevance of chemokine receptor dimerization involves the warts, hypogammaglobulinemia, infections and myelokathexis (WHIM) syndrome. WHIM syndrome is a rare immunodeficiency disease that has been linked in many cases to mutations in the C-terminus of CXCR4 that result in truncated receptor variants [*77*]. The truncated CXCR4 receptors exhibit enhanced signaling activity and fail to desensitize and internalize upon CXCL12 stimulation [*78*]. These truncated receptors are expressed, and thus likely coexist with WT receptors in heterozygous individuals. Interestingly, it was demonstrated that cells coexpressing WT and mutant CXCR4 also exhibit enhanced chemotaxis and ERK1/2 signaling responses, and that CXCL12 failed to induce internalization not only of the mutant receptor, but also of WT CXCR4 in these cells [*79*]. It was later demonstrated by CoIP and BRET studies that the mutant and WT CXCR4 form constitutive heterodimers, suggesting a mechanism whereby mutant CXCR4 can alter the function of the WT receptor in heterozygous WHIM leukocytes by preventing their internalization [*78*].

Other studies have implicated heterodimer formation in alternative G protein coupling besides Gi as well as receptor transinhibition. Contento et al. provide data to

suggest that CXCR4 and CCR5 recruitment to the immunological synapses (IS) of T cells, and subsequent receptor association, promote chemokine-induced costimulation of T cells. Specifically, at the IS, CXCR4/CCR5 can couple to G_q and/or G_{11} and generate stimulatory signals that can enhance T cell activation, thus providing a mechanism for modulating T cell behavior [*20, 74*]. Transinhibition through CXCR4/CCR2 heterodimers has also been reported [*68, 72*]. Competition binding assays on cells coexpressing CXCR4 and CCR2 demonstrated that addition of the CXCR4 specific ligand, CXCL12, decreased CCL2 (MCP-1) binding to CCR2, and vice versa. This cross-inhibition mechanism is considered allosteric in nature whereby agonist binding of one receptor in a dimer complex results in a conformational change affecting the agonist binding ability to the other receptor. An additional although unexpected consequence of CXCR4/CCR2 heterodimerization in heterologous expression systems was the transinhibition of CCR2 agonist binding upon the addition of a specific CXCR4 small molecule antagonist, AMD3100. Similarly, a CCR2 specific antagonist, TAK-779, also antagonized CXCL12 binding to CXCR4. Consistent with the competitive binding data, AMD3100 and TAK-779 inhibited agonist mediated CXCR4 and CCR2 calcium mobilization and migration assays similarly demonstrated cross inhibition of CXCR4 and CCR2 agonist-induced chemotaxis by TAK-779 and AMD3100, respectively [*72*]. Together, the antagonist mediated cross-inhibition of the CXCR4/CCR2 dimer complex is an intriguing mechanism for the modulation of chemokine receptor activity because it has broad biological consequences and significant implications for therapeutics.

In addition to their ability to form oligomers with each other, chemokine receptors can engage in direct interactions and indirect crosstalk with other GPCR and non-GPCR receptors. Evidence for cooperative interactions between receptors and signaling

pathways includes additivity, amplification and synergy in responses [*80-82*]. Although the occurrence of receptor crosstalk has long been established [*81, 83*], the importance and consequences of crosstalk for chemokine receptor signaling and function is only now becoming more appreciated both in the context of normal cellular function and in disease. Differential expression patterns of chemokines and their receptors are both tissue specific as well as environmentally regulated and allow chemokine receptors to partner with receptors and pathways in a cell-dependent manner [*52*]. Such added complexities create the possibility of unprecedented diversity and multifactorial responses that challenge the concept of redundancy in the chemokine system. Given the vast array of extracellular signaling molecules and target receptors, the potential for interactions between different networks, whether it be to amplify, inhibit, or alter a response, is significant. Nevertheless, there is a high degree of selectivity in crosstalk events, not only in terms of which receptors or signals may interact, but also in terms of cell-type specificity in the occurrence and degree of certain crosstalk events. Although the basic constituents of cells are the same, varying levels of G proteins, cytosolic tyrosine kinases, and other similar signaling molecules may dramatically affect crosstalk interactions and functional response.

As presented here, receptor crosstalk refers to the ability of a particular receptor to influence the signaling and function of another receptor. As summarized in Figure 1.7, potential mechanisms of chemokine receptor crosstalk allowing transactivation or transinhibition of implicated receptors may involve: A) Physical association with another receptor (oligomerization). B) Transcriptional regulation of ligands. C) Post-transcriptional regulation of ligand levels: metalloproteinase cleavage and release of tethered ligands (depicted), altered rates of degradation or translation/mRNA stability (not depicted). D) Transactivation of receptors via activation of cytosolic tyrosine kinase

signaling. E) Trafficking of receptors to/away from signaling microdomains of the plasma membrane (e.g. lipid rafts). F) Downstream signaling amplification (synergy).

One example of receptor crosstalk modulating chemokine receptor signaling is with epidermal growth factor (EGF) and platelet derived growth factor (PDGF) affecting CXCL12/CXCR4 function [*84-85*]. Stimulation with CXCL12 in several ovarian cancer cell lines resulted in cell proliferation through CXCR4 and biphasic activation of ERK1/2 and Akt, which decreased upon addition of an EGFR specific inhibitor, suggesting a relevant crosstalk between CXCR4 and EFGR. Similarly, CXCL8 stimulation of CXCR1 and CXCR2 expressing ovarian cancer cells activated ERK1/2, which was dependent on interactions with EGFR and c-Src [*86*].

Chemokine receptor crosstalk can influence the response a cell has to receptor agonists including the amplitude and duration of the signaling, rates of desensitization of receptors, and receptor trafficking [*83*]. The integration of signals downstream of chemokine and other receptors is key to understanding how cells fine-tune their response to a variety of stimuli, including therapeutics.

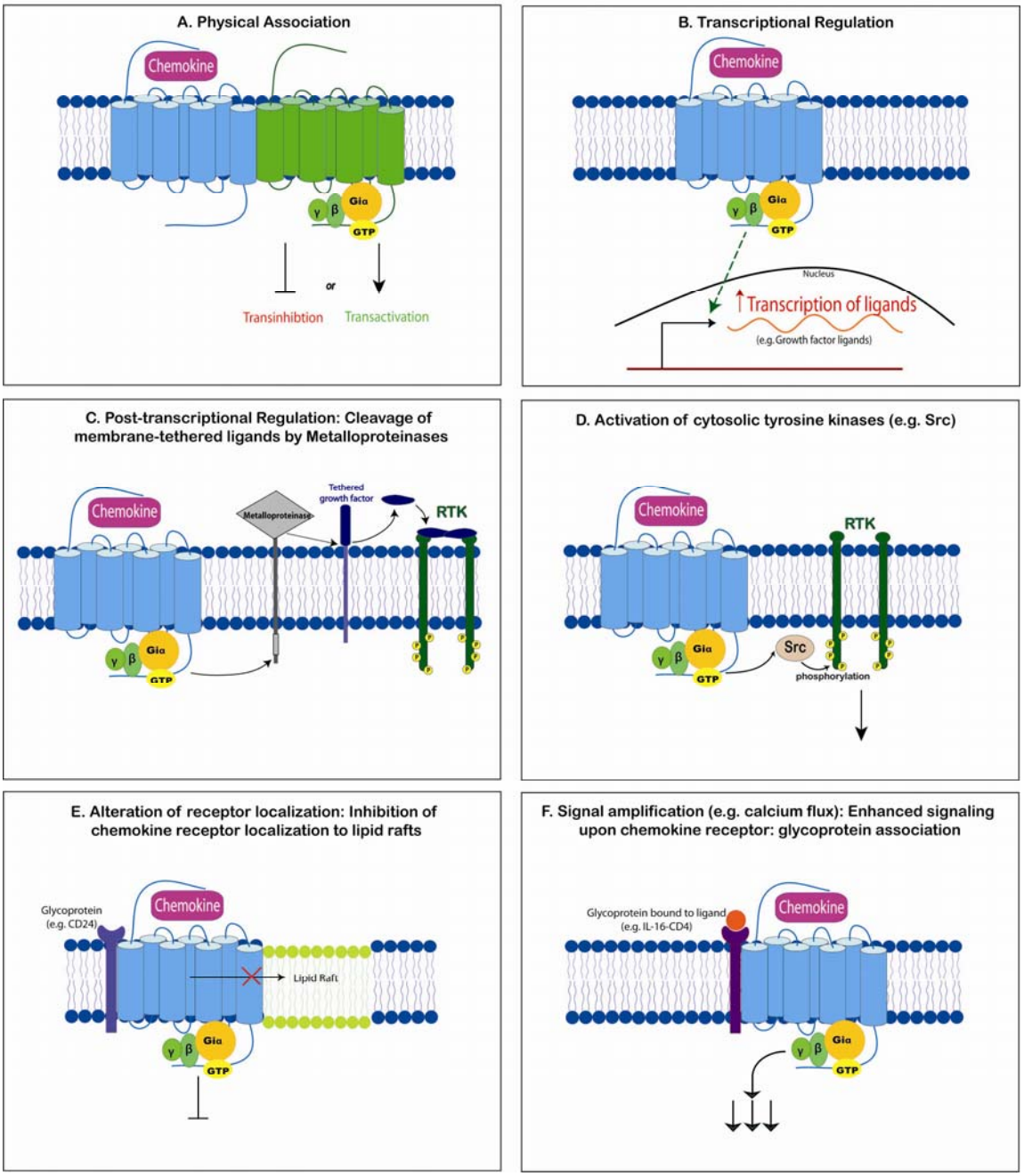

Figure 1.7 Different mechanisms and consequences of heterodimerization and crosstalk of chemokine receptors and other proteins. Figure as published in Salanga et al. (2009) *Cell Mol Life Sci* [*58*].

1.4 Chemokine Involvement in Disease and Cancer

In addition to the normal physiological functions of chemokines in immune system function, aberrant regulation and expression of chemokines and their receptors has been implicated in a number of diseases including chronic inflammatory diseases, atherosclerosis, cancer and HIV [*87*].

One of the most established disease implications involving chemokine receptors is AIDS where HIV enters leukocytes by exploiting two primary chemokine receptors, CXCR4 and CCR5, along with the HIV surface glycoprotein gp120 and the host receptor CD4. The observation that chemokines block viral entry suggested the concept of developing entry inhibitors for the treatment of AIDS, which has now been validated with an FDA approved drug [*88*]. Interestingly, *Plasmodium vivax,* the most widespread of the four human malaria species, enters red blood cells via the chemokine receptor DARC (Duffy Antigen Receptor for Chemokines) and can also be blocked by chemokines [*89*]. Thus similar entry inhibitors could provide viable treatments for malaria where new drugs are desperately needed [*90*]. Other viruses have exploited the chemokine system to help evade the immune system and spread by encoding chemokine binding proteins in their genomes, as in the case of US28 encoded by human cytomegalovirus (HCMV) and ORF74/vGPCR encoded by Kaposi's Sarcoma Herpes Virus (KSHV) [*91*].

Many inflammatory diseases, including rheumatoid arthritis, multiple sclerosis, Crohn's disease, fibrosis, transplant rejection and atherosclerosis are also related to the deregulation of the chemokine system where uncontrolled cell migration and activation can lead to collateral cell damage. Thus inhibitors of many inflammatory chemokine receptors have been extensively pursued for diseases related to chronic inflammation in order to dampen the inflammatory immune response.

Chemokines in Cancer

In the past few years, the involvement of chemokines and their receptors in cancer, particularly metastasis, has been firmly established [*92-94*]. The process by which tumors grow and metastasize is complex [*95*] with many steps required for primary tumor development and establishment of clinically significant secondary tumors (Figure 1.8). These steps include (i) survival and growth of the primary tumor (ii) detachment of tumor cells from the primary lesion (iii) invasion into vascular or lymphatic vessels (iv) homing and adherence to the destination organs and (v) survival, growth and "organogenesis" of the metastasized cells in their new environment [*93, 96*]. Since alternative environments like bone marrow and lymph node are not naturally compatible with cells from mammary tissue for example in the case of breast cancer, these cancer cells must both derive and provide signals to favorably shape the tumor microenvironment to become conducive to survival and growth [*97-99*].

The role of chemokines and their receptors in cancer can thus be divided into three broad categories which contribute to one or more of the above processes: providing directional cues for migration/metastasis, shaping the tumor microenvironment, and providing survival and/or growth signals. Table 1.2 summarizes chemokine receptors and respective ligands involved in cancer and their general mechanism of tumorigenesis. Although their involvement in these three categories is fairly well established, the exact mechanisms of action are not well understood and the underlying complexity of the chemokine network makes it difficult to characterize definitively. Consideration of some of these complexities may be crucial to elucidating more precise mechanisms and thus enable development of better cancer therapeutics.

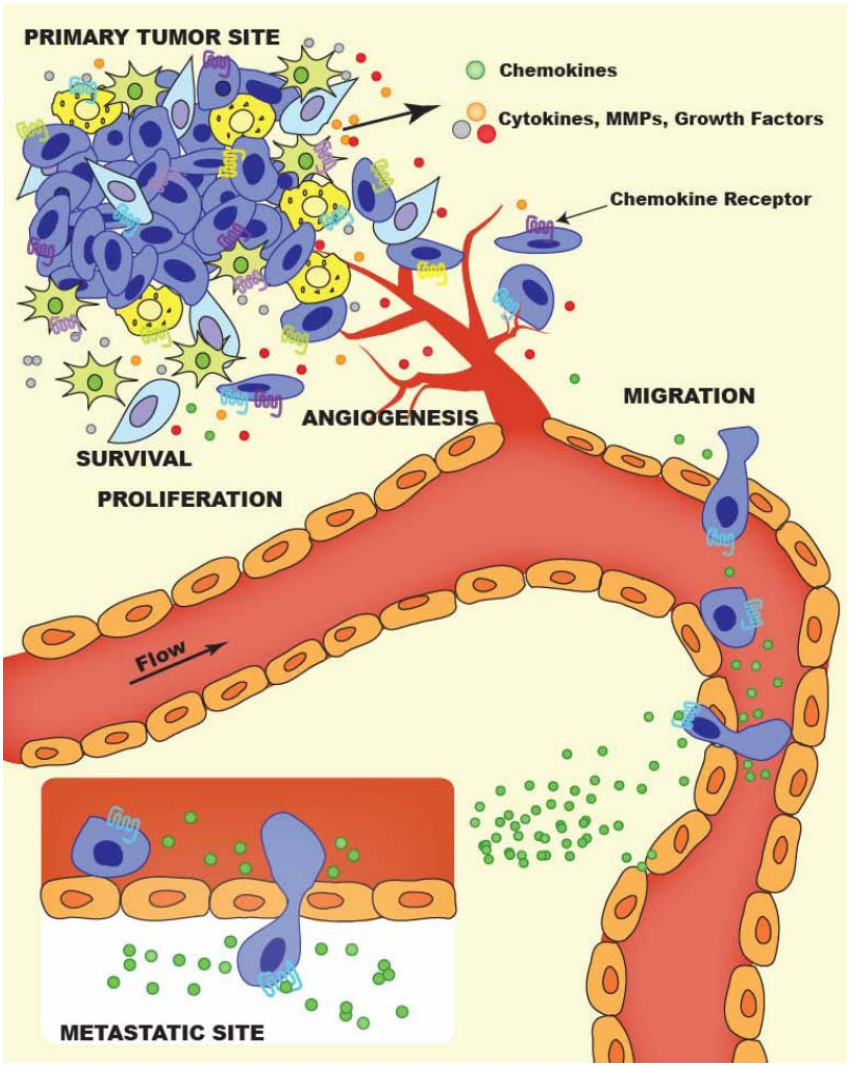

Figure 1.8 Illustration of various steps in cancer growth and metastasis where chemokines and their receptors play a role. Reprinted from O'Hayre et al. (2008) *Biochem Journal* [*10*].

Chemokines in Metastasis

It has been known since the early 1900s that metastasis is not a random process of cell migration and that cancer cells have a propensity to metastasize to specific organs [*100*]. When Müller and colleagues highlighted the role for chemokines in directing organ-specific metastasis, it became clear that chemokine receptor expression patterns on cancer cells and the localization of the corresponding ligands could provide

clues for understanding directional metastasis [*92*]. It has now been established that several chemokines and their receptors play a role in the metastatic process by directing the migration of receptor-bearing tumor cells to sites of metastases where the ligands are expressed. These findings make sense because of the parallels one can draw between lymphocyte trafficking and tumor migration.

Furthermore, metastasis has many features in common with normal cell migration. The general mechanisms involved in normal cell migration and metastasis are similar. Chemokines cause cell movement by inducing changes in cytoskeletal structure and dynamics. Actin polymerization leads to formation of protrusions (pseudopods) and with the help of integrins, form focal adhesions with the ECM to help propel the cell forward [*101*]. While multiple pathways contribute to chemokine-induced cell migration, PI3K, FAK (focal adhesion kinase), and the Rho family of GTPases (Rho, Rac, Cdc42) are particularly important [*102-105*]. ERK and PKC signaling, independently or in conjunction with PI3K may also be involved [*106-109*]. More detail regarding signaling involved in migration is shown in Figure 1.5. However, key differences/distinctions in cancer cells include abnormal chemokine receptor expression, regulation or utilization, often on cells that typically do not migrate. Chemokines then provide a physical address for the secondary destination of the tumor cells. Since metastasis is leading cause of death in cancer patients [*95*], understanding how chemokines are involved in this process and may designate organ selectivity is important.

In numerous types of cancer, the malignant cells exhibit increased or aberrant expression of particular chemokine receptors relative to their normal counterparts, notably CXCR4, CCR7, and CCR10 [*94, 96, 110-111*]. In a study of breast cancer, it was demonstrated that CXCR4 was strongly expressed on breast cancer cells compared to normal breast epithelial tissue, which does not express CXCR4; additionally, antibodies

against CXCR4 blocked metastasis in a mouse model of breast cancer [*92*]. Since that seminal publication, CXCR4 and its ligand, CXCL12 (SDF-1α) have been implicated in ~23 different types of cancer [*94*]. At least two other chemokine systems also play a direct role in metastatic homing of cancer cells: CCR10 in metastasis to skin where CCL27 (CTACK) is expressed (e.g. melanoma), and CCR7 in lymph node metastasis where CCL21 (SLC) is expressed [*92, 96, 111-112*].

Many reasons for altered chemokine/receptor expression in cancer have been identified. Chemokine receptor expression is regulated both at the transcriptional level and post-transcriptionally through RNA stability, translation, and receptor desensitization and internalization [*113-119*]. The tumor microenvironment, and mutant proteins or altered signaling in the cancer cell itself, can also affect chemokine receptor levels. Conditions present within a tumor, such as hypoxia and a rich cytokine environment including IL-2, can induce the transcription of certain chemokine receptors [*113, 116-117*]. For example, hypoxia induces upregulation of CXCR4 transcription via hypoxia inducible factor 1 (HIF-1) and through transcript stabilization [*114, 116*]. HIF-1 was also recently found to promote transcription of CCR7, CXCR1, and CXCR2 [*118-119*]. In renal carcinoma cells, it was demonstrated that mutation of the von Hippel-Lindau (pVHL) tumor suppressor protein, normally responsible for targeting HIF-1 for cell degradation, results in constitutive activation of HIF-1 target genes including CXCR4 [*116*]. Nuclear factor kappa B (NF-κB) is a key signaling pathway that is often activated in cancer cells and can contribute to the transcription of chemokines (e.g. CXCL1 (Gro-α), CXCL8 (IL-8), and CXCL12), and chemokine receptors, such as CXCR1, CXCR2, and CXCR4 [*111, 120*]. On a post-transcriptional level, changes in receptor translation and desensitization by internalization and degradation provide other mechanisms for regulating chemokine receptor expression. For example, enhanced CXCR4 translation in

breast cancer cells was shown to be associated with the oncogene, HER2, which may help to protect CXCR4 from ligand-induced ubiquitination and degradation [*114*].

Chemokines in the Tumor Microenvironment

An interest in understanding the interactions between cancer cells and their microenvironment has provided new insights into how cancer cells grow, survive and become invasive. Tumors are complex entities that are not only comprised of cancer cells, but numerous other cell types including stromal cells and infiltrating immune cells as well as extracellular matrix components. In fact, other cell types in the tumor are quite prevalent; for example, macrophages are estimated to comprise up to 80% of the cell mass in breast carcinomas [*121*]. Chemokines, which can be expressed by cancer cells, non-cancerous immune or stromal cells, or both depending on the tumor, became an interest in the tumor microenvironment field for their ability to recruit immune cells to the tumor and, more recently, for directly acting as growth and survival cues for cancer cells and promoting angiogenesis [*121-122*]. Although my work and the background information presented herein primarily focuses on the pro-tumorigenic roles of chemokines, it should be noted that some chemokines/receptors have anti-angiogenic and anti-tumorigenic effects as expected given their physiological role in protecting the host [*123*]. Along these lines, while recruitment of immune cells to a tumor can sometimes lead to the destruction and clearing of cancer lesions, oftentimes these immune cells can have counterproductive roles and actually promote tumor growth by releasing numerous cytokines (e.g. IL-6) and growth factors in an inflammatory-like response that the cancer cells use to survive and proliferate.

A link between inflammation and cancer was observed over 150 years ago when Rudolf Virchow noted that cancers tend to occur at sites of chronic inflammation [*124*].

Although the relationship between cancer and inflammation is complex, epidemiological studies indicate that inflammatory and infectious diseases are often associated with an increased risk of cancer [*125*]. In many ways, the microenvironment of tumors mimics that of tissues during the height of an inflammatory response to injury [*125*]. For example, they both contain a large number of cells from the innate and adaptive immune systems, which are recruited and activated by a complex profile of chemokines, cytokines, growth factors and proteases. However, unlike the organized morphology of normal tissue, and the ultimate resolution of the inflammation that occurs during healing, tumors exist in a state of chronic inflammation characterized by the presence of malignant cells, development of an aberrant vascular network and the persistence of inflammatory mediators. Within the tumor microenvironment, chemokines and their receptors play roles in modulating angiogenesis, cell recruitment, tumor survival and proliferation, and through these processes, help to define the progression of the cancer. For example, the CCL27/CCR10 system is known to attract melanoma cells to the skin, but recent studies suggest that these proteins also promote tumor cell survival by helping to circumvent anti-tumor processes and by providing protection against apoptosis [*112*].

As discussed above, there is significant overlap between the pathways that are operative in normal chemokine function and those that contribute to cancer. While cancer cells use much of the same machinery and signaling pathways as normal cells, they typically have altered characteristics, such as the expression of oncogenes or mutations in tumor suppressors that can change or exaggerate the response to chemokines. As already mentioned, the mutant pVHL tumor suppressor and the HER2 oncoprotein contribute to aberrant expression levels of chemokine receptors on cancer cells, thus altering how the cells would normally respond to chemokine signals. In

addition, such oncoproteins or mutant tumor suppressors could potentially have a dramatic effect on chemokine receptor signaling leading to prolonged or enhanced pathway activation, or even activation of unique pathways. For example, mutation of PTEN, a phosphatase that contributes to inactivation of Akt, could prolong chemokine-induced Akt activation, thus leading to aberrant activity [*126*].

Additionally, although inappropriate expression of particular chemokine receptors is certainly relevant to a variety of cancers, increased receptor levels do not always correlate with enhanced signaling [*127*]. For example, CXCR4 upregulation was observed on both metastatic and non-metastatic breast cancer cell lines; however, only the metastatic lines expressed functional CXCR4 [*127*]. Thus, an increase in receptor expression may not always translate into enhanced activity. Furthermore, there may be cancers in which receptor expression is unaltered, yet there are significant changes in the functional response and downstream signaling. Chemokine receptor mutations that cause constitutive activation or impair desensitization could potentially contribute to tumorigenicity [*128-130*]. While there are currently no known endogenously expressed chemokine receptors that exhibit these characteristics, the Kaposi's Sarcoma Herpes virus (KSHV) GPCR is a CXCR2-like receptor that is constitutively active and contributes to the pathogenesis of Kaposi's lesions [*128*]. Similarly, point mutations yielding constitutive activation of CXCR2 in NIH 3T3 cells resulted in cell transformation and induced proliferation [*131*]. Further adding to the complexity, many types of cancer cells express multiple chemokine receptors and/or chemokine ligands. CXCR1, CXCR2, CXCR3, CXCR4, CCR7, and CCR10 can all be expressed on melanoma cells and potentially contribute to malignancy [*132*]. Whether these different receptors contribute independently, redundantly, and/or in a coordinated manner to the disease remains to be determined.

Table 1.2 Cancer Promoting Properties of Chemokines and their Receptors. Only chemokines/receptors with pro-tumorigenic roles in cancer are listed. However, some of these chemokines/receptors are known to also mediate anti-tumorigenic effects depending on the context and these are indicated by the asterisk (*). Some of the chemokine receptors are directly expressed on cancer cells (D), while others function indirectly (I) by recruiting TAMs, DCs, or other non-malignant cells that can contribute to the tumor microenvironment. Abbreviations: dendritic cell (DC), tumor associated macrophage (TAM), chronic lymphocytic leukemia (CLL), cutaneous T cell lymphoma (CTCL), adult T cell leukemia/lymphoma (ATLL), Hepatocellular carcinoma (HCC), multiple myeloma (MM). Table from O'Hayre et al. (2008) *Biochem Journal* [*10*].

Chemokine Receptor	Ligands	Direct (D)/ Indirect (I) effects	Tumorigenic Properties	Types of Cancer
CXCR1/2	CXCL1, 2, 3, 5, 6, 7, 8	D & I	Angiogenesis (ELR+), invasion & metastasis, growth & proliferation, survival, MMP-2/9/MT1-MMP expression (CXCL8)	Colorectal, lung, melanoma, pancreatic, prostate, renal cell
CXCR3	*CXCL9, 10, 11	D	Invasion & metastasis, survival, proliferation	Colorectal, melanoma, leukemias
CXCR4	CXCL12	D & I	Angiogenesis, invasion & metastasis, growth & proliferation, survival, DC recruitment, MMP-9 expression	23 types
CXCR5	CXCL13	D	Invasion & metastasis, growth & proliferation	Carcinomas (pancreatic, colon, head & neck), CLL, lymphomas
CXCR7	CXCL12	D	Growth, survival	Breast, lung
CCR1	*CCL3, 4, 5, 7, 16, 23	D & I	TAM & DC recruitment, polarization, invasion & metastasis, angiogenesis, MMP-9/19 expression (CCL5)	Breast, cervical, HCC, lung, MM, prostate, T-cell leukemia
CCR2	*CCL2, 7, 8, 12	D & I	TAM & fibroblast recruitment, polarization, invasion & metastasis, angiogenesis, MMP-12/MT1-MMP expression (CCL2)	Breast, glioma, lung, melanoma, MM, prostate
CCR3	*CCL5, 7, 11, 24, 26	D & I	TAM & eosinophil recruitment, invasion & metastasis, angiogenesis, MMP-19 expression (CCL5)	Breast, cervical, CTCL, melanoma, renal cell
CCR4	CCL2, 3, 5, 17, 22	D & I	TAM & T cell recruitment, invasion & metastasis	ATLL, CTCL, Hodgkin's lymphoma, ovarian
CCR5	*CCL3, 4, 5, 8	D & I	TAM recruitment, polarization, invasion & metastasis, growth, MMP-19 expression (CCL5)	Breast, cervical, lung, MM, pancreatic, prostate
CCR6	CCL20	D & I	DC recruitment, invasion & metastasis proliferation,	Breast, colorectal, HCC
CCR7	CCL19, 21	D	Invasion & metastasis, survival	Breast, CLL, colorectal, gastric, head & neck, lung, melanoma
CCR9	CCL25	D	Invasion & metastasis, survival	Melanoma, prostate
CCR10	CCL27	D	Invasion & metastasis, growth, survival	ATLL, CTCL, melanoma
CX3CR1	*CX3CL 1	D	Invasion & metastasis, survival	Prostate

In a tumor microenvironment there is a milieu of growth factors, cytokines and chemokines that most likely function in concert to shape the growth, survival, and spread of cancer cells. Although it is critical to gain a solid understanding of the individual contributions of each factor to the progression of cancer, they do not function in isolation, and it will also be necessary to consider the global picture in the context of complexities such as receptor crosstalk, alterations in signaling pathways, and interactions with other cell types.

1.5 Interplay between CXCL12, CXCR4 and CXCR7

Since my research focuses predominantly on the chemokine, CXCL12 and its two receptors, CXCR4 and CXCR7, more details regarding these proteins are presented in this section. CXCL12, also known as SDF-1 for Stromal-cell Derived Factor 1, is a highly conserved and constitutively expressed chemokine. CXCR4 was originally thought to be the sole receptor for CXCL12, and thus they were believed to function as a non-redundant pair. Corroborating this notion, gene knockout mice of both *CXCL12* and *CXCR4* exhibit similar phenotypes, with embryonic lethality (~day 18.5) due to hematopoietic, neuronal and cardiac development defects. However, several years ago another chemokine receptor, CXCR7 (formerly the orphan GPCR, RDC-1), was characterized and found to bind CXCL12 with high affinity (kd in high picomolar range) [*133-134*]. CXCR7 also binds another chemokine, CXCL11 (ITAC), albeit with slightly lower affinity (kd in low nanomolar range). However, gene knockout of *CXCR7* in mice exhibit a milder phenotype to those observed with *CXCL12* and *CXCR4*. Studies revealed that targeted deletion of *CXCR7* results in postnatal death in >95% of the mice, and a different phenotype is observed compared to the *CXCR4* knockout mouse, consisting of heart valve defects but normal hematopoietic and neural development [*73*].

Furthermore, CXCL11, which can bind to CXCR7 and CXCR3, is not necessary for development in mice and is naturally absent in some mouse strains, including the C57BL/6 mouse strain which was used as the background *CXCR7* knockout mouse mentioned previously [*135*]. Additionally, both CXCL12 and CXCL11 fail to stimulate calcium flux or chemotaxis through CXCR7, two classic hallmarks of chemokine receptor function [*73, 133*].

One of the first indications that CXCR7 (RDC-1) might be a member of the chemokine receptor family was on the basis of sequence similarity (~43% similarity and 32% identity) with the chemokine receptor, CXCR2; *CXCR7* also shares ~31% sequence homology with *CXCR4* [*136-137*]. CXCR7 was independently identified as a chemokine receptor in an effort to understand why CXCL12 could still bind to fetal liver cells from *CXCR4* knockout mice [*133*]. Both CXCR4 and CXCR7 are conserved from zebrafish (*Danio rerio*) and frogs (*Xenops laevis*) through humans [*137*]. Gene conservation of *CXCL12, CXCR4* and *CXCR7* in mammals is high, respectively exhibiting 99%, 90% and 92% sequence identity between human and mouse genes [*138*]. Due to this high conservation, mouse studies likely provide relevant information to how the human receptors function. This also allows us to use human cancer cells bearing CXCR4 and CXCR7 receptors in immunocompromised mice and they will respond to endogenous mouse CXCL12.

CXCR4 is one of the best characterized chemokine receptors due to its importance in hematopoietic, neuronal and cardiac development and its implications in HIV and cancer. CXCR4 is also the first and only chemokine receptor structure solved to date [*139*]. CXCR4 exhibits classic chemokine receptor functions upon activation by CXCL12, including initiation of G-protein activation (typically G_i, but also $G_{12/13}$ and G_q) leading to calcium mobilization, cellular migration, β-arrestin recruitment and

internalization. However, as mentioned above, CXCR7 does not couple to Gi or induce calcium mobilization or migration upon ligand stimulation although it does recruit β-arrestin and internalize, indicating that CXCR7 does not signal through traditional chemokine receptor mechanisms (Figure 1.9) [*73, 133*]. Consistent with this concept, CXCR7 has a variation in the conserved DRY motif common to class A GPCRs (DRYLSIT instead of DRYLAIV), which is considered important for G protein coupling. However, replacement of the DRYSIT motif on the second intracellular loop of CXCR7 to correspond with the DRYLAIV sequence of CXCR4 failed to restore CXCL12-induced chemotaxis or calcium mobilization, suggesting that the signaling differences are more complicated than initially expected [*140*].

Many theories regarding CXCR7 function have been proposed including CXCR7 signaling through different pathways, functioning as a non-signaling decoy receptor and modulating CXCR4 function through heterodimerization [*73, 141*]. The possibility of CXCR7 functioning as a decoy receptor is not unprecedented since D6 and DARC serve such a function. However, this hypothesis seems less likely due to the importance of CXCR7 in development, and the selectivity of CXCR7 for CXCL12 and CXCL11 compared to D6 and DARC which bind multiple CC and CXC chemokines [*142-143*]. Given the distinct roles of CXCR4 and CXCR7 in developmental processes and their non-identical CXCL12 binding domains [*144*], it will be interesting to determine the differences between these receptors in terms of their roles in cancer and whether they function independently and/or synergistically in various contexts of cellular function.

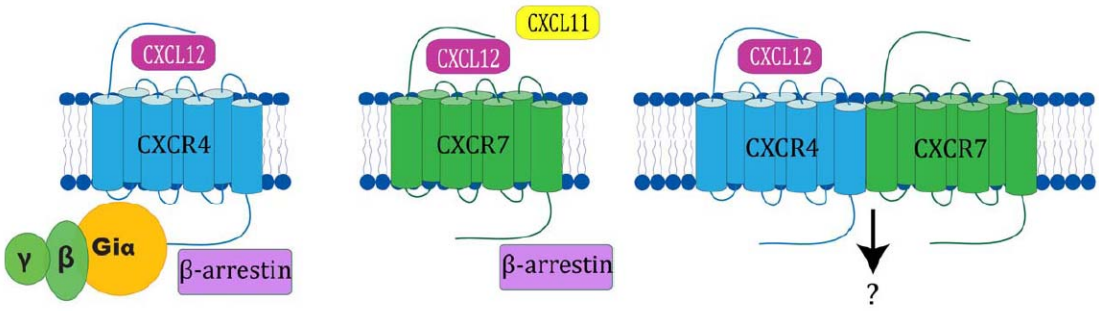

Figure 1.9 Comparison of CXCR4 and CXCR7 signaling. CXCR4 and CXCR7 both bind CXCL12 but signal differently. CXCR7 does not couple to G-proteins like most other chemokine receptors including CXCR4; however, both are thought to activate β-arrestin. CXCR4 and CXCR7 can heterodimerize, further complicating their individual and interactive functions.

CXCR4 and CXCR7 have been shown to form constitutive homodimers as well as heterodimers [*66-68, 145*]. Although the functional relevance of chemokine receptor dimerization is currently a controversial subject, there is strong evidence for their existence and potential implications as presented earlier in the chapter. Additionally, it was demonstrated by FRET analysis that homodimers of CXCR4 exist at the cell surface and intracellularly in HEK293 and HeLa cells. Furthermore, it was shown through FRET photobleaching and cholesterol depletion studies that CXCR4 dimers are present in lipid rafts, which are important signaling microdomains [*66*]. In attempt to disrupt homodimerization to examine functional effects of dimerization, several synthetic peptide of the CXCR4 transmembrane helix 4 (TM4), originally proposed to be involved in dimerization based on the structure of the rhodopsin receptor dimer, have been generated [*66, 68*]. Although results from these studies are somewhat ambiguous since it is difficult to determine whether the functional effects are a result of dimer disruption or simply due to altered conformations induced by the peptide, these data suggest that CXCL12 induces conformational changes in the CXCR4 homodimer and that disruption of this conformational change could inhibit function, at least in the context of calcium

mobilization [*68*]. More recently, the CXCR4 crystal structure was solved as a dimer, suggesting a dimer interface near the tops of transmembrane helices 5 and 6 [*139*]. These structural data provide insight into chemokine receptor dimerization and allows for more directed mutations aimed at disrupting the dimer interface in order to assess the functional consequences of monomeric versus dimeric states of the receptor.

Constitutively formed CXCR4/CXCR7 heterodimers have also been detected in HEK293 cells coexpressing labeled CXCR4 and CXCR7 [*73, 145*]. Ligand-independent dimer formation was further probed by CoIP experiments performed on untransfected HEK293 cells (possessing endogenous CXCR4), stably expressing CXCR7 HEK293 cells or IM-9 cells expressing endogenous CXCR4 and low levels of CXCR7. The HEK293 cells (parental control and stably-expressing CXCR7 lines) were then used to identify the functional impact of CXCR4/CXCR7 heterodimerization. Specifically, it was found that CXCL12 stimulation of the co-expressing cells caused enhanced calcium flux in comparison to the cells expressing CXCR4 only. CXCL12-induced CXCR4/CXCR7 signaling also demonstrated delayed ERK activation compared to CXCR4 signaling alone [*73*]. The lack of classical chemokine receptor signaling by CXCR7 suggests a distinct role for this receptor. Though unclear, CXCR7 activity may include signaling through alternative pathways or perhaps modulating CXCL12-induced CXCR4 activity through physical association. Since most investigations have examined the effects of CXCR4 or CXCR7 independently, the potential consequences of CXCR4 and CXCR7 co-expression through ligand sequestration, heterodimerization and/or crosstalk are largely unknown and present an important area for further investigation.

Functional implications of CXCL12, CXCR4 and CXCR7 in cancer have instigated considerable interest in these proteins. The CXCL12/CXCR4 axis is one of the most extensively studied chemokine-receptor systems with respect to cancer [*110*].

Groundbreaking work by Müller and colleagues demonstrated that breast cancer cells exhibit inappropriate CXCR4 expression, which is not expressed on normal breast tissue, and showed a critical role for CXCL12/CXCR4 in directing organ-specific cancer metastasis [*92*]. This work highlighted the tendency for breast cancer cells to metastasize to lymph nodes, bone marrow, lung and liver, all sites of constitutive CXCL12 expression [*92*]. Furthermore, breast cancer cells in the metastasized lesions have higher CXCR4 expression than in the primary tumor [*146*]. On the basis of this work and many subsequent studies, it is now well established that the CXCL12/CXCR4 axis contributes to the growth and metastatic potential of breast cancer cells, and in fact at least 22 other cancers [*110*]. Due to its more recent discovery, less is known regarding CXCR7 in cancer; however, CXCR7 was shown to promote tumor growth in models of several types of cancer including breast cancer, lung cancer and prostate cancer [*135, 147*]. Yet unlike CXCR4, CXCR7 is unlikely to directly promote metastasis since it does not promote cell migration.

However, both CXCR4 and CXCR7 have additional roles in cancer besides providing directional cues. In addition to promoting growth of the primary tumor, there is evidence that CXCR4 and CXCR7 can provide survival and proliferation cues to the primary tumor and possibly cancer cells at metastatic sites. Since CXCR4 and CXCR7 are important survival cues in developmental processes, it is understandable that they are also prominently involved in cancer cell survival. Molecular strategies for survival and metastasis are often the result of utilizing, and sometimes reprogramming, existing physiological mechanisms, which in this case are likely related to the role of CXCR4 and CXCR7 in survival and growth during development. Since alternative environments like bone marrow and lymph node are not normally compatible with cells from the breast, cancer cells must both derive and provide signals to favorably shape the tumor

microenvironment to a state conducive to tumor cell survival. Therefore, signals such as CXCL12 could induce or nurture the nascent metastases to become established lesions in the secondary sites through direct or indirect growth promoting and survival effects on tumor cells [*93, 148*].

Addition of CXCL12 to *in vitro* cultures of numerous types of CXCR4-expressing cancer cells, including pancreatic adenocarcinoma [*149*], glioma [*150*], leukemia cells [*151*] and breast cancer cells [*152*] results in their prolonged survival and protection from apoptosis when cultured in suboptimal conditions. It has also been demonstrated that CXCL12 promotes *in vivo* survival of numerous cancer cells. Administration of antagonists of CXCR4 synergized with chemotherapy in cell killing and tumor regression of glioblastoma multiforme-derived tumor cells [*153*] and in a B16 murine model of melanoma [*154*]. Knockdown of CXCR4 expression through RNAi or its pharmacologic inhibition via AMD3100 in a murine 4T1 breast cancer model also reduced formation of primary tumors and was found to delay and reduce the early growth and/or survival of the 4T1 cells in the lung [*152*]. These data clearly suggest a role for CXCL12/CXCR4 in survival and/or proliferation of both primary and metastasized cells.

Like CXCR4, CXCR7 plays a vital role in response to CXCL12 in various aspects of embryonic development [*73, 144*]. Furthermore, overexpression of CXCR7 is observed in several types of cancers and has been shown to contribute to cell survival and tumor development, independent of CXCR4 [*133, 135*]. Small molecule antagonists of CXCR7 interfere with tumor growth in mouse models of several different cancers. Overexpression of CXCR7 in the MDA-MB 435 breast cancer cell line, which normally has undetectable levels of CXCR7, resulted in a growth advantage due to increased cell survival in suboptimal growth conditions [*133*]. Implantation of CXCR7-overexpressing MDA-MB 435 cells induced formation of larger tumors in Severe Combined

Immunodeficiency Disease (SCID) mice than vector-control transfected cells, despite the absence of CXCR4. RNAi silencing of CXCR7 in the 4T1 breast cancer cells also resulted in reduced tumor size compared to the WT or control RNAi cells. Finally, similar effects of CXCR7 on cell growth/survival were observed in lung cancer cell lines [*135*].

There is considerable debate regarding the cross-modulation of CXCR4 and CXCR7, making it difficult to predict consequences of their co-expression in cancer cells. Evidence from zebrafish suggests CXCR7 is important for scavenging CXCL12 and modulating guidance of CXCR4-dependent migration [*140*]. On the other hand, CXCL11 and a synthetic small molecule ligand for CXCR7 called CCX771, can antagonize CXCR4-induced transendothelial migration of human tumor cells co-expressing CXCR4 and CXCR7, suggesting that there may be more direct effects of CXCR7 on CXCR4 function [*155*].

Overall, there is strong evidence implicating CXCL12 and its receptors CXCR4 and CXCR7 in cancer progression. However, the mechanisms and signaling pathways activated by CXCL12 to promote tumor growth, survival, and proliferation are not as well characterized. Additionally, it is largely unknown how CXCR4 and CXCR7 function together in the context of cancer and whether their co-expression correlates with neutral, additive/synergistic or inhibitory effects on cancer progression. Thus, a better understanding of CXCL12 signaling through CXCR4 and CXCR7 will provide valuable information on their role in cancer and potentially reveal molecular targets for therapeutic development.

1.6 Synopsis of the Dissertation

The goal of my dissertation research was to characterize the functions and signaling mechanisms by which the chemokine, CXCL12, contributes to the growth,

survival and metastasis of cancer cells, specifically CLL and breast cancer. This first chapter summarizes the known functions, complexities and disease implications of chemokines and their receptors. Chapter 2 provides an introduction to CLL and an overview of what is known regarding the underlying causes and current treatments of the disease. A description of the involvement of CXCL12 in CLL cell survival is also conveyed in Chapter 2 in addition to some preliminary data, which provided a basis for and guided the research presented in Chapters 3-6. The data in Chapters 3 and 4 represent targeted investigations of pathways known or predicted to be important to CLL cell survival. Specifically, in Chapter 3 we characterized differences in Raf/MEK/ERK pathway activation in aggressive versus indolent CLL and identified the multi-kinase inhibitor, sorafenib, as a potential new therapeutic for treatment for CLL (reprint of published article in *Blood*). In Chapter 4, the absence of a recently discovered Akt and PKC phosphatase, PHLPP1, in the majority of CLL patients' cells is described. In this chapter, the mechanisms and consequences of the loss of this potential tumor suppressor protein in CLL cells are examined.

A global profiling approach to elucidate CXCL12-mediated signaling events in CLL through phosphoproteomics methods is presented in Chapters 5 and 6. Chapter 5 provides details on the phosphoproteomics methods employed including the IMAC (immobilized-metal affinity chromatography) phospho-peptide enrichment technique, data collection on the LTQ mass spectrometer and data analysis using InsPecT (reprint of chapter published in *Methods in Enzymology*). The results from the phosphoproteomics analysis and follow-up of interesting findings including the phosphorylation of PDCD4, an important regulator of cell growth, are presented in Chapter 6.

While Chapters 2-6 are focused on CLL, Chapter 7 is devoted to understanding the role of CXCL12 and its receptors, CXCR4 and CXCR7, in breast cancer. In this chapter, we investigated the individual and combined contributions of CXCR4 and CXCR7 to breast cancer tumor growth and metastasis. Lastly, conclusions, perspectives and future directions are summarized in Chapter 8. Overall, this work has contributed to the understanding of chemokine signaling mechanisms and their implications in cancer.

ACKNOWLEDGMENTS

This chapter contains content and figures taken from previously published articles for which the dissertation author was a primary contributing author including:

O'Hayre, M., Salanga, C. L., Handel, T. M., and Hamel, D. J. (2010) Emerging Concepts and Approaches for Chemokine-Receptor Drug Discovery, *Expert Opin Drug Discov 5*, 1109-1122.

Salanga, C. L., O'Hayre, M., and Handel, T. (2009) Modulation of chemokine receptor activity through dimerization and crosstalk, *Cell Mol Life Sci 66*, 1370-1386.

O'Hayre, M., Salanga, C. L., Handel, T. M., and Allen, S. J. (2008) Chemokines and cancer: migration, intracellular signalling and intercellular communication in the microenvironment, *Biochem J 409*, 635-649.

REFERENCES

1. Rossi, D., and Zlotnik, A. (2000) The biology of chemokines and their receptors, *Annu Rev Immunol 18*, 217-242.

2. Moser, B., and Willimann, K. (2004) Chemokines: role in inflammation and immune surveillance, *Ann Rheum Dis 63 Suppl 2*, ii84-ii89.

3. Loetscher, P., Moser, B., and Baggiolini, M. (2000) Chemokines and their receptors in lymphocyte traffic and HIV infection, *Adv Immunol 74*, 127-180.

4. Proudfoot, A. E., Handel, T. M., Johnson, Z., Lau, E. K., LiWang, P., Clark-Lewis, I., Borlat, F., Wells, T. N., and Kosco-Vilbois, M. H. (2003) Glycosaminoglycan binding and oligomerization are essential for the in vivo activity of certain chemokines, *Proc Natl Acad Sci U S A 100*, 1885-1890.

5. Nagasawa, T., Hirota, S., Tachibana, K., Takakura, N., Nishikawa, S., Kitamura, Y., Yoshida, N., Kikutani, H., and Kishimoto, T. (1996) Defects of B-cell lymphopoiesis and bone-marrow myelopoiesis in mice lacking the CXC chemokine PBSF/SDF-1, *Nature 382*, 635-638.

6. Stover, A. G., Da Silva Correia, J., Evans, J. T., Cluff, C. W., Elliott, M. W., Jeffery, E. W., Johnson, D. A., Lacy, M. J., Baldridge, J. R., Probst, P., Ulevitch, R. J., Persing, D. H., and Hershberg, R. M. (2004) Structure-activity relationship of synthetic toll-like receptor 4 agonists, *J Biol Chem 279*, 4440-4449.

7. Allen, S. J., Crown, S. E., and Handel, T. M. (2007) Chemokine: receptor structure, interactions, and antagonism, *Annu Rev Immunol 25*, 787-820.

8. Lau, E. K., Allen, S., Hsu, A. R., and Handel, T. M. (2004) Chemokine-receptor interactions: GPCRs, glycosaminoglycans and viral chemokine binding proteins, *Adv Protein Chem 68*, 351-391.

9. Clore, G. M., Appella, E., Yamada, M., Matsushima, K., and Gronenborn, A. M. (1990) Three-dimensional structure of interleukin 8 in solution, *Biochemistry 29*, 1689-1696.

10. O'Hayre, M., Salanga, C. L., Handel, T. M., and Allen, S. J. (2008) Chemokines and cancer: migration, intracellular signalling and intercellular communication in the microenvironment, *Biochem J 409*, 635-649.

11. Appay, V., Brown, A., Cribbes, S., Randle, E., and Czaplewski, L. G. (1999) Aggregation of RANTES is responsible for its inflammatory properties. Characterization of nonaggregating, noninflammatory RANTES mutants, *J Biol Chem 274*, 27505-27512.

12. Murooka, T. T., Wong, M. M., Rahbar, R., Majchrzak-Kita, B., Proudfoot, A. E., and Fish, E. N. (2006) CCL5-CCR5-mediated apoptosis in T cells: Requirement for glycosaminoglycan binding and CCL5 aggregation, *J Biol Chem 281*, 25184-25194.

13. Wang, L., Fuster, M., Sriramarao, P., and Esko, J. D. (2005) Endothelial heparan sulfate deficiency impairs L-selectin- and chemokine-mediated neutrophil trafficking during inflammatory responses, *Nat Immunol 6*, 902-910.

14. Johnson, Z., Power, C. A., Weiss, C., Rintelen, F., Ji, H., Ruckle, T., Camps, M., Wells, T. N., Schwarz, M. K., Proudfoot, A. E., and Rommel, C. (2004) Chemokine inhibition--why, when, where, which and how?, *Biochem Soc Trans 32*, 366-377.

15. Thelen, M. (2001) Dancing to the tune of chemokines, *Nat Immunol 2*, 129-134.

16. Schwartz, T. W., Frimurer, T. M., Holst, B., Rosenkilde, M. M., and Elling, C. E. (2006) Molecular mechanism of 7TM receptor activation--a global toggle switch model, *Annu Rev Pharmacol Toxicol 46*, 481-519.

17. Reiter, E., and Lefkowitz, R. J. (2006) GRKs and beta-arrestins: roles in receptor silencing, trafficking and signaling, *Trends Endocrinol Metab 17*, 159-165.

18. Lefkowitz, R. J., and Whalen, E. J. (2004) beta-arrestins: traffic cops of cell signaling, *Curr Opin Cell Biol 16*, 162-168.

19. Lefkowitz, R. J., and Shenoy, S. K. (2005) Transduction of receptor signals by beta-arrestins, *Science 308*, 512-517.

20. Molon, B., Gri, G., Bettella, M., Gomez-Mouton, C., Lanzavecchia, A., Martinez, A. C., Manes, S., and Viola, A. (2005) T cell costimulation by chemokine receptors, *Nat Immunol 6*, 465-471.

21. Bacon, K. B., Premack, B. A., Gardner, P., and Schall, T. J. (1995) Activation of dual T cell signaling pathways by the chemokine RANTES, *Science 269*, 1727-1730.

22. Arai, H., and Charo, I. F. (1996) Differential regulation of G-protein-mediated signaling by chemokine receptors, *J Biol Chem 271*, 21814-21819.

23. Rodriguez-Frade, J. M., Mellado, M., and Martinez, A. C. (2001) Chemokine receptor dimerization: two are better than one, *Trends Immunol 22*, 612-617.

24. Mantovani, A. (1999) The chemokine system: redundancy for robust outputs, *Immunol Today 20*, 254-257.

25. Devalaraja, M. N., and Richmond, A. (1999) Multiple chemotactic factors: fine control or redundancy?, *Trends Pharmacol Sci 20*, 151-156.

26. D'Ambrosio, D., Albanesi, C., Lang, R., Girolomoni, G., Sinigaglia, F., and Laudanna, C. (2002) Quantitative differences in chemokine receptor engagement generate diversity in integrin-dependent lymphocyte adhesion, *J Immunol 169*, 2303-2312.

27. Rajagopal, S., Rajagopal, K., and Lefkowitz, R. J. Teaching old receptors new tricks: biasing seven-transmembrane receptors, *Nat Rev Drug Discov 9*, 373-386.

28. Kohout, T. A., and Lefkowitz, R. J. (2003) Regulation of G protein-coupled receptor kinases and arrestins during receptor desensitization, *Mol Pharmacol 63*, 9-18.

29. Bhattacharya, S., Hall, S. E., Li, H., and Vaidehi, N. (2008) Ligand-stabilized conformational states of human beta(2) adrenergic receptor: insight into G-protein-coupled receptor activation, *Biophys J 94*, 2027-2042.

30. Bhattacharya, S., Hall, S. E., and Vaidehi, N. (2008) Agonist-induced conformational changes in bovine rhodopsin: insight into activation of G-protein-coupled receptors, *J Mol Biol 382*, 539-555.

31. Kobilka, B. K., and Deupi, X. (2007) Conformational complexity of G-protein-coupled receptors, *Trends Pharmacol Sci 28*, 397-406.

32. Yao, X., Parnot, C., Deupi, X., Ratnala, V. R., Swaminath, G., Farrens, D., and Kobilka, B. (2006) Coupling ligand structure to specific conformational switches in the beta2-adrenoceptor, *Nat Chem Biol 2*, 417-422.

33. Kenakin, T., and Miller, L. J. (2010) Seven transmembrane receptors as shapeshifting proteins: the impact of allosteric modulation and functional selectivity on new drug discovery, *Pharmacol Rev 62*, 265-304.

34. O'Hayre, M., Salanga, C. L., Handel, T. M., and Hamel, D. J. (2010) Emerging Concepts and Approaches for Chemokine-Receptor Drug Discovery, *Expert Opin Drug Discov 5*, 1109-1122.

35. Kohout, T. A., Nicholas, S. L., Perry, S. J., Reinhart, G., Junger, S., and Struthers, R. S. (2004) Differential desensitization, receptor phosphorylation, beta-arrestin recruitment, and ERK1/2 activation by the two endogenous ligands for the CC chemokine receptor 7, *J Biol Chem 279*, 23214-23222.

36. Otero, C., Groettrup, M., and Legler, D. F. (2006) Opposite fate of endocytosed CCR7 and its ligands: recycling versus degradation, *J Immunol 177*, 2314-2323.

37. Zidar, D. A., Violin, J. D., Whalen, E. J., and Lefkowitz, R. J. (2009) Selective engagement of G protein coupled receptor kinases (GRKs) encodes distinct functions of biased ligands, *Proc Natl Acad Sci U S A 106*, 9649-9654.

38. Byers, M. A., Calloway, P. A., Shannon, L., Cunningham, H. D., Smith, S., Li, F., Fassold, B. C., and Vines, C. M. (2008) Arrestin 3 mediates endocytosis of CCR7 following ligation of CCL19 but not CCL21, *J Immunol 181*, 4723-4732.

39. Yoshida, R., Nagira, M., Kitaura, M., Imagawa, N., Imai, T., and Yoshie, O. (1998) Secondary lymphoid-tissue chemokine is a functional ligand for the CC chemokine receptor CCR7, *J Biol Chem 273*, 7118-7122.

40. Savino, B., Borroni, E. M., Torres, N. M., Proost, P., Struyf, S., Mortier, A., Mantovani, A., Locati, M., and Bonecchi, R. (2009) Recognition versus adaptive up-regulation and degradation of CC chemokines by the chemokine decoy receptor D6 are determined by their N-terminal sequence, *J Biol Chem 284*, 26207-26215.

41. Jarnagin, K., Grunberger, D., Mulkins, M., Wong, B., Hemmerich, S., Paavola, C., Bloom, A., Bhakta, S., Diehl, F., Freedman, R., McCarley, D., Polsky, I., Ping-Tsou, A., Kosaka, A., and Handel, T. M. (1999) Identification of surface residues

of the monocyte chemotactic protein 1 that affect signaling through the receptor CCR2, *Biochemistry 38*, 16167-16177.

42. Simmons, G., Clapham, P. R., Picard, L., Offord, R. E., Rosenkilde, M. M., Schwartz, T. W., Buser, R., Wells, T. N., and Proudfoot, A. E. (1997) Potent inhibition of HIV-1 infectivity in macrophages and lymphocytes by a novel CCR5 antagonist, *Science 276*, 276-279.

43. Mack, M., Luckow, B., Nelson, P. J., Cihak, J., Simmons, G., Clapham, P. R., Signoret, N., Marsh, M., Stangassinger, M., Borlat, F., Wells, T. N., Schlondorff, D., and Proudfoot, A. E. (1998) Aminooxypentane-RANTES induces CCR5 internalization but inhibits recycling: a novel inhibitory mechanism of HIV infectivity, *J Exp Med 187*, 1215-1224.

44. Gonzalez, E., Kulkarni, H., Bolivar, H., Mangano, A., Sanchez, R., Catano, G., Nibbs, R. J., Freedman, B. I., Quinones, M. P., Bamshad, M. J., Murthy, K. K., Rovin, B. H., Bradley, W., Clark, R. A., Anderson, S. A., O'Connell R, J., Agan, B. K., Ahuja, S. S., Bologna, R., Sen, L., Dolan, M. J., and Ahuja, S. K. (2005) The influence of CCL3L1 gene-containing segmental duplications on HIV-1/AIDS susceptibility, *Science 307*, 1434-1440.

45. Cocchi, F., DeVico, A. L., Garzino-Demo, A., Arya, S. K., Gallo, R. C., and Lusso, P. (1995) Identification of RANTES, MIP-1 alpha, and MIP-1 beta as the major HIV-suppressive factors produced by CD8+ T cells, *Science 270*, 1811-1815.

46. Proudfoot, A. E., Buser, R., Borlat, F., Alouani, S., Soler, D., Offord, R. E., Schroder, J. M., Power, C. A., and Wells, T. N. (1999) Amino-terminally modified RANTES analogues demonstrate differential effects on RANTES receptors, *J Biol Chem 274*, 32478-32485.

47. Elsner, J., Mack, M., Bruhl, H., Dulkys, Y., Kimmig, D., Simmons, G., Clapham, P. R., Schlondorff, D., Kapp, A., Wells, T. N., and Proudfoot, A. E. (2000) Differential activation of CC chemokine receptors by AOP-RANTES, *J Biol Chem 275*, 7787-7794.

48. Gaertner, H., Cerini, F., Escola, J.-M., Kuenzi, G., Melotti, A., Offord, R., Rossitto-Borlat, I. n., Nedellec, R., Salkowitz, J., Gorochov, G., Mosier, D., and Hartley, O. (2008) Highly potent, fully recombinant anti-HIV chemokines: Reengineering a low-cost microbicide, *Proceedings of the National Academy of Sciences 105*, 17706-17711.

49. Rajagopal, S., Kim, J., Ahn, S., Craig, S., Lam, C. M., Gerard, N. P., Gerard, C., and Lefkowitz, R. J. (2010) Beta-arrestin- but not G protein-mediated signaling by the "decoy" receptor CXCR7, *Proc Natl Acad Sci U S A 107*, 628-632.

50. Loetscher, P., Pellegrino, A., Gong, J. H., Mattioli, I., Loetscher, M., Bardi, G., Baggiolini, M., and Clark-Lewis, I. (2001) The ligands of CXC chemokine receptor 3, I-TAC, Mig, and IP10, are natural antagonists for CCR3, *J Biol Chem 276*, 2986-2991.

51. Galandrin, S., Oligny-Longpre, G., Bonin, H., Ogawa, K., Gales, C., and Bouvier, M. (2008) Conformational rearrangements and signaling cascades involved in ligand-biased mitogen-activated protein kinase signaling through the beta1-adrenergic receptor, *Mol Pharmacol 74*, 162-172.

52. Zlotnik, A., and Yoshie, O. (2000) Chemokines: a new classification system and their role in immunity, *Immunity 12*, 121-127.

53. Moore, B. B., Arenberg, D. A., Stoy, K., Morgan, T., Addison, C. L., Morris, S. B., Glass, M., Wilke, C., Xue, Y. Y., Sitterding, S., Kunkel, S. L., Burdick, M. D., and Strieter, R. M. (1999) Distinct CXC chemokines mediate tumorigenicity of prostate cancer cells, *Am J Pathol 154*, 1503-1512.

54. Kijowski, J., Baj-Krzyworzeka, M., Majka, M., Reca, R., Marquez, L. A., Christofidou-Solomidou, M., Janowska-Wieczorek, A., and Ratajczak, M. Z. (2001) The SDF-1-CXCR4 axis stimulates VEGF secretion and activates integrins but does not affect proliferation and survival in lymphohematopoietic cells, *Stem Cells 19*, 453-466.

55. Terrillon, S., and Bouvier, M. (2004) Roles of G-protein-coupled receptor dimerization, *EMBO Rep 5*, 30-34.

56. Milligan, G. (2004) G protein-coupled receptor dimerization: function and ligand pharmacology, *Mol Pharmacol 66*, 1-7.

57. Springael, J. Y., Urizar, E., and Parmentier, M. (2005) Dimerization of chemokine receptors and its functional consequences, *Cytokine Growth Factor Rev 16*, 611-623.

58. Salanga, C. L., O'Hayre, M., and Handel, T. (2009) Modulation of chemokine receptor activity through dimerization and crosstalk, *Cell Mol Life Sci 66*, 1370-1386.

59. El-Asmar, L., Springael, J. Y., Ballet, S., Andrieu, E. U., Vassart, G., and Parmentier, M. (2005) Evidence for negative binding cooperativity within CCR5-CCR2b heterodimers, *Mol Pharmacol 67*, 460-469.

60. Mellado, M., Vila-Coro, A. J., Martinez, C., and Rodriguez-Frade, J. M. (2001) Receptor dimerization: a key step in chemokine signaling, *Cell Mol Biol (Noisy-le-grand) 47*, 575-582.

61. Issafras, H., Angers, S., Bulenger, S., Blanpain, C., Parmentier, M., Labbe-Jullie, C., Bouvier, M., and Marullo, S. (2002) Constitutive agonist-independent CCR5 oligomerization and antibody-mediated clustering occurring at physiological levels of receptors, *J Biol Chem 277*, 34666-34673.

62. Vila-Coro, A. J., Mellado, M., Martin de Ana, A., Lucas, P., del Real, G., Martinez, A. C., and Rodriguez-Frade, J. M. (2000) HIV-1 infection through the CCR5 receptor is blocked by receptor dimerization, *Proc Natl Acad Sci U S A 97*, 3388-3393.

63. Wilson, S., Wilkinson, G., and Milligan, G. (2005) The CXCR1 and CXCR2 receptors form constitutive homo- and heterodimers selectively and with equal apparent affinities, *J Biol Chem 280*, 28663-28674.

64. Toth, P. T., Ren, D., and Miller, R. J. (2004) Regulation of CXCR4 receptor dimerization by the chemokine SDF-1alpha and the HIV-1 coat protein gp120: a fluorescence resonance energy transfer (FRET) study, *J Pharmacol Exp Ther 310*, 8-17.

65. Trettel, F., Di Bartolomeo, S., Lauro, C., Catalano, M., Ciotti, M. T., and Limatola, C. (2003) Ligand-independent CXCR2 dimerization, *J Biol Chem 278*, 40980-40988.

66. Wang, J., He, L., Combs, C. A., Roderiquez, G., and Norcross, M. A. (2006) Dimerization of CXCR4 in living malignant cells: control of cell migration by a synthetic peptide that reduces homologous CXCR4 interactions, *Mol Cancer Ther 5*, 2474-2483.

67. Babcock, G. J., Farzan, M., and Sodroski, J. (2003) Ligand-independent dimerization of CXCR4, a principal HIV-1 coreceptor, *J Biol Chem 278*, 3378-3385.

68. Percherancier, Y., Berchiche, Y. A., Slight, I., Volkmer-Engert, R., Tamamura, H., Fujii, N., Bouvier, M., and Heveker, N. (2005) Bioluminescence resonance energy transfer reveals ligand-induced conformational changes in CXCR4 homo- and heterodimers, *J Biol Chem 280*, 9895-9903.

69. Vila-Coro, A. J., Rodriguez-Frade, J. M., Martin De Ana, A., Moreno-Ortiz, M. C., Martinez, A. C., and Mellado, M. (1999) The chemokine SDF-1alpha triggers CXCR4 receptor dimerization and activates the JAK/STAT pathway, *FASEB J 13*, 1699-1710.

70. Chakera, A., Seeber, R. M., John, A. E., Eidne, K. A., and Greaves, D. R. (2008) The duffy antigen/receptor for chemokines exists in an oligomeric form in living cells and functionally antagonizes CCR5 signaling through hetero-oligomerization, *Mol Pharmacol 73*, 1362-1370.

71. Mellado, M., Rodriguez-Frade, J. M., Vila-Coro, A. J., Fernandez, S., Martin de Ana, A., Jones, D. R., Toran, J. L., and Martinez, A. C. (2001) Chemokine receptor homo- or heterodimerization activates distinct signaling pathways, *Embo J 20*, 2497-2507.

72. Sohy, D., Parmentier, M., and Springael, J. Y. (2007) Allosteric transinhibition by specific antagonists in CCR2/CXCR4 heterodimers, *J Biol Chem 282*, 30062-30069.

73. Sierro, F., Biben, C., Martinez-Munoz, L., Mellado, M., Ransohoff, R. M., Li, M., Woehl, B., Leung, H., Groom, J., Batten, M., Harvey, R. P., Martinez, A. C., Mackay, C. R., and Mackay, F. (2007) Disrupted cardiac development but normal hematopoiesis in mice deficient in the second CXCL12/SDF-1 receptor, CXCR7, *Proc Natl Acad Sci U S A 104*, 14759-14764.

74. Contento, R. L., Molon, B., Boularan, C., Pozzan, T., Manes, S., Marullo, S., and Viola, A. (2008) CXCR4-CCR5: a couple modulating T cell functions, *Proc Natl Acad Sci U S A 105*, 10101-10106.

75. Mellado, M., Rodriguez-Frade, J. M., Vila-Coro, A. J., de Ana, A. M., and Martinez, A. C. (1999) Chemokine control of HIV-1 infection, *Nature 400*, 723-724.

76. Agrawal, L., Lu, X., Qingwen, J., VanHorn-Ali, Z., Nicolescu, I. V., McDermott, D. H., Murphy, P. M., and Alkhatib, G. (2004) Role for CCR5Delta32 protein in resistance to R5, R5X4, and X4 human immunodeficiency virus type 1 in primary CD4+ cells, *J Virol 78*, 2277-2287.

77. Hernandez, P. A., Gorlin, R. J., Lukens, J. N., Taniuchi, S., Bohinjec, J., Francois, F., Klotman, M. E., and Diaz, G. A. (2003) Mutations in the chemokine receptor gene CXCR4 are associated with WHIM syndrome, a combined immunodeficiency disease, *Nat Genet 34*, 70-74.

78. Lagane, B., Chow, K. Y., Balabanian, K., Levoye, A., Harriague, J., Planchenault, T., Baleux, F., Gunera-Saad, N., Arenzana-Seisdedos, F., and Bachelerie, F. (2008) CXCR4 dimerization and beta-arrestin-mediated signaling account for the enhanced chemotaxis to CXCL12 in WHIM syndrome, *Blood 112*, 34-44.

79. Balabanian, K., Lagane, B., Pablos, J. L., Laurent, L., Planchenault, T., Verola, O., Lebbe, C., Kerob, D., Dupuy, A., Hermine, O., Nicolas, J. F., Latger-Cannard, V., Bensoussan, D., Bordigoni, P., Baleux, F., Le Deist, F., Virelizier, J. L., Arenzana-Seisdedos, F., and Bachelerie, F. (2005) WHIM syndromes with different genetic anomalies are accounted for by impaired CXCR4 desensitization to CXCL12, *Blood 105*, 2449-2457.

80. Flaherty, P., Radhakrishnan, M. L., Dinh, T., Rebres, R. A., Roach, T. I., Jordan, M. I., and Arkin, A. P. (2008) A dual receptor crosstalk model of G-protein-coupled signal transduction, *PLoS Comput Biol 4*, e1000185.

81. Hill, S. M. (1998) Receptor crosstalk: communication through cell signaling pathways, *Anat Rec 253*, 42-48.

82. Selbie, L. A., and Hill, S. J. (1998) G protein-coupled-receptor cross-talk: the fine-tuning of multiple receptor-signalling pathways, *Trends Pharmacol Sci 19*, 87-93.

83. Barnes, P. J. (2006) Receptor heterodimerization: a new level of cross-talk, *J Clin Invest 116*, 1210-1212.

84. Porcile, C., Bajetto, A., Barbieri, F., Barbero, S., Bonavia, R., Biglieri, M., Pirani, P., Florio, T., and Schettini, G. (2005) Stromal cell-derived factor-1alpha (SDF-1alpha/CXCL12) stimulates ovarian cancer cell growth through the EGF receptor transactivation, *Exp Cell Res 308*, 241-253.

85. Scotton, C. J., Wilson, J. L., Scott, K., Stamp, G., Wilbanks, G. D., Fricker, S., Bridger, G., and Balkwill, F. R. (2002) Multiple actions of the chemokine CXCL12 on epithelial tumor cells in human ovarian cancer, *Cancer Res 62*, 5930-5938.

86. Venkatakrishnan, G., Salgia, R., and Groopman, J. E. (2000) Chemokine receptors CXCR-1/2 activate mitogen-activated protein kinase via the epidermal growth factor receptor in ovarian cancer cells, *J Biol Chem 275*, 6868-6875.

87. Gerard, C., and Rollins, B. J. (2001) Chemokines and disease, *Nat Immunol 2*, 108-115.

88. Fatkenheuer, G., Pozniak, A. L., Johnson, M. A., Plettenberg, A., Staszewski, S., Hoepelman, A. I., Saag, M. S., Goebel, F. D., Rockstroh, J. K., Dezube, B. J., Jenkins, T. M., Medhurst, C., Sullivan, J. F., Ridgway, C., Abel, S., James, I. T., Youle, M., and van der Ryst, E. (2005) Efficacy of short-term monotherapy with maraviroc, a new CCR5 antagonist, in patients infected with HIV-1, *Nat Med 11*, 1170-1172.

89. Horuk, R., Chitnis, C. E., Darbonne, W. C., Colby, T. J., Rybicki, A., Hadley, T. J., and Miller, L. H. (1993) A receptor for the malarial parasite Plasmodium vivax: the erythrocyte chemokine receptor, *Science 261*, 1182-1184.

90. Handel, T. M., and Horuk, R. (2010) Duffy antigen inhibitors: useful therapeutics for malaria?, *Trends Parasitol 26*, 329-333.

91. Sodhi, A., Montaner, S., and Gutkind, J. S. (2004) Viral hijacking of G-protein-coupled-receptor signalling networks, *Nat Rev Mol Cell Biol 5*, 998-1012.

92. Muller, A., Homey, B., Soto, H., Ge, N., Catron, D., Buchanan, M. E., McClanahan, T., Murphy, E., Yuan, W., Wagner, S. N., Barrera, J. L., Mohar, A., Verastegui, E., and Zlotnik, A. (2001) Involvement of chemokine receptors in breast cancer metastasis, *Nature 410*, 50-56.

93. Zlotnik, A. (2006) Involvement of chemokine receptors in organ-specific metastasis, *Contrib Microbiol 13*, 191-199.

94. Balkwill, F. (2004) Cancer and the chemokine network, *Nat Rev Cancer 4*, 540-550.

95. Gupta, G. P., and Massague, J. (2006) Cancer metastasis: building a framework, *Cell 127*, 679-695.

96. Murakami, T., Cardones, A. R., and Hwang, S. T. (2004) Chemokine receptors and melanoma metastasis, *J Dermatol Sci 36*, 71-78.

97. Ben-Baruch, A. (2003) Host microenvironment in breast cancer development: inflammatory cells, cytokines and chemokines in breast cancer progression: reciprocal tumor-microenvironment interactions, *Breast Cancer Res 5*, 31-36.

98. Kulbe, H., Levinson, N. R., Balkwill, F., and Wilson, J. L. (2004) The chemokine network in cancer--much more than directing cell movement, *Int J Dev Biol 48*, 489-496.

99. Sica, A., Schioppa, T., Mantovani, A., and Allavena, P. (2006) Tumour-associated macrophages are a distinct M2 polarised population promoting tumour progression: potential targets of anti-cancer therapy, *Eur J Cancer 42*, 717-727.

100. Murphy, P. M. (2001) Chemokines and the molecular basis of cancer metastasis, *N Engl J Med 345*, 833-835.

101. Friedl, P., and Wolf, K. (2003) Tumour-cell invasion and migration: diversity and escape mechanisms, *Nat Rev Cancer 3*, 362-374.

102. Tan, W., Martin, D., and Gutkind, J. S. (2006) The Galpha13-Rho signaling axis is required for SDF-1-induced migration through CXCR4, *J Biol Chem 281*, 39542-39549.

103. Tanaka, T., Bai, Z., Srinoulprasert, Y., Yang, B. G., Hayasaka, H., and Miyasaka, M. (2005) Chemokines in tumor progression and metastasis, *Cancer Sci 96*, 317-322.

104. Li, S., Guan, J. L., and Chien, S. (2005) Biochemistry and biomechanics of cell motility, *Annu Rev Biomed Eng 7*, 105-150.

105. Zhao, M., Mueller, B. M., Discipio, R. G., and Schraufstatter, I. U. (2007) Akt plays an important role in breast cancer cell chemotaxis to CXCL12, *Breast Cancer Res Treat*.

106. Zipin-Roitman, A., Meshel, T., Sagi-Assif, O., Shalmon, B., Avivi, C., Pfeffer, R. M., Witz, I. P., and Ben-Baruch, A. (2007) CXCL10 promotes invasion-related properties in human colorectal carcinoma cells, *Cancer Res 67*, 3396-3405.

107. Laudanna, C., Mochly-Rosen, D., Liron, T., Constantin, G., and Butcher, E. C. (1998) Evidence of zeta protein kinase C involvement in polymorphonuclear

neutrophil integrin-dependent adhesion and chemotaxis, *J Biol Chem 273*, 30306-30315.

108. Scala, S., Giuliano, P., Ascierto, P. A., Ierano, C., Franco, R., Napolitano, M., Ottaiano, A., Lombardi, M. L., Luongo, M., Simeone, E., Castiglia, D., Mauro, F., De Michele, I., Calemma, R., Botti, G., Caraco, C., Nicoletti, G., Satriano, R. A., and Castello, G. (2006) Human melanoma metastases express functional CXCR4, *Clin Cancer Res 12*, 2427-2433.

109. Webb, D. J., Donais, K., Whitmore, L. A., Thomas, S. M., Turner, C. E., Parsons, J. T., and Horwitz, A. F. (2004) FAK-Src signalling through paxillin, ERK and MLCK regulates adhesion disassembly, *Nat Cell Biol 6*, 154-161.

110. Balkwill, F. (2004) The significance of cancer cell expression of the chemokine receptor CXCR4, *Semin Cancer Biol 14*, 171-179.

111. Kakinuma, T., and Hwang, S. T. (2006) Chemokines, chemokine receptors, and cancer metastasis, *J Leukoc Biol 79*, 639-651.

112. Murakami, T., Cardones, A. R., Finkelstein, S. E., Restifo, N. P., Klaunberg, B. A., Nestle, F. O., Castillo, S. S., Dennis, P. A., and Hwang, S. T. (2003) Immune evasion by murine melanoma mediated through CC chemokine receptor-10, *J Exp Med 198*, 1337-1347.

113. Loetscher, P., Seitz, M., Baggiolini, M., and Moser, B. (1996) Interleukin-2 regulates CC chemokine receptor expression and chemotactic responsiveness in T lymphocytes, *J Exp Med 184*, 569-577.

114. Li, Y. M., Pan, Y., Wei, Y., Cheng, X., Zhou, B. P., Tan, M., Zhou, X., Xia, W., Hortobagyi, G. N., Yu, D., and Hung, M. C. (2004) Upregulation of CXCR4 is essential for HER2-mediated tumor metastasis, *Cancer Cell 6*, 459-469.

115. Busillo, J. M., and Benovic, J. L. (2007) Regulation of CXCR4 signaling, *Biochim Biophys Acta 1768*, 952-963.

116. Staller, P., Sulitkova, J., Lisztwan, J., Moch, H., Oakeley, E. J., and Krek, W. (2003) Chemokine receptor CXCR4 downregulated by von Hippel-Lindau tumour suppressor pVHL, *Nature 425*, 307-311.

117. Schioppa, T., Uranchimeg, B., Saccani, A., Biswas, S. K., Doni, A., Rapisarda, A., Bernasconi, S., Saccani, S., Nebuloni, M., Vago, L., Mantovani, A., Melillo, G., and Sica, A. (2003) Regulation of the chemokine receptor CXCR4 by hypoxia, *J Exp Med 198*, 1391-1402.

118. Maxwell, P. J., Gallagher, R., Seaton, A., Wilson, C., Scullin, P., Pettigrew, J., Stratford, I. J., Williams, K. J., Johnston, P. G., and Waugh, D. J. (2007) HIF-1 and NF-kappaB-mediated upregulation of CXCR1 and CXCR2 expression promotes cell survival in hypoxic prostate cancer cells, *Oncogene*.

119. Wilson, J. L., Burchell, J., and Grimshaw, M. J. (2006) Endothelins induce CCR7 expression by breast tumor cells via endothelin receptor A and hypoxia-inducible factor-1, *Cancer Res 66*, 11802-11807.

120. Helbig, G., Christopherson, K. W., 2nd, Bhat-Nakshatri, P., Kumar, S., Kishimoto, H., Miller, K. D., Broxmeyer, H. E., and Nakshatri, H. (2003) NF-kappaB promotes breast cancer cell migration and metastasis by inducing the expression of the chemokine receptor CXCR4, *J Biol Chem 278*, 21631-21638.

121. Siveen, K. S., and Kuttan, G. (2009) Role of macrophages in tumour progression, *Immunol Lett 123*, 97-102.

122. Burger, J. A., and Kipps, T. J. (2006) CXCR4: a key receptor in the crosstalk between tumor cells and their microenvironment, *Blood 107*, 1761-1767.

123. Homey, B., Muller, A., and Zlotnik, A. (2002) Chemokines: agents for the immunotherapy of cancer?, *Nat Rev Immunol 2*, 175-184.

124. Balkwill, F., and Mantovani, A. (2001) Inflammation and cancer: back to Virchow?, *Lancet 357*, 539-545.

125. Coussens, L. M., and Werb, Z. (2002) Inflammation and cancer, *Nature 420*, 860-867.

126. Fox, J. A., Ung, K., Tanlimco, S. G., and Jirik, F. R. (2002) Disruption of a single Pten allele augments the chemotactic response of B lymphocytes to stromal cell-derived factor-1, *J Immunol 169*, 49-54.

127. Holland, J. D., Kochetkova, M., Akekawatchai, C., Dottore, M., Lopez, A., and McColl, S. R. (2006) Differential functional activation of chemokine receptor

CXCR4 is mediated by G proteins in breast cancer cells, *Cancer Res 66*, 4117-4124.

128. Arvanitakis, L., Geras-Raaka, E., Varma, A., Gershengorn, M. C., and Cesarman, E. (1997) Human herpesvirus KSHV encodes a constitutively active G-protein-coupled receptor linked to cell proliferation, *Nature 385*, 347-350.

129. Burger, J. A., Burger, M., and Kipps, T. J. (1999) Chronic lymphocytic leukemia B cells express functional CXCR4 chemokine receptors that mediate spontaneous migration beneath bone marrow stromal cells, *Blood 94*, 3658-3667.

130. Yang, T. Y., Chen, S. C., Leach, M. W., Manfra, D., Homey, B., Wiekowski, M., Sullivan, L., Jenh, C. H., Narula, S. K., Chensue, S. W., and Lira, S. A. (2000) Transgenic expression of the chemokine receptor encoded by human herpesvirus 8 induces an angioproliferative disease resembling Kaposi's sarcoma, *J Exp Med 191*, 445-454.

131. Burger, M., Burger, J. A., Hoch, R. C., Oades, Z., Takamori, H., and Schraufstatter, I. U. (1999) Point mutation causing constitutive signaling of CXCR2 leads to transforming activity similar to Kaposi's sarcoma herpesvirus-G protein-coupled receptor, *J Immunol 163*, 2017-2022.

132. Slettenaar, V. I., and Wilson, J. L. (2006) The chemokine network: a target in cancer biology?, *Adv Drug Deliv Rev 58*, 962-974.

133. Burns, J. M., Summers, B. C., Wang, Y., Melikian, A., Berahovich, R., Miao, Z., Penfold, M. E., Sunshine, M. J., Littman, D. R., Kuo, C. J., Wei, K., McMaster, B. E., Wright, K., Howard, M. C., and Schall, T. J. (2006) A novel chemokine receptor for SDF-1 and I-TAC involved in cell survival, cell adhesion, and tumor development, *J Exp Med 203*, 2201-2213.

134. Balabanian, K., Lagane, B., Infantino, S., Chow, K. Y., Harriague, J., Moepps, B., Arenzana-Seisdedos, F., Thelen, M., and Bachelerie, F. (2005) The chemokine SDF-1/CXCL12 binds to and signals through the orphan receptor RDC1 in T lymphocytes, *J Biol Chem 280*, 35760-35766.

135. Miao, Z., Luker, K. E., Summers, B. C., Berahovich, R., Bhojani, M. S., Rehemtulla, A., Kleer, C. G., Essner, J. J., Nasevicius, A., Luker, G. D., Howard, M. C., and Schall, T. J. (2007) CXCR7 (RDC1) promotes breast and lung tumor growth in vivo and is expressed on tumor-associated vasculature, *Proc Natl Acad Sci U S A 104*, 15735-15740.

136. Gravel, S., Malouf, C., Boulais, P. E., Berchiche, Y. A., Oishi, S., Fujii, N., Leduc, R., Sinnett, D., and Heveker, N. (2010) The peptidomimetic CXCR4 antagonist TC14012 recruits beta-arrestin to CXCR7: roles of receptor domains, *J Biol Chem 285*, 37939-37943.

137. Thelen, M., and Thelen, S. (2008) CXCR7, CXCR4 and CXCL12: an eccentric trio?, *J Neuroimmunol 198*, 9-13.

138. Heesen, M., Berman, M. A., Charest, A., Housman, D., Gerard, C., and Dorf, M. E. (1998) Cloning and chromosomal mapping of an orphan chemokine receptor: mouse RDC1, *Immunogenetics 47*, 364-370.

139. Wu, B., Chien, E. Y., Mol, C. D., Fenalti, G., Liu, W., Katritch, V., Abagyan, R., Brooun, A., Wells, P., Bi, F. C., Hamel, D. J., Kuhn, P., Handel, T. M., Cherezov, V., and Stevens, R. C. (2010) Structures of the CXCR4 chemokine GPCR with small-molecule and cyclic peptide antagonists, *Science 330*, 1066-1071.

140. Naumann, U., Cameroni, E., Pruenster, M., Mahabaleshwar, H., Raz, E., Zerwes, H. G., Rot, A., and Thelen, M. (2010) CXCR7 functions as a scavenger for CXCL12 and CXCL11, *PLoS One 5*, e9175.

141. Perlin, J. R., and Talbot, W. S. (2007) Signals on the move: chemokine receptors and organogenesis in zebrafish, *Sci STKE 2007*, pe45.

142. Locati, M., Torre, Y. M., Galliera, E., Bonecchi, R., Bodduluri, H., Vago, G., Vecchi, A., and Mantovani, A. (2005) Silent chemoattractant receptors: D6 as a decoy and scavenger receptor for inflammatory CC chemokines, *Cytokine Growth Factor Rev 16*, 679-686.

143. Mantovani, A., Bonecchi, R., and Locati, M. (2006) Tuning inflammation and immunity by chemokine sequestration: decoys and more, *Nat Rev Immunol 6*, 907-918.

144. Dambly-Chaudiere, C., Cubedo, N., and Ghysen, A. (2007) Control of cell migration in the development of the posterior lateral line: antagonistic interactions between the chemokine receptors CXCR4 and CXCR7/RDC1, *BMC Dev Biol 7*, 23.

145. Levoye, A., Balabanian, K., Baleux, F., Bachelerie, F., and Lagane, B. (2009) CXCR7 heterodimerizes with CXCR4 and regulates CXCL12-mediated G protein signaling, *Blood 113*, 6085-6093.

146. Kang, Y., Siegel, P. M., Shu, W., Drobnjak, M., Kakonen, S. M., Cordon-Cardo, C., Guise, T. A., and Massague, J. (2003) A multigenic program mediating breast cancer metastasis to bone, *Cancer Cell 3*, 537-549.

147. Maksym, R. B., Tarnowski, M., Grymula, K., Tarnowska, J., Wysoczynski, M., Liu, R., Czerny, B., Ratajczak, J., Kucia, M., and Ratajczak, M. Z. (2009) The role of stromal-derived factor-1--CXCR7 axis in development and cancer, *Eur J Pharmacol 625*, 31-40.

148. Zlotnik, A. (2006) Chemokines and cancer, *Int J Cancer 119*, 2026-2029.

149. Marchesi, F., Monti, P., Leone, B. E., Zerbi, A., Vecchi, A., Piemonti, L., Mantovani, A., and Allavena, P. (2004) Increased survival, proliferation, and migration in metastatic human pancreatic tumor cells expressing functional CXCR4, *Cancer Res 64*, 8420-8427.

150. Zhou, Y., Larsen, P. H., Hao, C., and Yong, V. W. (2002) CXCR4 is a major chemokine receptor on glioma cells and mediates their survival, *J Biol Chem 277*, 49481-49487.

151. Nishio, M., Endo, T., Tsukada, N., Ohata, J., Kitada, S., Reed, J. C., Zvaifler, N. J., and Kipps, T. J. (2005) Nurselike cells express BAFF and APRIL, which can promote survival of chronic lymphocytic leukemia cells via a paracrine pathway distinct from that of SDF-1alpha, *Blood 106*, 1012-1020.

152. Smith, M. C., Luker, K. E., Garbow, J. R., Prior, J. L., Jackson, E., Piwnica-Worms, D., and Luker, G. D. (2004) CXCR4 regulates growth of both primary and metastatic breast cancer, *Cancer Res 64*, 8604-8612.

153. Redjal, N., Chan, J. A., Segal, R. A., and Kung, A. L. (2006) CXCR4 inhibition synergizes with cytotoxic chemotherapy in gliomas, *Clin Cancer Res 12*, 6765-6771.

154. Lee, C. H., Kakinuma, T., Wang, J., Zhang, H., Palmer, D. C., Restifo, N. P., and Hwang, S. T. (2006) Sensitization of B16 tumor cells with a CXCR4 antagonist increases the efficacy of immunotherapy for established lung metastases, *Mol Cancer Ther 5*, 2592-2599.

155. Zabel, B. A., Wang, Y., Lewen, S., Berahovich, R. D., Penfold, M. E., Zhang, P., Powers, J., Summers, B. C., Miao, Z., Zhao, B., Jalili, A., Janowska-Wieczorek, A., Jaen, J. C., and Schall, T. J. (2009) Elucidation of CXCR7-mediated signaling

events and inhibition of CXCR4-mediated tumor cell transendothelial migration by CXCR7 ligands, *J Immunol 183*, 3204-3211.

CHAPTER 2

Targeted Investigation of CXCL12/CXCR4 Signaling in Chronic Lymphocytic Leukemia

2.1 Introduction to B Cell Chronic Lymphocytic Leukemia

B cell Chronic Lymphocytic Leukemia (CLL) is the most common leukemia in the Western world [*1*]. The disease is characterized by the accumulation of mature, CD5+, monoclonal B cells in the blood, bone marrow and secondary lymphoid tissues [*2*]. Approximately 7,800 people in the United States are diagnosed with the disease annually and ~5,000 CLL patients die each year; to date there is no cure and thus new therapeutic strategies are needed [*3*]. CLL mostly affects the older population with a median age of 72 at diagnosis and is rarely observed in people under age 35 [*4-5*]. Epidemiological studies have revealed biases in the incidence of CLL as it is much more prevalent in Caucasian than African, Native American, and Asian ethnicities and is nearly twice as common in men as women [*4-5*]. Additionally, CLL is a heterogeneous disease with highly variable clinical progression, which will be elaborated in more detail later in this section [*2*].

CLL is diagnosed based on high B lymphocyte count (>5000 B cells/μL) of small monoclonal B cells bearing a typical immunophenotype of CD19, CD20 (dim), CD5 (dim), CD23, CD43, and CD79a expression and low expression of surface immunoglobulin M (IgM) and IgD [*6*]. Some patients never exhibit major symptoms and do not require treatment whereas other patients exhibit a rapid and aggressive clinical course of the disease. The major symptoms experienced by different CLL patients

include lymphadenopathy (enlarged lymph nodes), anemia, thrombocytopenia (decrease in platelets), weight loss, fever, and extreme fatigue. CLL patients also generally have a decrease in immunoglobulin levels in the blood and an increased susceptibility to certain infections, which is the major cause of morbidity and mortality in CLL patients [*6*]. Since the majority of CLL patients are elderly, aggressive chemotherapeutics and treatment options are usually not possible. The current frontline chemotherapeutic used to treat CLL patients is fludarabine, a purine analog and DNA synthesis inhibitor [*7*]. Other therapeutic regiments include chlorambucil (alkylating agent), rituximab (chimeric monoclonal antibody against CD20), cyclophosphamide (alkylating agent), alemtuzumab (monoclonal antibody against CD52), as well as various combinations of these drugs [*6*]. Although these treatments can reduce the tumor burden, they are not curative and development of fludarabine-refractory disease is a major hurdle in providing long-term treatment to CLL patients.

The accumulation of CLL cells in patients was originally believed to be due to an apoptotic defect of the cells since the majority of CLL cells are arrested in the G_0/G_1 phase of the cell cycle and thus proliferation rates are very low. However, this theory was challenged as CLL cells will die rapidly in *in vitro* culture even under conditions that support culture of B cells from healthy donors [*8*]. Now it is believed that their accumulation is due, in large part, to protection and enhanced responsiveness to survival signals from the microenvironment accompanied by low rates of proliferation from precursor cells [*2*]. Supporting this notion, the apoptosis of CLL cells in culture can be rescued by accessory cells including "Nurse-Like cells" (NLCs), which provide CLL cells with survival factors that protect them from spontaneous and drug-induced apoptosis in culture (Figure 2.1) [*8*]. Correspondingly, the *in vivo* microenvironment is believed to provide protective niches where NLCs secrete survival factors that prolong

the longevity of CLL cells thereby limiting the effectiveness of therapeutic agents [*8-10*]. Interestingly, this process involves a two-way communication whereby CLL cells, in contrast to normal B cells, have the unique ability to shape their microenvironment. CLL cells secrete factors that induce differentiation of monocytes into NLCs, essentially the tumor-associated macrophages of CLL, which are phenotypically and functionally distinct from normal macrophages, the default path of cell differentiation (Figures 2.2 and 2.3).

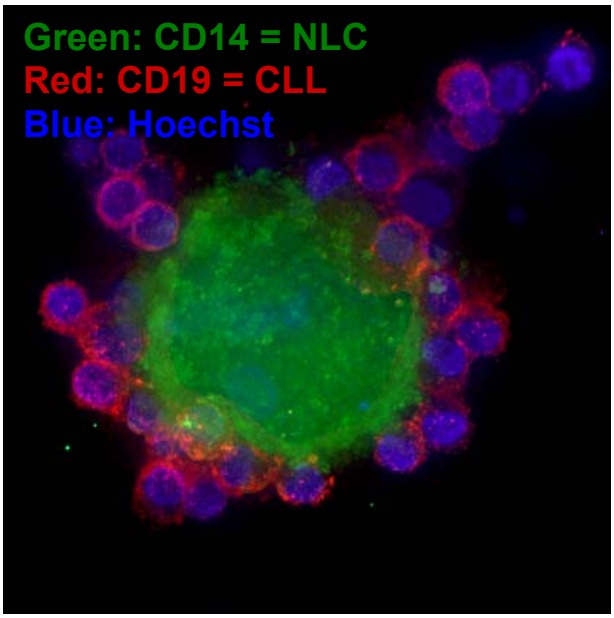

Figure 2.1 Image of CLL cells surrounding a NLC. Immunofluorescence image of CLL cells stained in red using a PE-conjugated antibody against CD19 and NLCs in green using a FITC-conjugated antibody against CD14. A Hoechst-DAPI nuclei stain is in blue. Image is reprinted from Tsukada et al. (2002) *Blood* [*11*].

The factors produced by CLL cells that are responsible for this transformation of monocytes to NLCs are still mostly unknown. Conditioned media from CLL cells in culture is sufficient to promote the differentiation of CD14+ monocytes from healthy donors into the NLCs that enhance CLL cell survival, providing support that the CLL cells

are modifying their environment (Figure 2.3). Based on preliminary data from Dr. Davorka Messmer's lab, TNF-α was found to be an important factor in this process, but it is not sufficient and so other contributing factors still need to be identified (unpublished data, personal communication). The factors produced by NLCs that in turn promote survival of CLL cells include BAFF, APRIL, and the chemokine CXCL12 (SDF-1) [*8, 10, 12*]. Furthermore, CXCR4 is overexpressed on CLL cells compared to healthy normal B cells, suggesting CLL cells may have enhanced responsiveness to CXCL12 signaling [*8-10*]. Additionally, CXCR4 antagonists sensitize CLL cells to killing by chemotherapeutic agents like fludarabine *in vitro* [*13*]. However, these factors do not fully recapitulate the survival benefits provided by NLCs [*10*], indicating that unidentified survival factors are secreted by the NLCs (Figure 2.4).

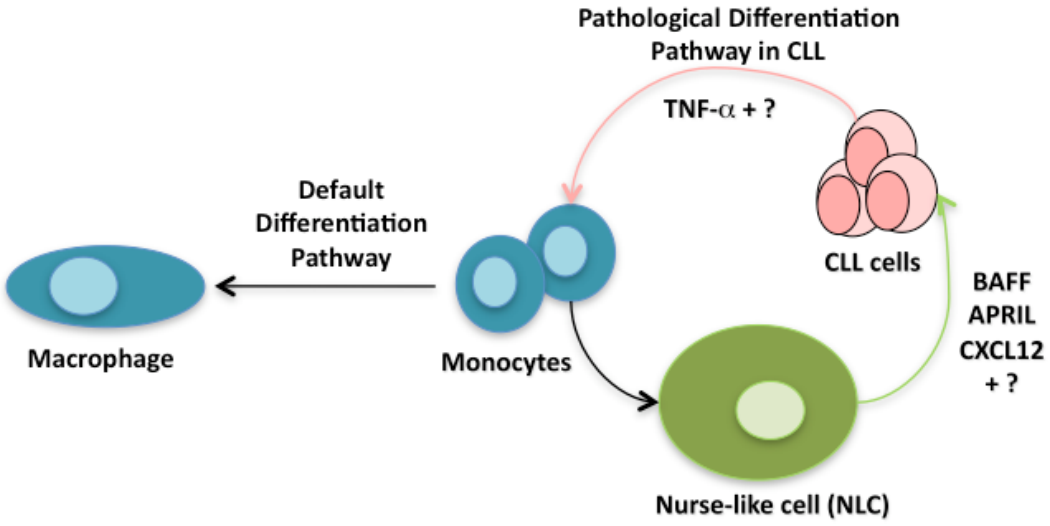

Figure 2.2 Illustration of the CLL-NLC crosstalk. In normal physiology, monocytes enter tissues where they differentiate into macrophages. However, the presence of CLL cells can drive monocytes to differentiate into CLL-modified macrophages, called Nurse-Like Cells (NLCs). TNF-α was identified as a factor produced by CLL cells that contributes to this transformation; however, additional factors are required. In turn, the NLCs produce proteins promoting CLL cell survival, including CXCL12, BAFF, APRIL, and additional factors that remain to be identified.

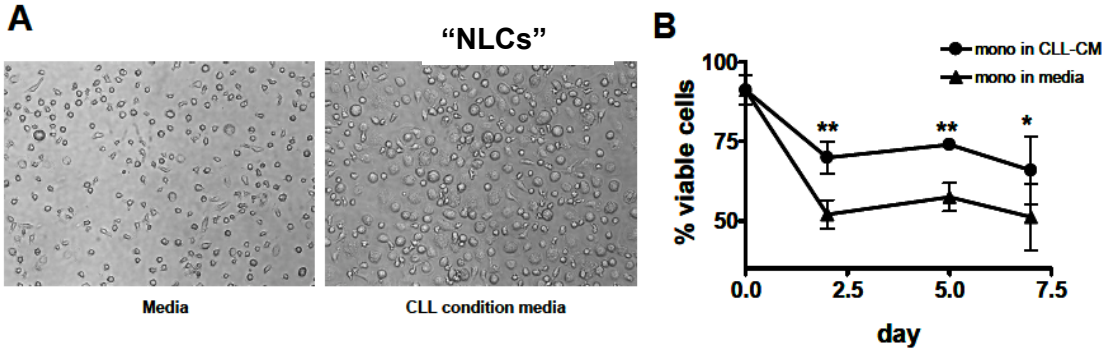

Figure 2.3 Monocytes cultured in CLL-conditioned media support CLL cell survival. A) Conditioned media from purified CLL cells induces morphological changes in monocytes resulting in differentiation into Nurse-Like Cells (NLCs). B) Monocytes cultured with CLL-conditioned media (NLCs) increases the survival of CLL cells compared to those in control media. The data shown are mean +/- SD of 6 independent experiments. (Unpublished data from D. Messmer)

NLCs were found to express much higher levels of CXCL12, BAFF and APRIL compared to normal monocytes. BAFF and APRIL belong to the tumor necrosis factor (TNF) family of proteins and are thought to promote CLL survival through distinct mechanisms compared to CXCL12 [*10*]. BAFF and APRIL, but not CXCL12, were found to induce activation of NF-κB, while only CXCL12 induced ERK1/2 and Akt phosphorylation in CLL cells [*10*]. In support of non-redundant functions of these proteins, combinations of CXCL12 (SDF-1) and BAFF/APRIL appeared to have additive contributions to CLL survival (Figure 2.4). Other chemokines including CCL19 and CCL21, which both bind to the chemokine receptor CCR7 expressed on CLL cells, are also believed to promote CLL cell survival. Whether these chemokines function similarly or through distinct mechanisms compared to CXCL12 is unclear. While CXCL12, CCL19 and CCL21 share the ability to induce Akt and ERK1/2 activation in CLL cells, it appears that CCL19 and CCL21 function as much stronger migratory cues, suggesting there are some differences in how these different chemokines influence CLL signaling [*14-15*].

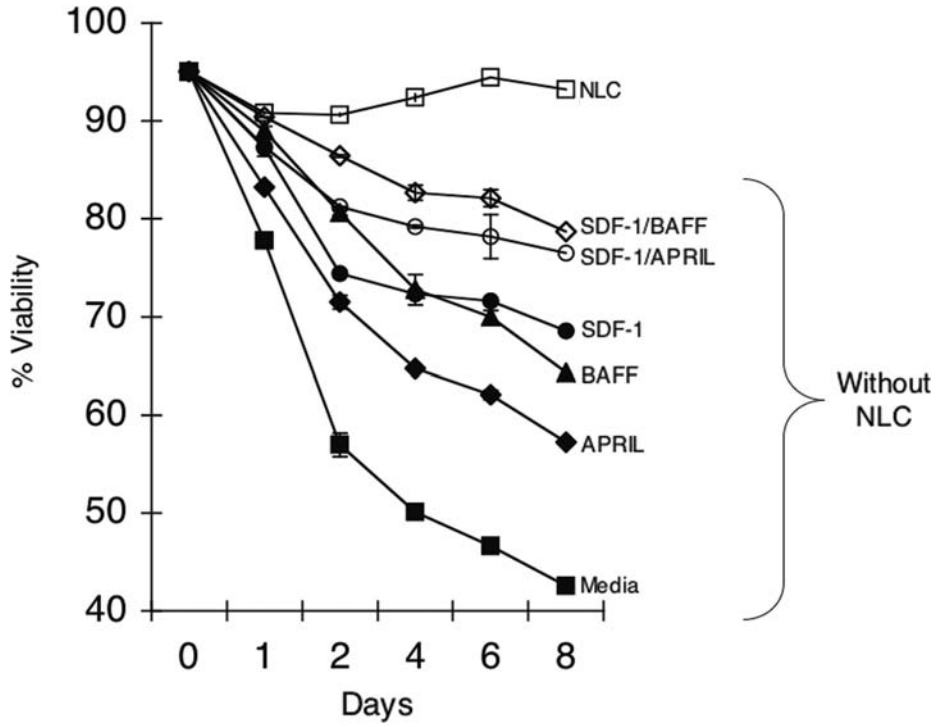

Figure 2.4 Effect of NLCs, CXCL12 (SDF-1), BAFF, and APRIL on CLL cell survival. CLL cells were cultured with or without NLCs. CLL cultures without NLCs were left untreated or were exposed to CXCL12, BAFF, and APRIL. The mean viability +/- SEM of replicate wells was determined following PI-$DiOC_6$ staining by flow cytometry for each time point. Figure is reprinted from Nishio et al. (2005) *Blood* [*10*].

As previously mentioned, CLL is a heterogeneous disease and patients exhibit strikingly different clinical progression and outcome. CLL patients can generally be segregated into two prognostic groups based on the number of mutations in the immunoglobulin heavy chain variable regions (IgV_H) of the B cell receptor (BCR) [*16-17*]. Those with unmutated IgV_H typically show an aggressive course and shorter survival time compared to patients with mutated IgV_H [*18-19*]. CLL cells with unmutated IgV_H often have stereotyped BCRs and the BCR is usually polyreactive to a variety of autoantigens, which may contribute to CLL pathogenesis of this more aggressive prognostic group [*5*].

Expression of the tyrosine kinase zeta-associated protein 70 (ZAP-70) and cell surface glycoprotein CD38 are also predictors of disease progression. High ZAP-70 expression (denoted by >20% of cells expressing ZAP-70) correlates with aggressive disease and low or no expression is observed in cells from patients with indolent disease [*20*]. Similarly, high CD38 expression is indicative of more aggressive disease [*21*]. ZAP-70 is a tyrosine kinase expressed in T cells, but generally not in B cells, that is recruited to the immunoreceptor tyrosine-based activation motifs (ITAMs) of an activated T-cell receptor (TCR). This process leads to activation of ZAP-70 through tyrosine phosphorylation by Lck, thereby inducing of a number of signaling cascades including PLC-γ and ERK1/2 [*22*]. The tyrosine kinase, $p72^{Syk}$, plays an analogous role to ZAP-70 in B cells, associating with the ITAMs of the BCR and mediating antigen-receptor signal transduction. Since $p72^{Syk}$ is expressed at similar levels in CLL cells and normal B cells and can efficiently mediate BCR signaling, it is unclear what role ZAP-70 expression may have in CLL cells although it has been proposed to enhance BCR signaling [*23*]. Interrogation of the role of ZAP-70 in CLL by Chen *et al.* revealed an interesting finding in which enhanced IgM signaling associated with ZAP-70 expression in CLL cells was independent of its kinase activity, as introduction of a kinase-defective mutant of ZAP-70 elicited the same effects as wild type ZAP-70 [*22*]. These results suggested that the effects of ZAP-70 in CLL might largely be attributed to a scaffolding role facilitating recruitment of other proteins to the BCR, and indeed the SH2 domain of ZAP-70 was found to be critical for enhanced calcium flux in stimulated CLL cells [*22*]. Although the mechanisms by which ZAP-70 may be linked to disease prognosis are largely unknown, these studies have provided some insight into how ZAP-70 may function in CLL.

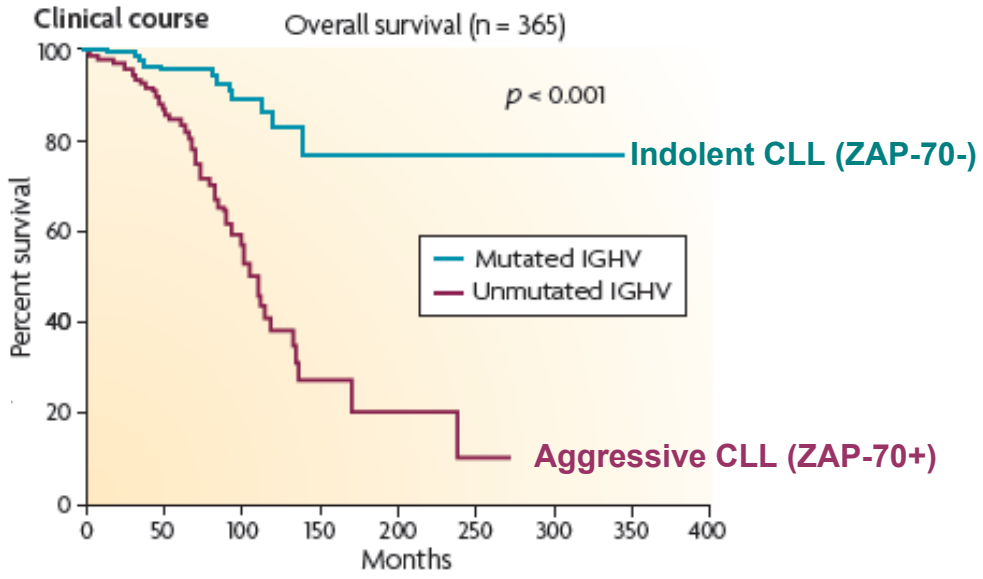

Figure 2.5 Clinical course of CLL. Percent survival of CLL patients classified with aggressive disease based on unmutated *IGHV* (IgV_H) status (maroon) versus indolent disease with mutated IGHV (blue). Modified from Zenz et al. (2010) *Nature Reviews* [*5*].

Although these three different markers (IgV_H, ZAP-70, and CD38) typically correlate with one another in terms of prognosis for disease progression, there are some discrepancies and certain limitations to their use as prognostic markers. The marker primarily used to distinguish between indolent and aggressive CLL in these studies is ZAP-70, although information regarding IgV_H, CD38 and other factors such as age, gender, Rai stage [*24*] and treatment are also known and considered when interpreting the data. Additional considerations for disease aggressiveness include *TP53* mutation leading to p53 inactivation, which generally coincides with chromosome 17p deletion. 17p deletion is observed in ~4-9% of untreated CLL patients, although this percentage can increase following chemotherapy due to selective pressure and clonal evolution [*5*]. As expected due to the importance of p53 in regulating apoptosis, these patients generally exhibit poor prognosis and refractory disease, which confers resistance to

chemotherapy (this prognosis is independent of IgV_H, ZAP-70 and CD38). Nevertheless, refractory CLL is also common among patients that do not have 17p deletions or *TP53* mutations, indicating that other factors are involved in this process [*5*]. The majority of CLL patients eventually become refractory to therapeutic treatment, which is one of the major hurdles in treating CLL [*5*]. Therefore, a better understanding of the biology of the disease and pathways that may be exploited and/or altered in CLL is important for the development of novel therapeutic agents for better and more effective treatment.

Although CXCL12 alone cannot recapitulate the NLC support of CLL survival, it provides a good starting point for characterizing how the CLL cells respond to survival signals. Therefore, we took two different approaches to addressing the functions and signaling mechanisms by which CXCL12 promotes survival of CLL cells: a targeted approach based on known survival mechanisms as presented in this chapter as well as chapters 3 and 4, and a more global and unbiased phosphoproteomics approach presented in chapters 5 and 6. Some preliminary work and future plans to explore what other factors are involved in the two-way communication between CLL cells and NLCs are also discussed in Chapter 8: Conclusions and Future Perspectives. Comparison of cells derived from both patient subgroups (aggressive and indolent) provides a unique opportunity for delineating specific signaling events contributing to aggressive disease and those that are shared attributes of CLL cell accumulation and survival.

Our goal was to characterize the signaling cascades activated by CXCL12 to provide a better understanding of the important pathways and molecular signatures contributing to CLL pathogenesis and ultimately identify new targets along these signaling pathways that if inhibited, will sensitize CLL cells to killing, alone or in combination with current chemotherapeutic treatments. Although CXCR4 antagonists have the potential for blocking pro-survival signals and conceivably mobilizing the most

resistant CLL cells from their protective microenvironments, they have been shown to effectively mobilize CXCR4 expressing hematopoietic progenitors in healthy individuals as well [*25-26*]. One must consider potential problems in targeting CXCR4 as a strategy, since the most likely side effect is that normal hematopoietic progenitor cells will be mobilized and thus experience increased cytotoxicity from chemotherapy. Therefore, characterizing the downstream signaling events following CXCR4 activation may identify potential molecular entities that would be better pharmacological targets for treating CLL.

2.2 Expression and Purification of CXCL12

In order to facilitate the investigation of CXCL12-mediated survival signaling in CLL, it was necessary to express and purify large quantities of CXCL12. The current cost of commercially available recombinant human CXCL12 is exorbitant, ranging from $200-400 for 10 μg of protein. The ability to produce large quantities of chemokines enabled us to interrogate CXCL12 signaling and perform the phosphoproteomics experiments described in later chapters, which would otherwise be cost limiting. Using an established protocol from a former graduate student in the Handel lab, Susan Crown, I was able to generate multi-milligram quantities of CXCL12 for these studies; a description of this procedure is presented here. For a more detailed protocol describing purification steps, see Appendix AI.1.

Human CXCL12 (SDF-1α) was codon optimized for expression in bacteria and cloned into a pET21a vector. It was expressed as a His-tag fusion with an enterokinase cleavage site (DDDDK) and purified from inclusion bodies in BL21 *E. coli*. Bacterial cultures were induced with 0.5 mM IPTG at an OD_{600} of ~0.6. Bacterial pellets were resuspended in 10 mM Tris-Cl pH 8.0, 1 mM $MgCl_2$ with 200 μg DNAse, and Complete protease inhibitor cocktail (EDTA-free) (Roche) and then sonicated and washed with

deoxycholate. Pellets were solubilized in 6 M guanadine-HCl, 100 mM sodium phosphate, 10 mM Tris-Cl, pH 8.0, using a dounce homogenizer. The protein was then filtered and purified over a Ni-NTA column eluting with buffer containing 6 M guanidine-HCl, 100 mM sodium phosphate, 10 mM Tris pH 4.0. Fractions containing protein were pooled and refolded with Hampton Fold-It Buffer #8 overnight at 4°C (Hampton Research, Aliso Viejo, CA). Following refolding, the CXCL12 was dialyzed and concentrated using Amicon Ultra centrifugal concentrators (MWCO=5000). The His-tag was removed by cleaving with enterokinase (NEB, Ipswich, MA) at a 1:100,000 molar ratio overnight at room temperature. The CXCL12 was then purified by reversed phase-HPLC and lyophilized for long-term storage (Figures 2.6 and 2.7). Verification of the identity and purity of the CXCL12 was assessed by mass spectrometry (MS) (MW= 7.96 kDa) (Figure 2.8). A more detailed protocol of CXCL12 expression and purification is presented in Appendix AI.1.

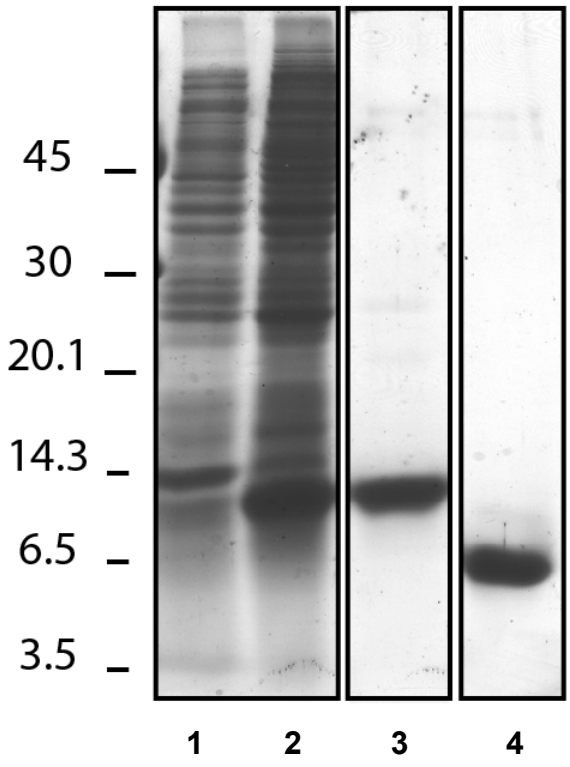

Figure 2.6 Gel showing steps of CXCL12 purification process. Gel with sample fractions from the purification procedure was Coomassie stained for proteins and lanes of interest were cropped. Lanes show steps of the purification procedure: 1) prior to IPTG induction 2) following IPTG induction but prior to purification 3) following purification but prior to enterokinase cleavage and 4) final enterokinase cleaved and HPLC purified CXCL12. Molecular weight indications are shown on the left hand side of the image.

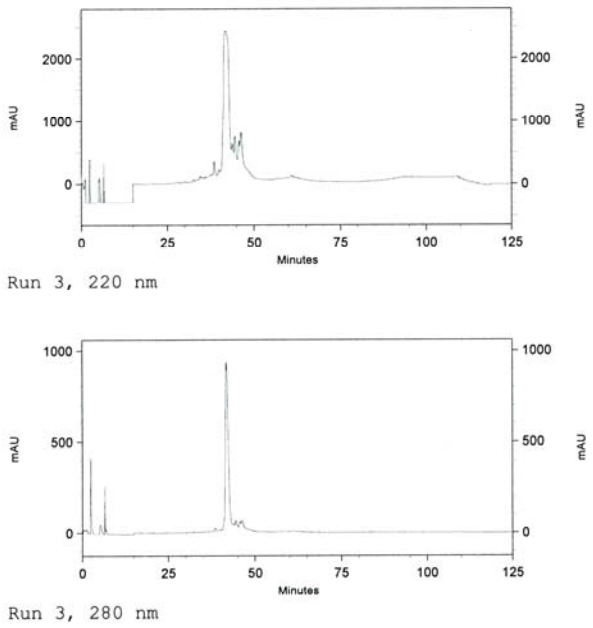

Figure 2.7 HPLC chromatograms of CXCL12. The A220 (top) and A280 (bottom) traces from the HPLC purification step of CXCL12 preparation are shown.

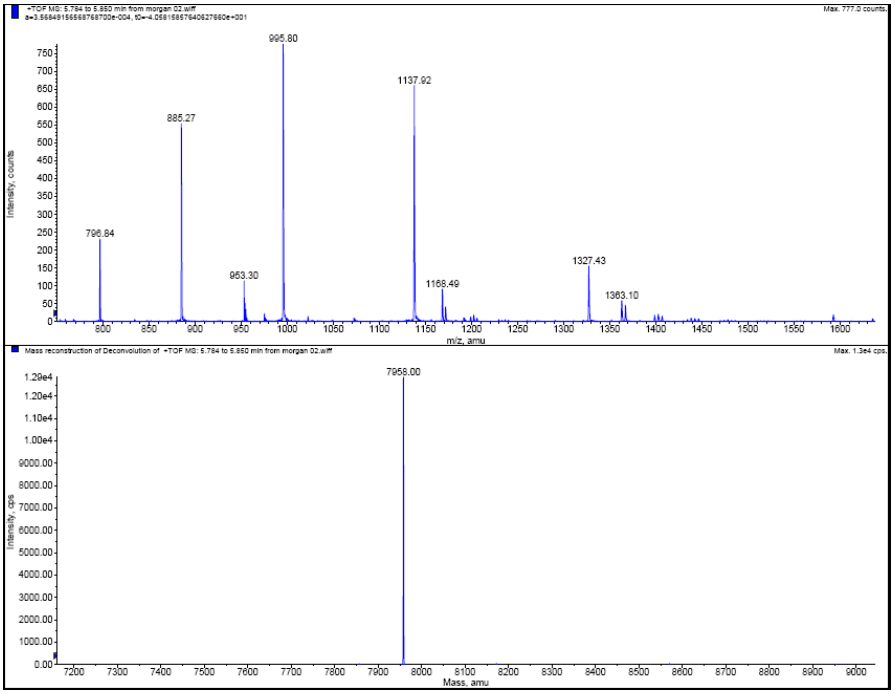

Figure 2.8 Mass spectrum of purified CXCL12. A sample of the purified CXCL12 was sent to the Scripps Institute Mass Spectrometry core for ESI MS analysis in order to verify and assess purity of the protein.

Since the molecular weight of 7958 Da determined by MS corresponded to that of recombinant CXCL12 and the purity looked very good, it was next necessary to verify functionality of the purified protein. Thus, transwell migration assays (Corning, Corning, NY) with Jurkat T cells were performed over a range of CXCL12 concentrations from 0-100 nM. As shown in Figure 2.9, the purified CXCL12 was functional and effectively elicited migration response of Jurkat cells.

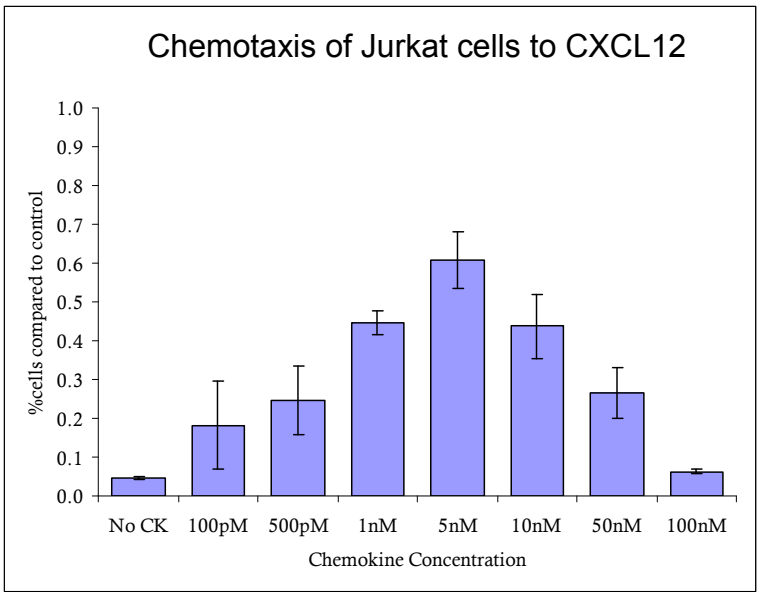

Figure 2.9 Chemotaxis of Jurkat cells to recombinant CXCL12. A transwell migration assay was performed on Jurkat cells in response to a range of CXCL12 concentrations (No CK= no chemokine up to 100 nM) and percent of cells migrated was calculated by counting cells migrated through via flow cytometry. Experiments were performed in triplicate and error represents standard deviation of the mean.

2.3 Characterization of CXCL12-Mediated Survival in Aggressive (ZAP-70+) Versus Indolent (ZAP-70-) CLL

Upon commencement of this project, it was established that CXCL12 could partially rescue the survival of CLL cells in culture (Figure 2.4), and that stimulation of CLL cells with CXCL12 induced phosphorylation and activation of well established growth and survival pathways, Akt and ERK1/2 [*8, 10*]. However, these early studies

were done on small patient sample sets and it was unknown whether there were differences in CXCL12-mediated survival and survival signaling between the aggressive and indolent prognostic groups (segregated based on ZAP-70 expression). Therefore, we first characterized the survival response of purified CLL cells in culture with 30 nM CXCL12 compared to media alone (Figure 2.10).

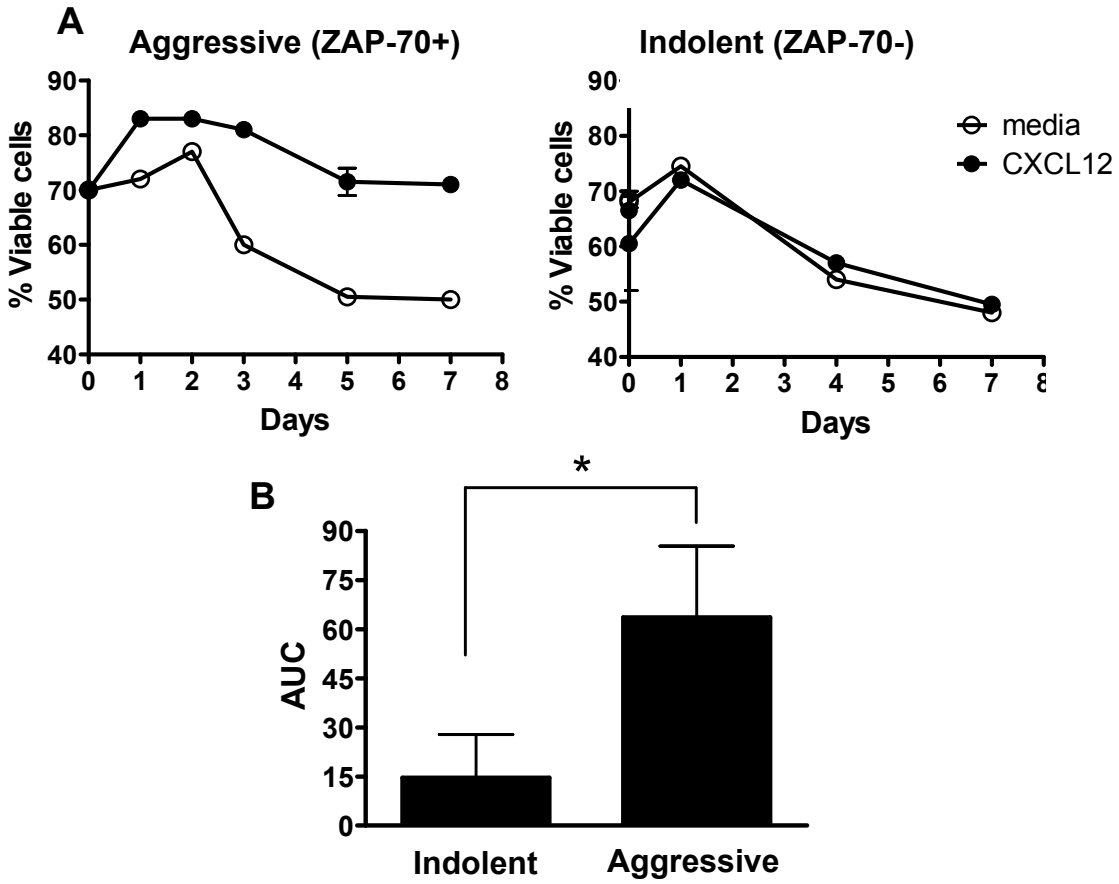

Figure 2.10 CXCL12 confers stronger survival advantage to aggressive ZAP-70+ CLL cells. Purified CLL cells were cultured in presence or absence of CXCL12 (30 nM). The effect of CXCL12 on CLL cell viability was measured at the indicated time points by flow cytometry measuring the mitochondrial transmembrane potential with $DiOC_6$ and membrane permeability to propidium iodine (PI). A) A representative survival experiment with a ZAP-70+ (left) and a ZAP-70- (right) patient's cells is shown. B) To quantitatively compare the CXCL12-mediated increase in viability over time, the area under the curve was measured with and without CXCL12 in ZAP-70+ CLL (n=6) and ZAP-70- CLL (n=5) samples and the increase in viability in response to CXCL12 is depicted. The * indicates a statistically significant difference with $p < 0.05$ based on a paired Student t-test. (Unpublished data from collaboration with Dr. Davorka Messmer's lab).

While CXCL12 generally provided survival benefit to both CLL subsets, it conferred a statistically significant stronger survival advantage to the aggressive (ZAP-70+) CLL cells. Figure 2.10B shows the average survival response to CXCL12 over multiple patients where the area under the curve (AUC) value is the difference between viability of CXCL12 stimulated and unstimulated CLL cells over time (0 would indicate no effect on survival and positive values indicate better survival with stimulation); Figure 2.10 A shows representative viability plots from individual ZAP-70+ and ZAP-70- patients. These findings have since been corroborated by another group [*14*]. We as well as several other groups noted that these differences in survival cannot be explained by differences in the levels of CXCR4 expression between the two prognostic groups [*14, 27*]. As described in our published article presented in Chapter 3, internalization and recycling kinetics of CXCR4 were similar between ZAP-70+ and ZAP-70- CLL patients' cells and surface levels of CXCR7 were undetectable on these cells [*27*]. Therefore, the differences in survival must be related to downstream signaling events as opposed to CXCR4 or CXCR7 expression levels or turnover/recycling kinetics.

Thus, we examined whether there were differences in downstream signaling events between the CLL prognostic groups. First we probed for CXCL12-mediated phosphorylation and activation of Akt and ERK1/2, well established growth and survival pathways known to be activated downstream of CXCL12 in CLL cells [*10*]. Although there is inherent heterogeneity in the signaling responses between patients, there was an evident trend in which the aggressive ZAP-70+ CLL cells appeared to have more robust and prolonged phosphorylation of ERK1/2, while Akt signaling was more comparable between the two subsets (representative western blots in Figure 2.11). With regard to ERK1/2 activation, all ZAP-70+ cells probed versus only ~80% of ZAP-70- CLL cells exhibited ERK1/2 phosphorylation in response to CXCL12 (n>20 for each subset).

These differences in ERK1/2 phosphorylation between ZAP-70- and ZAP-70+ CLL subsets were more quantitatively assessed and followed-up in greater detail as described in the published article reprinted in Chapter 3 [27].

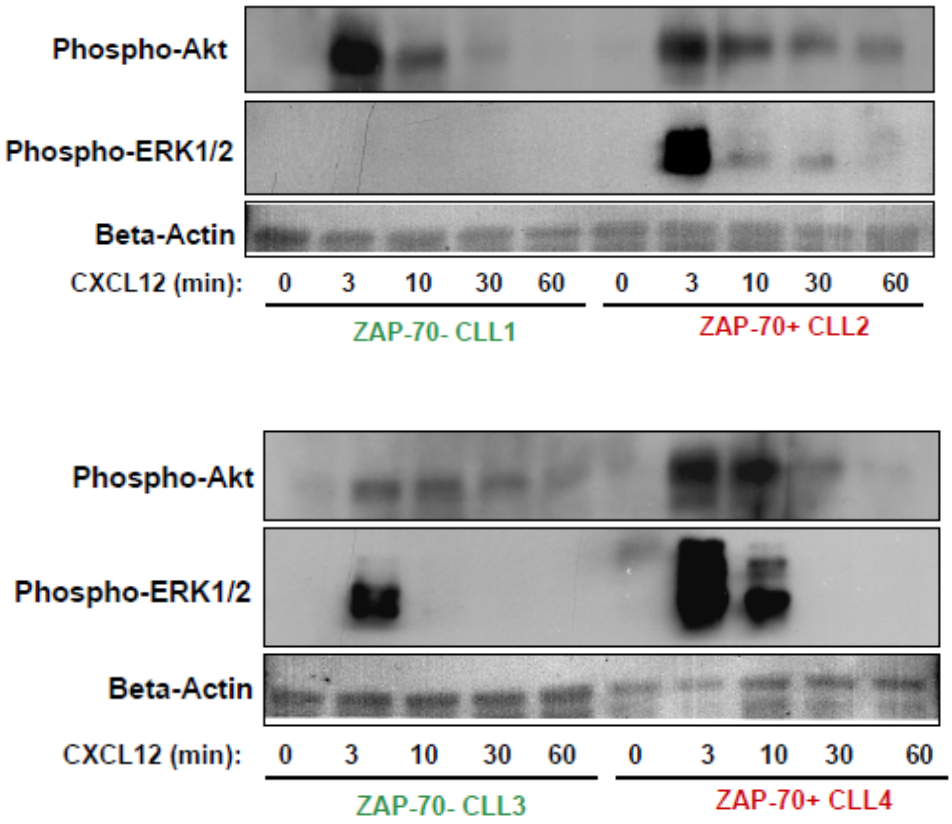

Figure 2.11 CXCL12-mediated phosphorylation of Akt and ERK1/2 in ZAP-70+ vs ZAP-70- CLL cells. Western blots of CLL cell lysates from 4 different patients (2xZAP-70+ on right and 2xZAP-70- on left) stimulated over an hour time course with CXCL12 (30 nM) and probed for Akt and ERK1/2 phosphorylation. β-actin served as a loading control.

Thus, while the differences in ERK1/2 signaling may help distinguish between aggressive and indolent CLL phenotypes, Akt signaling may underlie the accumulation and longevity of CLL cells in general, regardless of clinical course. In the following section, various known downstream targets of Akt, as shown in Figure 2.12, were characterized for CXCL12-mediated regulation. Additionally, we detected a global loss of the PHLPP1 phosphatase, which directly dephosphorylates Akt thereby negatively

regulating its activity, in the majority of CLL cells; the mechanisms and consequences of the loss of PHLPP1 in CLL are described in Chapter 4.

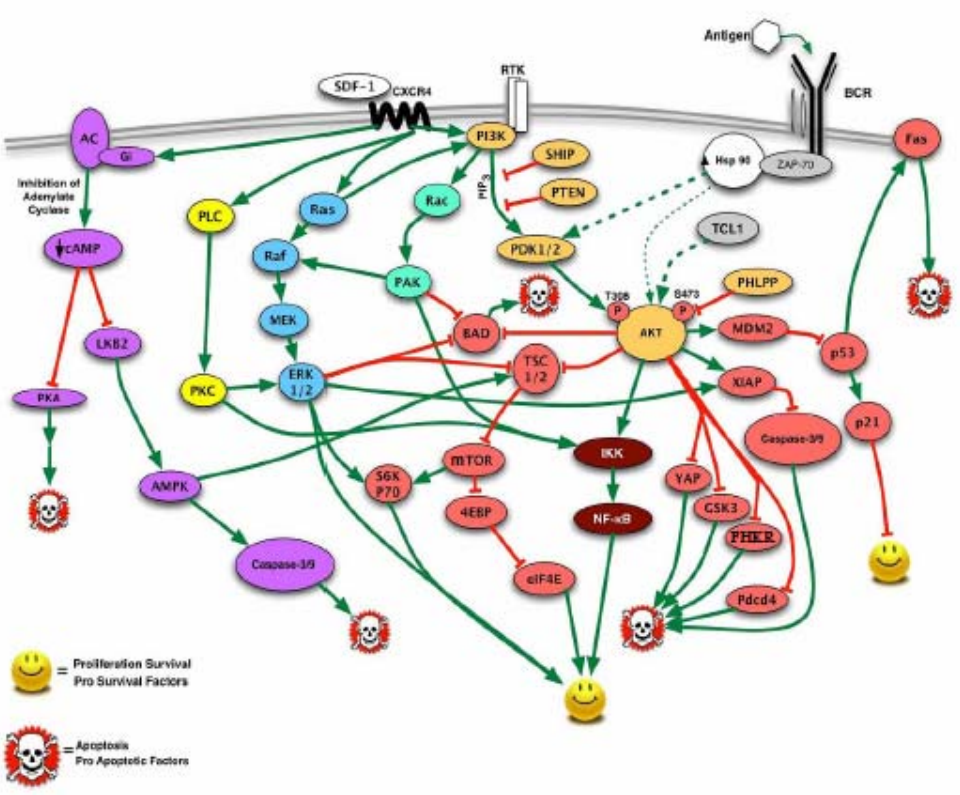

Figure 2.12 Potential CXCL12-mediated signaling pathways that enhance survival and/or inhibit apoptotic factors. Green arrows indicate factors that are induced and red lines ending with a bar indicate factors that are inhibited by the upstream factor. Binding of CXCL12 (SDF-1) to CXCR4 activates the G protein, Gi. Numerous survival pathways, activated by CXCR4 signaling through Gi are depicted in the figure above.

2.4 Elucidation of CXCL12-Induced Signaling Downstream of Akt

Several potential downstream targets of CXCL12 signaling were probed by western blot in order to more fully characterize the mechanisms mediating the survival and longevity effects in the CLL cells. Several classic targets downstream of Akt that are associated with regulation of apoptosis, including the pro-apoptotic Bcl-2-associated death promoter (BAD) and the mammalian target of rapamycin (mTOR), do not exhibit significant changes in phosphorylation in response to CXCL12-induced Akt activation

(Figure 2.13 A and B) [*28-29*]. However, this does not preclude an important role of these molecules to CLL survival, especially since the BAD antibodies are weak and other important phosphorylation sites besides S136 could not be effectively probed (e.g. S112). Furthermore, using small molecule inhibitors of mTOR signaling such as Rapamycin would more accurately reflect the contributions of the mTOR pathway. Nevertheless, due to lack of strong data implicating these proteins in CXCL12 signaling, they were not pursued any further in the context of this work.

Mcl-1, a pro-survival Bcl-2 family member and downstream target of the Akt pathway that has been previously implicated in CLL survival [*30*], was found to be constitutively expressed in all 17 CLL samples probed; yet, only 3 samples showed any CXCL12-induced Mcl-1 expression (data not shown), consistent with previous findings [*10*]. Expression levels of T cell leukemia-1 (TCL-1), a co-activator of Akt that is implicated in a number of leukemias [*31*], were also examined among the CLL patient samples. TCL-1 was found to be constitutively expressed in the CLL cells probed, yet overall there were few differences in TCL-1 expression between patient subsets based on ZAP-70 expression, and as expected, no changes in levels in response to a short 30 min time course of CXCL12 stimulation (a longer time course to determine if CXCL12 signaling altered TCL-1 stability was not performed) (Figure 2.14). Notably however, CXCL12 did induce a robust and prolonged phosphorylation and activation of HDM2/MDM2 (human/murine double minute 2) and phosphorylation and inhibition of GSK-3β (glycogen synthase kinase 3β) (Figure 2.13 C and D).

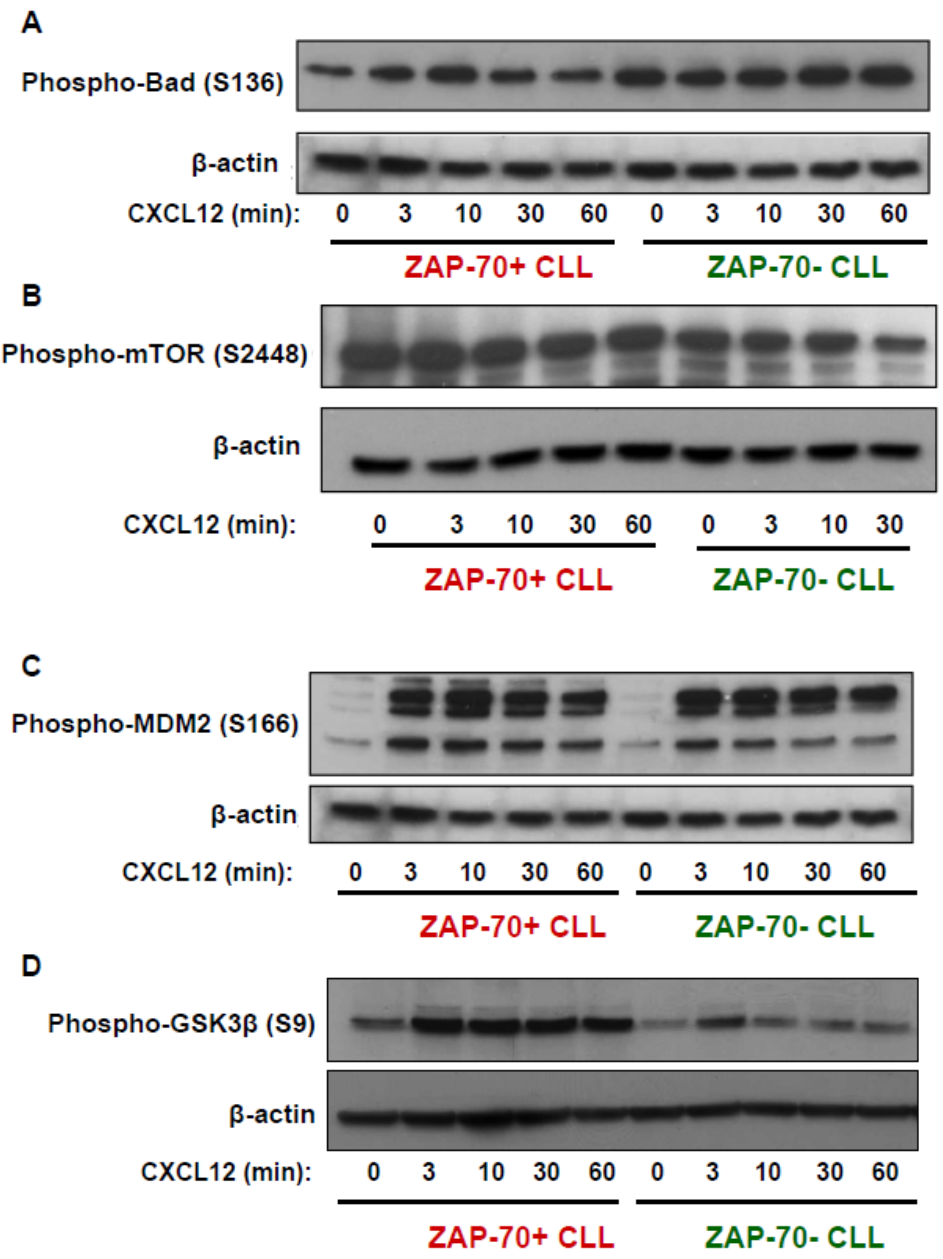

Figure 2.13 Analysis of potential targets of CXCL12 signaling downstream of Akt activation. ZAP-70+ (left) and ZAP-70- (right) CLL patient cells were stimulated over an hour time course with 30 nM CXCL12 and probed for A) phospho-Bad (S136) B) phospho-mTOR (S2448) C) phospho-MDM2 (S166) and D) phospho-GSK3β. β-actin served as a loading control.

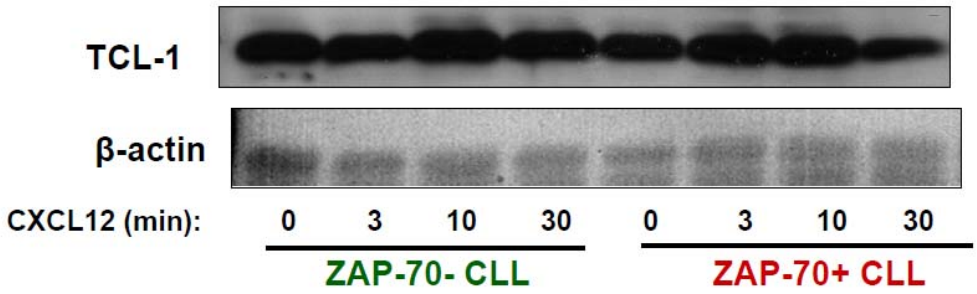

Figure 2.14 TCL-1 expression in ZAP-70- and ZAP-70+ CLL cells. Representative western blot depicting TCL-1 expression in from a ZAP-70- and a ZAP-70+ CLL patients' cells. Cells had been stimulated over a 30 min time course with 30 nM CXCL12. β-actin served as a loading control.

2.5 Characterization of CXCL12-Mediated MDM2 Phosphorylation

The strong phosphorylation of MDM2 that was observed in response to CXCL12 stimulation was intriguing (Figure 2.13 C). MDM2 is an E3 ligase responsible for degrading p53, which is an important modulator of cell cycle as well as apoptosis in response to a variety of stresses including DNA damage and certain extracellular death stimuli (Figure 2.15) [*32-33*]. Akt and MDM2 have also been shown to negatively regulate the forkhead transcription factor, Foxo3A (Figure 2.15) [*34*]. Foxo3A is believed to trigger cell death via upregulation of genes important for apoptosis including Bim and Puma [*35-36*]. Therefore, MDM2-mediated degradation of p53 and Foxo3A could play an important role in CXCL12-mediated CLL cell survival and protection from chemotherapeutic agents. Thus, we examined the effects of MDM2 on CLL survival by examining CXCL12 survival and p53 and Foxo3A response in CLL cells following DNA damage induced by gamma irradiation. Although the ultimate goal is to determine if the activation of MDM2 may be involved in CLL cell resistance to chemotherapeutic agents, we started by examining the effects of gamma irradiation since chemotherapeutics have

multifaceted and diverse effects towards promoting cell death besides DNA damage/p53 response.

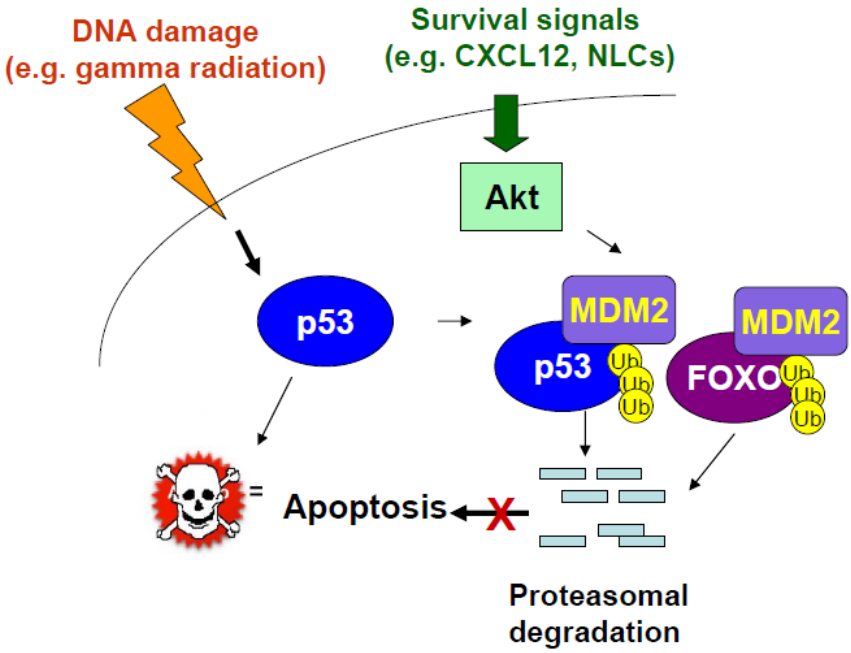

Figure 2.15 Figure illustrating the relationship between MDM2, p53 and Foxo3A. DNA damage induces expression of p53, a protein important for regulating DNA damage repair and promoting apoptosis when the damage is too severe. Signaling through Akt phosphorylates and activates MDM2, which ubiquitinates and thereby targets p53 and Foxo3A for proteasomal degradation.

We first more closely examined the phosphorylation response of MDM2 to CXCL12. As shown in Figure 2.16, stimulation of CLL cells with CXCL12 (3 min) induces phosphorylation of MDM2. This phosphorylation response, however, can be blocked by pre-incubation with the CXCR4 inhibitor, AMD3100, and by pertussis toxin treatment, an inhibitor of Gi signaling. These results confirm that this phosphorylation response is specifically related to CXCL12/CXCR4 signaling and occurs through a Gi-dependent pathway. To relate these findings to a situation more representative of the microenvironment, we also looked at MDM2 phosphorylation in the presence and

absence of NLC coculture. We found that coculture of CLL cells with NLCs in the absence of exogenous CXCL12 induced phosphorylation of MDM2 as well (Figure 2.16).

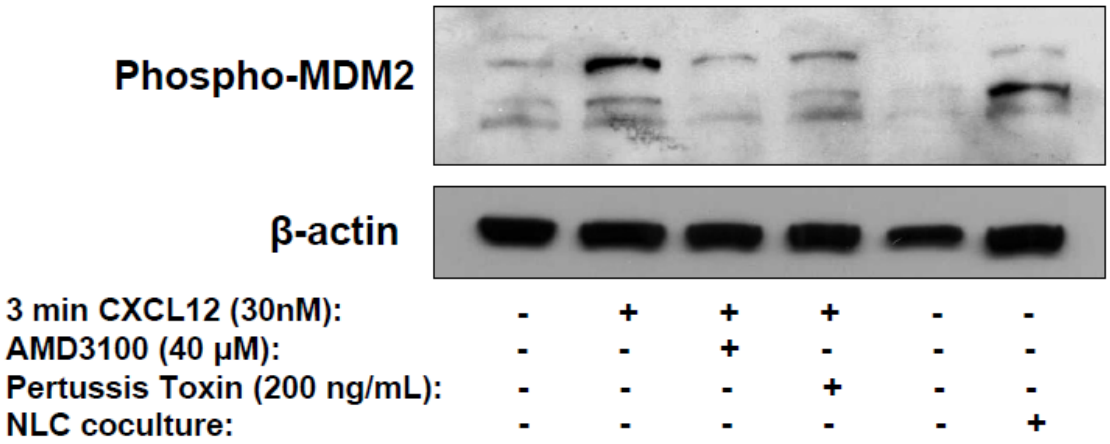

Figure 2.16 Phosphorylation of MDM2 by CXCL12 can be blocked by AMD3100 and Pertussis Toxin and is promoted by NLCs. Western blot detecting MDM2 phosphorylation of CLL cells cultured in the presence (+) or absence (-) of 3 min 30nM CXCL12, and 1 h pre-treatment with 40 μM AMD3100 or 200 ng/mL Pertussis Toxin. MDM2 phosphorylation in the absence (-) or presence (+) of NLC coculture is also shown. β-actin served as a loading control.

To examine the potential consequences of this CXCL12-mediated MDM2 phosphorylation, we compared the survival of gamma-irradiated (5 Gy) CLL cells cultured in the presence (+) or absence (-) of CXCL12 (non-irradiated cell survival is also shown as a control) (Figure 2.17). As expected, viability of CLL cells was worse following gamma-irradiation compared to the non-irradiated cells. CXCL12 did promote slight increases in CLL cell survival in both irradiated and non-irradiated cells (Figure 2.17). However, CXCL12 was not sufficient to fully rescue the CLL cells from radiation-induced cell death.

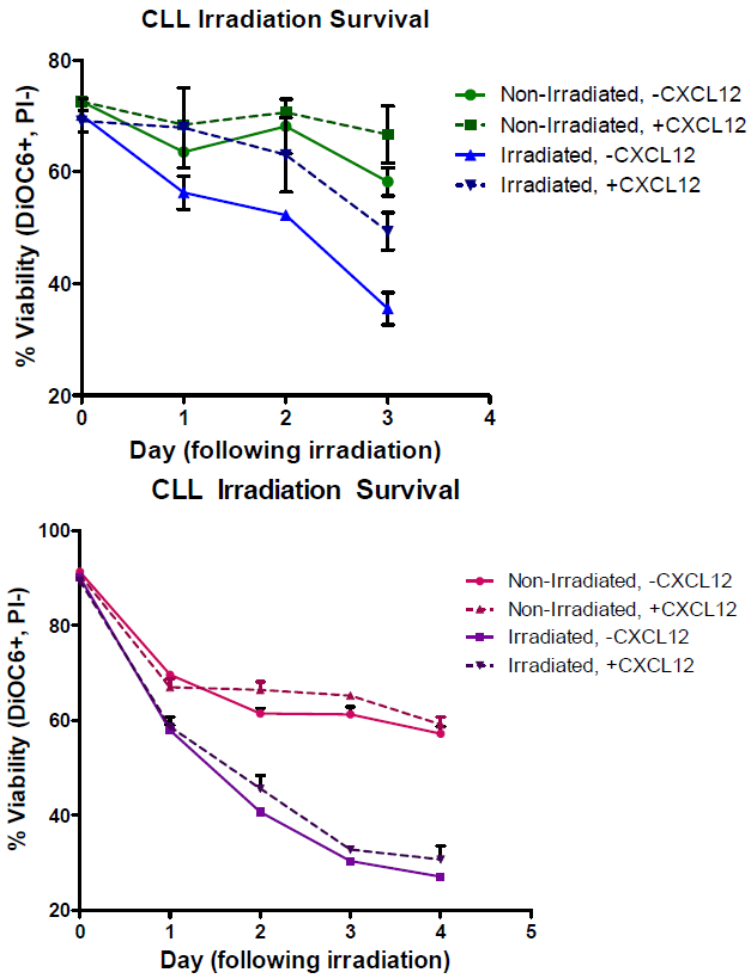

Figure 2.17 CLL cell survival following irradiation in the presence or absence of CXCL12. Representative survival profiles of CLL cells from two different patients (ZAP-70+ on top, ZAP-70- on bottom) γ-irradiated (5 Gy dose) or non-irradiated controls cultured in the presence (+, dashed lines) or absence (-, solid lines) of 75 nM CXCL12. Viability was measured at the indicated time points by flow cytometry measuring the mitochondrial transmembrane potential with $DiOC_6$ and membrane permeability to propidium iodine (PI). Error bars indicate standard deviation of duplicate or triplicate measurements.

Since γ-irradiation causes DNA damage, it should lead to an induction of p53 expression in CLL cells. Although, it was not surprising that CXCL12 alone could not completely rescue irradiation-mediated CLL cell death, we wanted to look more molecularly at its effects on p53 and Foxo3A, as downstream targets of MDM2 activation. Since MDM2 is responsible for the degradation of p53 and Foxo3A, we

expected there to be a decrease in the levels of these proteins in the CXCL12-treated cells. Our preliminary results indicated that, as expected, p53 is expressed following irradiation; however there are no significant differences in the levels of p53 between the CLL cells cultured in the presence or absence of CXCL12 (Figure 2.18). Although a 24 h time point post-CXCL12 treatment is shown in Figure 2.18, other time points out to 96 h were taken and probed for p53 expression and similarly, no differences in p53 levels were observed in these other time points (data not shown).

Foxo3A was previously shown to be phosphorylated and inhibited by CXCL12 as well as other chemokines, and that this inactivation of Foxo3A was related to chemokine-induced CLL cell survival effects [*37*]. I too have confirmed an increase in the phosphorylation and inhibition of Foxo3A upon CXCL12 stimulation in CLL cells (data not shown). Thus, there are multiple possible links between CXCL12 and Foxo3A regulation including Akt-mediated inhibition and MDM2-mediated degradation. Therefore, it was surprising to find that following 24 h of CXCL12 stimulation, no decreases in total Foxo3A protein were observed in the non-irradiated CLL cells and in fact, a strong increase in Foxo3A expression was observed following CXCL12 treatment in the irradiated CLL cells (Figure 2.18). In addition, we observed a similar effect whereby CXCL12 induced an increase in another forkhead transcription factor, Foxo4, following irradiation (data not shown). While the reasons for the observed increases in Foxo transcription factor expression upon CXCL12 stimulation specifically in irradiated CLL cells are unclear, it is possibly due to some feedback regulation. Nevertheless, the lack of striking data with p53 and Foxo3A regulation by CXCL12 reflects the only mild survival benefits of CXCL12 on the irradiated CLL cells (Figure 2.17). It is also possible that further optimization and use of a more relevant apoptotic agent, such as fludarabine

or another chemotherapeutic agent, could yield different results, but this has yet to be explored.

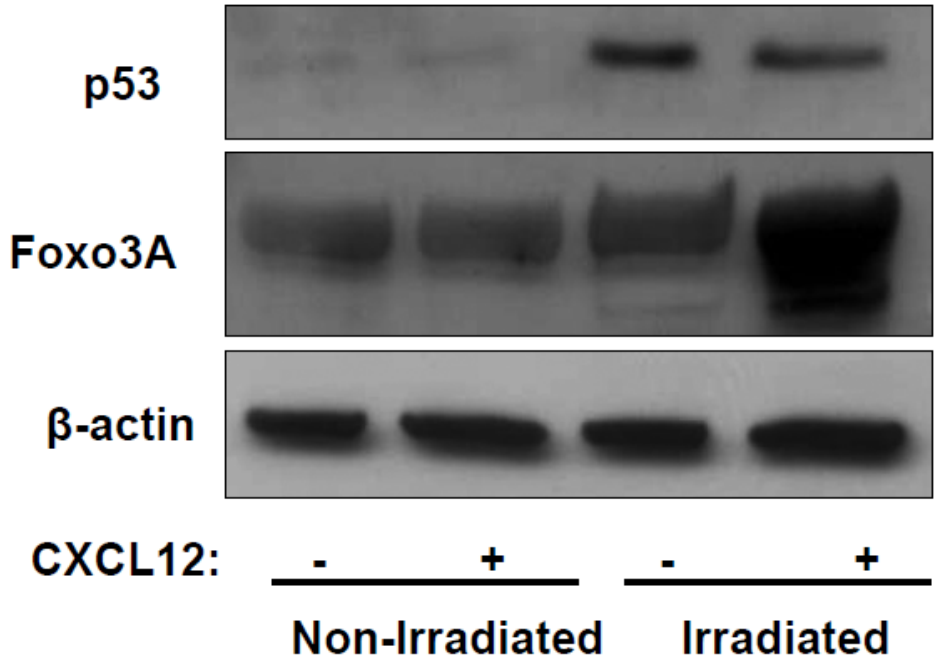

Figure 2.18 Effects of CXCL12 on p53 and Foxo-3A levels in the presence and absence of γ-irradiation. Western blot showing p53 and Foxo-3A levels in non-irradiated and irradiated (5 Gy) CLL cells 24 h following treatment, cultured in the presence (+) or absence (-) of 75 nM CXCL12. β-actin served as a loading control.

Using a different approach to examine potential effects of MDM2 and p53 on CLL cell survival in response to γ-irradiation-induced DNA damage, irradiated and non-irradiated control cells were cocultured with NLCs. First, we examined the ability of NLC coculture to rescue the irradiation-induced cell death in CLL cells and compared this to CLL cells that exhibited 17p deletion, indicative of p53 deletion/mutation, which should be refractory to irradiation-induced cell death. As mentioned previously, the 17p deletion and *TP53* mutations/deletions are present in ~4-9% of CLL cases, which underlies refractory disease in these patients. As shown in Figure 2.19 A, the CLL cells with the p53 mutation maintained good viability following irradiation, independent of NLC

coculture. CLL cells that do not have p53 mutation rapidly die following irradiation and this effect is partially rescued by coculture with NLCs (Figure 2.19 A). Although there was variability in the extent to which NLCs protected the CLL cells following irradiation, there was typically a population of at least 5-10% of cells that maintained viability even out to a week in culture (data not shown). Therefore, it appears that NLCs provide protection to at least a subset of CLL cells following γ-irradation.

To evaluate what role CXCL12 might have in this protection mediated by NLCs, irradiated CLL cells (5 Gy) were cultured in media alone (CLL) or cocultured with NLCs in the presence of absence of inhibitors of CXCL12/CXCR4 signaling. The CXCR4 inhibitor, AMD3100 (AMD), and the Gi signaling inhibitor, pertussis toxin (PTx) were assessed for their ability to reduce NLC-mediated protection of CLL cells from irradiation-induced apoptosis (Figure 2.19 B). AMD3100 slightly impaired the NLC protection from cell death and pertussis toxin more consistently and robustly impaired the NLC protection, resulting in lower CLL cell viability compared to coculture with NLCs alone (Figure 2.19 B). However, neither of these compounds eliminated the protection received from NLCs, so it is evident that other factors are important to the NLC protection from DNA-damage induced apoptosis from irradiation.

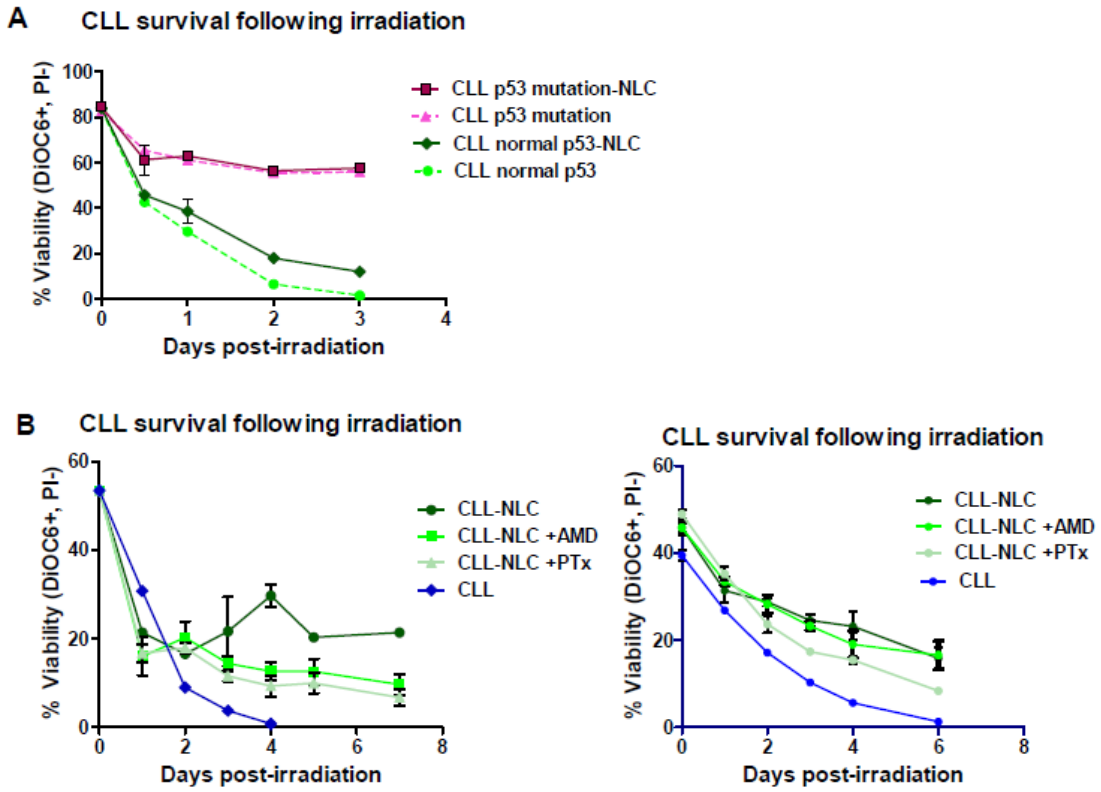

Figure 2.19 CLL survival profiles following irradiation when cocultured with NLCs and inhibitors of CXCL12/CXCR4 signaling. A) Representative survival profiles of γ-irradiated (5 Gy dose) CLL cells from two different patients, one with normal 17p/p53 (green) and one with 17p deletion/p53 mutation (magenta) cultured in media alone (dashed lines) or cocultured with NLCs (solid lines). B) Representative survival profiles for γ-irradiated (5 Gy dose) CLL cells cultured in media alone (blue) or cocultured with NLCs (green shades). NLC cocultures were left untreated or treated with 40 μM AMD3100 (AMD) or 200 ng/mL pertussis toxin (PTx). Viability was measured as previously described. Error bars indicate standard deviation of duplicate or triplicate measurements.

Since pertussis toxin appeared to reduce the viability of CLL cells cocultured with NLCs following γ-irradiation, and Gi is the G-protein to which chemokine receptors predominantly couple, we examined whether other chemokines in addition to CXCL12 could promote CLL survival following irradiation. CCL19 is a ligand for CCR7, which has been implicated in CLL survival and pathogenesis [*15*]. CXCL8 (IL-8) is a ligand for CXCR1 and CXCR2 that was found to be expressed by CLL cells themselves and may

promote longevity of CLL cells as well [*38*]. Comparing CLL cell viability 1 and 2 days following irradiation and cultured in the presence or absence of these various chemokines, we observed a trend for CCL19, like CXCL12, to promote CLL cell survival. CXCL8, however, did not have much influence on CLL cell viability (Figure 2.20). In order to determine if the different chemokines could promote synergistic or additive effects on CLL survival, since chemokines sometimes mediate non-redundant functions, survival was also monitored with the combination of all 3 chemokines. However, no additive or synergistic effects were observed (Figure 2.20). Nevertheless, it is important to note that these are preliminary results and replicates would have to be performed in order to gain statistical significance and validation of these effects.

It will be important to examine the effects of CXCL12 on survival following exposure to therapeutic agents such as fludarabine, since this provides a more relevant system for evaluating survival effects although it also complicates the interpretation of the molecular mechanisms mediating the survival effects. A selective inhibitor of MDM2, Nutlin-3, could also be used in future investigations to more definitively demonstrate its involvement in CLL survival in response to irradiation as well as response to chemotherapeutic treatment [*39*].

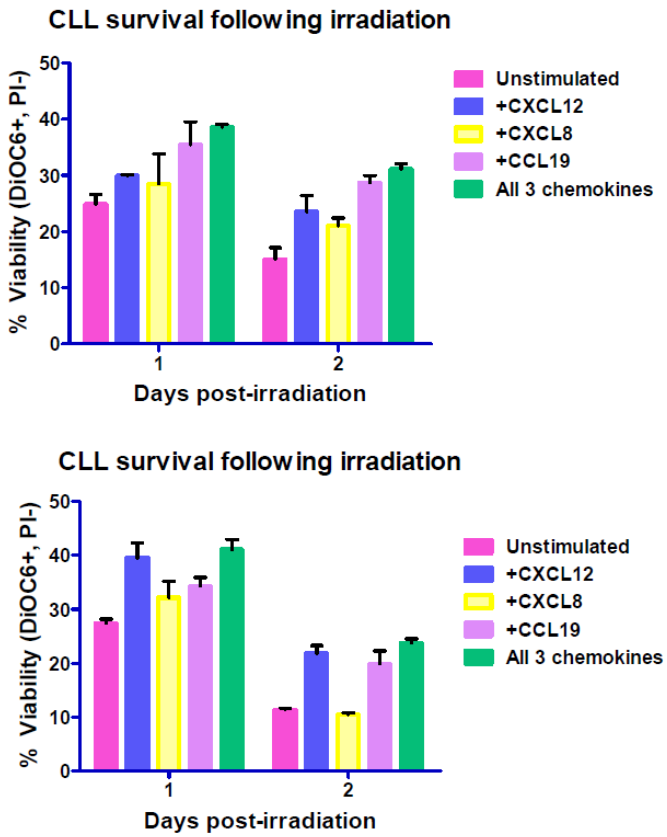

2.20 CLL survival profiles following irradiation and stimulation with the chemokines CXCL12, CXCL8 and CCL19. CLL cells from 2 representative patients (top and bottom profiles are 2 different CLL patients' cell survival profiles) were γ-irradiated (5 Gy dose), left unstimulated or stimulated with CXCL12 (75 nM), CXCL8 (100 nM), CCL19 (100 nM), or a combination of all 3 chemokines and viability was monitored 1 and 2 days following irradiation. Viability was measured by flow cytometry as previously described. Error bars indicate standard deviation of duplicate or triplicate measurements.

2.6 2-Dimensional Gel Electrophoresis (2DE) Imaging of Unstimulated and CXCL12-Stimulated CLL Cells

In order to more globally assess CXCL12-mediated signaling events in CLL cells and evaluate potential differences in the aggressive and indolent CLL subsets, we initially employed 2-dimensional gel electrophoresis in combination with tandem mass spectrometry (2DE-MS/MS). 2DE offers one method for profiling the proteome of whole cell lysates. In addition to being able to visually observe and quantify changes in

expression levels of proteins, it is particularly good for identifying post-translational modifications (PTMs), which is especially important for probing signaling events [*40*]. Operationally, the technique involves separation of complex protein mixtures according to charge by isoelectric focusing (IEF) on immobilized pH gels (IPG) in the first dimension, and separation in the second dimension according to mass by SDS PAGE. The result is a highly resolved 2-dimensional gel of intact proteins in which differentially regulated proteins can be detected, extracted and characterized by mass spectrometry. In addition, stains specific for phosphoproteins (Ser, Thr, Tyr) can be utilized to identify newly phosphorylated (or dephosphorylated) proteins [*40*].

However, due to limitations of phosphoprotein enrichments and staining and mechanical problems with the Q-STAR XL hybrid mass spectrometer, we ultimately decided to focus our proteomics efforts in a different direction. These alternative phosphoproteomics methods and results we employed are presented in Chapters 5 and 6, whereby we used immobilized metal affinity chromatography (IMAC) to enrich for phospho-peptides from the CLL cells (unstimulated versus stimulated with CXCL12), separated the enriched phospho-peptides by C18 liquid chromatography, and performed tandem mass spectrometry (LC-MS/MS) using an ion-trap (LTQ) mass spectrometer. In this manner, we were able to identify a large number of phosphorylated proteins in our CLL samples. Although this method in itself is not as quantitative as 2DE, spectral counting allowed us to assess relative amounts of specific phosphorylated proteins in unstimulated compared to stimulated samples. An advantage of this approach is that it is much higher throughput than 2DE, yields greater number of peptides since gel extraction can be inefficient, and ultimately gave the best success. However, representative 2DE gels are shown here for visualization of some of the differences in protein expression and protein shifts indicative of PTMs detected in unstimulated and 3 min CXCL12-

stimulated CLL cells from representative ZAP-70- and ZAP-70+ CLL patients' cells (Figure 2.21). Detailed protocols of 2DE methods are also included in Appendix AI.14.

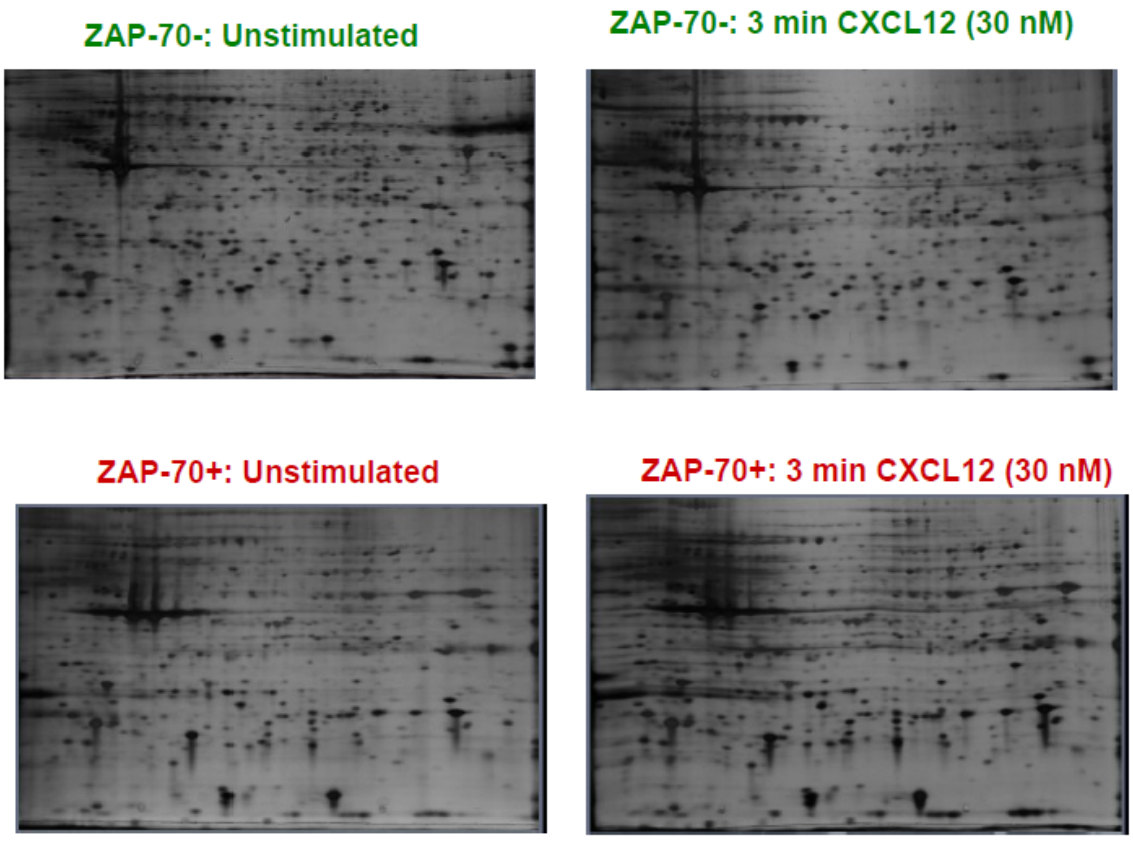

Figure 2.21 2DE gel profile of unstimulated and CXCL12-stimulated CLL cells. 2DE was performed on cytoplasmic lysates from ZAP-70- (top) and ZAP-70+ (bottom) patient's cells unstimulated (left) or stimulated for 3 min with 30 nM CXCL12 (right). Gels were silver stained and analyzed using PDQuest software (BioRad) to detect differences in spots (data not shown).

2.7 Summary

This chapter provides an introduction to CLL and an overview of how the microenvironment nurtures and protects these leukemia cells. One of the factors produced in the microenvironment that is known to promote survival of CLL cells is the chemokine, CXCL12. Our research has focused on elucidating the signaling pathways activated by CXCL12 in CLL cells, as this can provide important information regarding

the mechanisms by which these cells survive that if inhibited could promote apoptosis of CLL cells or enhance the efficacy of current therapeutics. Herein, details are provided regarding the expression and purification of CXCL12 process since purchasing chemokines can be cost prohibitive for such extensive signaling and phosphoproteomics analyses performed for this project. Additionally, many of the preliminary results shown in this chapter are what guided future research directions presented in the following 4 chapters. For one, we show that aggressive CLL cells appear to have enhanced survival responsiveness to CXCL12 compared to indolent CLL cells (based on ZAP-70 expression). Correspondingly, we noticed that ERK1/2 activation appeared to be more robust and prolonged in the aggressive CLL cells; however, activation of Akt was more comparable between the CLL subsets.

While the effects of the differential ERK1/2 activation are explored in the next chapter, some of the downstream targets of Akt signaling that could be responsible for CLL survival and accumulation common to both subsets of disease aggressiveness were described in this chapter. We found that CXCL12 induced a striking phosphorylation and activation of MDM2, an important regulator of p53 and thus, apoptosis. Although irradiation studies were performed to determine if CXCL12 may protect CLL cells from DNA damage induced cell death via an MDM2-dependent mechanism, results were fairly inconclusive and so more experiments would need to be performed in the context of irradiation or chemotherapeutic agents to assess CXCL12 or NLC-mediated protection. Lastly, some of the considerations regarding phosphoproteomics analysis of CXCL12-mediated signaling pathways are conveyed, including the initial 2DE-MS/MS approach used and the reasons for later employing the IMAC phosphopeptide enrichment and MS/MS analysis described in Chapters 5 and 6.

Overall, the results presented here and in the next 4 chapters provide information that increases our understanding of how CXCL12 contributes to CLL pathology.

2.8 Materials and Methods

Cells and reagents

Peripheral blood mononuclear cells (PBMCs) were obtained from consenting CLL patients at the Moores University of California San Diego (UCSD) Cancer Center in compliance with the Declaration of Helsinki and the institutional review board of UCSD. PBMCs were isolated by Ficoll-Paque (GE Healthcare) density gradient centrifugation (see Appendix AI.3). The isolated CLL PBMCs were frozen as liquid nitrogen stocks in 90% heat inactivated fetal bovine serum (FBS)/10% DMSO for later use. CLL B cells were purified from the PBMCs by negative selection using the magnetic associated cell sorting (MACS) (Miltenyi Biotec, Auburn, CA) by depletion of CD14+ (monocytes) and CD2+ (T cells) cells, leading to >99% CLL B cell purity (see Appendix AI.4), as assessed by flow cytometry analysis staining for CD19+/CD3-/CD14- cells. The expression levels of ZAP-70 in CLL cells were determined by flow cytometry as previously described, as part of the UCSD CLL Research Consortium headed by Dr. Thomas Kipps [*20*]. The cut-off was set at 20%; greater that 20% of CLL cells expressing ZAP-70 were defined as ZAP-70+ and less than 20% were defined as ZAP-70-. Jurkat cells used for migration assays to test function of recombinant human CXCL12 were obtained from ATCC. RPMI-1640 glutamax media and FBS were obtained from Gibco (Invitrogen, Carlsbad, CA).

Migration assays

Transwell migration assays (Corning, Corning, NY) were performed on Jurkat cells using inserts of 6.5 mm diameter, 5.0 μm pore size. Jurkat cells were resuspended in RPMI+10%FBS and 2.5 × 10^5 cells in a 100 μL volume was added to each insert. CXCL12 was diluted over a concentration range of 0 nM to 100 nM in a 600 μL total volume of RPMI+10%FBS in the bottom wells and all concentrations were prepared in triplicate. As a positive control and cell count reference, cells were added directly to the wells without inserts. Transwell migration was conducted for 2 h at 37°C/5%CO_2. Cells that had migrated into the bottom wells were then collected and counted by flow cytometry on a FACSCalibur (BD Biosciences, San Jose, CA). Data was normalized to no chemokine control and percent migration was calculated from the positive reference control.

Western blots and antibody reagents

For western blot analysis, purified CLL B cells were cultured in serum-free RPMI at 1 × 10^7 cells/mL for 3 h at 37°C/5%CO_2 and then stimulated with 30 nM CXCL12 over an hour time course (unstimulated, 3, 10, 30 and 60 min). For inhibitor studies, CLL cells were pre-treated with 40 μM AMD3100 (Sigma) or 200 ng/ml Pertussis toxin (List Biological Laboratories) for 1 h prior to stimulation with CXCL12. Cells were lysed on ice for 30 min in Ripa buffer (10 mM Tris pH 7.4, 150 mM NaCl, 1% Triton X, 0.1% Na-Deoxycholate, 0.1%SDS and 5 mM EDTA) containing Complete protease inhibitor cocktail (Roche, Palo Alto, CA) and Halt phosphatase inhibitors (Pierce). Lysates were clarified by centrifugation at 20,000 rcf for 10 min at 4°C. A BCA protein assay (Pierce) was performed to determine total protein concentration and 20 μg of total protein was loaded into each well of 10% SDS-PAGE gels. Gels were transferred onto PVDF membranes (Bio-Rad), blocked with 5% milk-TBST, and incubated overnight at 4°C with

primary antibodies. Blots were washed 3 times for 10 min with Tris Buffered Saline + 0.1% Tween (TBST) and then incubated for 1 h at room temperature with secondary antibodies conjugated to HRP, washed again 3 times with TBST and then developed with Amersham ECL-plus (GE-healthcare) or SuperSignal West femto-sensitivity reagent (Pierce). Blots were stripped with Restore western blot stripping solution (Pierce) for 10 min at room temperature and then re-probed with other antibodies and/or β-actin as a loading control. Primary antibodies were diluted into 5% BSA-TBST at recommended concentrations. The antibody against p53 was obtained from Santa Cruz Biotechnology and all other antibodies were obtained from Cell Signaling Technology (see Antibody Information in APPENDIX II).

Generation of nurse-like cells (NLCs)

PBMCs were isolated from the blood of normal volunteers (San Diego Blood Bank) over a Ficoll (GE Healthcare, Piscataway, NJ) density gradient. $CD14^+$ monocytes were isolated from PBMCs by positive selection using anti-CD14 beads (Miltenyi Biotech) following the manufacturer's instructions. To generate NLCs, 1.25×10^5/well (1 ml) $CD14^+$ cells were co-cultured with 3×10^6/well (1 ml) purified CLL B cells in a 24-well plate (BD, Franklin Lakes, NJ) in culture media (RPMI 1640 supplemented with: 10 mM HEPES (GIBCO-BRL), penicillin (100 U/ml)-streptomycin (100 µg/ml) (GIBCO-BRL), and 10% human serum (Omega Scientific, Tarzana, Ca) for 10-12 days. At this point the non-adherent B cells were gently washed off. More details are provided in Appendix AI.5.

Irradiation Experiments

Purified CLL cells were resuspended at $1x10^7$/mL and left untreated or dosed with 5 Gy of γ-radiation as part of a shared resource facility at UCSD. Cells were aliquoted into 24-well plates (1 mL/well) and treated accordingly (e.g. with 30 nM CXCL12) or added to 24-well plates with NLC monolayers in culture. For inhibitor studies, CLL cells were treated with 40 μM AMD3100 (Sigma) or 200 ng/ml pertussis toxin (List Biological Laboratories) prior to irradiation and then added to NLC cultures. Experiments were setup in duplicate or triplicate for each time point and cell viability was assessed as described below immediately following cell irradiation (D0) and subsequent days for up to 1 week.

Measurement of cell viability

Purified CLL cells were cultured at 1 x 10^6 cells/mL in 24-well plates (BD) under various conditions. Determination of CLL cell viability was based on the analysis of mitochondrial transmembrane potential ($\Delta\psi_m$) using 3,3'-dihexyloxacarbocyanine iodine ($DiOC_6$) (Invitrogen) and cell membrane permeability to propidium iodine (PI) (Sigma). For viability assays, 100 μL of the cell culture was collected at the indicated days and transferred to polypropylene tubes containing 100 μL of 40 μM $DiOC_6$ and 10 μg/mL propidium iodide (PI) in culture media. The cells were then incubated at 37°C for 15 minutes and analyzed within 30 minutes by flow cytometry using a FACSCalibur (Becton Dickinson). Fluorescence was recorded at 525 nm for $DiOC_6$ (FL-1) and at 600 nm (FL-2) for PI. Data was analyzed using the FlowJo 7.2.2 software (Tree Star). The percentage of viable cells was determined by gating on PI negative and $DiOC_6$ bright cells. More details are provided in Appendix AI.6.

2-dimensional gel electrophoresis

Representative 2DE images are from CLL cells that were serum starved for 4 hours and stimulated for 3 min with 30 nM CXCL12 or left unstimulated. Cells were harvested in ice cold cytoplasmic lysis buffer containing 10 mM HEPES, pH 7.9, 1.5 mM $MgCl_2$, 10 mM KCl, 0.5 mM dithiothreitol (DTT) (Sigma, St. Louis, MO), Complete protease inhibitor cocktail (Roche Diagnostics, Indianapolis, IN), and Halt phosphatase inhibitor cocktail (Pierce, Rockford, IL) for 30 min on ice. Lysates were clarified by centrifugation at 20,000 rcf for 20 min at 4°C. The supernatants were distributed into protein LoBind Eppendorf tubes (Eppendorf, Westbury, NY) and stored at –80°C. Protein concentrations were determined by a BCA protein assay, and 75 ug of protein extracts were separated in the first dimension on IPG strips (pI 5-8; BioRad) followed by separation in the second dimension by SDS-PAGE precast gels (BioRad). Gels were then silver stained, imaged on a VersaDoc 4000 (Bio-Rad) and analyzed using the PDQuest software (Bio-Rad). (See Appendix AI.14 for more detailed protocols on the 2DE methodology).

ACKNOWLEDGEMENTS

Susan Crown established the initial CXCL12 purification protocol and the dissertation author made minor modifications to the protocol and expressed and purified CXCL12 used for the studies. Data presented in Figures 2.3 and 2.10 were performed in Dr. Davorka Messmer's lab, as part of a collaboration. C.C. King provided instruction and use of equipment for 2DE experiments. The dissertation author designed and performed all other experiments presented in this chapter.

REFERENCES

1. Landis, S. H., Murray, T., Bolden, S., and Wingo, P. A. (1999) Cancer statistics, 1999, *CA Cancer J Clin 49*, 8-31, 31.

2. Chiorazzi, N., Rai, K. R., and Ferrarini, M. (2005) Chronic lymphocytic leukemia, *N Engl J Med 352*, 804-815.

3. Dighiero, G., and Binet, J. L. (2000) When and how to treat chronic lymphocytic leukemia, *N Engl J Med 343*, 1799-1801.

4. Dores, G. M., Anderson, W. F., Curtis, R. E., Landgren, O., Ostroumova, E., Bluhm, E. C., Rabkin, C. S., Devesa, S. S., and Linet, M. S. (2007) Chronic lymphocytic leukaemia and small lymphocytic lymphoma: overview of the descriptive epidemiology, *Br J Haematol 139*, 809-819.

5. Zenz, T., Mertens, D., Kuppers, R., Dohner, H., and Stilgenbauer, S. (2010) From pathogenesis to treatment of chronic lymphocytic leukaemia, *Nat Rev Cancer 10*, 37-50.

6. Gribben, J. G. (2010) How I treat CLL up front, *Blood 115*, 187-197.

7. Tournilhac, O., Cazin, B., Lepretre, S., Divine, M., Maloum, K., Delmer, A., Grosbois, B., Feugier, P., Maloisel, F., Villard, F., Villemagne, B., Bastit, D., Belhadj, K., Azar, N., Michallet, M., Manhes, G., and Travade, P. (2004) Impact of frontline fludarabine and cyclophosphamide combined treatment on peripheral blood stem cell mobilization in B-cell chronic lymphocytic leukemia, *Blood 103*, 363-365.

8. Burger, J. A., Tsukada, N., Burger, M., Zvaifler, N. J., Dell'Aquila, M., and Kipps, T. J. (2000) Blood-derived nurse-like cells protect chronic lymphocytic leukemia B cells from spontaneous apoptosis through stromal cell-derived factor-1, *Blood 96*, 2655-2663.

9. Burger, J. A., and Kipps, T. J. (2006) CXCR4: a key receptor in the crosstalk between tumor cells and their microenvironment, *Blood 107*, 1761-1767.

10. Nishio, M., Endo, T., Tsukada, N., Ohata, J., Kitada, S., Reed, J. C., Zvaifler, N. J., and Kipps, T. J. (2005) Nurselike cells express BAFF and APRIL, which can

promote survival of chronic lymphocytic leukemia cells via a paracrine pathway distinct from that of SDF-1alpha, *Blood 106*, 1012-1020.

11. Tsukada, N., Burger, J. A., Zvaifler, N. J., and Kipps, T. J. (2002) Distinctive features of "nurselike" cells that differentiate in the context of chronic lymphocytic leukemia, *Blood 99*, 1030-1037.

12. Endo, T., Nishio, M., Enzler, T., Cottam, H. B., Fukuda, T., James, D. F., Karin, M., and Kipps, T. J. (2007) BAFF and APRIL support chronic lymphocytic leukemia B-cell survival through activation of the canonical NF-kappaB pathway, *Blood 109*, 703-710.

13. Burger, M., Hartmann, T., Krome, M., Rawluk, J., Tamamura, H., Fujii, N., Kipps, T. J., and Burger, J. A. (2005) Small peptide inhibitors of the CXCR4 chemokine receptor (CD184) antagonize the activation, migration, and antiapoptotic responses of CXCL12 in chronic lymphocytic leukemia B cells, *Blood 106*, 1824-1830.

14. Richardson, S. J., Matthews, C., Catherwood, M. A., Alexander, H. D., Carey, B. S., Farrugia, J., Gardiner, A., Mould, S., Oscier, D., Copplestone, J. A., and Prentice, A. G. (2006) ZAP-70 expression is associated with enhanced ability to respond to migratory and survival signals in B-cell chronic lymphocytic leukemia (B-CLL), *Blood 107*, 3584-3592.

15. Till, K. J., Lin, K., Zuzel, M., and Cawley, J. C. (2002) The chemokine receptor CCR7 and alpha4 integrin are important for migration of chronic lymphocytic leukemia cells into lymph nodes, *Blood 99*, 2977-2984.

16. Fais, F., Ghiotto, F., Hashimoto, S., Sellars, B., Valetto, A., Allen, S. L., Schulman, P., Vinciguerra, V. P., Rai, K., Rassenti, L. Z., Kipps, T. J., Dighiero, G., HWJr, S., Ferrarini, M., and Chiorazzi, N. (1998) Chronic lymphocytic leukemia B cells express restricted sets of mutated and unmutated antigen receptors, *Journal Of Clinical Investigation 102*, 1515-1525.

17. Schroeder, H. W. J., and Dighiero, G. (1994) The pathogenesis of chronic lymphocytic leukemia: analysis of the antibody repertoire [see comments], *Immunology Today 15*, 288-294.

18. Damle, R. N., Wasil, T., Fais, F., Ghiotto, F., Valetto, A., Allen, S. L., Buchbinder, A., Budman, D., Dittmar, K., Kolitz, J., Lichtman, S. M., Schulman, P., Vinciguerra, V. P., Rai, K. R., Ferrarini, M., and Chiorazzi, N. (1999) Ig V gene

mutation status and CD38 expression as novel prognostic indicators in chronic lymphocytic leukemia, *Blood 94*, 1840-1847.

19. Hamblin, T. J., Davis, Z., Gardiner, A., Oscier, D. G., and Stevenson, F. K. (1999) Unmutated Ig V(H) genes are associated with a more aggressive form of chronic lymphocytic leukemia [see comments], *Blood 94*, 1848-1854.

20. Rassenti, L. Z., Huynh, L., Toy, T. L., Chen, L., Keating, M. J., Gribben, J. G., Neuberg, D. S., Flinn, I. W., Rai, K. R., Byrd, J. C., Kay, N. E., Greaves, A., Weiss, A., and Kipps, T. J. (2004) ZAP-70 compared with immunoglobulin heavy-chain gene mutation status as a predictor of disease progression in chronic lymphocytic leukemia, *N Engl J Med 351*, 893-901.

21. Matrai, Z. (2005) CD38 as a prognostic marker in CLL, *Hematology 10*, 39-46.

22. Chen, L., Huynh, L., Apgar, J., Tang, L., Rassenti, L., Weiss, A., and Kipps, T. J. (2008) ZAP-70 enhances IgM signaling independent of its kinase activity in chronic lymphocytic leukemia, *Blood 111*, 2685-2692.

23. Chen, L., Apgar, J., Huynh, L., Dicker, F., Giago-McGahan, T., Rassenti, L., Weiss, A., and Kipps, T. J. (2005) ZAP-70 directly enhances IgM signaling in chronic lymphocytic leukemia, *Blood 105*, 2036-2041.

24. Rai, K. R., Sawitsky, A., Cronkite, E. P., Chanana, A. D., Levy, R. N., and Pasternack, B. S. (1975) Clinical staging of chronic lymphocytic leukemia, *Blood 46*, 219-234.

25. Flomenberg, N., Devine, S. M., Dipersio, J. F., Liesveld, J. L., McCarty, J. M., Rowley, S. D., Vesole, D. H., Badel, K., and Calandra, G. (2005) The use of AMD3100 plus G-CSF for autologous hematopoietic progenitor cell mobilization is superior to G-CSF alone, *Blood 106*, 1867-1874.

26. Liles, W. C., Broxmeyer, H. E., Rodger, E., Wood, B., Hubel, K., Cooper, S., Hangoc, G., Bridger, G. J., Henson, G. W., Calandra, G., and Dale, D. C. (2003) Mobilization of hematopoietic progenitor cells in healthy volunteers by AMD3100, a CXCR4 antagonist, *Blood 102*, 2728-2730.

27. Messmer, D., Fecteau, J. F., O'Hayre, M., Bharati, I. S., Handel, T. M., and Kipps, T. J. (2011) Chronic lymphocytic leukemia cells receive RAF-dependent survival signals in response to CXCL12 that are sensitive to inhibition by sorafenib, *Blood 117*, 882-889.

28. Datta, S. R., Dudek, H., Tao, X., Masters, S., Fu, H., Gotoh, Y., and Greenberg, M. E. (1997) Akt phosphorylation of BAD couples survival signals to the cell-intrinsic death machinery, *Cell 91*, 231-241.

29. Aoki, M., Blazek, E., and Vogt, P. K. (2001) A role of the kinase mTOR in cellular transformation induced by the oncoproteins P3k and Akt, *Proc Natl Acad Sci U S A 98*, 136-141.

30. Longo, P. G., Laurenti, L., Gobessi, S., Sica, S., Leone, G., and Efremov, D. G. (2008) The Akt/Mcl-1 pathway plays a prominent role in mediating antiapoptotic signals downstream of the B-cell receptor in chronic lymphocytic leukemia B cells, *Blood 111*, 846-855.

31. Noguchi, M., Ropars, V., Roumestand, C., and Suizu, F. (2007) Proto-oncogene TCL1: more than just a coactivator for Akt, *FASEB J 21*, 2273-2284.

32. Mayo, L. D., and Donner, D. B. (2001) A phosphatidylinositol 3-kinase/Akt pathway promotes translocation of Mdm2 from the cytoplasm to the nucleus, *Proc Natl Acad Sci U S A 98*, 11598-11603.

33. Zhou, B. P., Liao, Y., Xia, W., Zou, Y., Spohn, B., and Hung, M. C. (2001) HER-2/neu induces p53 ubiquitination via Akt-mediated MDM2 phosphorylation, *Nat Cell Biol 3*, 973-982.

34. Yang, W., Dolloff, N. G., and El-Deiry, W. S. (2008) ERK and MDM2 prey on FOXO3a, *Nat Cell Biol 10*, 125-126.

35. Ekoff, M., Kaufmann, T., Engstrom, M., Motoyama, N., Villunger, A., Jonsson, J. I., Strasser, A., and Nilsson, G. (2007) The BH3-only protein Puma plays an essential role in cytokine deprivation induced apoptosis of mast cells, *Blood 110*, 3209-3217.

36. Myatt, S. S., and Lam, E. W. (2007) The emerging roles of forkhead box (Fox) proteins in cancer, *Nat Rev Cancer 7*, 847-859.

37. Ticchioni, M., Essafi, M., Jeandel, P. Y., Davi, F., Cassuto, J. P., Deckert, M., and Bernard, A. (2007) Homeostatic chemokines increase survival of B-chronic lymphocytic leukemia cells through inactivation of transcription factor FOXO3a, *Oncogene 26*, 7081-7091.

38. Secchiero, P., Corallini, F., Barbarotto, E., Melloni, E., di Iasio, M. G., Tiribelli, M., and Zauli, G. (2006) Role of the RANKL/RANK system in the induction of interleukin-8 (IL-8) in B chronic lymphocytic leukemia (B-CLL) cells, *J Cell Physiol 207*, 158-164.

39. Verma, R., Rigatti, M. J., Belinsky, G. S., Godman, C. A., and Giardina, C. (2010) DNA damage response to the Mdm2 inhibitor nutlin-3, *Biochem Pharmacol 79*, 565-574.

40. Gorg, A., Weiss, W., and Dunn, M. J. (2004) Current two-dimensional electrophoresis technology for proteomics, *Proteomics 4*, 3665-3685.

CHAPTER 3

Chronic Lymphocytic Leukemia Cells Receive Raf-Dependent Survival Signals in Response to CXCL12 that Are Sensitive to Inhibition by Sorafenib

This chapter is a reprint of the published article: Messmer D*, Fecteau JF*, O'Hayre M**,** Bharati I, Handel TM, Kipps TJ. Chronic Lymphocytic Leukemia Cells Receive Raf-Dependent Survival Signals in Response to CXCL12 that Are Sensitive to Inhibition by Sorafenib. (2011) *Blood* 117(3): 882-9. **Authors contributed equally.*

Chronic lymphocytic leukemia cells receive RAF-dependent survival signals in response to CXCL12 that are sensitive to inhibition by sorafenib

*Davorka Messmer,[1] *Jessie-F. Fecteau,[1] *Morgan O'Hayre,[2] Ila S. Bharati,[1] Tracy M. Handel,[2] and Thomas J. Kipps[1]

[1]Moores Cancer Center and [2]Skaggs School of Pharmacy and Pharmaceutical Sciences, and School of Medicine, University of California San Diego, La Jolla, CA

The chemokine CXCL12, via its receptor CXCR4, promotes increased survival of chronic lymphocytic leukemia (CLL) B cells that express high levels of ζ-chain–associated protein (ZAP-70), a receptor tyrosine kinase associated with aggressive disease. In this study, we investigated the underlying molecular mechanisms governing this effect. Although significant differences in the expression or turnover of CXCR4 were not observed between ZAP-70$^+$ and ZAP-70$^-$ cell samples, CXCL12 induced greater intracellular Ca^{2+} flux and stronger and more prolonged phosphorylation of extracellular signal-regulated kinase (ERK) and mitogen-activated protein kinase/ERK kinase (MEK) in the ZAP-70$^+$ CLL cells. The CXCL12-induced phosphorylation of ERK and MEK in ZAP-70$^+$ CLL cells was blocked by sorafenib, a small molecule inhibitor of RAF. Furthermore, ZAP-70$^+$ CLL cells were more sensitive than ZAP-70$^-$ CLL cells to the cytotoxic effects of sorafenib in vitro at concentrations that can readily be achieved in vivo. The data suggest that ZAP-70$^+$ CLL cells may be more responsive to survival factors, like CXCL12, that are elaborated by the leukemia microenvironment, and this sensitivity could be exploited for the development of new treatments for patients with this disease. Moreover, sorafenib may have clinical activity for patients with CLL, particularly those with ZAP-70$^+$ CLL. (*Blood*. 2011;117(3):882-889)

Introduction

Chronic lymphocytic leukemia (CLL) is a disease characterized by the accumulation of mature monoclonal B cells in the blood, secondary lymphoid tissue, and marrow.[1,2] Regardless of their apparent longevity in vivo, CLL B cells undergo apoptosis in vitro unless rescued by monocyte-derived nurse-like cells (NLCs) or marrow stromal cells.[3-6] In line with this hypothesis, the marrow is invariably infiltrated with CLL cells in patients, and the extent of infiltration correlates with clinical stage and prognosis.[5,7] These accessory cells also protect CLL cells from drug-induced apoptosis in vitro.[8] Thus, it has been postulated that CLL cells receive survival signals from these accessory cells, which constitute part of the CLL B-cell microenvironment in secondary lymphoid tissue and marrow.[6] Such niches could protect leukemia cells from spontaneous or drug-induced apoptosis in vivo, motivating the current study to better understand the survival pathways triggered by the microenvironment.

Accessory cells such as NLCs protect CLL cells from apoptosis in vitro in part through the secretion of the stromal cell-derived factor-1α (renamed as CXCL12).[9,10] CXCL12 is a highly conserved chemokine that signals through the chemokine receptor CXCR4, which is expressed at high levels by CLL cells.[3,10,11] Although most noted for its role in directing cell migration, CXCL12 also provides survival stimuli to CLL cells and partially protects them from spontaneous or drug-induced apoptosis or both in vitro.[3,9] Further, the enhanced viability of these cells in the presence of CXCL12 can be blocked by antibodies to CXCL12[3] or peptide inhibitors of CXCR4.[8]

In prior studies, it was found that treatment of CLL cells with CXCL12 induced activation of extracellular signal-regulated kinase (ERK).[8,12] In this study, we further examined the survival and signaling responses of CLL cells to CXCL12 to characterize the mechanism for the survival benefit. In addition, we compared the CXCL12-induced responses of CLL cells from 2 subgroups of patients, with high or low expression levels of ζ-chain–associated protein of 70 kDa (ZAP-70), a tyrosine kinase whose high-level expression is correlated with increased risk of early disease progression and relatively short survival [12,13].

Methods

Preparation of CXCL12

CXCL12 was prepared as previously described.[14] Briefly, CXCL12 was expressed as a His-tag fusion protein and purified from inclusion bodies in BL21 *Escherichia coli*. Bacterial pellets were resuspended in 10mM Tris (tris(hydroxymethyl)aminomethane) pH 8.0, 1mM $MgCl_2$ with 200 μg of DNAse, and complete protease inhibitor cocktail (free of EDTA [ethylenediaminetetraacetic acid]; Roche Applied Science) and then sonicated and washed with deoxycholate. Pellets were solubilized in 6M Guanadine-HCl, 100mM sodium phosphate, 10mM Tris-Cl, pH 8.0, with the use of a dounce homogenizer. The protein was then filtered and purified over a nickel-nitriloacetic acid column and refolded with Hampton Fold-It Buffer no. 8 (Hampton Research). After refolding, CXCL12 was dialyzed and concentrated with the use of Amicon Ultra centrifugal concentrators (molecular weight cutoff = 5000). The His-tag was removed by cleaving with

Submitted April 27, 2010; accepted October 17, 2010. Prepublished online as *Blood* First Edition paper, November 15, 2010; DOI 10.1182/blood-2010-04-282400.

*D.M., J.-F.F., and M.O. contributed equally to this study.

The online version of this article contains a data supplement.

The publication costs of this article were defrayed in part by page charge payment. Therefore, and solely to indicate this fact, this article is hereby marked "advertisement" in accordance with 18 USC section 1734.

enterokinase (NEB) at a 1:100 000 molar ratio overnight at room temperature. CXCL12 was then purified by high-performance liquid chromatography, and the purity was assessed by mass spectrometry. Transwell migration assays (Corning) with Jurkat cells were performed to verify the functionality of the purified protein.

Isolation of CLL B cells, cell culture, and reagents

Blood samples were collected from patients at the University of California San Diego (UCSD) Moores Cancer Center who satisfied diagnostic and immunophenotypic criteria for common B-cell CLL after providing written informed consent in compliance with the Declaration of Helsinki[1] and the institutional review board of UCSD. Peripheral blood mononuclear cells (PBMCs) were isolated from patients with CLL by density centrifugation with Ficoll-Hypaque (GE Healthcare) and were resuspended in 90% fetal calf serum and 10% dimethylsulfoxide (DMSO) for viable storage in liquid nitrogen. If not otherwise indicated, the CLL cells were isolated from thawed PBMCs by negative selection with the use of anti-CD2 and anti-CD14 magnetic beads (Miltenyi Biotech).

The B-RAF and C-RAF inhibitor KG5 and the control kinase inhibitor KG1 were kindly provided by Dr D. Cheresh (UCSD). The RAF inhibitor GW5074 was purchased from Sigma. Sorafenib and sunitinib were purchased from LC Laboratories. All inhibitors were solubilized in DMSO, which was used in all experiments as a negative control.

Generation of NLCs

PBMCs were isolated from the blood of healthy volunteers (San Diego Blood Bank) over a Ficoll (GE Healthcare) density gradient. $CD14^+$ monocytes were isolated from PBMCs by positive selection with the use of anti-CD14 beads (Miltenyi Biotech) following the manufacturer's instructions. To generate NLCs, 1.25×10^5/well $CD14^+$ cells were cocultured with 3×10^6/well purified CLL B cells in 1 mL of media in a 24-well plate (BD) in culture media (RPMI 1640 supplemented with 10mM HEPES [N-2-hydroxyethylpiperazine-N′-2-ethanesulfonic acid]; Invitrogen), penicillin (100 U/mL) and streptomycin (100 μg/mL; Invitrogen), 50uM Beta-mercaptoethanol, and 10% pooled human serum (Omega Scientific) for 12 days. At this point CLL B cells were gently washed off, and the adherent NLCs were used for coculture experiments with the use of freshly purified CLL cells.

Analysis of ZAP-70 expression by flow cytometry

The expression levels of ZAP-70 in CLL cells were determined by flow cytometry as previously described. The cutoff was set at 20%: $>20\%$ of CLL cells expressing ZAP-70 were defined as ZAP-70^+ and $<20\%$ were defined as ZAP-70^-.[13]

CXCR4 expression turnover measurement

CLL cells were incubated with 30nM CXCL12 for 30 minutes and either collected immediately and stained for CXCR4 expression (0 minutes) to assess receptor down-modulation or washed and recultured for another 30, 60, or 240 minutes and then collected and stained for CXCR4 expression, to assess receptor reexpression after ligand removal. CLL cells (1×10^5) were incubated for 20 minutes at 4°C in 100μL of phosphate-buffered saline (PBS)/5% fetal calf serum/0.1% sodium azide (staining buffer) with phycoerythrin–conjugated immunoglobulin G specific for human CXCR4, or the appropriate phycoerythrin-conjugated isotype control (R&D Systems). Cells were then washed 4 times with staining buffer, fixed in 3.7% formaldehyde in PBS (pH 7.2-7.4), and examined by flow cytometry with the use of a FACSCalibur (Beckon Dickinson). Data were analyzed with the FlowJo 7.2.2 software (TreeStar Inc).

Calcium flux measurements

Calcium flux assays were performed with the Molecular Devices Calcium 4 assay kit and measurements were acquired with a Molecular Devices FlexStation3 (Molecular Devices Corporation). Purified CLL B cells were washed twice in 0.5% bovine serum albumin/PBS and then suspended at 2.5×10^6 cells/mL in assay buffer (1× Hanks Balanced salt solution, 20mM HEPES, pH 7.4, 0.1% bovine serum albumin). One hundred microliters of cell suspension plus 10 μL of calcium 4 dye were distributed into wells of a 96-well Biocoat plate (BD Biosciences) and incubated at 37°C/5%CO_2 for 1 hour before analysis. CXCL12 was diluted in ddH_2O and distributed into wells of a 300-μL V-bottom 96-well plate (Corning Inc) and 50 μL of CXCL12 (8nM) or ddH_2O was distributed into the assay plate with cells at the start of measurements with the use of the liquid handling capabilities of the FlexStation3. Calcium flux measurements were averaged between triplicate data points and normalized against the ddH_2O control calcium flux response. CLL cells from 12 separate patients were analyzed for calcium flux, and, although there is variability in the overall maximum fluorescence signal observed between runs, the trend was the same as the one shown for 3 ZAP-70^+ and 3 ZAP-70^- CLL cells, which were analyzed together in one run. All statistics were determined with GraphPad Prism software Version 5.00 for Windows (GraphPad Software).

Immunoblot

CLL cells stimulated with 30nM CXCL12 were lysed for 20 minutes on ice in RIPA lysis buffer (10mM Tris pH 7.4, 150mM NaCl, 1% TritonX-100, 0.1% sodium deoxycholate, 0.1% sodium dodecylsulfate (SDS), 5mM EDTA supplemented with 1mM phenylmethylsulfonyl fluoride, Halt phosphatase inhibitor (Thermo Fisher Scientific), 1mM sodium vanadate, 1mM sodium fluoride, and complete protease inhibitor cocktail (Roche). Protein concentration was determined with the DC (Detergent Compatible) protein assay (Bio-Rad). The lysates were snap-frozen and stored at −80°C. Equal amounts of protein lysates (~ 30 μg) were separated by gel electrophoresis with the use of a NuPAGE Novex 4%-12% Bis-Tris Midi Gel (Invitrogen) and transferred to polyvinylidene fluoride membranes (Bio-Rad). Membranes were washed with 1× TBST (Tris-Buffered Saline Tween-20) and blocked for 1 hour at room temperature in 5% milk/TBST. Membranes were probed overnight for phospho p44/p42 (ERK1/2; Thr202/Tyr 204), phospho (p)–mitogen-activated protein kinase/ERK kinase 1 and 2 (MEK1/2; Ser 217/221), MEK1/2, p44/p42 (ERK1/2), and β-actin or glyceraldehyde-3-phosphate dehydrogenase (GAPDH), using antibody from Cell Signaling Technology. The next day, membranes were washed with 1× TBST and incubated with goat anti–rabbit or anti–mouse horseradish peroxidase–conjugated secondary antibodies (Santa Cruz Biotechnology) diluted to 1:5000 and 1:2000, respectively, in 5%milk/TBST for 1 hour at room temperature. Antibodies were detected with the use of either an enhanced chemiluminescence detection kit (GE Healthcare) or SuperSignal West Femto Maximum Sensitivity Substrate (Thermo Fisher Scientific).

p-ERK and p-MEK enzyme-linked immunoabsorbent assay

For each patient, the induction of p-MEK or p-ERK after CXCL12 stimulation (30nM) was measured with p-MEK1 (Ser217/221) and p-p44/42 mitogen-activated protein kinase (Thr202/Tyr204) sandwich enzyme-linked immunoabsorbent assay kits (Cell Signaling). The kinetics are displayed as the amount of p-MEK measured (optical density [OD] at 450 nm) for each time point after CXCL12 stimulation (0, 3, 10, 30, and 60 minutes.). For each patient, the overall p-MEK and p-ERK expression kinetics were compared by calculating the area under the curve with the use of GraphPad Prism software.

Measurement of cell viability

Purified CLL cells were cultured at 1×10^6 cells/mL in 24-well plates (BD) under various conditions. Determination of CLL cell viability was based on the analysis of mitochondrial transmembrane potential ($\Delta\Psi_m$) with the use of 3,3′-dihexyloxacarbocyanine iodide ($DiOC_6$; Invitrogen) and cell membrane permeability to propidium iodide (PI; Sigma). For viability assays, 100 μL of the cell culture was collected at the indicated days and transferred to polypropylene tubes containing 100 μL of 40μM $DiOC_6$ and 10 μg/mL PI in culture media. The cells were then incubated at 37°C for 15 minutes and analyzed within 30 minutes by flow cytometry with the use of a FACSCalibur (Becton Dickinson). Fluorescence was recorded at 525 nm for $DiOC_6$ and at 600 nm for PI. Data were analyzed with the

FlowJo 7.2.2 software (TreeStar). The percentage of viable cells was determined by gating on PI-negative and $DiOC_6$-bright cells.

Statistical analysis

Unless indicated otherwise, data are presented as either the mean ± standard deviation (SD) or the median ± SD. Statistical significance was determined with the use of paired or unpaired Student *t* test or 2-way analysis of variance. *P* values < .05 were considered significant.

Results

Influence of CXCL12 on calcium flux and receptor turnover in ZAP-70$^+$ CLL cells versus ZAP-70$^-$ CLL cells

The goal of this study was to understand differences in signaling in CLL cells from patients with aggressive versus indolent diseases. Because expression of high levels of the receptor tyrosine kinase ZAP-70 is associated with aggressive disease,[13] ZAP-70 expression is used to segregate the 2 groups of patients (see "Methods"). Consequently, in referring to the cells as being ZAP-70$^+$ and ZAP-70$^-$, we refer to the disease category not the exact expression levels of ZAP-70 in individual cells. We previously showed that CXCL12 could enhance the survival of CLL cells in vitro.[3,9] Furthermore, subsequent studies showed that CLL cells which expressed high levels of ZAP-70 appeared more responsive to the survival stimulus provided by CXCL12 than ZAP-70$^-$ CLL cells.[12] Because of this difference, we examined the capacity of CXCL12 to induce intracellular Ca^{2+} flux in ZAP-70$^+$ versus ZAP-70$^-$ CLL cells in vitro, because this is a common response of chemokine receptors to their ligands. Whereas CXCL12 could induce a robust intracellular Ca^{2+} flux in ZAP-70$^+$ CLL cells, it induced only modest-to-poor calcium flux in ZAP-70$^-$ CLL cells (Figure 1A). The maximum calcium flux signal induced by CXCL12 in ZAP-70$^+$ CLL cells (31 ± 3, median maximal fluorescence ± SD; n = 3) was significantly greater than that observed in ZAP-70$^-$ CLL cells (2 ± 3, median maximal fluorescence ± SD; n = 3; *P* = .0069) (Figure 1B). Within 90 seconds after exposure to the chemokine, the calcium flux returned back to baseline levels.

The difference in calcium flux could be caused by differences in receptor expression levels or turnover kinetics. Thus, we examined ZAP-70$^+$ and ZAP-70$^-$ CLL cells for expression of CXCR4 and CXCR7, which are the only known receptors for CXCL12.[15,16] In agreement with previous work, the cells from each patient expressed CXCR4[17] and the expression levels of CXCR4 on ZAP-70$^+$ CLL cells were similar to the levels on ZAP-70$^-$ CLL cells, as described[12] (data not shown). However, CLL cells did not express detectable surface levels of CXCR7 in contrast to normal B cells[18] (data not shown). Therefore, we examined the relative capacity of CXCL12 to induce down-modulation of CXCR4 (Figure 2A) and whether CXCR4 reexpression on the cell surface, through de novo synthesis and recycling (Figure 2B), differed between CLL cells from the 2 groups. A similar rapid down-modulation of CXCR4 was observed on both CLL populations (Figure 2A), and the reexpression of CXCR4 on the surface of both cell populations was not significantly different after removal of CXCL12 (Figure 2B). Therefore, the differences in the response of ZAP-70$^+$ and ZAP-70$^-$ CLL cells must be because of differences in downstream signaling.

Intracellular signaling in response to CXCL12

Prior studies have shown that CXCL12 could induce activation of ERK in CLL cells.[3,9] Because activation of this pathway can

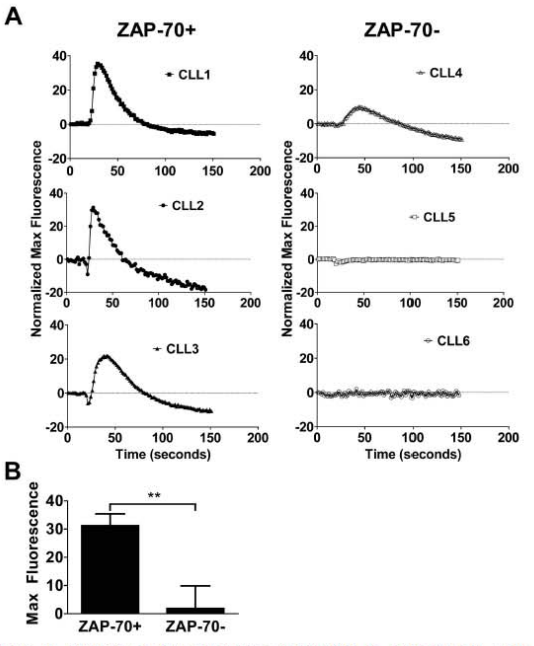

Figure 1. CXCL12 confers stronger calcium flux in ZAP-70$^+$ CLL cells. (A) Representative calcium flux profiles of 3 ZAP-70$^+$ (filled symbols) and 3 ZAP-70$^-$ (open symbols) CLL cells in response to 8nM CXCL12 stimulation. Measurements represent an average of triplicate data points that have been normalized to buffer controls. (B) The maximal fluorescence signal from the calcium flux was averaged between the ZAP-70$^+$ (n = 3) and ZAP-70$^-$ (n = 3) CLL cells and was found to be significantly different on the basis of unpaired Student *t* test (*P* < .01). Data shown are median ± SD.

enhance cell survival, we reasoned that ERK activation could account for the enhanced survival of ZAP-70$^+$ CLL cells after stimulation with CXCL12. First, we examined the relative magnitude and duration of ERK phosphorylation in ZAP-70$^+$ versus ZAP-70$^-$ CLL cells in response to CXCL12 via immunoblot analyses. CXCL12 induced increased and prolonged ERK phosphorylation in ZAP-70$^+$ CLL cells compared with that observed with ZAP-70$^-$ CLL cells (Figure 3A). Such differences were also observed with enzyme-linked immunoabsorbent assay–based measurements (Figure 3B). Although increased ERK activation was noted at 3 minutes in both ZAP-70$^+$ (*P* = .007) and ZAP-70$^-$ CLL samples (*P* = .003), at 10 minutes after exposure, significantly higher levels of p-ERK were measured in ZAP-70$^+$ CLL cells (n = 7) compared with ZAP-70$^-$ CLL cells (n = 10) (*P* < .05) (Figure 3B left). In addition to comparing the ERK response at the individual time points we also examined the complete ERK response to CXCL12, taking into account the intensity and duration of ERK activation. For this comparison we measured the integrated response over time (see "Methods") and observed that ZAP-70$^+$ CLL cells showed an increased amplitude of ERK activation (36 ± 16; n = 8) than ZAP-70$^-$ CLL cells (20 ± 7; n = 10; *P* = .015) (Figure 3B right). The individual kinetics of CXCL12-induced p-ERK for each patient are shown in supplemental Figure 1 (available on the *Blood* Web site; see the Supplemental Materials link at the top of the online article).

We next examined differences between ZAP-70$^+$ versus ZAP-70$^-$ CLL cells in the CXCL12-induced activation of kinases that

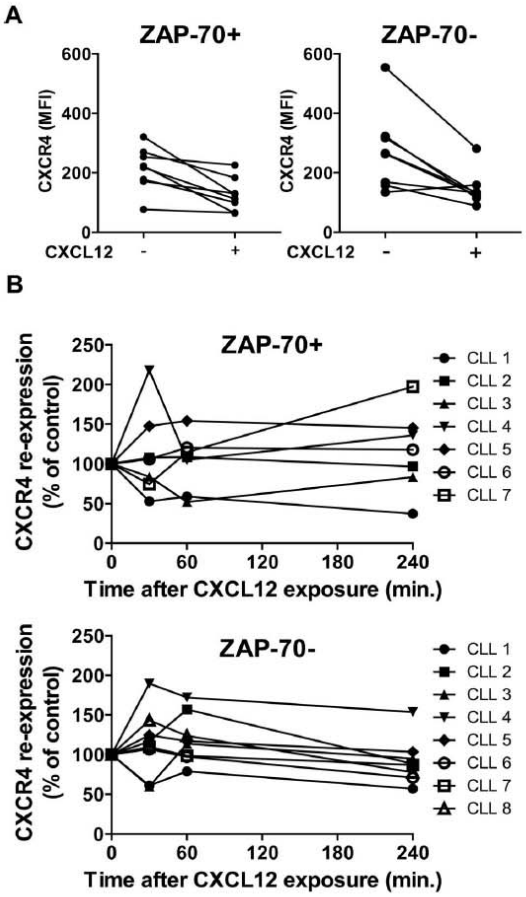

Figure 2. CXCR4 expression and down-modulation in response to CXCL12. Purified CLL cells from ZAP-70$^+$ CLL samples (n = 7) or ZAP-70$^-$ CLL samples (n = 8) were incubated with or without CXCL12 (80nM) for 30 minutes. The CLL cells were either collected immediately and stained to assess CXCR4 down-modulation after incubation with its ligand (A) or washed and recultured for another 30, 60, or 240 minutes and then collected and stained to study CXCR4 reexpression overtime in the absence of the ligand (B). Cells were analyzed by flow cytometry, and the data shown depict CXCR4 expression as mean fluorescence intensity (MFI). (A) CXCR4 expression level is compared in the presence or absence of CXCL12 for 30 minutes. (B) CXCR4 reexpression is expressed as a percentage of control, which is the level of CXCR4 remaining on the surface after 30 minutes of CXCL12 stimulation, and corresponds to time 0.

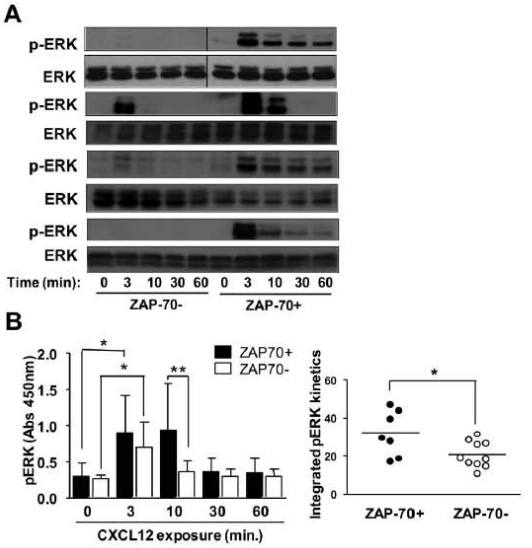

Figure 3. CXCL12 induces increased and prolonged ERK activation in ZAP-70$^+$ CLL cells. CLL cells were exposed to 30nM CXCL12 for 0-60 minutes at which point the cells were harvested, lysed, and analyzed for p-ERK. (A) Immunoblots were probed with anti–p-ERK and total ERK (ERK) antibody. Representative data of 4 ZAP-70$^+$ and 4 ZAP-70$^-$ CLL samples are shown. Vertical lines have been inserted to indicate repositioned gel lanes to align ZAP-70$^-$ and ZAP-70$^+$ samples. (B) To obtain quantitative results, cell lysates were analyzed by a p-ERK–specific enzyme-linked immunoabsorbent assay. (Left) Depicted is the absorbance measured at 450 nm. Data are shown as mean ± SD of ZAP-70$^-$ CLL samples (n = 9) and ZAP-70$^+$ CLL samples (n = 7). * indicates a statistically significant difference; $P < .05$ paired Student *t* test. Two-way analysis of variance was used for the comparison ZAP-70$^+$ vs ZAP-70$^-$ CLL samples at 10 minutes. (Right) The integral under the curve was measured as described in "Methods" and is depicted for all ZAP-70$^+$ and ZAP-70$^-$ CLL cases shown on the left. Data shown are median ± SD; * indicates a statistically significant difference; $P < .05$ unpaired Student *t* test.

can contribute to ERK activation, starting with p-MEK. At 3 minutes after stimulation with CXCL12, ZAP-70$^+$ CLL cells (n = 8) had significantly higher levels of p-MEK ($P = .01$) than did ZAP-70$^-$ CLL cells (n = 7; $P < .01$) (Figure 4 left). The response pattern closely mimicked the induction of p-ERK, with the strongest signal at 3 minutes. Furthermore, as with p-ERK, the CXCL12-induced MEK phosphorylation was prolonged in ZAP-70$^+$ CLL cells compared with ZAP-70$^-$ CLL cells (Figure 4 left). When investigating the amplitude of the p-MEK response as a function of time (see "Methods") we found that ZAP-70$^+$ CLL cells expressed significantly higher levels of p-MEK (79 ± 35; n = 8) than ZAP-70$^-$ CLL cells (45 ± 15; n = 7; $P = .03$) (Figure 4 right). The individual kinetics of CXCL12-induced p-MEK for each patient are represented in supplemental Figure 2.

CXCL12-mediated MEK activation in ZAP-70$^+$ CLL cells is RAF dependent

Because phosphorylation of MEK could depend on the activity of RAF, we evaluated whether sorafenib, a small molecule inhibitor of RAF,[19] could block CXCL12-induced activation of CLL cells in vitro. Because ZAP-70$^-$ CLL cells did not show significant MEK activation, we focused on ZAP-70$^+$ CLL cells. Sorafenib,[19] was found to block CXCL12-induced activation of MEK and ERK in ZAP-70$^+$ CLL cells (Figure 5A). Because sorafenib also targets non-RAF kinases,[19] additional RAF inhibitors were tested. Consistent with the notion that the effect of sorafenib was because of its action on RAF, CXCL12-induced activation of MEK/ERK was not affected by sunitinib (Figure 5B). Sunitinib is an inhibitor of non-RAF kinases that are also inhibited by sorafenib,[20] including vascular epidermal growth factor receptors, platelet-derived growth factor receptors, Flt3 and c-Kit, but it does not target RAF.[21] As a positive control, the activity of sunitinib in CLL cells was demonstrated by its capacity to block CXCL12-induced activation of cAMP response element-binding in the same experiment (data not shown). Thus, these shared kinase targets are not involved in the activation of MEK after treatment with CXCL12.

We also examined whether other inhibitors of RAF could block CXCL12-induced MEK activation in CLL cells with the use of KG5, a kinase inhibitor of RAF signaling through B-RAF and C-RAF in addition to platelet-derived growth factor receptors α and β, Flt3 and Kit.[22] As a control we used KG1, a kinase inhibitor

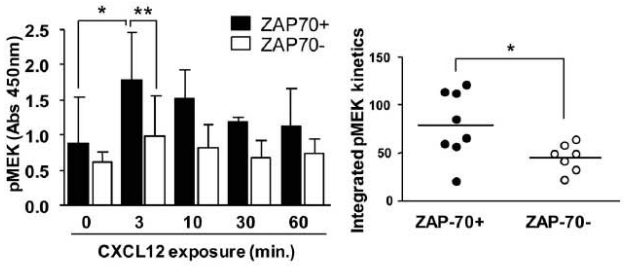

Figure 4. CXCL12 induces pronounced MEK activation in ZAP-70$^+$. CLL cells were exposed to 30nM CXCL12 for 0-60 minutes at which point the cells were harvested, and the lysates were analyzed for p-MEK protein expression by enzyme-linked immunoabsorbent assay. Depicted is the absorbance measured at 450 nm. Results are shown as mean ± SD of ZAP-70$^-$ CLL samples (n = 7) and ZAP-70$^+$ CLL (n = 8); * indicates a statistically significant difference; $P < .05$ paired Student *t* test. Two-way analysis of variance was used for the comparison ZAP-70$^+$ CLL vs ZAP-70$^-$ CLL at 3 minutes. (Right) The integral under the time curve was measured as described in "Methods" and is depicted for all ZAP-70$^+$ and ZAP-70$^-$ CLL cases shown on the left. Data shown are median ± SD; * indicates a statistically significant difference; $P < .05$ unpaired Student *t* test.

that targets all of these kinases except B- and C-RAF.[22] Whereas KG5 blocked MEK/ERK activation, KG1 did not (Figure 5C). Finally, we tested GW5074, an inhibitor of B-RAF and C-RAF, and found that it also inhibited CXCL12-induced MEK activation in ZAP-70$^+$ CLL cells (Figure 5C). Collectively, these data imply that CXCL12-induced activation of MEK/ERK in CLL depends on the activity of RAF.

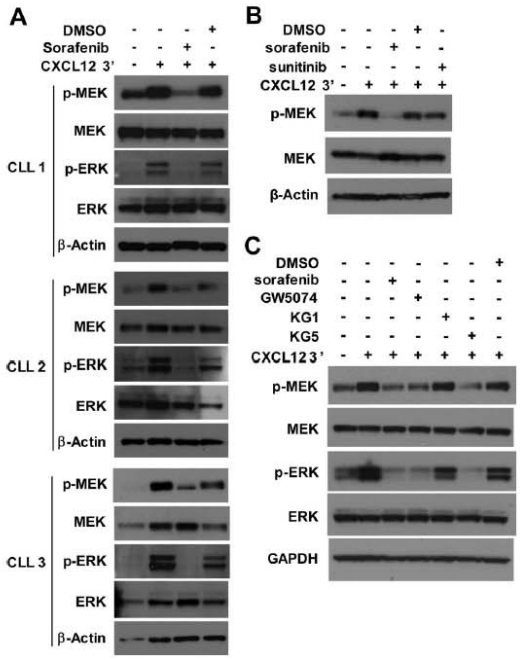

Figure 5. CXCL12-mediated MEK and ERK activation in ZAP-70$^+$ CLL cells is RAF dependent. (A) CLL cells were pretreated with 10μM sorafenib or DMSO as solvent control for 30 minutes before the addition of CXCL12 or media control. After exposure of CLL cells to CXCL12 for 3 minutes, the cells were harvested, lysed, and analyzed for the presence of the indicated proteins by immunoblot. Results are shown from 3 ZAP-70$^+$ CLL samples. (B) ZAP-70$^+$ CLL cells were pretreated with 10μM sorafenib, 10μM sunitinib, or DMSO as solvent control for 30 minutes before the addition of CXCL12 or media control. After exposure of CLL cells to CXCL12 for 3 minutes, cells were harvested and analyzed as above. Results are shown from 1 representative of 3 ZAP-70$^+$ CLL samples, all showing similar responses. (C) ZAP-70$^+$ CLL cells were pretreated with sorafenib, GW5074, KG1, KG5 (all inhibitors were used at 10μM), or DMSO as solvent control for 30 minutes before the addition of CXCL12 or media control. After exposure of CLL cells to CXCL12 for 3 minutes, cells were harvested and analyzed as above. Results are shown from 1 representative of 6 ZAP-70$^+$ CLL samples; all but 1 sample showed similar responses. GAPDH indicates glyceraldehyde-3-phosphate dehydrogenase.

Sorafenib causes enhanced apoptosis in ZAP-70$^+$ CLL cells

Because sorafenib could inhibit activation of MEK/ERK in ZAP-70$^+$ CLL cells, we examined whether it was selectively cytotoxic for ZAP-70$^+$ CLL cells in vitro. Indeed, 5μM sorafenib induced significantly higher levels of apoptosis in ZAP-70$^+$ CLL cells than in ZAP-70$^-$ CLL cells (Figure 6A-B). After 24 hours the mean viability (± SD) of the ZAP-70$^+$ CLL cells in the presence of sorafenib was 65% (± 22%; n = 5; $P = .02$ vs DMSO) compared with 82% (± 17%; n = 6; P = NS vs DMSO) for the ZAP-70$^-$ CLL cells. After 48 hours, these numbers dropped to 62% (± 18%; n = 5; $P = .03$ vs DMSO) and 73% (± 33%; n = 6; P = NS vs DMSO) for the ZAP-70$^+$ and ZAP-70$^-$ CLL cells, respectively. Thus, at both time points the ZAP-70$^+$ CLL cells showed enhanced sorafenib-induced apoptosis compared with the ZAP-70$^-$ CLL cells (Figure 6B). Although we noticed increased sensitivity to sorafenib at 5μM (Figure 6A-B), higher concentrations were cytotoxic to all CLL samples examined, following a dose- and time-dependent pattern (Figure 6C; supplemental Figure 4). However, ZAP-70$^+$ CLL cells were more sensitive than ZAP-70$^-$ CLL cells to sorafenib at concentrations ≤ 5μM.

Sorafenib causes apoptosis of CLL cells in the presence of NLCs

Because cells of the microenvironment can protect CLL cells from spontaneous and drug-induced apoptosis,[8] we examined whether sorafenib could kill CLL cells even when cocultured with NLCs, which presumably exist in the CLL microenvironment and can protect them from apoptosis in vitro. As expected NLCs protected CLL cells from spontaneous apoptosis in vitro (Figure 7A). However, the addition of sorafenib to these NLC/CLL cocultures rapidly and significantly reduced the viability of the CLL cells. After 4 days, most CLL cells were dead, using 10μM sorafenib in the presence of NLCs (Figure 7A; supplemental Figure 5 shows individual patient responses).

Because the frontline therapy for CLL is fludarabine,[23] we compared fludarabine and sorafenib for their potential to induce the apoptosis of CLL cells in the presence of NLCs and asked whether sorafenib could enhance fludarabine-induced CLL cell death. When tested at the same dose of 10μM, CLL cell viability was

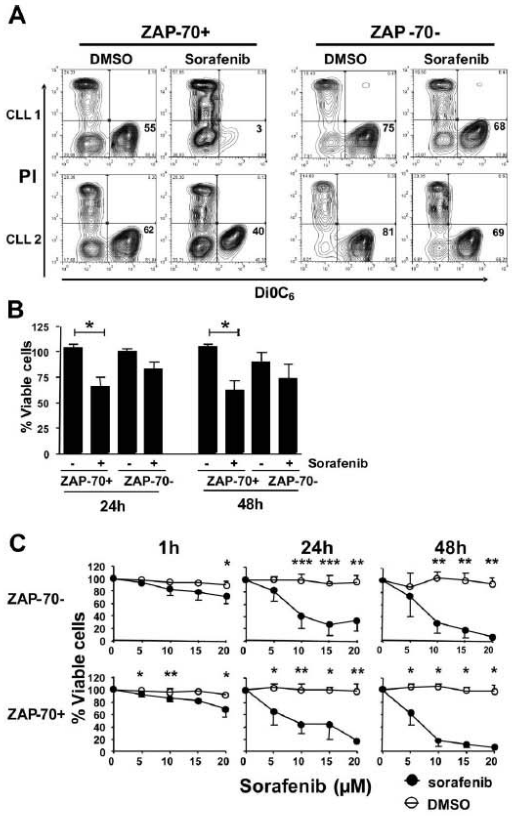

Figure 6. Sorafenib causes increased apoptosis in ZAP-70$^+$ CLL cells. CLL cells were cultured in the presence of sorafenib or DMSO control, added once at the beginning of the culture. CLL cells were harvested at the indicated times and stained with $DiOC_6$/PI and analyzed by flow cytometry. (A) Presented are contour maps from 2 representative ZAP-70$^+$ and 2 ZAP-70$^-$ CLL samples treated with DMSO or 5μM sorafenib for 24 hours. The relative $DiOC_6$ and PI fluorescence intensities are depicted on the x- and y-axis, respectively. Cells in the lower right quadrant, which are $DiOC_6$ bright and PI negative, are viable, and those numbers were used for the generation of the plots shown below. (B) CLL cells were cultured in the presence of 5μM sorafenib or DMSO control and harvested after 24 and 48 hours for analysis of viability as above. Results are represented relative to untreated control at day 0, which was set as 100%. Data shown are mean ± SD from ZAP-70$^-$ (n = 5) and ZAP-70$^+$ CLL cells (n = 5); * indicates a statistically significant difference; $P < .05$ paired Student *t* test. (C) CLL cells were cultured in increasing doses of sorafenib and analyzed for viability as above.

lower in the presence of sorafenib (38 ± 19%) compared with fludarabine (60 ± 23%; $P = .0002$) after 24 hours (Figure 7B). Although increased apoptosis by sorafenib compared with fludarabine was still observed after 2 and 3 days, the differences were not significant. A combination of sorafenib and fludarabine caused a small but insignificant additional increase in apoptosis (Figure 7B).

Discussion

It has been postulated that CLL cells receive survival signals from their microenvironment and that these signals limit the activity of antileukemia drugs in vivo. Such microenvironmental interactions could be a major impediment to the eradication of minimal residual disease in patients with CLL using current therapies. Therefore, identifying the mechanism(s) whereby CLL cells respond to microenvironmental survival signals could reveal novel targets for therapy. One of the survival factors elaborated in the microenvironment is CXCL12,[3,9] a chemokine that enhances the survival of CLL cells in vitro, particularly CLL cells that express high levels of ZAP-70 which is associated with aggressive disease[13] compared with ZAP-70$^-$ CLL cells.[12] Our goal was to understand differences in signaling in CLL cells from patients segregated as having aggressive versus indolent diseases on the basis of their ZAP-70 status.

Cell surface expression of CXCR4 does not differ between ZAP-70$^+$ and ZAP-70$^-$ CLL cells,[12] and we found no significant differences in the extent of receptor down-regulation or surface reexpression of CXCR4 of both, implicating downstream signaling events in the differential effects observed on CXCL12-induced survival of these 2 subgroups of cells. The effects of CXCL12 are mediated exclusively by CXCR4, because the other receptor for CXCL12, CXCR7,[15,16] is not expressed on the CLL cells[18] (data not shown). A genetic analysis of CXCR4 sequences in CLL showed no common variations in the sequences that correlate with risk of CLL (data not shown).[24] Therefore, signaling differences are not likely to be because of receptor mutations but rather downstream events. Prior studies showed that CXCL12 signaling causes ERK activation in CLL cells.[9,12] However, because the overall signaling cascade linking CXCL12 to ERK activation and ultimately to the survival of CLL cells has not fully explored, it became the focus of our studies.

We found that CXCL12 induced high levels of intracellular calcium flux in ZAP-70$^+$ CLL cells, whereas most ZAP-70$^-$ CLL cells showed little or no intracellular calcium flux. Calcium-induced ERK activation has been described in B cells[25] and T cells.[26] We have previously shown that aberrant expression of ZAP-70 in CLL cells leads to increases in intracellular calcium flux

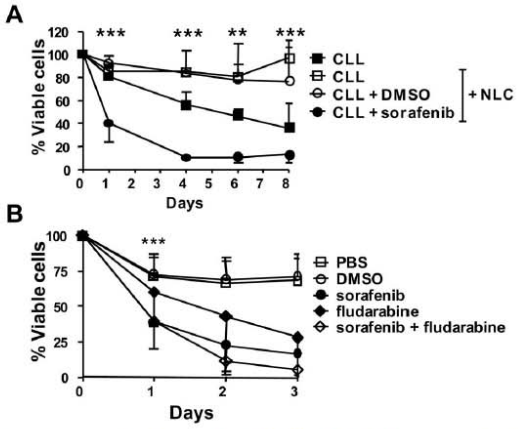

Figure 7. Sorafenib causes apoptosis of CLL cells in the presence of NLCs. (A) CLL cells were cultured for 8 days alone or in the presence of NLCs with or without 10μM sorafenib or DMSO control added only once at the beginning of the culture. Viability was measured and analyzed as above. Data shown are mean ± SD from 4 different CLL samples. The mean viability ± SD of CLL cells cultured in presence of NLCs + sorafenib was 40% ± 16% (day 1), 10% ± 3% (day 4), 11% ± 6% (day 6), and 12% ± 6% (day 8). The * indicates a statistically significant difference; $P < .05$ paired Student *t* test. (B) CLL cells were cultured for 3 days in the presence of NLCs with or without 10μM sorafenib and 10μM fludarabine alone or in combination added only once at the beginning of the culture. Viability was measured and analyzed as above. Data shown are mean ± SD from 4 different CLL samples. The * indicates a statistically significant difference between sorafenib and fludarabine at day 1 ($P = .0002$, paired Student *t* test).

in response to B-cell receptor engagement.[27] Furthermore, ionomycin, a calcium ionophore that opens calcium channels, induced MEK activation in ZAP-70$^+$ CLL cells (data not shown). Taken together, these data suggest that increased CXCL12-mediated ERK signaling might be attributed to increased calcium flux, which in turn may lead to increased phospholipase C activity in ZAP-70$^+$ CLL cells relative to ZAP-70$^-$ CLL cells, a hypothesis currently under investigation.

In concordance with findings by Richardson et al,[12] we found that CXCL12 caused increased and prolonged activation of ERK in CLL cells, particularly those CLL cells that express ZAP-70. Extending these observations, we showed that CXCL12 induces increased RAF-dependent p-MEK levels in ZAP-70$^+$ CLL cells compared with ZAP-70$^-$ CLL cells, a finding that could explain the increased levels of p-ERK downstream of MEK. Although originally developed as a RAF inhibitor, sorafenib was subsequently found to inhibit other tyrosine kinases, including vascular epidermal growth factor receptor 2 and 3, platelet derived growth factor receptor-β, Flt3, and c-Kit.[19] That these kinases do not play a role in the MEK signaling induced by CXCL12 is indicated by the lack of activity on the MEK/ERK pathways of another drug, sunitinib, which inhibits these other kinases,[21] but not RAF. Two other RAF inhibitors also blocked CXCL12-induced activation of MEK/ERK in CLL cells, providing additional support for this model.

Conceivably, CLL cells from patients with ZAP-70$^+$ or ZAP-70$^-$ may have differential expression of other kinases, phosphatases, or adapter proteins that play a role in the signaling cascade triggered by exposure to CXCL12. For example, the differences in MEK activation between ZAP-70$^+$ and ZAP-70$^-$ CLL cells could be attributed to higher levels or activity of phosphatases in the ZAP-70$^-$ CLL cells. One possible candidate is the SH2-containing inositol 5′-phosphate (SHIP) phosphatase, which has been implicated in suppression of RAF and ERK activation in mouse pre-B cells[28] and in signaling lymphocyte activation molecule–mediated ERK activation in a B-cell line.[29] Furthermore, increased SHIP-1 protein levels were reported in ZAP-70$^-$ CLL cells, and it was found to be constitutively tyrosine phosphorylated to a greater extent than in ZAP-70$^+$ CLL cells.[30] Thus, increased SHIP-1 levels in ZAP-70$^-$ CLL cells could be responsible for the short or absent CXCL12-induced ERK activation.

In any case, the relative sensitivity of ZAP-70$^+$ CLL cells to CXCL12 compared with CLL cells lacking ZAP-70 appears rooted in the differential CXCL12-induced activation of the RAF/MEK/ERK signaling pathway, making this pathway an attractive target for development of new treatments for patients with CLL, particularly those with ZAP-70$^+$ CLL who have a tendency for relatively rapid disease progression and shorter survival. To this end, we found that sorafenib blocked CXCL12-induced activation of the RAF/MEK/ERK pathway and sorafenib induced more pronounced apoptosis in ZAP-70$^+$ CLL than in ZAP-70$^-$ CLL cells, suggesting an increased dependence on CLL cells from patients with ZAP-70$^+$ on this pathway for survival. However, at higher doses sorafenib dramatically reduces CLL cell survival in both ZAP-70$^+$ and ZAP-70$^-$ CLL cells.

Importantly, a single dose of 10μM sorafenib induced apoptosis of most CLL cells even when cocultured with NLCs, which can protect CLL cells from fludarabine-induced apoptosis in vitro.[8] These results suggest that sorafenib could be an effective novel therapeutic for CLL. Although our data support the involvement of RAF in CXCL12-mediated activation of MEK/ERK, the sorafenib-induced apoptosis of CLL cells could be a consequence of inhibition of other sorafenib targets in addition to MEK/ERK.

In summary, our data show that the extent and duration of MEK and ERK activation and subsequent survival of CLL cells after treatment with CXCL12 is significantly greater in CLL cells from patients with ZAP-70$^+$ than in CLL cells from patients with ZAP-70$^-$. Furthermore, the RAF-dependent MEK activation suggests a new method for the treatment of CLL with the inhibitor sorafenib. Conceivably, ZAP-70$^+$ CLL cells might be more sensitive/responsive than ZAP-70$^-$ CLL cells to other survival factors produced by the microenvironment in addition to CXCL12; thus, further identification of such factors and their effects on CLL may provide fertile ground for the development of additional strategies to improve the outcome of patients with CLL, particularly those with an aggressive form of the disease.

Acknowledgments

We thank Dr Laura Z. Rassenti (Chronic Lymphocytic Research Consortium) for assistance with CLL samples and Lloyd Howard Wang for his excellent technical assistance.

This work was supported by the Lymphoma Research Foundation (grant CLL-07-029; D.M., T.M.H., and T.J.K.), RO1-AI37113 (T.M.H.), and "Le Fond de la Recherche en Santé du Québec" (J.-F.F).

Authorship

Contribution: D.M. designed the research, supervised the study, analyzed the data, designed figures, and wrote the paper; J.-F.F. and M.O. performed experiments, analyzed data, designed figures, and revised the manuscript; I.S.B. performed experiments, analyzed data, and designed figures; T.M.H. designed experiments, analyzed data, and revised the manuscript; T.J.K. provided patient samples, contributed to scientific discussion, and revised the manuscript.

Conflict-of-interest disclosure: The authors declare no competing financial interests.

Correspondence: Davorka Messmer, Moores UCSD Cancer Center, 3855 Health Science Dr no. 0820, La Jolla, CA 92093-0820; e-mail: dmessmer@ucsd.edu.

References

1. Kipps TJ. Chronic lymphocytic leukemia and related diseases. In: Beutler E, Lichtman MA, Coller BA, Kipps TJ, Seligsohn U, eds. *Williams Hematology*. 6th ed. New York, NY: McGraw Hill Publishers; 2001:1163-1194.
2. Chiorazzi N, Rai KR, Ferrarini M. Chronic lymphocytic leukemia. *N Engl J Med*. 2005;352(8):804-815.
3. Burger JA, Tsukada N, Burger M, Zvaifler NJ, Dell'Aquila M, Kipps TJ. Blood-derived nurse-like cells protect chronic lymphocytic leukemia B cells from spontaneous apoptosis through stromal cell-derived factor-1. *Blood*. 2000;96(8):2655-2663.
4. Lagneaux L, Delforge A, Bron D, De Bruyn C, Stryckmans P. Chronic lymphocytic leukemic B cells but not normal B cells are rescued from apoptosis by contact with normal bone marrow stromal cells. *Blood*. 1998;91(7):2387-2396.
5. Pedersen IM, Kitada S, Leoni LM, et al. Protection of CLL B cells by a follicular dendritic cell line is dependent on induction of Mcl-1. *Blood*. 2002;100(5):1795-1801.
6. Tsukada N, Burger JA, Zvaifler NJ, Kipps TJ. Distinctive features of "nurselike" cells that differentiate in the context of chronic lymphocytic leukemia. *Blood*. 2002;99(3):1030-1037.
7. Han T, Barcos M, Emrich L, et al. Bone marrow infiltration patterns and their prognostic significance in chronic lymphocytic leukemia: correlations with clinical, immunologic, phenotypic, and cytogenetic data. *J Clin Oncol*. 1984;2(6):562-570.
8. Burger M, Hartmann T, Krome M, et al. Small

peptide inhibitors of the CXCR4 chemokine receptor (CD184) antagonize the activation, migration, and antiapoptotic responses of CXCL12 in chronic lymphocytic leukemia B cells. *Blood.* 2005;106(5):1824-1830.

9. Nishio M, Endo T, Tsukada N, et al. Nurselike cells express BAFF and APRIL, which can promote survival of chronic lymphocytic leukemia cells via a paracrine pathway distinct from that of SDF-1alpha. *Blood.* 2005;106(3):1012-1020.
10. Burger JA, Kipps TJ. CXCR4: a key receptor in the crosstalk between tumor cells and their microenvironment. *Blood.* 2006;107(5):1761-1767.
11. Bleul CC, Farzan M, Choe H, et al. The lymphocyte chemoattractant SDF-1 is a ligand for LESTR/fusin and blocks HIV-1 entry. *Nature.* 1996;382(6594):829-833.
12. Richardson SJ, Matthews C, Catherwood MA, et al. ZAP-70 expression is associated with enhanced ability to respond to migratory and survival signals in B-cell chronic lymphocytic leukemia (B-CLL). *Blood.* 2006;107(9):3584-3592.
13. Rassenti LZ, Huynh L, Toy TL, et al. ZAP-70 compared with immunoglobulin heavy-chain gene mutation status as a predictor of disease progression in chronic lymphocytic leukemia. *N Engl J Med.* 2004;351(9):893-901.
14. O'Hayre M, Salanga CL, Dorrestein PC, Handel TM. Phosphoproteomic analysis of chemokine signaling networks. *Methods Enzymol.* 2009;460:331-346.
15. Balabanian K, Lagane B, Infantino S, et al. The chemokine SDF-1/CXCL12 binds to and signals through the orphan receptor RDC1 in T lymphocytes. *J Biol Chem.* 2005;280(42):35760-35766.
16. Burns JM, Summers BC, Wang Y, et al. A novel chemokine receptor for SDF-1 and I-TAC involved in cell survival, cell adhesion, and tumor development. *J Exp Med.* 2006;203(9):2201-2213.
17. Burger JA, Burger M, Kipps TJ. Chronic lymphocytic leukemia B cells express functional CXCR4 chemokine receptors that mediate spontaneous migration beneath bone marrow stromal cells. *Blood.* 1999;94(11):3658-3667.
18. O'Hayre M, Salanga CL, Kipps TJ, Messmer D, Dorrenstein PC, Handel TM. Elucidating the CXCL12/CXCR4 signaling network in chronic lymphocytic leukemia through phosphoproteomics analysis. *PLoSOne.* 2010;5(7):e11716.
19. Wilhelm SM, Carter C, Tang L, et al. BAY 43-9006 exhibits broad spectrum oral antitumor activity and targets the RAF/MEK/ERK pathway and receptor tyrosine kinases involved in tumor progression and angiogenesis. *Cancer Res.* 2004;64(19):7099-7109.
20. Faivre S, Demetri G, Sargent W, Raymond E. Molecular basis for sunitinib efficacy and future clinical development. *Nat Rev Drug Discov.* 2007;6(9):734-745.
21. Hartmann JT, Kanz L. Sunitinib and periodic hair depigmentation due to temporary c-KIT inhibition. *Arch Dermatol.* 2008;144(11):1525-1526.
22. Murphy EA, Shields DJ, Stoletov K, et al. Disruption of angiogenesis and tumor growth with an orally active drug that stabilizes the inactive state of PDGFRbeta/B-RAF. *Proc Natl Acad Sci U S A.* 2010;107(9):4299-4304.
23. Tsimberidou AM, Keating MJ. Treatment of fludarabine-refractory chronic lymphocytic leukemia. *Cancer.* 2009;115(13):2824-2836.
24. Crowther-Swanepoel D, Qureshi M, Dyer MJ, et al. Genetic variation in CXCR4 and risk of chronic lymphocytic leukemia. *Blood.* 2009;114(23):4843-4846.
25. Franklin RA, Tordai A, Mazer B, Terada N, Lucas JJ, Gelfand EW. Activation of MAP2-kinase in B lymphocytes by calcium ionophores. *J Immunol.* 1994;153(11):4890-4898.
26. Atherfold PA, Norris MS, Robinson PJ, Gelfand EW, Franklin RA. Calcium-induced ERK activation in human T lymphocytes. *Mol Immunol.* 1999;36(8):543-549.
27. Chen L, Huynh L, Apgar J, et al. ZAP-70 enhances IgM signaling independent of its kinase activity in chronic lymphocytic leukemia. *Blood.* 2008;111(5):2685-2692.
28. Oki S, Limnander A, Yao PM, Niki M, Pandolfi PP, Rothman PB. Dok1 and SHIP act as negative regulators of v-Abl-induced pre-B cell transformation, proliferation and Ras/Erk activation. *Cell Cycle.* 2005;4(2):310-314.
29. Mikhalap SV, Shlapatska LM, Yurchenko OV, et al. The adaptor protein SH2D1A regulates signaling through CD150 (SLAM) in B cells. *Blood.* 2004;104(13):4063-4070.
30. Gabelloni ML, Borge M, Galletti J, et al. SHIP-1 protein level and phosphorylation status differs between CLL cells segregated by ZAP-70 expression. *Br J Haematol.* 2008;140(1):117-119.

SUPPLEMENTAL INFORMATION

Messmer D*, Fecteau JF*, O'Hayre M**,** Bharati I, Handel TM, Kipps TJ. Chronic Lymphocytic Leukemia Cells Receive Raf-Dependent Survival Signals in Response to CXCL12 that Are Sensitive to Inhibition by Sorafenib. (2011) *Blood* 117(3): 882-9. **Authors contributed equally.*

Figure S1

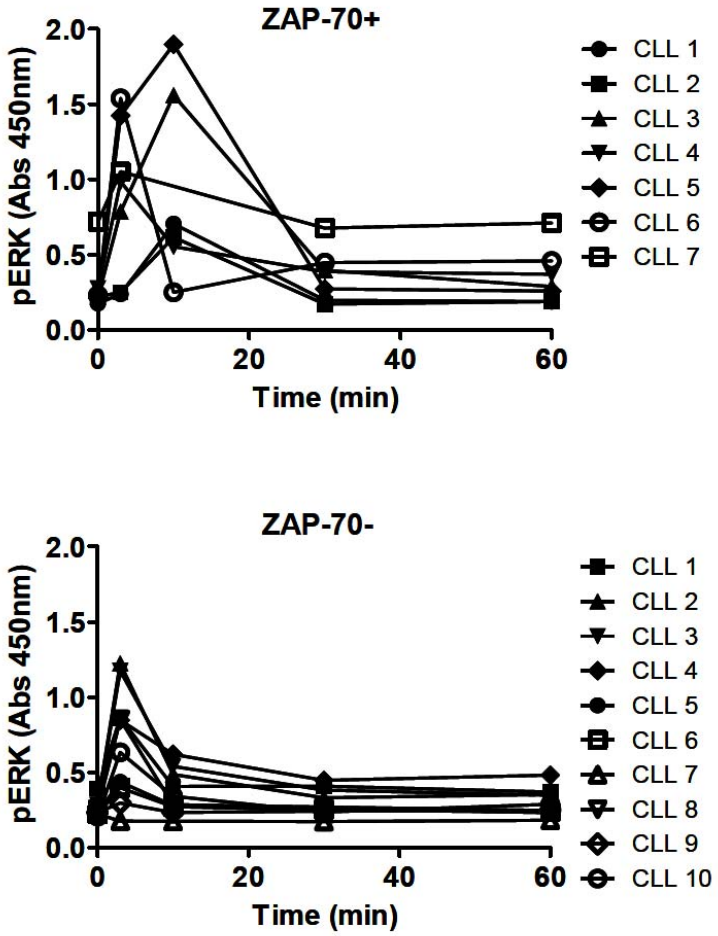

Figure S1. CXCL12 induces increased and prolonged ERK activation in ZAP-70+ CLL cells. The same data are shown as in Figure 2 from ZAP-70- CLL samples (n=10) and ZAP-70+ CLL samples (n=7), showing individual patient responses; each line represents one patient sample measured over time.

Figure S2

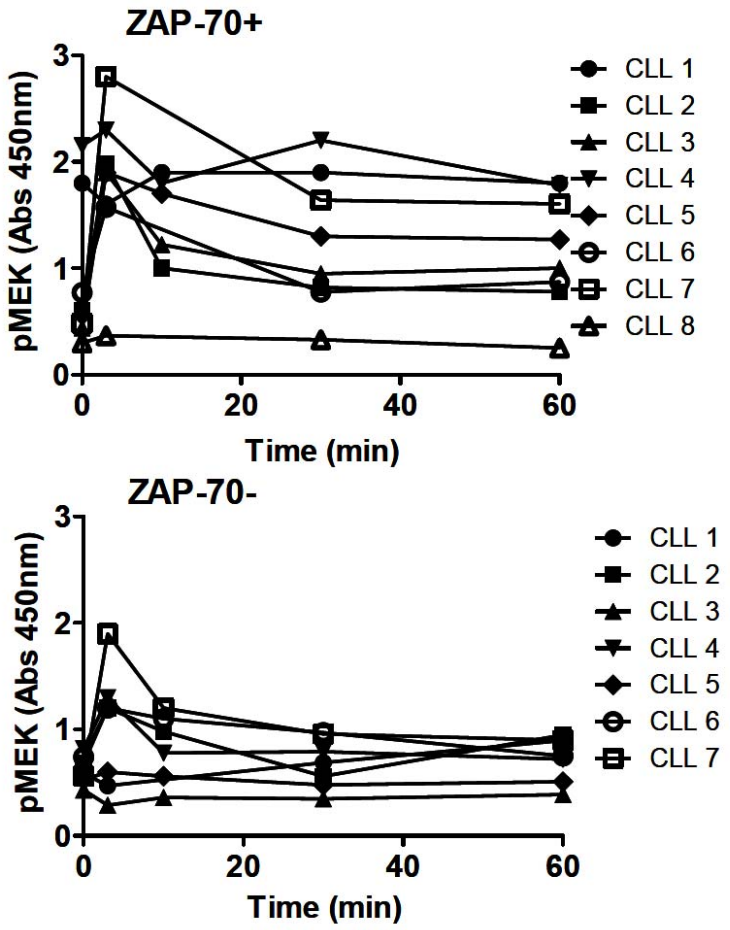

Figure S2. CXCL12 induces pronounced MEK activation in ZAP-70+ CLL cells. Depicted are the same data as in Figure 3 showing the individual patient responses; each line represents one patient sample measured over time (n= 8 for ZAP-70+ and n=7 for ZAP-70-).

Figure S3

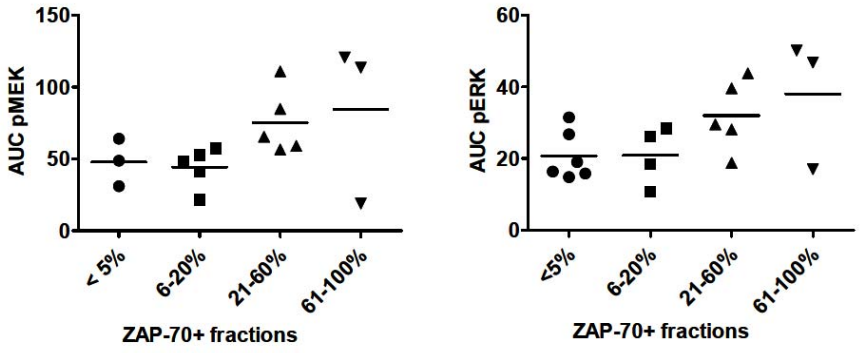

Figure S3. Amplitude of pMEK and pERK responses to CXCL12 based on the fraction of ZAP-70+ CLL cells in the patient samples. Shown are levels of pMEK and pERK using data shown in Figures 2B and 3, where the samples were divided based on the 20% cut-off. Here the samples were divided into 4 groups based on the percentage of ZAP-70+ cells to examine if there is a correlation between the percentage of ZAP-70+ and the phosphorylation level.

Figure S4

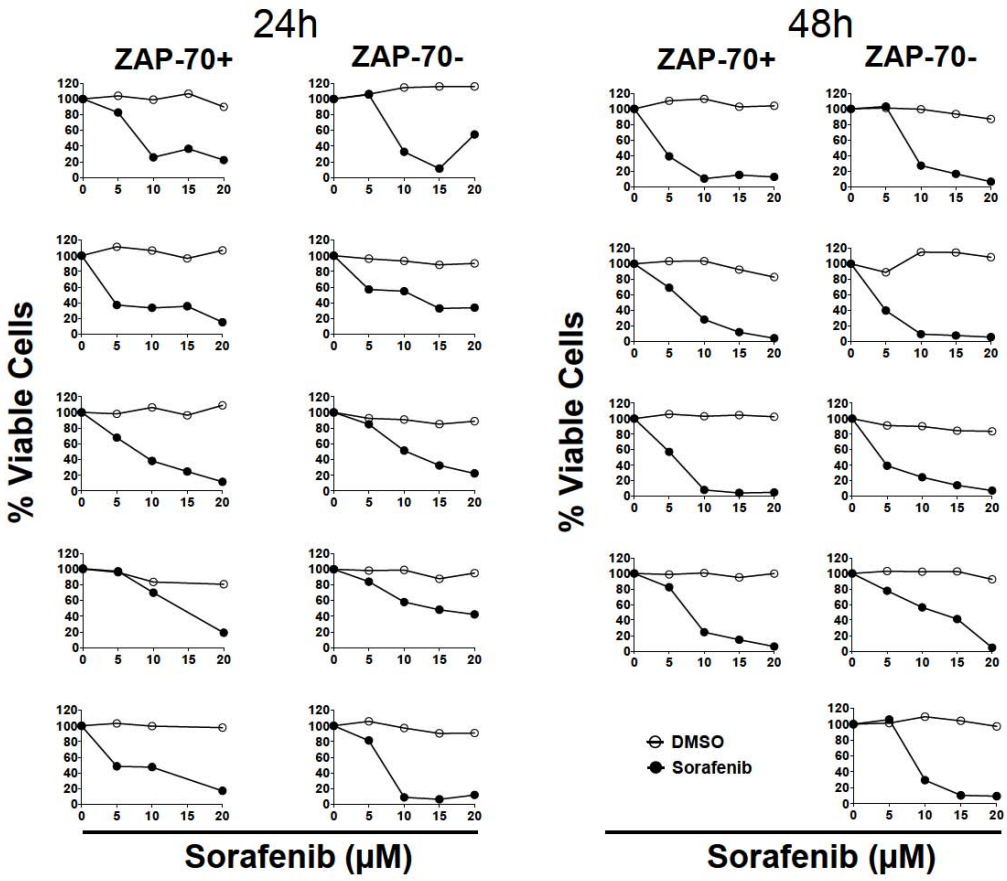

Figure S4. Sorafenib causes increased apoptosis in ZAP-70+ CLL cells. Depicted are the same data as in Figure 5B showing individual patient responses.

Figure S5

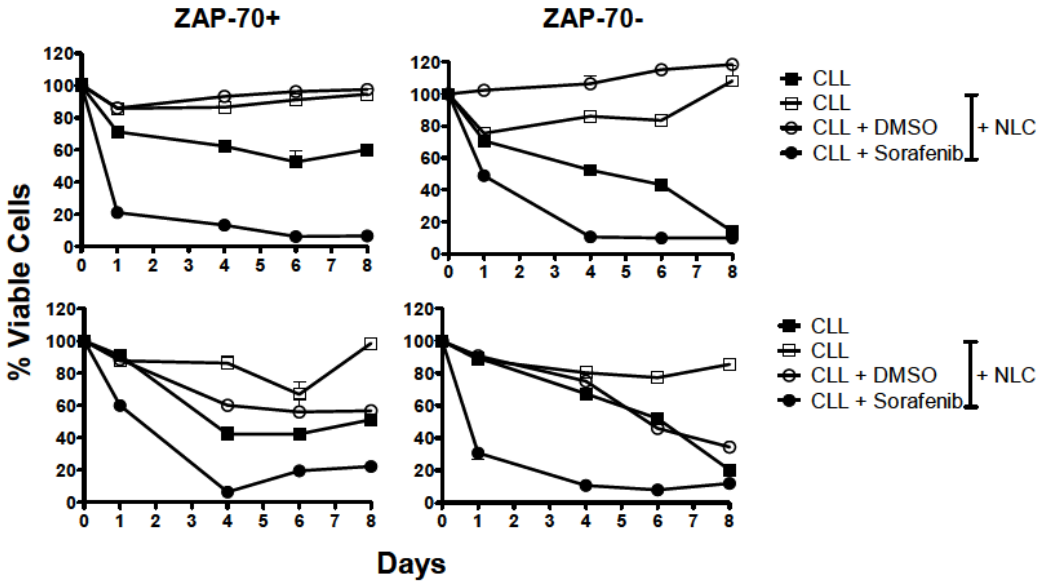

Figure S5. Sorafenib cause apoptosis of CLL cells in presence of NLCs.

Depicted are the same data as in Figure 5C showing individual patient responses.

ACKNOWLEDGEMENTS

Chapter 3 is a reprint of the material as it appears in *Blood*, 2011, Davorka Messmer*, Jessie-F Fecteau*, Morgan O'Hayre*, Ila S Bharati, Tracy M Handel and Thomas J Kipps. Chronic Lymphocytic Leukemia Cells Receive Raf-Dependent Survival Signals in Response to CXCL12 that Are Sensitive to Inhibition by Sorafenib, 117(3): 882-9. **Authors contributed equally.*

The dissertation author was one of the primary authors on the article and designed and performed experiments characterizing the differential ERK1/2 activation and calcium flux responses to CXCL12, prepared CXCL12 for all experiments, wrote corresponding sections for the manuscript and edited the manuscript. Jessie-F Fecteau and Ila S Bharati designed and performed experiments examining effects of sorafenib on MEK and ERK activation and CLL survival and edited the manuscript. Davorka Messmer designed experiments and wrote the manuscript. Tracy M Handel and Thomas J Kipps contributed to experimental design and edited the manuscript.

CHAPTER 4

Mechanisms and Consequences of the Loss of PHLPP1 Phosphatase in Chronic Lymphocytic Leukemia

4.1 Abstract

Chronic Lymphocytic Leukemia (CLL) is an adult leukemia characterized by the accumulation of mature monoclonal B cells that is primarily attributed to their enhanced responsiveness to survival cues and/or apoptotic resistance *in vivo*. Activation of survival pathways such as Akt and ERK1/2 by factors produced in the microenvironment, including cytokines and chemokines, is known to be important for the survival of CLL cells. Therefore, a better understanding of how these key survival pathways are activated and/or misregulated in CLL is critical for understanding the mechanisms contributing to disease progression. The PH domain and Leucine-rich repeat Protein Phosphatase 1 (PHLPP1) is a phosphatase that directly de-phosphorylates Akt and PKC at their hydrophobic motifs and thereby inactivates them, and also indirectly regulates ERK1/2 activation. PHLPP1 is a proposed tumor suppressor protein and thus alterations in PHLPP1 expression or activity could have significant implications in cancer malignancy. Herein, we describe the loss of detectable PHLPP1 protein expression in >90% of CLL patients' cells examined. This loss of PHLPP1 protein correlated with significant decreases in PHLPP1 transcript levels compared to normal B cell controls these decreases do not appear to be a result of genetic mutations. Additionally, we provide evidence suggesting that the observed loss of PHLPP1 expression may be due, in part, to DNA methylation of the *PHLPP1* gene as well as decreased transcript stability.

As an important regulator of Akt, PKC and ERK1/2 signaling, the loss of PHLPP1 expression may enable CLL cells to have more enhanced responsiveness to survival stimuli.

4.2 Introduction

The PHLPP (Pleckstrin Homology domain and Leucine-rich repeat Protein Phosphatase) family is comprised of novel Ser/Thr phosphatases that serve as important regulators of cell survival and apoptosis [*1-2*]. The PHLPP family consists of two main isoforms, PHLPP1 (also known as SCOP) and PHLPP2, which both dephosphorylate Akt and PKC on their hydrophobic motifs. However, these phosphatases vary in their selectivity for different Akt isoforms, whereby PHLPP1 preferentially targets Akt2 and Akt3, selectively regulating downstream targets such as HDM2 and GSK3α, while PHLPP2 targets Akt1 and Akt3 [3]. Additionally, PHLPP1 has been shown to negatively regulate the Ras/Raf/MEK/ERK pathway, potentially by directly binding and inhibiting Ras guanine nucleotide exchange and activation [4]. Recent evidence from Dr. Alexandra Newton's lab indicates that PHLPP1 also regulates the transcription of various growth factor receptors, including epidermal growth factor receptor (EGFR), and thus may indirectly affect ERK1/2 activation as well as cell growth and survival through regulation of receptor tyrokine kinase expression (unpublished data). By negatively regulating Akt, PKC, and ERK1/2 signaling (directly or indirectly), the PHLPP phosphatases have been proposed to function as tumor-suppressors [*2, 5*]. Indeed, a decrease in PHLPP1 and/or PHLPP2 expression levels has been detected in a number of cancers including colon cancer, breast cancer, glioblastoma, and several lymphomas and leukemias [*5-8*]. Furthermore, overexpression of PHLPP phosphatases suppresses growth and increases apoptosis of non-small-cell lung and breast cancer cell

lines, while reduction of PHLPP levels enhances proliferation and survival responses [*2, 5, 9*].

Chronic Lymphocytic Leukemia is an adult B cell leukemia and the most common leukemia in the Western world [10]. The disease is characterized by an accumulation of monoclonal CD5+ B cells in the blood, secondary lymphoid tissue, and marrow. This accumulation is believed to be predominately attributed to their enhanced survival/apoptotic resistance *in vivo* [*11-12*]. Factors from the microenvironment, including chemokines such as CXCL12, are believed to play important roles in the survival of CLL cells; by activating a number of pro-survival and growth-promoting pathways including Akt and ERK1/2, these signals from the microenvironment can protect cells from spontaneous as well as drug-induced apoptosis [*11, 13-14*]. As such, any disruptions in the balance between pro-survival and apoptotic pathways may be key factors in CLL pathogenesis. Consequently, alterations in the expression or function of proteins regulating these pathways, including the PHLPP phosphatases, can influence how CLL cells respond to growth and survival cues (Figure 4.1).

Recently, a reduction in PHLPP1 protein levels in CLL cells was reported [*15*]. Herein, we provide further evidence with cells from a separate set of CLL patients to support the loss of PHLPP1 expression in the majority of CLL cases. We show that introduction of PHLPP1 into primary CLL cells via adenoviral expression results in a decrease in the intensity of Akt and ERK1/2 activation in response to CXCL12 stimulation. Furthermore, we observe higher levels of DNA methylation of the *PHLPP1* gene in CLL cells compared to normal B cells and the few CLL patients' cells that do express PHLPP1. Hypermethylation of CpG islands is frequently observed in cancers and it was recently demonstrated that CLL cells exhibit a number of aberrantly methylated genes [*16-17*]. In particular, methylation of tumor suppressor genes leading

to repressed expression of the corresponding proteins can contribute to cancer progression [*17-18*].

Overall, our results suggest that the loss of PHLPP1 expression in CLL cells may enhance their responsiveness to growth and survival factors. Additionally, we propose DNA methylation, a yet unpublished mechanism for regulation of PHLPP1 expression, may in part account for the decrease in PHLPP1 mRNA and protein levels observed in CLL. Our data suggests that lower PHLPP1 mRNA stability may also account for decreased PHLPP1 expression in the CLL cells.

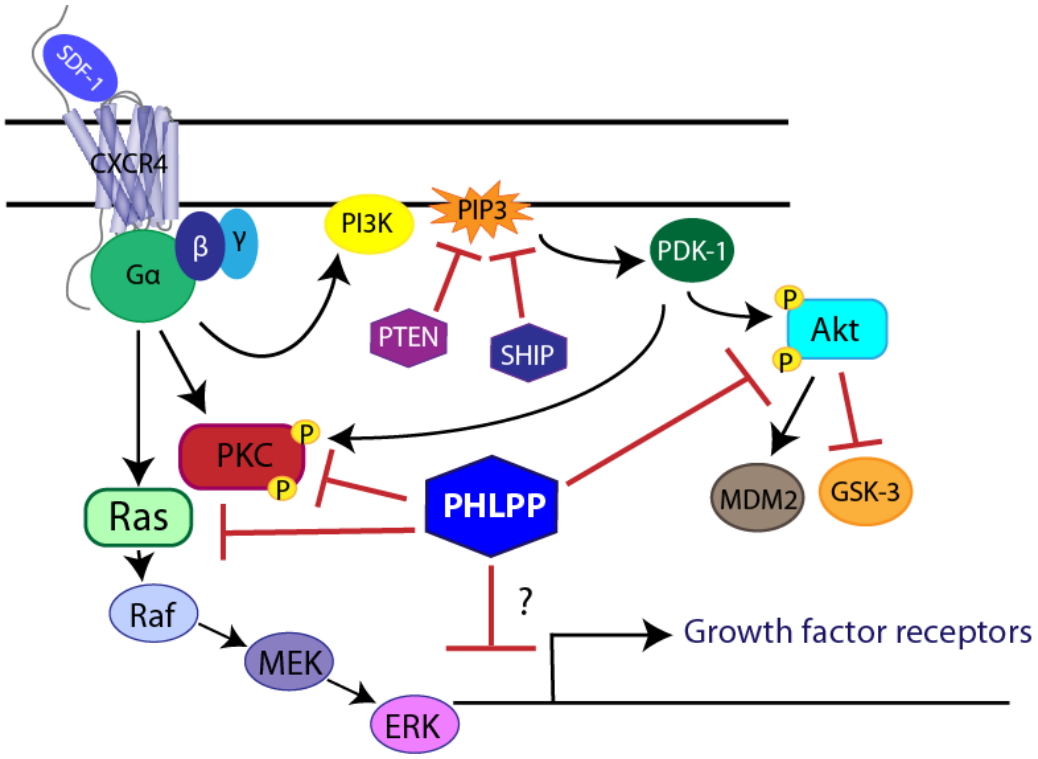

Figure 4.1 Diagram illustrating potential mechanisms by which PHLPP could regulate signaling events downstream of the CXCL12/CXCR4 axis. PHLPP phosphatases directly dephosphorylate and regulate Akt and PKC, respectively leading to inactivation or degradation. Akt and PKC are known targets of CXCL12/CXCR4 signaling and so differences in PHLPP expression may alter signaling responsiveness to CXCL12.

4.3 Results

4.3.1 PHLPP1 Protein is Absent in >90% of Patients' CLL Cells

Since the PHLPP phosphatases are reduced in several types of cancer, regulate pathways critical to CLL survival, and have proposed tumor suppressor functions, PHLPP1 and PHLPP2 protein levels were probed in CLL B cells [3]. Additionally, since PTEN, a phosphatase that acts on the lipid phosphatidylinositol (3,4,5,) triphosphate (PIP_3) upstream of Akt activation, is deleted or mutated in a number of cancers, we also examined expression levels of PTEN [*19*]. Overall, we detected PHLPP1 protein expression in only 4 out of the 43 CLL patients' B cells probed, corresponding to a loss in >90% of patients, whereas it was detected in all healthy B cells and highly expressed in Ramos cells, a Burkitt's lymphoma B cell line (representative blot in Figure 4.2). PHLPP2 expression, on the other hand, was detected in all CLL cells probed, although the levels were found to be somewhat variable between different patients' cells. Additionally, no differences in PTEN expression levels were observed among the CLL patients or between healthy B cells, although it was previously suggested to be lost in CLL cells in approximately a quarter of patients (Figure 4.2) [*20*]. These observed differences may be due to a number of factors including a different CLL patient pool and different PTEN antibodies used. We also did not specifically look for cells exhibiting loss of heterozygosity at 10q23.3, which corresponds to the chromosomal location of *PTEN*. Overall, these results demonstrate a dramatic loss of PHLPP1 expression in CLL cells from most patients, although PTEN and PHLPP2 expression appear to be maintained.

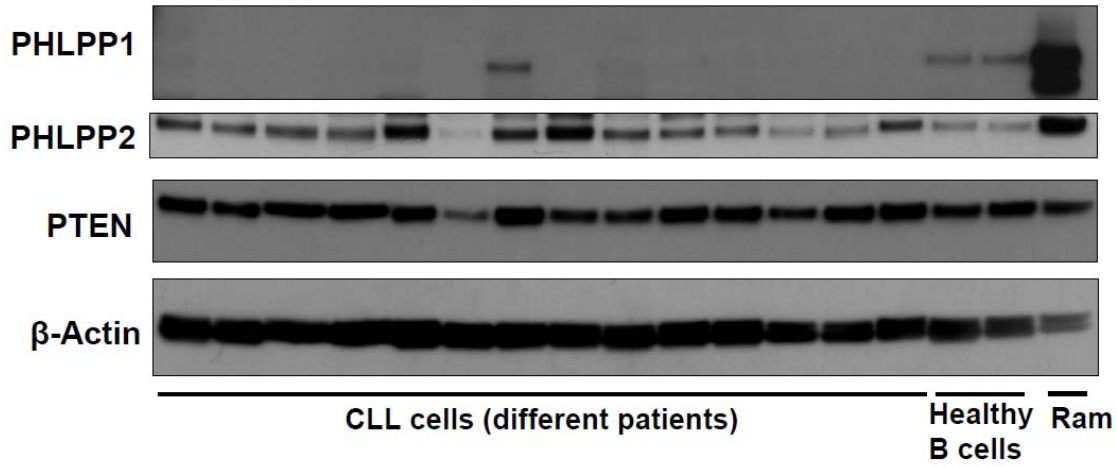

Figure 4.2 PHLPP1 expression is lost in the majority of CLL patients' cells. Representative western blot profiling PHLPP1, PHLPP2 and PTEN expression in CLL patients' cells compared to B cells from healthy donors and Ramos B cell line (Ram). β-actin served as a loading control

4.3.2 Loss of PHLPP1 Protein Expression Corresponds with a Decrease in mRNA Expression

In order to determine if the loss of PHLPP1 protein corresponds with a decrease in transcript levels of PHLPP1 or whether it might be related to a decrease in protein stability, we performed quantitative reverse-transcription PCR (RT-PCR) on RNA isolated from purified CLL B cells and B cells from healthy donors. In healthy B cells and the 4 CLL patients' cells in which PHLPP1 protein levels were detectable by western blot (top panel Figure 4.3), significant levels of mRNA transcripts were also observed (bottom panel Figure 4.3). CLL cells with undetectable PHLPP1 protein had significantly reduced or undetectable PHLPP1 mRNA levels. This is in contrast to what Suljagic *et al*. reported in which PHLPP1 protein was not detected in any of their patients' CLL cells although mRNA expression was sometimes observed; however it is consistent with their findings that proteasomal and calpain inhibitors had no effect on PHLPP1 protein accumulation [*15*].

Additionally, we examined PHLPP1 mRNA expression in Ramos cells and two CLL cell lines, WaC3CD5+ and EHEB. These cell lines were not directly compared to the CLL cells due to significant differences in GAPDH levels, despite equivalent amounts of mRNA and converted cDNA used in the reactions (~20x higher GAPDH in cell lines versus primary cells). The Ramos cells and WaC3CD5+ cells, which both express PHLPP1 protein, also exhibit significant levels of PHLPP1 mRNA; in contrast, the EHEB CLL cell line, which has significantly lower PHLPP1 protein detection, also has significantly reduced mRNA expression (Figure 4.4). (Note: when comparing GAPDH normalized Ct (threshold cycle) values, the EHEB cells have ~3x higher levels of PHLPP1 mRNA to CLL cells whereas direct Ct comparisons indicate ~60x higher PHLPP1 mRNA in the EHEBs).

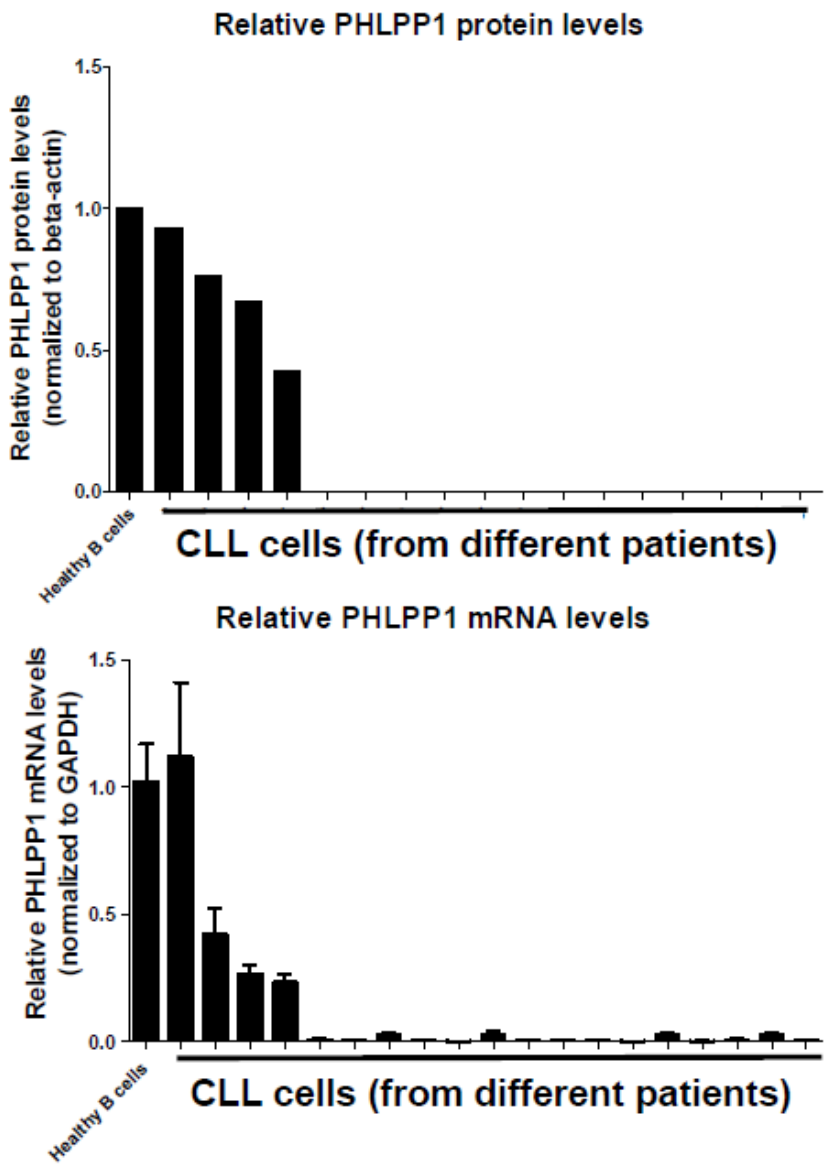

Figure 4.3 Loss of PHLPP1 protein expression correlates with a loss in mRNA expression. PHLPP1 protein expression quantified by densitometry from western blots of healthy B cells (n=4), the 4 CLL patient's cells expressing PHLPP1 and other CLL patients' cells is shown in the top panel. The correlating mRNA expression from these cells determined by quantitative RT-PCR is shown in the bottom panel. Data presented is an average of 3 experiments performed in triplicate and normalized to GAPDH, and the levels are relative to an average of normal B cells.

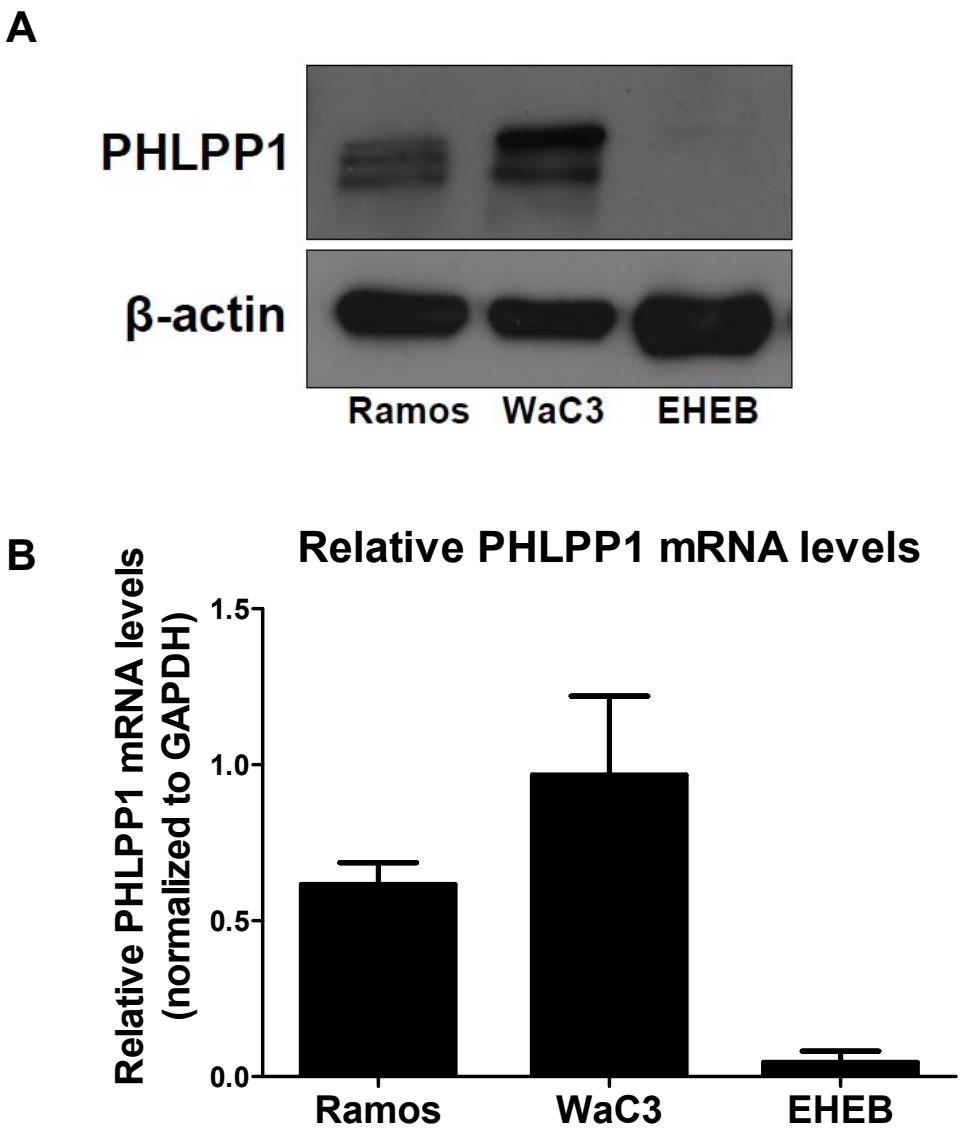

Figure 4.4 PHLPP1 expression in leukemic B cell lines. Western blot of relative PHLPP1 protein expression in Ramos Burkitt's lymphoma line and two CLL cell lines, EHEB and WaC3CD5+ (WaC3) cells (top panel) and corresponding relative mRNA expression as assessed by quantitative RT-PCR (bottom panel).

Overall, our results indicate that PHLPP1 protein expression in CLL cells largely correlates with mRNA levels, suggesting that the mechanism for its loss is likely due to genetic mutation(s), epigenetic modification (e.g. DNA methylation) or alterations in mRNA stability rather than changes in translation efficiency or protein stability. As

alluded to earlier, these results are consistent with findings from Suljagic *et al*. in which calpain and proteasomal inhibitors, used to determine if there were differences in the stability of PHLPP1 protein in CLL cells compared to normal B cells and leukemic cell lines, had no effect on PHLPP1 protein accumulation in CLL cells [*15*].

4.3.3 Expression of PHLPP1 in CLL Cells Decreases Their Signaling Response to CXCL12

In order to elucidate the potential consequences of the loss of PHLPP1 expression in CLL cells, fresh CLL cells were adenovirally transduced with PHLPP1 or GFP control, stimulated over a 1 h time course with CXCL12, and probed for phosphorylation and activation of Akt (S473) and ERK1/2. In order to control that the adenovirus was specifically upregulating PHLPP1 and that there was not a compensatory decrease in PHLPP2 levels, we noted that expression of PHLPP2 in the CLL cells was not altered upon PHLPP1 adenoviral expression (data not shown). We observed that expression of PHLPP1 in CLL cells reduced the CXCL12-induced phosphorylation of Akt and ERK1/2, although there was variability in the extent to which phosphorylation was affected (representative blot from n=4 in Figure 4.5). Additionally, over-expression of PHLPP1 in the WaC3CD5+ CLL cell line, expresses endogenous PHLPP1, resulted in a decrease in basal as well as CXCL12-mediated Akt (S473) phosphorylation, corresponding to previous observations (Figure 4.6) [*2*]. Nevertheless, CXCL12 stimulation response and/or constitutive Akt and ERK1/2 phosphorylation was observed in the CLL cells that endogenously expressed PHLPP1 (data not shown). It is possible that there are alterations in other signaling components that compensate for the expression of PHLPP1 and permit constitutive activity and/or good stimulation response

in these cells. It is also possible that there is some degree of compensation from PHLPP2 activity in CLL cells that lack PHLPP1 expression.

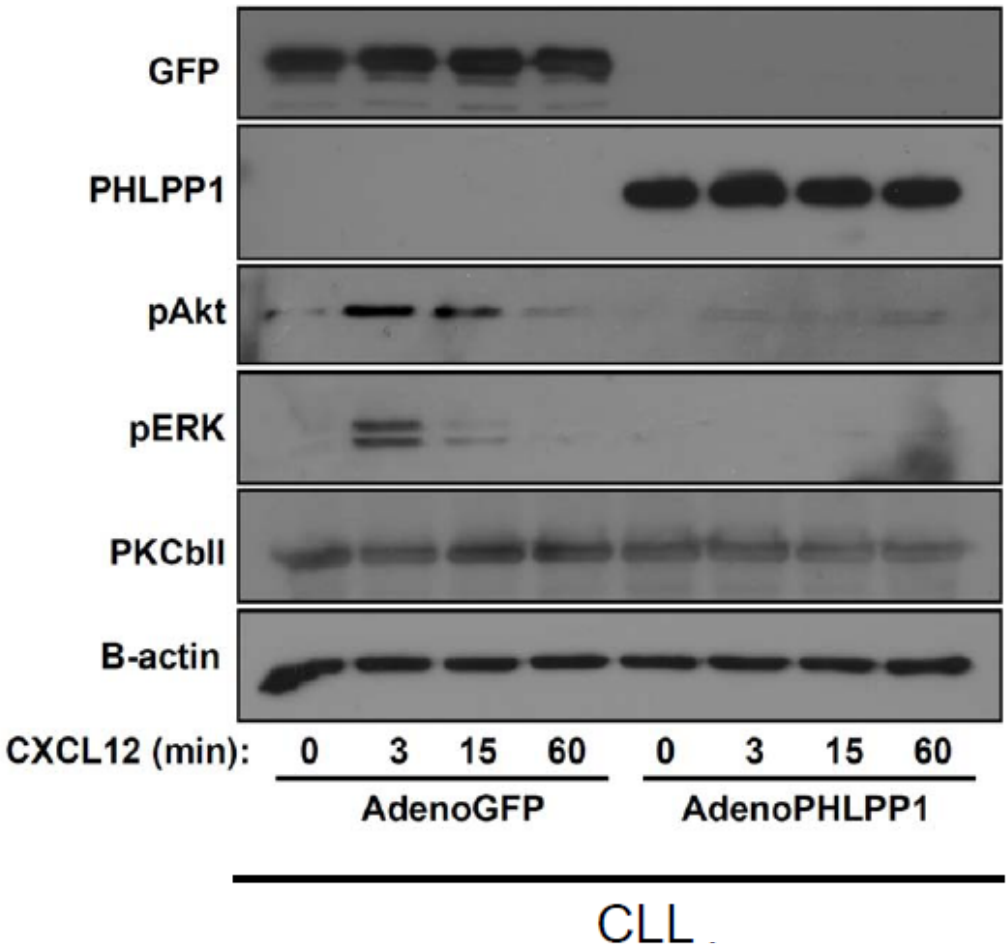

Figure 4.5 PHLPP1 expression reduces CXCL12-induced Akt and ERK1/2 activation in CLL cells. Western blot comparing phospho-Akt (S473), phospho-ERK1/2 and PKC-βII levels in a representative (n=4) CLL patient's cells adenovirally transduced with PHLPP1 or GFP control and unstimulated or stimulated with 30 nM CXCL12 for 3, 15 or 60 min. β-actin served as a loading control and GFP and PHLPP1 demonstrate successful adenoviral transduction.

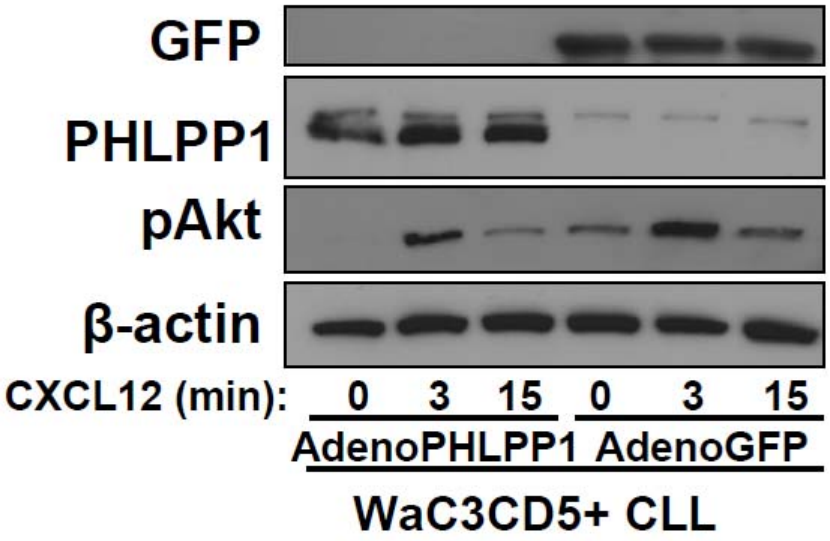

Figure 4.6 PHLPP1 over-expression reduces basal and CXCL12-induced Akt phosphorylation (S473) in WaC3CD5+ cells. Western blot comparing phospho-Akt (S473) at 0, 3 and 15 min of 30 nM CXCL12 stimulation in adenoviral PHLPP1 or adenoviral GFP transduced WaC3CD5+ cells. β-actin served as a loading control and GFP and PHLPP1 demonstrate successful adenoviral transduction.

Since PHLPP1 expression has been shown to reduce PKC stability and PKCβII is strongly expressed in CLL cells, PKCβII levels were also probed (Figure 4.5) [1]. However, PKCβII levels were found to be maintained in the PHLPP1 expressing cells compared to control cells. Given that 72 h following adenoviral transduction of PHLPP1 may not be long enough to observe notable decreases in the PKCβII expression since PKC has a very stable half life [*21*], we also compared endogenous PKCβII in CLL cells compared to normal B cells (Figure 4.7). In general, a stronger signal and banding pattern of PKCβII expression was observed in CLL cells compared to normal B cells, and the Ramos cells, which expressed really high PHLPP1 levels, had no detectable PKCβII. Therefore, there is a trend for stronger PKCβII expression in CLL cells, in correlation with the loss of PHLPP1 expression in these cells.

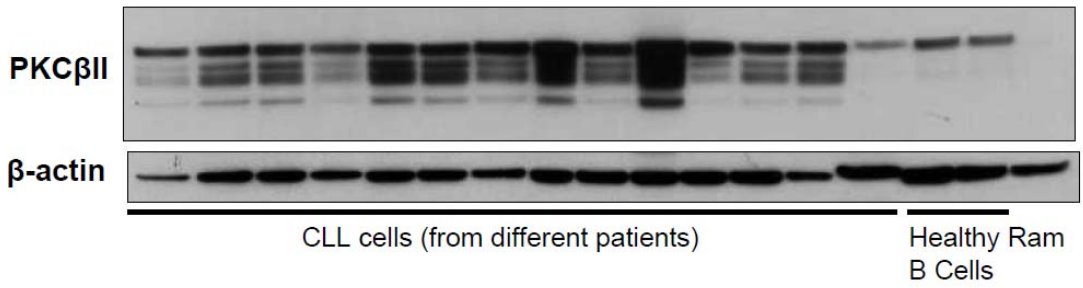

Figure 4.7 PKCβII expression in CLL cells compared to B cells from healthy donors and Ramos B cell line. Western blot profiling PKCβII levels in CLL cells, B cells from healthy donors and Ramos B cells (Ram). β-actin served as a loading control.

Although ERK is not a direct target of PHLPP phosphatase activity, expression of PHLPP1 in CLL cells significantly reduced CXCL12-mediated ERK1/2 phosphorylation. It has been proposed that effects of PHLPP1 expression on ERK activation may be mediated through regulation of Ras activity [4]; we also have evidence that PHLPP1 negatively regulates the transcription and expression of growth factor receptors such as EGFR, thereby altering ERK1/2 activation by growth factors (e.g. EGF) (unpublished data from Dr. Alexandra Newton's lab). To determine whether PHLPP1 may be regulating CXCR4 expression levels and thereby altering cellular response to CXCL12, we compared CXCR4 expression in CLL cells expressing adenoviral PHLPP1 versus adenoviral LacZ or GFP. Our results indicated that neither CXCR4 protein levels nor CXCR4 transcription were altered by PHLPP1 expression in CLL cells following 72 h of adenoviral infection (Figure 4.8 and data not shown). We also examined expression of CXCR4 in mouse embryonic fibroblasts from control and *PHLPP1-/-* mice and observed no differences in CXCR4 expression (data not shown), providing additional confirmation that CXCR4 is not regulated by PHLPP1.

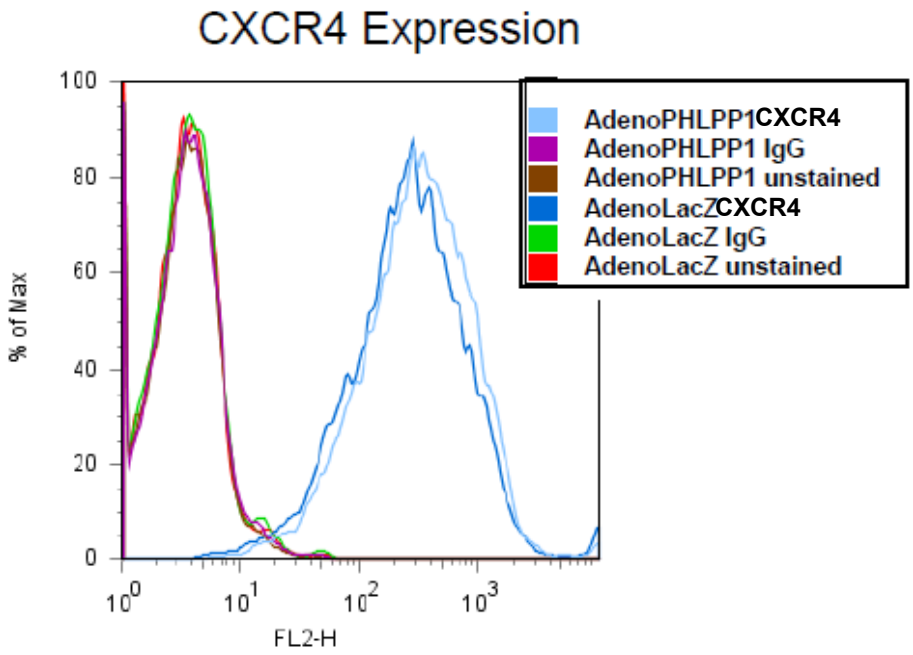

Figure 4.8 PHLPP1 does not appear to regulate CXCR4 levels. CLL cells were infected for 72 h with an adenovirus encoding PHLPP1 or LacZ as a control. The cells were then stained for surface expression of CXCR4, an IgG isotype control (IgG) or left unstained and analyzed by flow cytometry. Both the PHLPP1 and LacZ infected cells stained for CXCR4 (in light and dark blue, respectively) exhibit similar, high levels of CXCR4 compared to unstained and IgG controls.

4.3.4 Sequencing for Potential Mutations in the *PHLPP1* Gene

DNA sequence alterations leading to premature translational stop or decreased mRNA stability of an mRNA have been characterized in a number of diseases, notably cancer [*22-23*]. To address the possibility of genetic mutation as the source of decreased PHLPP1 levels in CLL, we sequenced the 17 exons that comprise the PHLPP1 gene. Twenty-three PCR reactions covering the genomic sequence for PHLPP1 were carried out on 15 CLL samples as well as 3 normal B cell controls and the Ramos B cell line. Subsequent DNA sequencing analysis uncovered several alterations to the exonic sequence, all of which had been previously characterized as single nucleotide polymorphisms (in the NCBI database), indicating that these changes were present in the normal B cells and that there were no somatic mutations in *PHLPP1* exon

regions in the CLL samples (Figure 4.9). Our analysis included the additional 1500 base pairs of the longer PHLPP1β splice variant [*9*]. To our knowledge this is the first study to sequence this region due to its high GC content and requirement for additional PCR additives for amplification. Since we were able to amplify each exon, it is unlikely that bi-allelic loss of the PHLPP1 gene was responsible for the absence of PHLPP1 mRNA and protein in the CLL cells. Taken together, these data suggest that unlike glioblastoma and colon cancer where several somatic mutations to *PHLPP1* have been characterized [*3, 24-25*], there were no mutations to *PHLPP1* in CLL, indicating that other mechanisms are responsible for loss of PHLPP1 expression.

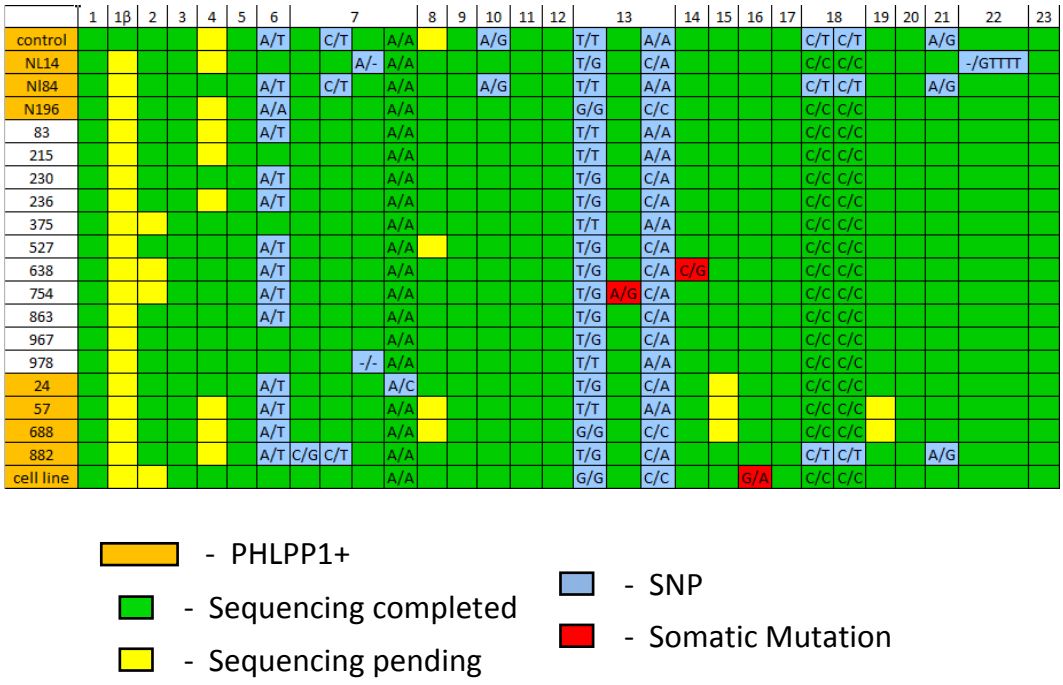

Figure 4.9 DNA sequencing analysis of PHLPP1. Table of sequencing reactions performed to cover the PHLPP1 gene including the PHlPP1β extension. In the left column, boxes colored in orange represent cells expressing PHLPP1 while white boxes indicate loss of PHLPP1 in those cells probed. Regions highlighted in blue or red represent SNP or potential somatic mutations, respectively found in those sequencing reactions and yellow regions indicate sequencing reactions are still pending.

4.3.5 CLL B Cells Exhibit Higher Levels of *PHLPP1* Gene Methylation Compared to B cells from Healthy Donors and PHLPP1-Expressing CLL Cells

Since a correlation between the loss of PHLPP1 protein expression and a reduction in PHLPP1 mRNA levels was observed and no likely responsible genetic mutations were detected, we examined whether methylation of the *PHLPP1* promoter or gene could account for the reduced transcript levels in CLL cells. Methylation of CpG islands is a common mechanism for regulation of gene expression and hypermethylation of tumor suppressor genes is frequently observed in cancers [*17-18*].

In order to evaluate levels of *PHLPP1* methylation, bisulfite treatment of DNA from purified CLL cells, B cells from healthy donors or cell lines was performed, which results in the conversion of un-methylated cytosines to uracil/thymine while methylated cytosines are protected from conversion (Figure 4.10). PCR amplification of 250-400 bp regions within the CpG islands of the *PHLPP1* promoter and gene was performed, PCR products were gel purified and cloned into a TOPO/TA vector and then 5-10 colonies from each DNA sample were sequenced and the fraction of methylated CpGs was quantified (Figure 4.10). Although regions throughout the *PHLPP1* promoter and gene were screened and assessed for methylation (Figure 4.11), the majority of methylation observed was in the last ~750 bp of exon 1 while very little methylation was observed in the promoter or early exon 1 regions probed. Due to the large time requirements, sample limitations, and expense of this process and the sequencing, the focus of the methylation analysis for quantitative comparisons was on the last ~340 bp region of exon 1 highlighed in Figure 4.12. However, based on preliminary screening, it appears that ~400 bp upstream of this region also reflect a similar degree of methylation and similar differences between CLL cells and healthy B cells. These results indicate that the end of

exon 1 region of *PHLPP1* exhibits a high degree of methylation that is potentially important for gene expression. In agreement with these results, Dr. Christiane Knobbe and Dr. Guido Reifenberger observed a reduction in PHLPP1 transcription in a number of primary glioblastomas and glioblastoma cell lines and while no differences in promoter methylation were identified, there appeared to be enhanced methylation near the end of exon 1 of the *PHLPP1* gene (personal communication).

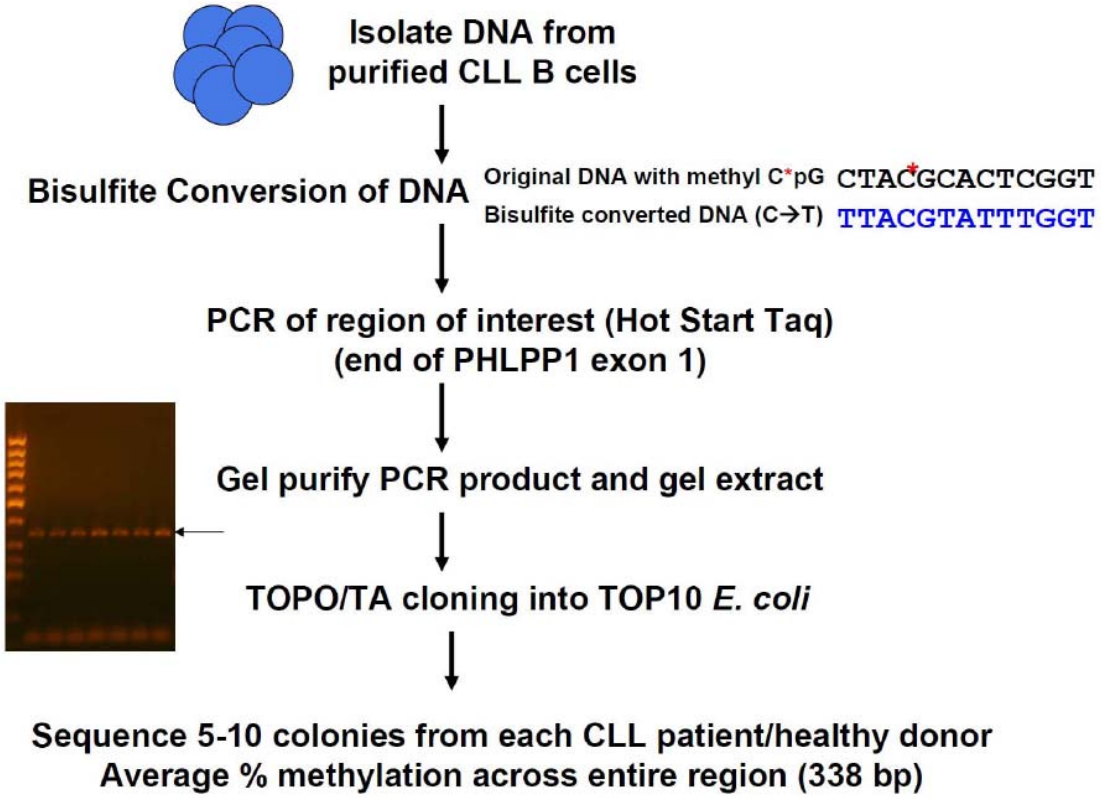

Figure 4.10 Methylation analysis of the PHLPP1 gene. A flow diagram of the experimental procedure for methylation analysis of the PHLPP1 gene: DNA from purified CLL B cells was bisulfite converted and PCR amplified over the region of interest (end of exon 1), PCR products were gel purified, cloned into a TOPO/TA vector and 5-10 colonies from each sample were sequenced and fraction of CpG methylation was quantified.

Figure 4.11 Relative percent CpG methylation across regions of the bisulfite converted *PHLPP1* gene and promoter. DNA sequence of bisulfite converted *PHLPP1* gene and promoter. Boxed sequences indicate the primers used to probe these regions (forward and reverse primers) and red highlight indicates the ATG start site. Highlighted regions represent: white- not probed, yellow- <15% CpG methylation across the region, green- >30% CpG methylation across the region, blue- >20% CpG methylation across region and this is the region used in quantitative analysis. *In vitro* DNA methylation using Sss1 (NEB) performed as a positive control results in ~45-50% CpG methylation across these regions.

```
   1    ATGGA GCCCG CCGCC GCGGC CACGG TACAG CGACT CCCCG AGCTC GGCAG
  51    GGAGG ACCGA GCTTC GGCTC CGGCG GCCGC CGCTG CGGCA GCAGC AGCAG
 101    CAGCG GCGGC CGCGG CGGCT CTGGC GGCGG CGGCC GGGGG CGGCC GGAGT
 151    CCGGA GCCCG CGCTG ACCCC GGCGG CCCCG AGCGG CGGGA ACGGC AGCGG
 201    CAGCG GGGCG CGGGA AGAGG CCCCA GGCGA GGCGC CGCCG GGGCC GCTGC
 251    CGGGC AGAGC GGGGG GTGCC GGGCG CAGGA GGCGG CGCGG GGCGC CCCAG
 301    CCCAT TGCCG GCGGG GCTGC CCCCG TACCC GGGGC CGGCG GCGGC GCCAA
 351    CTCCC TCCTG CTGAG GAGAG GGCGG CTGAA GAGGA ATCTG TCCGC GGCCG
 401    CCGCG GCCGC CTCCT CGTCG TCGTC GTCCT CGGCC GCTGC TGCCT CGCAC
 451    TCCCC CGGCG CTGCC GGCCT CCCCG CCTCC TGCTC GGCCT CGGCG TCGCT
 501    GTGCA CCCGG AGCCT GGACA GGAAG ACGCT GCTTC TGAAG CACCG GCAGA
 551    CGCTG CAGCT GCAGC CGTCG GACCG GGACT GGGTG AGGCA CCAGC TCCAG
 601    CGCGG CTGCG TGCAC GTCTT CGACC GCCAC ATGGC CTCGA CCTAC CTGCG
 651    CCCGG TGCTC TGCAC ACTGG ACACC ACGGC CGGCG AGGTG GCCGC CCGCC
 701    TGCTG CAGCT GGGCC ACAAA GGCGG CGGCG TGGTG AAGGT GCTGG GCCAG
 751    GGGCC CGGAG CCGCC GCCGC CCGGG AGCCC GCTGA ACCGC CCCCC GAGGC
 801    CGGCC CCCGG CTGGC GCCCC CGGAG CCGCG GGACT CGGAG GTACC GCCCG
 851    CGAGG AGCGC GCCGG GTGCC TTCGG GGGGC CTCCG CGCGC GCCCC CCGCC
 901    GACCT ACCCC TGCCC GTCGG CGGCC CGGGC GGGTG GTCGC GCCGC GCCAG
 951    CCCAG CGCCC TCGGA CTCCA GCCCC GGCGA GCCGT TCGTT GGGGG CCCTG
1001    TCTCT TCGCC CCGCG CCCCA CGGCC TGTGG TCTCC GACAC CGAGA GCTTC
1051    AGTCT GAGTC CCAGC GCCGA GAGCG TGTCT GACCG GTTGG ACCCC TACAG
1101    CAGCG GCGGC GGCTC CTCGT CGTCG TCGGA AGAGC TCGAG GCCGA CGCAG
1151    CCTCG GCCCC GACGG GGGTC CCGGG CCAGC CCCGC CGTCC CGGCC ACCCC
1201    GCGCA GCCCC TCCCG CTTCC CCAGA CGGCT TCCTC GCCTC AGCCG CAGCA
1251    GAAAG CCCCG AGGGC CATTG ACAGC CCGGG CGGGG CCGTC CGCGA GGGGT
1301    CGTGC GAGGA GAAGG CAGCG GCAGC CGTGG CCCCG GGAGG CCTCC AGTCT
1351    ACCCC CGGGA GGAGC GGGGT GACCG CGGAG AAGGC GCCTC CGCCG CCCCC
1401    GCCGC CCACC CTGTA CGTGC AGCTC CACGG AGAGA CCACC CGGCG CTTGG
1451    AGGCG GAGGA GAAGC CATTG CAGAT CCAAA ATGAC TACCT CTTCC AACTG
1501    GGATT TGGGG AGCTG TGGAG GGTGC AGGAG GAAGG CATGG ACTCG GAGAT
1551    TGGCT GCCTC ATCCG CTTCT ATGCA GGTAA GGAAG TCACC TGCCT TGACG
```

Figure 4.12 Region of PHLPP1 gene analyzed for quantitative methylation comparison. Highlighted in gray is the region of the PHLPP1 gene (non bisulfite converted) near the end of exon 1 that exhibited significant levels of CpG methylation and was probed for quantification.

Upon comparing the degree of methylation in the region at the end of exon 1 between B cells from healthy donors (n=3), the 4 CLL patients' cells expressing PHLPP1, and a set of CLL cells in which PHLPP1 expression was lost (n=9), we found that the CLL cells with no/reduced PHLPP1 mRNA and protein levels also had a significantly higher degree of CpG methylation compared to healthy B cells and CLL cells expressing PHLPP1 (Figure 4.13). Ramos cells, which have very high levels of

PHLPP1, had no detectable methylation and the WaC3CD5+ CLL line, which also expresses high levels of PHLPP1, had very low levels of CpG methylation compared to the CLL cells. Additionally, the EHEB CLL line, which had lower levels of PHLPP1 protein and mRNA compared to Ramos and WaC3CD5+ cells, correspondingly exhibited a higher degree of *PHLPP1* methylation compared to the other cell lines (Figure 4.13). However, the degree of methylation in the EHEB cells was still not to the same extent as observed in the primary CLL cells, correlating with the even lower levels of PHLPP1 expression in the primary CLL cells.

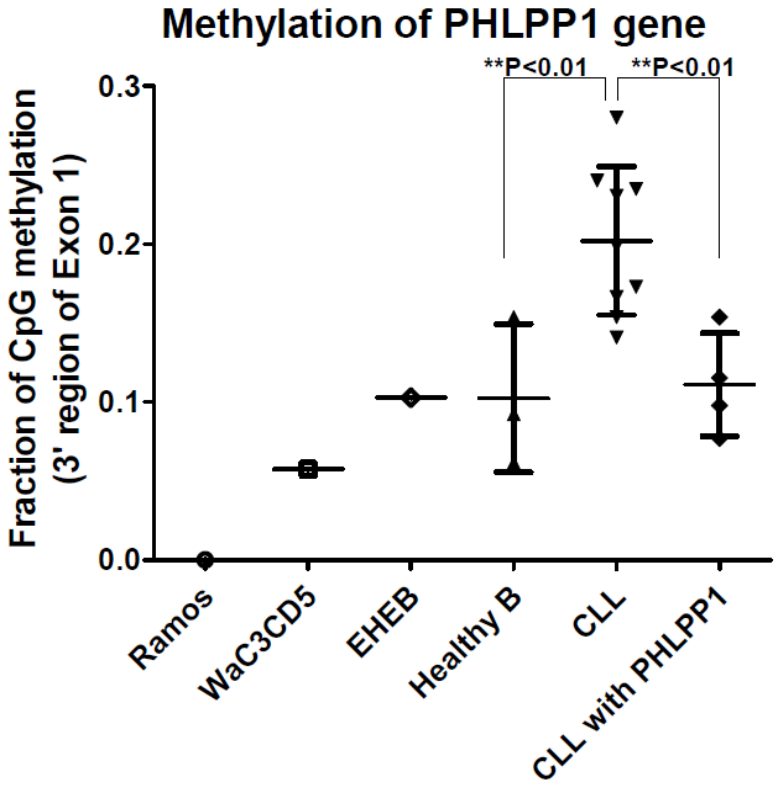

Figure 4.13 Comparison of CpG methylation detected in region of the *PHLPP1* gene near the end of exon 1. The average fraction of CpG sites methylated across the entire region of interest highlighted in 4.12 (quantified over the 5-10 colonies from each sample) is shown for Ramos cells, WaC3CD5 cells, EHEB cells, healthy B cells (n=3), CLL cells expressing PHLPP1 (n=4) and a set of CLL cells with low/no PHLPP1 expression (n=9). Each dot represents a separate patient/donor and the bar indicates the average +/- SD. A student's t-test was performed to determine statistical significance.

Therefore, there was a strong correlation between the loss of PHLPP1 transcription and a higher degree of *PHLPP1* methylation at the end of exon 1. Repression of gene transcription due to CpG methylation is usually a result of methylation across a region as opposed to specific loci [*26*]. Correspondingly, we found that while methylation of certain CpG sites at the beginning of the exon were fairly evenly represented among the different cells, the CLL cells lacking PHLPP1 expression had greater PHLPP1 methylation throughout the region, as shown by the relative distributions of methylation at individual CpG sites shown in Figure 4.14.

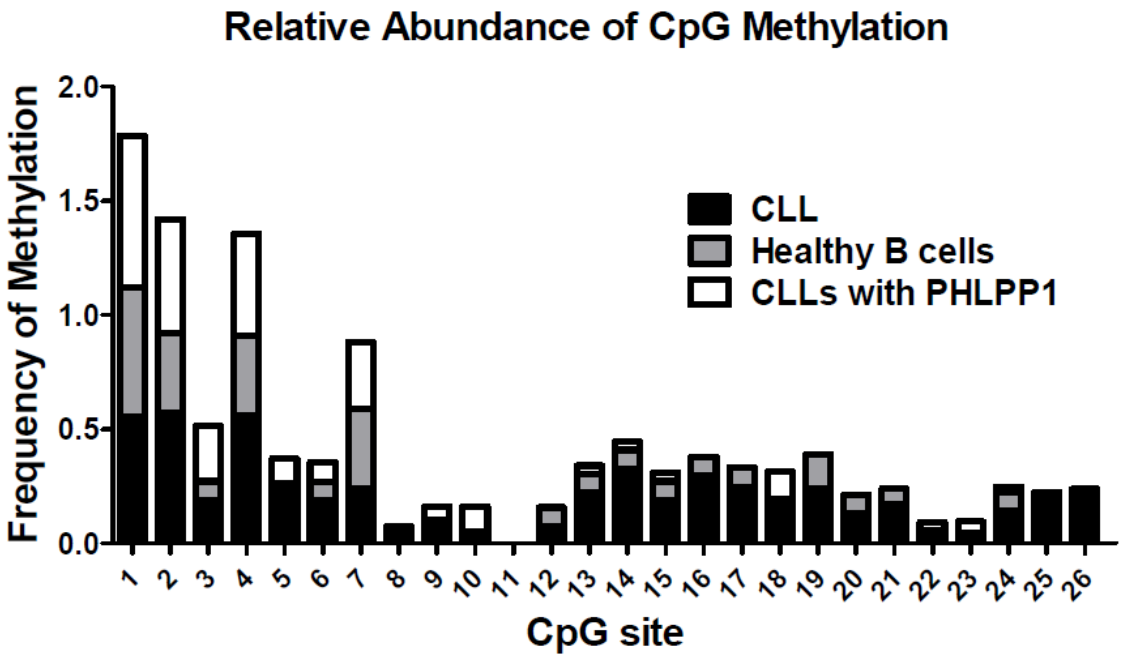

Figure 4.14 Relative abundance of methylation at individual CpG sites within the region of *PHLPP1* probed. Fraction of cells exhibiting methylation at each CpG site in the region highlighted in 4B is compared between CLL cells (black), healthy B cells (gray), and PHLPP1-expressing CLL cells (white). The data represents an average (between different patients/donors) of the frequency at which methylation is observed at the individual CpG sites.

Evident correlations between the degree of gene methylation and PHLPP1 transcription were observed; yet, to more directly assess the effects of methylation on PHLPP1 expression the DNA methyltransferase inhibitor, 5-aza-2'-deoxycytidine (5-aza DC), is generally employed. However, 5-aza DC only works on dividing cells and since the primary CLL cells are non-dividing, this was not a viable option. The 5-aza DC could be used on the cell lines, although the levels of PHLPP1 and methylation patterns in these lines do not directly correlate with the primary CLL cells. Despite these limitations, we examined the effects of 5-aza DC on PHLPP1 mRNA levels in the EHEB CLL cell line, which has reduced PHLPP1 levels compared to the WaC3CD5+ and Ramos cells. As shown in Figure 4.15, a small dose-dependent increase in PHLPP1 mRNA expression was observed in the EHEB cells, but only resulted in a 1.72 fold increase in PHLPP1 mRNA following a 25 μM treatment with 5-aza DC for 72 h. Although a longer treatment with 5-aza DC may be required to see significant increases in PHLPP1 mRNA expression, as shown for DAPK1 expression in the WaC3CD5+ CLL cell line in which increases in DAPK1 mRNA were observed following 6 days (but not at 3 days) of 5-aza DC treatment [*27*], the EHEB cells died upon prolonged exposure to 5-aza DC. Since Ramos cells exhibit no/very little methylation and higher PHLPP1 expression relative to the EHEB cells, the effects of 5-aza DC on Ramos cells were compared. However, even low concentrations of 5-aza DC significantly reduced the viability of the Ramos cells and resulted in a concurrent decrease in both the GAPDH and PHLPP1 mRNA and so could not be accurately compared (data not shown).

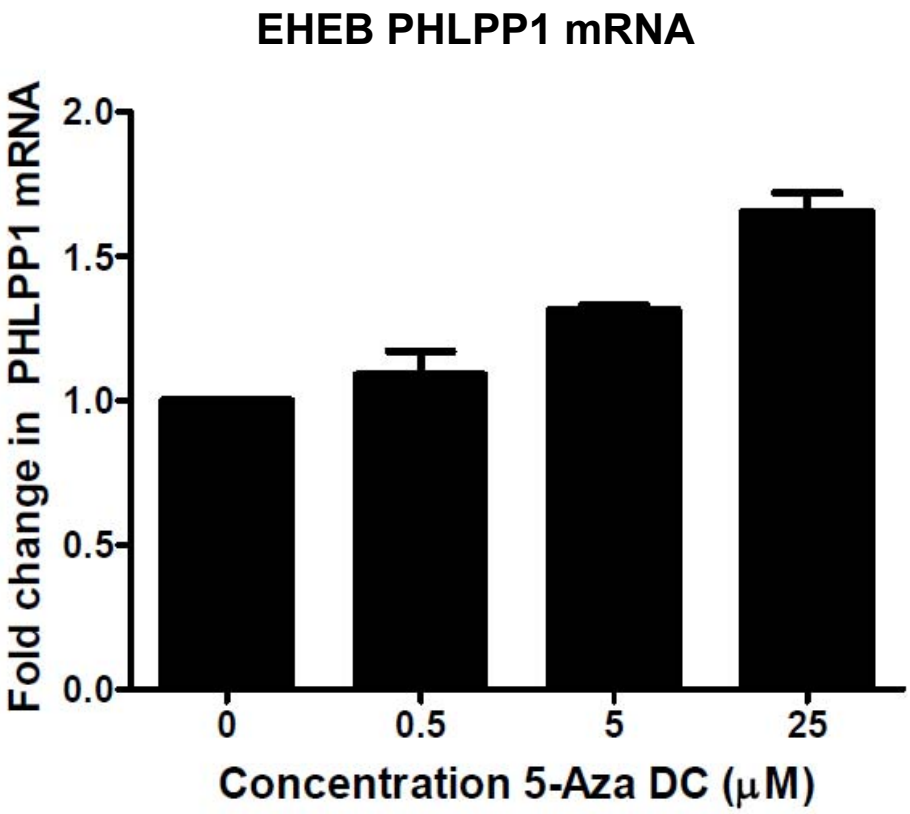

Figure 4.15 PHLPP1 mRNA levels in EHEB cells treated with 5-Aza DC. EHEB cells were treated with varying concentrations of 5-Aza DC from 0.5-25 μM or DMSO control (0) for 72 h and levels of mRNA were compared by quantitative RT-PCR. Results indicate fold changes in PHLPP1 mRNA levels after normalization to GAPDH.

As an alternative to 5-aza DC, valproate (VPA) has been shown to indirectly induce active replication-independent DNA demethylation [*28*]. Therefore, we tested varying concentrations of VPA from 0-20 mM for 72h on CLL cells from 2 different patients in order to examine whether demethylation would result in an increase in the PHLPP1 mRNA expression. Although the DMSO control treated CLL cells maintained ~90% viability over this 72 h time course based on trypan blue staining, the VPA treated cells were <10% viable and so we were unable to collect reliable data regarding the effects of DNA demethylation on PHLPP1 mRNA expression (Figure 4.16). Since the RNA and DNA yield and quality were low in the VPA treated cells, the experiment was

not repeated again because it did not yield information regarding the effects of DNA methylation of PHLPP1 expression. Nevertheless, the dramatic reduction in cell viability upon VPA treatment suggests the possibility that DNA methylation may be repressing a variety of growth and survival regulating genes in CLL cells; thus, demethylation and inhibition of histone deacetylation by VPA results in a dramatic increase in cell death.

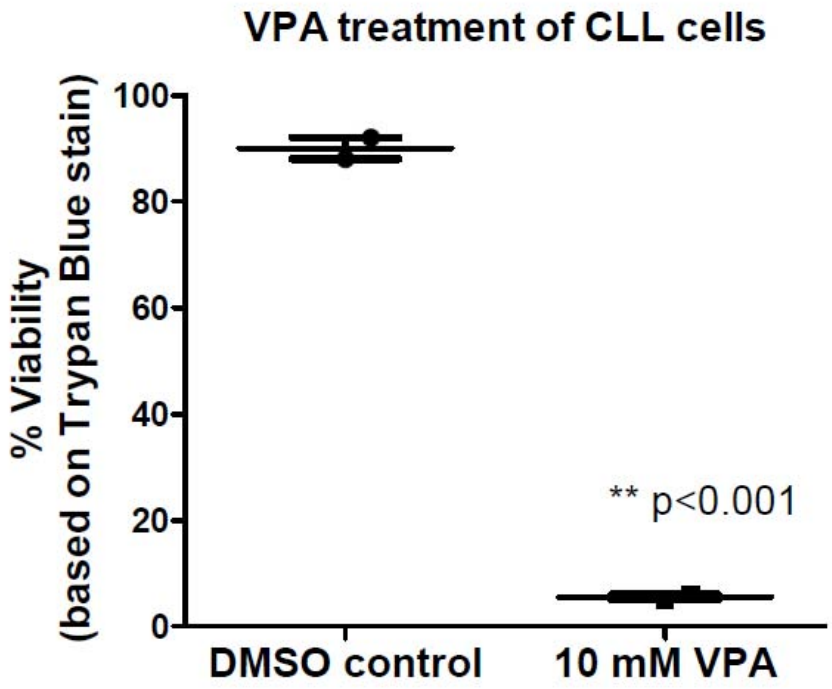

Figure 4.16 Viability of CLL cells following treatment with VPA. Purified CLL cells from 2 patients were treated with 10 mM (on right) and 20 mM (not shown) VPA or DMSO control (on left) and cultured for 72 h. Cell viability was measured based on cell count and trypan blue staining (% viability= non blue cells/total # of cells). Statistical significance was calculated based on a student's t-test.

4.3.6 PHLPP1 mRNA Stability Differs between CLL Cells, Healthy B Cells and B Cell Lines

Since differences in mRNA stability could also account for the loss of PHLPP1 transcript and protein levels in CLL cells, we assessed the decay of PHLPP1 mRNA relative to GAPDH mRNA following inhibition of transcription by Actinomycin D. We found that CLL cells expressing low, but detectable PHLPP1 mRNA, and CLL cells adenovirally expressing PHLPP1 had matching mRNA decay profiles in which a rapid reduction in PHLPP1 mRNA levels was observed within 2 h following Actinomycin D treatment. In contrast, B cells from healthy donors, CLL cells expressing PHLPP1 and the leukemia cell lines exhibited a much slower decay profile (Figure 4.17). The rapid decay of adenovirally expressed PHLPP1 in CLL cells supports our findings that genetic alterations of the *PHLPP1* gene are not likely responsible for the decrease in PHLPP1 expression in CLL; thus, it is possible that other factors such as miRNAs may lead to rapid transcript degradation. PHLPP1 mRNA decay was monitored out to 24 h following Actinomycin D treatment, but the levels stabilize after 4 h (and in some cases start to increase relative to GAPDH), so just these earlier time points are shown (Figure 4.17). These data suggest that a decrease in PHLPP1 mRNA stability may also contribute to the lower levels of PHLPP1 transcription and protein expression observed in the majority of CLL patient B cells. These experiments still need to be repeated in order to validate these results. Additionally, to confirm that these differences in mRNA stability are selectively towards PHLPP1, we will also monitor the mRNA stability of PHLPP2 as a comparison in these samples.

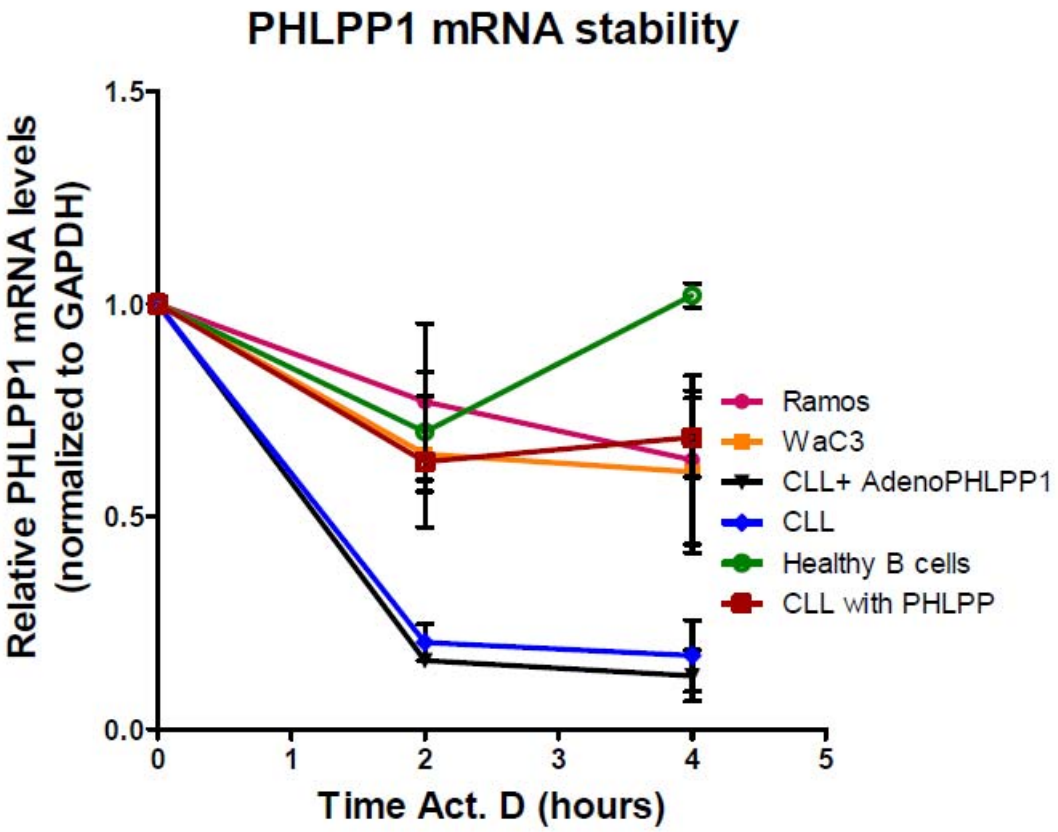

Figure 4.17 PHLPP1 transcript stability following Actinomycin D treatment in CLL cells compared to healthy B cells and B cell lines. Levels of PHLPP1 mRNA relative to GAPDH mRNA at 0 h, 2 h, 4 h , 6 h, and 8 h following 5 µg/mL Actinomycin D treatment were compared between Ramos (pink), WaC3CD5 (orange), healthy B cells (green), CLL cells expressing PHLPP1 (red), CLL cells transduced with adenoviral PHLPP1 (black) and CLL cells expressing low but detectable PHLPP1 mRNA (blue).

4.4 Discussion

CLL B cell accumulation depends on survival cues from the microenvironment, which activate key growth and survival pathways including Akt, ERK1/2 and PKC. Herein, we demonstrate the loss of protein and mRNA expression of an important negative regulator of these pathways, the PHLPP1 phosphatase. Reduction in PHLPP1 expression has previously been associated with an increased signaling response to various growth factors and enhanced survival and proliferation of a number of cancer

cells [*2, 5-9*]. Meanwhile, over-expression of PHLPP1 correlates with an increase in apoptosis [*2, 29*]. Overall, these observations suggest that the loss of PHLPP1 in CLL cells may increase responsiveness to growth and survival stimuli thereby promoting the accumulation of these cells. Accordingly, we demonstrated that adenoviral expression of PHLPP1 in primary CLL patients cells resulted in a decrease in the activation of Akt and ERK1/2 in response to CXCL12, a chemokine associated with CLL cell survival. Despite the strong differences in activation of survival signaling pathways upon adenoviral expression of PHLPP1, there was not a statistically significant difference in CLL survival response to CXCL12 in adenoviral PHLPP1 versus adenoviral GFP infected cells (data not shown). This may be due to the already poor viability of the CLL cells in culture following infection with adenovirus and/or limited correspondence between *in vitro* and *in vivo* conditions. Nevertheless, Suljagic *et al*. reported a statistically significant decrease in CLL survival in response to B cell receptor (BCR) activation following nucleofection of PHLPP1 into CLL cells [*15*]. Therefore, the observed loss of PHLPP1 expression conceivably contributes *in vivo* to the enhanced survival of CLL cells.

A number of mechanisms by which PHLPP1 is regulated have been previously described. At the protein level, PHLPP1 is stabilized by its substrate, Akt. This feedback regulation is mediated via GSK-3β and the E3 ligase β-TrCP and is preferentially lost in high-grade glioblastomas [*30-31*]. PHLPP1 protein levels are also controlled by the de-ubiquitinase UCH-L1 [*6*]. Additionally, the translation of both PHLPP1 and PHLPP2 is sensitive to rapamycin-induced inhibition of the mTORC1 complex [*32*]. Conversely, little has been reported about how PHLPP is regulated at the transcriptional level. One exception involves two studies revealing that PHLPP1 mRNA levels oscillate with the circadian cycle [*33-34*]. We demonstrate that the loss of PHLPP1 protein expression in CLL cells correlates well with a reduction in mRNA expression, suggesting that this loss

in expression is related to a decrease in mRNA stability/increase in mRNA degradation or a decrease in transcription, for example via epigenetic modulation. We also probed for genetic mutations that may account for differences in PHLPP1 stability, but did not identify any likely important somatic mutations. The success in generating PCR product and sequence for all samples renders bi-allelic deletion of PHLPP1 an unlikely source of the loss of expression. In addition, studies of chromosomal loss in CLL have not identified 18q21 (where PHLPP1 is found) as a region of frequent deletion [*35*].

However, our data suggest that DNA methylation and/or reduced mRNA stability (or increased mRNA degradation) may account for the reduced PHLPP1 protein and mRNA expression in CLL cells. To our knowledge, this work, along with unpublished data from Dr. Christiane Knobbe and Dr. Guido Reifenberger, provide the first indications that PHLPP1 expression may be regulated at the level of DNA methylation, although it is not surprising since the promoter and exon 1 contain extensive CpG island regions. An increase in methylation at the end of exon 1 of the *PHLPP1* gene correlated with reduced mRNA and protein expression. Although there did not appear to be significant levels of methylation in the CLL cells in the promoter region as most of the methylation was detected later in the first exon, a recent investigation of DNA methylation patterns in mammalian cells suggests that methylation of the first exon region is actually more tightly linked to transcriptional silencing than methylation of the promoter region [*36*]. Additionally, aberrant methylation of a number of genes in CLL cells has previously been described [*16, 27*], and a higher DNA methylation index has been linked to disease progression suggesting that a number of tumor suppressor genes may be repressed by DNA methylation in CLL cells [*37*]. While PHLPP1 was not identified in previous global profiling analyses for aberrant methylation patterns in CLL,

these profiling techniques rely on the use of restriction enzymes that do not cleave at most of the CpG sites in the regions we observed to be highly methylated.

Lastly, CLL cells with low but detectable PHLPP1 mRNA and adenovirally expressed PHLPP1 in CLL cells exhibited a more rapid decrease in transcript levels following Actinomycin D treatment compared to normal B cells and B cell lines. This suggests that there may be a more rapid degradation of PHLPP1 transcript in CLL cells, perhaps by miRNAs. Therefore, future investigations to identify potential miRNAs targeting PHLPP1 would be worthwhile.

Overall, our results confirm the absence of the PHLPP1 phosphatase in the majority of CLL patients' B cells. We demonstrate that reconstitution of PHLPP1 into CLL cells through adenoviral transduction dramatically reduces CXCL12-mediated activation of Akt and ERK1/2, suggesting that its absence in CLL cells may enhance their ability to respond to survival stimuli. Additionally, we show that the decrease in PHLPP1 protein expression correlated with a loss of PHLPP1 mRNA in CLL cells and to our knowledge, provide the first indications that DNA methylation and regulation of transcript stability may be important means of PHLPP1 regulation. Since decreased PHLPP1 mRNA levels have been described in a variety of other cancer types, gene methylation and/or regulation of transcript stability (e.g. via miRNAs) may be commonly used mechanisms to suppress PHLPP1 levels [*38-42*].

4.5 Materials and Methods

Cells and Reagents

Peripheral blood mononuclear cells (PBMCs) were acquired from consenting CLL patients at the Rebecca and John Moores Cancer Center at the University of California San Diego (UCSD) in compliance with the Declaration of Helsinki and the

institutional review board of UCSD. PBMCs were isolated from blood by Ficoll-Paque (GE Healthcare) density gradient centrifugation as previously described [14]. The isolated PBMCs were used fresh for adenoviral infections or frozen for later use as liquid nitrogen stocks in 90% heat inactivated fetal bovine serum (FBS)/10% DMSO. RPMI-1640 glutamax media and FBS were obtained from Gibco (Invitrogen, Carlsbad, CA) and DMSO was supplied by Sigma-Aldrich (St. Louis, MO). Ramos cells were acquired from ATCC. EHEB cells were a gift from Dr. Paul Insel at UCSD and WaC3CD5+ cells were generated by Dr. John Byrd at Ohio State University.

DNA and RNA Isolation

Prior to DNA and RNA isolation, CLL B cells were purified from PBMCs by negative selection using magnetic associated cell sorting (MACS) (Miltenyi Biotec, Auburn, CA) to remove CD14+ monocytes and CD2+ T cells cells, leading to >99% CLL cell purity. Normal B cells were purified from PBMCs from healthy donors (San Diego Blood Bank) using the MACS B cell Isolation Kit II according to the manufacturer's protocol and were determined to be >90% pure by flow analysis staining for CD19+/CD3-/CD14- cells. QIAshredders were used to lyse $1x10^7$ cells and DNA and RNA were isolated using the AllPrep DNA/RNA mini kit, according to manufacturer's protocol (Qiagen). RNA was treated for 30 min with RNAse-free DNase (Qiagen).

Quantitative PCR

One microgram of RNA was reverse transcribed using the High Capacity cDNA Reverse Transcription Kit (Applied Biosystems). The cDNAs generated were then analyzed in triplicates using SYBR-Green PCR mix (Applied Biosystems). All values were normalized to GAPDH expression. Primers used are as follows: GAPDH (Forward

5'-GAGAGACCCTCACTGCTG-3', Reverse 5'- GATGGTACATGACAAGGTGC-3') and PHLPP1 (Forward 5'-ACTGGGATTTGGGGAGCTG-3', Reverse 5'-CGTCTTGTCCATCGGTTCACT-3'). Quantitative PCR experiments were performed using the 7500-Fast Real-time PCR system from Applied Biosystems. Samples from each experiment were run in triplicate and relative mRNA concentrations were calculated by the $2^{-\Delta\Delta Ct}$ method, where Ct is the mean threshold cycle value and GAPDH was used to normalize.

Adenoviral Infection of CLL Cells

PHLPP1 adenovirus was prepared by Dr. Atsushi Miyanohara at the UCSD Viral Vector Core. Fresh CLL PBMCs were infected in 50 ul drops at $5x10^7$ cells/mL with an MOI of 300 pfu/cell and incubated for 2h at 37°C/5%CO_2. Following adenoviral infection, CLL cells were resuspended at $1x10^7$ cells/mL and cultured in plates containing a 3T3 fibroblast layer at ~70% confluence. After 72h following infection, GFP expression of the control adenoviral GFP CLL cells was confirmed by flow cytometry and the CLL cells were then collected for stimulations and western blot analysis.

CXCL12 Stimulations, Protein Lysates and Western Blots

Purified CLL B cells were lysed in ice cold RIPA buffer for profiling PHLPP1, PHLPP2 and PTEN levels. CLL cells infected with adenoviral-GFP or adenoviral-PHLPP1 for 72 h were cultured in serum-free RPMI at $1x10^7$ cells/ml for 5h at 37°C/5%CO_2 and then stimulated with 30 nM CXCL12 over an hour time course: unstimulated, 3, 10, 30 and 60 min. Cells were then collected and harvested on ice for 30 min in ice cold RIPA buffer. CXCL12 used for stimulations was expressed recombinantly in BL21 E. coli as previously described [*43*]. A BCA protein assay (Pierce)

was performed to determine total protein concentration of the lysates and 20 µg of total protein was loaded. PHLPP1 and PHLPP2 (PHLPPL) antibodies were obtained from Bethyl Laboratories, phospho-ERK1/2 and ERK1/2 antibodies were from Upstate, PKC antibodies were from Santa Cruz, and all other antibodies were acquired from Cell Signaling Technology and used according to manufacturer's recommendations. Secondary antibodies conjugated to HRP were obtained from Perkin Elmer or Thermo Fisher Scientific and blots were developed using an enhanced chemiluminescence (ECL) detection kit (GE Healthcare) or SuperSignal West Femto Maximum Sensitivity Substrate (Thermo Fisher Scientific), respectively. Blots were stripped with Restore western blot stripping solution (Thermo Fisher Scientific) for 10 min at room temperature and then re-probed. Densitometry analysis was performed using ImageJ (NIH) and normalized to β-actin loading controls.

Bisulfite DNA Conversion and Sequencing

Genomic DNA (500 ng) was bisulfite converted using the EZ DNA Methylation Kit (Zymo Research) according to the manufacturer's protocol. PCR amplification of bisulfite-converted DNA was carried out using Hot Start Taq (Qiagen) in 1x reaction buffer, 250 µM dNTP mix, 1 µM of each primer, 2.5 mM $MgCl_2$, and 5% DMSO. Primers for the region of interest in which the majority of methylation was detected are as follows: Forward 5'-GAGGGTTATTGATAGTT-3' and Reverse 5'-CAAAACAAATAACTTCCTTACC-3'. Primers used to probe the PHLPP1 promoter and other CpG regions in exon 1 are included in Appendix AI.22. The PCR reactions were performed under the following conditions: 95°C for 15 min, then 40 cycles of 95°C for 1 min, 58°C for 1 min, and 72°C for 1 min, followed by 72°C for 7min. PCR products were gel purified (Qiagen gel extraction kit) and cloned into a TOPO/TA vector (Invitrogen)

according to manufacturer's protocol. Five to ten colonies from each patient DNA sample were sequenced and the fraction of methylated CpGs was calculated across the entire region. As a positive control for bisulfite conversion, in vitro methylation of DNA using SSSI (NEB) was performed according to manufacturer's instructions. DNA sequencing was performed by the DNA Sequencing Shared Resource, UCSD Cancer Center, which is funded in part by NCI Cancer Center Support Grant # 2 P30 CA023100-23.

Analysis of PHLPP1 mRNA Stability and Inhibition of DNA Methylation

To assess PHLPP1 mRNA stability, cells were treated with 5 μg/mL of Actinomycin D (Calbiochem) and RNA was harvested at 0 h, 2 h, 4 h, 6 h, 8 h and 24 h following Actinomycin D treatment. Reverse transcription and quantitative PCR was carried out as described above in the "Quantitative PCR" methods section. PHLPP1 transcript levels were normalized to GAPDH levels at each time point so that transcript stability relative to GAPDH is compared between the different samples. To examine the effects of DNA methylation on PHLPP1 mRNA expression, EHEB and Ramos cell lines were left untreated or treated with 5-aza-2'-deoxycytidine (Sigma) (0 to 25 μM) for 72 h. RNA isolation, cDNA synthesis, and quantitative PCR were performed as described above.

DNA sequencing for mutations

The primers used to amplify the genomic regions of PHLPP1 were designed using designed using Primer 3, to cover the exonic regions plus at least 50 bp of intronic sequences on both sides of intron-exon junctions. The PCR reactions were carried out using the Hotstart Kapa Fast Taq kit per the manufacturer's protocol. DNA sequencing

was completed by the UCSD cancer center shared DNA sequencing resource (see above).

Statistical analysis

Results are presented as mean +/- standard deviation. Data were analyzed for statistical significance using a Student's t-test. P-values <0.05 were considered statistically significant.

ACKNOWLEDGEMENTS

This manuscript is being prepared for submission: Morgan O'Hayre, Matthew Niederst, Jessie-F Fecteau, Thomas J Kipps, Davorka Messmer, Alexandra C Newton, Tracy M Handel. Mechanisms and Consequences of the Loss of PHLPP1 Phosphatase in Chronic Lymphocytic Leukemia.

The dissertation author designed and performed most experiments and wrote the manuscript. Matthew Niederst and his undergraduate student, Victoria Nguyen, designed and performed DNA sequencing analysis of the *PHLPP1* gene in the CLL samples (Figure 4.9). Thomas J Kipps provided the CLL patient cells used in experiments and all other authors contributed ideas and reviewed the material presented in this chapter.

REFERENCES

1. Gao, T., Brognard, J., and Newton, A. C. (2008) The phosphatase PHLPP controls the cellular levels of protein kinase C, *J Biol Chem 283*, 6300-6311.

2. Gao, T., Furnari, F., and Newton, A. C. (2005) PHLPP: a phosphatase that directly dephosphorylates Akt, promotes apoptosis, and suppresses tumor growth, *Mol Cell 18*, 13-24.

3. Brognard, J., and Newton, A. C. (2008) PHLiPPing the switch on Akt and protein kinase C signaling, *Trends Endocrinol Metab 19*, 223-230.

4. Shimizu, K., Okada, M., Nagai, K., and Fukada, Y. (2003) Suprachiasmatic nucleus circadian oscillatory protein, a novel binding partner of K-Ras in the membrane rafts, negatively regulates MAPK pathway, *J Biol Chem 278*, 14920-14925.

5. Liu, J., Weiss, H. L., Rychahou, P., Jackson, L. N., Evers, B. M., and Gao, T. (2009) Loss of PHLPP expression in colon cancer: role in proliferation and tumorigenesis, *Oncogene 28*, 994-1004.

6. Hussain, S., Foreman, O., Perkins, S. L., Witzig, T. E., Miles, R. R., van Deursen, J., and Galardy, P. J. (2010) The de-ubiquitinase UCH-L1 is an oncogene that drives the development of lymphoma in vivo by deregulating PHLPP1 and Akt signaling, *Leukemia 24*, 1641-1655.

7. Hirano, I., Nakamura, S., Yokota, D., Ono, T., Shigeno, K., Fujisawa, S., Shinjo, K., and Ohnishi, K. (2009) Depletion of Pleckstrin homology domain leucine-rich repeat protein phosphatases 1 and 2 by Bcr-Abl promotes chronic myelogenous leukemia cell proliferation through continuous phosphorylation of Akt isoforms, *J Biol Chem 284*, 22155-22165.

8. Qiao, M., Iglehart, J. D., and Pardee, A. B. (2007) Metastatic potential of 21T human breast cancer cells depends on Akt/protein kinase B activation, *Cancer Res 67*, 5293-5299.

9. Brognard, J., Sierecki, E., Gao, T., and Newton, A. C. (2007) PHLPP and a second isoform, PHLPP2, differentially attenuate the amplitude of Akt signaling by regulating distinct Akt isoforms, *Mol Cell 25*, 917-931.

10. Zenz, T., Mertens, D., Kuppers, R., Dohner, H., and Stilgenbauer, S. (2010) From pathogenesis to treatment of chronic lymphocytic leukaemia, *Nat Rev Cancer 10*, 37-50.

11. Burger, J. A., Tsukada, N., Burger, M., Zvaifler, N. J., Dell'Aquila, M., and Kipps, T. J. (2000) Blood-derived nurse-like cells protect chronic lymphocytic leukemia B cells from spontaneous apoptosis through stromal cell-derived factor-1, *Blood 96*, 2655-2663.

12. Chiorazzi, N., Rai, K. R., and Ferrarini, M. (2005) Chronic lymphocytic leukemia, *N Engl J Med 352*, 804-815.

13. Messmer, D., Fecteau, J. F., O'Hayre, M., Bharati, I. S., Handel, T. M., and Kipps, T. J. (2011) Chronic lymphocytic leukemia cells receive RAF-dependent survival signals in response to CXCL12 that are sensitive to inhibition by sorafenib, *Blood 117*, 882-889.

14. Nishio, M., Endo, T., Tsukada, N., Ohata, J., Kitada, S., Reed, J. C., Zvaifler, N. J., and Kipps, T. J. (2005) Nurselike cells express BAFF and APRIL, which can promote survival of chronic lymphocytic leukemia cells via a paracrine pathway distinct from that of SDF-1alpha, *Blood 106*, 1012-1020.

15. Suljagic, M., Laurenti, L., Tarnani, M., Alam, M., Malek, S. N., and Efremov, D. G. (2010) Reduced expression of the tumor suppressor PHLPP1 enhances the antiapoptotic B-cell receptor signal in chronic lymphocytic leukemia B-cells, *Leukemia 24*, 2063-2071.

16. Rush, L. J., Raval, A., Funchain, P., Johnson, A. J., Smith, L., Lucas, D. M., Bembea, M., Liu, T. H., Heerema, N. A., Rassenti, L., Liyanarachchi, S., Davuluri, R., Byrd, J. C., and Plass, C. (2004) Epigenetic profiling in chronic lymphocytic leukemia reveals novel methylation targets, *Cancer Res 64*, 2424-2433.

17. McCabe, M. T., Brandes, J. C., and Vertino, P. M. (2009) Cancer DNA methylation: molecular mechanisms and clinical implications, *Clin Cancer Res 15*, 3927-3937.

18. Taberlay, P. C., and Jones, P. A. (2011) DNA methylation and cancer, *Prog Drug Res 67*, 1-23.

19. Keniry, M., and Parsons, R. (2008) The role of PTEN signaling perturbations in cancer and in targeted therapy, *Oncogene 27*, 5477-5485.

20. Leupin, N., Cenni, B., Novak, U., Hugli, B., Graber, H. U., Tobler, A., and Fey, M. F. (2003) Disparate expression of the PTEN gene: a novel finding in B-cell chronic lymphocytic leukaemia (B-CLL), *Br J Haematol 121*, 97-100.

21. Marengo, B., De Ciucis, C., Ricciarelli, R., Pronzato, M. A., Marinari, U. M., and Domenicotti, C. (2011) Protein Kinase C: An Attractive Target for Cancer Therapy, *Cancers 3*, 531-567.

22. Hanahan, D., and Weinberg, R. A. (2011) Hallmarks of cancer: the next generation, *Cell 144*, 646-674.

23. Stratton, M. R. (2011) Exploring the genomes of cancer cells: progress and promise, *Science 331*, 1553-1558.

24. Parsons, D. W., Jones, S., Zhang, X., Lin, J. C., Leary, R. J., Angenendt, P., Mankoo, P., Carter, H., Siu, I. M., Gallia, G. L., Olivi, A., McLendon, R., Rasheed, B. A., Keir, S., Nikolskaya, T., Nikolsky, Y., Busam, D. A., Tekleab, H., Diaz, L. A., Jr., Hartigan, J., Smith, D. R., Strausberg, R. L., Marie, S. K., Shinjo, S. M., Yan, H., Riggins, G. J., Bigner, D. D., Karchin, R., Papadopoulos, N., Parmigiani, G., Vogelstein, B., Velculescu, V. E., and Kinzler, K. W. (2008) An integrated genomic analysis of human glioblastoma multiforme, *Science 321*, 1807-1812.

25. (2008) Comprehensive genomic characterization defines human glioblastoma genes and core pathways, *Nature 455*, 1061-1068.

26. Wong, D. J., Foster, S. A., Galloway, D. A., and Reid, B. J. (1999) Progressive region-specific de novo methylation of the p16 CpG island in primary human mammary epithelial cell strains during escape from M(0) growth arrest, *Mol Cell Biol 19*, 5642-5651.

27. Raval, A., Tanner, S. M., Byrd, J. C., Angerman, E. B., Perko, J. D., Chen, S. S., Hackanson, B., Grever, M. R., Lucas, D. M., Matkovic, J. J., Lin, T. S., Kipps, T. J., Murray, F., Weisenburger, D., Sanger, W., Lynch, J., Watson, P., Jansen, M., Yoshinaga, Y., Rosenquist, R., de Jong, P. J., Coggill, P., Beck, S., Lynch, H., de la Chapelle, A., and Plass, C. (2007) Downregulation of death-associated protein kinase 1 (DAPK1) in chronic lymphocytic leukemia, *Cell 129*, 879-890.

28. Detich, N., Bovenzi, V., and Szyf, M. (2003) Valproate induces replication-independent active DNA demethylation, *J Biol Chem 278*, 27586-27592.

29. Qiao, M., Wang, Y., Xu, X., Lu, J., Dong, Y., Tao, W., Stein, J., Stein, G. S., Iglehart, J. D., Shi, Q., and Pardee, A. B. (2010) Mst1 is an interacting protein that mediates PHLPPs' induced apoptosis, *Mol Cell 38*, 512-523.

30. Li, X., Liu, J., and Gao, T. (2009) beta-TrCP-mediated ubiquitination and degradation of PHLPP1 are negatively regulated by Akt, *Mol Cell Biol 29*, 6192-6205.

31. Warfel, N. A., Niederst, M., Stevens, M. W., Brennan, P. M., Frame, M. C., and Newton, A. C. (2011) Mislocalization of the E3 ligase, beta-transducin repeat containing protein 1 ({beta}-TrCP1) in glioblastoma uncouples negative feedback between the PH domain Leucine-rich repeat Protein Phosphatase 1 (PHLPP1) and Akt, *J Biol Chem*.

32. Liu, J., Stevens, P. D., and Gao, T. (2011) mTOR-dependent regulation of PHLPP expression controls the rapamycin sensitivity in cancer cells, *J Biol Chem 286*, 6510-6520.

33. Masubuchi, S., Gao, T., O'Neill, A., Eckel-Mahan, K., Newton, A. C., and Sassone-Corsi, P. (2010) Protein phosphatase PHLPP1 controls the light-induced resetting of the circadian clock, *Proc Natl Acad Sci U S A 107*, 1642-1647.

34. Shimizu, K., Okada, M., Takano, A., and Nagai, K. (1999) SCOP, a novel gene product expressed in a circadian manner in rat suprachiasmatic nucleus, *FEBS Lett 458*, 363-369.

35. Gunn, S. R., Bolla, A. R., Barron, L. L., Gorre, M. E., Mohammed, M. S., Bahler, D. W., Mellink, C. H., van Oers, M. H., Keating, M. J., Ferrajoli, A., Coombes, K. R., Abruzzo, L. V., and Robetorye, R. S. (2009) Array CGH analysis of chronic lymphocytic leukemia reveals frequent cryptic monoallelic and biallelic deletions of chromosome 22q11 that include the PRAME gene, *Leuk Res 33*, 1276-1281.

36. Brenet, F., Moh, M., Funk, P., Feierstein, E., Viale, A. J., Socci, N. D., and Scandura, J. M. (2011) DNA methylation of the first exon is tightly linked to transcriptional silencing, *PLoS One 6*, e14524.

37. Yu, M. K., Bergonia, H., Szabo, A., and Phillips, J. D. (2007) Progressive disease in chronic lymphocytic leukemia is correlated with the DNA methylation index, *Leuk Res 31*, 773-777.

38. Hao, Y., Triadafilopoulos, G., Sahbaie, P., Young, H. S., Omary, M. B., and Lowe, A. W. (2006) Gene expression profiling reveals stromal genes expressed in common between Barrett's esophagus and adenocarcinoma, *Gastroenterology 131*, 925-933.

39. Bredel, M., Bredel, C., Juric, D., Harsh, G. R., Vogel, H., Recht, L. D., and Sikic, B. I. (2005) High-resolution genome-wide mapping of genetic alterations in human glial brain tumors, *Cancer Res 65*, 4088-4096.

40. Talantov, D., Mazumder, A., Yu, J. X., Briggs, T., Jiang, Y., Backus, J., Atkins, D., and Wang, Y. (2005) Novel genes associated with malignant melanoma but not benign melanocytic lesions, *Clin Cancer Res 11*, 7234-7242.

41. Karnoub, A. E., Dash, A. B., Vo, A. P., Sullivan, A., Brooks, M. W., Bell, G. W., Richardson, A. L., Polyak, K., Tubo, R., and Weinberg, R. A. (2007) Mesenchymal stem cells within tumour stroma promote breast cancer metastasis, *Nature 449*, 557-563.

42. Richardson, A. L., Wang, Z. C., De Nicolo, A., Lu, X., Brown, M., Miron, A., Liao, X., Iglehart, J. D., Livingston, D. M., and Ganesan, S. (2006) X chromosomal abnormalities in basal-like human breast cancer, *Cancer Cell 9*, 121-132.

43. O'Hayre, M., Salanga, C. L., Dorrestein, P. C., and Handel, T. M. (2009) Phosphoproteomic analysis of chemokine signaling networks, *Methods Enzymol 460*, 331-346.

CHAPTER 5

Phosphoproteomics Methodology: Phosphoproteomic Analysis of Chemokine Signaling Networks

This chapter is a reprint of the published chapter: O'Hayre M*, Salanga CL*, Dorrestein PC, Handel TM. Phosphoproteomic analysis of chemokine signaling networks. (2009) *Methods Enzymol* 460:331-46. **Authors contributed equally.*

CHAPTER SIXTEEN

Phosphoproteomic Analysis of Chemokine Signaling Networks

Morgan O'Hayre,*,[1] Catherina L. Salanga,*,[1] Pieter C. Dorrestein,* *and* Tracy M. Handel*

Contents

Abstract

Chemokines induce a number of intracellular signaling pathways by activating second messengers (e.g. calcium) and phosphorylation cascades in order to mediate a myriad of functions including cell migration, survival and proliferation. Although there is some degree of overlap in chemokine receptor–mediated pathway activation, different chemokines will often elicit distinct signaling events. Factors such as cell type, receptor expression levels, G protein availability, and disease state will also influence the signaling response from chemokine-induced receptor activation. Improvements in mass spectrometry, enrichment strategies, and database search programs for identifying phosphopeptides have made phosphoproteomics an accessible biological tool for studying chemokine-induced phosphorylation cascades. Although signaling pathways involved in chemokine-mediated migration have been fairly well characterized, less is known regarding other signaling cascades elicited by chemokines (e.g. to induce proliferation) or the potential for distinct pathway activation in a disease state such as cancer. CXCL12(SDF-1)/CXCR4 signaling

* Skaggs School of Pharmacy and Pharmaceutical Science, University of California, San Diego, La Jolla, California, USA
[1] Both authors contributed equally

Methods in Enzymology, Volume 460
ISSN 0076-6879, DOI: 10.1016/S0076-6879(09)05216-1

has been shown to play an important role in the survival of chronic lymphocytic leukemia (CLL) cells, and thus provides a good system for exploring chemokine signaling, particularly in the interest of survival pathway activation. In this chapter, we describe the use of immobilized metal affinity chromatography (IMAC) phosphopeptide enrichment followed by reversed-phase liquid chromatography and tandem mass spectrometry (LC-MS/MS) analysis for exploring CXCL12-mediated signaling in human CLL patient cells.

1. Introduction

As chemokines bind their respective chemokine receptors, they induce conformational changes in the receptors leading to activation of intracellular signaling molecules including G proteins and β-arrestins (Thelen, 2001). These intracellular signaling molecules activate a variety of downstream signaling pathways primarily through the initiation of phosphorylation cascades.

In eukaryotic organisms, phosphorylation, a key reversible post-translational modification, is critical for the rapid transduction of messages from extracellular stimuli to elicit a cellular response. Thus, it is not surprising that an estimated 2 to 3% of the human genome is directly involved in phosphorylation (kinases, which catalyze the addition of phosphate groups, and phosphatases, which catalyze their removal) (Hubbard and Cohen, 1993; Manning *et al.*, 2002), and an estimated 30 to 50% of proteins are proposed to exhibit phosphorylation at some point in time (Kalume *et al.*, 2003). Phosphorylation is known to alter the activity, stability, localization, and interaction properties of molecules, and has been linked to a number of cellular processes including cell growth, metabolism, differentiation, movement, and apoptosis (de Graauw *et al.*, 2006; Schreiber *et al.*, 2008). However, the study of protein phosphorylation has been limited due to a number of challenges, including low abundance of many phosphoproteins, the low stoichiometry of phosphorylation, the heterogeneity of phosphorylation sites on a given protein, and the transient/reversible nature of phosphorylation (Mann *et al.*, 2002).

Classically, immunoblot (Western blot) analysis using phosphorylation-specific antibodies to a target of interest has been the gold standard for probing phosphorylation cascades activated in response to extracellular stimuli. Immunohistochemistry, immunofluorescence, and flow cytometry are additional methods for probing these signaling events; however, all of these techniques target specific proteins and require highly specific phosphoantibodies. The high costs and limited availability of phosphoantibodies restrict the use of these techniques, which are generally used when there is prior knowledge or association with a particular signaling pathway.

These methods are not amenable to global examination of phosphorylation events or for the identification of new phosphorylation sites. Classic methods to identify new phosphorylation sites including Edman sequencing and ^{32}P mapping are generally tedious and not commonly performed (Mann *et al.*, 2002). These limitations in understanding global (as opposed to *a priori* knowledge and targeted) protein phosphorylation events and in identifying novel phosphorylation sites have been a strong driving force for the development and implementation of phosphoproteomics techniques.

Utilizing phosphoproteomics to investigate intracellular signaling provides an unbiased approach for globally investigating cellular response to stimuli. The ability to simultaneously examine many phosphoproteins within a single sample and discover novel phosphorylations has also made phosphoproteomics a very attractive alternative from traditional approaches. However, implementation of mass spectrometry (MS)–based phosphoproteomics has its own set of challenges including negative ion suppression effects, limited dynamic range of detection, and difficulties in confidently identifying phosphopeptides (Paradela and Albar, 2008; Schreiber *et al.*, 2008). Nevertheless, the development and improvement of phosphoprotein and phosphopeptide enrichment strategies to counteract dynamic range problems and database search algorithms incorporating post-translational modifications have made this technique more accessible and feasible for signaling studies (Paradela and Albar, 2008; Schreiber *et al.*, 2008).

Given the improvements in phosphoproteomics strategies, this technique can be employed to generate a wealth of information on cellular response to stimuli such as chemokines. Although there is some functional redundancy in the chemokine system given the approximate 50 chemokine ligands and 20 chemokine receptors (Allen *et al.*, 2007), many chemokine/receptor pairs will activate distinct pathways and responses (O'Hayre *et al.*, 2008). Furthermore, differences in cell type and factors such as G protein availability and expression of specific isoforms and/or levels of particular signaling molecules can have dramatic effects on the signaling pathways utilized and functional response to chemokine stimulation (Salanga *et al.*, 2008). It is also largely unknown how different disease states such as chronic inflammation or cancer may alter the response to chemokines, potentially through misregulation of known pathways, activation of alternative pathways, or targeting of different downstream effectors.

Here we present the use of MS-based phosphoproteomics method to investigate the signaling pathways induced by CXCL12 in chronic lymphocytic leukemia (CLL) cells. CLL is the most common form of adult leukemia in the Western world and is characterized by the accumulation of a monoclonal population of $CD5^+$ B cells in the blood, bone marrow, and secondary lymphoid tissues (Burger *et al.*, 2000). CLL cells are known to overexpress the chemokine receptor, CXCR4 (Mohle *et al.*, 1999), and its

ligand, CXCL12, is thought to be an important microenvironmental factor contributing to the survival of these cells (Burger *et al.*, 2000). Access to primary CLL cells (not immortalized or passaged cell lines) and the relevance of the CXCL12/CXCR4 axis to cancer pathogenesis (Burger and Kipps, 2006) make this an ideal system for studying phosphorylation signaling cascades induced by CXCL12. It is important to note that while the method described here is specific to CXCL12 stimulation of CLL cells, it can also be used as a starting point for alternative studies involving chemokine/receptor signaling networks as well as non–chemokine signaling networks. Within these methods, there are many possibilities for optimization, as well as additional manipulations that can be exploited to obtain the most comprehensive results possible.

2. Methods

2.1. Isolation of chronic lymphocytic leukemia cells

Primary CLL cells were obtained in collaboration with Dr. Thomas Kipps at the University of California, San Diego, Moores Cancer Center. Briefly, leukopheresis blood was collected from consenting CLL patients, in agreement with institutional guidelines. Peripheral blood mononuclear cells (PBMCs) were isolated by Ficoll-Paque (Amersham Biosciences, Piscataway, NJ) density gradient centrifugation. Any contaminating red blood cells were lysed at room temperature (RT) for 5 min with red blood cell lysis buffer (Roche Diagnostics, Indianapolis, IN). The PBMCs from the CLL patient used for this particular phosphoproteomics data were determined to contain more than 90% $CD19^+/CD5^+/CD3^-$ B cells as assessed by flow cytometry.

2.2. CXCL12 stimulation of CLL cells and lysate preparation

2.2.1. CXCL12 preparation

CXCL12 was insolubly expressed in inclusion bodies as a His tag fusion in *Escherichia coli*. The protein was purified over a Ni-NTA column and refolded with Hampton Fold-It Buffer #8 (Hampton Research, Aliso Viejo, CA). Following dialysis and protein concentration, the His tag was cleaved at RT overnight using enterokinase (NEB, Ipswich, MA) at a 1:100,000 molar ratio. CXCL12 was purified by HPLC, and MS was performed to verify protein identity and purity. Transwell migration assays (Corning, Corning, NY) using Jurkat cells (ATCC, Manassas, VA) were performed to validate the functionality of purified CXCL12.

2.2.2. Stimulation of CLL cells

To prepare cell lysates for phosphoproteomic analysis, 3×10^9 CLL PBMCs were washed with sterile PBS, and resuspended at 1×10^7 cells/ml in serum-free, RPMI-1640 media (Gibco, Rockville, MD). Sixty milliliters of CLL cell suspension were distributed into each of five 15 cm plates (Corning Inc, Corning, NY) and cultured for 2 h at 37 °C/5% CO_2 prior to stimulation with CXCL12. A CXCL12 stimulation time course was conducted such that one plate remained unstimulated and the other four were stimulated for 3 min, 10 min, 30 min, or 60 min, with 30 n*M* CXCL12, and all plates were harvested at the same time on ice. Cells were lysed on ice for 30 min with 3 ml ice cold cytoplasmic lysis buffer containing 10 m*M* HEPES, pH 7.9, 1.5 m*M* $MgCl_2$, 10 m*M* KCl, 0.5 m*M* dithiothreitol (DTT) (Sigma, St. Louis, MO), Complete protease inhibitor cocktail (Roche Diagnostics, Indianapolis, IN), and Halt phosphatase inhibitor cocktail (Pierce, Rockford, IL). Plates were scraped with cell scrapers (Sarstedt, Newton, NC) and the cell lysates were collected, sonicated on ice for 15 s pulse (3 s on, 2 s off), and then centrifuged at 20,000 rcf for 20 min at 4 °C. The supernatants were distributed into protein LoBind Eppendorf tubes (Eppendorf, Westbury, NY) and lysates and pellets were stored at −80 °C. Finally, the total protein concentration of the CLL lysates was determined using a BCA protein assay (Pierce, Rockford, IL). Two milligrams of CLL lysate from each time point were used for phosphoproteomic analysis.

2.3. IMAC phosphopeptide enrichment of CLL samples

The IMAC methods presented herein are based on the protocol described by Payne *et al.* (2008); however, adjustments to the protocol have been made for our system using CLL cells. Given that several phosphoproteomic platforms are available (Schmelzle and White, 2006), factors such as sample amount/availability, instrument access, time, and cost must be considered in determining the best approach for a particular study. The strategy (Fig. 16.1) employed for the current study was selected based on available resources as well as the primary goal to rapidly identify many potentially interesting downstream targets of CXCL12 stimulation in CLL cells. Several other techniques could be used in conjunction with, or alternatively to, the methods described below, and will be mentioned throughout.

2.3.1. Denaturation, reduction, and alkylation

To prepare lysates for tryptic digest and IMAC enrichment, CLL lysates were denatured with 1% sodium dodecyl sulfate (SDS) (Fisher Scientific, Pittsburgh, PA). Disulfides were then reduced by the addition of freshly prepared DTT (final concentration = 10.5 m*M*) and heated to 60 to 65 °C.

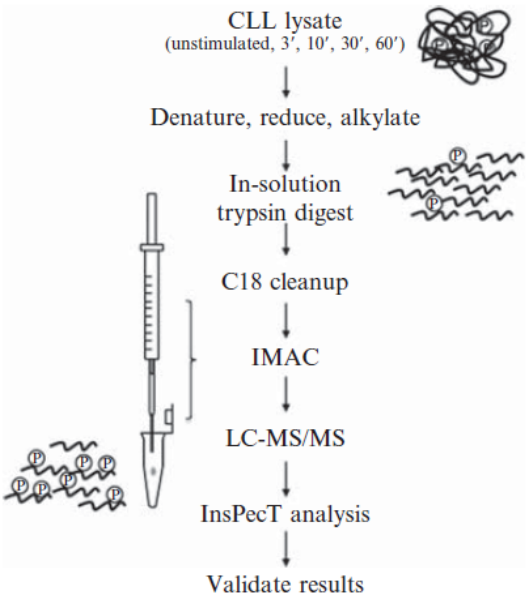

Figure 16.1 IMAC phosphoenrichment strategy. Brief outline of the MS-based methods using IMAC for phosphoenrichment of CXCL12-stimulated CLL cells. Following enrichment and LC-MS/MS analysis, phosphopeptides were identified by InsPecT and then manually validated.

After 20 min, lysates were cooled to RT for ~30 min. Because reduction is reversible, samples were alkylated with fresh iodoacetamide (Sigma, St. Louis, MO) to a final concentration of 100 m*M* and left to incubate at 25 °C for 30 min in the dark. Following SDS, DTT, and iodoacetamide treatment, protein was precipitated by addition of 3 to 4× the starting volume of 50% ethanol/50% acetone/0.1% acetic acid (HAC) in order to remove the detergent. To aid precipitation, samples were thoroughly mixed and stored at –80 °C for 10 min. The precipitation reactions were then centrifuged at 1500 rcf for 10 min. The supernatants were removed and the pellets were washed again with an equivalent volume of 50% ethanol/50% acetone/0.1% HAC plus 20% volume of H_2O. The washed pellets were centrifuged at 1500 rcf for 10 min, the supernatant was completely removed and the protein pellets were left to dry overnight.

2.3.2. Trypsin digest

Protein pellets were resuspended in 200 μl of 6 *M* urea/0.1 *M* Tris, pH 8.0, and vortexed (volume dependent on amount of starting material). Prior to trypsin digest, the urea concentration was diluted five-fold by addition of 50 m*M* Tris, pH 8.0. Protein was digested using sequencing- grade modified trypsin (Promega, Madison, WI) by resuspending trypsin in 50 m*M* Tris,

pH 8.0, and 1 m*M* $CaCl_2$ (final concentration) and adding to sample at a ratio of 1:50 (trypsin: protein). Digests were vortexed, parafilmed, and stored at 37 °C while shaking. Following an overnight incubation, trypsin was inactivated by acidification of the digests with trifluoroacetic acid to 0.3 to 0.5% (v/v) and stored at 4 °C (for long-term storage, freeze and store at −80 °C).

2.3.3. C18 cleanup

Peptide mixtures were desalted with 50 mg Sep-pak C18 cartridges (Waters Corp, Milford, MA). Prior to use, C18 cartridges (one per time point) were hydrated with methanol, and then rinsed with 80% acetonitrile (ACN) /1% HAC and equilibrated with 1% HAC. Peptides were loaded onto the columns, washed twice with 1% HAC, and eluted with 400 μl of 80% ACN/0.1% HAC. Fractions were collected in LoBind Eppendorf tubes, dried on a speed-vac at 50 °C for ~1 h, and stored at 4 °C. Pellets were resuspended in 100 μl of 1% HAC and centrifuged at 1500 rcf for 2 min. Supernatants were saved and used for subsequent IMAC enrichment steps.

2.3.4. IMAC bead preparation and enrichment

IMAC beads were prepared by removing the resin from 2 Ni-NTA spin columns (Qiagen, Valencia, CA) and replacing the Ni for Fe. Nickel resin was stripped by rotating with 50 m*M* EDTA, 1 *M* NaCl in 50 ml for 1 h, and then centrifuged in a swinging bucket rotor at 1500 rcf for 2 min. The supernatant was removed and the pellet was washed with 50 ml of Milli-Q H_2O followed by 50 ml of 0.6% HAC. The resin was then charged with 50 ml of 100 m*M* $FeCl_3$ (Fluka reagent, Sigma, St. Louis, MO) in 0.3% HAC for 1 h while rotating (Note: prior to $FeCl_3$ stock use, allow any impurities to settle from the solution for at least 1 month). Finally, supernatant was removed to make a 50:50 IMAC bead slurry (~600 μl). Individual IMAC columns were generated with the freshly prepared IMAC beads using gel-loading tips (Fisher Scientific, Pittsburgh, PA) affixed with a 1 cc syringe to control flow rate. Each column was plugged with a small amount of glass wool and pinched at the tip before adding 60 μl of IMAC bead slurry. Before each sample was loaded onto its own gel loading tip, the IMAC beads were conditioned with 25% ACN/0.1% HAC. Nonspecific peptides were removed by washing twice with 30 μl of 25% ACN/0.1% HAC/0.1 *M* NaCl, and then twice with 0.1% HAC, and finally twice with 30 μl of Milli-Q H_2O. Phosphopeptides were eluted with a total volume of 50 μl over three elutions with 1% phosphoric acid. All fractions were collected in protein LoBind Eppendorf tubes, speed-vac dried, and stored at −20 °C until MS analysis.

2.3.5. Additional phosphoenrichment strategies and considerations

In addition to Fe^{3+}, Ga^{3+} is another commonly used metal for IMAC (Paradela and Albar, 2008); ZrO_2 (Feng *et al.*, 2007) and TiO_2 (Klemm *et al.*, 2006; Larsen *et al.*, 2005) have also been widely used for phosphopeptide enrichment, typically in a tip or column format. To obtain optimal enrichment, each approach must be tested and optimized individually to determine its suitability for a given application. Each of these phosphoenrichment strategies has slightly different phosphopeptide selectivity based on their variable chemistry, which leads to identification of some nonoverlapping phosphopeptides (Bodenmiller *et al.*, 2007). Therefore, utilization of multiple phosphoenrichment strategies will yield complementary data (Paradela and Albar, 2008). Phosphoprotein enrichment, particularly for phosphotyrosine proteins, performed by immunoprecipitation with phosphotyrosine antibodies, in conjunction with phosphopeptide enrichment, has also been quite successful (Paradela and Albar, 2008). An important consideration and potential shortcoming to IMAC phosphoenrichment is the ability of IMAC resin to bind to highly acidic peptides (i.e. rich in Asp and/or Glu), which can "contaminate" a data set. However, methyl esterification is one option for reducing this phenomenon (Ficarro *et al.*, 2002). In our work, despite not doing methyl esterification, we were still able to obtain an average phosphoenrichment of ~30% for all data sets (Table 16.1). Preferential enrichment and strong binding of multiply phosphorylated peptides has also been considered a drawback to IMAC enrichment (Paradela and Albar, 2008). However, we mostly recovered peptides containing a single phosphate, consistent with observations that acidic elution conditions mostly yield monophosphorylated peptides (Thingholm *et al.*, 2008), and may also be related to retention of multiply phosphorylated

Table 16.1 Summary of phosphorylations identified in CXCL12-stimulated CLL cells

30 n*M* CXCL12 Time point	Unstimulated	3′	10′	30′	60′
Total peptides	550	734	770	754	737
Phosphopeptides	161	249	236	209	158
False positives[a]	8	9	11	13	11
False discovery rate (%)	1.5	1.2	1.4	1.7	1.5
Phosphoenrichment (%)	29.3	33.9	30.6	27.7	21.4
Phosphoproteins[b]	93	131	133	104	103

[a] Estimated by use of a decoy database approach.
[b] Number of phosphoproteins identified within a time point data set.
Notes: The total number of phosphorylation events and correlating false discovery rate and percent of phosphoenrichment are summarized for each time point data set of CXCL12-stimulated CLL cells.

peptides or the challenge of proteomics software to provide a confident identification of multiphosphorylated peptides. Therefore, additional strategies, such as SIMAC (sequential elution from IMAC) can be employed to isolate multiple phosphorylated peptides from monophosphorylated peptides in a complex sample (Thingholm *et al.*, 2008). Additionally, LC-MS/MS analysis of IMAC flow-through and wash fractions recovered few phosphopeptide identifications (1 phosphopeptide per 1000 peptides). The few phosphopeptides identified from the wash fractions were highly abundant in IMAC elution fractions, suggesting efficient enrichment.

2.4. Reversed-phase liquid chromatography and tandem mass spectrometry

Phosphoenriched CLL peptides were analyzed by reversed-phase, capillary liquid chromatography and tandem mass spectrometry (LC-MS/MS) on a Thermo Finnigan LTQ ion trap mass spectrometer. The capillary LC columns (~17 cm) were packed in-house using deactivated fused silica (100 μm) (Agilent, Santa Clara, CA) with C18 resin (5 μm, 300 Å) (Michrom Bioresources, Auburn, CA). Capillary columns were prepared by drawing a 360 μm O.D., 100 μm I.D. deactivated, fused silica tubing with a Model P-2000 laser puller (Sutter Instruments, Novato, CA) (heat: 330, 325, 320; vel: 45; del: 125) and were packed at ~600 psi to a length of ~10 cm with C18 reversed-phase resin suspended in methanol. While purchasing capillary columns has distinct advantages, such as improved column-to-column reproducibility, they are about 150 times more expensive than the columns prepared in our laboratory. To prepare samples for running on LC-MS/MS, dried eluate was resuspended in 50 μl of Milli-Q H_2O. The resuspension volume should be adjusted according to the amount of starting material and column capacity, as well as the sensitivity of the mass spectrometer used. Approximately 15 μl of the resuspension was added to a 96-well plate (Axygen, Union City, CA) of which 10 μl was loaded onto the capillary column for LC-MS/MS analysis. To minimize sample evaporation, the 96-well plate was covered with a sealing film (Axygen, Union City, CA). Angiotensin II (Sigma-Aldrich, St. Louis, MO) was used as a control for column performance and run after every two CLL sample runs. The standard method used for all samples was as follows: 95% A/5% B (buffer A = 0.1% HAC in HPLC-grade Milli-Q H_2O, buffer B = 0.1% HAC in HPLC-grade ACN) for 20 min, 60% A/40% B for 30 min, 20% A/80% B for 6 min, followed by a final washing step of 95% A/5% B for 30 min at 250 μl/min. The flow of solvent was split before it reached the column resulting in a flow rate of 200 to 500 nl/min through the capillary column. Samples were run in data-dependent mode, where the spectrometer performed one full MS scan followed by six MS/MS scans of the top six most intense ions in the parent spectrum with a m/z ranging from 400 to 2000.

A dynamic exclusion list was applied with a repeat count of 1, a repeat duration of 30 s, an exclusion size of 100, exclusion duration of 180 s, and an exclusion mass width of 1.50. The spray voltage was 1.8 kV. Because the instrument cannot fragment all the peptides in the parent spectrum, the sample can be run several times to saturate the proteomic space for a given method. At this time, the gold standard in proteomics is three runs for each sample, but one will miss some of the possible phosphopeptides that can be identified. Five runs on a given method and identical sample will nearly saturate all the possible candidate peptides and 10 would be better for a higher degree of confidence.

On average, the scan rate in this experiment ranged from four to eight scans per second. The higher the scan rate, the more peptides one will be able to identify for a given LC run, which is an important consideration when designing an experiment and/or purchasing a mass spectrometer for proteomics. While we have provided the parameters for a starting method for the phosphoproteomic analysis, changing the HPLC gradient, changing the data-dependent analysis of different top intensity ions (e.g. 7th to the 13th most intense ions in the parent spectrum) and dynamic exclusion parameters influences the type and amount of data collected. Once the data is collected, prior to InsPecT analysis, RAW data files were converted to mzXML data files using the program ReAdW (http://tools.proteomecenter.org/ReAdW.php).

2.4.1. Additional phosphopeptide separation techniques

Additional separation of phosphopeptides, which can be carried out prior to LC-MS/MS, include strong cation exchange (SCX) chromatography (Motoyama *et al.*, 2007) and hydrophilic interaction liquid chromatography (HILIC) (Albuquerque *et al.*, 2008). Both techniques produce an orthogonal method of separation to reversed-phase LC and have been shown to significantly increase the number of phosphopeptides identified. However, given the limited amount of starting material from the primary CLL cells (these are not a renewable source) and increased risk of sample loss associated with additional steps, these techniques were not utilized in the present study. Nevertheless, SCX and HILIC present an attractive means for enhanced phosphopeptide separation and detection.

2.4.2. Phosphopeptide identification with InsPecT

Data analysis was carried out with the open-access database search tool, InsPecT (http://proteomics.ucsd.edu/index.html), which allows for rapid identification of post-translationally modified peptides such as phosphopeptides (Tanner *et al.*, 2005). InsPecT is particularly useful for identification of post-translational modifications on peptides in a complex mixture. Its employment of tag-based filters reduces the overall number of peptides considered from the database early on, significantly reducing the processing

time compared to most other search algorithms available (Tanner *et al.*, 2005). Additionally, modifications to the InsPecT program have been made recently to specifically improve the recognition of phosphopeptides. A highly enriched and validated phosphopeptide data set was used to develop better recognition and scoring parameters for phosphopeptide spectra (Payne *et al.*, 2008). This is important because during collision-induced dissociation (CID) MS/MS, phosphoric acid is typically lost. The resulting spectral patterns of phosphopeptides are characterized by a strong neutral loss peak and weaker y- and b-ion fragments. Because of the decreased intensity of the various fragments, it becomes a difficult and time consuming task for search databases to correctly identify phosphopeptides. However, since the training set for improving the phosphopeptide identification and scoring was collected on an ion trap using CID to generate MS/MS data, the program is especially good at recognizing these phosphopeptide signatures. Gentler dissociation methods, like electron capture dissociation (ECD) and electron transfer dissociation (ETD) are alternative methods to CID, and generally retain the phosphate group on a phosphopeptide facilitating a more precise phosphate localization on a peptide (Paradela and Albar, 2008).

MS/MS spectra were processed using the UniProt human database, the UniProt shuffled human decoy database as well as common contaminants databases (e.g. keratin). Peptide sequencing searches were also defined for variable modification of up to two phosphorylation sites (Ser, Thr, or Tyr) on a peptide, and tryptic cleavage search restraints. Using the target decoy database as a measure of the overall quality of MS/MS data, spectra from each time point were sorted by *p*-values. Peptides with a false discovery rate (FDR) of less than 1 to 2% were manually validated for positive identification. Although there are some drawbacks associated with the use of decoy databases (Kall *et al.*, 2008; Kim *et al.*, 2008), they are generally an acceptable approach for approximating the confidence of reliable spectra assignments particularly for tryptic digests (Wang *et al.*, 2009).

Positive hits from each stimulation time point were combined into a comprehensive list and sorted by protein. Collectively, the five time points resulted in the identification of 1036 unique phosphopeptides and a total of 251 unique proteins (Table 16.1). Taking into consideration the limited amount of starting material used in this study, the overall number of phosphorylation events detected in our analysis is comparable to other phosphoproteomic studies involving complex biological samples (Moser and White, 2006). Phosphorylated protein targets of interest were further probed by alternative mechanisms. In some instances, phospho-specific antibodies were available for the phosphorylated protein of interest and could be probed by Western blot for validation. However, in most cases, no phosphoantibodies existed, and comparisons between time points had to be determined by other means. The CLL peptide samples were rerun three

times, and exclusion list restraints were varied in order to obtain more data for spectral counting comparison. Spectral counting is a straightforward, cost-saving, semi-quantitative approach to determining the differential levels of relatively abundant proteins in a dataset (Balgley *et al.*, 2008; Liu *et al.*, 2004a; Zhang *et al.*, 2006; Zybailov *et al.*, 2006). However, less abundant peptides are not ideal for this method because there is too much stochastic variation. Alternatively, a $^{16}O/^{18}O$ trypsin digest can be used. This semi-quantitative method involves postdigestion labeling of peptides by exchanging ^{16}O for ^{18}O in a trypsin-catalyzed reaction (Liu *et al.*, 2004b). The exchange of ^{16}O for ^{18}O is a specific process in which the C-termini of tryptic peptides are generally labeled with two ^{18}O atoms, resulting in a 4-Da shift between coeluting labeled and unlabeled peptides. Other chemical modification methods available for quantitative proteomics include isotope-coded affinity tags (ICAT), isobaric tags for quantification (iTRAQ), and phosphoramidate chemistry (PAC), and have been reviewed elsewhere (Ong and Mann, 2005; Schreiber *et al.*, 2008). Lastly, the development of stable isotope labeling with amino acids in cell culture (SILAC) has provided an effective and reproducible means of quantification between sample sets (e.g. unstimulated vs. stimulated) for proteomics studies (Olsen *et al.*, 2006). This technique involves the metabolic incorporation of isotopically labeled amino acids, generally ^{13}C or ^{15}N labeled Lys and/or Arg, and then comparison of the peak intensities of mixed unlabeled and labeled samples. However, several disadvantages of SILAC include the expense of growing cells in labeled media and the requirement for proliferating cells in culture preventing its use in primary tissue samples such as the CLL cells.

2.4.3. Considerations for selecting an appropriate search database program

An additional consideration in choosing the appropriate search database is cost. Currently, there are several available open source search databases, such as InsPecT, X!Tandem, and OMSSA (Geer *et al.*, 2004; Matthiesen and Jensen, 2008). InsPecT is particularly effective for the identification of phosphopeptides and runs in a fraction of the time compared to other search databases. However, use of a Windows browser interface is a distinct advantage to programs like X!Tandem, if the user is unfamiliar with command lines as in InsPecT, although a current version with a user-friendly Web interface is being developed at the UCSD center for computational mass spectrometry. InsPecT tutorials to aid in installation and data processing are available online. There are also commercially available search database programs including SEQUEST, Mascot, and Spectrum Mill. Comparisons using a number of search database programs have been previously carried out (Bakalarski *et al.*, 2007; Payne *et al.*, 2008).

In many instances, a combination of strategies that include various data analysis platforms is likely to yield the most comprehensive approach

to phosphoproteomics. In particular, the use of several database search engines for peptide identification is an excellent way to gather the most information from a data set, because often different database search engines will identify nonoverlapping peptides due to the inherent differences in detection and scoring strategies (Payne *et al.*, 2008). For example, Payne *et al.* demonstrated that the use of three different search algorithms—X! Tandem, SEQUEST, and InsPecT (filtered to a 1% false discovery rate)—collectively identified 1371 phosphopeptide spectra, of which 92, 116, and 203 spectra were nonoverlapping, respectively. The drawback to running a MS/MS data set against several databases is the run time. For example, in their studies, SEQUEST required 72 times longer to process the same data compared to InsPecT, a distinct advantage to using the InsPecT software package.

2.4.4. Additional proteomics data analysis tools

Following phosphopeptide identification, proteins can be classified through online bioinformatics tools such as Database for Annotation, Visualization, and Integrated Discovery (DAVID) (http://david.abcc.ncifcrf.gov/) and Cytoscape (http://cytoscape.org/). In addition, the phosphorylation site databases (e.g. Phosida, www.phosida.com, and Phosphobase, http://phospho.elm.eu.org/) have been developed as a repository for phosphopeptide identifications and corollary information. Together, these tools allow data to be more easily evaluated, categorized, and visualized in different formats, thus enabling a global and/or in-depth view of particular proteins identified in various biological pathways. For example, classification of our phosphopeptide results using DAVID revealed many candidates involved in cell death, survival, growth, proliferation, and cell cycle (Table 16.2).

3. Summary

Phosphorylation is a critical post-translational modification regulating protein activation as well as protein–protein interactions for a variety of biological responses. With the advances in MS-based phosphoproteomics, as well as the development of improved enrichment strategies for targeted or novel identification of phosphorylated peptides, phosphoproteomics has become an increasingly used application for dissecting signaling networks in a variety of biological tissues. In this chapter, we have described a general protocol for IMAC phosphopeptide enrichment followed by LC-MS/MS analysis for the study of CXCL12 stimulated primary CLL cells. This method is an excellent starting point for probing a particular phosphoproteome and generating hypothesis driven targets for further analysis.

Table 16.2 Functional annotation of phosphoproteomics data

Functional annotation (GO with DAVID)	Protein count	% of Proteins
G-protein modulator	25	10.4
Cell death	23	9.6
Regulation of gene expression	46	19.3
Leukocyte activation	8	3.4
Cell cycle	23	9.7
Cell growth	8	3.4
Cell proliferation	18	7.6
Lymphocyte proliferation	4	1.7
Cell motility	11	4.6
Immune system development	11	4.6
Cell development	28	11.8
B-cell activation	4	1.7
Leukocyte differentiation	8	3.3

Notes: A subset of interesting categories from DAVID gene ontology functional annotation of phosphoproteins identified in the CLL cells is displayed. The number and percent of phosphoproteins implicated in regulation of particular cellular processes are indicated.

Thus far, we have identified many novel downstream targets that are currently under investigation. However, depending on the circumstances (i.e. model system and resources available), some modifications and/or optimization to this method may be required and should be empirically determined. For the most comprehensive analysis of a phosphoproteome, either to identify novel or targeted phosphorylation events, a combination of various techniques, MS detection, and search algorithms is recommended (Schmelzle and White, 2006).

ACKNOWLEDGMENTS

We gratefully acknowledge the contributions of Dr. Thomas Kipps and Dr. Davorka Messmer for access to the primary CLL cells used in these studies; Dr. Huilin Zhou and Marie Reichart for guidance with the IMAC technique; Dr. Larry Gross and Dario Meluzzi for training on the preparation of capillary LC columns; Dario Meluzzi, David Gonzalez, and Wei-Ting Liu for assistance with LC-MS/MS and InsPecT analysis; Angel Lee for help with DAVID functional annotation; and Dr. Steve Bark for many useful discussions and critical reading of this work. This work was funded by a California Breast Cancer Research Program Dissertation Award (14GB-0147) to M.O.; a Ruth L. Kirschstein NIGMS MARC Predoctoral Fellowship (F31) to C.L.S.; awards from the National Institutes of Health (RO1-AI37113), Department of Defense (BC060331), and Lymphoma Research Foundation to T.M.H.; and The V-Foundation of Cancer Research scholar award to P.C.D.

REFERENCES

Albuquerque, C. P., Smolka, M. B., Payne, S. H., Bafna, V., Eng, J., and Zhou, H. (2008). A multidimensional chromatography technology for in-depth phosphoproteome analysis. *Mol. Cell. Proteomics* **7,** 1389–1396.

Allen, S. J., Crown, S. E., and Handel, T. M. (2007). Chemokine: Receptor structure, interactions, and antagonism. *Annu. Rev. Immunol.* **25,** 787–820.

Bakalarski, C. E., Haas, W., Dephoure, N. E., and Gygi, S. P. (2007). The effects of mass accuracy, data acquisition speed, and search algorithm choice on peptide identification rates in phosphoproteomics. *Anal. Bioanal. Chem.* **389,** 1409–1419.

Balgley, B. M., Wang, W., Song, T., Fang, X., Yang, L., and Lee, C. S. (2008). Evaluation of confidence and reproducibility in quantitative proteomics performed by a capillary isoelectric focusing-based proteomic platform coupled with a spectral counting approach. *Electrophoresis* **29,** 3047–3054.

Bodenmiller, B., Mueller, L. N., Mueller, M., Domon, B., and Aebersold, R. (2007). Reproducible isolation of distinct, overlapping segments of the phosphoproteome. *Nat. Methods* **4,** 231–237.

Burger, J. A., and Kipps, T. J. (2006). CXCR4: A key receptor in the crosstalk between tumor cells and their microenvironment. *Blood* **107,** 1761–1767.

Burger, J. A., Tsukada, N., Burger, M., Zvaifler, N. J., Dell'Aquila, M., and Kipps, T. J. (2000). Blood-derived nurse-like cells protect chronic lymphocytic leukemia B cells from spontaneous apoptosis through stromal cell-derived factor-1. *Blood* **96,** 2655–2663.

de Graauw, M., Hensbergen, P., and van de Water, B. (2006). Phospho-proteomic analysis of cellular signaling. *Electrophoresis* **27,** 2676–2686.

Feng, S., Ye, M., Zhou, H., Jiang, X., Zou, H., and Gong, B. (2007). Immobilized zirconium ion affinity chromatography for specific enrichment of phosphopeptides in phosphoproteome analysis. *Mol. Cell. Proteomics* **6,** 1656–1665.

Ficarro, S. B., McCleland, M. L., Stukenberg, P. T., Burke, D. J., Ross, M. M., Shabanowitz, J., Hunt, D. F., and White, F. M. (2002). Phosphoproteome analysis by mass spectrometry and its application to *Saccharomyces cerevisiae*. *Nat. Biotechnol.* **20,** 301–305.

Geer, L. Y., Markey, S. P., Kowalak, J. A., Wagner, L., Xu, M., Maynard, D. M., Yang, X., Shi, W., and Bryant, S. H. (2004). Open mass spectrometry search algorithm. *J. Proteome Res.* **3,** 958–964.

Hubbard, M. J., and Cohen, P. (1993). On target with a new mechanism for the regulation of protein phosphorylation. *Trends Biochem. Sci.* **18,** 172–177.

Kall, L., Storey, J. D., MacCoss, M. J., and Noble, W. S. (2008). Assigning significance to peptides identified by tandem mass spectrometry using decoy databases. *J. Proteome Res.* **7,** 29–34.

Kalume, D. E., Molina, H., and Pandey, A. (2003). Tackling the phosphoproteome: Tools and strategies. *Curr. Opin. Chem. Biol.* **7,** 64–69.

Kim, S., Gupta, N., and Pevzner, P. A. (2008). Spectral probabilities and generating functions of tandem mass spectra: A strike against decoy databases. *J. Proteome Res.* **7,** 3354–3363.

Klemm, C., Otto, S., Wolf, C., Haseloff, R. F., Beyermann, M., and Krause, E. (2006). Evaluation of the titanium dioxide approach for MS analysis of phosphopeptides. *J. Mass. Spectrom.* **41,** 1623–1632.

Larsen, M. R., Thingholm, T. E., Jensen, O. N., Roepstorff, P., and Jorgensen, T. J. (2005). Highly selective enrichment of phosphorylated peptides from peptide mixtures using titanium dioxide microcolumns. *Mol. Cell. Proteomics* **4,** 873–886.

Liu, H., Sadygov, R. G., and Yates, J. R. 3rd (2004). A model for random sampling and estimation of relative protein abundance in shotgun proteomics. *Anal. Chem.* **76,** 4193–4201.

Liu, T., Qian, W. J., Strittmatter, E. F., Camp, D. G. 2nd, Anderson, G. A., Thrall, B. D., and Smith, R. D. (2004). High-throughput comparative proteome analysis using a quantitative cysteinyl-peptide enrichment technology. *Anal. Chem.* **76,** 5345–5353.

Mann, M., Ong, S. E., Gronborg, M., Steen, H., Jensen, O. N., and Pandey, A. (2002). Analysis of protein phosphorylation using mass spectrometry: Deciphering the phosphoproteome. *Trends Biotechnol.* **20,** 261–268.

Manning, G., Plowman, G. D., Hunter, T., and Sudarsanam, S. (2002). Evolution of protein kinase signaling from yeast to man. *Trends Biochem. Sci.* **27,** 514–520.

Matthiesen, R., and Jensen, O. N. (2008). Analysis of mass spectrometry data in proteomics. *Methods Mol. Biol.* **453,** 105–122.

Mohle, R., Failenschmid, C., Bautz, F., and Kanz, L. (1999). Overexpression of the chemokine receptor CXCR4 in B. cell chronic lymphocytic leukemia is associated with increased functional response to stromal cell-derived factor-1 (SDF-1). *Leukemia* **13,** 1954–1959.

Moser, K., and White, F. M. (2006). Phosphoproteomic analysis of rat liver by high capacity IMAC and LC-MS/MS. *J. Proteome Res.* **5,** 98–104.

Motoyama, A., Xu, T., Ruse, C. I., Wohlschlegel, J. A., and Yates, J. R. 3rd (2007). Anion and cation mixed-bed ion exchange for enhanced multidimensional separations of peptides and phosphopeptides. *Anal. Chem.* **79,** 3623–3634.

O'Hayre, M., Salanga, C. L., Handel, T. M., and Allen, S. J. (2008). Chemokines and cancer: Migration, intracellular signalling and intercellular communication in the microenvironment. *Biochem. J.* **409,** 635–649.

Olsen, J. V., Blagoev, B., Gnad, F., Macek, B., Kumar, C., Mortensen, P., and Mann, M. (2006). Global, *in vivo*, and site-specific phosphorylation dynamics in signaling networks. *Cell* **127,** 635–648.

Ong, S. E., and Mann, M. (2005). Mass spectrometry-based proteomics turns quantitative. *Nat. Chem. Biol.* **1,** 252–262.

Paradela, A., and Albar, J. P. (2008). Advances in the analysis of protein phosphorylation. *J. Proteome Res.* **7,** 1809–1818.

Payne, S. H., Yau, M., Smolka, M. B., Tanner, S., Zhou, H., and Bafna, V. (2008). Phosphorylation-specific MS/MS scoring for rapid and accurate phosphoproteome analysis. *J. Proteome Res.* **7,** 3373–3381.

Salanga, C. L., O'Hayre, M., and Handel, T. (2008). Modulation of chemokine receptor activity through dimerization and crosstalk. *Cell. Mol. Life Sci.* [Epub ahead of print].

Schmelzle, K., and White, F. M. (2006). Phosphoproteomic approaches to elucidate cellular signaling networks. *Curr. Opin. Biotechnol.* **17,** 406–414.

Schreiber, T. B., Mausbacher, N., Breitkopf, S. B., Grundner-Culemann, K., and Daub, H. (2008). Quantitative phosphoproteomics--an emerging key technology in signal-transduction research. *Proteomics* **8,** 4416–4432.

Tanner, S., Shu, H., Frank, A., Wang, L. C., Zandi, E., Mumby, M., Pevzner, P. A., and Bafna, V. (2005). InsPecT: Identification of posttranslationally modified peptides from tandem mass spectra. *Anal. Chem.* **77,** 4626–4639.

Thelen, M. (2001). Dancing to the tune of chemokines. *Nat. Immunol.* **2,** 129–134.

Thingholm, T. E., Jensen, O. N., Robinson, P. J., and Larsen, M. R. (2008). SIMAC (sequential elution from IMAC), a phosphoproteomics strategy for the rapid separation of monophosphorylated from multiply phosphorylated peptides. *Mol. Cell. Proteomics* **7,** 661–671.

Wang, G., Wu, W. W., Zhang, Z., Masilamani, S., and Shen, R. F. (2009). Decoy methods for assessing false positives and false discovery rates in shotgun proteomics. *Anal. Chem.* **81,** 146–159.

Zhang, B., VerBerkmoes, N. C., Langston, M. A., Uberbacher, E., Hettich, R. L., and Samatova, N. F. (2006). Detecting differential and correlated protein expression in label-free shotgun proteomics. *J. Proteome Res.* **5,** 2909–2918.

Zybailov, B., Mosley, A. L., Sardiu, M. E., Coleman, M. K., Florens, L., and Washburn, M. P. (2006). Statistical analysis of membrane proteome expression changes in *Saccharomyces cerevisiae*. *J. Proteome Res.* **5,** 2339–2347.

ACKNOWLEDGEMENTS

Chapter 5 is a reprint of the chapter as it appears in Methods in Enzymology, 2009, Morgan O'Hayre, Catherina L Salanga, Pieter C Dorrestein, Tracy M Handel. Chapter 16: Phosphoproteomic analysis of chemokine signaling networks, 460:331-46.

The dissertation author and Catherina L Salanga equally contributed to this work, designing and performing experiments and writing the chapter. Pieter C Dorrestein and Tracy M Handel contributed to experimental design and edited the material.

CHAPTER 6

Elucidating the CXCL12/CXCR4 Signaling Network in Chronic Lymphocytic Leukemia through Phosphoproteomics Analysis

This chapter is a reprint of the published article: O'Hayre M, Salanga CL, Kipps TJ, Messmer D, Dorrestein PC, Handel TM. Elucidating the CXCL12/CXCR4 Signaling Network in Chronic Lymphocytic Leukemia through Phosphoproteomics Analysis. (2010) *PLoS One* 5(7): e11716.

OPEN ACCESS Freely available online

PLoS one

Elucidating the CXCL12/CXCR4 Signaling Network in Chronic Lymphocytic Leukemia through Phosphoproteomics Analysis

Morgan O'Hayre[1], Catherina L. Salanga[1], Thomas J. Kipps[2], Davorka Messmer[2], Pieter C. Dorrestein[1], Tracy M. Handel[1]*

1 Skaggs School of Pharmacy and Pharmaceutical Sciences, University of California San Diego, La Jolla, California, United States of America, **2** Rebecca and John Moores Cancer Center, University of California San Diego, La Jolla, California, United States of America

Abstract

Background: Chronic Lymphocytic Leukemia (CLL) pathogenesis has been linked to the prolonged survival and/or apoptotic resistance of leukemic B cells *in vivo*, and is thought to be due to enhanced survival signaling responses to environmental factors that protect CLL cells from spontaneous and chemotherapy-induced death. Although normally associated with cell migration, the chemokine, CXCL12, is one of the factors known to support the survival of CLL cells. Thus, the signaling pathways activated by CXCL12 and its receptor, CXCR4, were investigated as components of these pathways and may represent targets that if inhibited, could render resistant CLL cells more susceptible to chemotherapy.

Methodology/Principal Findings: To determine the downstream signaling targets that contribute to the survival effects of CXCL12 in CLL, we took a phosphoproteomics approach to identify and compare phosphopeptides in unstimulated and CXCL12-stimulated primary CLL cells. While some of the survival pathways activated by CXCL12 in CLL are known, including Akt and ERK1/2, this approach enabled the identification of additional signaling targets and novel phosphoproteins that could have implications in CLL disease and therapy. In addition to the phosphoproteomics results, we provide evidence from western blot validation that the tumor suppressor, programmed cell death factor 4 (PDCD4), is a previously unidentified phosphorylation target of CXCL12 signaling in all CLL cells probed. Additionally, heat shock protein 27 (HSP27), which mediates anti-apoptotic signaling and has previously been linked to chemotherapeutic resistance, was detected in a subset (~25%) of CLL patients cells examined.

Conclusions/Significance: Since PDCD4 and HSP27 have previously been associated with cancer and regulation of cell growth and apoptosis, these proteins may have novel implications in CLL cell survival and represent potential therapeutic targets. PDCD4 also represents a previously unknown signaling target of chemokine receptors; therefore, these observations increase our understanding of alternative pathways to migration that may be activated or inhibited by chemokines in the context of cancer cell survival.

Citation: O'Hayre M, Salanga CL, Kipps TJ, Messmer D, Dorrestein PC, et al. (2010) Elucidating the CXCL12/CXCR4 Signaling Network in Chronic Lymphocytic Leukemia through Phosphoproteomics Analysis. PLoS ONE 5(7): e11716. doi:10.1371/journal.pone.0011716

Editor: Syed A. Aziz, Health Canada, Canada

Received June 14, 2010; **Accepted** June 29, 2010; **Published** July 22, 2010

Funding: This work was funded by a California Breast Cancer Research Program Dissertation Award (14GB-0147) to MO (http://www.cbcrp.org), a Ruth L. Kirschstein NIGMS MARC Predoctoral Fellowship (F31) to CLS, and awards from the National Institutes of Health (RO1-AI37113), the Department of Defense (BC060331), and the Lymphoma Research Foundation (http://www.lymphoma.org) to TMH, TJK and DM and the V-Foundation Scholar Award (http://www.jimmyv.org) to PCD. These funders had no role in study design, data collection and analysis, decision to publish, or preparation of the manuscript.

Competing Interests: The authors have declared that no competing interests exist.

* E-mail: thandel@ucsd.edu

Introduction

B cell Chronic Lymphocytic Leukemia (CLL) is an adult leukemia characterized by the accumulation of B cells in the blood, bone marrow and secondary lymphoid tissues due to apparent survival advantages and/or apoptosis resistance of these cells *in vivo* [1]. There is significant heterogeneity in the disease progression between CLL patients. A more aggressive form of the disease, which results in lower patient survival time, correlates with markers including unmutated immunoglobulin heavy chain variable region (IgHV) status and high expression of the tyrosine kinase ZAP-70 (ZAP-70+). Although the accumulation of a monoclonal population of CD5+/CD19+ B cells is characteristic of both prognostic groups, aggressive CLL appears to have some distinct characteristics and signaling properties compared to indolent CLL [2].

Despite their enhanced survival *in vivo*, when CLL cells from patients are cultured *in vitro*, they rapidly undergo apoptosis under conditions that support the survival of normal B cells, underscoring the dependence of these cells on survival cues from the microenvironment [3,4]. In the microenvironment, marrow stromal cells are believed to secrete factors that promote CLL cell survival in patients; correspondingly, when monocytes isolated from peripheral blood of CLL patients are cultured, they differentiate into "Nurse-like cells" (NLCs) that promote CLL survival *in vitro* [3]. One of the factors known to be secreted by

these NLCs and to support CLL survival, is the chemokine, CXCL12 (SDF-1). Additionally, CXCR4, the receptor for CXCL12, is overexpressed on CLL cells compared to normal B cells, and thus has the potential for enhanced responsiveness to CXCL12 signaling [5]. Although another chemokine receptor, CXCR7, can also bind CXCL12 and was previously shown to be expressed on B cells [6], surface expression of CXCR7 was not observed on CLL B cells (Figure 1). Therefore the CXCL12 signaling effects are likely mediated exclusively by CXCR4 in these cells.

While chemokines and their G-protein coupled receptors are best known for their role in directing the migration of immune cells, it is clear that these proteins are involved in many other biological functions. The CXCL12/CXCR4 axis is critical for developmental processes including lymphopoiesis, and central nervous system and cardiac development, and knockout of either the ligand or receptor in mice results in embryonic lethality [7]. Due to the involvement of CXCL12/CXCR4 in migration, angiogenesis, and development, it is not surprising that this axis is often exploited by cancer cells for metastasis as well as survival and proliferation [8]. However, the specific molecular mechanisms by which these various functions are effectuated and how these signaling pathways target different downstream signaling molecules in cancer cells compared to non-malignant counterpart cells is largely unknown. Similarly, while it is known that Akt and ERK1/2 are activated by CXCL12 in CLL, the downstream targets of these pathways and activation of other pathways have not been elucidated [9].

Despite the upregulation of CXCR4 and strong Akt and ERK signaling demonstrated by CLL cells in response to CXCL12, the CLL cells actually migrate less efficiently to CXCL12 than B cells from healthy donors in a transwell migration assay (Figure 2). Thus, in CLL cells, it appears that signaling downstream of CXCL12/CXCR4 may be redirected towards survival signaling in lieu of cell migration. To better characterize the signaling responses to CXCL12 stimulation, primary CLL cells isolated from 5 patients were subjected to phosphoproteomic analysis by

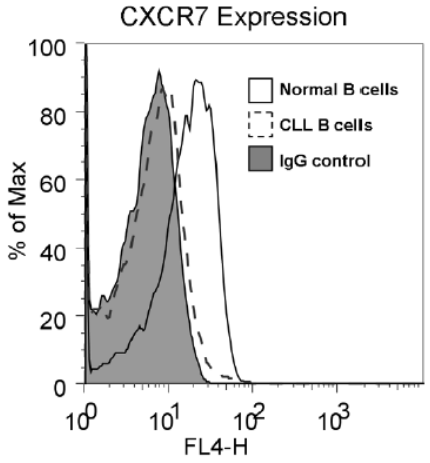

Figure 1. CXCR7 Expression on Normal B cells and CLL B Cells. Surface CXCR7 expression on Normal B cells (solid line) and CLL B cells (dashed line) was analyzed by flow cytometry and referenced to an IgG1 isotype control (filled histogram). Profiles are representative of B cells from 4 healthy donors (normal B cells) and 10 CLL patients' B cells.
doi:10.1371/journal.pone.0011716.g001

A

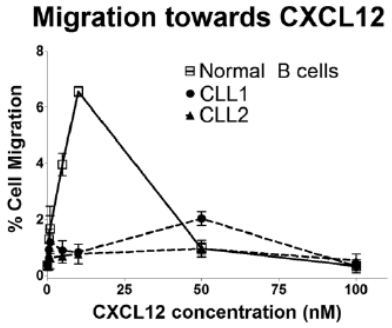

B

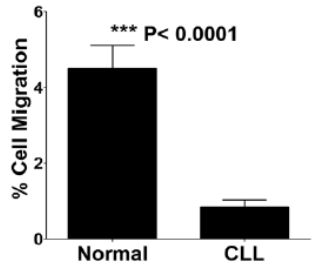

C

	B cell	CLL B cell
Max efficacy	4.5 +/- 1.2%	0.85 +/- 0.5%
Potency	10 nM	50 nM

Figure 2. CXCL12-mediated Migration of CLL B Cells and Normal B Cells. A) Representative migration assay profiles for normal B cells (solid line) compared to 2 different CLL patients' cells (dashed lines) performed in triplicate over a range of 0–100 nM CXCL12 and normalized to no chemokine. Data represents the percent of cells migrated through the transwell filter. B) Bar graph comparing the maximum percent cell migration observed in normal B cells and CLL B cells. Data represents an average of multiple transwell migration assays from separate donors, normal B cells $n=5$, CLL B cells $n=7$, each performed in triplicate. Differences were found to be statistically significant ($p<0.0001$) based on Student's t-test. C) Table depicting the maximum percent migration to CXCL12 (efficacy) and the concentration at which maximal migration is achieved (potency) observed in normal B cells compared to CLL B cells.
doi:10.1371/journal.pone.0011716.g002

liquid chromatography and tandem mass spectrometry (LC-MS/MS). Rather than attempting to characterize the complete phosphoproteome of CLL cells, this approach was designed to generate new hypotheses about the CXCL12/CXCR4 signaling network in CLL survival, and to identify downstream proteins that might be good therapeutic targets. While many phosphoproteins were identified in the CLL cells, comparison of spectral counts between CXCL12 stimulated and unstimulated cells allowed identification of proteins phosphorylated as a consequence of CXCL12/CXCR4 signaling. With follow-up experiments, the

tumor suppressor PDCD4 was validated as a downstream phosphorylation target of CXCL12 signaling in all CLL patient cells examined (n = 10) and HSP27 was similarly validated in a subset of CLL patients (~25%). Although these proteins have been previously linked to cancer cell survival, they have not been previously associated with CLL nor has PDCD4 been established as a downstream phosphorylation target of CXCL12 signaling. Furthermore, a number of other proteins (many of which do not have commercially available phospho-specific antibodies available) have been proposed as potential downstream phosphorylation targets of CXCL12 stimulation based on spectral count analysis of the CLL phosphoproteomics data.

Methods

Cells and reagents

Peripheral blood mononuclear cells (PBMCs) were obtained from leukopheresis samples of CLL patients following written consent at the Rebecca and John Moores Cancer Center at the University of California San Diego (UCSD), in compliance with the Declaration of Helsinki. These studies were approved by the Institutional Review Board of UCSD. PBMCs were isolated by Ficoll-Paque (GE Healthcare) density gradient centrifugation as previously described [9]. The isolated PBMCs were used fresh and cultured for phosphoproteomics analysis or frozen as liquid nitrogen stocks in 90% heat inactivated fetal bovine serum (FBS)/10% DMSO for follow-up analysis by western blot. PBMCs used in the proteomics experiments were determined to be >90% CLL B cells as assessed by CD5+/CD19+ staining and flow cytometry analysis. For western blot validation, CLL B cells were purified from the PBMCs by negative selection using the magnetic associated cell sorting (MACS) (Miltenyi Biotec, Auburn, CA) by depletion of CD14+ (monocytes) and CD2+ (T cells) cells, leading to >99% CLL B cell purity. Normal B cells were purified from PBMCs from healthy donors (San Diego Blood Bank) using the MACS B cell Isolation Kit II (Miltenyi Biotec, Auburn, CA) according to the manufacturer's protocol and were determined to be >90% pure by flow analysis staining for CD19+/CD3-/CD14- cells. RPMI-1640 glutamax media and FBS were obtained from Gibco (Invitrogen, Carlsbad, CA).

Recombinant CXCL12 preparation

CXCL12 was expressed recombinantly in BL21 *E. coli* as previously described [10]. In brief, CXCL12 was expressed as a His-tag fusion protein and purified from inclusion bodies. Bacterial cell pellets were sonicated and washed with deoxycholate following resuspension in 10 mM Tris pH 8.0 with 1 mM $MgCl_2$, 200 µg DNAse, and Complete Protease Inhibitor Cocktail (EDTA-free) (Roche, Indianapolis, IN). Protein was then solubilized in 6 M Guanadine-HCl, 100 mM sodium phosphate, 10 mM Tris-Cl, pH 8.0, using a dounce homogenizer. CXCL12 was purified over a Ni-NTA column and refolded with Hampton Fold-It Buffer #8 (Hampton Research, Aliso Viejo, CA), then dialyzed and concentrated using Amicon Ultra centrifugal concentrators (MWCO = 5000). The His-tag was removed by cleaving with enterokinase (NEB, Ipswich, MA) at a 1:100,000 molar ratio overnight at room temperature. CXCL12 was then purified by HPLC and the identity and purity was validated by ESI mass spectrometry. Transwell migration assays on Jurkat cells were used to validate functionality of the purified CXCL12.

Migration assays

Transwell migration assays (Corning, Corning, NY) were performed on purified CLL B cells and B cells from healthy donors using inserts with a 6.5 mm diameter, 5.0 µm pore size. Cells were resuspended at 2.5×10^6 cells/mL in RPMI+10%FBS and 100 µL of cell suspension was added to the inserts. CXCL12 was diluted over a concentration range of 0 nM to 500 nM in a 600 µL total volume of RPMI+10%FBS in the bottom wells. As a positive control and cell count reference, cells were added directly to the wells without inserts. Transwell migration was conducted for 2 h at 37°C/5%CO_2. Cells that had migrated into the bottom wells were then collected and counted by flow cytometry on a FACSCalibur (BD Biosciences, San Jose, CA). Data was normalized to no chemokine control and percent migration was calculated from the positive reference control.

Preparation of CLL lysates for proteomics

CLL cell lysates for phosphoproteomic analysis were prepared as previously described [10]. Briefly, 3×10^9 total CLL PBMCs were washed with sterile PBS and resuspended at 1×10^7 cells/mL in serum-free RPMI-1640 media. The CLL cell suspension was distributed evenly into five 15 cm plates (6×10^8 cells/plate) (Corning Inc, Corning, NY) and cultured for 2 h at 37°C/5% CO_2 prior to stimulation with CXCL12. CLL cells were then either unstimulated or stimulated for 3 min, 10 min, 30 min, or 60 min with 30 nM CXCL12. All plates were harvested at the same time with 3 mL ice cold cytoplasmic lysis buffer containing 10 mM HEPES, pH 7.9, 1.5 mM $MgCl_2$, 10 mM KCl, 0.5 mM dithiothreitol (DTT) (Sigma, St. Louis, MO), Complete Protease Inhibitor Cocktail (Roche Diagnostics, Indianapolis, IN), and Halt Phosphatase Inhibitor Cocktail (Pierce, Rockford, IL) for 30 min on ice. Lysates were clarified by centrifugation at 20,000 rcf for 20 min at 4°C. The supernatants were distributed into protein LoBind Eppendorf tubes (Eppendorf, Westbury, NY) and stored at −80°C. The total protein concentration of the CLL lysates was determined using a BCA protein assay (Pierce, Rockford, IL).

IMAC phosphopeptide enrichment

IMAC enrichment was performed as previously described [10]. Briefly, 2 mg of CLL lysates were denatured with 1% sodium dodecyl sulfate (SDS) (Fisher Scientific, Pittsburgh, PA), reduced with 10 mM DTT, and alkylated with iodoacetamide (Sigma, St. Louis, MO). Proteins were then precipitated with 50% ethanol/ 50% acetone/0.1% acetic acid (HAC). The pellets were resuspended in 6 M urea/0.1 M Tris, pH 8.0, and vortexed to solubilize the protein. The urea concentration was then diluted five-fold by addition of 50 mM Tris, pH 8.0 and protein was digested overnight at 37°C using sequencing-grade modified trypsin (Promega, Madison, WI) at a ratio of 1:50 (trypsin:protein). Trypsin was inactivated by acidification of the digests with trifluoroacetic acid to 0.3 to 0.5% (v/v). Prior to IMAC enrichment, peptide mixtures were desalted with 50 mg Sep-pak C18 cartridges (Waters Corp, Milford, MA). IMAC beads were prepared by stripping Ni-NTA spin column resin (Qiagen, Valencia, CA) and recharging the beads with 100 mM $FeCl_3$ (Fluka reagent, Sigma, St. Louis, MO). IMAC beads were then packed into gel loading tips with glass wool and conditioned with 25% Acetonitrile (ACN)/0.1% HAC. Nonspecific peptides were removed by washing twice with 30 µL of 25% ACN/0.1% HAC/ 0.1 M NaCl, twice with 0.1% HAC, and twice with 30 µL of Milli-Q H_2O. Phosphopeptides were eluted with a total volume of 50 µL over three elutions with 1% phosphoric acid. All fractions were collected in protein LoBind Eppendorf tubes, speed-vac dried, and stored at −20°C until MS analysis. Analysis of IMAC washes and flow through by LC-MS/MS confirmed successful binding of phosphopeptides to the IMAC columns as less than 0.1% of these peptides were found to be phosphorylated, and the

few that were detected were redundant with phosphopeptides identified in the IMAC enriched samples.

Mass spectrometry and data processing

IMAC-enriched CLL peptides were resuspended in Milli-Q H_2O +0.1%HAC and analyzed by reversed-phase, C18 capillary liquid chromatography and tandem mass spectrometry (LC-MS/MS) on a Thermo-Finnigan LTQ ion trap mass spectrometer. The capillary LC columns (~17 cm) were pulled and packed in-house using deactivated fused silica (100 µm) (Agilent, Santa Clara, CA) as previously described [10]. Angiotensin II (Sigma-Aldrich, St. Louis, MO) was run after every two CLL sample runs as a control for column performance. The standard method used for all samples was as follows: 95% A/5% B (buffer A = 0.1% HAC in HPLC-grade Milli-Q H_2O, buffer B = 0.1% HAC in HPLC-grade ACN) for 20 min, 60% A/40% B for 30 min, 20% A/80% B for 6 min, followed by a final washing step of 95% A/5% B for 30 min at 250 µl/min. A flow rate of 200 to 500 nL/min through the capillary column was achieved by splitting the flow of solvent before it reached the column. Samples were run in data-dependent mode in which the spectrometer performed one full MS scan followed by six MS/MS scans of the top six most intense ions in the parent spectrum with an m/z ranging from 400 to 2000. The dynamic exclusion list was varied in order to get a range of coverage and spectral counts. The standard dynamic exclusion list applied had a repeat count of 1, a repeat duration of 30 s, an exclusion size of 100, an exclusion duration of 180 s, and an exclusion mass width of 1.50. Other variations included a list of the top 25 peptides with a repeat duration of 60 s, an exclusion of the top 5 most abundant peptides, and a dynamic exclusion list turned off. The spray voltage was 1.8 kV. On average, the scan rate in this experiment ranged from four to eight scans per second.

A comprehensive phosphoproteomics data set from cells of one particular patient (CLL A) with unmutated IgHV and ZAP-70+ status (indicative of more aggressive disease) was collected from two separate triplicate runs and one duplicate run in order to obtain good coverage and number of spectra for comparison. Phosphoproteomics analyses of 4 additional CLL patients' cells (CLL B – E) (each run in single triplicate experiments) were also performed to ensure reproducibility between different patient cells and stimulations. CLL B, D and E also had more aggressive (high ZAP-70) characteristics (high ZAP-70) while CLL C was of the indolent (low ZAP-70) subgroup. Following data collection, RAW data files were converted to mzXML data files using the program ReAdW (http://tools.proteomecenter.org/ReAdW.php). Data analysis of the MS/MS spectra was performed using the open-access database search tool, InsPecT [11,12], with the UniProt human database, the UniProt shuffled human decoy database as well as common contaminants databases (e.g. keratin). Peptide sequencing searches were defined for tryptic cleavage restraints and to allow for modification of up to two phosphorylation sites (Ser, Thr, or Tyr) on a peptide. Spectra were sorted by p-values according to the InsPecT scoring function and the target decoy database was used as a measure of the overall quality of MS/MS data. Peptides smaller than 7 amino acids and peptides with more than one missed cleavage were excluded from analysis. Peptides with a false discovery rate (FDR) of less than 1–2% were manually validated for positive identification.

Western blots and antibody reagents

For western blot analysis, patient CLL cells used for phosphoproteomics as well as additional patient's cells were used. Purified CLL B cells were cultured in serum-free RPMI at 1×10^7 cells/mL for 2 h at 37°C/5%CO_2 and then stimulated with 30 nM CXCL12 over an hour time course (unstimulated, 3, 10, 30 and 60 min) or for 4 h, 10 h, and 24 h for PDCD4 degradation analysis. For inhibitor studies, CLL cells were pre-treated with 40 µM AMD3100 (Sigma) or 200 ng/ml Pertussis toxin (List Biological Laboratories) for 1 h prior to stimulation with CXCL12. Coculture of CLL cells with NLCs was performed as previously described [3,9] and then the CLL cells were collected and centrifuged for harvest. Cells were lysed on ice for 30 min in Ripa buffer (10 mM Tris pH 7.4, 150 mM NaCl, 1% Triton X, 0.1% Na-Deoxycholate, 0.1%SDS and 5 mM EDTA) containing Complete Protease Inhibitor Cocktail (Roche, Palo Alto, CA) and Halt Phosphatase Inhibitors (Pierce). Lysates were clarified by centrifugation at 20,000 rcf for 10 min at 4°C. A BCA protein assay (Pierce) was performed to determine total protein concentration and 20 µg of total protein was loaded into each well of a Criterion 4–12% Bis-Tris gel and run with the XT MES buffer system (Bio-Rad, Hercules, CA). Gels were transferred onto PVDF membranes (Bio-Rad), blocked with 5% milk-TBST, and incubated overnight at 4°C with primary antibodies. Blots were washed 3 times for 10 min with Tris Buffered Saline +0.1% Tween (TBST) and then incubated for 1 h at room temperature with secondary antibodies conjugated to HRP, washed again 3 times with TBST and then developed with

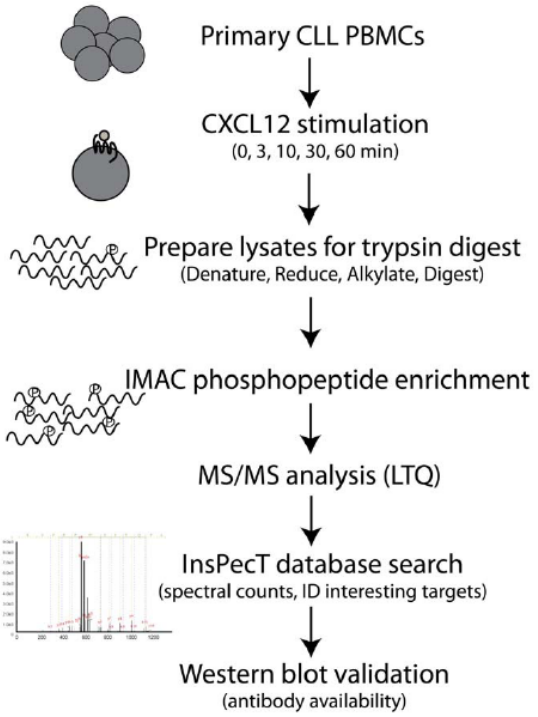

Figure 3. Flow Chart of CLL Phosphoproteomics Analysis. Lysates were prepared from primary CLL B cells that had been stimulated over an hour time course with 30 nM CXCL12. Lysates were denatured, reduced and alkylated in preparation for trypsin digest. Tryptic peptides were then enriched for phosphopeptides by IMAC and LC-MS/MS was performed. Data was analyzed using the InsPecT database search algorithm for phosphorylations on Ser, Thr, or Tyr. A decoy database and manual validation of the spectra were used as quality control. Spectral count comparisons were made as a qualitative assessment of CXCL12 stimulation response and interesting target proteins were selected for follow-up studies if antibodies were available.
doi:10.1371/journal.pone.0011716.g003

Amersham ECL-plus (GE-healthcare) or SuperSignal West femto-sensitivity reagent (Pierce). Blots were stripped with Restore western blot stripping solution (Pierce) for 10 min at room temperature and then re-probed with other antibodies and/or β-actin as a loading control. Primary antibodies were diluted into 5% BSA-TBST at recommended concentrations. Phospho-PDCD4 and PDCD4 antibodies were obtained from Rockland Immunochemicals. Phospho-p38, phospho-HSP27, HSP27, phospho-S6K, and β-actin were obtained from Cell Signaling Technology. Densitometry analysis was performed using ImageJ software (NIH) and normalized to β-actin loading controls.

Flow cytometry

CLL B cells or normal B cells were purified for flow cytometry analysis. Cells were washed and resuspended in a 0.5% bovine serum albumin (BSA) (Sigma) in Phosphate Buffered Saline (PBS) solution and stained for CXCR7 expression using an APC-conjugated antibody (clone 11G8) (R&D systems) or an APC-conjugated IgG1 isotype control according to manufacturer's protocol (R&D systems). Flow cytometry data was collected on a FACSCalibur cytometer (BD Biosciences) and analyzed using FlowJo software.

Results

Normal B cells migrate with higher efficacy and potency to CXCL12 than CLL B cells, despite having lower levels of CXCR4

Chemokines, including CXCL12, are best known for their role in directing cell migration, but it is well established that they can also induce cell survival and proliferation [8]. This observation can be rationalized by the fact that some of the major pathways involved in cell migration (e.g. PI3K/Akt and Raf/MEK/ERK), are also important for survival and proliferation signaling [13]. However, little is known regarding the extent to which there is

A

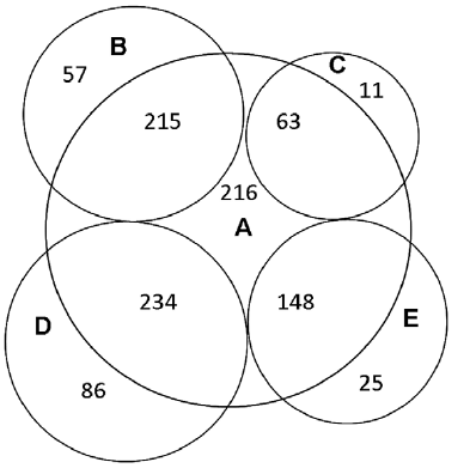

B

SAMPLE	A	B	C	D	E
A	538	215	63	234	148
B	215	271	56	178	97
C	63	56	74	58	37
D	234	178	58	320	104
E	148	97	37	104	173

Figure 4. Overlap in Phosphoprotein Identification between CLL cells from Different Patients. A) Venn diagram illustrating the degree of overlap between the phosphoproteins identified in CLL A compared to the phosphoproteins identified in CLL B, C and D. B) Matrix table outlining the number of overlapping phosphoproteins identified for CLL A, B, C and D.
doi:10.1371/journal.pone.0011716.g004

overlap or divergence of the upstream and downstream effectors of these pathways in the context of migration versus survival/proliferation. Since it has been established that CLL cells have up-regulated expression of CXCR4 compared to normal B cells, and that CXCL12 stimulation of CLL cells activates Akt and ERK1/2 pathways, transwell migration assays were performed on purified CLL B cells and normal B cells to compare their ability to migrate towards CXCL12 [5,8,9].

Surprisingly, the normal B cells showed a significantly greater ($p<0.0001$) ability to migrate to CXCL12, with respect to both efficacy (4.5+/−1.2% migration in normal vs. 0.85+/−0.48% migration in CLL cells) and potency (~10 nM in normal vs ~50 nM in CLL cells) (Figure 2). Although it was expected that the CLL cells would have the stronger migratory response due to higher CXCR4 expression, these results are consistent with previously published observations that showed weak migration of CLL cells to CXCL12 compared to a much more robust response to the CCR7 ligands, CCL19 and CCL21 [14,15]. These data suggest that the downstream effects of CXCR4 may be redirected for survival rather than migration, and led us to consider what other pathways or downstream targets of Akt or ERK1/2 might be activated to bias the CXCL12 signaling response towards survival. Taking a global approach to this question, we performed mass spectrometry-based phosphoproteomics analysis of unstimulated and CXCL12-stimulated CLL cells.

Characterization of phosphopeptides/phosphoproteins in CXCL12-stimulated CLL cells via mass spectrometry

Fresh PBMCs from 5 CLL patients were stimulated over an hour time course with CXCL12, and lysates were generated for IMAC enrichment and LC-MS/MS analysis. Multiple (3 separate duplicate or triplicate experiments with variable acquisition methods) phosphoproteomics data sets were acquired on lysates from the cells of a patient with ZAP-70+ aggressive CLL, referred to as "CLL A", in order to ensure good coverage of the proteomic space. Smaller phosphoproteomics data sets (single triplicate experiments) were collected from cells of 4 additional patients (CLL B to E) for comparison.

Protein lysates from the CLL cells were trypsin digested and enriched for phosphopeptides via immobilized metal affinity chromatography (IMAC) to yield a highly enriched population of phosphorylated peptides. Phosphopeptides were analyzed by LC-MS/MS using a linear iontrap (LTQ) mass spectrometer. Data was processed using the InsPecT database search algorithm and the spectra were manually inspected for validation (see flow diagram Figure 3).

Over 10,000 spectra were collected from the combined phosphoproteomics analysis of unstimulated as well as stimulated CLL cells, which was comprised of 1470 phosphopeptides (>1200 unique phosphosites) from 696 phosphoproteins (Table S1). In general, a >30% enrichment of annotated phosphopeptides was achieved from our IMAC procedure, which is on par with other phosphopeptide enrichment studies of mammalian cells [16].

To ensure that good coverage of the CLL A data set was obtained, a comparison was made of the overlapping phosphoproteins identified in the CLL A data sets and the smaller CLL B - E data sets. 538 of the 696 total phosphoproteins (>77%) identified in the CLL A data sets were also identified in data sets B - E, suggesting detection of the majority of phosphopeptides detectable by these methods. Also, many of the non-overlapping phosphoproteins identified in CLL B to E but not in CLL A were isoform variants of phosphoproteins detected in CLL A. Figure 4 depicts the overlap of CLL B - E with CLL A (Figure 4A) and the matrix shows overlap between all of the CLL samples (Figure 4B).

Identification of phosphoproteins with prior correlations to CLL and other leukemias

Adding confidence to our phosphoproteomics results, a number of hematopoietic-specific phosphoproteins as well as phosphoproteins with prior implications in CLL and other leukemias were identified. Table 1 highlights 9 of the phosphoproteins detected with previous links to CLL/leukemia, including Hematopoietic cell-specific Lyn substrate (Hcls1) and SH2-containing inositol phosphatase-1 (SHIP-1). The phosphorylation status of both Hcls1

Table 1. Phosphoproteins identified by LC-MS/MS analysis with prior implications in CLL/leukemia disease.

Protein	Gi Accession	Implications in CLL/leukemia	References
B cell novel protein 1 (BCNP1)	31542207	Overexpressed in CLL and other B cell malignancies compared to normal B cells	Boyd et al 2003
Formin-like 1 (FMNL1)	33356148	Akt interacting partner found to be overexpressed in CLL	Favaro et al 2003
Hematopoietic cell-specific Lyn substrate (Hcls1 or HS1)	4885405	Phosphorylation correlated with shorter mean patient survival time in CLL	Scielzo et al 2005
HSP-90 alpha	92859630	Stabilizes Akt and ZAP-70 signaling in CLL, highly activated in CLL, and role in CLL survival	Castro et al 2005
Lyn (Yamaguchi sarcoma viral (v-yes-1))	4505055	Overexpressed in CLL compared to normal B cells, potential anti-apoptotic function in CLL	Contri et al 2005
Minichromosome maintenance protein 2 (Mcm2)	33356547	Role in DNA replication, marker for proliferation and prognosis in B-cell lymphoma	Obermann et al 2005
promyelocytic leukemia protein (PLZF)	4505903	Correlates with apoptotic resistance, higher expression of PLZF associated with lower CLL patient survival	Parrado et al 2000
SH2 containing inositol phosphatase 1 (SHIP-1)	64085167	Phosphorylation status segregated with ZAP-70, correlated with aggressive disease in CLL	Gabelloni et al 2008
Stathmin 1 (oncoprotein 18)	44890052	Overexpressed in acute leukemia cells compared to normal lymphocytes, involved in cell growth and proliferation	Melhem et al 1991

Table listing select proteins identified by LC-MS/MS with prior implications in CLL or other related leukemias along with the GI accession number, a brief description of biological implications, and references [17,19–20,22,41–45].
doi:10.1371/journal.pone.0011716.t001

and SHIP-1 have been shown to correlate with disease aggressiveness and shorter mean survival [17,18,19], consistent with the aggressive characteristics of CLL A.

Also included in Table 1 are phosphoproteins which have been linked to CLL but not necessarily phosphorylation status, including HSP90, B cell novel protein 1, promyelocitic leukemia protein, and formin-like 1 (FMNL1) [20,21,22]. These proteins have general implications in CLL, but whether differences in phosphorylation status affect the activity or function in disease is unclear. A few additional proteins including minichromosome maintenance protein 2 and stathmin 1 have been linked to disease progression of other leukemias, but not directly to CLL and thus warrant further investigation in CLL. Many of these phosphoproteins did not appear to exhibit changes in phosphorylation in response to CXCL12 or spectral numbers were too low to make an assessment of stimulation response, but HSP-90 and Mcm2 could be potential phosphorylation targets and are thus also highlighted as proteins of interest in Table 2.

Identification of novel downstream targets of CXCL12/CXCR4 signaling in CLL

To semi-quantitatively assess whether phosphorylation of some of the proteins is a consequence of CXCL12 stimulation, spectral counts from the mass spectrometry runs on the stimulated samples off CLL A were compared to those from unstimulated samples. Select candidate targets of CXCL12-induced phosphorylation are reported in Table 2 along with their associated spectral counts. A number of known targets of survival signaling pathways including programmed cell death factor 4 (PDCD4) and heat shock protein 27 (HSP27) were identified as having more spectral counts in the stimulated versus unstimulated samples, and were selected for validation by western blot and further analysis, discussed in detail later. Validation was performed on lysates from CLL cells used in phosphoproteomics analysis (lettered CLL A to E) as well as additional patient cells not examined by phosphoproteomics (CLL1, CLL2, etc) in order to determine consistency of these responses across different patients, since CLL is a heterogeneous disease [1].

Table 2. Select phosphoproteins from phosphoproteomics analysis with spectral count numbers and known functions.

Adenylyl cyclase-associated protein (CAP1)	5453595	5; 8; 14; 17; 12	Invovled in cAMP pathway, overexpressed in pancreatic cancer, correlated with poor prognosis	Yamazaki et al 2009
Heat shock protein 27 kDa (HSP27)	7706687	1; 10; 13; 7; 7	Downstream target of p38-MAPKAPK2 pathway; involvement in IkB degradation, protection from apoptosis, sequestering and inhibiting cytochrome c release, interacts with Akt	Parcellier et al 2003; Garrido et al 2006
Heterogeneous nuclear ribonuclear proteins (U, D, A1)	U (14141161), D (14110414), A1 (45044445)	U (0; 14; 11; 6; 7), D (3; 21; 25; 20; 14), A1 (13; 33;16; 40; 17)	Nucleocytoplamic shuttling proteins that shuttle mRNAs from site of transcription to start of translation; hnRNPA1 levels are increased in chronic myelogenous leukemia (CML), implications in apoptotic resistance and tumorigenesis; potentially regulated by phosphorylation by various MAPKs	Lervolino et al 2002; Eiring et al 2008; Van der Houven van Oordt et al 2000
HSP90-alpha	92859630	2; 24; 18; 21; 12	Stabilizes PI3K and Akt, pro-proliferative and tumorigenic effects, important for Jak-STAT signaling, Implicated with ZAP-70 stability and signaling in aggressive CLL, less known regarding phosphorylation	Castro et al 2005; Fujita et al 2002; Sato et al 2000; Schoof et al 2009
L-Plastin (lymphocyte cytosolic protein 1)	4504965	0; 4; 9; 1; 1	Actin binding protein expressed in hematopoietic lineage cells as well as malignant cells of non-hematopoietic origin; important for cell polarization and motility	Lin et al 1993; Morley et al 2010
Lymphocyte specific protein 1 (LSP1) (S252)	61742789	1; 9; 11; 5; 8	Downstream target of p38-MAPKAPK2 pathway, PKC, GSK3; F-actin binding protein involved in chemotaxis	Wu et al 2007
Minichromosome maintenance protein 2 (Mcm2)	33356547	2; 7; 2; 4; 2	Role in DNA replication, marker for proliferation and prognosis in B-cell lymphoma	Obermann et al 2005
Programmed cell death factor 4 (PDCD4)	21735596	5; 11; 10; 9; 14	Inhibition of AP1 transcription and eiF4A translational activity, phosphorylation by Akt and p70 S6K is inhibitory and promotes its degradation	Yang et al 2001; Yang et al 2003; Palamarchuk et al 2005; Lankat-Buttgereit et al 2009
serine/arginine repetitive matrix 1 (SRm160)	42542379	15; 57; 57; 40; 30	RNA splicing coactivator; regulates CD44 alternative splicing with potential role in tumor cell invasion	Cheng and Sharp 2006
Small acidic protein	7657234	1; 18; 10; 14; 6	Very little information available, unknown function	
Splicing factor 1 (SF)	42544125	0; 14; 13; 21; 13	Regulates premesseger RNA splicing and gene transactivation and including that of b-catenin/TCF4 complex. Phosphorylated by protein kinase KIS enhances binding to U2AF65	Shitashige et al 2007; Manceau et al 2006
UV excision repair protein RAD23 homolog A (RAD23A, hHR23)	4826964	0; 19; 10; 12; 3	Involved in nucleotide excision repair, recognition of DNA damage; implicated in p53 degradation; phosphorylation function unknown	Glockzin et al 2003

Spectral count numbers for select phosphoproteins of interest are presented for each CXCL12 (30 nM) stimulation time point (0; 3; 10; 30; 60 min). A brief description of known functions and corresponding references are also provided [21–24,26,28–29,43,46–60].

doi:10.1371/journal.pone.0011716.t002

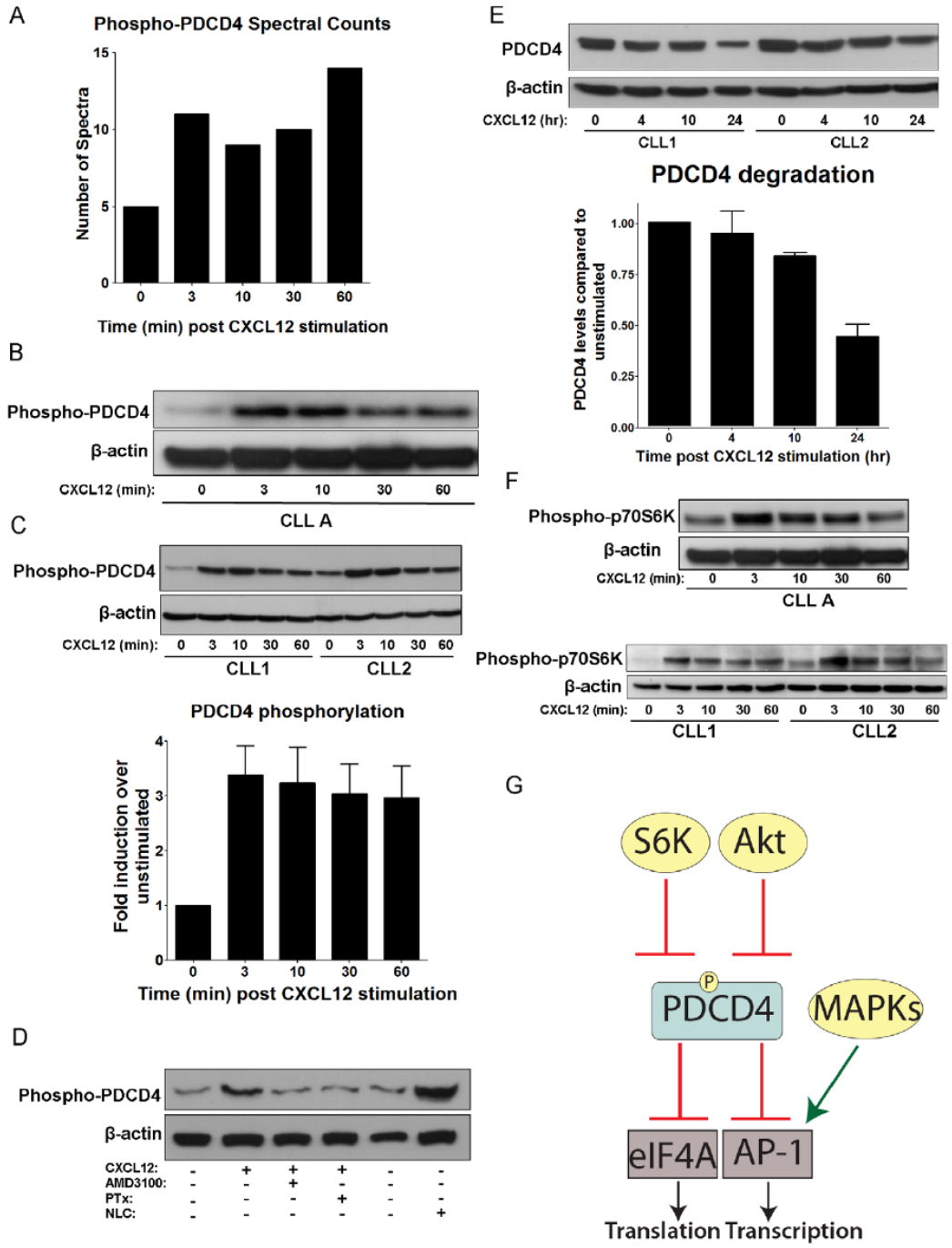

Figure 5. CXCL12 Induces Phosphorylation of PDCD4 at Ser457. A) Bar graph depicting the spectral counts of PDCD4 phosphopeptides observed in the LC-MS/MS analysis at time points of CXCL12 stimulation. B) Western blot of PDCD4 phosphorylation over time course of 0 to 60 min CXCL12 stimulation (30 nM) from CLL A patient cells. β-actin served as a loading control. C) Top panel: Representative western blot of PDCD4 phosphorylation in CLL cells from 2 different CLL patients not used in LC-MS/MS analysis over 30 nM CXCL12 stimulation time course. β-actin served

as a loading control. Bottom panel: Densitometry analysis of PDCD4 phosphorylation levels CXCL12 stimulation (30 nM) time points relative to unstimulated controls and averaged from 10 separate CLL patient cells. Error bars represent standard error of the mean (SEM). D) Western blot of PDCD4 phosphorylation in unstimulated/untreated CLL cells or 3 min CXCL12 stimulations (30 nM) in the presence (+) or absence (−) of preincubation (1 h) with AMD3100 (40 μM) or Pertussis toxin (PTx) (200 ng/ml). NLC lysate represents CLL cells cultured in presence of NLCs with no further stimulation or treatment. CLL cells were removed from the adherent NLCs and lysed. β-actin served as a loading control. E) Top panel: Representative western blot detecting total levels of PDCD4 in CLL cells following 0, 4, 10 or 24 h of 30 nM CXCL12 stimulation. β-actin served as a loading control. Bottom panel: Bar graph quantifying total PDCD4 levels over 24 h time course of 30 nM CXCL12 stimulation compared to 0 h unstimulated controls and normalized to β-actin levels by densitometry analysis of western blots. Data represented are mean +/− SD of 3 separate CLL patients' cells. F) Western blot stripped and reprobed from Figure 4B for p70S6K phosphorylation (Thr389) over time course of 30 nM CXCL12 stimulation from CLL A patient cells (Top panel) and 2 other representative CLL patients' cells (bottom panel). β-actin served as a loading control. G) Diagram of PDCD4 signaling showing known upstream regulators as well as downstream targets. Akt and p70S6K are known to phosphorylate PDCD4, thereby inhibiting its function in repressing eIF4A translational activity and AP-1 transcription.
doi:10.1371/journal.pone.0011716.g005

Some of the phosphoproteins identified in this study have been previously implicated in cancer malignancy such as Mcm2 and adenylyl cyclase associated protein (CAP1), while little information is available on some of the other potential targets including small acidic protein (Table 2). Although two of the proteins (PDCD4 and HSP27) are validated herein as targets of CXCL12-signaling in CLL, the remaining phosphoproteins, while beyond the scope of this work, pose interesting targets for future investigations.

CXCL12 induces the phosphorylation and degradation of PDCD4

PDCD4 is one of the phosphoproteins that appeared to be induced by CXCL12 stimulation based on spectral counts (Figure 5A and Table 2). It is a known tumor suppressor, and downstream phosphorylation target of Akt, which is known to be activated by CXCL12 in CLL cells [9]. A phospho-specific antibody is also commercially available, making it attractive for follow-up studies [23,24]. As a tumor suppressor protein, PDCD4 has been implicated in a number of cancers where it is often inhibited and/or downregulated, disrupting its ability to inhibit eIF4A translational and AP-1 transcriptional activity, processes that are important for cell growth and survival (Figure 5G). Phosphorylation of PDCD4 is known to occur by Akt and p70 S6Kinase (p70S6K) which inhibits its activity and leads to its ubiquitination and proteosomal degradation [23,24,25,26].

Three separate phosphopeptides from PDCD4 were detected from our analysis: R.FVSpEGDGGR.V (Ser457), R.SGLTVPTSpPK.G (Ser94) and R.DSGRGDSpVSDSGSDALR.S (Ser76) (Figure S1). The R.FVSpEGDGGR.V phosphopeptide corresponds to Ser457 phosphorylation, a site known to be phosphorylated by Akt [23]. Therefore, multiple CLL patient samples were examined for PDCD4 phosphorylation in response to CXCL12 by western blot. An increase in phosphorylation of PDCD4 at Ser457 was observed upon CXCL12 stimulation in CLL A cells (Figure 5B), as well as all 9 additional CLL patient cells examined (representative western blot in Figure 5C). Increases in PDCD4 phosphorylation levels was variable between patients and ranged from 1.7-fold to 7.4-fold and averaged to approximately 3.4-fold (n = 10), as quantified by densitometry analysis of western blots (Figure 5C). Although variability was noted, this variation did not cluster according to disease aggressiveness.

As a control to ensure that the phosphorylation was dependent on CXCL12/CXCR4 signaling and to determine if the effects were dependent on signaling through the G-protein, Gi, CLL cells were pretreated with the small molecule CXCR4 antagonist, AMD3100, or the Gi-inhibitor, pertussis toxin (PTx) prior to a 3 min stimulation with CXCL12. As shown in Figure 5D, both AMD3100 and PTx completely abrogated phosphorylation suggesting it is CXCR4 and G-protein signaling dependent. Furthermore, to ensure that phosphorylation of PDCD4 has relevance in a more physiological context, the levels of PDCD4 phosphorylation were examined in CLL cells that had been cultured with NLCs (+) compared to those without NLCs (−). As with CXCL12 stimulation, the coculture of CLL cells with NLCs led to an increase in the phosphorylated levels of PDCD4 (Figure 5D).

Since the phosphorylation of PDCD4 is known to lead to its ubiquitination and degradation [23,25], we examined levels of total PDCD4 over a 24 h time period (0, 4, 10 and 24 h) following CXCL12 stimulation. As shown in Figure 5E, 24 h post-stimulation resulted in PDCD4 degradation to ~45% of starting levels.

Additionally, although it is well established that Akt is phosphorylated downstream of CXCL12 signaling in CLL cells [9], it has not been established whether p70S6K, another kinase known to phosphorylate PDCD4 leading to its ubiquitination and degradation, is activated in CLL cells by CXCL12. Western blot analysis revealed that phosphorylation and thus activation of p70S6K (Thr389) was induced by CXCL12-stimulation in the CLL cells (Figure 5F).

HSP27 expression and phosphorylation is variable in CLL cells

The other phosphoprotein investigated further was HSP27 (phosphopeptide: R.QLSphosSGVEIR.H, Ser82) (mass spectrum shown in Figure S2). HSP27 was also selected due to spectral counts indicative of phosphorylation upon CXCL12 activation of CXCR4 (Figure 6A), its implications in cancer and protection from apoptosis, and the availability of a phospho-specific antibody at the Ser82 phosphorylation site [27,28,29]. Additionally, HSP27 is an interesting target since it is downstream of p38-MAPK signaling [27] which has not received much attention in association with CLL and therefore represents a pathway with potentially novel implications in CLL survival.

Interestingly, while PDCD4 was found to be a common target of CXCL12 signaling in all CLL samples examined, phospho-HSP27 and total HSP27 protein were only detectable by western blot in a subset of ~25% (3 out of 12) of CLL patients examined (representative western blot Figure 6B). Nevertheless, HSP27 was indeed present and did exhibit an increase in phosphorylation upon CXCL12 stimulation in the CLL A patient samples from which the phosphoproteomics data was collected (Figure 6B). Since p38-MAPK is known to be upstream of HSP27 phosphorylation, we also examined p38 phosphorylation among the CLL patient samples (Figure 6C); correspondingly, we observed detectable p38 phosphorylation only in the samples that also exhibited the HSP27 phosphorylation (CLL A, Figure 6B). Although no common factor could be determined among the patients examined with detectable HSP27, a larger sample size might identify common features of these cells and determine whether HSP27 is influencing the survival of this subset of CLL patients.

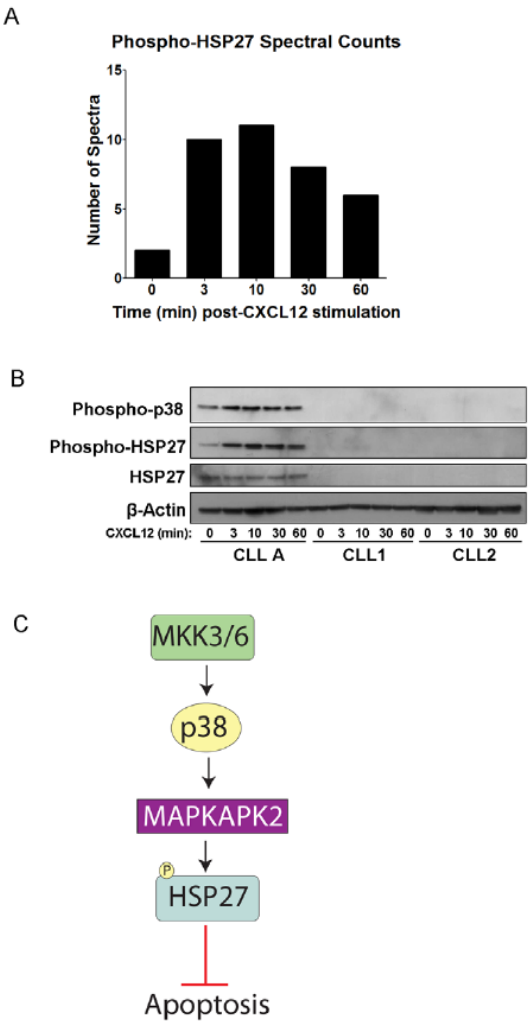

Figure 6. Phosphorylation of HSP27 in Subset of CLL Patients. A) Bar graph depicting the spectral counts of HSP27 phosphopeptides (Ser82) observed in the LC-MS/MS analysis after CXCL12 stimulation. B) Western blot detecting phosphorylation of HSP27 and the upstream p38-MAPK, and total HSP27 over time course of 0 to 60 min CXCL12 stimulation (30 nM) from CLL A patient cells and 2 other representative CLL patients' cells. β-actin was run as a loading control. C) Signaling diagram of HSP27, which can protect from apoptosis, and its upstream regulation by p38-MAPK and MAPKAPK2.
doi:10.1371/journal.pone.0011716.g006

Discussion

CLL is the most common leukemia in the Western world [1]. The accumulation of CLL B cells is believed to result from low rates of precursor cell proliferation and via recruitment of accessory cells that create a supportive microenvironment by producing factors that foster CLL survival [1,2]. The chemokine, CXCL12, is one of the cytokines produced by cells in the microenvironment that enhances CLL survival *in vitro* and likely *in vivo* [9]. Although chemokines are best known for their role as chemoattractants, we show here that CLL cells are much less capable of migrating to CXCL12 compared to CLL B cells, despite an upregulation of CXCR4 on the CLL cells [5]. While the low levels of migration may still play a role *in vivo* [30], it is evident that the CXCL12/CXCR4 axis is also networked into pathways involved in survival. In contrast, CXCR7, the other receptor of CXCL12, is not expressed on the surface of CLL cells although it is expressed on normal B cells [6]. Thus, while there is overlap in signaling pathways activated by CXCL12 in CLL cells and normal B cells, the differences in migration and CXCR7 expression, and the potential bias towards survival in CLL cells, suggest significant differences in the role that the CXCL12/CXCR4 axis plays in the context of the normal and pathological cells.

Phosphoproteomics analysis of CXCL12-stimulated CLL cells was performed in an effort to determine potential downstream signaling targets that could contribute to the survival and malignancy of CLL cells. As these are precious non-renewable primary patient cells, the intent of our phosphoproteomics approach was to generate hypotheses rather than an exhaustive analysis of the CLL phosphoproteome. Therefore, while it would be ideal to use a number of phospho-enrichment strategies in addition to IMAC (e.g. TiO_2) and to employ additional liquid chromatography separation steps besides C18 (e.g. hydrophilic interaction liquid chromatography (HILIC)) to expand the number of phosphoproteins identified, we focused our efforts on well established methods [10,31]. Along these lines, the use of quantitative phosphoproteomics strategies is limited since these cells do not replicate and cannot be cultured long term. Thus, stable isotope labeling of amino acids in cell culture (SILAC) is not possible [32]. Post-digest labeling with iTRAQ or ICAT isotopic labels [32] is also difficult due to limited sample availability, limitations in instrumentation (one-third rule with the LTQ spectrometer restricting detection of the labels in the low molecular weight range) [33], and the labile nature of phosphates and labels which causes reduced fragmentation and detection in MS/MS spectra [34]. While understanding its limitations, spectral counting was employed as a semi-quantitative assessment of the CXCL12-stimulation responses [35] and several candidates were followed up by western blot validation. In addition to the above examples with PDCD4 and HSP27, which showed that the spectral counting provides a relatively good approximation of stimulation response, spectral counts reflecting fairly even levels of phosphorylated p21-activated kinase (PAK2), another target of the PI3K pathway, was also confirmed by western blot in all six patient cells probed for phospho-PAK2 (Ser141) (Figure S3).

Through this phosphoproteomics approach, we were able to confidently identify close to 700 phosphoproteins in the CLL samples, including numerous proteins previously implicated in CLL disease. Additionally, we identified many proteins that appear to exhibit changes in phosphorylation levels in response to CXCL12. This data led to the identification and validation of several previously unknown phosphorylation targets of CXCL12 signaling. Typical approaches (e.g. western blot) for investigating signaling in response to stimuli require *a priori* knowledge of specific targets and the availability of phospho-specific antibodies, which limits the ability to globally assess cellular signaling events. Furthermore, validation studies of CLL cells are difficult since their viability in culture is limited. They are also difficult to manipulate through transfection and transduction since they do not divide in culture or infect well (e.g. they require high MOI and/or pre-activation of cells with CD40L and IL-4 [36] which could complicate interpretation of signaling analysis). Therefore, this mass-spectrometry-based approach seemed the most effective method for gaining new insight into the function of CXCL12 on CLL cell survival and possibly disease aggressiveness. Although

not done in this study, comprehensive MS analysis of many patients may help to distinguish variations between patients, and with disease stratification and the identification of judicious therapeutic targets.

To our knowledge, this is the first report demonstrating that PDCD4 is a phosphorylation target downstream of CXCL12 signaling in CLL or other cell types. This finding is exciting due to the established role of PDCD4 as a tumor suppressor and as a substrate of Akt [23,25]. Although little is known regarding the function of two of the phosphorylation sites of PDCD4 (Ser94 and Ser76) identified from the LC-MS/MS analysis, phosphorylation at Ser457 near the C-terminus of the protein is a well-established site with known functional implications. Phosphorylation at Ser457 by Akt has been shown to result in nuclear translocation of PDCD4 and a decrease in its ability to inhibit AP-1-mediated transcription and eIF4A-mediated translation [24,26]; although Ser67 phosphorylation was not directly identified in our LC-MS/MS analysis, it is likely that this sight is also phosphorylated in response to CXCL12 stimulation since PDCD4 degradation was observed following stimulation [23,25]. In combination, these effects may reduce the growth regulating/tumor-suppressor capacity of PDCD4, thereby contributing to CLL cell survival and the malignancy phenotype. Validation of PDCD4 phosphorylation also led to the identification of p70S6K phosphorylation and activation downstream of CXCL12 signaling in CLL cells.

Based on the phosphoproteomics analysis, HSP27 appeared to be another promising phosphorylation target of CXCL12-signaling. HSP27 and several other HSPs have received attention in the context of cancer due to their cytoprotective/anti-apoptotic functions. Specifically, HSP27 indirectly inhibits cytochrome c release and caspase activation and it sequesters cytosolic cytochrome c. It also promotes degradation of the inhibitor of NF-kB (IkB) and p27kip, and interacts with and supports the activity of Akt under stressful conditions, all leading to protection from apoptosis [29,37]. We identified the presence of phosphorylated and total HSP27 protein and its upstream activator p38-MAPK in a subset (~25%) of cell samples from different CLL patients. Of note, the observed variability in signaling between different CLL patient cells highlights the underlying heterogeneity of the disease. Furthermore, it serves as a reminder of how different parameters including patient differences (age and gender), variations in clinical course such as aggressiveness, stage and prognosis, and different treatments (e.g. chemotherapy, gene therapy, etc) may alter how the cells respond to different stimuli. Such variability is not unprecedented as Messmer *et al* (submitted manuscript) have demonstrated differences in CXCL12-mediated MEK and ERK activation in different ZAP-70 subgroups of CLL, and Montresor *et al* demonstrated differences in CXCL12-mediated lymphocyte function-associated antigen-1 (LFA-1) activation in normal B cells compared to CLL B cells and amongst the cells of different CLL patients [38]. Thus, it is reasonable to expect that different patients will exhibit different responses to stimuli, whether it is a survival stimulus from the microenvironment or a therapeutic agent used to treat the disease.

These results showing patient variability in HSP27 expression emphasize the strength of utilizing primary cells for understanding

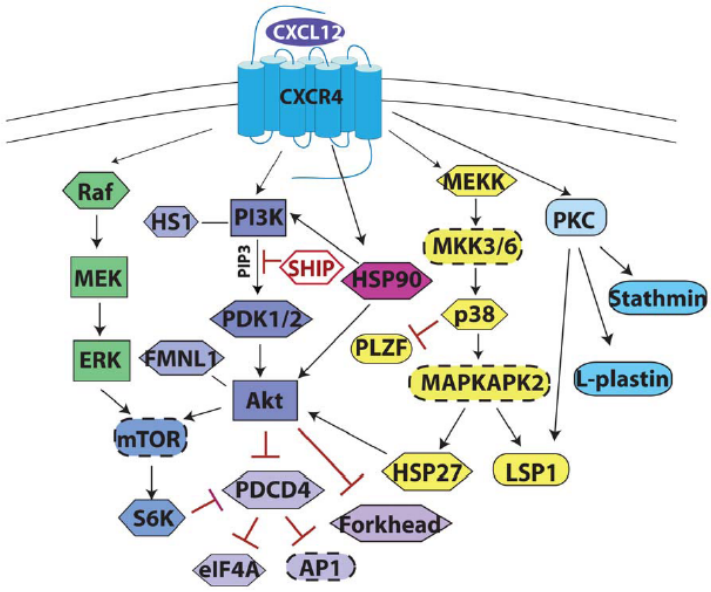

Figure 7. Summary of CXCL12-mediated Signaling in CLL. Signaling diagram depicting pathways activated downstream of CXLC12. Through direct or indirect mechanisms, arrows indicate factors that are activated, red lines ending with a bar indicate factors that are inhibited by the upstream factor, and lines (no arrowhead) indicate interactions. Proteins in hexagons were identified and validated herein or were previously known targets also detected in the LC-MS/MS. Proteins in rectangles are known key signaling molecules of these pathways that were not detected in this LC-MS/MS data set. Proteins in ovals with dashed lines are likely intermediates/targets of the pathways based on previous studies. Proteins in oval shape were also identified by LC-MS/MS but have yet to be validated. Much of our focus has been on the PI3K/Akt and Raf/MEK/ERK pathways due to known implications in CLL cell survival and resistance to apoptosis. Furthermore, the potential involvement of the p38-MAPK pathway in some CLL patients with activation of HSP27 and LSP1 is outlined.
doi:10.1371/journal.pone.0011716.g007

disease pathogenesis as opposed to cell lines, which are much more homogenous, but can be less insightful and sometimes misleading. While there was considerable overlap in the phosphoproteins identified from LC-MS/MS analysis between different patients (CLL A – E), more comprehensive MS analysis of multiple patients may help to distinguish variations in signaling responses between patients. Along these lines, since HSP27 is often induced following stressful cellular events such as treatment with chemotherapeutics, its induction in certain patients could reflect a response to treatment. For example, lymphoma cells which did not express Hsp27 were sensitive to apoptosis while those expressing Hsp27 were resistant to apoptosis induced by Bortezomib (PS-341), a proteasome inhibitor [39]. Silencing of Hsp27 in the resistant lymphoma cells then rendered them susceptible to Bortezomib-induced death, demonstrating its link in resistance to this chemotherapeutic treatment [39]. Thus, a larger patient sample size may reveal if expression of HSP27 is induced by certain chemotherapeutics or in particular subsets of patients and whether there is any correlation to refractory disease, as resistance to chemotherapy is one of the major hurdles in treating CLL [2].

Herein we present follow-up data to PDCD4 and HSP27, although there are numerous other candidate phosphoprotein targets of CXCL12 signaling in CLL cells that have been proposed (Table 2). A summary of our findings from phosphoproteomics analysis combined with some previously established pathways of CXCL12 signaling in CLL are summarized in a signaling diagram (Figure 7). Overall, our data suggests that CXCL12 may preferentially activate survival signaling pathways rather than those involved in cell migration in CLL cells, although some of the pathway components (Gi, Erk, Akt) are common nodes. We have demonstrated that the use of phosphoproteomics is a feasible and informative means of evaluating signaling responses to CXCL12 in CLL, which could be employed for investigating a variety of other stimuli in these or other primary cells. Through phosphoproteomics detection and western blot validation, PDCD4 was found to be a common phosphorylation target of CXCL12-signaling in CLL while HSP27 was present in only a subset of CLL patients. Although our focus was on CXCL12 as a survival factor, it is likely that other growth and survival stimuli may synergistically activate these pathways and downstream targets. Therefore, PDCD4 and HSP27, which have previous implications in regulation of apoptosis and carcinogenesis, may represent potential therapeutic targets for treatment of CLL. In fact, small molecule stabilizers of PDCD4, that enhance its function as a tumor suppressor by inhibiting its degradation, are currently being developed due to its potential as a therapeutic target for numerous cancers. Such agents could prove to be useful agents in combination with other therapeutic modalities for the treatment of CLL [40].

Supporting Information

Table S1 Table of all phosphoproteins and corresponding phosphopeptides identified by LC-MS/MS analysis on IMAC enriched CLL samples.
Found at: doi:10.1371/journal.pone.0011716.s001 (0.18 MB XLS)

Figure S1 Mass spectra of PDCD4 phosphopeptides. Mass spectra from the 3 phosphopeptides from PDCD4 that were identified in the LC-MS/MS analysis. The top spectrum (A) represents the phosphopeptide with Ser457, which is the phosphosite detected by the antibody used in follow-up western blot analysis. B) Spectrum for Ser94 phosphorylation site. C) Spectrum for Ser76 phosphorylation site.
Found at: doi:10.1371/journal.pone.0011716.s002 (0.10 MB DOC)

Figure S2 Mass spectrum of HSP27 phosphopeptide. Mass spectrum from the HSP27 phosphopeptide (Ser 82) that was identified in the LC-MS/MS analysis.
Found at: doi:10.1371/journal.pone.0011716.s003 (0.04 MB DOC)

Figure S3 Phosphorylation of PAK2 is present but not induced by CXCL12 in CLL cells. A) Mass spectrum of the phosphopeptide K.YLSpFTPPEK.D (Ser141) of PAK2, which was present in all proteomics runs but had fairly even spectral counts (1–3 spectra) in each CXCL12 stimulation time point). B) Representative western blot of PAK2 phosphorylation (Ser141) over 60 min time course of 30 nM CXCL12 stimulation in 3 different CLL patient's cells reflects no changes in phospho-PAK2 upon stimulation, although total phospho-PAK2 levels were variable between different patients' cells. β-actin served as a loading control.
Found at: doi:10.1371/journal.pone.0011716.s004 (0.08 MB DOC)

Acknowledgments

We gratefully acknowledge the contributions of Dr. Huilin Zhou and Marie Reichart for guidance with the IMAC technique, Larry Gross, Dario Meluzzi and Mike Meehan for assistance with LC-MS/MS and Dr. Steve Bark and Dr. Elizabeth Komives for many useful discussions and critical reading of this work.

Author Contributions

Conceived and designed the experiments: MO CLS DM PCD TMH. Performed the experiments: MO CLS. Analyzed the data: MO CLS. Contributed reagents/materials/analysis tools: TJK DM PCD. Wrote the paper: MO.

References

1. Chiorazzi N, Rai KR, Ferrarini M (2005) Chronic lymphocytic leukemia. N Engl J Med 352: 804–815.
2. Zenz T, Mertens D, Kuppers R, Dohner H, Stilgenbauer S (2010) From pathogenesis to treatment of chronic lymphocytic leukaemia. Nat Rev Cancer 10: 37–50.
3. Burger JA, Tsukada N, Burger M, Zvaifler NJ, Dell'Aquila M, et al. (2000) Blood-derived nurse-like cells protect chronic lymphocytic leukemia B cells from spontaneous apoptosis through stromal cell-derived factor-1. Blood 96: 2655–2663.
4. Collins RJ, Verschuer LA, Harmon BV, Prentice RL, Pope JH, et al. (1989) Spontaneous programmed death (apoptosis) of B-chronic lymphocytic leukaemia cells following their culture in vitro. Br J Haematol 71: 343–350.
5. Mohle R, Failenschmid C, Bautz F, Kanz L (1999) Overexpression of the chemokine receptor CXCR4 in B cell chronic lymphocytic leukemia is associated with increased functional response to stromal cell-derived factor-1 (SDF-1). Leukemia 13: 1954–1959.
6. Infantino S, Moepps B, Thelen M (2006) Expression and regulation of the orphan receptor RDC1 and its putative ligand in human dendritic and B cells. J Immunol 176: 2197–2207.
7. Zou YR, Kottmann AH, Kuroda M, Taniuchi I, Littman DR (1998) Function of the chemokine receptor CXCR4 in haematopoiesis and in cerebellar development. Nature 393: 595–599.
8. O'Hayre M, Salanga CL, Handel TM, Allen SJ (2008) Chemokines and cancer: migration, intracellular signalling and intercellular communication in the microenvironment. Biochem J 409: 635–649.
9. Nishio M, Endo T, Tsukada N, Ohata J, Kitada S, et al. (2005) Nurselike cells express BAFF and APRIL, which can promote survival of chronic lymphocytic leukemia cells via a paracrine pathway distinct from that of SDF-1alpha. Blood 106: 1012–1020.
10. O'Hayre M, Salanga CL, Dorrestein PC, Handel TM (2009) Phosphoproteomic analysis of chemokine signaling networks. Methods Enzymol 460: 331–346.

11. Payne SH, Yau M, Smolka MB, Tanner S, Zhou H, et al. (2008) Phosphorylation-specific MS/MS scoring for rapid and accurate phosphoproteome analysis. J Proteome Res 7: 3373–3381.
12. Tanner S, Shu H, Frank A, Wang LC, Zandi E, et al. (2005) InsPecT: identification of posttranslationally modified peptides from tandem mass spectra. Anal Chem 77: 4626–4639.
13. Lee JT, Jr., McCubrey JA (2002) The Raf/MEK/ERK signal transduction cascade as a target for chemotherapeutic intervention in leukemia. Leukemia 16: 486–507.
14. Till KJ, Lin K, Zuzel M, Cawley JC (2002) The chemokine receptor CCR7 and alpha4 integrin are important for migration of chronic lymphocytic leukemia cells into lymph nodes. Blood 99: 2977–2984.
15. Richardson SJ, Matthews C, Catherwood MA, Alexander HD, Carey BS, et al. (2006) ZAP-70 expression is associated with enhanced ability to respond to migratory and survival signals in B-cell chronic lymphocytic leukemia (B-CLL). Blood 107: 3584–3592.
16. Moser K, White FM (2006) Phosphoproteomic analysis of rat liver by high capacity IMAC and LC-MS/MS. J Proteome Res 5: 98–104.
17. Gabelloni ML, Borge M, Galletti J, Canones C, Calotti PF, et al. (2008) SHIP-1 protein level and phosphorylation status differs between CLL cells segregated by ZAP-70 expression. Br J Haematol 140: 117–119.
18. Ghia P, Circosta P, Scielzo C, Vallario A, Camporeale A, et al. (2005) Differential effects on CLL cell survival exerted by different microenvironmental elements. Curr Top Microbiol Immunol 294: 135–145.
19. Scielzo C, Ghia P, Conti A, Bachi A, Guida G, et al. (2005) HS1 protein is differentially expressed in chronic lymphocytic leukemia patient subsets with good or poor prognoses. J Clin Invest 115: 1644–1650.
20. Favaro PM, de Souza Medina S, Traina F, Basseres DS, Costa FF, et al. (2003) Human leukocyte formin: a novel protein expressed in lymphoid malignancies and associated with Akt. Biochem Biophys Res Commun 311: 365–371.
21. Sato S, Fujita N, Tsuruo T (2000) Modulation of Akt kinase activity by binding to Hsp90. Proc Natl Acad Sci U S A 97: 10832–10837.
22. Castro JE, Prada CE, Loria O, Kamal A, Chen L, et al. (2005) ZAP-70 is a novel conditional heat shock protein 90 (Hsp90) client: inhibition of Hsp90 leads to ZAP-70 degradation, apoptosis, and impaired signaling in chronic lymphocytic leukemia. Blood 106: 2506–2512.
23. Lankat-Buttgereit B, Goke R (2009) The tumour suppressor Pdcd4: recent advances in the elucidation of function and regulation. Biol Cell 101: 309–317.
24. Yang HS, Jansen AP, Nair R, Shibahara K, Verma AK, et al. (2001) A novel transformation suppressor, Pdcd4, inhibits AP-1 transactivation but not NF-kappaB or ODC transactivation. Oncogene 20: 669–676.
25. Dorrello NV, Peschiaroli A, Guardavaccaro D, Colburn NH, Sherman NE, et al. (2006) S6K1- and betaTRCP-mediated degradation of PDCD4 promotes protein translation and cell growth. Science 314: 467–471.
26. Yang HS, Jansen AP, Komar AA, Zheng X, Merrick WC, et al. (2003) The transformation suppressor Pdcd4 is a novel eukaryotic translation initiation factor 4A binding protein that inhibits translation. Mol Cell Biol 23: 26–37.
27. Concannon CG, Gorman AM, Samali A (2003) On the role of Hsp27 in regulating apoptosis. Apoptosis 8: 61–70.
28. Parcellier A, Schmitt E, Gurbuxani S, Seigneurin-Berny D, Pance A, et al. (2003) HSP27 is a ubiquitin-binding protein involved in I-kappaBalpha proteasomal degradation. Mol Cell Biol 23: 5790–5802.
29. Garrido C, Brunet M, Didelot C, Zermati Y, Schmitt E, et al. (2006) Heat shock proteins 27 and 70: anti-apoptotic proteins with tumorigenic properties. Cell Cycle 5: 2592–2601.
30. Burger JA, Burkle A (2007) The CXCR4 chemokine receptor in acute and chronic leukaemia: a marrow homing receptor and potential therapeutic target. Br J Haematol 137: 288–296.
31. Smolka MB, Albuquerque CP, Chen SH, Zhou H (2007) Proteome-wide identification of in vivo targets of DNA damage checkpoint kinases. Proc Natl Acad Sci U S A 104: 10364–10369.
32. Matthiesen R, Carvalho AS (2010) Methods and algorithms for relative quantitative proteomics by mass spectrometry. Methods Mol Biol 593: 187–204.
33. Want EJ, Cravatt BF, Siuzdak G (2005) The expanding role of mass spectrometry in metabolite profiling and characterization. Chembiochem 6: 1941–1951.
34. Macek B, Mann M, Olsen JV (2009) Global and site-specific quantitative phosphoproteomics: principles and applications. Annu Rev Pharmacol Toxicol 49: 199–221.
35. Zhu W, Smith JW, Huang CM (2010) Mass spectrometry-based label-free quantitative proteomics. J Biomed Biotechnol 2010: 840518.
36. Huang MR, Olsson M, Kallin A, Pettersson U, Totterman TH (1997) Efficient adenovirus-mediated gene transduction of normal and leukemic hematopoietic cells. Gene Ther 4: 1093–1099.
37. Bruey JM, Ducasse C, Bonniaud P, Ravagnan L, Susin SA, et al. (2000) Hsp27 negatively regulates cell death by interacting with cytochrome c. Nat Cell Biol 2: 645–652.
38. Montresor A, Bolomini-Vittori M, Simon SI, Rigo A, Vinante F, et al. (2009) Comparative analysis of normal versus CLL B-lymphocytes reveals patient-specific variability in signaling mechanisms controlling LFA-1 activation by chemokines. Cancer Res 69: 9281–9290.
39. Chauhan D, Li G, Shringarpure R, Podar K, Ohtake Y, et al. (2003) Blockade of Hsp27 overcomes Bortezomib/proteasome inhibitor PS-341 resistance in lymphoma cells. Cancer Res 63: 6174–6177.
40. Blees JS, Schmid T, Thomas CL, Baker AR, Benson L, et al. (2010) Development of a high-throughput cell-based reporter assay to identify stabilizers of tumor suppressor Pdcd4. J Biomol Screen 15: 21–29.
41. Boyd RS, Adam PJ, Patel S, Loader JA, Berry J, et al. (2003) Proteomic analysis of the cell-surface membrane in chronic lymphocytic leukemia: identification of two novel proteins, BCNP1 and MIG2B. Leukemia 17: 1605–1612.
42. Contri A, Brunati AM, Trentin L, Cabrelle A, Miorin M, et al. (2005) Chronic lymphocytic leukemia B cells contain anomalous Lyn tyrosine kinase, a putative contribution to defective apoptosis. J Clin Invest 115: 369–378.
43. Obermann EC, Went P, Zimpfer A, Tzankov A, Wild PJ, et al. (2005) Expression of minichromosome maintenance protein 2 as a marker for proliferation and prognosis in diffuse large B-cell lymphoma: a tissue microarray and clinico-pathological analysis. BMC Cancer 5: 162.
44. Parrado A, Noguera ME, Delmer A, McKenna S, Davies J, et al. (2000) Deregulated expression of promyelocytic leukemia zinc finger protein in B-cell chronic lymphocytic leukemias does not affect cyclin A expression. Hematol J 1: 15–27.
45. Melhem RF, Zhu XX, Hailat N, Strahler JR, Hanash SM (1991) Characterization of the gene for a proliferation-related phosphoprotein (oncoprotein 18) expressed in high amounts in acute leukemia. J Biol Chem 266: 17747–17753.
46. Yamazaki K, Takamura M, Masugi Y, Mori T, Du W, et al. (2009) Adenylate cyclase-associated protein 1 overexpressed in pancreatic cancers is involved in cancer cell motility. Lab Invest 89: 425–432.
47. Eiring AM, Neviani P, Santhanam R, Oaks JJ, Chang JS, et al. (2008) Identification of novel posttranscriptional targets of the BCR/ABL oncoprotein by ribonomics: requirement of E2F3 for BCR/ABL leukemogenesis. Blood 111: 816–828.
48. Iervolino A, Santilli G, Trotta R, Guerzoni C, Cesi V, et al. (2002) hnRNP A1 nucleocytoplasmic shuttling activity is required for normal myelopoiesis and BCR/ABL leukemogenesis. Mol Cell Biol 22: 2255–2266.
49. van der Houven van Oordt W, Diaz-Meco MT, Lozano J, Krainer AR, Moscat J, et al. (2000) The MKK(3/6)-p38-signaling cascade alters the subcellular distribution of hnRNP A1 and modulates alternative splicing regulation. J Cell Biol 149: 307–316.
50. Fujita N, Sato S, Ishida A, Tsuruo T (2002) Involvement of Hsp90 in signaling and stability of 3-phosphoinositide-dependent kinase-1. J Biol Chem 277: 10346–10353.
51. Schoof N, von Bonin F, Trumper L, Kube D (2009) HSP90 is essential for Jak-STAT signaling in classical Hodgkin lymphoma cells. Cell Commun Signal 7: 17.
52. Lin CS, Park T, Chen ZP, Leavitt J (1993) Human plastin genes. Comparative gene structure, chromosome location, and differential expression in normal and neoplastic cells. J Biol Chem 268: 2781–2792.
53. Morley SC, Wang C, Lo WL, Lio CW, Zinselmeyer BH, et al. (2010) The actin-bundling protein L-plastin dissociates CCR7 proximal signaling from CCR7-induced motility. J Immunol 184: 3628–3638.
54. Wu Y, Zhan L, Ai Y, Hannigan M, Gaestel M, et al. (2007) MAPKAPK2-mediated LSP1 phosphorylation and FMLP-induced neutrophil polarization. Biochem Biophys Res Commun 358: 170–175.
55. Palamarchuk A, Efanov A, Maximov V, Aqeilan RI, Croce CM, et al. (2005) Akt phosphorylates and regulates Pdcd4 tumor suppressor protein. Cancer Res 65: 11282–11286.
56. Cheng C, Sharp PA (2006) Regulation of CD44 alternative splicing by SRm160 and its potential role in tumor cell invasion. Mol Cell Biol 26: 362–370.
57. Glockzin S, Ogi FX, Hengstermann A, Scheffner M, Blattner C (2003) Involvement of the DNA repair protein hHR23 in p53 degradation. Mol Cell Biol 23: 8960–8969.
58. Manceau V, Swenson M, Le Caer JP, Sobel A, Kielkopf CL, et al. (2006) Major phosphorylation of SF1 on adjacent Ser-Pro motifs enhances interaction with U2AF65. FEBS J 273: 577–587.
59. Shitashige M, Naishiro Y, Idogawa M, Honda K, Ono M, et al. (2007) Involvement of splicing factor-1 in beta-catenin/T-cell factor-4-mediated gene transactivation and pre-mRNA splicing. Gastroenterology 132: 1039–1054.
60. Shitashige M, Satow R, Honda K, Ono M, Hirohashi S, et al. (2007) Increased susceptibility of Sf1(+/-) mice to azoxymethane-induced colon tumorigenesis. Cancer Sci 98: 1862–1867.

SUPPLEMENTAL INFORMATION

O'Hayre M, Salanga CL, Kipps TJ, Messmer D, Dorrestein PC, Handel TM. Elucidating the CXCL12/CXCR4 Signaling Network in Chronic Lymphocytic Leukemia through Phosphoproteomics Analysis. (2010) *PLoS One* 5(7): e11716.

Table S1 Found online at doi: 10.1371/journalpone.0011716.s001

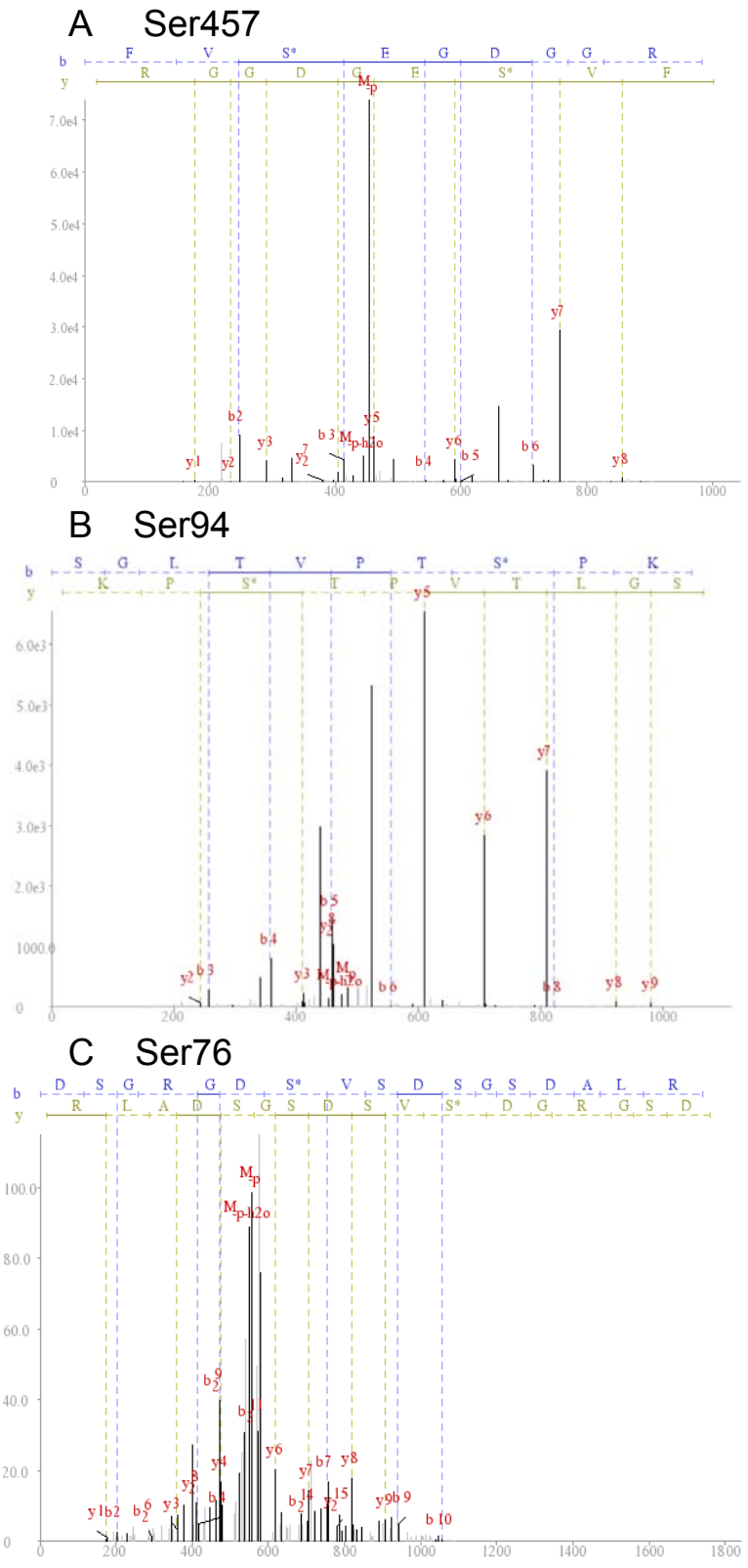

Figure S1 Mass Spectra of PDCD4 Phosphopeptides.

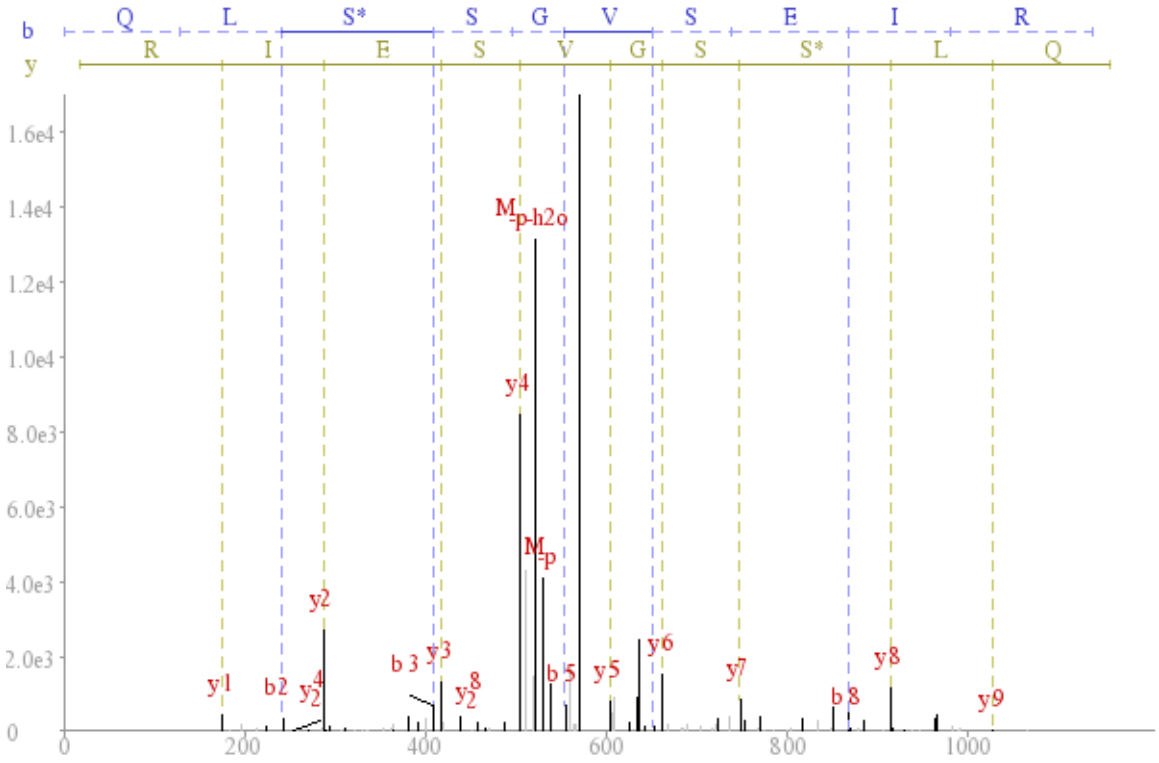

Figure S2 Mass Spectrum of HSP27 Phosphopeptide.

A

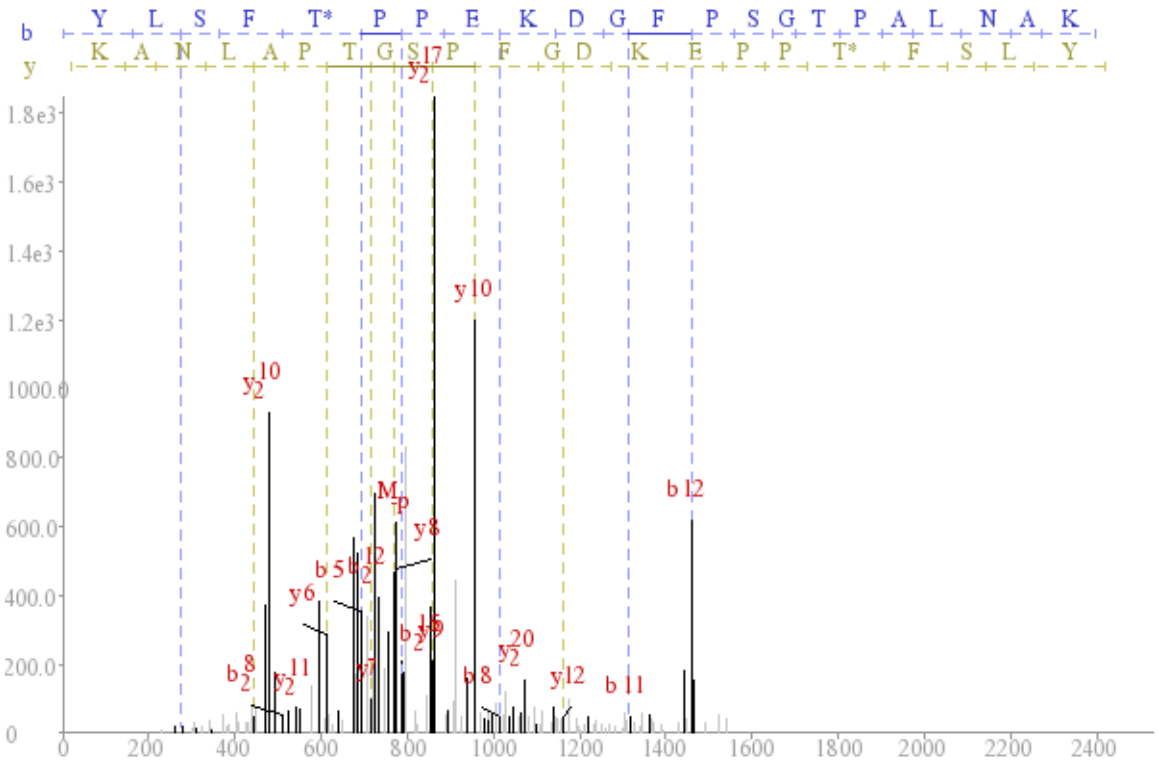

B

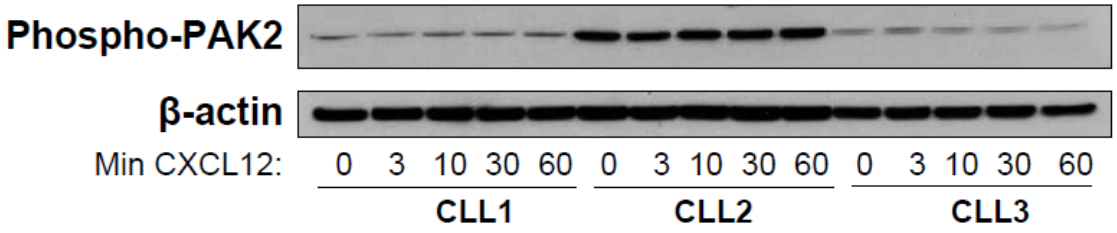

Figure S3 Phosphorylation of PAK2 Is Present but Not Induced by CXCL12 in CLL cells. A) Mass spectrum for PAK2 phosphopeptide. B) Western blot of phosphorylated PAK2 levels over 60 min time course of CXCL12 stimulation for 3 different CLL patients' cells.

ACKNOWLEDGEMENTS

Chapter 6 is a reprint of the article as it appears in PLoS ONE, 2010, Morgan O'Hayre, Catherina L Salanga, Thomas J Kipps, Davorka Messmer, Pieter C Dorrestein, Tracy M Handel, 5(7): e11716. doi:10.1371/journal.pone.0011716.

The dissertation author prepared the CLL stimulations and lysates, performed phosphoproteomics data collection and analysis, carried out the follow-up analysis and wrote the article. Catherina L Salanga contributed to the phosphoproteomics data collection and analysis. The other authors provided guidance and/or resources contributing to the article.

CHAPTER 7

Elucidating the Roles of CXCR4 and CXCR7 in Breast Cancer Progression

7.1 Overview

Chemokines and their receptors play an important role in the immune system by guiding the migration of cells involved in routine immune surveillance and inflammatory responses. However, they can also be exploited by cancer cells to facilitate metastasis and enhance tumor growth. Work presented in this chapter focuses on elucidating the roles of the chemokine, CXCL12, and its receptors, CXCR4 and CXCR7, in breast cancer. Although CXCR4 and CXCR7 are not normally expressed in breast tissue, they are often expressed on breast cancer cells and are known to contribute to metastasis and primary tumor growth, respectively. However, the extent to which CXCR4 and CXCR7 serve redundant versus distinct functions has not been established, nor have the underlying mechanisms of how they contribute to disease. Thus, our goal is to explore how these two chemokine receptors function independently and in conjunction in breast cancer progression.

In order to address these questions, we derived sublines from the MDA-MB-231 human breast cancer cell line that express low levels of both receptors, high levels of CXCR4, high levels of CXCR7 or high levels of both receptors. Consistent with previously published observations, our results indicate that high expression of either CXCR4 or CXCR7 in breast cancer cells results in accelerated tumor growth compared to those with low expression. Furthermore, we found that high CXCR4 but not high

CXCR7 resulted in increased metastasis, consistent with previous findings from studies of the individual receptors. However, we observe striking effects of dual receptor expression on metastasis, in which CXCR7 expression appears to inhibit metastasis potentially through negative regulation of CXCR4-promoted metastasis. In order to better understand the molecular mechanisms underlying these contrasting results, we have also examined how co-expression of the two receptors alters CXCL12-induced signaling events such as calcium flux, ERK activation, and PDCD4 inhibition. Furthermore, we provide evidence to suggest these effects are not simply due to CXCL12 sequestration by CXCR7, but likely also involve direct interactions between CXCR4 and CXCR7 receptors.

These data suggest that CXCR4 and CXCR7 do not serve redundant functions although they influence the functions of each other both at the cellular level and in breast cancer growth and metastasis. These findings could have significant implications in terms of disease aggressiveness and the effectiveness of targeting the receptors and downstream signaling pathways for the treatment of breast cancer.

7.2 Introduction

Aside from skin cancers, breast cancer is the most common cancer and the second leading cause of cancer related deaths among American women. Approximately 12% of women will develop invasive breast cancer at some point in their life (American Cancer Society). Metastasis of primary tumors to secondary organs is the leading cause of death in breast cancer patients [*1*]; therefore, a better molecular understanding of the process of metastasis and the mechanisms by which metastasized cells survive and proliferate would contribute to the development of drugs that enhance patient survival. Chemokine receptors in general have been implicated in enhancing and directing the

metastasis of cancer cells to distant sites from the primary tumor; in particular, CXCR4 is associated with promoting metastasis in at least 23 different types or cancer [*2*]. The role of chemokine receptors in directing metastasis makes sense since it parallels their normal role in controlling cell migration during immune responses. In the context of breast cancer, CXCR4 was shown to be expressed in numerous breast cancer cells, although it is not expressed in normal breast epithelia and there is preferential metastasis of breast cancer cells to sites where the ligand, CXCL12, is constitutively expressed [*3*]. CXCR7, the other receptor to which CXCL12 binds, is also absent on normal breast epithelia but is frequently expressed on breast cancer cells as well as on tumor associated vasculature (endothelial cells) [*4-5*]. In contrast to CXCR4, which has widespread tissue distribution during and after development [*6-7*] surface CXCR7 expression after development is more limited in normal tissues, primarily to activated endothelium and peripheral blood mononuclear cells (PBMCs). However, the expression of CXCR7 on tumors and tumor vasculature in several types of cancer including glioma, lung cancer, breast cancer, renal cell carcinoma, and other cancers suggests it may have an important role in cancer progression [*4-5, 8-9*].

It is well established that expression of CXCR4 on breast cancer cells promotes metastasis of these cells to sites of constitutive CXCL12 production [*3*]. For example, knockdown of CXCR4 expression in the MDA-MB-231 breast cancer cell line through siRNA and through neutralizing antibodies against CXCR4 impaired lung and lymph node metastasis in mice [*3, 10*]. Administration of antagonists of CXCR4 also synergize with chemotherapy in cell killing and tumor regression of glioblastoma multiforme-derived tumor cells and in a B16 murine model of melanoma, and CXCR4 was shown to be required for outgrowth of colon carcinoma micrometastases [*11-13*]. Furthermore, CXCR4 expression has been associated with enhanced survival and proliferation of

various cancer cells [*14-16*], so it is likely that chemokine receptor signaling may provide more than just a migrational advantage in breast cancer as well. CXCR4 may also help the metastasized cells establish and survive in secondary environments. Since alternative environments like bone marrow and lymph node are not normally compatible with cells from the breast, cancer cells must both derive, and provide signals to favorably shape the tumor microenvironment to a state conducive to tumor cell survival [*2*].

Due to its more recent discovery, much less is known about CXCR7; however, CXCR7 was shown to promote tumor growth in breast cancer and lung cancer [*5*]. Introduction of CXCR7 into the human breast cancer cell line, MDA-MB-435 conferred a growth advantage to these cells and promoted cell adhesion *in vitro* and small molecule antagonists of CXCR7 reduced tumor growth and increased survival of mice engrafted with CXCR7-expressing tumor lines (IM9 human B lymphoma, A549 human lung carcinoma, and LL/2 mouse lung carcinoma) [*4*]. Additionally, knockdown of CXCR7 by RNA interference of 4T1 murine breast cancer cells introduced into mice (both immunodeficient and immunocompetent) reduced the tumor formation compared to siRNA control and wild type mice [*5*].

Although CXCL12 can bind to both CXCR4 and CXCR7, it is likely that these receptors act through different signaling mechanisms. For one, CXCR4 and CXCR7 contribute to different aspects of development, as previously described (see Chapter 1) [*17*]. Also, CXCR7 does not activate migration or calcium mobilization pathways typically associated with chemokine receptors, and consistent with this observation, it contains a modified sequence motif for G protein coupling (“DRY” motif) compared to most other chemokine receptors [*4, 17*]. Nevertheless, CXCR7 does appear to signal, as it promotes tumor cell proliferation, survival and adhesion [*5*]. Yet, unlike CXCR4, CXCR7 is unlikely to directly promote metastasis since it does not directly activate cell migration.

The mechanisms and downstream pathways of CXCR7 activation are largely unknown at this time as is its role in cancer [*18*]. As such, examining whether CXCR7 and CXCR4 activate distinct signaling pathways and function independently and/or through cross-regulation in the context of breast cancer is important.

The effects of CXCR7 and CXCR4 co-expression on signaling and function has been debated for some time, although it remains unclear whether they function independently, additively/synergistically, or in a trans-inhibitory manner and may likely be context/cell type dependent. CXCR7 has been proposed as a decoy receptor that sequesters CXCL12 from activating CXCR4 and constitutively internalizes and recyles to degrade chemokine [*19-20*]. Additionally, CXCR7 and CXCR4 were shown to heterodimerize, potentially leading to transinhibition of CXCR4 signaling, as previously described in more detail (Chapter 1) [*20-22*]. On the other hand, co-expression of CXCR4 and CXCR7 was found to correlate with poor prognosis in renal cell carcinoma, suggesting they may have independent and/or additive effects on cancer progression [*8*]. Therefore, it remained to be determined how coexpression of both CXCR4 and CXCR7 on breast cancer cells would influence the signaling and tumor growth promoting properties of these receptors, since direct comparisons between CXCR4, CXCR7 and co-expressing breast cancer cells has not been performed.

The detailed mechanisms of how CXCR4 and CXCR7 enhance metastasis and/or tumor growth and their full implications for disease progression are unknown. Molecular strategies for survival and metastasis through well appreciated angiogenic and growth factor-mediated pathways are often the result of utilizing, and sometimes reprogramming, existing physiological mechanisms, which in this case are likely related to the role of CXCR4 and CXCR7 in survival and growth during development. Such signals could induce or nurture the nascent metastasis to become established lesions in

the secondary sites through direct or indirect growth promoting and survival effects on tumor cells [*23-24*]. Thus, characterizing the downstream signaling targets of CXCR4 and CXCR7 involved in survival and/or growth and elucidating potential consequences of their co-expression should yield a better understanding of their function in breast cancer and potentially reveal new opportunities for therapeutic intervention.

7.3 Generation of MDA-MB-231 Cell Sublines Expressing Varying Levels of CXCR4 and/or CXCR7

In order to elucidate the individual and combined effects of CXCR4 and CXCR7 in breast cancer cells, we first acquired and derived sublines of the MDA-MB-231 human breast cancer cell line. In addition to acquiring the parental cell line from ATCC, we were also provided a highly metastatic line of MDA-MB-231 (MDA-HM or High_Met) that was originally selected *in vivo* for the ability to metastasize to the lung (from Dr. Anja Müller, personal communication). One of the main differences between these cells and the ATCC cells is a much higher level of CXCR4 expression as determined by microarray (7th most upregulated gene), RT-PCR and flow cytometry (Figure 7.1). These data support that CXCR4 is advantageous for metastasis of breast cancer cells. In studies of MDA-MB-231 cells from ATCC, it was found that only a small population expressed CXCR4; these ATCC cells produced tumors and metastasized very slowly compared to cells that had been pre-selected for their ability to metastasize *in vivo* and showed high levels of CXCR4 (Figure 7.2). However, once the ATCC-derived cells began to form tumors and metastasize, they also expressed high CXCR4 suggesting a growth contribution from this receptor (data not shown).

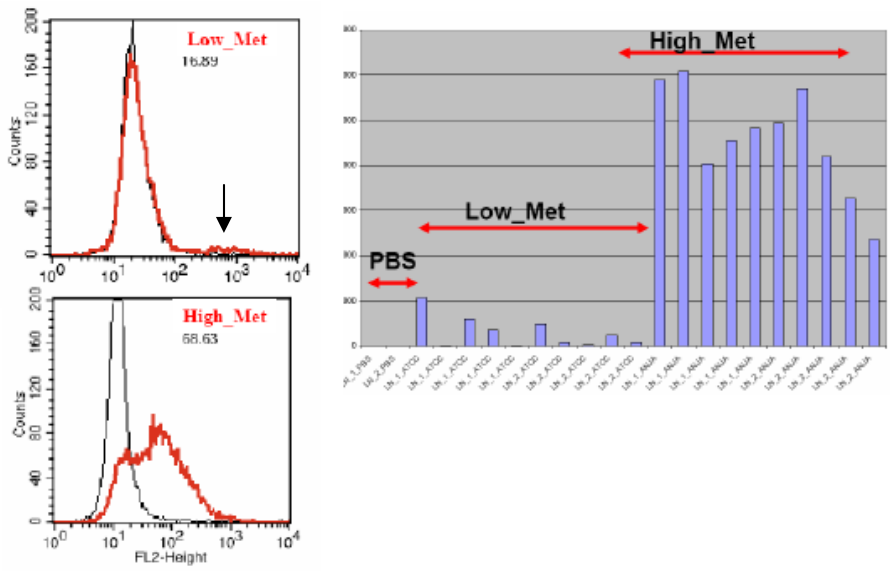

Figure 7.1 CXCR4 expression in MDA-MB-231 and MDA-HM cells. CXCR4 expression levels on MDA-MB-231 cells selected for metastatic potential (High_Met, MDA-HM) or unselected ATCC line (Low_Met – black arrow) as assessed by flow cytometry with CXCR4 expression in red and IgG control in black (left panels) and by RT-PCR using an Hu CXCR4 TaqMan probe (right panel). These are unpublished data from Dr. Tracy Handel and Dr. Albert Zlotnik.

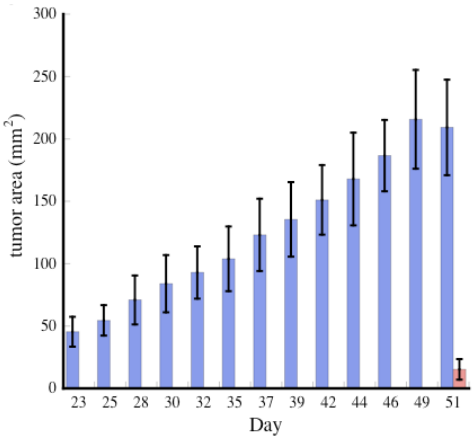

Figure 7.2 Comparison of primary tumor growth rates in ATCC MDA-MB-231 and MDA-HM cells in SCID mice. Growth (y-axis) of MDA-HM (blue) versus MDA-MB-231 (ATCC, red) in vivo as a function of time (x-axis). These are unpublished data from Dr. Tracy Handel and Dr. Albert Zlotnik.

Since these preliminary data were collected before CXCR7 was characterized, we examined CXCR7 expression in the various MDA-MB-231 lines. We determined that both the ATCC and MDA-HM cells have very low/no detectable surface CXCR7 expression based on flow cytometry analysis. However, these cells were found to have high intracellular levels of CXCR7 as determined by immunofluorescence (Figure 7.3) and flow cytometry (Figure 7.8) of permeabilized cells; these observations are consistent with other reports indicating presence of high intracellular populations and stores of CXCR7 [*19-20, 25*].

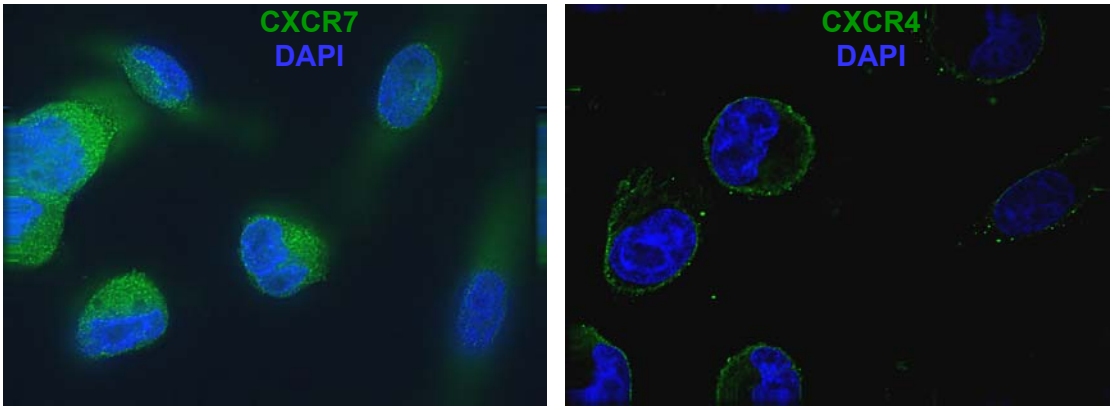

Figure 7.3 CXCR4 and CXCR7 localization in MDA-MB-231 cells. Immunofluorescence staining of CXCR7 (green, left panel) and CXCR4 (green, right panel) in permeabilized MDA-MB-231 cells. Results indicate significant intracellular localization of CXCR7 while CXCR4 is mostly surface expressed. DAPI staining of nuclei is shown in blue.

Thus, we sought to derive sublines of the ATCC MDA-MB-231 and MDA-HM cells to express high CXCR4 only, high CXCR7 only, or high of both receptors. Interestingly, we found that although the MDA-MB-231 cells directly from ATCC express low levels of CXCR4, an increase in CXCR4 expression was observed in these cells over passage in culture (an increase from <20% CXCR4+ cells to ~55% CXCR4+ cells was observed following ~20 passages in cell culture) (Figure 7.4). This indicates that there may be a selective advantage for the growth and proliferation of the CXCR4-expressing MDA-MB-231 cells in culture.

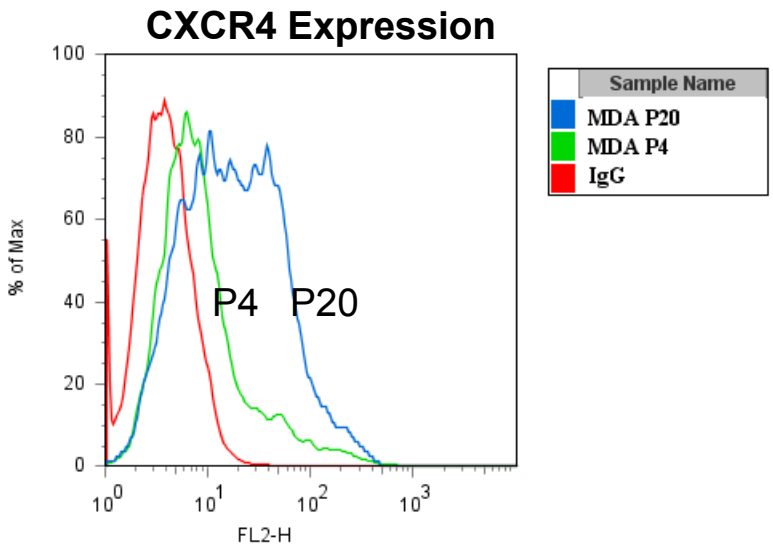

Figure 7.4 Increase in CXCR4 expression in MDA-MB-231 cells following passage in culture. Flow cytometry staining for surface expression of CXCR4 was performed to compare MDA-MB-231 cells that had been passaged 20 times (P20, brown) or 4 times (P4, blue) in culture compared to isotype control (green) and unstained (red) cells.

Due to this increase in CXCR4 expression over time, we initially attempted to sort MDA-MB-231 cells by fluorescence-activated cell sorting (FACS) to derive the various populations of CXCR4 and CXCR7 expressing sublines while still maintaining native/non-overexpressed levels of receptor. However, we found that these FACS-sorted lines did not maintain stable populations of selected receptor expression over time (data not shown). Nevertheless, an MTT proliferation assay on these initially FACS sorted sublines was performed to examine potential consequences of CXCR4 and CXCR7 expression on cell proliferation in culture. As shown in Figure 7.5, it appeared that the FACS sorted cells for CXCR7 expression had more rapid cell proliferation compared to unsorted cells, and this proliferation was independent of ligand stimulation. On a cautionary note, the commercially available CXCR7 antibody originally used to FACS sort these cells was recently reported to have non-specific binding effects in a number of cell lines including the MDA-MB-231s [*26*], so solid conclusions cannot be drawn from

these data. However, these proliferation assays may be worth repeating on the more recently generated sublines described below.

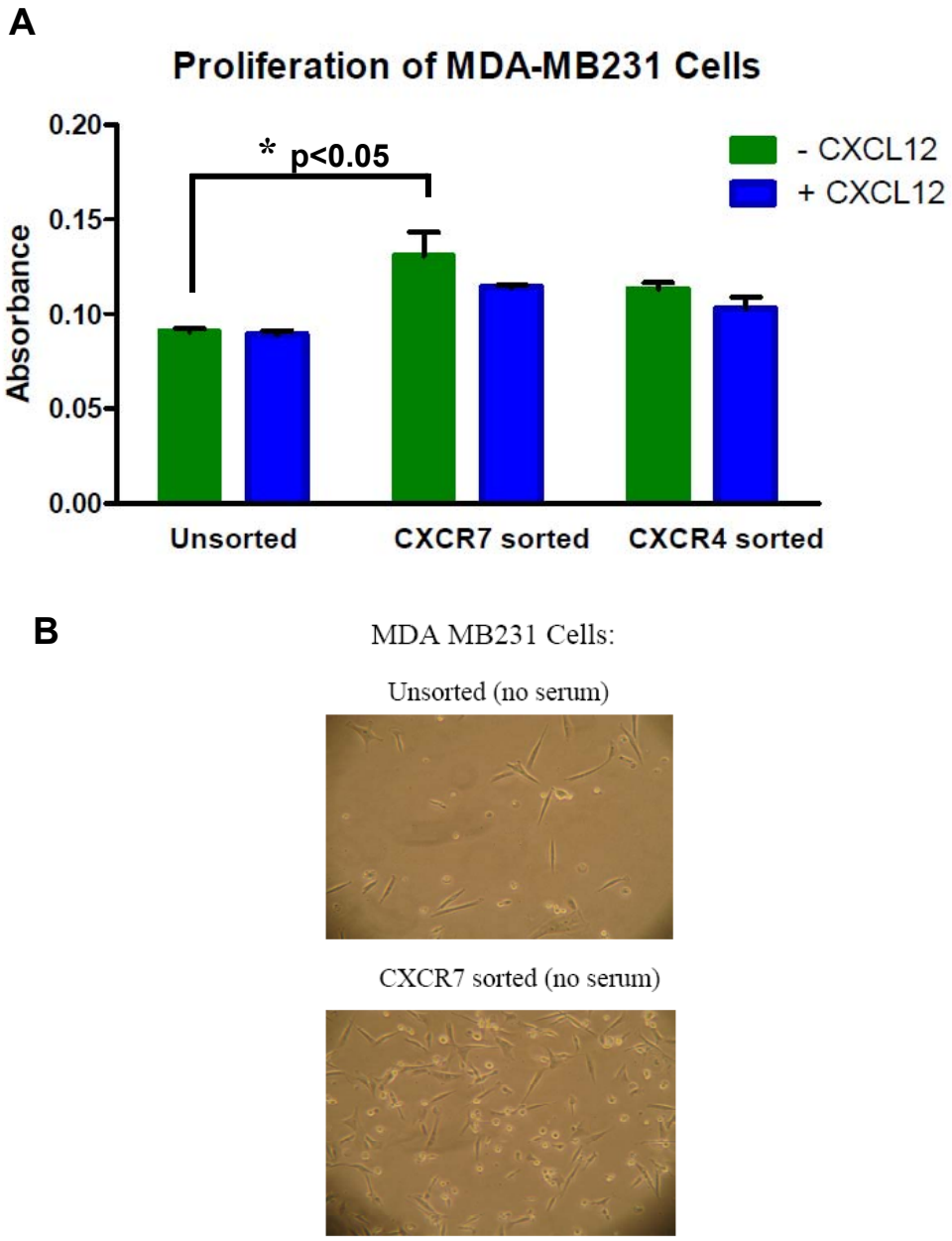

Figure 7.5 Proliferation of MDA-MB-231 cells FACS sorted for high CXCR7 or CXCR4 expression. A) Proliferation of unsorted, CXCR7 sorted and CXCR4 sorted MDA-MB-231 cells with and without 15 nM CXCL12 stimulation was assessed by MTT assay (average of 3 experiments each performed in triplicate). B) Image of unsorted compared to CXCR7 sorted MDA-MB-231 cells (equal numbers of cells seeded from the two populations) following 72 h of culture in serum-free media.

Since FACS sorting failed to generate sublines that maintained stable receptor expression, we generated sublines using a retroviral overexpression system instead. Additionally, a different CXCR7 antibody clone (11G8) became commercially available and was used to assess CXCR7 expression in all future experiments. First, we clonally selected for an MDA-MB-231 subline that had low CXCR7 levels and maintained low CXCR4 expression over repeated passage (termed “clonal line”). This clonal line was then retrovirally transduced with CXCR4, CXCR7, or both receptors (Figure 7.6). We also retrovirally expressed CXCR7 into the MDA-HM cells (which have endogenously high CXCR4) (Figure 7.7 and 7.11). This retroviral expression system enabled generation of sublines that maintained stable receptor expression levels over passage. Interestingly, we noticed that in generating these stable lines, selection with neomycin led to lower receptor levels than when selecting with puromycin (Figure 7.7). Although data presented herein involve the higher expressing, puromycin-selected cells, using different drug selections could allow for probing dose-dependent effects of receptor expression in future investigations. Additionally, while the majority of CXCR7 expression in ATCC MDA-MB-231 cells was intracellular, retroviral expression of CXCR7 results in high surface expression of the receptor (Figure 7.8).

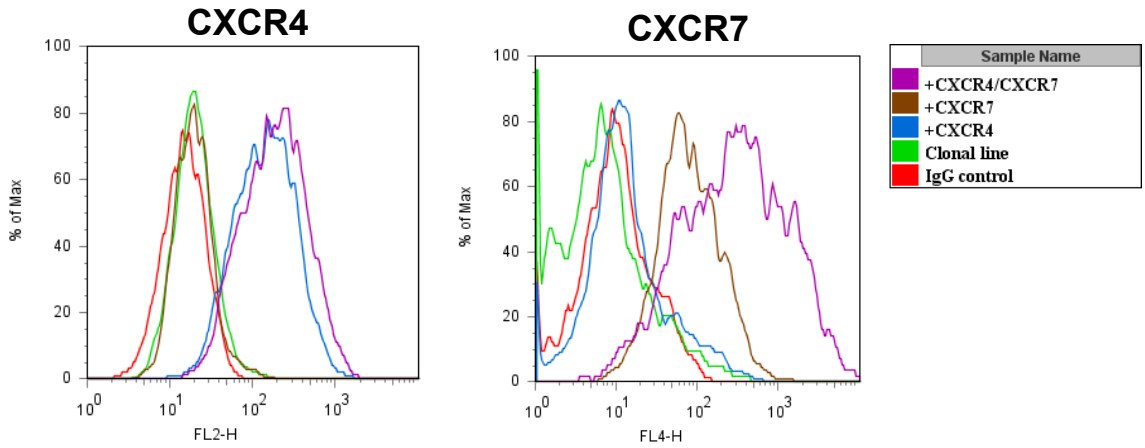

Figure 7.6 CXCR4 and CXCR7 expression in MDA sublines. Surface expression CXCR4 and CXCR7 expression in parental clonal MDA line and this line retrovirally transduced with CXCR4 and/or CXCR7 as monitored by flow cytometry.

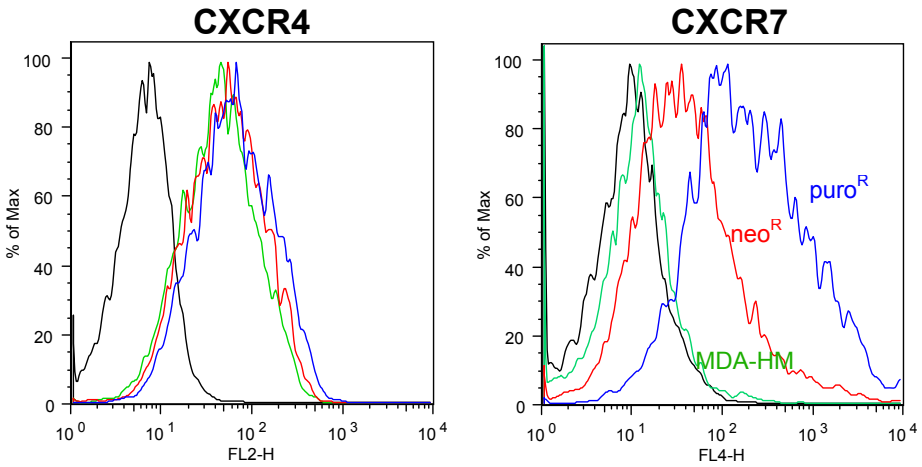

Figure 7.7 Differential expression of MDA-HM + CXCR7 transductions selected with either neomycin or puromycin. CXCR7 was cloned into a retroviral expression vector (pBABE) with neomycin- or puromycin-resistance genes and used to generate stable lines of MDA-HM cells with high (puro^R – blue) or moderate (neo^R – red) CXCR7 expression compared to MDA-HM cells (green) and IgG isotype control (black). CXCR4 (left) and CXCR7 (right) expression in these sublines was assessed by flow cytometry.

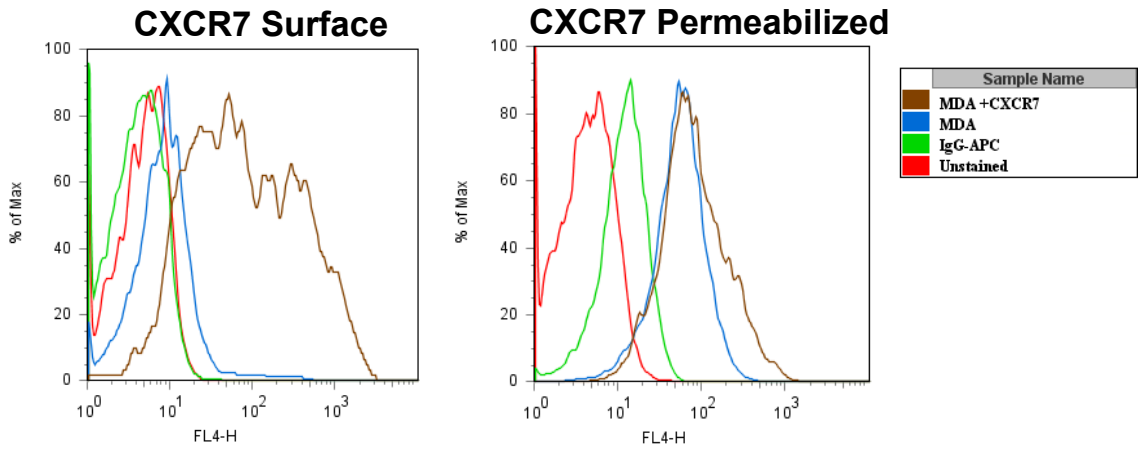

Figure 7.8 Surface and intracellular expression of CXCR7 in MDA-MB-231 cells. MDA-MB-231 cells (MDA, blue) and these cells retrovirally transduced with CXCR7 (brown) were stained for surface (left) or permeabilized and stained for total (right) CXCR4 expression and analyzed by flow cytometry. Unstained (red) and IgG (green) controls are both shown for reference.

7.4 CXCR4 and CXCR7 Accelerate Primary Tumor Growth

In order to assess the contributions of CXCR4 and CXCR7 to breast cancer tumor growth and metastasis, these MDA sublines described above were retrovirally transduced with GFP to enable visualization of metastases. These cells were then injected into the mammary fat pads of immunocompromised SCID mice and tumor growth and metastasis were monitored. First, primary tumor growth progression was compared between mice injected with the MDA clonal cell line (selected for low CXCR4 and CXCR7 expression) and mice injected with the clonal line stably expressing high levels of CXCR4, CXCR7, or both receptors. Our results supported previous findings that the CXCR4-high expressing cells had accelerated rates of primary tumor growth and metastasis; CXCR7 expressing cells also exhibited higher primary tumor growth rates compared to the parental clonal cells, but lower than the CXCR4 expressing cells (Figure 7.9). Surprisingly, the cells with both CXCR4 and CXCR7 yielded much slower

primary tumor growth rates and reduced metastasis compared to all other populations, including the parental clonal line with very low CXCR4 and CXCR7 (Figure 7.9 and data not shown). These results suggest these receptors could potentially have transinhibitory effects on one another.

A

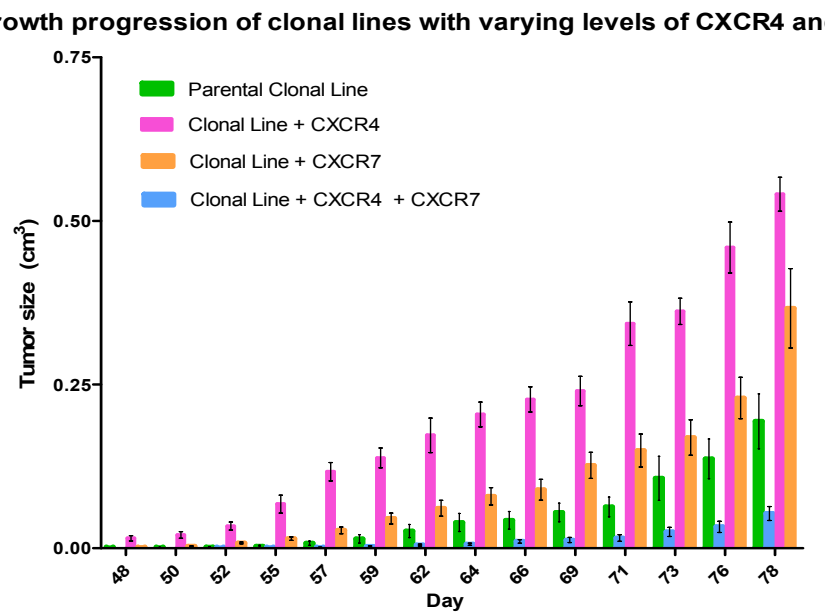

B

Population	%CXCR4+	%CXCR7+
Clonal line	4.2	4.1
Clonal line+CXCR4	84.5	7.5
Clonal line+CXCR7	4.2	70
Clonal line+CXCR4+CXCR7	89	87

Figure 7.9 Analysis of primary tumor growth and metastasis of MDA sublines expressing different levels of CXCR4 and CXCR7. A) Primary tumor growth curves between mice injected with the MDA-MB-231 parental clonal cell line (selected for low CXCR4 and CXCR7 expression) and mice injected with clonal lines stably expressing high levels of CXCR4, CXCR7, or CXCR4 and CXCR7. Size estimates were measured by caliper. B) Percent of cells expressing CXCR4 and CXCR7 receptors in the clonal line and the clonal line with retroviral expression of CXCR4 and/or CXCR7. Percentages were calculated based on flow cytometry data relative to an IgG isotype control.

.

Additionally, while lymph nodes (LNs), lung, spleen, and liver were collected for analysis of metastasis, the vast majority of metastases were observed in the LNs and lungs and not many were seen in the liver or spleen; therefore, we focused our future analyses on lung and LN metastases. Although tumors were allowed to grow to ~1.5 cm in diameter before euthenizing the mice and examining metastases (so populations of mice were sacrificed at different times), there were overall limited amounts of metastases from all of the populations of cells derived from the clonal cell line. While some metastases were observed in the CXCR4 expressing lines, it was difficult to quantitiatively compare the levels of metastases in the various different populations. The primary tumor growth rates of the clonal lines were also slower compared to ATCC MDA-MB-231 cells (parental clonal cells taking ~120 days to reach 1.5 cm diameter), suggesting that other factors limiting tumor growth and metastatic potential may have been selected with this clone besides just low CXCR4 expression. Nevertheless, lung and LN metastases harvested from mice injected with the parental clonal cells exhibited a large increase in CXCR4 expression compared to the primary tumor cells, reconfirming the importance of CXCR4 to the metastatic capacity of these breast cancer cells (Figure 7.10). However, the limitations in being able to fully quantify levels of metastases led us to employ the more aggressive MDA-HM cells, with or without retroviral CXCR7 expression, in order to better elucidate functions of CXCR4 and CXCR7 on metastasis.

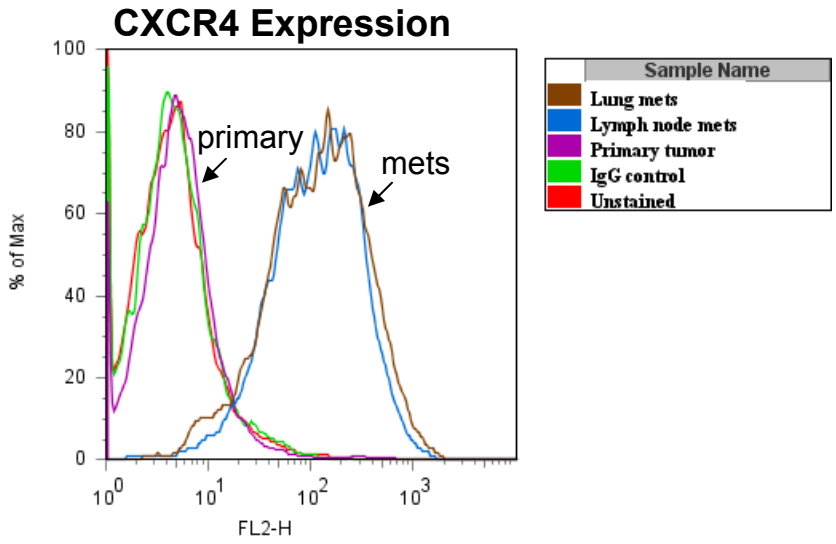

Figure 7.10 Comparison of CXCR4 expression in primary tumors and metastases. Expression of CXCR4 in primary tumors from the parental clonal line versus metastatic lesions ("mets") were compared between primary tumors, lymph node and lung metastases by flow cytometry, showing an increase in CXCR4 expression upon metastasis. CXCR7 expression remained low in all cells (data not shown).

As previously described, the MDA-HM cells have endogenously high CXCR4 levels, accelerated primary tumor growth rates and aggressive metastatic potential. Thus, these cells offered a faster and more conducive means for examining the effects of CXCR4 and CXCR7 coexpression on tumor growth and metastasis. MDA-HM cells and MDA-HM +CXCR7 cells (both expressing GFP) were injected into SCID mice, as previously described (Figure 7.11). Interestingly, although the dual receptor expressing cells led to an initial delay in primary tumor growth, they eventually yielded slightly larger tumor masses compared to the MDA-HM cells when the mice were euthenized after ~46-50 days. Tumor size based on caliper measurements and final tumor masses from a representative experiment (n=3) are shown in Figures 7.12 and 7.13. Therefore, in these highly metastatic cells, CXCR7 expression did not appear to have an overall inhibitory effect on tumor growth, and actually slightly enhanced tumor growth in the long term.

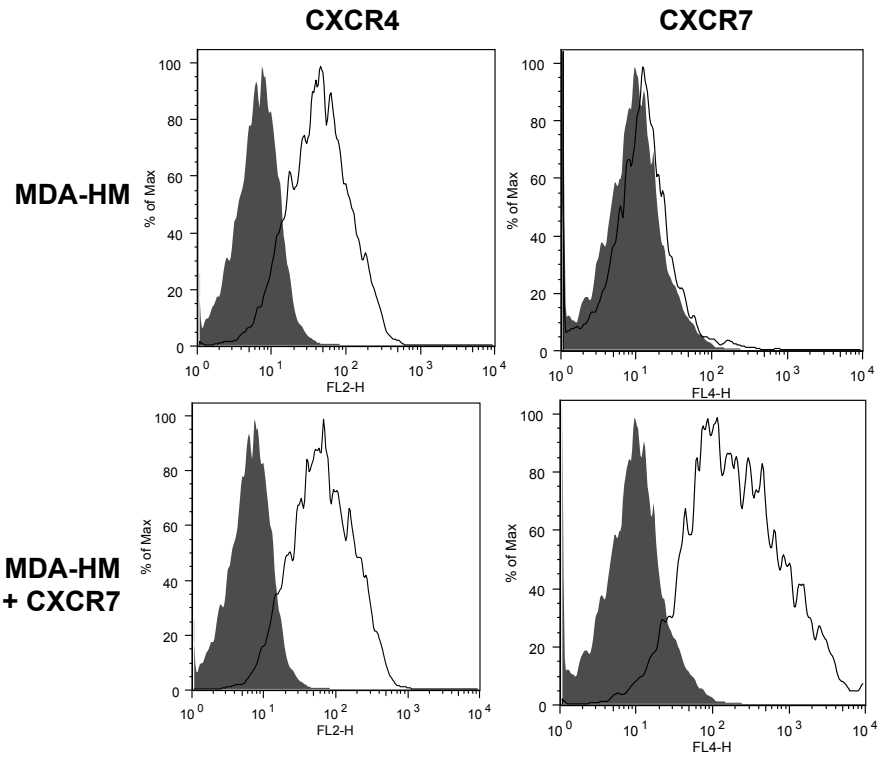

Figure 7.11 Comparison of CXCR4 and CXCR7 expression for MDA cell lines used for *in vivo* tumor metastasis mouse studies. CXCR4 expression is maintained for MDA-HM and MDA-HM + CXCR7 (top left, bottom left), while CXCR7 expression is elevated in the MDA-HM + CXCR7 line (bottom right) and not in MDA-HM (top right), as determined by flow cytometry analysis.

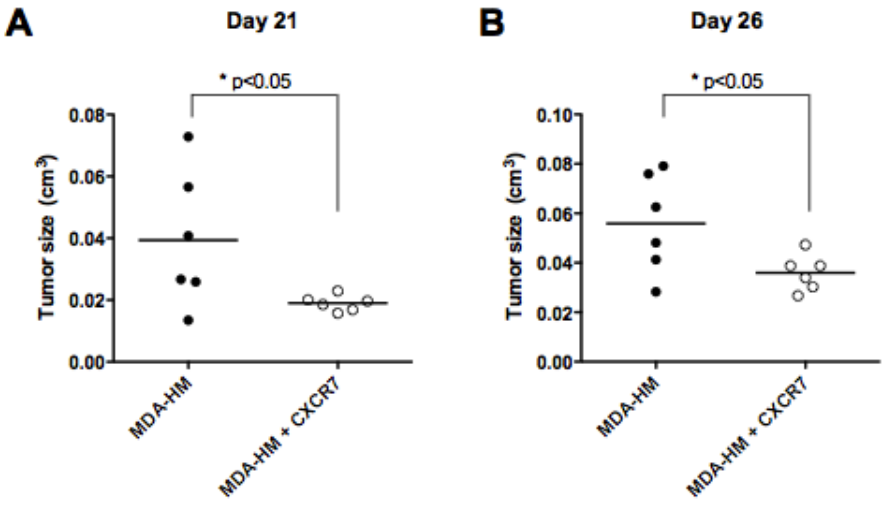

Figure 7.12 MDA-HM + CXCR7 cells exhibit an initial delay in primary tumor growth. Comparison of MDA-HM and MDA-HM + CXCR7 tumor sizes at day 21 and day 26 post injection.

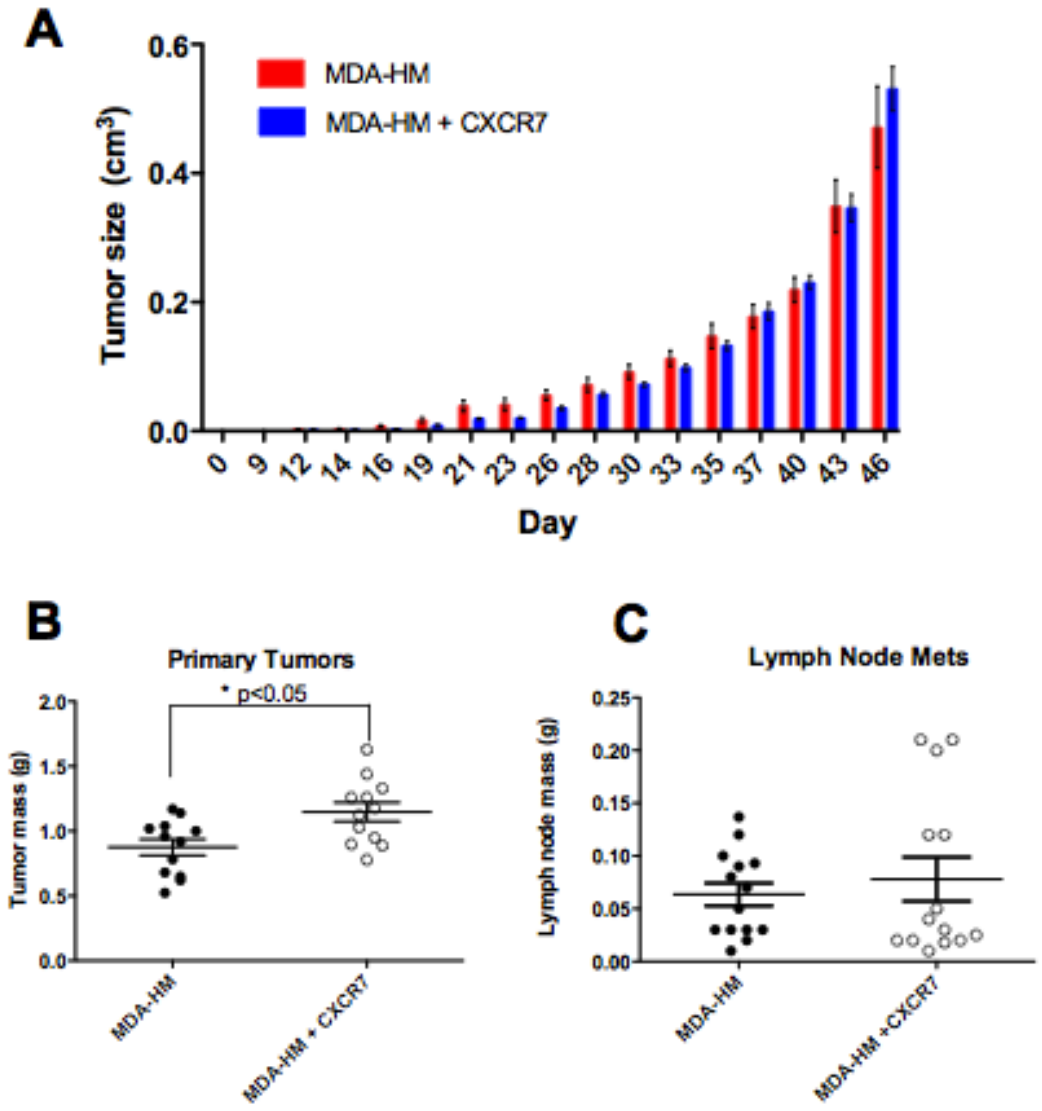

Figure 7.13 Effects of CXCR7 expression on primary tumor growth of MDA-HM cells. A) Primary tumor growth of MDA-HM and these cells retrovirally transduced with CXCR7 (MDA-HM +CXCR7) in SCID mice were compared. B) Although similar growth patterns were observed between these lines (4A), the final tumor masses after 48 days were slightly larger in the CXCR7-expressing cells. C) No significant differences in Lymph node metastasis was noticed between the MDA-HM and MDA-HM +CXCR7 cells.

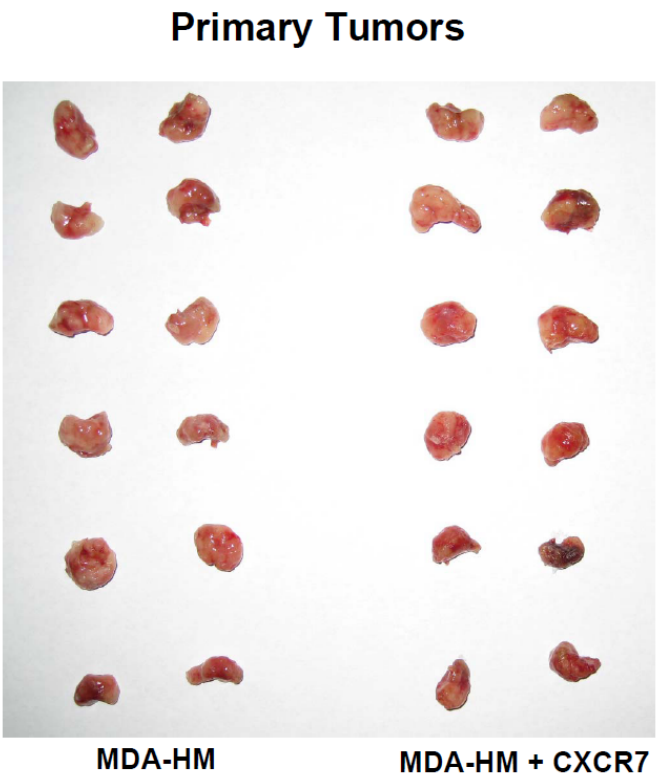

Figure 7.14 Comparison of primary growth from MDA-HM or MDA-HM +CXCR7 cells. Image comparing primary tumor size from SCID mice injected with MDA-HM (left) and MDA-HM + CXCR7 (right) cells. Data is from a representative experiment of 3 performed.

7.5 CXCR7 Expression Reduces Extent of Lung Metastasis

Since CXCR7 expression in the context of these highly metastatic MDA-MB-231 cells did not appear to have much of an inhibitory effect on primary tumor growth as was observed for cells from the co-receptor expressing clonal line (Figures 7.13 and 7.14), we next examined whether it had an effect on metastasis. Although CXCR7 expression in the MDA-HM line did not have an effect on size or number of lymph node metastases observed as quantified by lymph node tumor masses in Figure 7.13C, it led to a striking decrease in the levels of lung metastases observed (Figures 7.15 and 7.16). This observation cannot be attributed to differences in primary tumor size, since the MDA-HM +CXCR7 tumors were slightly larger. Additionally, the difference observed in the effects

of CXCR7 on lymph node metastasis (no effect) versus lung metastasis (inhibitory effect) is intriguing. It is possible that metastasis to the lymph nodes is more rapid and so could be lower in the CXCR7-expressing cells at earlier stages in the tumor progression. It could also be due to differences in how cells migrate through the lymphatic system versus blood vessels and how CXCR7 may be involved in/modulate these processes.

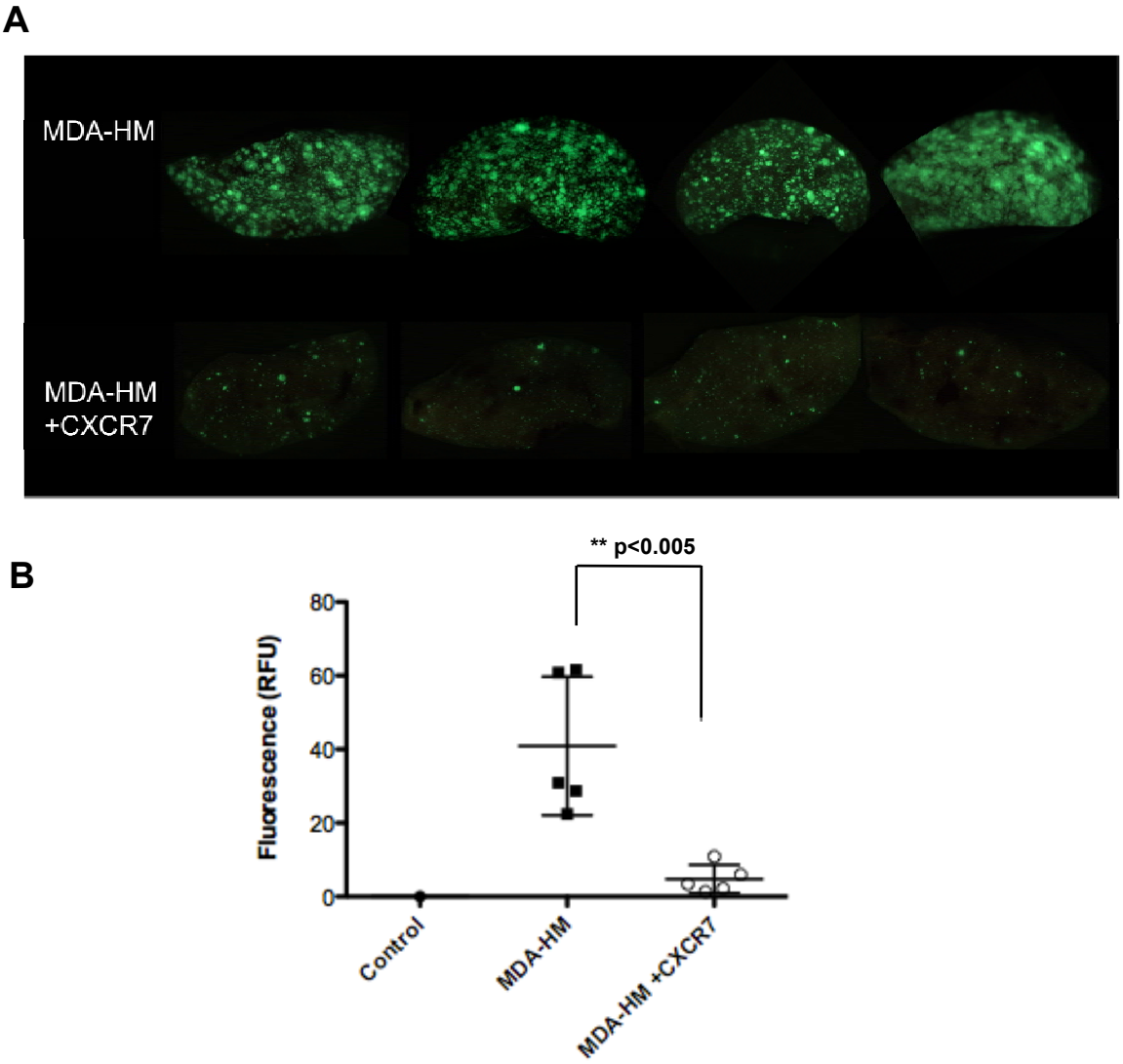

Figure 7.15 Comparison of lung metastasis of MDA-HM and MDA-HM + CXCR7 cells. A) Representative images of GFP+ metastases in lung lobes from 4 mice injected with MDA-HM cells (top) and 4 mice injected with MDA-HM+CXCR7 cells. B) Quantification of fluorescence from GFP+ metastases in lungs from mice injected with MDA-HM cells compared to MDA-HM+CXCR7 cells. Data from a representative experiment out of 3 performed. Statistical significance was determined by a student's t-test.

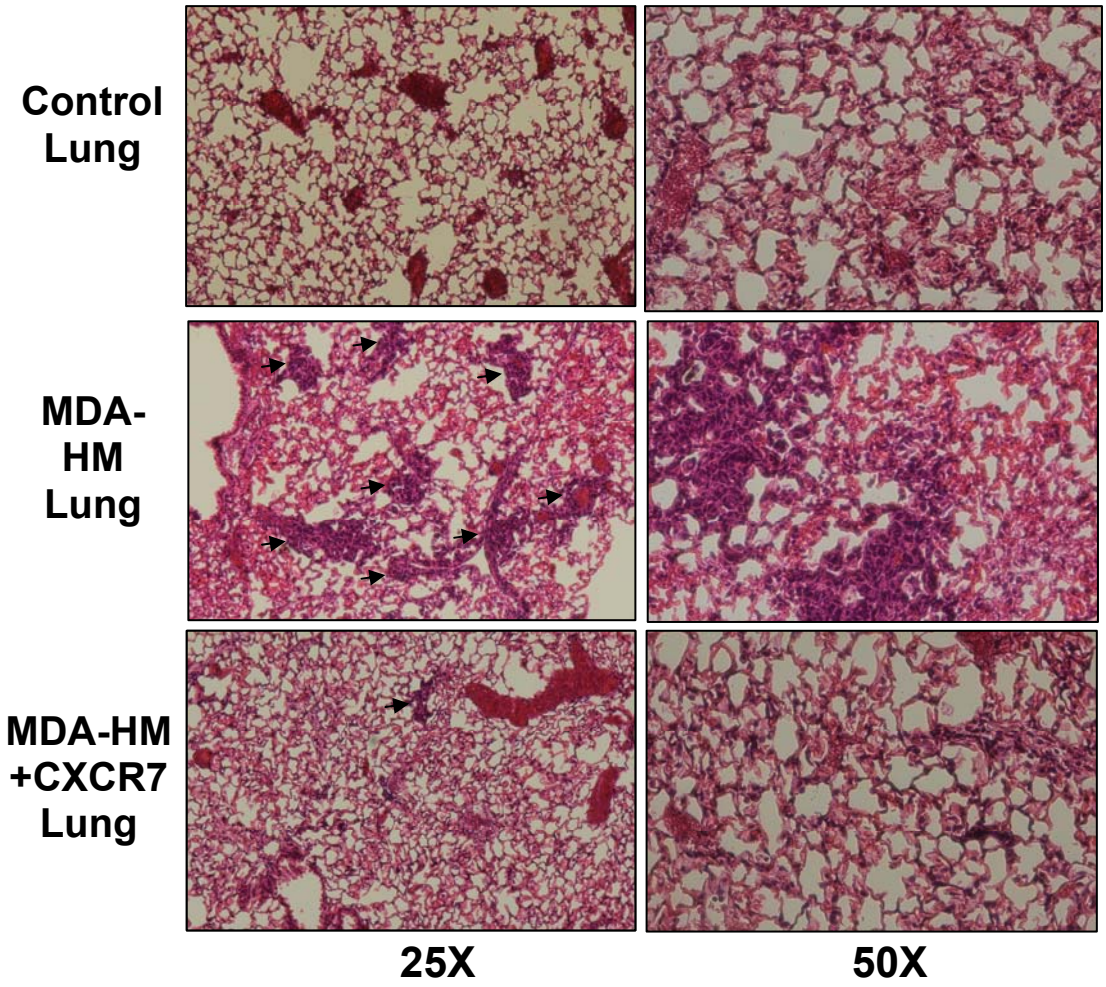

Figure 7.16 Histology of lung sections from control mice and mice injected with MDA-HM or MDA-HM +CXCR7 cells. Images (at 25x (left) and 50x (right) magnification) of hematoxylin and eosin (H&E) stained lung cross-sections from control mice (top) and mice injected MDA-HM (middle) or MDA-HM + CXCR7 (bottom) cells. Regions of dark purple staining as indicated by black arrows indicate sites of metastases.

7.6 *In Vitro* Analysis of CXCR4 and CXCR7 Signaling

In order to investigate potential mechanisms by which CXCR7 may have the observed inhibitory effects on lung metastasis and better evaluate the underlying molecular effects, we performed several *in vitro* internalization and signaling assays. Calcium mobilization (calcium flux) is a well-established consequence of CXCR4 activation by CXCL12 that is not observed upon stimulation of CXCR7. Therefore, we

compared calcium flux response to CXCL12 in the MDA-HM and MDA-HM+CXCR7 cells to see if the presence of CXCR7 affected CXCR4-mediated signaling responses. Consistent with the inhibitory effects of CXCR7 on metastasis to the lung, the MDA-HM +CXCR7 cells exhibited a lower maximal calcium flux response to CXCL12 compared to the MDA-HM cells (Figure 7.17). Even at saturating concentrations of CXCL12 (1 and 4 μM), the MDA-HM+CXCR7 cells did not reach the same levels of calcium flux response, suggesting that ligand sequestration alone cannot account for the inhibitory effects observed. Additionally, the EC50 response between the MDA-HM and MDA-HM+CXCR7 cells were well within an order of magnitude (56 nM vs 130 nM, respectively), so CXCR7 primarily influenced the efficacy rather than the potency of CXCL12-mediated calcium flux (Figure 7.17 C).

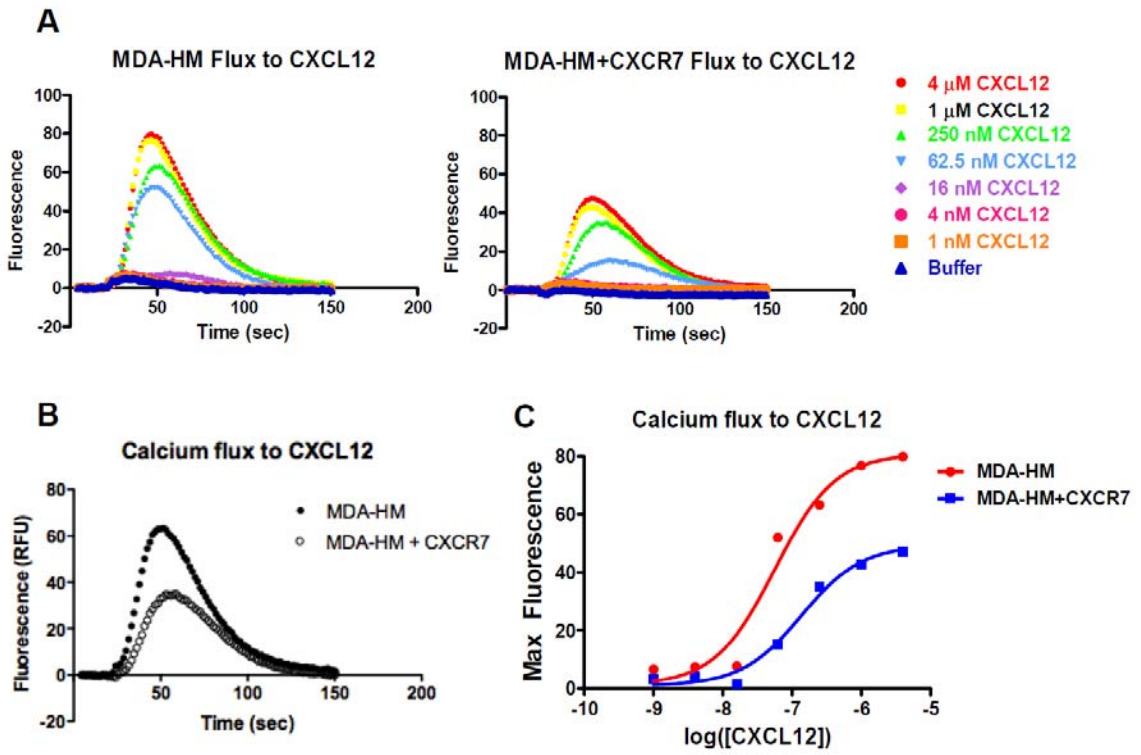

Figure 7.17 Calcium flux response to CXCL12 in MDA-HM and MDA-HM+CXCR7 cells. A) Calcium flux of MDA-HM (left) and MDA-HM+CXCR7 (right) cells was measured in response to varying concentrations of CXCL12 (0 nM- 4 μM) using a calcium sensitive fluorescent dye (FLIPR system) and monitoring fluorescence using a Molecular Devices flex station. B) Direct comparison of calcium flux response in MDA-HM (solid circle) versus MDA-HM+CXCR7 (open circle) cells to 250 nM CXCL12 stimulation. C) Graph depicting dose response for maximal fluorescence/calcium flux in MDA-HM (red) and MDA-HM+CXCR7 (blue) cells. Max fluorescence is plotted against the log of CXCL12 concentration (M).

In addition to calcium mobilization, CXCL12 is known to activate a number of intracellular kinase signaling cascades leading to phosphorylation and activation of Akt and ERK1/2 and inactivation of PDCD4 [*14, 27-28*]. These proteins are known to be important for mediating growth and survival of cells. Therefore, we examined phosphorylation of these proteins over a time course of CXCL12 stimulation (0-30 min) in the ATCC MDA-MB-231 (MDA) cells and these cells transduced with CXCR4, CXCR7 or both receptors. (Note: the MDA-HM cells have very high basal levels of Akt and

ERK1/2 phosphorylation even following long (48 h) serum starve conditions, so it is difficult to observe strong CXCL12-induced phosphorylation responses in these cells). Overall, the strongest CXCL12-mediated phosphorylation responses were observed in the MDA+CXCR4 cells and this response was generally slightly reduced in the dual receptor expressing cells (Figure 7.18). Another interesting observation was that the lines expressing CXCR4 and/or CXCR7 had higher basal levels of ERK1/2 and PDCD4 phosphorylation, suggesting that these overexpressed receptors, including CXCR7, may have some constitutive/basal level of activity over the MDA cells. Although Akt phosphorylation was not observed in the MDA cells without additional CXCR4 expression, the low levels of endogenous CXCR4 were enough to observe CXCL12-mediated ERK1/2 and PDCD4 phosphorylation in these cells (Figure 7.18).

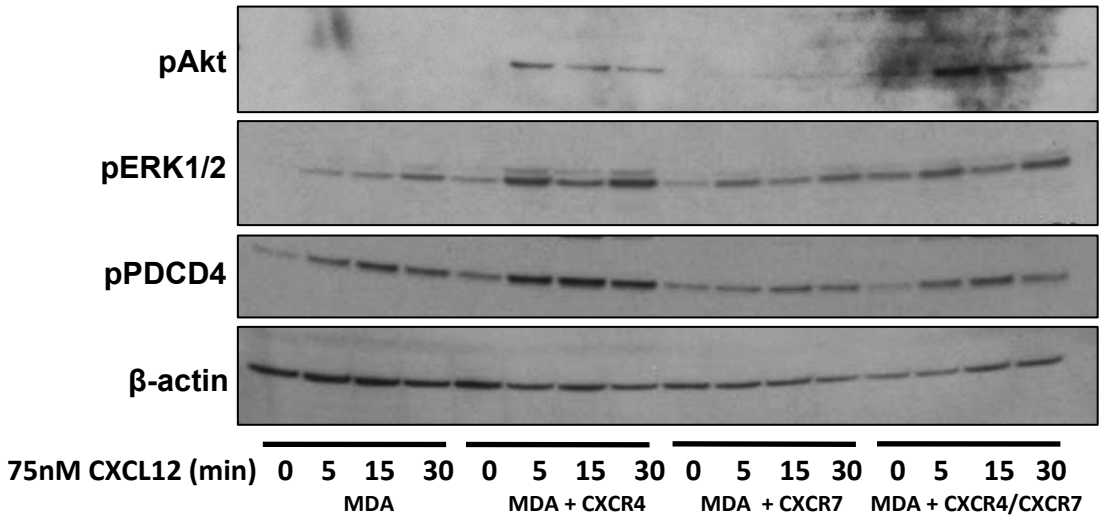

Figure 7.18 CXCL12-mediated phosphorylation of Akt, ERK1/2 and PDCD4 in MDA sublines. ATCC MDA-MB-231 (MDA) cells and these cells retrovirally transduced with CXCR4, CXCR7, or both receptors (CXCR4/CXCR7) were left unstimulated or stimulated for 5, 15 or 30 min with CXCL12. Western blots were performed to detect phosphorylated levels of Akt, ERK1/2 and PDCD4 and β-actin served as a loading control.

We further investigated the effects of CXCR7 expression on CXCL12-mediated PDCD4 phosphorylation and inhibition. Phosphorylation of PDCD4 by Akt and p70-S6K results in its inhibition, thereby relieving inhibition of AP-1 transcription and eIF4A translation by PDCD4. As described previously in Chapter 6, CXCL12 induces a robust phosphorylation and inhibition of PDCD4 in CLL cells, and as we show here, in the MDA-MD231 breast cancer cells as well. Since a slight delay in PDCD4 phosphorylation was observed in the MDA cells expressing CXCR7 (Figure 7.18), we decided to investigate this effect further in the MDA-HM and MDA-HM+CXCR7 cells. Similarly, we found that the CXCR7-expressing cells showed a delay in the CXCL12-mediated PDCD4 phosphorylation, as very little phosphorylation was detected at 3 min although a good response was observed a little later at 15 min following stimulation (Figure 7.19 A). Additionally, we used small molecule inhibitors to better dissect the mechanisms of the PDCD4 phosphorylation response in these cells: pertussis toxin (PTx) is an inhibitor of Gi signaling, AMD3100 (AMD) is an inhibitor of CXCR4 and CCX-771 (771) is an inhibitor of CXCR7. Both PTx and AMD were able to block CXCL12-mediated PDCD4 phosphorylation in the MDA-HM cells and 771 led to a slight, perhaps non-specific reduction in phosphorylation. Interestingly, although AMD still completely abrogated the CXCL12-mediated PDCD4 phosphorylation in the MDA-HM +CXCR7 cells, PTx and 771 were not able to fully inhibit the phosphorylation response (Figure 7.19 B). Although CXCR7 does not appear to interfere with binding of AMD to CXCR4, the observed decrease in pertussis toxin-sensitivity with CXCR7 expression suggests that there could be some interference with pertussis toxin sensitivity and perhaps G-protein accessibility.

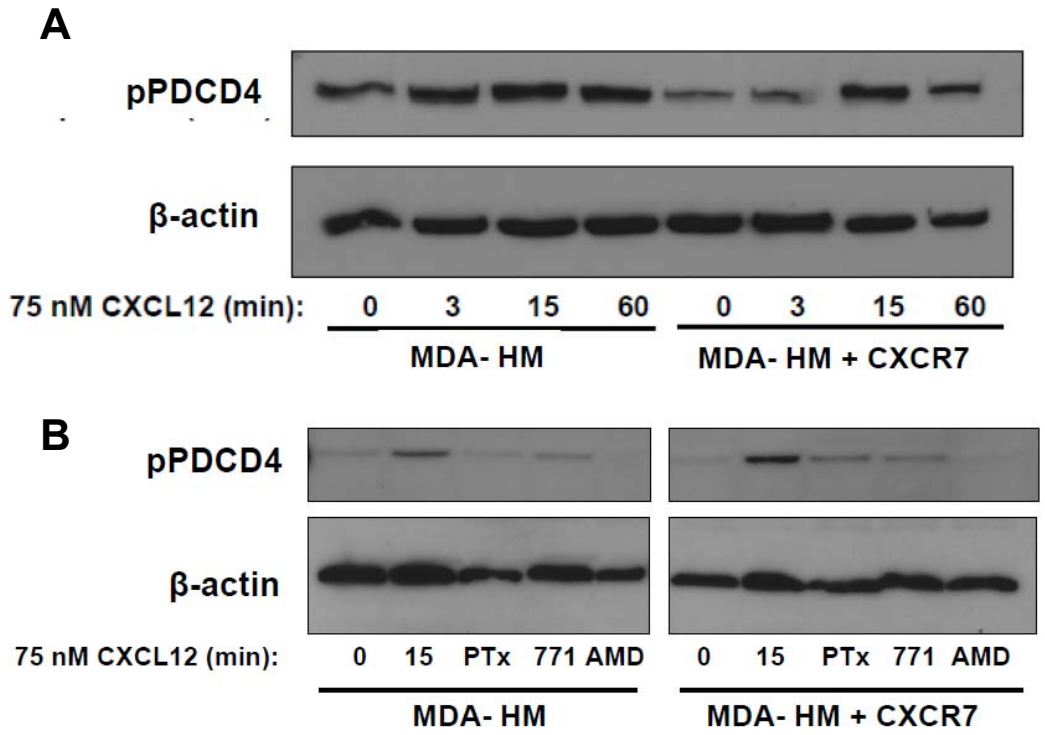

Figure 7.19 CXCL12-mediated PDCD4 phosphorylation in MDA-HM versus MDA-HM+CXCR7 cells. A) Western blot detecting phosphorylated PDCD4 (pPDCD4) in MDA-HM and MDA-HM+CXCR7 cells stimulated over a 60 min time course with 75 nM CXCL12. β-actin served as a loading control. B) MDA-HM and MDA-HM+CXCR7 cells were left unstimulated (0) or stimulated for 15 min with CXCL12 following 1 h pretreatment with DMSO control (15), 200 ng/mL Pertussis toxin (PTx), 1 μM CCX-771 (771), or 40 μM AMD3100 (AMD). Western blots were performed probing for PDCD4 phosphorylation and β -actin as a loading control.

7.7 CXCR4 WHIM Mutant Reduces CXCR7 Internalization in Response to CXCL12

It is clear from our data as well as previously published results that CXCR7 expression can alter CXCR4-mediated signaling and function. However, there is considerable debate in the field regarding whether CXCR7 merely sequesters CXCL12 ligand thereby modulating CXCR4 activation or has a more direct effects on CXCR4 signaling through heterodimerization. Based on our results demonstrating a loss of pertussis-toxin sensitivity in CXCR7-expressing cells and data showing a reduction in

calcium flux efficacy in cells expressing both CXCR4 and CXCR7 versus just CXCR4, it seems that CXCR7 may have more direct effects on CXCR4 function rather than simply ligand sequestration.

Thus, to better assess the relevance of CXCR4-CXCR7 heterodimerization beyond the previously published BRET and FRET studies indicating association of the receptors [*17, 22*], we used a mutant of CXCR4 based on WHIM syndrome that exhibits defective internalization properties [*29*]. WHIM syndrome (warts, hypogammaglobulinemia, immunodeficiency, myelokathexis) is an immunodeficiency disease characterized by neutropenia, hypogammaglobulinemia, and high HPV susceptibility that is caused by mutations leading to the truncation of the C-terminus of CXCR4. These mutations in CXCR4 impair desensitization of the receptor, leading to enhanced and prolonged responses to CXCL12. Interestingly, the majority of WHIM patients exhibit heterozygous genetic mutations in the *CXCR4* gene and therefore co-express wild-type (WT) and mutant receptors [*29*]. Since the WT-receptor also showed prolonged surface expression and loss of desensitization, this suggested that these mutations had dominant effects and that WT and mutant CXCR4 could heterodimerize [*30-31*].

Therefore, we used a WHIM-guided CXCR4 truncation mutant, CXCR4 R334X, to determine if it could alter CXCR7 internalization properties in a similar manner to WT-CXCR4, as this would suggest a physical association of CXCR4 and CXCR7. First, we performed a control experiment to assess CXCL12-mediated internalization in CXCR4 R334X versus WT CXCR4 expressing MDA cells as well as in cells co-expressing CXCR7. As expected, addition of CXCL12 led to a significant decrease in WT CXCR4 surface expression while CXCR4 R334X remained on the cell surface similar to unstimulated cells. Similar results were observed for WT CXCR4 and CXCR4 R334X

internalization properties in MDA cells also expressing CXCR7 (Figure 7.20). We next determined whether CXCR7 still internalizes or maintains surface expression in the presence of CXCR4 R334X. Since CXCR4 R334X was expressed with puromycin selection, CXCR7 was expressed with neomycin selection in these cells and so CXCR7 levels were lower (as described in Figure 7.7). It will be important to repeat this experiment with cells expressing higher levels of CXCR7 using puromycin selection and the CXCR4 R334X with neomycin selection in order to get better separation of surface CXCR7 levels in the presence or absence of CXCL12. Nevertheless, the results indicated that while CXCL12 induced CXCR7 internalization in the MDA+CXCR7/CXCR4 cells, this internalization was disrupted in the MDA cells co-expressing CXCR7 and the mutant CXCR4 R334X receptors (Figure 7.21). Quantifications of these data based on MFI are shown in Figure 7.22. These data provide evidence supporting the existence of a relevant CXCR4-CXCR7 heteromer. Therefore, it is possible that CXCR7 may mediate trans-inhibitory effects on CXCR4, for example via altering conformation changes in the receptor which could alter its ability to signal.

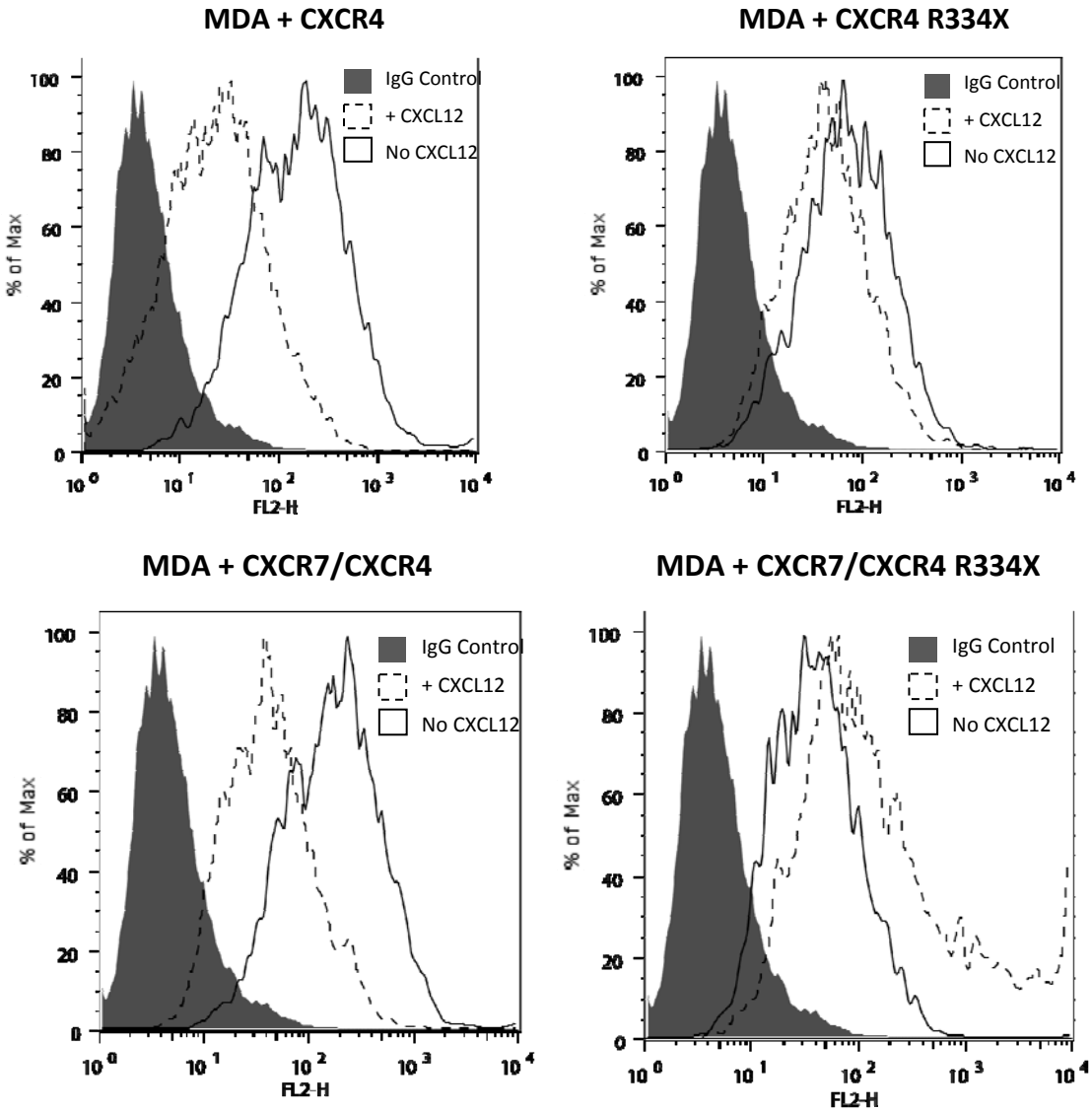

Figure 7.20 CXCR4 R334X disrupts CXCL12-mediated CXCR4 internalization. MDA (top) or MDA+CXCR7 (bottom) cells were transduced with WT CXCR4 or CXCR4 R334X and CXCR4 internalization in response to 45 min incubation with 200 nM CXCL12 was monitored by detecting a decrease in surface expression of CXCR4 as assessed by flow cytometry. IgG control stained cells (solid gray) and CXCR4-stained cells with no ligand stimulation (solid line) serve as reference points for the CXCR4 levels of CXCL12-stimulated cells (dashed line).

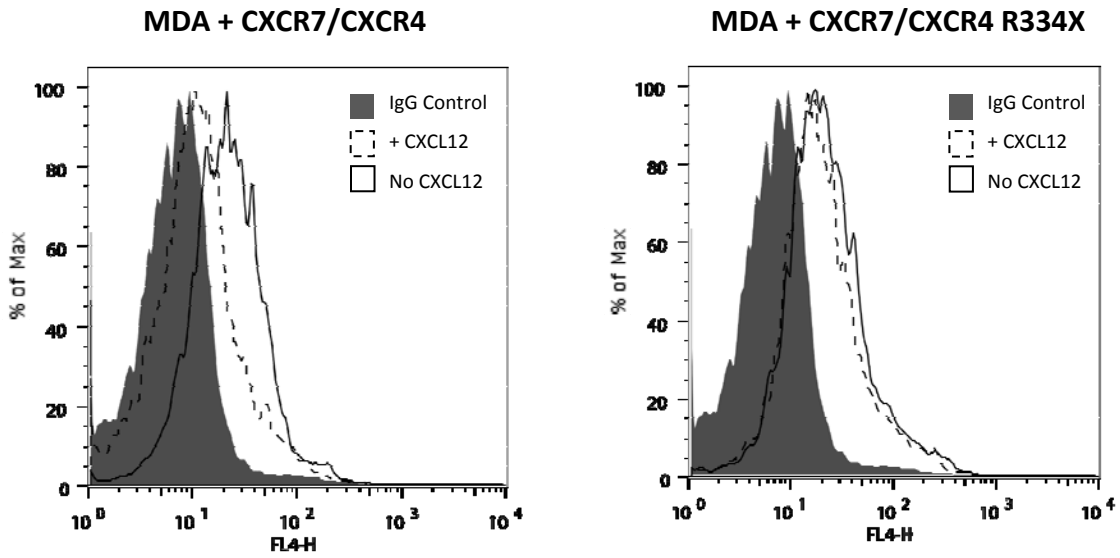

Figure 7.21 CXCR4 R334X disrupts CXCL12-mediated CXCR7 internalization. MDA+CXCR7 cells were transduced with WT CXCR4 or CXCR4 R334X and CXCR4 internalization in response to 45 min incubation with 200 nM CXCL12 was monitored by detecting a decrease in surface expression of CXCR7 as assessed by flow cytometry. IgG control stained cells (solid gray) and CXCR7-stained cells with no ligand stimulation (solid line) serve as reference points for the CXCR7 levels of CXCL12-stimulated cells (dashed line).

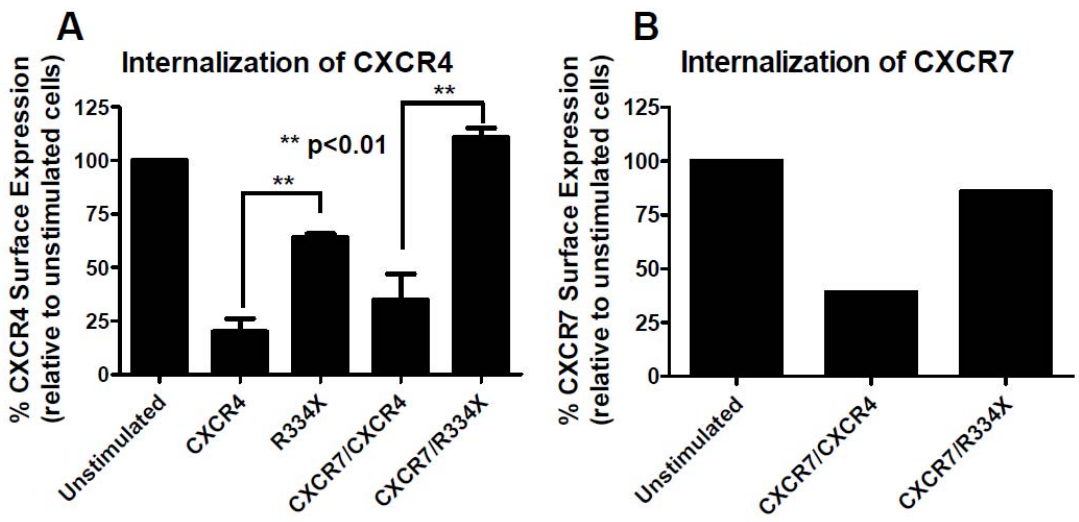

Figure 7.22 Percent of chemokine receptor remaining on surface after treatment with CXCL12. Cells incubated for 40 min in the presence or absence of 200 nM CXCL12 were stained with antibodies against CXCR4 or CXCR7 and receptor surface expression was assessed by flow cytometry. The relative % CXCR4 (A) or CXCR7 (B) surface expression was calculated as 100 x (Ft – Fi)/(Fu – Fi) where Fu = Mean fluorescence intensity of unstimulated cells, Fi = Mean fluorescence intensity of isotype control and Ft= Mean fluorescence intensity of CXCL12 treated cells. Mean fluorescent intensity was determined using FlowJo software. CXCR4 internalization data (panel A) represents average of 3 independent experiments and differences between WT CXCR4 and CXCR4 R334X were found to be statistically significant based on a student's t-test ($p<0.01$). Only a single experiment is shown for CXCR7 internalization (will be repeated).

7.8 Summary and Future Plans

In agreement with previous findings, we found that enhanced expression of CXCR4 or CXCR7 on MDA-MB-231 human breast cancer cells accelerated primary tumor growth [*4-5, 32*]. Interestingly, while high expression of CXCR4 promoted extensive metastasis to the lungs, cells co-expressing CXCR4 and CXCR7 exhibited a dramatic reduction in lung metastases. Since CXCR7 does not couple to Gi or directly activate migration and calcium mobilization responses like typical chemokine receptors, it was not too surprising that CXCR7 failed to promote tumor metastasis. However, the effects of co-expression of CXCR4 and CXCR7 is largely unexplored and the current literature presents conflicting data, implicating inhibitory [*17, 22*] as well as additive or

independent effects of CXCR7 [*18, 33-34*] on CXCR4-mediated cell migration and signaling. Additionally, it has been proposed that while CXCR7 does not directly promote cell migration, it may be critical for directional migration of primordial germ cells in zebrafish by sequestering and internalizing CXCL12 to shape the chemokine gradient [*21, 35*]. Recently, Zabel *et al* have also proposed an important function for CXCR7 in the transendothelial migration of human cancer cells, as addition of ligands selective for CXCR7 but not CXCR4 (the small molecule CCX-771 or endogenous ligand CXCL11) to B-lymphoblastoid cells (NC-37) endogenously co-expressing CXCR4 and CXCR7 blocked transendothelial migration of these cells to CXCL12 [*36*]. Therefore, this striking inhibition of lung metastasis in highly metastatic cells expressing CXCR4 and CXCR7, independent of effects on tumor growth, was intriguing.

In order to examine if the inhibitory effects of CXCR7 expression on metastasis were potentially due to inhibitory effects on CXCR4 signaling and function, a variety of *in vitro* cell signaling and internalization assays were performed. First, we showed that the cells co-expressing CXCR4 and CXCR7 (MDA-HM+CXCR7) had significantly reduced efficacy of calcium mobilization in response to CXCL12 stimulation than the cells expressing CXCR4 alone (MDA-HM), even at saturating concentrations of ligand. Furthermore, we observed an overall reduction in the CXCL12-induced phosphorylation of growth and survival regulating proteins Akt, ERK1/2 and PDCD4 in the co-receptor expressing cells. A delay in PDCD4 phosphorylation in the MDA-HM+CXCR7 versus MDA-HM cells was also observed and pertussis toxin sensitivity of the phosphorylation response was reduced in the cells expressing both receptors. One of our future plans is to perform transwell migration assays to compare migration of the MDA-HM and MDA-HM+CXCR7 cells to CXCL12 to provide complementary data to the lung metastasis results. This *in vitro* system also provides an opportunity to confirm that the observed

effects are due to inhibition of CXCR4 function rather than some other mechanism whereby CXCR7 may inhibit metastasis *in vivo*.

Overall, these data suggest a more direct transinhibitory effect of CXCR7 on CXCR4, for example through receptor heterodimerization [*17, 22*] as opposed to simply sequestration of CXCL12 [*19, 25, 35*]. To more definitively assess a functional role of CXCR4 and CXCR7 heterodimerization beyond BRET and FRET studies already published [*17, 22*], we performed internalization assays using a CXCR4 truncation mutant, CXCR4 R334X, that has impaired desensitization and prolonged signaling properties. Thus, if CXCR4 and CXCR7 form functional and stable heterodimers we would expect that expression of CXCR7 with CXCR4 R334X would impair its internalization in response to CXCL12 stimulation. Indeed, we found that similar to the impaired internalization of CXCR4 R334X in MDA-MB-231 cells and cells co-expressing CXCR7, CXCR7 internalization was also impaired in the CXCR7/CXCR4 R334X co-expressing cells. We would like to repeat these experiments in order to confirm these results and also perform internalization experiments using CXCL11, the other ligand for CXCR7 that does not bind to CXCR4. In this case, we would expect that if CXCR4 and CXCR7 are forming stable heteromers, CXCR4 will also be internalized along with CXCR7 in response to CXCL11 stimulation.

Additionally, we have demonstrated that a key distinction between the endogenous expression of these two receptors is that CXCR4 primarily localizes at the surface of MDA-MB-231 breast cancer cells, while CXCR7 largely localizes inside the cell. Therefore, receptor localization may be important for understanding the functions of CXCR7 and may influence how CXCR7 influences CXCR4 function, since functions of intracellular CXCR7 may be separate from its functions at the cell surface. Nevertheless, recent studies have demonstrated the ability of CXCR7 to shuttle between the cytosol

and the surface, suggesting that a large population of intracellular receptor may still be important to its biological function [*25*].

To more mechanistically investigate the individual and combined functions of CXCR4 and CXCR7, we also plan to perform more signaling analyses and *in vitro* functional assays (migration, proliferation, etc.) employing receptor antagonists selective for CXCR4 (AMD3100 or T140) or CXCR7 (CCX-771). These antagonists will allow us to better dissect the distinct signaling mechanisms and functions of these two receptors. Additionally, CXCR4 mutants to disrupt dimer formation but preserve ligand binding capabilities are being designed Irina Kufareva, a project scientist working with Dr. Ruben Abagyan and our lab; such mutants could aid in determining the function of the CXCR4/CXCR7 heterodimer and whether CXCR7 expression may have direct inhibitory effects on CXCR4 function. We are also in the process of expressing HA-tagged CXCR4 and CXCR7 receptors for the purpose of performing immunoprecipitations on the receptors to identify potential novel/distinguishing interacting partners (especially for CXCR7 since this is largely unknown) via mass spectrometry. Furthermore, microarray data collected by Dr. Tracy Handel during her sabbatical with Dr. Albert Zlotnik indicated that CXCR4 activation may have indirect effects on promoting tumor growth through the upregulation of other receptors known to be important in breast cancer including prolactin receptor, growth hormone receptor, and prostaglandin E3 receptor. While we were unable to confirm these results through Q-PCR analysis, it is likely that CXCR4 and/or CXCR7 could have numerous indirect effects on transcription of various proteins important for tumorigenesis and collecting new microarray data may be worthwhile for future endeavors.

Overall, these data suggest that CXCR7 can modulate the activity of CXCR4 signaling and function in human breast cancer cells. While expression of CXCR4 or

CXCR7 in MDA-MB-231 cells enhanced primary tumor growth, CXCR4 had much more pronounced effects on promotion of tumor growth. Additionally, our results suggest that tumor cells expressing CXCR4 alone or both CXCR4 and CXCR7 may have different metastatic potentials; specifically, CXCR7 expression on CXCR4-expressing cancer cells may actually reduce the ability of these cells to metastasize to distant sites. Experiments to determine whether these inhibitory effects of CXCR7 expression on CXCR4 signaling and function are direct or indirect are currently in progress, although preliminary data suggests more direct mechanisms.

7.9 Materials and Methods

Cells and Reagents

MDA-MB-231 and HEK293t cells were acquired from the American Tissue Cultture Collection (ATCC). MDA-HM cells were kindly provided by Dr. Anja Müller and Dr. Albert Zlotnik. Pertussis toxin was purchased from List Biological Laboratories, AMD3100 from Sigma, and CCX-771 was kindly provided by Mark Penfold at Chemocentrix. Tissue culture media and FBS were from Gibco. Retroviral GFP, CXCR4, CXCR7 and CXCR4 R334X constructs were cloned into pBABEblast (GFP), pBABEpuro or pBABEneo vectors (Addgene), kindly provided by Dr. Jing Yang. Retrovirus was packaged by transfection of 1 μg of plasmid DNA, 0.9 μg of pUCMV3 and 0.1 μg VSVG into HEK293t cells in a 6 cm dish. Viral supernatants were collected 48 h and 72 h following transfection and used to infect the MDA-MB-231 cells. Cells were stably selected using 5 μg/mL Blasticidin (Invitrogen), 5 μg/mL puromycin (Invitrogen) or 0.7 mg/mL Geneticin/neomycin (Gibco). Details of retroviral transfection and infection procedure are provided in Appendix AI.8.

Flow Cytometry

Cells were lifted with 1 mM EDTA, centrifuged at 250 x g for 10 min at 4°C and cell pellets were resuspended in a 0.5% bovine serum albumin (BSA) (Sigma) in Phosphate Buffered Saline (PBS) solution. Cells (250,000-500,000) were stained for CXCR4 expression using a PE-conjugated antibody (BD Pharmingen) or CXCR7 expression using an APC-conjugated antibody (clone 11G8) (R&D systems). Corresponding PE-conjugated and APC-conjugated IgG isotype controls were also used according to manufacturer's protocol, as a reference point (BD Pharmingen and R&D systems). Cells were washed 3 times with 0.5% BSA-PBS solution and then resuspended in 400 µL volume for flow analysis. Flow cytometry data was collected on a FACSCalibur cytometer (BD Biosciences) and analyzed using FlowJo software.

MTT Proliferation Assay

Cells were resuspended in RPMI media without phenol red and 100,000 cells per well (100 µl volume) were seeded into a 96-well plate in triplicate samples and incubated overnight at 37°C/5%CO_2. Add 10 µL of 5 mg/mL MTT reagent (Sigma) prepared in RPMI (without phenol red) to each well and let cells incubate with reagent at 37°C/5%CO_2 for 2.5 – 3 h. Reagent was aspirated and cells were resolubilized and mixed well with buffer containing 0.04 M HCl in isopropanol. Absorbances at 570 nm and 650 nm were read using a Molecular Devises SpectraMax M5 plate reader. See Appendix AI.29.

Immunofluorescence

Cells were grown on a cover slip for 24 h, fixed with 4% paraformaldehyde (PFA) for 15 min, permeabilized with 0.5% Triton X-100 in PBS for 10 min, washed and

blocked with SeaBlock (Pierce/Thermo Scientific). Samples were incubated with primary antibodies for 2 h at room temperature, washed and then incubated with AlexaFluor488 secondary antibody (Invitrogen) for 30-45 min. After washing, cover slips were mounted onto slides with Prolong Gold (Invitrogen) and allowed to dry overnight in the dark. Images were acquired on a DeltaVision deconvolution microscope as part of the UCSD Cancer Center shared resource (see Appendix AI.25).

Tumor Growth and Metastasis Studies

Severe Combined Immunodeficiency (SCID) mice were obtained from Charles River and 7-8 week old female mice were anesthetized with continuous isoflurane administration during surgical procedure. Two million GFP-expressing cells in a 50:50 mix with matrigel (BD Biosciences) were injected into both 4^{th} inguinal mammary fat pads of the mice. Tumor size was estimated by caliper measurements 3 times per week until tumors reached 1.5 cm diameter, at which point the mice were euthanized. Primary tumors and lymph node metastases were weighed and measured for final size and imaged using a fluorescence dissection scope (Zeiss) to confirm MDA tumor cell origin based on GFP fluorescence. Lungs were perfused with 4% PFA for fixation and histology analysis or collected for imaging metastases by fluorescence dissection scope (Zeiss) and fluorescence quantification. For quantification of lung metastases based on GFP fluorescence, lungs were homogenized as previously described [*37*] and fluorescence was measured using a Molecular Devices SpectraMax M5 plate reader. Values were normalized against lungs from control mice (no cells injected). H&E stained slides for histology were prepared by the UCSD Histology Shared Resource. Representative data from a total of 3 independent experiments with the MDA-HM and

MDA-HM +CXCR7 cells are shown. All mouse studies were approved by UCSD IACUC. More detailed protocols are included in Appendix AI.30-32.

Calcium Flux Measurements

Calcium flux assays were performed using the Molecular Devices Calcium 4 assay kit and measurements were acquired using a Molecular Devices FlexStation3 (Molecular Devices Corporation, Sunyvale, CA). Cells were lifted with 1 mM EDTA, washed twice in 0.5%BSA-PBS, and then resuspended at $2.5x10^6$ cells/mL in assay buffer (1x Hanks Balanced salt solution, 20 mM Hepes, pH7.4, 0.1% BSA). One hundred microliters of cell suspension and 100 µL of Calcium 4 dye were distributed to each well in a 96-well Biocoat plate (BD Biosciences, San Jose, CA) and incubated at 37°C/5%CO_2 for 1 hr prior to analysis. CXCL12 was diluted in ddH_2O and distributed into a 0.3 mL v-bottom 96-well plate (Corning Inc., Corning, NY) and 50 µL of CXCL12 or buffer was distributed to the assay plate with cells at the start of measurements with the use of the liquid handling capabilities of the FlexStation3. Calcium flux measurements were averaged between triplicate data points and normalized against the buffer control calcium flux response. A more detailed calcium flux protocol is provided in Appendix AI.33.

Western Blots and Antibody Reagents

MDA-MB-231 cells at ~70-80% confluency were serum starved for 24 h at 37°C/5%CO_2 and then stimulated with 75 nM CXCL12 over an hour time course. For inhibitor studies, cells were pre-treated with 40 µM AMD3100 (Sigma), 1 µM CCX-771 or 200 ng/ml Pertussis toxin (List Biological Laboratories) for 1 h prior to stimulation with 75 nM CXCL12 for 15 min. Cells were lysed on ice for 30 min in Ripa buffer (10 mM Tris-Cl

pH7.4, 150 mM NaCl, 1% Triton X, 0.1% Na-Deoxycholate, 0.1%SDS and 5 mM EDTA) containing Complete protease inhibitor cocktail (Roche, Palo Alto, CA) and Halt phosphatase inhibitors (Pierce). Lysates were clarified by centrifugation at 20,000 rcf for 10 min at 4°C. A BCA protein assay (Pierce) was performed to determine total protein concentration and 20 µg of total protein was loaded into each well of 10% SDS-PAGE gels. Gels were transferred onto PVDF membranes (Bio-Rad), blocked with 5% milk-TBST, and incubated overnight at 4°C with primary antibodies. Blots were washed 3 times for 10 min with Tris Buffered Saline + 0.1% Tween (TBST) and then incubated for 1 h at room temperature with secondary antibodies conjugated to HRP, washed again 3 times with TBST and then developed with Amersham ECL-plus (GE-healthcare) or SuperSignal West femto-sensitivity reagent (Pierce). Blots were stripped with Restore western blot stripping solution (Pierce) for 10 min at room temperature and then re-probed with other antibodies and/or β-actin as a loading control. Primary antibodies were diluted into 5% BSA-TBST at recommended concentrations. The antibody against phospho-PDCD4 (S457) was obtained from Rockland, phospho-ERK1/2 was from Upstate and all other antibodies were obtained from Cell Signaling Technology (see Antibody Information in Appendix II). Detailed wester blot protocol is provided in Appendix AI.23.

Internalization Assay

A decrease in surface expression of receptor following CXCL12 stimulation was used to assess internalization. Cells were seeded into 6-well plates for internalization assay and the next day were stimulated with 200 nM CXCL12 for 40 min at 37°C/5%CO_2. After this time, cells were washed with PBS to remove any unbound CXCL12 and harvested with 1 mM EDTA on ice. Cells were either washed first with an

acid wash buffer (50 mM glycine + 100 mM NaCl pH 3) to remove any surface bound CXCL12 that could interfere with antibody binding or directly resuspended in 0.5%BSA-PBS for antibody staining. (Note CXCR4-PE antibody, clone 1D9 does not interfere with CXCL12 binding and so acid wash is not required). Staining and flow cytometry analysis were performed as described above. More experimental details are provided in Appendix AI.24.

ACKNOWLEDGEMENTS

Experiments presented in this chapter represent equal contributions from Catherina Salanga and the dissertation author. Figures 7.1 and 7.2 show unpublished data collected by Dr. Tracy Handel during her sabbatical with Dr. Albert Zlotnik. Dr. Jing Yang also provided considerable guidance and resources for the experiments performed in this chapter.

REFERENCES

1. Gupta, G. P., and Massague, J. (2006) Cancer metastasis: building a framework, *Cell 127*, 679-695.

2. Balkwill, F. (2004) The significance of cancer cell expression of the chemokine receptor CXCR4, *Semin Cancer Biol 14*, 171-179.

3. Muller, A., Homey, B., Soto, H., Ge, N., Catron, D., Buchanan, M. E., McClanahan, T., Murphy, E., Yuan, W., Wagner, S. N., Barrera, J. L., Mohar, A., Verastegui, E., and Zlotnik, A. (2001) Involvement of chemokine receptors in breast cancer metastasis, *Nature 410*, 50-56.

4. Burns, J. M., Summers, B. C., Wang, Y., Melikian, A., Berahovich, R., Miao, Z., Penfold, M. E., Sunshine, M. J., Littman, D. R., Kuo, C. J., Wei, K., McMaster, B. E., Wright, K., Howard, M. C., and Schall, T. J. (2006) A novel chemokine receptor for SDF-1 and I-TAC involved in cell survival, cell adhesion, and tumor development, *J Exp Med 203*, 2201-2213.

5. Miao, Z., Luker, K. E., Summers, B. C., Berahovich, R., Bhojani, M. S., Rehemtulla, A., Kleer, C. G., Essner, J. J., Nasevicius, A., Luker, G. D., Howard, M. C., and Schall, T. J. (2007) CXCR7 (RDC1) promotes breast and lung tumor growth in vivo and is expressed on tumor-associated vasculature, *Proc Natl Acad Sci U S A 104*, 15735-15740.

6. Gupta, S. K., and Pillarisetti, K. (1999) Cutting edge: CXCR4-Lo: molecular cloning and functional expression of a novel human CXCR4 splice variant, *J Immunol 163*, 2368-2372.

7. Lu, W., Gersting, J. A., Maheshwari, A., Christensen, R. D., and Calhoun, D. A. (2005) Developmental expression of chemokine receptor genes in the human fetus, *Early Hum Dev 81*, 489-496.

8. D'Alterio, C., Consales, C., Polimeno, M., Franco, R., Cindolo, L., Portella, L., Cioffi, M., Calemma, R., Marra, L., Claudio, L., Perdona, S., Pignata, S., Facchini, G., Carteni, G., Longo, N., Pucci, L., Ottaiano, A., Costantini, S., Castello, G., and Scala, S. (2010) Concomitant CXCR4 and CXCR7 expression predicts poor prognosis in renal cancer, *Curr Cancer Drug Targets 10*, 772-781.

9. Hattermann, K., Held-Feindt, J., Lucius, R., Muerkoster, S. S., Penfold, M. E., Schall, T. J., and Mentlein, R. (2010) The chemokine receptor CXCR7 is highly

expressed in human glioma cells and mediates antiapoptotic effects, *Cancer Res 70*, 3299-3308.

10. Liang, Z., Yoon, Y., Votaw, J., Goodman, M. M., Williams, L., and Shim, H. (2005) Silencing of CXCR4 blocks breast cancer metastasis, *Cancer Res 65*, 967-971.

11. Redjal, N., Chan, J. A., Segal, R. A., and Kung, A. L. (2006) CXCR4 inhibition synergizes with cytotoxic chemotherapy in gliomas, *Clin Cancer Res 12*, 6765-6771.

12. Lee, C. H., Kakinuma, T., Wang, J., Zhang, H., Palmer, D. C., Restifo, N. P., and Hwang, S. T. (2006) Sensitization of B16 tumor cells with a CXCR4 antagonist increases the efficacy of immunotherapy for established lung metastases, *Mol Cancer Ther 5*, 2592-2599.

13. Zeelenberg, I. S., Ruuls-Van Stalle, L., and Roos, E. (2001) Retention of CXCR4 in the endoplasmic reticulum blocks dissemination of a T cell hybridoma, *J Clin Invest 108*, 269-277.

14. Nishio, M., Endo, T., Tsukada, N., Ohata, J., Kitada, S., Reed, J. C., Zvaifler, N. J., and Kipps, T. J. (2005) Nurselike cells express BAFF and APRIL, which can promote survival of chronic lymphocytic leukemia cells via a paracrine pathway distinct from that of SDF-1alpha, *Blood 106*, 1012-1020.

15. Zhou, Y., Larsen, P. H., Hao, C., and Yong, V. W. (2002) CXCR4 is a major chemokine receptor on glioma cells and mediates their survival, *J Biol Chem 277*, 49481-49487.

16. Kulbe, H., Levinson, N. R., Balkwill, F., and Wilson, J. L. (2004) The chemokine network in cancer--much more than directing cell movement, *Int J Dev Biol 48*, 489-496.

17. Sierro, F., Biben, C., Martinez-Munoz, L., Mellado, M., Ransohoff, R. M., Li, M., Woehl, B., Leung, H., Groom, J., Batten, M., Harvey, R. P., Martinez, A. C., Mackay, C. R., and Mackay, F. (2007) Disrupted cardiac development but normal hematopoiesis in mice deficient in the second CXCL12/SDF-1 receptor, CXCR7, *Proc Natl Acad Sci U S A 104*, 14759-14764.

18. Balabanian, K., Lagane, B., Infantino, S., Chow, K. Y., Harriague, J., Moepps, B., Arenzana-Seisdedos, F., Thelen, M., and Bachelerie, F. (2005) The chemokine

SDF-1/CXCL12 binds to and signals through the orphan receptor RDC1 in T lymphocytes, *J Biol Chem 280*, 35760-35766.

19. Naumann, U., Cameroni, E., Pruenster, M., Mahabaleshwar, H., Raz, E., Zerwes, H. G., Rot, A., and Thelen, M. (2010) CXCR7 functions as a scavenger for CXCL12 and CXCL11, *PLoS One 5*, e9175.

20. Luker, K. E., Steele, J. M., Mihalko, L. A., Ray, P., and Luker, G. D. (2010) Constitutive and chemokine-dependent internalization and recycling of CXCR7 in breast cancer cells to degrade chemokine ligands, *Oncogene*.

21. Dambly-Chaudiere, C., Cubedo, N., and Ghysen, A. (2007) Control of cell migration in the development of the posterior lateral line: antagonistic interactions between the chemokine receptors CXCR4 and CXCR7/RDC1, *BMC Dev Biol 7*, 23.

22. Levoye, A., Balabanian, K., Baleux, F., Bachelerie, F., and Lagane, B. (2009) CXCR7 heterodimerizes with CXCR4 and regulates CXCL12-mediated G protein signaling, *Blood 113*, 6085-6093.

23. Muller, A., Sonkoly, E., Eulert, C., Gerber, P. A., Kubitza, R., Schirlau, K., Franken-Kunkel, P., Poremba, C., Snyderman, C., Klotz, L. O., Ruzicka, T., Bier, H., Zlotnik, A., Whiteside, T. L., Homey, B., and Hoffmann, T. K. (2006) Chemokine receptors in head and neck cancer: association with metastatic spread and regulation during chemotherapy, *Int J Cancer 118*, 2147-2157.

24. Zlotnik, A. (2006) Involvement of chemokine receptors in organ-specific metastasis, *Contrib Microbiol 13*, 191-199.

25. Hartmann, T. N., Grabovsky, V., Pasvolsky, R., Shulman, Z., Buss, E. C., Spiegel, A., Nagler, A., Lapidot, T., Thelen, M., and Alon, R. (2008) A crosstalk between intracellular CXCR7 and CXCR4 involved in rapid CXCL12-triggered integrin activation but not in chemokine-triggered motility of human T lymphocytes and CD34+ cells, *J Leukoc Biol 84*, 1130-1140.

26. Berahovich, R. D., Zabel, B. A., Penfold, M. E., Lewen, S., Wang, Y., Miao, Z., Gan, L., Pereda, J., Dias, J., Slukvin, II, McGrath, K. E., Jaen, J. C., and Schall, T. J. (2010) CXCR7 protein is not expressed on human or mouse leukocytes, *J Immunol 185*, 5130-5139.

27. Messmer, D., Fecteau, J. F., O'Hayre, M., Bharati, I. S., Handel, T. M., and Kipps, T. J. (2011) Chronic lymphocytic leukemia cells receive RAF-dependent survival signals in response to CXCL12 that are sensitive to inhibition by sorafenib, *Blood 117*, 882-889.

28. O'Hayre, M., Salanga, C. L., Kipps, T. J., Messmer, D., Dorrestein, P. C., and Handel, T. M. (2010) Elucidating the CXCL12/CXCR4 signaling network in chronic lymphocytic leukemia through phosphoproteomics analysis, *PLoS One 5*, e11716.

29. Hernandez, P. A., Gorlin, R. J., Lukens, J. N., Taniuchi, S., Bohinjec, J., Francois, F., Klotman, M. E., and Diaz, G. A. (2003) Mutations in the chemokine receptor gene CXCR4 are associated with WHIM syndrome, a combined immunodeficiency disease, *Nat Genet 34*, 70-74.

30. Diaz, G. A. (2005) CXCR4 mutations in WHIM syndrome: a misguided immune system?, *Immunol Rev 203*, 235-243.

31. Diaz, G. A., and Gulino, A. V. (2005) WHIM syndrome: a defect in CXCR4 signaling, *Curr Allergy Asthma Rep 5*, 350-355.

32. Orimo, A., Gupta, P. B., Sgroi, D. C., Arenzana-Seisdedos, F., Delaunay, T., Naeem, R., Carey, V. J., Richardson, A. L., and Weinberg, R. A. (2005) Stromal fibroblasts present in invasive human breast carcinomas promote tumor growth and angiogenesis through elevated SDF-1/CXCL12 secretion, *Cell 121*, 335-348.

33. Wang, Y., Li, G., Stanco, A., Long, J. E., Crawford, D., Potter, G. B., Pleasure, S. J., Behrens, T., and Rubenstein, J. L. (2011) CXCR4 and CXCR7 have distinct functions in regulating interneuron migration, *Neuron 69*, 61-76.

34. Tarnowski, M., Grymula, K., Reca, R., Jankowski, K., Maksym, R., Tarnowska, J., Przybylski, G., Barr, F. G., Kucia, M., and Ratajczak, M. Z. (2010) Regulation of expression of stromal-derived factor-1 receptors: CXCR4 and CXCR7 in human rhabdomyosarcomas, *Mol Cancer Res 8*, 1-14.

35. Boldajipour, B., Mahabaleshwar, H., Kardash, E., Reichman-Fried, M., Blaser, H., Minina, S., Wilson, D., Xu, Q., and Raz, E. (2008) Control of chemokine-guided cell migration by ligand sequestration, *Cell 132*, 463-473.

36. Zabel, B. A., Wang, Y., Lewen, S., Berahovich, R. D., Penfold, M. E., Zhang, P., Powers, J., Summers, B. C., Miao, Z., Zhao, B., Jalili, A., Janowska-Wieczorek,

A., Jaen, J. C., and Schall, T. J. (2009) Elucidation of CXCR7-mediated signaling events and inhibition of CXCR4-mediated tumor cell transendothelial migration by CXCR7 ligands, *J Immunol 183*, 3204-3211.

37. Borsig, L., Wong, R., Hynes, R. O., Varki, N. M., and Varki, A. (2002) Synergistic effects of L- and P-selectin in facilitating tumor metastasis can involve non-mucin ligands and implicate leukocytes as enhancers of metastasis, *Proc Natl Acad Sci U S A 99*, 2193-2198.

CHAPTER 8

Conclusions and Future Perspectives

8.1 Perspectives and Summary

Approximately 10 years ago, Hanahan and Weinberg described six hallmarks of cancer: sustaining proliferation, resisting cell death, evading growth suppression, enabling replicative immortality, inducing angiogenesis, and activating invasion and metastasis [*1*]. Over the past decade, research in the cancer field has expanded these concepts to incorporate genome instability, reprogramming energy metabolism, tumor-promoting inflammation and evading immune destruction [*2*]. In particular, the concepts of tumor-promoting inflammation and evasion of immune destruction are at the center of a booming field directed towards understanding the tumor microenvironment. A link between cancer and inflammation and the immune system was proposed over 100 years ago, when Rudolf Virchow noted an infiltration of immune cells in neoplastic tissues and suggested the origin of cancer was at sites of chronic inflammation [*3*]. We are now starting to understand the importance of this link as it is becoming clear that the microenvironment and non-neoplastic cells can have a major role in shaping the growth and invasive properties of tumors.

Although the immune system is capable of recognizing abnormal properties of cancer cells leading to destruction of the tumor, and major efforts are being made to manipulate the immune system to this end [*4*], immune cells can also have tumor-promoting effects, particularly in the context of inflammation [*2-4*]. Under an inflammatory state, a milieu of growth factors, cytokines and chemokines are released by immune cells and stromal cells; these molecules can enhance the growth,

proliferation and survival of cancer cells as well as promote matrix remodeling and angiogenesis leading to invasive and metastatic capacities of these neoplastic cells [*2-4*]. Therefore, immune cells, stromal cells and extracellular matrix constituents can have "enabling" characteristics on tumor progression and invasion [*2*]. The intricacies of how non-neoplastic constituents of the tumor modify properties of cancer cells and vice versa, of how cancer cells may manipulate their surroundings to enable their growth and invasion, will be a major focus of research efforts in the years to come.

While a number of cytokines and growth factors in the extracellular milieu of the tumor microenvironment can extend growth, survival and invasive properties to cancer cells, my research has focused on the role of chemokines in this process [*5*]. Herein, the effects and signaling mechanisms downstream of the chemokine, CXCL12, on promoting the survival, growth, and metastasis of cancer cells were investigated and described. In particular, we elucidated some of the survival effects of CXCL12 on CLL cells and investigated the interplay between its two receptors, CXCR4 and CXCR7, in breast cancer growth and metastasis. By probing CXCL12-mediated signaling mechanisms and functions, we have unveiled a number of interesting considerations and potential targets for new therapeutic strategies for treatment of these cancers.

8.2 Summary and Future Directions for the Involvement of CXCL12 in CLL Survival

We investigated the response of CLL cells to CXCL12, a key factor that enhances CLL viability and is secreted by NLCs, cells of the CLL microenvironment that nurture CLL cell accumulation and survival [*6-7*]. We found that aggressive CLL cells, characterized by high ZAP-70 expression, derive increased survival benefits from CXCL12 compared to cells from patients with indolent disease. The enhanced survival is

accompanied by increased activation of the MEK/ERK survival pathway [*8*], while activation of Akt is more similar between the two subgroups in response to CXCL12. Strikingly, we found that the survival of CLL cells cultured in the presence of NLCs is blocked by the Raf inhibitor, sorafenib.

Future investigations to better understand the pathophysiology of aggressive-CLL will involve elucidating the origin of the differences in ERK/MEK signaling between aggressive and indolent CLL cells by examining the involvement of upstream molecules like Ras and PKC, and testing the contribution of ZAP-70 in the cascade (Figure 8.1). Comparison of cells derived from both patient subgroups (aggressive and indolent) therefore provides a unique opportunity for delineating specific signaling events contributing to aggressive disease. In turn, these findings will translate into a better understanding of the molecular signatures that distinguish cells from patients with aggressive versus indolent disease, and further provide a biological/functional explanation for the poor clinical outcome of aggressive CLL.

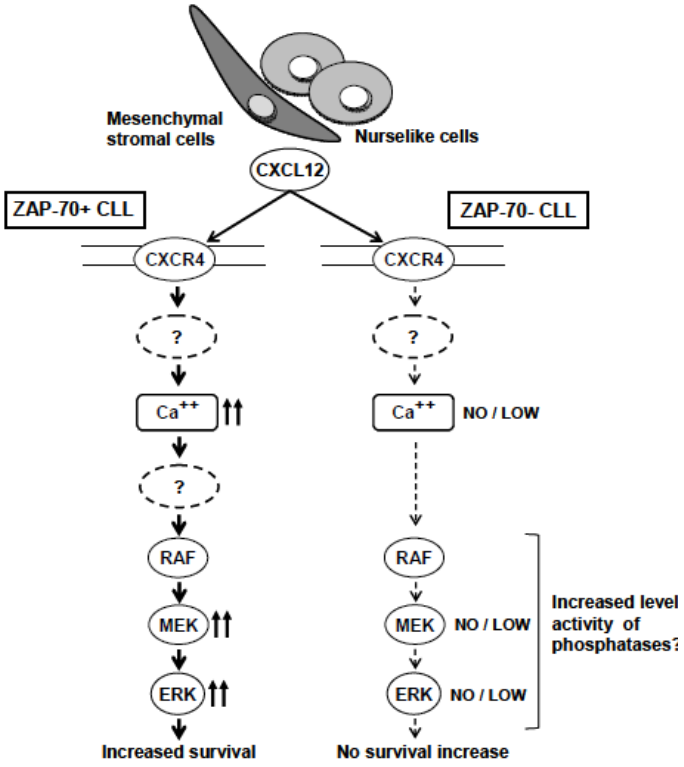

Figure 8.1 CXCL12-induced signaling in ZAP-70+ and ZAP-70- CLL cells. CXCL12 protects ZAP-70+ but not ZAP-70- CLL cells from spontaneous apoptosis. CXCR4 expression levels and turnover kinetics do not differ between ZAP-70+ and ZAP-70- CLL cells. However, in ZAP-70+ CLL cells CXCL12 induces calcium flux and increased and prolonged MEK and ERK activation. In ZAP-70+ CLL cells, MEK and ERK activation are RAF-dependent. Figure from Dr. Jessie-F Fecteau.

Additionally, since sorafenib is a promising drug for the treatment of CLL, the mechanisms underlying sorafenib-mediated apoptosis of CLL cells in co-culture with NLCs will also be investigated. Notably, we found that a single dose of 10 μM sorafenib, a concentration reachable *in vivo* [*9-11*], resulted in dramatic apoptosis of CLL cells. We also found that aggressive CLL cells exposed to a single low 5 μM dose [*12*] or to a repeated addition of 1 μM in the presence of NLCs were more sensitive to sorafenib-mediated apoptosis than indolent-CLL cells, suggesting a heightened sensitivity of the aggressive cells to this survival pathway. These observed effects of sorafenib on CLL cells are exciting findings because sorafenib was approved by the FDA for treatment of

advanced hepatocellular carcinoma in 2007, and our data strongly suggests that it might be a potential drug for the treatment of CLL. Due to the promising effects of sorafenib on mediating CLL cell death and since sorafenib is already an FDA approved drug for treating other types of cancer, our collaborators Dr. Thomas Kipps and Dr. Davorka Messmer at the UCSD Moore's Cancer Center have received funding from the private sector and will conduct a Phase I/II clinical trial testing sorafenib in CLL patients as part of a future study.

Although sorafenib is a Raf inhibitor and blocks the downstream ERK pathway, it is also a multi-kinase inhibitor that can inhibit Akt as well [*13-14*]. In later studies, we found that sorafenib reduced the expression of Mcl-1 (Figure 8.2), a pro-survival molecule downstream of Akt and other kinases, in CLL cells cultured with NLCs. The effects of sorafenib on other potential downstream targets besides Raf, including Mcl-1 STAT3, will be investigated as this could provide valuable information on the mechanisms by which sorafenib promotes CLL cell death and insight into how CLL cells survive and respond to signals from the NLCs. Furthermore, it is becoming clear that single target approaches for therapeutic agents are often limiting due to cancer cell evolution and development of cell populations resistant to those agents. Therefore, use of drugs like sorafenib that target multiple different proteins and pathways may provide more effective treatment strategies. A multifaceted approach, by combining different therapeutic agents such as sorafenib with other drugs like fludarabine, could also have added beneficial effects on killing CLL cells and enhancing patient survival. These are important considerations for future investigations.

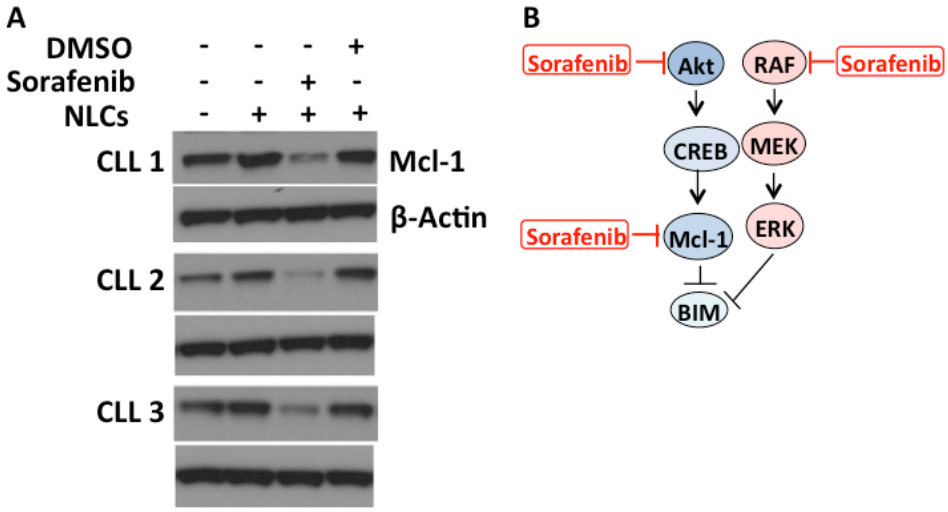

Figure 8.2 Sorafenib downregulates the expression of Mcl-1. A) CLL cells from 3 different patients were cultured alone or with NLCs in the presence of 10 μM sorafenib. Cell lysates were analyzed by western blot for Mcl-1 expression after 24 h. B) Schematic of known targets of sorafenib. Unpublished data from collaboration with Dr. Davorka Messmer.

Additionally, we broadly investigated the phosphoproteome of CLL cells in response to CXCL12 and identified phosphorylation of several survival-associated signaling proteins, which have not been previously described in the context of CXCL12 or CLL. Downstream of the pro-survival kinase Akt, MDM2, involved in the degradation of pro-apoptotic molecules, is activated; furthermore, the tumor suppressor PDCD4 is inactivated by Akt phosphorylation (S457) and degraded by p70S6K phosphorylation (S67) following CXCL12 stimulation [*15-17*]. We also found that PHLPP1, a phosphatase that negatively regulates Akt and PKC, is not expressed in most CLL patient samples, which would amplify the survival effects of cytokines that impinge on these kinases.

Through phosphoproteomics analysis and western blot validation, we discovered that PDCD4 is phosphorylated in response to CXCL12 in CLL cells [*18*]. PDCD4 is a tumor suppressor; its phosphorylation by Akt and p70S6K disrupts its ability to inhibit eIF4A translational and AP-1 transcriptional activity, which in turn impairs its growth

regulating/tumor-suppressor function thereby linking it to survival [*19-20*]. Loss of PDCD4 expression/activity has been linked to a number of cancers and PDCD4 stabilizers are currently being pursued as potential cancer therapeutics [*21*].

PDCD4 phosphorylation was found to be strongly induced by CXCL12 in all CLL patients' cells examined. It is also induced by NLCs as well as two other chemokines important for CLL survival CCL19 and CCL21 (Figure 8.3), reinforcing the importance of its inhibition. This also suggests that PDCD4 inhibition may be a common mechanism by which chemokines signal and exert some of their effects; thus, determining which chemokines stimulate phosphorylation of PDCD4 is currently being pursued. Stimulation of CLL cells with CXCL12 also led to a decrease in total PDCD4 levels. Therefore, we have future plans to determine if phosphorylation and degradation of PDCD4 via chemokines and NLCs influence CLL survival, using a non-phosphorylatable mutant of PDCD4 S67A/S457A that stabilizes PDCD4 and prevents its degradation. Furthermore, we plan to validate whether stimulation with chemokines and NLCs alters the rate of AP-1 transcripts through real-time PCR analysis and global protein translation by examining [^{35}S]-methionine incorporation in unstimulated and stimulated CLL cells. Although there are currently no direct pharmacological stabilizers of PDCD4, inhibitors of PI3K-Akt (LY294002) and mTOR-p70-S6K (Rapamycin) pathways can be used to indirectly stabilize PDCD4 and determine if these inhibitors sensitize CLL cells to apoptosis.

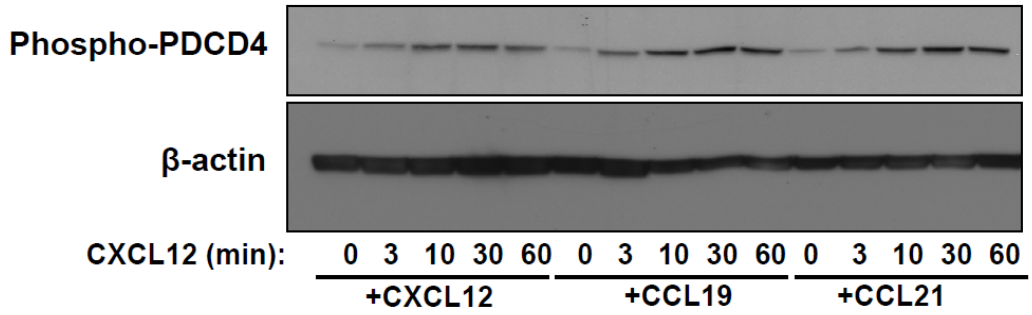

Figure 8.3 PDCD4 is phosphorylated by multiple different chemokines. Western blot detecting PDCD4 phosphorylation in CLL cells treated over a 60 min time course with 30 nM CXCL12, 1 μg/mL (~100 nM) CCL19 or 1 μg/mL (~100 nM). β-actin served as a loading control.

We also demonstrated that HSP27 is expressed and becomes phosphorylated in a subset of CLL cells in response to CXCL12; however, not much is known regarding the function/consequences of HSP27 phosphorylation. While the expression of HSP27 has been implicated in protection of cells from apoptosis as well as in resistance of cancer cells to chemotherapeutics [*22-23*], it has not been previously associated with CLL survival. Thus, it will be interesting to determine whether exposure of CLL cells to different chemotherapeutic agents, such as fludarabine, can induce expression of HSP27 and if CLL samples that already express HSP27 are more resistant to fludarabine-induced apoptosis. HSP27 is a downstream target of the p38-MAPK pathway which gets activated by CXCL12 in CLL cells from the same subset patients; thus, we would also like to examine the effects of p38 inhibition by the small molecule inhibitor SB203580 on cells that exhibit HSP27 phosphorylation compared to those that do not, to confirm the link and potential effects of inhibiting the p38/HSP27 pathway.

Overall, we have made significant progress in characterizing the CXCL12/CXCR4 signaling axis in CLL cells. A summary of our analysis of CXCL12-mediated signaling through directed as well as phosphoproteomics methods is represented in Figure 8.4. Although CXCL12 is just one of many factors that promotes

survival of CLL cells, it provides clues as to how CLL cells generally respond to survival cues and importantly led to the identification of therapeutic strategies, such sorafenib, that promote CLL cell death in the context of the more complex NLC environment.

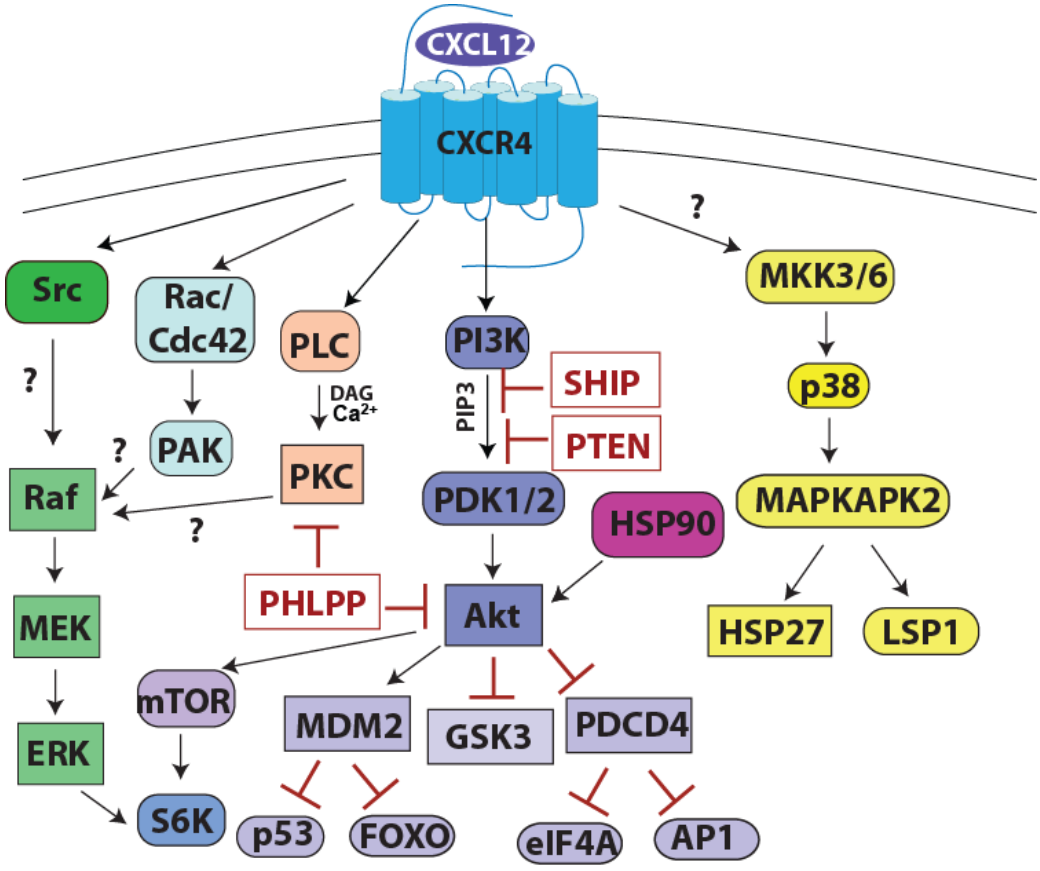

Figure 8.4 CXCL12-mediated signaling pathways investigated in these studies that enhance growth and survival and/or inhibit apoptosis. Arrows indicate factors that are induced and red lines ending with a bar indicate factors that are inhibited by the upstream factor. Proteins boxed in rectangles have already been probed and are described in preliminary data based on western blot and/or phosphoproteomics validation while rounded rectangles are other pathway components and proteins of interest. Much of our focus has been on the PI3K/Akt and Raf/MEK/ERK pathways for involvement in CLL cell survival and resistance to apoptosis. These pathways enhance activities of proteins important for growth/survival, for example S6K and MDM2, and inhibit factors involved in apoptosis/growth inhibition such as GSK3 and PDCD4. PHLPP is a phosphatase that dephosphorylates and inhibits Akt and was also found to dephosphorylate and thus destabilize PKC, and PHLPP1 expression is lost in the majority of CLL cases. PKC activation downstream of phospholipase C (PLC) also feeds into several pro-survival and anti-apoptotic pathways. Furthermore, potential involvement of the p38-MAPK pathway in a subset of patients will be probed based on HSP27 and LSP1 implications from phosphoproteomics data.

In addition to following up on CXCL12 signaling mechanisms described above, we are also interested in further characterizing the two-way molecular communication between CLL cells and NLCs to understand how their interplay contributes to disease progression and aggressiveness. Since CLL B cells undergo apoptosis *in vitro* unless rescued from by monocyte-derived NLCs or Marrow Stromal Cells (MSCs) [*7, 24-26*], it has been postulated that *in vivo,* CLL cells receive survival signals from microenvironments such as secondary lymphoid tissue and the marrow, where these accessory cells reside. In line with this hypothesis, the marrow is invariably infiltrated with CLL cells in patients, and the extent of infiltration correlates with clinical stage and prognosis [*27-28*]. Such protective niches could prevent current therapies from achieving complete remission in patients. Therefore, interfering with the microenvironmental signals may allow for a more effective depletion of the CLL cells, thus preventing recurrence.

CLL cells not only derive survival signals from accessory cells, they also manipulate these cells, promoting cooperative phenotypes that are highly supportive of CLL cell viability. CLL cells secrete factors that induce monocytes to differentiate into NLCs [*29*], which in turn protect them from apoptosis by the elaboration of factors such as CXCL12, BAFF, and APRIL [*7-8*]. However, little is known about the key factors produced by CLL cells that induce the transformation of monocytes into NLCs. Furthermore, the factors produced by the NLCs identified thus far do not fully recapitulate the survival benefits of NLCs. Therefore, future investigations are aimed at more comprehensively identifying the factors in the bi-directional CLL:NLC secretome using a combination of approaches involving proteomics as well as multi-analyte profiling using a Luminex or similar ELISA-based screening technologies. Preliminary efforts have been made to reduce the signal from abundant serum proteins (14 most abundant

serum proteins that account for ~94% of serum content) to enable detection of the much less abundant proteins of interest by mass spectrometry. Ultimately, use of the albumin/immunoglobulin depletion columns with a gel-free fractionation system from Protein Discovery may significantly aid these efforts (Figure 8.5).

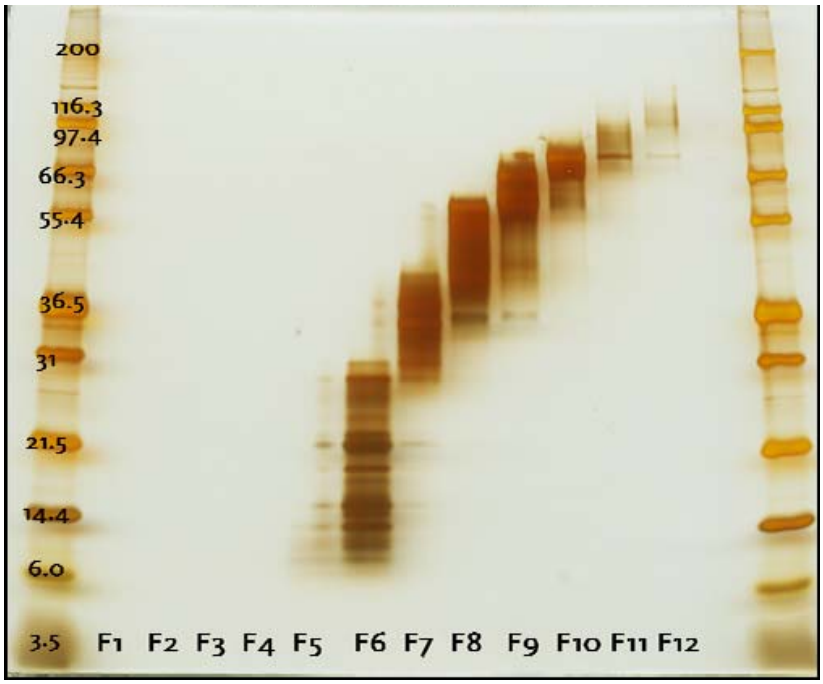

Figure 8.5 Silver stained SDS PAGE gel of gel-free separated CLL:NLC co-cultures fractions after albumin/IgG depletion.

We would also like to determine if different patients' CLL cells (e.g. patients with more aggressive disease) can uniquely shape their microenvironment, for example by generating more potent NLCs marked by an increased secretion of survival factors. Determining whether therapeutics such as fludarabine and sorafenib may alter this two-way communication will also be an interesting future direction. Identifying the proteins secreted by NLCs, and the downstream signaling pathways induced by these factors in CLL cells, will likely reveal novel therapeutic targets as well as facilitate a better global understanding of crosstalk that occurs within a tumor microenvironment.

As described above, HSP27 was identified in our phosphoproteomics study of the response of CLL cells to CXCL12 [*18*]. Interestingly, it was recently demonstrated that HSP27 is released in large quantities by breast cancer cells and further that it causes differentiation of monocytes into macrophages with an immunotolerizing phenotype [*30*]. Thus, it is also conceivable that CLL produced HSP27 could be involved in conversion of monocytes to NLCs. We therefore plan to examine whether HSP27 is released from CLL cells and whether it helps to promote monocyte differentiation into NLCs. In line with determining whether there are differences in NLCs generated by coculture with aggressive CLL cells compared to indolent CLL cells, we would also like to compare co-cultures of monocytes with CLL cells expressing HSP27 versus those that do not.

Overall, these future aims should provide a detailed understanding of the factors that enhance the survival of CLL cells and the mechanisms by which these factors elicit their functions. These efforts may lead to the identification of potential new therapeutic targets for CLL as well as characterization of a currently promising treatment for the disease, sorafenib. In the future, we also hope to gain a better understanding of the importance of the microenvironment and the two-way communication between CLL and accessory cells that fuel CLL accumulation and malignancy.

8.3 Summary and Future Directions for Understanding the Interplay between CXCL12, CXCR4 and CXCR7 in Breast Cancer Progression

We also investigated the individual and combined contributions of the two receptors to which CXCL12 binds, CXCR4 and CXCR7, in breast cancer progression. Overall, our data suggest that CXCR4 and CXCR7 contribute to the growth, survival, and metastasis of MDA-MB231 breast cancer cells through different mechanisms. While

CXCR4 appears to be most important in terms of the primary tumor growth and metastatic potential of these cells, the presence of CXCR7 on its own also confers additional advantages on growth. However, it appears that co-expression of CXCR7 with CXCR4 may actually have inhibitory effects on tumor metastasis and causes a delay in primary tumor growth. Whether this phenomenon could be attributed to sequestration of CXCL12 from CXCR4 and/or transinhibitory effects from receptor heterodimerization remains to be fully determined and is a current and future direction of our work on this project. However, our results demonstrating a decrease in calcium flux in response to CXCL12 in cells co-expressing CXCR4 and CXCR7 compared to CXCR4 alone, even at saturating ligand concentrations, would suggest a more direct trans-inhibition mechanism as opposed to just ligand sequestration. Additionally, data from internalization studies of the CXCR4 WHIM mutant, R334X, and CXCR7 indicate these two receptors can form stable heterodimers that can influence the internalization properties of the receptors. We are continuing to compare how differential levels of CXCR4 and CXCR7 receptor expression influences intracellular signaling events and would like to investigate the effects of endogenous, intracellular stores of CXCR7 compared to surface levels of CXCR7 on the growth and survival properties of the cells. A summary of our findings thus far regarding CXCR4, CXCR7 and dual receptor expression on breast cancer tumor growth, metastasis and signaling is presented in Figure 8.5. Using selective/differentiating inhibitors and agonists of the receptors should allow us to better delineate the transinhibitory and/or transactivating effects of CXCR4 and CXCR7. For example, we plan to determine if stimulation of CXCR4 and CXCR7 expressing cells with CXCL11, which binds CXCR7 but not CXCR7, can mediate internalization of CXCR4, adding further support to the idea that these receptors form

functionally relevant heterodimers that can alter the signaling or internalization properties of the other receptor.

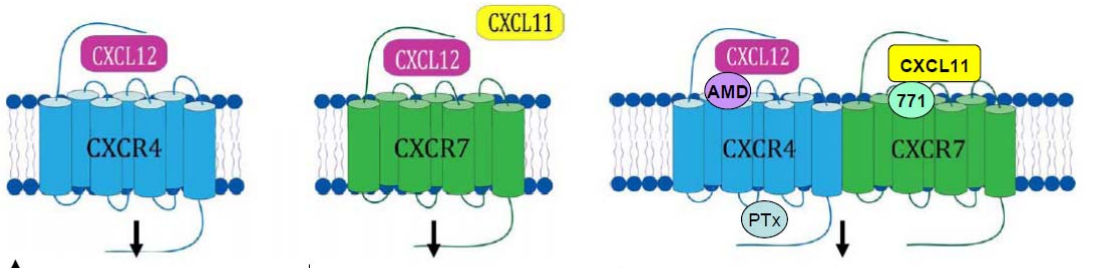

↑ Primary tumor growth	↑ Primary tumor growth	↑ Primary tumor growth (initial delay)
↑ Metastasis (*LN, lung)	No effect on metastasis	↓ Metastasis
Signaling: -Calcium flux -Survival and growth (pAkt, pERK, pPDCD4)	Signaling: - No calcium flux - Basal pERK, pPDCD4 higher	Signaling: - ↓ Calcium flux - ↓ and/or delay for pERK, pAkt, pPDCD4 - Sequester CXCL12? - Transinhibition?

Figure 8.6 Summary of the effects of CXCR4 and CXCR7 on tumor growth, metastasis and signaling of breast cancer cells. Both CXCR4 and CXCR7 on breast cancer cells correlates with an acceleration in primary tumor growth, although CXCR4 appears to have a more significant contribution. Coexpression of the receptors leads to an initial delay in primary tumor growth although an eventual increase in tumor size. On the other hand, while CXCR4 strongly drives metastasis to the lungs, CXCR7 alone has no effect and receptor coexpression has an inhibitory effect on metastasis. Calcium flux was similarly inhibited in the CXCR4 and CXCR7 coexpressing cells. Signaling analysis reveals that although basal levels of ERK and PDCD4 phosphorylation are higher in cells expressing CXCR7, the coexpression of CXCR7 with CXCR4 leads to a decrease and/or delay in the phosphorylation of ERK, Akt and PDCD4 compared to cells just expressing CXCR4. Future plans to further investigate the combined effects of CXCR4 and CXCR7 on breast cancer progression and signaling and better evaluate inhibitory effects of CXCR7 will involve use of various ligands and inhibitors of these receptors including CXCL11 (the other ligand for CXCR7), AMD3100 (AMD, CXCR4 antagonist), CCX-771 (771, CXCR7 antagonist/agonist), and pertussis toxin (PTx, Gi inhibitor).

While the results thus far are interesting and have led to insight into the individual and combined effects of CXCR4 and CXCR7 expression, there are still many unanswered questions and future directions remaining. We are currently in the process of expressing HA-tagged CXCR4 and CXCR7 receptors for the purpose of performing

immunoprecipitations on the receptors to identify potential novel/distinguishing interacting partners via mass spectrometry, especially since CXCR7 interactions and signaling complexes are largely unknown. A variety of tools are currently being developed in the lab that should aid future work in elucidating the effects of CXCR7 in combination with CXCR4 in breast cancer cells, both biochemically and mechanistically. Receptor antagonists selective for CXCR4 or CXCR7 and antagonists targeting both receptors have been developed by a post-doc in the lab through phage display in addition to the small molecule inhibitors we currently possess for CXCR4 (AMD3100) and CXCR7 (CCX-771, kind gift from Chemocentryx). These antagonists should allow us to better dissect the distinct functions of these two receptors. Additionally, CXCR4 mutants to disrupt dimer formation but preserve ligand binding capabilities are being designed in the lab; such mutants could aid in determining the function of the CXCR4/CXCR7 heterodimer and whether high levels of CXCR7 may have direct inhibitory effects on CXCR4 function. Investigating the complexities of chemokine signaling and functional consequences of chemokine receptor heterodimerization will constitute major efforts of future investigations.

8.4 Concluding Remarks

A boom in the field of tumor microenvironment has sparked a renewed interest in chemokines. While once predominantly appreciated for their role in directing cell migration, it is now clear that chemokines can have broad implications on cancer progression. Chemokines can be secreted by cancer cells, stromal cells, and/or immune cells at local or distant sites to promote tumor growth, cell survival, and angiogenesis in addition to metastasis and localization of cancer cells to protective microenvironmental niches. Due to their multifaceted roles in cancer, deciphering signaling pathways

activated by chemokines in various cancer cells to better understand how chemokines influence disease progression is important; furthermore, this can reveal potential downstream therapeutic targets and consequences of therapeutic intervention. Studies presented herein were directed at understanding how one particular chemokine, CXCL12, influences CLL and breast cancer progression. Nevertheless, there is a milieu of other chemokines, growth factors, cytokines and extracellular matrix within the tumor microenvironment that influence the development and progression of cancer. How these factors contribute in distinct, synergistic or redundant manners will be important considerations for future research. Overall, we are beginning to understand mechanisms through which cancer cells and non-neoplastic cells of the tumor microenvironment communicate. Furthermore, recent research efforts have started to unveil previously underappreciated insights into the complexities and intricacies of the chemokine network that contribute to a diverse array of physiological and pathophysiological processes.

REFERENCES

1. Hanahan, D., and Weinberg, R. A. (2000) The hallmarks of cancer, *Cell 100*, 57-70.

2. Hanahan, D., and Weinberg, R. A. (2011) Hallmarks of cancer: the next generation, *Cell 144*, 646-674.

3. Balkwill, F., and Mantovani, A. (2001) Inflammation and cancer: back to Virchow?, *Lancet 357*, 539-545.

4. Callahan, M. K., Wolchok, J. D., and Allison, J. P. (2010) Anti-CTLA-4 antibody therapy: immune monitoring during clinical development of a novel immunotherapy, *Semin Oncol 37*, 473-484.

5. O'Hayre, M., Salanga, C. L., Handel, T. M., and Allen, S. J. (2008) Chemokines and cancer: migration, intracellular signalling and intercellular communication in the microenvironment, *Biochem J 409*, 635-649.

6. Burger, J. A., and Kipps, T. J. (2006) CXCR4: a key receptor in the crosstalk between tumor cells and their microenvironment, *Blood 107*, 1761-1767.

7. Burger, J. A., Tsukada, N., Burger, M., Zvaifler, N. J., Dell'Aquila, M., and Kipps, T. J. (2000) Blood-derived nurse-like cells protect chronic lymphocytic leukemia B cells from spontaneous apoptosis through stromal cell-derived factor-1, *Blood 96*, 2655-2663.

8. Nishio, M., Endo, T., Tsukada, N., Ohata, J., Kitada, S., Reed, J. C., Zvaifler, N. J., and Kipps, T. J. (2005) Nurselike cells express BAFF and APRIL, which can promote survival of chronic lymphocytic leukemia cells via a paracrine pathway distinct from that of SDF-1alpha, *Blood 106*, 1012-1020.

9. Clark, J. W., Eder, J. P., Ryan, D., Lathia, C., and Lenz, H. J. (2005) Safety and pharmacokinetics of the dual action Raf kinase and vascular endothelial growth factor receptor inhibitor, BAY 43-9006, in patients with advanced, refractory solid tumors, *Clin Cancer Res 11*, 5472-5480.

10. Haouala, A., Zanolari, B., Rochat, B., Montemurro, M., Zaman, K., Duchosal, M. A., Ris, H. B., Leyvraz, S., Widmer, N., and Decosterd, L. A. (2009) Therapeutic Drug Monitoring of the new targeted anticancer agents imatinib, nilotinib,

dasatinib, sunitinib, sorafenib and lapatinib by LC tandem mass spectrometry, *J Chromatogr B Analyt Technol Biomed Life Sci 877*, 1982-1996.

11. Strumberg, D., Clark, J. W., Awada, A., Moore, M. J., Richly, H., Hendlisz, A., Hirte, H. W., Eder, J. P., Lenz, H. J., and Schwartz, B. (2007) Safety, pharmacokinetics, and preliminary antitumor activity of sorafenib: a review of four phase I trials in patients with advanced refractory solid tumors, *Oncologist 12*, 426-437.

12. Messmer, D., Fecteau, J. F., O'Hayre, M., Bharati, I. S., Handel, T. M., and Kipps, T. J. (2011) Chronic lymphocytic leukemia cells receive RAF-dependent survival signals in response to CXCL12 that are sensitive to inhibition by sorafenib, *Blood 117*, 882-889.

13. Ulivi, P., Arienti, C., Amadori, D., Fabbri, F., Carloni, S., Tesei, A., Vannini, I., Silvestrini, R., and Zoli, W. (2009) Role of RAF/MEK/ERK pathway, p-STAT-3 and Mcl-1 in sorafenib activity in human pancreatic cancer cell lines, *J Cell Physiol 220*, 214-221.

14. Yang, F., Van Meter, T. E., Buettner, R., Hedvat, M., Liang, W., Kowolik, C. M., Mepani, N., Mirosevich, J., Nam, S., Chen, M. Y., Tye, G., Kirschbaum, M., and Jove, R. (2008) Sorafenib inhibits signal transducer and activator of transcription 3 signaling associated with growth arrest and apoptosis of medulloblastomas, *Mol Cancer Ther 7*, 3519-3526.

15. Fu, W., Ma, Q., Chen, L., Li, P., Zhang, M., Ramamoorthy, S., Nawaz, Z., Shimojima, T., Wang, H., Yang, Y., Shen, Z., Zhang, Y., Zhang, X., Nicosia, S. V., Zhang, Y., Pledger, J. W., Chen, J., and Bai, W. (2009) MDM2 acts downstream of p53 as an E3 ligase to promote FOXO ubiquitination and degradation, *J Biol Chem 284*, 13987-14000.

16. Mayo, L. D., and Donner, D. B. (2001) A phosphatidylinositol 3-kinase/Akt pathway promotes translocation of Mdm2 from the cytoplasm to the nucleus, *Proc Natl Acad Sci U S A 98*, 11598-11603.

17. Dorrello, N. V., Peschiaroli, A., Guardavaccaro, D., Colburn, N. H., Sherman, N. E., and Pagano, M. (2006) S6K1- and betaTRCP-mediated degradation of PDCD4 promotes protein translation and cell growth, *Science 314*, 467-471.

18. O'Hayre, M., Salanga, C. L., Kipps, T. J., Messmer, D., Dorrestein, P. C., and Handel, T. M. (2010) Elucidating the CXCL12/CXCR4 signaling network in

chronic lymphocytic leukemia through phosphoproteomics analysis, *PLoS One 5*, e11716.

19. Yang, H. S., Jansen, A. P., Komar, A. A., Zheng, X., Merrick, W. C., Costes, S., Lockett, S. J., Sonenberg, N., and Colburn, N. H. (2003) The transformation suppressor Pdcd4 is a novel eukaryotic translation initiation factor 4A binding protein that inhibits translation, *Mol Cell Biol 23*, 26-37.

20. Yang, H. S., Jansen, A. P., Nair, R., Shibahara, K., Verma, A. K., Cmarik, J. L., and Colburn, N. H. (2001) A novel transformation suppressor, Pdcd4, inhibits AP-1 transactivation but not NF-kappaB or ODC transactivation, *Oncogene 20*, 669-676.

21. Blees, J. S., Schmid, T., Thomas, C. L., Baker, A. R., Benson, L., Evans, J. R., Goncharova, E. I., Colburn, N. H., McMahon, J. B., and Henrich, C. J. (2010) Development of a high-throughput cell-based reporter assay to identify stabilizers of tumor suppressor Pdcd4, *J Biomol Screen 15*, 21-29.

22. Parcellier, A., Schmitt, E., Gurbuxani, S., Seigneurin-Berny, D., Pance, A., Chantome, A., Plenchette, S., Khochbin, S., Solary, E., and Garrido, C. (2003) HSP27 is a ubiquitin-binding protein involved in I-kappaBalpha proteasomal degradation, *Mol Cell Biol 23*, 5790-5802.

23. Garrido, C., Brunet, M., Didelot, C., Zermati, Y., Schmitt, E., and Kroemer, G. (2006) Heat shock proteins 27 and 70: anti-apoptotic proteins with tumorigenic properties, *Cell Cycle 5*, 2592-2601.

24. Burger, M., Hartmann, T., Krome, M., Rawluk, J., Tamamura, H., Fujii, N., Kipps, T. J., and Burger, J. A. (2005) Small peptide inhibitors of the CXCR4 chemokine receptor (CD184) antagonize the activation, migration, and antiapoptotic responses of CXCL12 in chronic lymphocytic leukemia B cells, *Blood 106*, 1824-1830.

25. Lagneaux, L., Delforge, A., Bron, D., De Bruyn, C., and Stryckmans, P. (1998) Chronic lymphocytic leukemic B cells but not normal B cells are rescued from apoptosis by contact with normal bone marrow stromal cells, *Blood 91*, 2387-2396.

26. Pedersen, I. M., Kitada, S., Leoni, L. M., Zapata, J. M., Karras, J. G., Tsukada, N., Kipps, T. J., Choi, Y. S., Bennett, F., and Reed, J. C. (2002) Protection of CLL B cells by a follicular dendritic cell line is dependent on induction of Mcl-1, *Blood 100*, 1795-1801.

27. Han, T., Barcos, M., Emrich, L., Ozer, H., Gajera, R., Gomez, G. A., Reese, P. A., Minowada, J., Bloom, M. L., Sadamori, N., and et al. (1984) Bone marrow infiltration patterns and their prognostic significance in chronic lymphocytic leukemia: correlations with clinical, immunologic, phenotypic, and cytogenetic data, *J Clin Oncol 2*, 562-570.

28. Pangalis, G. A., Roussou, P. A., Kittas, C., Mitsoulis-Mentzikoff, C., Matsouka-Alexandridis, P., Anagnostopoulos, N., Rombos, I., and Fessas, P. (1984) Patterns of bone marrow involvement in chronic lymphocytic leukemia and small lymphocytic (well differentiated) non-Hodgkin's lymphoma. Its clinical significance in relation to their differential diagnosis and prognosis, *Cancer 54*, 702-708.

29. Tsukada, N., Burger, J. A., Zvaifler, N. J., and Kipps, T. J. (2002) Distinctive features of "nurselike" cells that differentiate in the context of chronic lymphocytic leukemia, *Blood 99*, 1030-1037.

30. Banerjee, S., Lin, C. F., Skinner, K. A., Schiffhauer, L. M., Peacock, J., Hicks, D. G., Redmond, E. M., Morrow, D., Huston, A., Shayne, M., Langstein, H. N., Miller-Graziano, C. L., Strickland, J., O'Donoghue, L., and De, A. K. (2011) Heat shock protein 27 differentiates tolerogenic macrophages that may support human breast cancer progression, *Cancer Res 71*, 318-327.

APPENDIX I

Protocols

AI.1 CXCL12 Purification

pET21a (pMS2) His-CXCL12

MKKKHHHHHHHHDDDDKPVS LSYRCPCRFF ESHVARANVK HLKILNTPNC ALQIVARLKNNNRQVCIDPK LKWIQEYLEK ALNK

DNA sequence
gaaataattttgtttaactttaagaaggagatatacatATGAAAAAGAAACACCACCACCATCACCACCA
CCATGATGATGATGACAAAAAACCGGTGAGCCTGAGCTATCGCTGCCCGTGCCGC
TTCTTTGAAAGCCATGTGGCCCGCGCGAACGTGAAACATCTGAAAATTCTGAATAC
GCCGAACTGTGCCCTGCAGATTGTTGCCCGCCTGAAGAACAATAACCGCCAAGTGT
GCATTGATCCGAAACTGAAATGGATTCAGGAATATCTGGAAAAAGCGCTGAACAAA
TAATGAagcttgcggccgcactcgagcaccaccaccaccaccactgagatc

His-tag CXCL12 (pre-enterokinase cleavage)
MW: 10036.6
Ex. Coeff: 8480

CXCL12 (enterokinase cleaved)
MW: 7963.4 (reduced), 7959.4 (oxidized)
Ex. Coeff: 8480 (reduced), 8730 (oxidized)

BUFFERS:
Inclusion Body Resuspension Buffer:
(store at 4°C)
- 10 mM Tris 8.0
- 1 mM $MgCl_2$ (add fresh)
- 200 µg of DNAse (add fresh)
- Complete protease inhibitor tablet (Roche, 1 tablet/50mL)

Tetsuya's:
- 10 mM Tris 8.0
- 200 µg of DNAse (add fresh)

"Spin Purifying Buffer":
(Store at 4°C)
- 10 mM Tris pH 8
- 0.25% deoxycholate
- (Before use add: Protease Inhibitor Tablets 1 per 50 ml, stable for 1-2 weeks at 4°C)

Ni-NTA Buffers:
Buffer A (equilibration and wash 1):
10 mM Tris
100 mM NaPhos
6 M GuHCl
pH 8

Buffer B (elution):
10 mM Tris
100 mM NaPhos
6 M GuHCl
pH 4

Tetsuya's :
Buffer A (equilibration and wash 1):
10 mM Tris
6 M GuHCl
4mM DTT
pH 8

Buffer B (elution):
10 mM Tris
6 M GuHCl
4mM DTT
pH 4

Fold It Buffer #8:
Sterile filter and store at 4°C

55 mM MES pH 6.5
264 mM NaCl, 11 mM KCl
0.055% PEG 3350
1.1 mM EDTA
550 mM L-arginine-HCl

Add fresh:
1 mM GSH
0.1 mM GSSG
0.3 mM lauryl maltoside

Note: Tetsuya found that the above refolding conditions take ~3 days to get complete refolding based on analytical column, so he used modified conditions and refold at room temp- only takes 30 min-1 h (or O/N at 4°C)

Tetsuya's Revised Fold-It buffer:
50 mM Tris
1 mM EDTA
Arginine-HCl
pH 7.5-8

(No NaCl, no KCl, no PEG…)

Add fresh:
1 mM GSSG

Dialysis Buffer:

20 mM Tris pH 8.0
50 mM NaCl
2 mM $CaCl_2$

HPLC Buffers:

A: 0.1% TFA
B: 90% acetonitrile, 0.1% TFA

DAY 1: TRANSFORMATION

1. Transform BL21(DE3)pLysS Cells with 1 uL of plasmid. Plate 200 uL on LB/Carb plates

2. Prepare 6 x 5 mL cultures, 3 x 100 mL and 6 x 1 L cultures for the next day with LB+100 µg/ml Carb (1:1000 dilution).

DAY 2: GROWTH

1. Inoculate each of the 5 mL cultures with a swipe of colonies from the plate, shake at 37 °C
2. ~1h-1.5 later, pool 5 mL cultures and evenly divide to inoculate into 3 x 100 mL cultures
3. ~1-1.5h later, pool the cultures and inoculate 1L cultures (prewarmed)
4. Take timepoints (doubles every 20min), monitor growth by A600
5. Induce with 0.5 mM IPTG (0.5 mL of 1 M stock) when OD reaches ~0.6-0.7
6. Harvest after ~3-4 h of growth
7. Spin down pellets at 5.5k rpm, 15 min, 4°C
8. Resuspend in ~50 mL of Resuspension buffer (for 6 L culture)
9. Divide into 2 x 50 mL conicals, store at -80°C

DAY 3: INITIAL PURIFICATION

10. Thaw the cells by placing conicals in H_2O on ice

11. Pour thawed cells into small metal sonication cup, bring volume up to ~100 mL with resuspension buffer

12. Lyse cells by sonication on ice: 4 x 30s (with 3s on, 2s off, speed 8) resting in between cycles for ~1 min

13. Add Triton-X to a final concentration of 0.1% and incubate for 15 minutes on gel shaker at room temperature or add stir bar to the metal cup and stir for 15 min. To mix the triton-X completely in, you may have to add drop by drop or sonicate to mix 1X by 30 sec pulse.

14. Distribute into centrifuge tubes and spin lysate for 15 min in the Beckman JA25.5 rotor at 15,000 rpm, 4 °C

15. Resuspend the pellet in ~100 mL of "Spin-purifying Buffer". Sonicate and spin as above repeatedly until supernatant is clear (~3-4 times).

16. Solubilize Pellet in ~20 mL of "Buffer A" (see above) using a Dounce homogenizer. Spin as in step 14 to remove insoluble particles. Filter supe through a 0.22 uM PVDF filter (Millipore durapore membrane).

17. Purify over benchtop Ni-NTA gravity column

a. Use a 10-20 mL Ni-NTA Column re-equilibrated with 2 CV of Buffer A (above).
b. Load protein onto the column with gravity flow (turns brown).
c. Wash with 2 CV Buffer A
d. Elute with Buffer B. Collect 2 mL fractions in glass tubes until brown color goes away (can spec A280 to ID fractions containing protein)—pool these together. Add to 1 mM DTT final concentration.

   At this point, the protein can be stored at 4°C (stable for several days in GuHCl)

DAY 4: PROTEIN REFOLDING

18. Treat with either 1mM DTT or 5 mM TCEP. Store at 4 °C O/N in reducing conditions before refolding.

19. Refold in 20 volumes of cold FoldIt Buffer #8 (e.g. for 50 mL of protein fractions, need ~1 L of buffer). Generally,for 1-3 L preps, refold into 500 mL, for 4-6 L preps, refold into 1 L. Remember to add Arginine-HCl, lauryl maltoside, GSH and GSSG fresh to the refolding buffer right before use. Note--Because of the ArgHCl, the buffer needs to be pH'd (6.5).

20. Dropwise add chemokine in GuHCl into the Hampton FoldIt #8 refolding buffer with stirring, and let sit overnight at 4°C with stirring.

DAY 5: DIALYSIS

21. Dialyze the protein into 20 mM Tris pH 8.0, 50 mM NaCl and 2 mM $CaCl_2$ using dialysis membranes (MWCO=3500). Can add ~100 mL of protein into each dialysis membrane, leave some air at top so it floats.

22. Dialyze twice against 100 X volume of protein (for 50 ml, dialyze 2 times in 5000 ml—one in the day and one overnight).

23. Filter the content of the dialysis bag with a millipore durapore membrane.

24. Concentrate the protein (using amicon Ultra-15 centrifugal filter devices, MWCO=5000). Concentrate to ~1 mg/ml for the following step (get volume down to about 15 mL from the ~280 mL after dialysis).

a. Note:The filter devices take 15 ml at a time, spin for 40 min at 4°C at 5000rcf. Save retentate and discard the flow through.

25. Alternatively: concentrate protein after refolding in an Amicon concentrator (10kD YM10 membrane, 350 mL concentrator, 50psi; resistant to GuHCl) in delicase (4 °C) and dialyze against Dialyze against 3 L of 20 mM Tris pH 8.0, 50 mM NaCl, 2 mM $CaCl_2$ for 1 h at 4°C with stirring.

DAY 6: ENTEROKINASE CLEAVAGE

26. Concentrate chemokine to ~1 mg/mL concentration (A280 ~0.845). Determine concentration via absorbance readings.

27. Add enterokinase (NEB cat#P8070 or made in-house see protocol AI.42) to a ratio of 1:100,000 (molar ratio). Digest overnight at room temperature.

a. For 1mg/mL protein concentration, add 0.25 µl of EK for every 100 µl of protein solution.

DAY 7: HPLC

28. Purify by RP-HPLC: acidify protein with 1 M HCL to a pH of 2.5-3.0. Filter with a syringe filter.

29. Load ~4 mL volumes of acidified, filtered protein onto C18 column by repeatedly filling (up to 20 mg total protein) under constant 2.5 ml/min flow rate in 25% buffer B/75% buffer A.

30. Run over HPLC, using a slow linear gradient over ~30 min from about 25-65% B then bump everything else off by going up to 100% B faster, hold there for a 10min or so to remove any contaminants, then re-equilibrate back down to 25% B. Method altogether ~120min long

31. Freeze HPLC fractions and lyophilize

32. Store lyophilized protein in -80 °C until ready for use

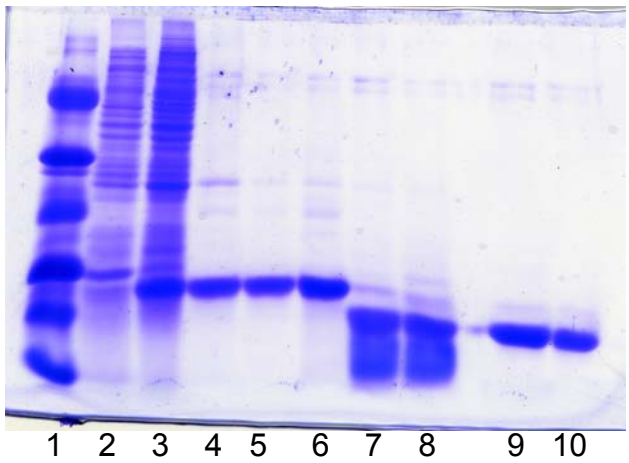

Figure AI.1.1 Coomassie gel of samples from the CXCL12 purification process. Lanes: 1) protein ladder 2) pre-induction 3) IPTG Induced 4) Ni-NTA purified 5) dialyzed 6) concentrated protein prior to EK cleavage 7&8) EK cleaved CXCL12 9&10) HPLC purified EK cleaved CXCL12. Sample aliquots were resuspended in Tris buffer: for OD of 0.5, use 50 µl.

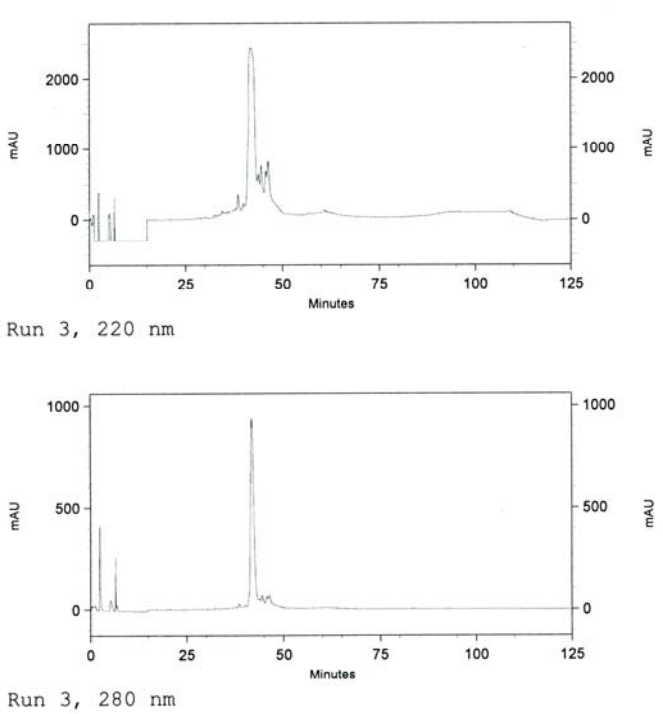

Figure AI.1.2 HPLC chromatogram of CXCL12. The A220 (top) and A280 (bottom) traces from the HPLC purification of CXCL12 are shown.

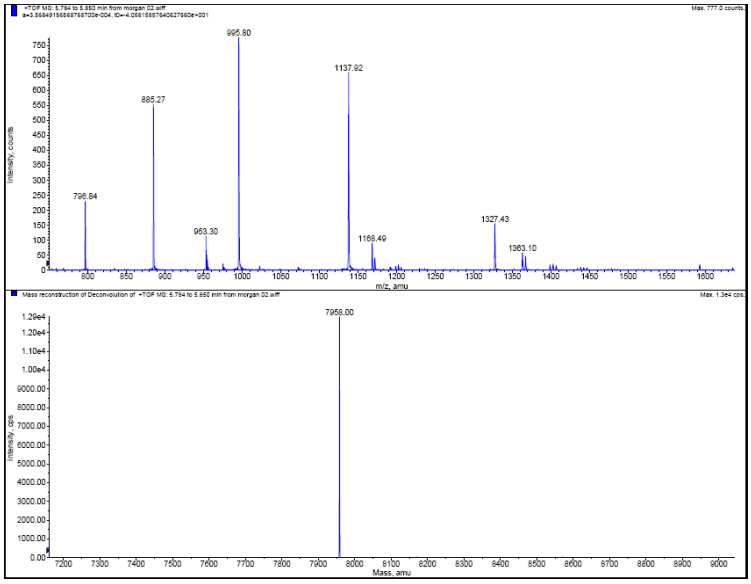

Figure AI.1.3 Mass spectrum of purified CXCL12.

AI.2 ITAC Purification

pCEV33 ITAC (3D3-Ub)
MGSSHHHHHHHHQLFVKTLTGKTITLELEPSDTVENVKAKIQDKEGIPPDQQRLIFAGK
QLEDGRTLSDYNIQKESTLHLVLRLRGGFPMFKRGRCLCIGPGVKAVKVADIEKASIMY
PSNNCDKIEVIITLKENKGQRCLNPKSKQARLIIKKVERKNF

pCEV33 ITAC 4-73 (3D3-Ub)
MGSSHHHHHHHHQLFVKTLTGKTITLELEPSDTVENVKAKIQDKEGIPPDQQRLIFAGK
QLEDGRTLSDYNIQKESTLHLVLRLRGGFKRGRCLCIGPGVKAVKVADIEKASIMYPSN
NCDKIEVIITLKENKGQRCLNPKSKQARLIIKKVERKNF

Ub-ITAC
MW: 18182.1
Ex. Coeff: 3230

ITAC
MW: 8307
Ex. Coeff: 1740

Ub-ITAC 4-73
MW: 17806
Ex. Coeff: 3230

ITAC
MW: 7931
Ex. Coeff: 1740

BUFFERS:

Inclusion Body Resuspension Buffer:
(store at 4°C)
500 mL Stock *without* DNAse, $MgCl_2$:
50 mM Hepes pH 7.2
200 mM NaCl

(Before use add: a pinch of DNAse, 1µL 0.5M $MgCl_2$(10 uM final))

"Spin Purifying Buffer":
(Store at 4°C)
10 mM Tris pH 8
0.25% deoxycholate

(Before use add: Protease Inhibitor Tablets 1 per 50 ml, stable for 1-2 weeks at 4°C)

Ni-NTA Buffers:

Buffer A (equilibration and wash 1):

10 mM Tris
100 mM NaPhos
6 M GuHCl
pH 8

Buffer B (elution):
10 mM Tris
100 mM NaPhos
6 M GuHCl
pH 4

1L Hampton Foldit Buffer 13
(without Arg, reduced and oxidized Glutathione) (or make a 10X stock)
1X Stock:
55 mM Tris pH 8
264 mM NaCl
11 mM KCl
1.1 mM EDTA
Last minute add the following and re-pH because arginine drops the pH:
1 mM GSH
0.1 mM GSSG
550 mM Arginine HCl

DAY 1: TRANSFORMATION

1. Transform BL21(DE3)pLysS Cells with 1 µL of plasmid. Plate 200 µL on LB/Kan plates

2. Prepare 6 x 5 mL cultures, 3 x 100 mL and 6 x 1 L cultures for the next day with 30ug/ml Kan (1:1000 dilution).

DAY 2: GROWTH

33. Inoculate each of the 5 mL cultures with a swipe of colonies from the plate, shake at 37 °C

34. ~1h-1.5 later, pool 5 mL cultures and evenly divide to inoculate into 3 x 100 mL cultures

35. ~1-1.5h later, pool the cultures and inoculate 1L cultures (prewarmed)

36. Take timepoints (doubles every 20min), monitor growth by A600

37. Induce with 0.5 mM IPTG (0.5 mL of 1 M stock) when OD reaches ~0.7

38. Harvest after ~3-4 h of growth

Figure AI.2.1 Growth and induction of ITAC.

39. Spin down pellets at 5.5k rpm, 15 min, 4°C

40. Resuspend in ~50 mL of Resuspension buffer (for 6 L culture)

41. Divide into 2 x 50 mL conicals, store at -80°C

DAY 3: INITIAL PURIFICATION

42. Thaw the cells by placing conicals in H_2O on ice

43. Pour thawed cells into small metal sonication cup, bring volume up to ~100-125 mL with resuspension buffer

44. Lyse cells by sonication on ice: 6 x 30s (with 3s on, 2s off) resting in between cycles for ~1 min

45. Distribute into centrifuge tubes and spin lysate for 30 min in the Beckman JA25.5 rotor at 18,000 rpm, 4 °C

46. Resuspend the pellet in ~100-150 mL of “Spin-purifying Buffer”. Sonicate and spin as above

47. Solubilize Pellet in ~20 mL of “Buffer A” (see above) using a Dounce homogenizer. Spin to remove insoluble particles. Filter supe through a 0.22 uM PVDF filter

48. Purify over benchtop Ni-NTA gravity column

a. Use a 10-20 mL Ni-NTA Column re-equilibrated with 2 CV of Buffer A (above).
b. Load protein onto the column with gravity flow (turns brownish).
c. Wash with 2 CV Buffer A
d. Elute with Buffer B. Collect 2 mL fractions in glass tubes until brown color goes away (can spec to ID fractions containing protein)—pool these together.

At this point, the protein can be stored at 4°C (stable for several days in GuHCl)

DAY 4: PROTEIN REFOLDING

49. Treat with either 1mM DTT or 5 mM TCEP. Store at 4 °C O/N in reducing conditions before refolding.

50. For 1-3 L preps, refold into 500 mL. For 4-6 L preps, refold into 1 L. Remember to add Arginine-HCl, GSH and GSSG fresh to the refolding buffer right before use. Note--Because of the ArgHCl, the buffer needs to be pH'd.

51. Dropwise add chemokine in GuHCl into the Hampton FoldIt #13 refolding buffer with stirring, and let sit overnight at 4°C with stirring.

DAY 5: CONCENTRATION/BUFFER EXCHANGE OF REFOLDED PROTEIN

52. Concentrate protein after refolding in an Amicon concentrator (10kD YM10 membrane, 350 mL concentrator, 50psi; resistant to GuHCl) in delicase (4 °C)

DAY 6: USP2CC CLEAVAGE AND HPLC

53. Dialyze against 3 L of 20 mM Tris, 200 mM NaCl (cleavage conditions) for 1 h at 4°C with stirring

54. Cleave with 1:100 Usp2cc for ~4 h at RT (Do see some ppt here form over time...could try to decrease cleavage time to reduce loss), no stirring

55. Cleanup cleavage reaction by running over Ni-NTA benchtop gravity column (use column devoted to Usp2-cc cleanup for this application)

a. Equilibrate column with 20 mM Tris, 300 mM NaCl, 40 mM Imidazole.
b. Filter cleavage reaction and load onto Ni column
c. Collect flow through (should contain ITAC)
d. Wash with 1CV of 20mM Tris, 300mM NaCl, 40mM Imidazole, collect
e. Elute Ub with 20mM Tris 300mM NaCl, 250mM Imidazole
f. Strip and regenerate Ni column, store in 20% EtOH

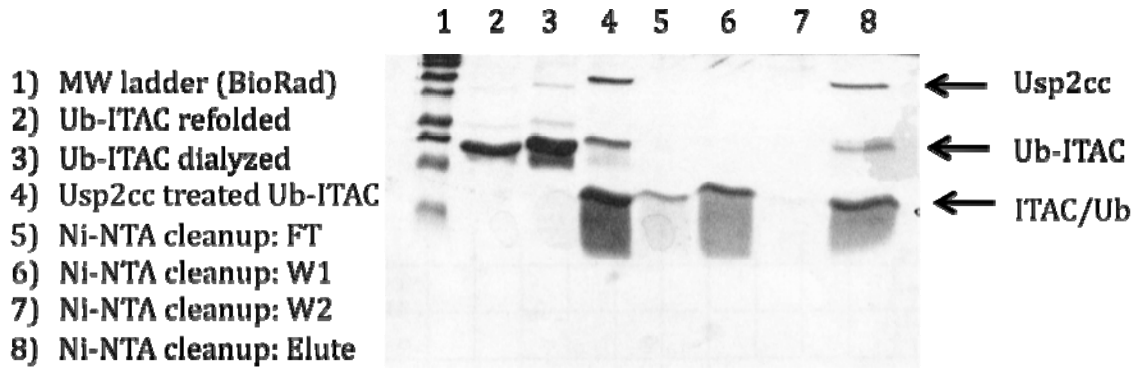

Figure A1.2.2 Coomassie gel of ITAC purification process.

56. Concentrate the ITAC FT with a 3K MWCO spin filter at 4 °C until volume is appropriate to load on to HPLC

57. Acidify HPLC load with 1 M HCl to pH 2-4; filter, and load in ~4 mL aliquots (up to 20 mg total protein)

58. Run over HPLC, using a slow linear gradient from about 25-50% B then bump everything else off by going up to 100% B faster, hold there for a 10min or so to remove any contaminants, then re-equilibrate back down to 25% B (should elute around ~30-35% B). Method ~90min long

59. Freeze HPLC fractions and lyophilize

60. Store lyophilized protein in -80 °C until ready for use

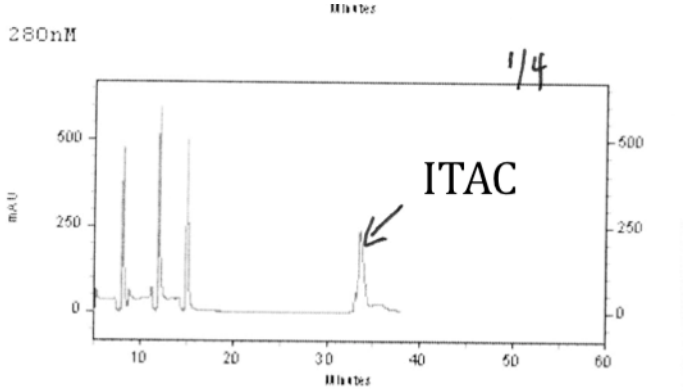

Figure A1.2.3 HPLC chromatogram of ITAC.

AI.3 Isolation of PBMCs by Ficoll-Hypaque

MATERIALS:

Ficoll-Paque Plus – GE Healthcare 17-1440-03

Red Blood Cell (RBC) lysis buffer – Roche 1-1814389-001

Phosphate Buffered Saline (PBS) – Cellgro 21-020-CV

PROTOCOL:

1. Obtain room temperature blood (usually from leukapheresis of CLL patients).
2. For leukapheresis blood, aliquot 5 mL of blood into 50 mL conicals (for normal blood can have ~15 mL aliquots of blood).
3. Add to 40 mL with room temperature PBS. Recap and mix well.
4. Carefully underlay with 10 mL of **room temperature** ficoll:
    a. Release slowly so as not to disrupt the interphase
    b. Use the Drummond pipet aids, not the Pipetboy since the Pipetboy releases too quickly at the end and disrupts the interphase
5. Centrifuge at 2000 rpm (931 rcf) in swinging bucket centrifuge for 20 min at **room temperature** with the **brake OFF**. Note: spin takes ~30-40 min total (no brake).
6. If needed, plasma can be collected from top layer (e.g. for macrophage protocols).
7. Harvest the PBMCs at the interphase – middle thick white layer. Use a 5 mL pipet to collect the PBMCs and swirl tube to help collect interphase and avoid taking up platelets, neutrophils, RBCs from lower layer.

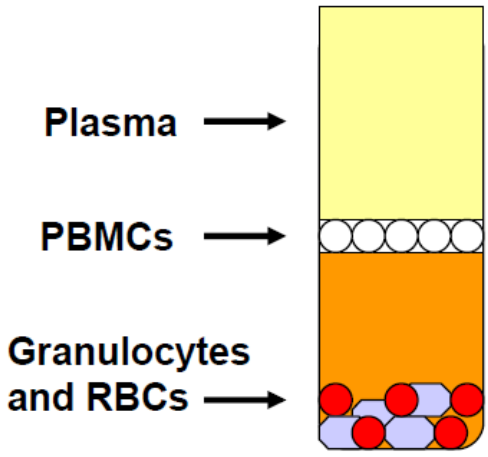

Figure AI.3.1 Illustration of cell separation by Ficoll gradient.

8. Transfer the PBMCs to a fresh 50 mL conical. Add fresh **ice cold** PBS to 50 mL and centrifuge for 10 min at 1500 rpm (524 rcf) at 4°C with the **brake ON**. This spin helps cells wash through any leftover ficoll.
9. Decant supernatants. If have contaminating RBCs (red color in PBMC layer), then resuspend cell pellets in ~5 mL of RBC lysis buffer and let incubate at RT for 5-10 min. If no RBCs, proceed to step 10.
10. Resuspend cells in ice cold PBS, making sure to brake up all cell clumps. Can pool cell pellets from 2 tubes at this point. Fill tubes to 50 mL with ice cold PBS.
11. Centrifuge cells for 10 min at 900 rpm (189 rcf) at 4°C for 10 min. Decant gently since this is a softer pellet.
12. Repeat steps 10-11 at least 2 more times until the supernatants are clear. Supernatant is cloudy from contaminating platelets, so wash out thoroughly.
13. Take a 10 µL aliquot of cell resuspension for cell count- it is best to first dilute 1 mL into 10 mL with PBS so have a 1:10 dilution for doing the cell count on leukapheresis PBMCs since high cell number.
    a. Cell count by mixing 10 µL cells with 10 µL of Trypan blue. Pipet up and down.
    b. Add 10 µL of cell-trypan blue mix to hemacytometer with cover slip
    c. Count cells in the 5x5 square grid. To calculate the total cell number: # of cells in grid x 2 (dilution with TB) x 10^4 = # of cells/mL

14. For freezing LN_2 stocks, freeze $3x10^7$ – $4x10^7$ cells per mL to 1 mL LN_2 vials. Aliquot enough PBMCs for freezing 25 stocks at a time (don't want to do all at once since the cells start dying if left too long in DMSO) and wash a final time with PBS, spin 10 min at 1000 rpm at 4°C.

a. Freeze cells in 90% heat inactivated FBS +10% DMSO
b. To heat inactivate serum:
    i. Thaw FBS in fridge or at room temperature
    ii. Prepare 50 mL aliquots for heat inactivation
    iii. Heat in circulating water bath at 56°C for 30 min. Mix throughout so heats evenly.
    iv. Cool on ice for preparing freezing media.
c. Have tubes labeled and caps loose. Resuspend pellets for 25 stocks in 25 mL of freezing media and quickly aliquot 1 mL per vial. It is best to have someone help freeze by closing the caps while aliquoting in order to speed up the process. Quickly place the stocks in the -80°C freezer in Styrofoam container. After 1 day at -80°C, can transfer the stocks to LN_2. Best to store the vials in the vapor phase rather than the liquid phase.

AI.4 Purification of CLL B cells

MATERIALS:

MACS buffer – 0.5% BSA, 2 mM EDTA in PBS (store at 4°C)

Human CD14 Microbeads – Miltenyi 130-050-201 (store at 4°C)

Human CD2 Microbeads – Miltenyi 130-091-114 (store at 4°C)

MACS dead cell removal kit – Miltenyi 130-090-101 (store at 4°C)

MACS B cell isolation kit II – Miltenyi 130-091-151 (store at 4°C)

- use this instead for purifying B cells from healthy donors

LS magnetic columns – Miltenyi #130-042-401

- can cool these columns to help reduce cell stickiness

PROTOCOL:

1. Thaw appropriate number of LN_2 stocks of CLL cells for number of CLL B cells needed quickly in 37°C water bath until they just begin to thaw (do not leave very long or let thaw completely since this reduces the viability of the cells).
    a. Estimate ~$3x10^7$ PBMCs per vial
    b. Can generally assume ~70% recovery of CLL cells from cell purification (~60-90%)
    c. For 1-2 vials, thaw into ~10-12 mL ice cold PBS; If using vials, thaw into 50 mL conical and fill with ice cold PBS
    d. Take a 10 µL aliquot and mix with 10 µL of Trypan blue for cell count using hemacytometer
    e. Note: if <75-80% cell viability, either don't use cells (dead cells do not stimulate well) or use MACS dead cell removal system to get rid of dead cells (recovery with dead cell removal generally not great 10-30%)
2. Spin at 250 x g (~1000 rpm) for 10 min at 4°C in swinging bucket centrifuge.
3. Resuspend cells in MACS buffer and magnetic beads:
    a. Per 10^7 cells: add 90 µL MACS buffer+ 5 µL anti CD14 beads (monocytes) + 5 µL anti-CD2 beads (T cells)

b. Note: Miltenyi recommends 80 µL of MACS and 10 µL of each set of beads, but this is much in excess since CLL PBMCs are generally >85% CLL B cells anyway.
c. Mix cells and beads well and incubate in fridge (4-8°C, not on ice) for 15 min.

4. Wash cells with ice cold PBS to remove unbound beads and spin 10 min at 1000rpm at 4°C.
5. During the last 5 min of spin, assemble LS columns in magnetic stand and rinse columns with 3 mL MACS buffer. Wait until it finishes dripping before adding sample.
6. Aspirate cell pellets and resuspend at a concentration of $2x10^8$ cells/mL or less and load sample on column, wait until it finishes dripping.
   a. Note: LS column capacity is to bind up to 10^8 magnetically labeled cells from up to $2x10^9$ total cells
   b. Safe to assume that the magnetically labeled T cells and B cells will represent <30% of the total PBMCs (generally only 2-15%)
7. Wash column 3 times with 3 mL MACS buffer (each time before adding more buffer, wait till it finishes dripping)
8. Keep negative fraction (=flow through), count and use it to proceed

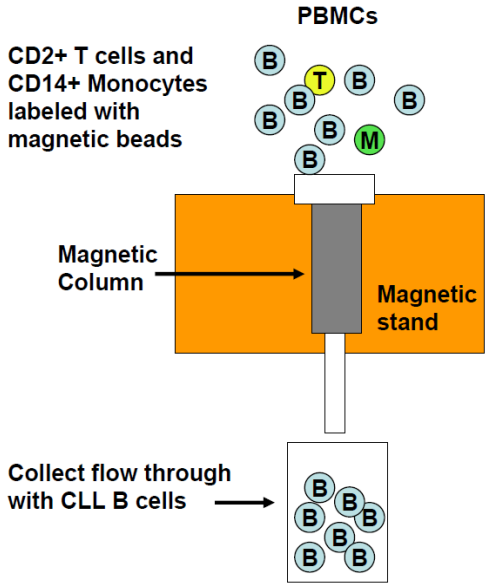

Figure AI.4.1 Diagram of CLL B cell purification by negative selection using magnetic assisted cell sorting (MACS).

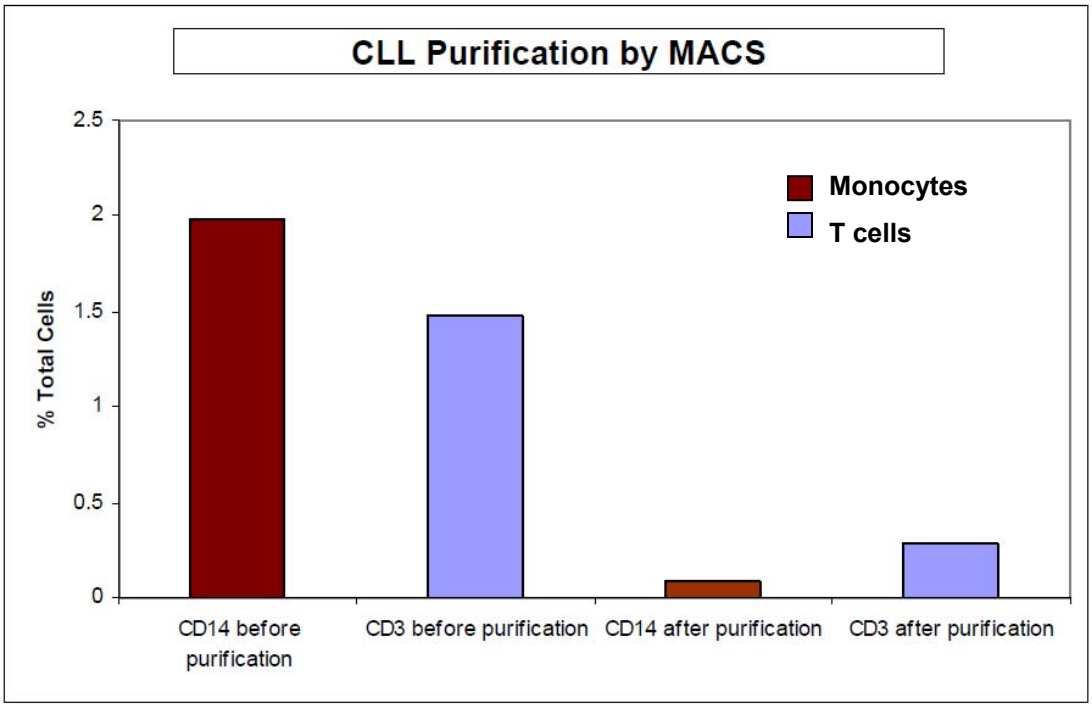

Figure AI.4.2 CLL purification by MACS. Quantification of % CD14+ monocytes (red) and CD3+ T cells (blue) in CLL PBMCs (before purification) and purified CLL cells (following negative selection by MACS). Representative data from one purification set, percentages quantified from flow cytometry data staining for the surface markers.

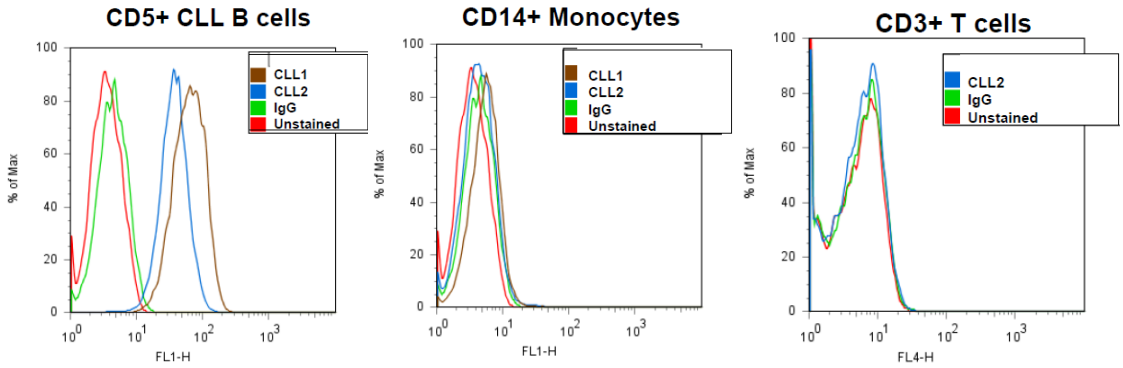

Figure AI.4.3 Representative flow cytometry data of purified CLL cells (following negative selection by MACS). Representative data from purification of two patient's cells staining for CD5+ CLL B cells (high expression), CD14+ monocytes (no staining) and CD3+ T cells (no staining).

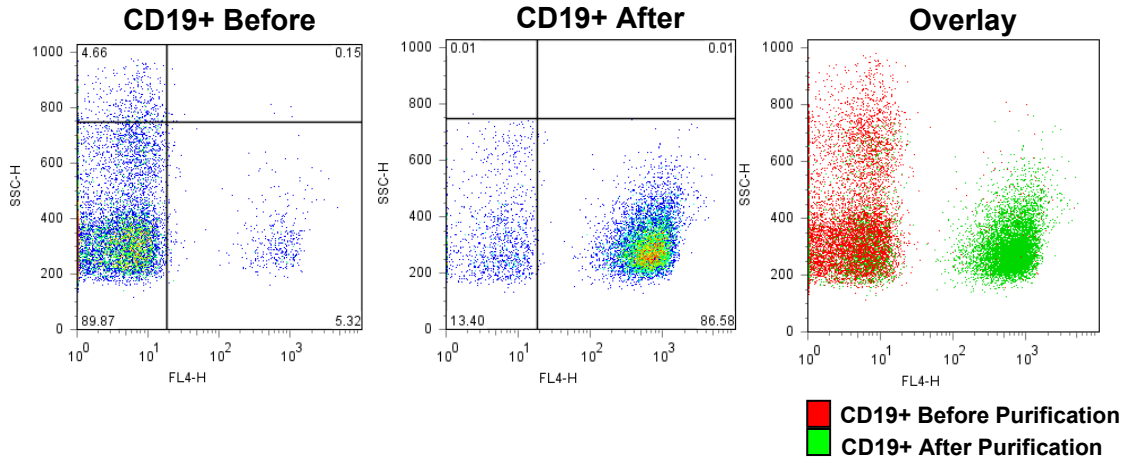

Figure AI.4.4 Representative purification data of normal B cells from healthy donors using MACS system (Miltenyi B cell Isolation Kit II). PBMCs from healthy donors were stained for CD19+ B cells prior to purification (left) and following purification via B cell Isolation Kit II (middle), and an overlay image showing distribution of cells before (red) and after (green) purification procedure, demonstrating good enrichment of B cells. Numbers in corners are percentages of total cell counts in given quadrants.

AI.5 Generation of Nurse-like Cells

MATERIALS:

PSG (pen strep L glutamine 100x) – Invitrogen 10378-016

Hepes (100x)- Gibco 15630

Human ab serum--male donors – Omega Scientific HS-20

Tissue culture grade Hepes (100x) – Sigma H0887

MACS buffer – 0.5% BSA, 2 mM EDTA in PBS (store at 4°C)

Human CD14 Microbeads – Miltenyi 130-050-201

Human CD2 Microbeads – Miltenyi 130-091-114

LS magnetic columns – Miltenyi #130-042-401

PROTOCOL:

1. Prepare the PBMCs from normal blood donors (from San Diego Blood Bank) by ficoll-hypaque density gradient centrifugation.
2. Isolate the CD14+ monocytes (positive selection) from the normal PBMCs at the same time as isolating the B cells from the CLL cells (negative selection) for generating the NLCs. Always keep a 1:25 ratio of monocytes:CLLs for generating the NLCs. Plate CD14+ monocytes at $1.25x10^5$/mL and then plate purified B cells on them at $3.1x10^6$/mL:
    a. Thaw ~2-3 vials of CLL liquid nitrogen stocks for each 24-well plate of NLCs, since need $3.1x10^6$ cells/mL x24 mL= $7.44x10^7$ cells.
    b. Need $1.25x10^5$ cells/mL of monocytes x24mL= 3x10^6 monocytes for a 24-well plate. Assume ~10% recovery of monocytes (usually ~15-20%) from the PBMC positive selection, so need to start with at least $3x10^7$ PBMCs.
    c. Isolate the CLL B cells using the Miltenyi MACS system: use 90 µL cold MACS buffer + 5 µL CD14 microbeads +5 µL CD2 microbeads (15 min incubation in fridge), wash out unbound beads with ~10 mL MACS buffer, spin cells at 250 x g for 10 min at 4°C, load onto column, wash 3x3mL with MACS buffer and keepithe negative fraction flow through. Note: manufacturer uses more beads, but we found this amount is sufficient especially since CLL cells are already so enriched.

d. Isolate the monocytes by positive selection using the MACS system: use 90 µL cold MACS buffer + 10 µL CD14 microbeads (15 min incubation in fridge), wash out unbound beads with ~10 mL MACS buffer, spin cells at 250 x g for 10 min at 4°C, load onto column, wash 3x3mL with MACS buffer. The flow through (negative selection) can be saved since it has B cells and T cells and you can purify normal B cells from this portion. After the 3x3mL washes, remove the column from the magnet and add 5 mL of MACS buffer to elute off the monocytes into new 15 mL tube.

3. Once the CLL cells and monocytes have been purified, take their cell count via hemacytometer (not the ViCell).

4. Resuspend the CLL cells and monocytes together in 10% Human Serum +Hepes +PSG so CLLs are at a final concentration of $3.1x10^6$ cells/mL and monocytes are at $1.25\ x10^5$cells/mL.

5. Plate 1mL of mixed cell suspension into each well of a 24-well plate (change volume appropriately for different size wells).

6. Let the monocytes differentiate into NLCs over time course of 7-12 days. No need to change media unless keeping in culture past ~day 14. NLCs should differentiate into fat, rounded, adherent cells.

7. When ready to use NLCs, gently rinse off the CLL cells with warm PBS (several rinses).

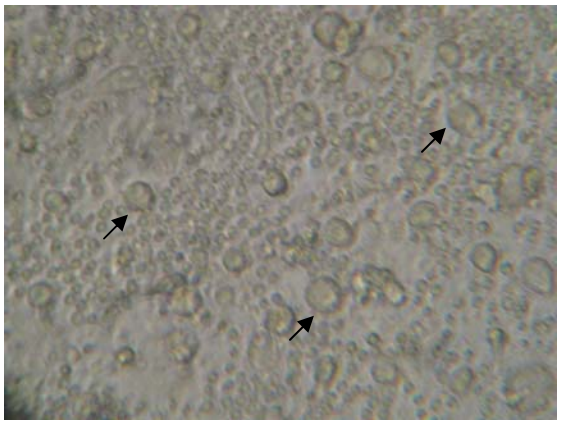

Figure AI.5.1 Image of NLCs. Following 7-12 days of monocyte-CLL coculture, monocytes differentiate into the fat, rounded NLCs shown above (a few select NLCs are indicated with black arrows).

AI.6 Monitoring CLL Cell Survival

MATERIALS:

DiOC6 (reconstitute at 40 µM) – Invitrogen D-273

Propidium iodide (PI) – Sigma P4864

CLL B cells- 10^6 cells/time point

PROTOCOL:

Thaw CLL cell stocks for survival assay

1. Get vials from LN_2, thaw quickly in 37°C water bath, as soon as there is still a little ice left, take the vials to the tissue culture hood, spray the vial with ethanol, wipe it dry and transfer the content to a 15 ml tube with cold PBS
2. Take a 10 µl aliquot for counting before spin
3. Spin cells 10 min at 1000 rpm (250 x g) (can be at 4°C or RT)
4. If cell viability is <80% based on trypan blue staining, should do dead cell removal to get rid of the dead cells (if already a lot of dead cells, the cells all die very quickly and can't distinguish differences in viability between treated and untreated).
5. Proceed with cell purification

Purification of CLL B cells

6. Resuspend cell pellet with 90 ul MACS buffer per 10^7 cells and 5 ul CD14-beads, and 5ul CD2 beads
7. Incubate cells with beads for 15 min at 4^oC (**fridge**, not on ice!!)
8. Add 10 times the volume of MACS buffer to cells and spin 10 min 1000 rpm
9. Assemble column and pre-wash columns with 3 ml MACS buffer
10. Resuspend cell pellet at $2x10^8$ cells/ml in MACS buffer and load on column, wait until last drop is "hanging".
11. Note: Load a maximum of 10^9 cells on one big column, only 10^8 cells can bind!!
12. For CLL cells safe to assume that <30% of total population will bind
13. Wash column 3 times with 3 ml MACS buffer, each time wait until last drop is "hanging" before adding next 3 ml

14. Take negative fraction (these are the B cells, need 1 x10^6 cells per stimulation time point)
15. Determine final cell count
16. Spin negative fraction 10 min at 1000 rpm and resuspend cells in XVIVO or 10% heat inactivated FCS or serum free RPMI media at 10^6/ml
17. Add 1 ml per well into a 24-well plate, one well per timepoint, incubate for 1hr before adding CXCL12 (or other stimulus)
18. Add CXCL12 stock to each +CXCL12 well for final concentration of 75nM
19. Samples are set up in duplicate or triplicate wells for the following time points: d0,1,2,3, 4,7, and 9 (or other time points depending on the experiment)

Plate setup:

-CXCL12	**D0**	**D1**	**D2**	**D3**	**D4**	**D7**	**D9**
+CXCL12	**D0**	**D1**	**D2**	**D3**	**D4**	**D7**	**D9**

Measure viability by DiOC6/PI and flow cytometry analysis

20. Transfer 100 µl from the d0 well into 3 FACS tubes and add 100 µl $DiOC_6$/PI mix for 15 min
    a. Prepare enough $DiOC_6$/PI mix for all necessary time points
    b. Add 2 µl $DiOC_6$ (40 µM) and 2 µl PI (10 µg/ml) per 1 mL of media
21. Analyze by FACS: settings 100,000 cells or 30 sec on high
22. Statistics: % $DiOC_6$dim of total , and total cell number collected
23. Day 0: set up triplicate wells for facs, use the first sample to set up FACS and the other two acquire the data

AI.7 Maintenance of MDA-MB-231 cells

MATERIALS:

Media: RPMI-1640 with Glutamax + 10% FBS (Invitrogen/Gibco)

DMSO- Sigma D2650

Selection Media for Neo^R, Puromycin^R, or Blasticidin^R transfected cells:

+ 5 µg/mL Puromycin (Invitrogen)

+ 5 µg/mL Blasticidin (Invitrogen)

+ 1mg/mL Geneticin (G418) (Invitrogen)

PROTOCOL:

Propagation (for cells >70-75% confluent):

1. Aspirate media
2. Rinse with 5 mL of PBS, aspirate
3. Add 1 mL of Trypsin-EDTA to plate, rock to distribute evenly
4. Incubate plate at 37°C for 2-3 min or until cells have lifted
5. Add 4 mL of media to plate and resuspend cells evenly
6. Add 8 mL of media to new 10cm plate
7. Seed the new plate with an aliquot of the resuspension (e.g. 1:12 is usually good, so cells only need to be split once/week) *
8. Change media on cells 3 x per week (M, W, F is good) until confluent again. Monitor number of passages.

Freezing Down

Materials needed:

Freezing media: 90% FBS/ 10% DMSO

Labeled cryovials (include cell line, date, initials) with labeled cap insert

2 x 15 mL conical styrofoam racks

9. Expand confluent cells from a 10cm plate to a 15 cm plate (can also seed a new 10cm plate for propagation at this time)
10. Bring media up to ~40 mL on the 15 cm plate and grow to >70% confluency
11. (1 x 15 cm plate = 5 LN2 stocks)

12. Rinse plate with PBS

13. Add 2 mL Trypsin-EDTA

14. Incubate at 37 °C until cells have lifted

15. Add 10 mL media to plate and resuspend cells evenly

16. Transfer cells to 15 mL conical and spin on low for several min to pellet

17. Meanwhile, prepare freezing media (or can do beforehand). For 1 x 15 cm plate, we prepare 6 mL of freezing media so there is a bit extra (can freeze extra at -20°C for later use, but avoid multiple freeze/thaws).

18. EtOH tube before bringing back into hood, aspirate media

19. Resuspend pellet in 5 mL of freezing media

20. Once evenly resuspended, distribute 1 mL of cell suspension into each cryovial

21. Place cryovials into 1 styrofoam rack; cover with an additional rack

22. Place at -80°C O/N (can be at -80°C for longer if necessary)

23. Transfer cells to LN_2 storage rack

AI.8 Retroviral Transfection and Infection Procedure

Original protocol from Dr. Jing Yang

MATERIALS:

TransIT-LT1 REAGENT - Mirius, # MIR2305

Serum free DMEM- Invitrogen/Gibco 10564

Sterile eppe tubes

HEK293t cells

DNA: pBABE vector construct, VSV-G and pUCMV3 (retro) or pCMVΔ8.2R (lenti)

Protamine sulfate (6mg/ml stock) in PBS- Sigma #P3369

PROTOCOL:

1. On the day before transfection, plate 1 x 10^6 HEK293T cells onto 6cm dishes in 4-5 ml DMEM/10%FBS. The cells are ready for transfection after 18-20 hours. For 10 cm dishes, double the quantities given here.
2. Pipette 6 μl TransIT-LT1 reagent into 150 μl serum-free medium, mix by gentle pipetting, incubate at room temperature for 10-20min. DO NOT TOUCH THE TUBE WITH UNDILUTED LT1.
3. Add 2 μg total DNA (in TE). For making VSV-G retroviruses by triple transfection use 0.9 μg gag/pol expression vector (use pUMCV3 for retrovirus and use pCMVΔ8.2R for lentivirus), 0.1 μg VSV-G expression vector, and 1 μg transfer vector. It is ok to add the plasmids separately.
4. Mix by gently pipetting
5. Incubate the LT1/Medium/DNA solution at Room Temperature for 30 min
6. Drip the mixture onto the HEK293T cells that were seeded the day before
7. Incubate the cells overnight at 37 °C

The day after transfection—

8. Change the transfected HEK293T media to 4-5 mL of fresh media
9. Seed targeting cells at 2-5 X 10^5 per 6cm plate. The next day, cells should be about 20% confluency and ready to be infected with the harvested viral supes.

48h post transfection—

10. Filter the viral supes from the HEK293T plates through 0.45um filter to get rid of floating HEK293T cells and put onto target cells. Add protamine sulfate at

6ug/ml (Sigma, #P3369, make protamine sulfate stock at 6mg/ml in PBS). After 4-6 hr infection, change to fresh media.

72h post transfection—

11. Repeat the infection as in step (10) using the 72h viral supe

12. Once the infected cells are confluent, cells can be expanded to a 10cm dish and proper drug will be added to select the resulting infected cells. Be sure to also seed a control plate of target cells not infected with viral supe and treat with selection media.

13. Once cells are selected, verify protein expression by flow cytometry or other means.

NOTES ON TransIT-LT1 REAGENT (Mirius, # MIR2305):

- Always make the reaction mix by first adding serum-free-media. It's ok to add the plasmids separately to the mix.
- The transfection efficiency with LT1 is comparable to that of Calcium Phosphate, but LT1 is not toxic to HEK293T cells.
- TransIT-LT1 is the same as Fugene6 from Roche, but cheaper.

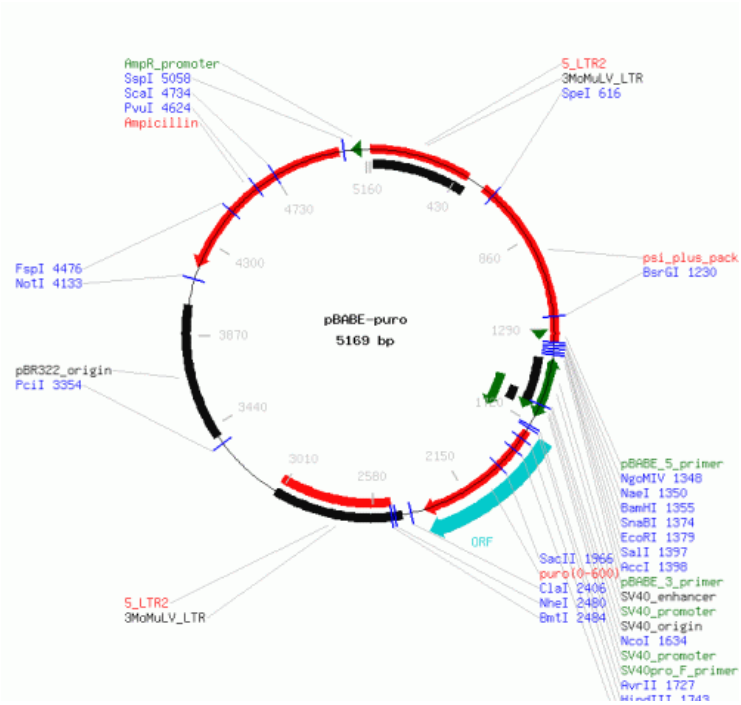

Figure AI.8.1 Vector map for pBABEpuro (from Adgene website).

AI.9 RNA Isolation and cDNA Synthesis

Original Procol from Etienne Danis, Dr. Jing Yang's lab

MATERIALS:

QIAshredder – Qiagen Cat. No. 79654 (for 50 units) or Cat. No. 79656 (for 250 units)

RNeasy Mini kit – Qiagen Cat. No. 74104 (for 50 units) or Cat. No. 74106 (for 250 units)

AllPrep DNA/RNA Mini kit – Qiagen Cat. No. 80204

β-mercaptoethanol/2-mercaptoethanol (RNA work only) – Sigma Cat. No. 60-24-2

Cell lifters – Sterile cell lifter from Corning/Costar Cat. No. 3008

Molecular Biology Grade (MG) Water – Cellgro 46-000-CM/CL

Ethanol (RNA work only, prepare 70% EtOH with MG Water) – Sigma E7023

RNase-free DNase set – Qiagen Cat. No. 79254

DNA/RNA LoBbind eppendorf tubes – Eppendorf 0.5 ml: 0030 108.035; 1.5 ml: 0030 108.051

High capacity cDNA reverse transcription kit – Applied Biosystems (1000 reactions) Part. No.: 4368813

*Use filter tips for pipetman in all steps of procedure

PROTOCOL (based on using the Qiagen RNeasy mini kit):

Cell lysis for RNA purification

1. Check availability for QIashredder columns, RLT lysis buffer, β -mercaptoethanol, cell lifters
2. Prepare the RLT lysis buffer + β-mercaptoethanol
    a. For $5x10^6$-$1x10^7$ cells, a 6-cm or a 10-cm plate: add 600 µL of RLT buffer
    b. For $<5x10^6$ cells or 6-well plates: use 350 µL of RLT buffer
    c. For each mL of RLT lysis buffer: add 10 µL of β -mercaptoethanol.
    d. Note: if using the AllPrep kit for DNA and RNA isolation, use the modified RLT Plus lysis buffer and add 10 µL of β –mercaptoethanol per 1 mL as above
3. Label QIashredder columns, one for each sample
4. Take plates containing cells at 80-90% of confluence from incubator and remove medium by aspiration or spin down appropriate number of suspension cells at 250 x g for 10 min and aspirate

5. Add directly RLT lysis buffer (600 µL or 350 µL) containing β -mercaptoethanol on the cells
6. Tilt the plate to make the RLT lysis buffer cover all the cells
7. Scrape the cells with a sterile disposable cell lifter, one new for each sample
8. Collect lysed cells with a Pipetman and a 1000-mL filter tip
9. Transfer the lysate in the QIashredder column to homogenize the lysate
10. Centrifuge at maximum speed (~14,000 g) and RT in a benchtop centrifuge machine for 2 min
11. Remove the column from the 2mL tube (discard column) and put a cap on the tube
12. Proceed to RNA purification step or put the tubes at -80^{o}C until later the next step, the RNA purification

RNA Purification Protocol

13. Put tubes containing cell lysates in Buffer RLT from -80°C to 37°C for ~5-10 min
14. Add 350 or 600 µL 70% Ethanol (equal volume to QIAshredded lysate) , mix gently by pipetting
15. Put up to 750 µL of this mix into the column
16. Centrifuge for 15 s at >10,000 g, discard FT
17. If necessary, put the remaining mix on the corresponding column and centrifuge again for 15 s at >10,000 g, discard FT
18. Add 350 µL Buffer RW1 into column
19. Centrifuge for 15 s at 10,000 g, discard FT
20. Add 80 µL DNaseI - Buffer RDD mix
    a. Stock Solution of RNase-free DNase I: Add 550 µL RNase-free water to the lyophilized DNaseI (RNAse free), mix by inversion. Aliquot 50 µL into small epper tubes and store at -20^{o}C
    b. For each sample, add 10 µL DNase I stock solution to 70 µL Buffer RDD
    c. Mix gently and keep on ice
21. Incubate at RT for 30 min
22. Add directly 350 µL Buffer RW1 into the column
23. Centrifuge for 15 s at 10,000 g, discard FT
24. Tranfer column into a new 2 mL collection tube (supplied)

25. Add 500 µL Buffer RPE into column

26. Centrifuge for 15 s at 10,000 g, discard FT

27. Add another 500 µL Buffer RPE

28. Centrifuge for 2 min at 10,000 g, discard FT

29. Transfer column into a new 1.5 mL collection tube (not supplied) (cap removed)

30. Centrifuge for 1 min at maximum speed, discard FT

31. Transfer column to a new 1.5 mL collection tube (not supplied) (cap removed)

32. Add directly 30 µL RNase free water on membrane

33. Incubate 5 min at RT

34. Centrifuge for 1 min at 13,000 g to elute

35. Quantification with nanophotometer using filter tips. A260/280 should be ~2

36. Store in -80°C or proceed to reverse transcription reaction

Reverse transcription protocol

37. cDNA synthesis with the ABI RT kit (without RNasin)

cDNA synthesis with the ABI RT kit (without RNasin)- 2x Master Mix		
10X RT buffer	2	µL
25X dNTP (100 mM)	0.8	µL
10X Random Primers	2	µL
MultiScribe Reverse Transcriptase (50 U/µL**)**	1	µL
RNase free H_2O	4.2	µL
2X RT Mix	**10**	**µL**
1 or 2 µg RNA plus RNase free H_2O to 10 µL	**10**	**µL**
Total reaction volume	20	µL

38. Mix well by pipetting up and down (no vortex!) and keep on ice

39. Set up thermal cycle run:

Thermal cycle run in the PCR machine
25°C for 10 min
37°C for 120 min
85°C for 5 min
4°C hold

40. Determine by standard curve the appropriate dilutions of cDNA to be in linear range. In general, for the 2 µg adding ~180 µL H_2O to reach 200 µL of final cDNA and use 4 µL of cDNA per real-time PCR reaction is in the linear range.

41. "-RT" cDNA synthesis without reverse transcriptase should be performed as a control for genomic DNA contamination the first time the RNA is used.

AI.10 Quantitative Real-time PCR

Original Procol from Etienne Danis, Dr. Jing Yang's lab

MATERIALS:

Power Sybr Green 2 X Master Mix – Applied Biosystems Cat. No 4367659

Molecular Biology Grade (MG) Water – Cellgro 46-000-CM/CL

RT PCR plates – Applied Biosystems 4346906

Plate Cover strip – Applied Biosystems 4311971

Filter tips

REAL TIME PCR PROTOCOL NOTES (for Applied Biosystems 7500 Fast):

- Use specific plates from Applied biosystems
- Set up samples in either duplicate or triplicate
- Always have a GAPDH control for each sample
- Have a non-template water control for each set of primers (tells you if there is any contamination in the water)
- Use filter tips on pipetman for all procedures, ethanol down bench before use, and prepare on RNA bench with pipetman, etc. for RNA work only
- Can prepare plate with template and mix ahead of time, sequence not important
- Contents of wells should be stable O/N at 4°C
- The necessity for samples to be prepared on ice is primer dependent, in most cases, ok to be prepared at RT but to be safe **prepare on ice**
- ABI recommends 50 µL volume, but 10 µL volume using a master mix is also reproducible
- Melting curve is found under "dissociation curve" results—want a single peak, if you see multiple, could be a result of primer-dimers, non-specific binding to dsDNA

COCKTAIL:

2 X Sybr Green Master Mix	5 µL
Primer Forward (5 µM)	0.4 µL
Primer Reverse (5 µM)	0.4 µL
RNAse free H_2O	0.2 µL
Mix per well to add	6 µL/well
Template	4 µL
TOTAL	10 µL

PROTOCOL:

Sample Preparation

1. Prepare primers, template, etc. at correct concentrations using molecular grade water for any dilutions. Note: if using primers for the first time, should set up a standard dilution curve to determine the linear range of cDNA amount to use
2. Add 6 µL of mix (including master mix, primers, and H_2O to each well)
3. Add DNA template to each well. For reproducible data, use new filter tip for every well even if using the same sample in triplicate
4. Start Real Time PCR machine for "pre-heating"
5. Cover plate with the adhesive covers being sure to align properly (cover all edges of circles surrounding wells—this will ensure that there are no leaks)
    a. Use plate film applicator to press film firmly over wells and around edges
6. Spin plate in benchtop centrifuge: 4000 rpm for 1-5 min (spin longer if there are persistent bubbles, best to eliminate them but should pop when the plate heats up anyway
7. Place plate in machine

Running Samples

8. Open Applied Biosystems 7500 Fast icon on desktop
9. Select "new document"
10. Select template: Use 2 Step RT protocol (from Yang Lab), in "Handel Lab" → "Rina_Morgan" → "Templates"
    a. PROGRAM:

i.	Activation of DNA polymerase	10 min at 95°C
ii.	DNA Amplification (x 40)	15 sec at 95°C
		1 min at 60°C
iii.	Melting Curve	15 sec at 95°C
		1 min at 60°C
		Increase gradually over 15 min to 95°C

11. Fill in well setup information; right click and select "well inspector":

a. Name contents in each well
b. Select what it is (e.g. U=unknown, S=standard, or NTC=non-template control)
c. For wells being assayed: select by check marking with GAPDH-sybr (should see green square in specific wells on template)
d. For wells that have nothing in them: uncheck (should not see green square in those wells—makes run faster)

12. Save as (be sure saved as an .sds file)

13. Start run (will want to save again, press “save and continue”)

14. Takes about 3 h to run

15. Turn off instrument after run (don’t keep on overnight)

16. Can keep plate O/N at 4°C

17. Can test amplification:

a. Load on gel
b. No need to stain (sybr green fluoresces under UV lamp)
c. Should see single band

AI.11 mRNA Stability Assay using Actinomycin D

MATERIALS:

Actinomycin D (*streptomyces* sp.)– Calbiochem 11466

DMSO-Sigma D2650

RPMI 1640- Gibco/Invitrogen 21875

QIAshredder – Qiagen Cat. No. 79654 (for 50 units)

RNeasy Mini kit – Qiagen Cat. No. 74104

PROTOCOL:

1. Resuspend Actinomycin D in DMSO at a 5 mg/mL stock concentration.
    a. Note: bright orange color when resuspended
    b. Store in fridge or freezer (I generally keep in -20°C) following resuspension
    c. Before use, thaw out at room temperature since it stays frozen on ice
2. Collect cells for Actinomycin D treatment: note, each time point is an RNA sample, so want ~$5x10^6$-$1X10^7$ cells for each time point.
    a. Primary CLL cells and B cells try to have $1X10^7$ cells since RNA yield is poor for these cells
    b. Cell lines can use fewer ~$5x10^6$ cells
3. Centrifuge cells at 250 x g for 10 min
4. Resuspend cells in media + Actinomycin D (Act D):
    a. Collect 0 h time point cells beforehand if don't want to waste Act D
    b. Concentration of Act D will vary depending on cell type, for CLL cells and leukemia cell lines, used 5 µg/mL final concentration (so stock is 1000x)
    c. Aliquot cells into wells to incubate over time course with Act D
        i. Note: for CLL cells, I used a 24 well plate with 1 mL media containing $1X10^7$ cells per well
    d. Cell lines can also use 12-well plates with 2 mL media and $5x10^6$ cells total
5. Incubate over time course with Act D at 37°C/5%CO_2: try time points such as 0, 2, 4, 6, 8, 12, 24 h

6. Collect time points, spin down cells at 250 x g for 10 min and resupend in RLT buffer. QIAshred and store homogenized lysate in -80°C until all time points are collected
7. Isolate RNA and perform Q-PCR according to protocols described above (AI.9 and AI.10)

AI.12 Inhibition of DNA Methylation by 5-Aza DC

MATERIALS:

5-Aza-2'-deoxycytidine (5-aza DC)- Sigma A3656

Valproic acid sodium salt (valproate)- Sigma P4543

DMSO-Sigma D2650

RPMI 1640- Gibco/Invitrogen 21875

QIAshredder – Qiagen Cat. No. 79654 (for 50 units)

RNeasy Mini kit – Qiagen Cat. No. 74104

PROTOCOL:

1. Resuspend 5-aza DC in DMSO* at 50 mM (11.41 mg/mL) stock concentration. Then prepare diluted working stocks at 5 mM (can dilute in PBS) and store in -20°C for later use (not stable very long)
   a. *Note: can also resuspend in 50% acetic acid or at 0.25 mg/mL in water
   b. 5 mg container, resuspend in 438 µL of DMSO for 50 mM stock
   c. Dilute 10 µL of 50 mM stock in 90 µL of PBS for 5 mM stock
2. Collect cells for 5-aza DC treatment: note, each time point is an RNA sample, so want ~$5x10^6$-$1X10^7$ cells for each time point.
   a. Note: this doesn't work on primary CLL cells since they don't actively divide, need dividing cells, can alternatively try 10 mM and 20 mM Valproate treatment for primary CLL cells
   b. Use cell lines only for this experiment e.g. EHEB
3. For EHEBs, resuspend so have ~$5x10^6$ cells total in T25 flask, 10 mL volume
4. Try different doses of 5-aza DC in 0.1-50 µM range and use DMSO as an untreated control (e.g. 0.5, 1, 5, 10 and 25 µM)
5. Incubate for ~72 h and harvest the RNA and DNA using RLT Plus buffer, Qiashredd to homogenize. Isolate RNA/DNA using All-prep Qiagen kit. Prepare cDNA and perform Q-PCR as described above (AI.9 and AI.10). Can verify inhibition of methylation by bisulfite sequencing analysis as described below (AI.21).
6. Note: may need to adjust time course depending on gene of interest and cell type. 72 h is a good starting point, but best to try multiple times ranging from 24 h to 12 days (DAPK1: 6 days to see effects of 5-aza DC in WaC3 cells)

AI.13 Adenoviral Infection of CLL Cells

MATERIALS:

CLL media: RPMI + 10% heat inactive FBS +PSG (pen-strep-glutamine) + hepes

GFP adenovirus, LacZ adenovirus, PHLPP1 adenovirus – all Ad5 vectors prepared by Atsushi Miyanohara at the UCSD viral vector core; viral titer and plaque forming units (pfu) determined by Atshushi as well

PROTOCOL:

Day 1:

1. Grow 3T3 fibroblasts in T-75 for seeding or prepare NLCs in 6-well plate.
2. Seed 250,000 3T3 fibroblast cells to each well of 6-well plate and culture for 24 h at 37°C/5% CO_2. (Note: Need 1xwell for AdenoPHLPP and 1xwell for AdenoGFP control per CLL patient per stimulation time point)

Day 2:

3. Thaw CLL cells for adenoviral infection:
    a. Want ~$1x10^7$ cells for each lysate ($1x10^7$ cells for each time point and need for Adenoviral GFP and PHLPP), but will only infect $2.5x10^6$ cells/drop
    b. Assume ~$3x10^7$ CLLs/vial for # of vials to thaw. Thaw CLLs into ice cold PBS.
4. Cell count and centrifuge 10 min at 250 x g.
5. Infect $2.5x10^6$ CLLs per 50 µl drop with adenovirus MOI= 300 pfu/cell.
    a. Resuspend cells at $5x10^7$ cells/mL ($2.5x10^6$ cells in 50 µl) in RPMI + 10% heat inactive FBS +PSG (pen-strep-glutamine) + hepes.
    b. Add appropriate amount of adenovirus for MOI of 300. Mix and distribute 50 µL drops in 10 cm plate so that they stay as a drop (be careful not to disrupt drop or surface tension).
    c. Note: usually do 4 drops (so $1x10^7$ cells) per time point x 4 time points for each adenovirus= 16 drops, which can fit into one 10 cm plate)
6. Incubate at 37°C/5% for 2h.
7. Resuspend drops in complete media and add onto 3T3 fibroblasts at ~70-80% confluency
8. Culture ~72 h for good protein expression (48-72 h)

AI.14 2D Gel Electrophoresis Protocols

MATERIALS:

FD cytoplasmic lysis buffer:

20 mM Hepes pH 7.9
10 mM KCl, 1.5 mM $MgCl_2$
0.1 mM EDTA
0.1 mM PMSF
Protease Inhibitor Cocktail (sigma p2714)
Halt phosphatase inhibitor cocktail (Pierce) containing sodium orthovanadate, sodium fluoride, βglycerophosphate, and sodium pyrophosphate

FD nuclear lysis buffer:

20mM Hepes pH7.9
420 mM NaCl, 1.5 mM $MgCl_2$
0.1 mM EDTA
25% glycerol
0.1 mM PMSF
Protease Inhibitor Cocktail (sigma p2714)
Halt phosphatase inhibitor cocktail (Pierce) containing sodium orthovanadate, sodium fluoride, βglycerophosphate, and sodium pyrophosphate

MM pellet lysis buffer:

5M Urea
2 M Thiourea
2% CHAPS
2% SB-3
0.1 mM PMSF
Protease Inhibitor Cocktail (sigma p2714)
Halt phosphatase inhibitor cocktail (Pierce) containing sodium orthovanadate, sodium fluoride, βglycerophosphate, and sodium pyrophosphate.

TEMD buffer:

50mM Tris-HCl
1mM EDTA
5 mM $MgCl_2$
1mM DTT

BCA assay kit – Pierce/Thermo Scientific 23227

Sepharose Q beads- GE Healthcare 17-1014-01

IPG strips: BioRad cat # 163-2018 (11 cm, pH 5-8, 10 per container)

Precast gels: BioRad cat # 345-0102 (12.5%trisHCl, 1mm, 1 per order)

Gnu sample buffer

2M thiourea
5 M urea
0.25% CHAPS
0.25% Tween-20
0.25% SB-3
10% isopropanol
12.5% water-saturated butanol
5% glycerol
bromophenol blue
Add fresh:
100 mM DTT
0.5% ampholytes 5-8 (biorad 163-1153)

Gel equilibration buffers 1 and 2:

#1: 15 M urea, 50 mM Tris-HCl pH 9.4, 2%SDS, 16% glycerol + 0.13 M DTT

#2: 15 M urea, 50 mM Tris-HCl pH 9.4, 2%SDS, 16% glycerol + 0.16 M iodoacetamide

9 g urea
8.5 ml water
1.25 ml 1 M Tris-HCl pH9.4 (dissolve at 37°C)
5 ml 10% SDS
4 ml glycerol to 25 ml total
Add DTT or iodoacetamide depending on buffer #

Overlay agarose- BioRad # 163-2111

Mineral oil- BioRad #162-2129

SDS-PAGE running buffer

Gel fixation buffer: 50% MeOH, 10% acetic acid, and 0.5 ml/L of 37% Formaldehyde

Silver stain rehydration buffer: 0.13g/L $Na_2S_2O_3$ (anhydrous) or 0.2 g/L of

$Na_2S_2O_3.5H_2O$ in dH_2O

Silver stain (prepare fresh):

0.1 g $AgNO_3$/50ml of buffer
1 µl/ml 37% formaldehyde

Developing buffer for silver stain:

60g/L Na_2CO_3 (sodium carbonate)
1 ml/L of 37% formaldehyde
30 ml/L rehydration buffer

Roche trypsin modified sequencing grade, Cat #11 418 025 001

4-alpha hydroxy cinnamic acid- Agilent G2037A

C_{18} ZipTips- Millipore ZTCO4S024

Microplate uniplate 250µl- Whatman Cat # 7701-6250

PROTOCOL:

Stimulation

Need 200-500 µg per set of 2DE
~300 µg of protein can be extracted from ~3-5X10^7 CLL cells
Need unstimulated and 3-4 time points of CXCL12-stimulated cells, in triplicate

1. Resuspend CLL cells at 1X10^7 cells/mL in serum free media and serum starve for ~ 3 h prior to stimulation
2. Stimulate with 30 nM CXCL12 over time course of 1 h (0 min, 3 min, 10 min, 30 min and 60 min)

Cell lysis and Fractionation

3. Wash cells gently with PBS. Note: CLL cells become adherent following serum starve, so can treat as adherent cells if gentle with them. Check, if have a lot of floating CLL cells too, collect these cells in tube and spin for lysis.
4. Lyse cells in FD cytoplasmic lysis buffer (~ 250 µl for a 10 cm plate) on ice for 30 min.
5. Spin at 13,000 rpm or greater. Collect supernatant as cytosolic fraction.
6. Resuspend pellet in FD nuclear lysis buffer if want to collect nuclear proteins
7. Spin at 13,000 rpm or greater. Collect supernatant as nuclear fraction.
8. Resuspend pellet in insoluble MM pellet lysis buffer. This is the insoluble protein fraction.
9. Perform BCA protein assay (for cytosolic and nuclear fractions) to determine total protein concentration of the lysates, or proceed to batch ion exchange for further fractionation of lysates.

Batch Ion Exchange (BIEX)

Note: (optional) to separate cytosolic extract into 4 further fractions and improve overall resolution and number of proteins identified

10. Sonicate samples (4 times with 30 second pulses of 3 sec on, 2 sec off; wait 2 minutes between each repetition)
11. Add cytosolic extract to washed Sepharose Q beads. Mix well at 4°C, then add 200 µl of 50 mM Tris-HCl, 1 mM EDTA, 1 mM DTT, 5 mM $MgCl_2$= TEMD buffer
12. Centrifuge at 4000 rpm for 1-2 min.

13. Collect different elutions by varying concentration of NaCl added to beads and lysate mix. Save first supernatant (no NaCl added) as FT fraction.

14. Resuspend pellet in 200 µl TEMD +200 mM NaCl and mix by pipeting and gentle vortex. Centrifuge @ 4000 rpm for 1-2 min. Save supernatant as Elute 200.

15. Add 200 µl TEMD +400 mM NaCl to pellet. Mix. Centrifuge @ 4000 rpm for 1-2 min. Save supernatant as Elute 400.

16. For final elution, add 200 µl TEMD +650 mM NaCl. Mix. Centrifuge @ 4000 rpm for 1-2 min. Save supernatant as Elute 650.

17. After collection, centrifuge fractions at 13,000 rpm to pellet any remaining beads.

18. Perform Chloroform Methanol Precipitation to remove salt and detergents from the cytoplasmic and nuclear extracts.

19. Perform BCA protein assay (Pierce) in 96-well plates to determine protein concentration

Isoelectric Focusing

20. Prepare 75 µg protein sample to run on gel for silver staining. Run ~200 µg for colloidal coomassie stain and spot picking for MS.

21. Dilute 75 µg of sample into “gnu” sample buffer for total of 200 µl

22. Start with the IPG (immobilized pH gradient) strips, using the pI 5-8 strips (can also use pI 3-10)

23. Run IPG strips on the Protean IEF:

a. Add strips to wells of Protean IEF system with 200 µl of protein sample solution in “Gnu” buffer
b. 4 hours of passive rehydration at room temperature
c. Overlay with 1.5 mL mineral oil to each well
d. 8 hours of active rehydration at 50V
e. No pause after rehydration
f. Run at 20°C at 250V for 15 min,
g. 8000V for 2.5 hours
h. hold at 500V
i. Note: if set up late in the afternoon, it should be done first thing in the morning

j. Remove the gel strips from the oil, gently blot off the excess mineral oil on a paper towel and place in the disposable gel strip tray
k. Can store IPG strips in -20°C if need to run on gels at a later date.

2D Gels

24. Before running gels, soak the IPG strips in the gel equilibration buffers in order to properly run on SDS-PAGE

25. Soak membranes with Buffer #1 (15 M urea, 50 mM Tris-HCl pH 9.4, 2%SDS, 16% glycerol + 0.13 M DTT) 2 times with 2 mL Buffer 1 per strip for a total of 15 minutes. Rinse with SDS-running buffer

26. Add Buffer #2 to the gel strips. Soak 2 times with 2 mL for a total of 15 minutes in Buffer 2. (15 M urea, 50 mM Tris-HCl pH 9.4, 2%SDS, 16% glycerol + 0.16 M iodoacetamide). The 5-8 strip like should turn from green-yellow color to blue color.

27. Note: do sequentially since iodoacetamide can inhibit DTT from reducing the proteins.

28. Load IPG strips on to 12.5% precast gels

a. Rinse IPG strips in SDS-PAGE running buffer
b. Warm overlay agarose buffer (purple) in microwave until liquid (0.5% agarose in 1X SDS Sample Buffer)
c. Fill well with overlay agarose and load IPG strip onto gel, position so even when running into gel. Insert the gel strip into the well so that the +5-8 are to the right of the marks for the ladder dye and press with tweezers to remove air bubbles
d. Add 10 µl of protein ladder to ladder lane
e. Top off wells with running buffer

29. Run for 54 min at 200V

Silver stain

30. Fix gels with 50% MeOH, 10% acetic acid, and 0.5 ml/L of 37% Formaldehyde

a. Rock at room temperature in the destain/fix buffer for ~30 min

31. Dehydrate gels with 50% ethanol washes

a. Do 5 X 30 min washes with 50% ethanol

b. At this point the gels should look dehydrated (brown/opaque or white band at the top) and should have shrunk to ~2/3 the original size

32. Rehdrate gels with rehydration buffer (0.13g/L Na2S2O3 (anhydrous) or 0.2 g/L of Na2S2O3.5H20 in dH2O)

a. Rehydrate gels for 60-90 sec.
b. Shake vigorously.
c. Should see the gel expand back to normal size and the top should turn clear again.
d. Wash 2X for 20 sec with dH_2O

33. Silver stain (0.1 g AgNO3/50ml of buffer, 1 ul/ml 37% formaldehyde)

a. Use clean gloves when doing silver stain
b. Incubate gels for 15-20 min with shaking
c. Should see it start to turn slightly brown
d. Empty waste into silver waste (not down drain)
e. Rinse briefly 2X with dH_2O

34. Develop (60g/L Na2CO3 (sodium carbonate), 1 ml/L of 37% formaldehyde, 30 ml/L rehydration buffer) with developing solution, shaking. Watch for resolution of bands so dark enough to see a number of spots but not overexposed (~0.5-10 min). Use clean gloves.

35. When ready to stop developing reaction rinse briefly 2X with dH_2O

36. Add 10% acetic acid to gel with water and leave gel in acetic acid solution for 30 min, after can transfer to just water and store.

37. Analyze gels using PDQuest program, versaDoc imaging system with spot cutter

38. For phospho proteins can use proQ diamond stain and phospho-tyr specific antibodies instead of silver staining, etc

Spot Picking

39. If running gels for spot picking, do a colloidal coomassie stain instead of a silver stain.

Colloidal Coomassie per 100 ml:

17 g ammonium sulfate

Dissolve in 66 ml mqH2O

Separately dissolve: 0.1 g g coomassie G250 in ~3-4 mL of methanol (best to use small glass beaker).
Add 3 ml phosphoric acid (should turn brownish now)
Once ammonium sulfate is dissolved, add ~30 ml methanol slowly to the ammonium sulfate solution (white precipitate that then goes back into solution)

40. Stain in colloidal overnight, rocking, room temperature

41. Destain for 5-10 min

42. Then water with Kimwipes for ~1 hour

43. Then leave in water for as long as want.

44. Scan colloidal coomassie stained gels. Make sure the zoom is set to 80, otherwise the gels won't match properly. For coomassie stained gels use the 11 setting. For spot picking, do not crop the gel image!

45. Prepare analysis sets for spot picking:

a. Spot detection wizard
-click on faintest spot (really just a faint spot- but still of interest and detection level)
-box the largest spot (actin)
-Will detect spots- check the vertical and horizontal streaking boxes, adjust the sensitivity, diameter, etc
-manually go through and edit/select spots you actually want to pick

b. Right click on master gel and choose "Analysis set manager".

c. Select "arbitrary". Select gel being imaged under "member. Check on box "all spots in membrane". Click save and done.

46. Make sure PD Quest is closed and Turn on the Spot cutter.

47. Open up the Spot Cutter and fill the 3 eppe tubes in back left with mqH2O.

a. Make sure the small cutting tip (~1 mm) is on (this is for gel cutting- if larger than this it is probably the one for nitrocellulose cutting).

b. Make sure a plastic cutting sheet is down on the cutting surface, then place gel on the plastic sheet and clamp in on sides of gel with the metal clamps to hold the gel in place. Make sure gel is parallel to the edge (not skewed).

44. Open PD Quest and open the appropriate analysis set for gel your cutting.

a. Go to “Identify”→”Analysis set excision tool”; analysis set= all spots. Everything should be set properly already, shouldn’t need to alter settings (1.5 mm tip, free gel, read down (A1, B1, C1…), etc)

b. Make plate- done. Makes cuts by quantity- 50µl.

c. First time in day using the spot cutter, first “Prime the Pump”.

d. Hit “Go”. “Acquire Image” and make sure set for white trans→ ”Proceed”

e. Right click on image and transform to make spots darker in order to better align. Align Green box and then click “Auto Align” for first run. For the spots that don’t match up, use “Jump and confirm”, threshold should be set at 88. Move blue targets to where spots should align.

f. Proceed with Plate- save. Position 96 well plate in front-right corner as indicated by PDquest. If cutting more than 96 spots, next plate is positioned in the rear-right, etc. as shown by the PD Quest software. Make sure A1 is facing you and it should be in the upper lefthand corner. Use the Microplate uniplate 250µl (Whatman Cat # 7701-6250)

g. Continue and spot picking should proceed ~9 min/96 well plate.

45. Once the spot picking is complete, it will ask you “Acquire confirmation Image?”, click “No” unless you want to see image of gel with holes cut from it.

46. ***Then be sure to EXPORT Data to an Excel file: Save as “…All spots Data”.

47. Delete the useless columns and sort by quantity (and then by plate # if >1 plate)

48. Cover the plate and store in -20°C freezer or continue with washes and tryptic digest.

Preparing the trypsin digest

49. Ethanol working area, change gloves, try to be as clean as possible and not to breathe on or reach over open plate to avoid keratin contamination.

50. Rinse out tray for multichannel pipettor.

51. Prepare ACN-NH_4HCO_3 wash solution to rinse out the coomassie stain from excised gel pieces: 50% ACN, 0.05 M NH_4HCO_3 (so mix 1:1, the ACN and 0.1 M NH_4HCO_3) (0.1 M NH_4HCO_3=3.93 g/500ml)

52. Remove the liquid from the wells using the 8 tip multichannel pipettor, being careful not to suck up the gel piece itself. Keep pipet tips off to one side and slowly take up liquid, scrape to make sure gel is not attached.

53. Wash the gel pieces with ~85 µl of 50% ACN, 0.05 M NH_4HCO_3 solution.

- **a.** Note- For washes can reuse the tips in the wells since just removing coomassie and not protein, so shouldn't cross contaminate.

54. Cover plate after adding 50% ACN, 0.05 M NH_4HCO_3 solution to all the wells and rock in 37°C for 30 min.

55. Gel pieces should be clear now. So be very careful when removing the wash solution from the wells since difficult to see the gel pieces.

56. Wash again with ~85µl of ACN, 0.05 M NH_4HCO_3 solution for 30 min at 37°C, rocking.

57. Remove the wash, again being careful not to take up the gel piece.

58. Optional- if want to make sure all the gel pieces are still there, then can add 100% ACN, should turn opaque and you can see them. Remove the ACN before adding trypsin solution.

59. Trypsin is stored in large -20°C freezer (Roche trypsin modified sequencing grade, Cat #11 418 025 001)

60. Normally, trypsin is prepared in an acid solution to delay its activity, but causes issues with having to add more bicarbonate at end- more salts, lead to more trouble getting rid of that in order to have good MS data. So, resuspend the trypsin (25µg bottle) in 250 µl of sterile, autoclaved water (small vial- black cap) so at a concentration of 0.1 µg/µl.

61. Prepare working trypsin solution: 100 µl of trypsin in 900 µl of sterile autoclaved water. Freeze remaining trypsin stock (0.1µg/µl) in -20°C which can be frozen and thawed one time- get into freezer ASAP.

62. Add 3 µl of diluted trypsin solution to gel pieces- individually add 3µl to each well.

63. Add 80 µl of 25mM NH_4HCO_3 +10% ACN solution to each well (multichannel pipettor).

64. Parafilm and incubate rocking at 37°C overnight.

Spotting MALDI plate

65. Grease MALDI plate with a coat of Lansinol so that the drops will bead up.

66. Obtain the Agilent Tech HCCA matrix from the fridge (αCHC, agilent cat # G2037A)

67. Prepare Matrix +ACN + Diammonium acetate + TFA as follows (should be more than enough for 96 well plate):
100 µl HCCA Agilent matrix

68. 256 µl 60% ACN

69. 40 µl diammonium acetate (100mM)

70. 4 µl of 10% TFA

71. Add 2.1-2.3µl of the matrix mix to 0.5 ml eppe tubes (enough for each spot picked) and quickly close the tubes so that the ACN does not evaporate.

72. Prepare buffers (good for ~2 weeks):

- **a.** 50% ACN
- **b.** 5% ACN + 0.1% TFA

73. Set out 3 trays for multichannel pipettor as follows:

- **a.** 50% ACN tray
- **b.** 5% ACN tray
- **c.** 5% ACN wash tray

74. Set out box of C18 Zip tips (for p10, Millipore Cat #ZTC185096) and empty box of zip tips. Fit zip tips securely to the 5-50 µl multichannel pipettor set at 40 µl.

75. Rinse Zip tips 3X with the 50% ACN, trying not to get air bubbles and discarding waste in tray lined with paper towel. Be sure to keep thumb pressed down on pipettor after ejection of wash in order to prevent introduction of unnecessary air bubbles.

76. Rinse Zip tips 3X in the 5% ACN solution (+0.1%TFA) and discard waste.

77. Pipet up and down in the peptide sample several times (3-6) and then eject in waste. Repeat with remaining sample. Eject all the way out.

78. Wash 3X with 5% ACN solution (3rd tray). On last wash, only eject ~1/2 of liquid in order to keep the tips moist.

79. Manually release the zip tips from the multichannel pipettor into the empty Zip tip container, keeping thumb pressed down on the pipettor in order to keep air from coming up (keep liquid in the tip).

80. Fit tip to a p20, eject the waste. Then use zip tip to pipet matrix-ACN solution from 0.5 ml eppe tubes 9-10 times to get the peptides out and spot the entire ~2 µl onto the MALDI plate.

81. Order should be A1, B1, C1…etc on the MALDI plate

82. Once finished, spot Angiotensin control peptide onto the plate in 2 wells (97 and 98).

83. Dry in the speed vac for several minutes.

84. Ready for MS analysis. Can store in wrapped in parafilm in dessicator for later use as well.

Mass Spec using the QSTAR (MALDI source)

85. Open up Analyst QS and oMALDI Server 4.0.

86. Open up virtual monitor to see the plate.

87. Click on Change Plate. Open with black knob and slide MALDI plate into place- A1 in the top left corner.

88. Check the voltages, etc on the machine to make sure everything looks ok before using (open up door).

89. Start pump down. MALDI plate should go in to low pressure compartment now.

90. In Analyst, go to "Manual tuning"→Open tune method→CC tune method X. Look at positions 97 or 98 where the angiotensin control is spotted. Set for 900-3000 mass parent ion (in MS TOF setting).

91. Laser power should be set for ~10-15% (something may be wrong if have to increase much more than that to see spectra).

92. Once have a good parent mass spectra in "MS TOF" setting, then change to "Product Ion" setting. Set that mass to 100 to 1300 (since angiotensin parent mass is 1296.6 so nothing should be larger than 1300). Go to "Advanced MS" and check both "suggest" boxes. Set collision energy to 58-60.

93. Masses should be within 0.05 or so. Hit "recalibrate" from the product ion AngioMSMS.

94. To move laser around and see where it's hitting, using "Shift + the arrow keys".

95. MALDI-TOF fingerprint data can be analyzed with the online database at Rockefeller University (http://prowl.rockefeller.edu) and MS/MS data was analyzed with the Mascot online database (http://www.matrixscience.com).

Notes: Plate Image shows up backwards (notice the numbering), keep in mind for what samples are. Trypsin is at 2163.05 Da, Angiotensin is at 1296.6 Da

AI.15 Preparing Cap-LC Columns

MATERIALS:

Deactivated fused silica .100mm X10m, Agilent P/N 160-2635-10, go to http://www.chem.agilent.com/scripts/Pcol.asp?lPage=2672, select Column Accessories, then Fused Silica (there is no direct link)

Column Packing Material Magic 5u 300A C18 (.50gm), Michrom Bioresources P/N PM5/66300/00**, http://www.michrom.com/catalog/index.php?cPath=22_124**

Ceramic scribe column cutter, Agilent # 5181-8836

PROTOCOL:

1. On bench, measure and mark cut length desired
    a. Suggested length- 17 cm per column
    b. For 17 cm column, cut 34 cm to make 2 columns
2. Pull out some of fused silica (be careful to only unravel a bit at a time) and measure to desired length, cut with ceramic scribe (pyromicro tecnolologies)
    a. To cut with scribe, press material into finger while passing scribe in other hand at 45deg angle over material. Adjust pressure/speed as necessary to scratch the top coating and gently tap off with finger. Don't try to cut with scribe. Should yield smooth straight edge with no jagged edges (look under microscope if necessary). Cut back further, if necessary, to obtain smooth edge.
    b. Fused silica comes in a 10 m pack – should yield approx. 60 columns (30 pieces to cut)
3. Once all pieces are cut to length, mark the middle point with black marker
4. Remove top coating of fused silica at middle point, to length of ~1 in. by *briefly* passing over medium, above blue flame
    a. Will see very brief spark of yellow/red
    b. Avoid keeping on flame for too long—don't want silica to bend or break
5. Wipe clean burned off coating with kimwipe and MeOH
    a. May need to work back/forth with kimwipe to remove all the black bits
6. ----------
7. Pull column (Tsien lab- Larry Gross) in Urey Hall, 2nd floor.
8. Use Sutter Instrument Co. Model P-2000 laser puller.

9. Turn on LHS

10. Enter in program 53 for pulling the CapLC columns:

a. Heat 330 vel 45 125pUL

b. Heat 325 vel 45 125pUL

11. Place clear region of column into the center section. Starting with left side, place the column into the grooves and hold into place with fingers, then tighten the knob to secure. Slide toward the center, then, while holding the two knobs to secure, adjust the right side of the column into the grooves. Press firmly and tighten the right knob.

12. Lower the shield and press “Pull”.

a. Should see the light flash 2-3 times and then pull the column apart

b. If the light stays on or flashes more than 3x, then it is not properly aligned, so press stop and try readjusting

c. Unscrew the pulled columns and carefully store so the tips don’t break.

d. Turn off the machine and cover.

---

13. Prepare packing material: place small spatula tip full of resin into 1.5 mL eppi; fill with ~0.5 mL MeOH to get resin suspension

14. Let resin equilibrate in MeOH for ~1 h or so prior to packing the columns

15. Use packing vessel to pack C18 resin into pulled column

a. Use goggles to protect eyes when packing (columns can shoot out of vessel)

b. Place open eppi with resin into center hole of vessel (may need to place something underneath to elevate to appropriate height)

c. Screw top of vessel into place

d. Tighten bolts

e. Place column into vessel, pulled side up, and tighten screw around column so doesn’t fly away when pressure is applied

f. Push column down until column bottom touches bottom of eppi

g. Make sure both right hand (RH) and left hand (LH) valve are closed, then open main tank valve to pressure of ~600 psi

h. Now open LH valve but keep RH valve closed

i. Ensure that slow drip of liquid is coming out from top of column

i. If not, hold scribe at 45deg angle and make upward sweeping motion against very top of tip...if cut, should begin to see flow

j. Begin moving column up and down in packing vessel to help mix resin (settles over time). To do this, hold column firmly with one hand while loosening screw around column with other. Lift up/down.

k. Should only take a few minutes to pack 17 cm column, check progress of the resin moving up the column

l. Let column pack further in vapor phase for ~15-20 min (this prevents loss of material out the end of the column)

m. To remove column: close LH valve and open RH valve (should vent).

n. Hold column up to light against an unpacked column, move around until you can detect a difference between the two

i. Packed column= glowing

ii. Not-packed= dark

16. Store columns flat until ready for use

AI.16 Running Samples on LTQ

CALCULATING PEPTIDE CONCENTRATION
(based on Wadell, 1956 paper)

- Using a 10 µL quartz cuvette, add 20 µL of sample (this give most reproducible readings)
- Measure A_{214} and A_{224}
- Equation: $(A_{214} - A_{224}) \times 144 = c$ (in ug/mL +/- 10-100 µg/mL)
    - 2 fold difference from actual concentration is reasonable

Sample assignments:
7 µL/well for samples (ending up adding to ~20 µL total with 0.1% HAc)
40 µL/well for AngII standards (refilled for each run) (0.5 µM)
7 µL/well for BSA digest (1 µM)

GENERAL NOTES:

Prior to starting run:

- Added new capillary column to instrument
- Experienced some difficulties with getting a tight seal at the union junction of the end of the column
    - Tested flow and seal by going to Direct control under MS surveyor pump (set at 250 uL/min flow rate)
    - Tried several times but continued to get leakage (pressure reading ~150bar) from both ends, finally got end sealed but continued leakage from front, regardless of tightening/positioning
    - Tried new fitting for union part and front (extra parts are in plastic compartment box or in small cardboard box), twice when flow was applied, the front end where back of column is inserted popped out. On the third try, held column firmly in place, and this did not happen. Pressure increased to ~230 bar with no evident leaks.
    - Rechecked LTQ tune, all parameters seemed good when turned on
- So, started queue for Ang x2 and BSA
- Verified that BSA digest looked good by Inspect (against cow database): Got 59 peptides and ~40% coverage at a p-value of 0.95.
- Part way through run “b” runs (after 0-10 had run), only ~2-3 uL of sample remaining in wells. Tray cooler is definitely not working!
    - Added 6.5 uL of 0.1 % HAc to 0’, 3’, 10’, waited on 30’ and 60’ since they will have to sit for longer before their final run
    - After 30’ run, added 6.5 uL of 0.1 % HAC to 30’ well
    - Kept 60’ as is, for some reason, volume hasn’t really decreased as dramatically as the other wells
    - Later in the day, added 1 uL of additional peptide samples to 0’, 3’, 10’, 30’, and 1 uL of 0.1 % HAc to 0’-30’, plus an additional 1 uL of HAc to 30’ to compensate for large sample evaporation

    - Let run until tomorrow morning
- Brought AngII volume in well A12 up to 40 uL for remaining runs (added 0.1 % HAc and a bit more AngII)
- Added two additional runs to new sample queue (should finish at ~10am on 3/30):
- Removed plate from tray, resuspended dry wells with 4 uL of 0.1 % HAc and added to original suspension
- Noticed that column performance dramatically diminished around run 3a
    - AngII_13a looked good
    - AngII_14 had a lot of noise and no strong peak (after 0a and 3a runs)
    - Can tell also b/c there is a decrease in file size. Good runs yield ~60 KB raw file sizes while the noisy data yields ~30 KB files...
- Overall, will definitely need to rerun TJK24 replicates as well as run TJK527.

LOADING COLUMNS

Changed column to put our own column on the MS. First need to remove column on the instrument:

If nanomate is present-

- Right-hand side lever with knob- use this to unlock nanomate from base setting
- Carfully lift nanomate and place on top of spectrometer
- Next, place two notches (pressed against front of instrument) to upright position to release base of the nanomate, lift out and place on right hand upper shelf

Fixing new base on-

- Place black base on to fittings (be very carful with wire and capillary connections, these are fragile (especially near the left hand portion of the instrument near the injection port, etc.)
- Secure the two notches to stabilize base
- Plug left hand side electrical port in, also connect voltage into righthand side hole (circular)
- If manipulating later on (e.g. fixing leaks or readjusting columns), be sure to unplug right hand side connection, when done, be sure to replug or won't see any ions
    1. Unscrew the column from the fitting
    2. Loosen fittings to slide column back from injection port
    3. Always remove and load column through the front
    4. Remove green fitting and feed column from the back through the fitting, stop when almost or at the clear part
    5. Feed column into base

6. Be careful not to hit the tip against anything so that it won't chip or break, and feed the back end through the unit until it comes out
7. Screw the top part of the column in.
8. Adjust/slide base forward so easier to access end of column
9. Feed end of column into fingertight fitting so cone part is at end
10. Use scribe to cut end of column to ensure that end is not jagged
11. Screw the back part into the union fittings and make sure this is really tight in order to avoid sample loss (but not too tight or may break capillary column and cause problems).
12. Also, when adjusting into the fitting, be sure to completely unscrew the fittings, slide the screws onto the column end and then screw in tightly, otherwise it can come loose and sample won't load properly.
13. Bring the unit very close to the injection port by sliding the right portion forward and following by sliding the left part forward until the column tip is ~5mm from the injection port.
14. Use the fine adjustment knobs to adjust the column so the tip is centered with the injection port and ~1mm from the port.

LTQ TUNE

- Open LTQ Tune on desktop
- Check the following:
  - Convection gauge: Want to be >0.95, heated capillary behind metal cone
    - If less than this, need to replace, indicates that it is beginning to get clogged (looks like ~5-6 in rod with an end round piece, this round piece on the rod is oriented in the front of the cone)
    - Needs to be changed ~1week (not cheap, $750, but save old ones)
  - FT Perring gauge: Want <3 E-9 torr
    - The better it is, the better the data you get
    - If it increases a lot when comparing run to run, something is wrong
  - Photon multiplier (Ion Detection System): Want <1700
    - If >1900, means the photon multiplier has died
    - Red X when not running, this is ok, should have green check once started
  - Always one marked with red X, -300V (this is ok—reads wrong)

- Also, X next to these ok FT Prani gauge and FT- turbo pumps 1 and 2
- If any other X's are indicated, something is wrong, issue with communication, etc. Need to figure out before starting

DIRECT CONTROL/ EQULIBRATION

General Notes:

If encounter issues with pressure, etc- Check fittings, usually the one that directly connects to the column (union fitting)

1. Check that there are plenty of buffers. Buffer A= 0.1% AcOH in HPLC grade water. Buffer B= 0.1% AcOH in HPLC grade Acetonitrile
2. Also need to have secondary water container for the instrument, even though this isn't part of the buffer system.
3. Open up LTQ Tune to check that the nanospray is working properly
4. Use the direct control to get the pumps going. Run at 95%A, 5% B. Start at 150ul/min flow rate, pressure should be at ~80 bar for this flow rate (it was good ~75-80 bar).
5. Check flow from column:
6. When you're not collecting samples, but pump is on, remove voltage connection and adjust column position away from vacuum inlet...should see droplet forming on tip of column if things are running normally; if not, filters or column may be clogged (can replace filters)
7. To make tray arm move out:
8. surveyor AS $\rightarrow$Go to Direct control $\rightarrow$ position arm
9. To manually cool tray:
10. Go to Direct control $\rightarrow$ Set tray temp $\rightarrow$ set to 10 °C (can't really go below this)

***Pathway to direct control*:**

11. X-Caliber (icon on desktop)
12. Instrument setup
13. Surveyor pump (left hand side)
14. Surveyor MS pump (toolbar)
15. Scroll to Direct control and select (direct control box should appear)

16. Set conditions at 50% A and B, 200uL/min

17. Monitor pressure. If too high, indicates leak. Stop and readjust/tighten connector pieces.

18. Make sure liquid is coming out of tip...

19. Pressure starting higher ~235bar, but decreases as column packs and becomes equilibrated (normal pressure is ~180bar)

20. After few minutes, started AngII runs (x 2)

21. Look at profile: make sure there's signal (~E5-E6)

22. If both 2nd AngII run looks good, add other samples to Queue (already added to wells)...samples looked fine, started running other samples O/N

23. Reduce flow rate to 20ul/min in order to test connection. Pressure should increase to ~200 bar. Shouldn't go over 300bar. Emergency shut-off is already set for 400 bar, but make sure below 300 bar because otherwise may have issues. (our pressure was fine, a little on the low side, but still fine at ~180 bar). Wait a few minutes. If something is wrong with the fittings or the connection, then the pressure will quickly drop down to 0. (Pressure maintained though and seemed fine).

24. In order to make sure the nanospray is working, should see noise peaks coming up on the screen. If there is contamination, then will have large peaks, but if clean, then have just background noise, the highest peaks at lowest MW, this is fine.

25. Since we had a brand new column that had only been exposed to MeOH, the first run (first AngII control run) is essentially wasted in setting properties of the column and wetting it with ACN.

26. Another thing to keep in mind are the microfilters that prevent large particles and clogs from going into the instrument (one set before the split flow, one set after the split flow). These don't need changed too often, but they can become clogged and cause increase in pressure, so if there is an issue with pressure, this may be something that needs changed.

27. Once everything has been checked and seems to be running properly, then you're ready to start the run. Press OK (or start) on the direct control.

28. The LTQ, Surveyor AS and Surveyor MS pump controls should all read "ready to download".

29. After 1-2 min, should see green light on the instrument switch to injection mode (no split), this should cause the pressure to increase to what we saw before with the 20ul/min flow rate (~200 bar). Injection mode lasts for ~20 min.

30. After 20 min, the light will switch back to the split flow run, should drop pressure back down to ~80 bar.

SETTING UP METHOD

- Go to Roadmaps → instrument settings → here you can update or make a new method**—**Can open up an older method (though generally want it to be something that has worked recently)
- To obtain the most comprehensive data sets, Pieter recommends running several methods (>3) in which you vary the dynamic exclusion list parameters (e.g. time, abundant ion #, etc.), gradient (the longer the gradient, the more data you can generally obtain, but sacrifice the number of samples you can run, if defined MS time), vary the number of scan events
- MS detector setup:
  - For scan event 1:
  - can choose Ion Trap or FT
  - FT, generally obtain 1/4th of the data, but very high quality
- Set resolution to 12500 (narrows time domain resulting in a faster scan rate)
- Set mass range from 200-2000 (probably don't adjust this range)
- Set to centroid (otherwise files are too large)
- Ion Trap, generally obtain many peptides, though confidence level may be lower for these
- Set resolution to normal
- Mass range from 400-2000 ok (can narrow range to 400/500-~1500; here you will be getting most of the +2's peptides and faster scan rate by eliminating the poorer quality +1, and higher charge states—the higher charge states are not able to be processed by current search databases; 1500 m/z allows the largest peptides- usually ~3000Da to be detected in the +2 state)
- Set to centroid (otherwise files are too large)
- For all other scan events:
  - Choose Ion Trap

    - Can vary number of events depending on experiment (recommended is 10-20 events, For FT do at least 10 scan events)
- Our original settings included:
- Fragment- 1 (can set two 2, will increase confidence for a peptide ID)
- Repeat count-30
- Dynamic exclusion size- 200
- Dynamic exclusion time- 180 s
- Mass width- 1.5 Da (after 30-60s, if a peptide elutes within a mass width of 1.5 Da of another peptide, it is probably a different one)
- If adding scan events on top of the default 5 that appear, be sure to set the scan event details → check data dependent MS → Go to settings → Current scan events →
- Mass determined from scan event 1 (should read this for all)
- Nth most intense ion (current scan event minus 1, e.g. for scan event 7, set this number to 6)
- Sometimes may default to check APCI corona... (unsure what this does, for consistency, keep off as first five scan events default to off)
- Setting gradient:
- Have to go out to main page (bottom left hand, surveyor button), click gradient:
- Can adjust this:
        - Gradient used on 3/27/09 (for TJK24 and FBS) “090327...really 105”
        - 0 min 95% A 5% B 250 uL/min
        - 15 min 95% A 5 % B 250 uL/min
        - 90 min 30% A 70% B 350 uL/min
        - 95 min 5% A 95% B 500 uL/min
        - 98 min 5% A 95% B 500 uL/min
        - 98.1 min 95% A 5% B 350 uL/min
        - 105 min 95% A 5 % B 350 uL/min
        - 100 350 uL/min

- NOTE: Increased uL/min when at high % B because the back pressure decreases with Increased AcCN, so this compensates for that difference

RUNNING STANDARDS

- BSA digest at 1 uM to test how well column and gradient are working
  - 18-23 peptides is generally good
  - On our digest (stored at -20°C box) got 39 peptides, more than half had good p-values
  - Run inspect against cow_protein.trie file in Inspect_bestPhos folder
  - Should take ~30 min
- AngII at 0.5 uM is a good control between runs, if something goes wrong, can isolate when this happened by looking at the controls. Can also show if you have a lot of carryover and how well the column is doing
  - Elution time for 85 min gradient, for our column lengths, ~35-36 min elution, but can vary to elute from 30-50 min
  - Want strong peak (~E6, E5 still usually ok) and good peak shape with little noise

SETTING UP SAMPLE QUEUE

1. Go to Roadmaps → sequence setup → generate queue here...
2. Be sure to save sample queue list once you make it
3. Sample ID should be 1 for each sample
4. 5 uL injection volume
5. If for any reason you need to stop the queue, stop and delete the runs on the queue and set up a new queue with what you want following the original queue (although stopping the queue doesn't always work, may require restarting or resetting computer). Don't try to change and save existing queue while it's running.
6. Double-check data file save path and method path are correct (avoid spaces and apostrophes when naming files)
7. Pausing run sometimes works, but sometimes requires restarting or resetting (try to avoid)

8. Sample and AngII (or BSA digest) runs differ, be sure they are assigned correctly

LOADING/RUNNING SAMPLES

9. Always spin down samples prior to adding to well

10. Always make sure slits are in cover slip over each well with sample in the plate

11. Always make sure tray is cooled

12. Capillary temp should be ~200

13. Volume in wells should be at least ~15-20uL if leaving samples for several hours (e.g. o/n run) (best if 30-50uL); can dilute samples with 0.1% HAc

14. Navigating data:

15. Can view real-time plot to see data that is currently being collected

16. Once started, leave on sequence view instead of Real-time plot, saves computer energy

17. Monitor pressure: Generally 70-180 recommended but ~200-250 is ok too (if over 400 it will automatically stop; if this happens, system will stop collecting data but pump will continue to run, have to stop manually)

Specific Runs and trouble shooting

DAY 1 (032608):

- Originally loaded TJK375 and TJK863 0'-60' samples
  - AngII_01, BSA digest, AngII_02 ran well
  - Experienced LTQ-FT MS communication issue during first experimental run (TJK375 0' sample had been injected, nothing remaining in well)
    - Also had sample loss due to evaporation, tray cooling was not activated for some reason
  - Removed remaining TJK375 samples and put back into original eppes (placed at 4 °C, to load later)
  - Eventually got MS connected to computer again (see details below)

- Once communication problem was resolved, continued with experimental samples:
  - Brought up volume of TJK863 wells to ~20 uL with additional sample and 0.1% HAc to ensure samples didn't evaporate overnight
    - Added 5 uL of additional sample to each wells A6-A10 as well as 10 uL of 0.1% HAc to each to bring up the sample volume
    - Added more AngII to each well
  - Added 10 uL of MQ H20 to well A1 as a "testwater" run in case there was any residual sample on column or in well, ran this one first. Definitely still had peptides present.
  - Started new sequence queue with TJK863 samples only and let run O/N—finished Fri morning

- Realized that "method" we used for this set of sample was originally only an 85 min gradient where we set the run time to 105 min, but the gradient ended at 85. Therefore, for the last 20 min, only running 100% A

Run Sequence:

COLUMN 1/DAY 1
(First run of TJK375 and TJK863)

Sample ID	Position	Method	Time	Folder saved to	Comments
AngII_01	A:A11	Angio or BSA.meth	85	c:\MS\Handel\090326TJK375A863	Don't really see anything
BSA dig	A:B12	Angio or BSA.meth	85	c:\MS\Handel\090326TJK375A863	Looks really good, get ~39 peptides
AngII_02	A:A11	Angio or BSA.meth	85	c:\MS\Handel\090326TJK375A863	Looks good, 5E5 signal; strong peak, elutes at ~35 min
AngII_03	A:A11	Angio or BSA.meth	85	c:\MS\Handel\090326TJK375A863	Looks good, E5 signal
TJK375-0'	A:A1	LTQ_105gradient_090327.meth	105	c:\MS\Handel\090326TJK375A863	Encountered problem, no communication with LTQ-FT MS (see explanation below for resolving issue)

****NO COMMUNICATION WITH LTQ-FT MS****

- Following AngII_02 run, spectrometer tried running TJK375_0' but did not acquire data
  - If tried to view real time plot, says no data acquisition
  - Error messages read "FT mass calibration for this mode is more than two days old" (Pieter says this one was fine, should operate anyways), and "scan merge error" (he had not seen this one before)
  - Also, in LTQ tune, there were X's next to FT turbo pump, but everything else looked ok, this shouldn't be a problem
- However, pressure looked fine and appeared that gradient was still running
- Allowed run to finish, however, the pump did not stop after 105 min (despite this being the run time for the given method)

- Assumed some FT issue since method for TJKJ375_0' included FT for the scan event 1 with 2-11 being ion trap and error seemed to be associated with the FT component of the MS
- Set up a new method that was exactly the same as before except scan event 1 was set to collect by Ion trap
- Called Pieter for guidance
    - Reset MS (small black button on right hand side of spectrometer), logged out of programs, but never close LTQ console and LTQ Tune...did not fix, although the MS did seem to be operating fine despite communication problem
    - Next, tried restarting computer (removed network cable beforehand) (NOTE: instructions on wall for how to safely reboot)
    - Still wouldn't start a new queue—on XCalibur, where it says "surveyor MS", "surveyor pump", etc, (on left hand side) it said LTQ-FTMS was "not connected", although it seemed ok
        - If properly working, when starting a run: should read "ready to download", "waiting for contact closure", "running" (in ~1-2min), if it doesn't, there's some problem
    - Once computer initialized and programs were opened again, rebooted MS again...LTQ MS finally connected and recognized (LTQ MS status changed)
    - LTQ-MS computer generally unstable has to communicate with LTQ instrument (2 computers inside it), so may take several rounds of resetting and rebooting computer. Also, computer has had several viruses and affects the startup (pings the network constantly, which can cause it to crash and not successfully start programs up).
    - Once everything was running properly, plugged the network back in to the computer

Sample ID	Position	Method	Time	Folder saved to	Comments
Test water	A:A1	LTQ_105gradient_090327.meth	105	c:\MS\Handel\090326TJK375A863	Definitely some peptides present
TJK863 0'	A:A6	LTQ_105gradient_090327.meth	105	c:\MS\Handel\090326TJK375A863	
AngII_04	A:A12	Angio or BSA.meth	85	c:\MS\Handel\090326TJK375A863	
TJK863 3'	A:A7	LTQ_105gradient_090327.meth	105	c:\MS\Handel\090326TJK375A863	
TJK863 10'	A:A8	LTQ_105gradient_090327.meth	105	c:\MS\Handel\090326TJK375A863	
AngII_05	A:A12	Angio or BSA.meth	85	c:\MS\Handel\090326TJK375A863	
TJK863 30'	A:A9	LTQ_105gradient_090327.meth	105	c:\MS\Handel\090326TJK375A863	
TJK863 60	A:A10	LTQ_105gradient_090327.meth	105	c:\MS\Handel\090326TJK375A863	
AngII_06	A:A12	Angio or BSA.meth	85	c:\MS\Handel\090326TJK375A863	Looks good,

					~1E6, strong peak, a little background

COLUMN 2/DAY 2-3:
(TJK863 runs, FBS secretome run, MCP-3 footprinting runs)

- For the TJK873 samples that were run on Day 1, there were ~2-3 uL remaining in the well, recovered this and placed in original suspension (eppe). Also rinsed well with 4 uL fo 0.1% Acetic acid and added to original
- Added TJK375 samples (store in 4°C O/N): 9uL of sample + 9uL of 0.1%HAc
    - Ran with the 105 (but really 85 min gradient)
- Added all of remaining A12 AngII well to A11
- Once completed, recovered ~2 uL of TJK375_60 and rinsed well with 4 uL of 0.1%HAc and added back to original suspension, had removed remaining sample for 0-30min earlier and added back to suspension (recovered ~6 uL of sample from well, washed with ~3uL with 0.1% HAc)

Generated new run sequence for FBS and MCP-3 runs (090327_FBSandMCP3.sld)...Added to queue...should begin once previous queue has completed

- Loaded 30 uL of sample to wells C1-C3
    - FBS- used 0.02 ug/mL stock, added approx. 0.1 ug with a small amount of 0.1%HAc to bring up the volume
    - MCP3-
- Added 30uL more of 0.5 uM AngII to A11

AI.17 Using InsPeCT

1. Connect to LTQ-MS in PSB basement by opening “My network places” on office computer (Blackdog)
    a. NOTE: In order to look at the raw data with the qual browser and in order to generate the mzxml data, must have XCalibur installed on computer
    b. Once XCalibur software is copied into the Inspect folder, then register the following files:
        i. Using the command prompt, go into the Inspect folder and XCalibur subfolder→ System→programs
    c. Then to register type: regsvr32 XRawfile.ocx
        regsvr32 XRawfile2.dll
2. Copy .RAW files to Inspect folder on lab computer
3. Convert files to python script that is Inspect compatible (.mzXML) (note: can begin typing and select tab, will bring up correct file name...)
    a. Go to “Run” → cmd → Enter
    b. Type “cd My documents”→ enter →..... enter →“cd Inspect” (use “cd” command to change directory to until you reach the subfolder for Inspect)
    c. Type ReadW.exe <raw file path> <c/p> → Enter
        i. Select “c” = centroid profile
    d. Generates 3 files in Inspect folder. One is mzXML, and then two other formats of it. Use the mzXML file created.
4. Prepare normal and shuffled databases (e.g. human uniprot database designated “protein.trie”, contaminants database).
    a. Preparing a shuffle database: >python ShuffleDB.py –r Database\(database to shuffle.trie – so protein.trie in this case) –w Database\(name – humanshuffleDB.RS.trie)
        i. Need to then copy this generated Shuffle database into the main Inspect directory as well so it can be located
    b. Creating a new database:
        i. Download database from website (e.g. Uniprot download page)
        ii. Select the .FASTA folder to download
        iii. Copy .FASTA file into main inspect folder

iv. In command prompt type: >python PrepDB.py FASTA "uniprot_sprot".fasta (this will create the .trie and .index files of the database that are necessary to have for inspect runs

5. Open input text file and fill out information according to each sample, save by "input_name_txt". Can adjust specifications for Inspect here, to have it run based on what you want to look for (e.g. PTM)

a. Select databases: (for example, we used protein.trie, commoncontaminants.trie, shufflehumproteinDB.RS.trie)
b. Account for phosphorylation modification (80) (e.g. mod,80,STY,opt,phosphorylation)
c. Allow 1 modification per peptide
d. Make sure to copy this input file into the main inspect folder.

6. In script line, type "inspect.exe -i input file name.txt –o output file name.txt"

a. Press enter, will eventually read, initialization successful

7. Data Processing:

a. Can open up the output file in excel to get an idea of how many peptides you have and their quality (should cleave before and after R or K) and # of phosphorylation events (look for +80 in peptide). xxx designates a "fake" sequence. For phospho-peptides, can go back and look at spectra to see if looks reasonable- look for strong phospho peak and neutral loss of 49 Da (for 2+ charge state- H_3PO_4)

8. Generate a summary file (NOTE: be sure Python v2.5 is installed):

a. >python Summary.py –r outputfile.txt –d Database\protein.trie –w resultsname.html (may want to add folder for this in which case use –w Summary(folder name)\resultsname.html –v 1 –i .\ -p 0.99
b. v indicates except anything for which there is 1 peptide, could make more stringent by using 2, so need to see 2 peptides for it to be considered a result. –p is for the p-value and can also be changed. p 0.99 is not that significant of a p value, but it doesn't really mean that much with Inspect

AI.18 In-gel Trypsin Digest

MATERIALS:

Reduction Buffer:

10 mM DTT (Sigma- D5545) in 25 mM ammonium bicarbonate

50% ACN, 0.05 M NH_4HCO_3:

Mix 1:1, the ACN and 0.1 M NH_4HCO_3

0.1 M NH_4HCO_3=3.93 g/500ml

Alkylation Buffer:

100 mM iodoacetamide (Sigma- 16125) in 25 mM ammonium bicarbonate

Trypsin- Promega V5111 or Roche trypsin modified sequencing grade #11 418 025 001

PROTOCOL:

1. Rinse the gel with distilled water for 10 min to remove any particulate matter.
2. Excise bands of interest with a clean razor. Cut as close to the edge of the band as possible to reduce the amount of "background" gel. Place gel pieces in protein LoBind eppe tubes- if you want good recovery of the peptides, you should use protein LoBind tubes, otherwise a lot of the material will just stick to the tubes.
    a. Note: I did 2DE so everything was in 96-well plate format, so just scale up volumes: volumes should be ~3-4x the volume of your gel pieces
3. Prepare ACN-NH_4HCO_3 wash solution to rinse out the coomassie stain from excised gel pieces:
        i. 50% ACN, 0.05 M NH_4HCO_3 (so mix 1:1, the ACN and 0.1 M NH_4HCO_3) (0.1 M NH_4HCO_3=3.93 g/500ml)
4. Wash the gel pieces with ~85 µl (for 96-well plate, so use more like 300ul or so, enough to immerse your piece) of 50% ACN, 0.05 M NH_4HCO_3 solution.
5. Cover plate after adding 50% ACN, 0.05 M NH_4HCO_3 solution to all the wells and rock in 37°C for 30 min. Spin down the gel particles at 500 xg in a microcentrifuge for 5 min
6. Gel pieces should be clear now. So be very careful when removing the wash solution from the wells since difficult to see the gel pieces.

7. Wash again with ~85µl of ACN, 0.05 M NH_4HCO_3 solution for 30 min at 37°C, rocking. Spin down the gel particles at 500 xg in a microcentrifuge for 5 min.
8. Remove the wash, again being careful not to take up the gel piece.
9. Add 100% ACN for 10min, gel pieces should turn opaque and shrink. Remove the ACN. Need to reduce and alkylate before trypsin digest.
10. Swell the gel pieces in 50 ul of ***Reduction Buffer*** (10 mM DTT in 25 mM ammonium bicarbonate) and incubate for 30 min at 56°C to reduce the proteins.

    i. *Reduction Buffer: (For 10 mL)*
        i. *10 mL of 25 mM ammonium bicarbonate*
        ii. *15.4 mg DTT*

11. Spin down the gel particles, and discard all liquid.
12. Shrink the gel pieces with 50 ul of ACN, spin down the gel particles, and discard all liquid.
    i. *Gel pieces visibly shrank and became opaque.*
13. Add 50 ul of ***Alkylation Buffer*** (100 mM iodoacetamide in 25 mM ammonium bicarbonate) to block reactive cysteines, and incubate for 20 min at room temperature in the dark (iodo is light sensitive!).
    i. *Alkylation Buffer: (For 10 mL)*
        i. *0.185 g*
        ii. *10 mL of 25 mM ammonium bicarbonate*
        iii. *(Stored in 15 mL foiled tube)*

14. Spin down the gel particles and discard all liquid.
15. Add 100 ul of AcN and incubate for 5 min until the gel pieces shrink, spin down the gel particles at maximum speed in a microcentrifuge for 10 s, and discard all liquid.
16. Repeat step 15 two more times.
17. Rehydrate the gel particles in ***Trypsin Digestion Buffer***: 20 ug of trypsin (Roche trypsin modified sequencing grade, Cat #11 418 025 001) in 200 ul of 1 mM HCl and keep on ice. Just before use, dilute this stock solution in 25 mM ammonium bicarbonate to a final trypsin concentration of 6.5 ng/ul), add to gel pieces, and

incubate on ice for 30 to 45 min. After 15 to 20 min, check the samples to make sure they are absorbing the solution and add more Digestion Buffer if all liquid has been absorbed by the gel pieces. Once saturated, add 25 mM ammonium bicarbonate to cover the pieces and let the trypsin digest proceed at 37° C overnight. Keep covered to prevent dehydration.

i. *Immediately before use, diluted Trypsin into 6.5 ng/uL.*
ii. *Digestion Buffer:* *3.07 mL*
20 ug trypsin aliquot

18. Scaled up digest by 2.5 x. In 15 ml tube, had 6.25 mL of 25 mM ammonium bicarbonate. When samples were ready to be digested, added ~500 uL solution of resuspended lyophilized trypsin (200 uL/20 ug x 2.25= 2 + vials) into 15 mL conical.

19. Gel pieces required ~100 uL of buffer to be covered.

20. Peptides should now be in the supernatant. Add 100 µl of extraction buffer (1:2 (vol/vol) 5% formic acid/acetonitrile) to each tube and incubate for 15 min at 37 °C in a shaker. For samples with much larger (or smaller) volume of gel matrix, add the extraction buffer such that the approximate ratio of 1:2 between volumes of the digest and extraction is achieved. Transfer the supernatant to new tube. This can be speed-vac dried and stored in -20 until ready to resuspended for MS analysis.

AI.19 Bisulfite Treatment of DNA

Original Protocol from Christiane Knobbe

MATERIALS:

Sodium Bisulfite (Sigma-Aldrich #243973)

Hydroquinone (Sigma-Aldrich)

Mineral oil

Wizard DNA Clean-Up Kit- Promega #A7280

NaAc

EtOH

Solutions (freshly made each time):

10 N NaOH	4 g in 10 ml H2O
10 mM Hydroquinone	0.11 g in 100 ml
3 M Sodium Bisulfite, pH5.0	6.24 g in 20 ml H2O Adjust pH with NaOH Test with pH paper

PROTOCOL:

Bisulfite Treatment of DNA. Alternatively, use Zymo EZ DNA methylation Kit according to Manufacturer's Protocol.

1. Prepare solutions of NaOH, hydroquinone, and sodium bisulfite fresh.
2. Denaturation of DNA samples
    a. 1 ug DNA from each sample
    b. 1.5 ul 10 N NaOH
    c. 38.5 ul H_2O
    d. Mix in 1.5 ml eppendorf tube
    e. Incubate at 40°C for 15 min in heating block (1.5 N NaOH final concentration)
3. Bisulfite Treatment
    a. Add: 30 ul 10 mM Hydroquinone (mix turns yellow)
    520 ul 3 M Sodium Bisulfite
    b. Mix

c. Overlay with 2-3 drops of mineral oil
d. Incubate for 16 hours (O/N) at 55°C eg in a hybridization oven

4. Clean up DNA with Wizard DNA Clean-Up Kit, #A7280 according to protocol
a. elute DNA in 50 µl H2O
b. add 1.5 µl of 10 N NaOH to DNA
c. denature DNA for 15 min at 40C ➔ PCR possible

5. Salt precipitation of DNA
a. Add 1/10 vol (5 µl) 3 M NaAc and 2 vol 100% EtOH (100 µl)
b. mix well
c. store at -20°C for 30 min (or longer and/or colder)
d. spin down DNA for 30 min at 4°C with 14000 rpm
e. wash pellet with 70% EtOH
f. resuspend DNA in 15 ul H2O ➔ PCR possible

AI.20 General Bisulfite PCR Protocol

Original Protocol from Christiane Knobbe

MATERIALS:

Qiagen Hot Start Taq – Qiagen 203203

50% DMSO solution (in mq water)

10 mM dNTP mix

25 mM $MgCl_2$

PROTOCOL:

As CpG islands even after bisulfite treatment are GC rich and hard to amplify, use QIAGEN Hot Star Taq, 5% DMSO and long denaturation, annealing and elongation as well as about 40 cycles for PCR amplification.

Typical PCR conditions:

PCR mix	1x
10xbuffer	2 µl
dNTPs 10 mM	0.5 µl
forward primer 10 µM	2 µl
reverse primer 10 µM	2 µl
MgCl2	2 µl
DMSO 50%	2 µl
Hot Star Taq	0.2 µl
H2O	8.3 µl
DNA (bisulfite treated)	1 µl
	20 µl

PCR conditions:

95°C	15 min	
95°C	1 min	
58°C	1 min	40x
72°C	1 min	
72°C	7 min	
4°C	forever	

AI.21 PHLPP1 Methylation Analysis Protocol

MATERIALS:

Purified CLL B cells/normal B cells

AllPrep DNA/RNA mini kit – Qiagen 80204

Zymo EZ DNA methylation kit- Zymo Research D5001

50% DMSO (in water)

Prepare a 1.5% agarose gel

TAE/TBE buffer

TOPO/TA cloning kit – Invitrogen K4575-01

Qiagen Hot Start Taq – Qiagen 203203

QIAquick Gel Extraction Kit – Qiagen 28706

LB+carb/LB +kan plates

LB media, kan or carb selection

QIAprep Spin Miniprep Kit– Qiagen 27106

CpG methyltransferase M.SssI (In vitro methylation as positive control)- NEB M0226S

PROTOCOL:

1. Purify CLL B cells using MACS purification binding CD2+ and CD14+ cells, collect flow through.
2. Use to RLT-Plus buffer to lyse and QIAshredders to homogenize $1x10^7$ CLL cells per patient and isolate DNA and RNA using the ALL Prep Qiagen kit.
    a. Note: be sure to use DNAse with the RNA
    b. Save the RNA for RT-PCR
    c. Keep DNA for methylation studies
3. Bisulfite conversion of DNA for methylation analysis using the Zymo EZ methylation kit.
    a. Add M-dilution buffer (5 µL), DNA (500 ng) and H_2O (to 50 µL volume), incubate at 37°C for 15min
    b. Add 100 µL CT conversion reagent and incubate at 50°C for 12-16 hrs

    c. Incubate samples on ice for 10min
    d. Add 400 µL of Binding buffer to column
    e. Add samples into column and centrifuge full speed (~13,000rpm) for 30 s
    f. Add 100 µL wash buffer to column and centrifuge 30s

g. Add 200 µL Desulphonation buffer and let stand at room temp for 20 min
h. After incubation, centrifuge for 30 s
i. Repeat previous step
j. Place column in new eppe tube and add 10 µL elution buffer, centrifuge for 30 s to elute the DNA
k. Store DNA at -20°C

4. If necessary, prepare a nested PCR with Bisulfite converted DNA. Use primers without the Not1 site first. If have issues with sequencing (inserting Cs randomly), then do second PCR with the Not1 primer. For this work, primarily focused on regions between the Bis13 and Bis10 primers.

PCR Mix:

a. 10x Buffer	2 µl
b. dNTPs (10 mM)	0.5 µl
c. Fwd Primer (10 µM)	2 µL
d. Rev Primer (10 µM)	2 µL
e. MgCl2 (25 mM)	2 µL
f. DMSO (50%)- fresh	2 µL
g. Hot Start Taq	0.2 µL
h. H2O	8.3 µL
i. DNA	1 µL
Final volume=	20 µL

(If using 50 mM MgCl2, then 1 µL MgCl2 and 9.3 µL H2O)

PCR conditions:

95°C for 15 min

95°C for 1 min
58°C for 1 min
72°C for 1 min
X40 cycles

72°C for 7 min
4°C forever (hold)

5. Repeat PCR using 1 µg of DNA from 1st PCR reaction now using the Not1 primers *if having issues with sequencing reactions, otherwise, continue on to step 6 and skip the 2nd PCR amplification step with Not1 primers
6. Run gel (1.5% agarose- so 0.75 g agarose in 50 mL TAE/TBE buffer, heat in microwave, mix, add 2.5 µL ethidium bromide) of PCR products
7. Excise bands and gel purify the DNA before doing the TOPO/TA cloning
8. TOPO/TA cloning kit for sequencing into TOP10 cells using kit from Invitrogen.
    a. PCR product: 4 µL
    b. Salt solution: 1 µL
    c. Topo vector: 1 µL
    d. Mix reaction and incubate for 5 min at RT
    e. Place rxn on ice
9. Transform 2 µL of TOPO/TA mix into TOP10 E. coli
    a. Add 2 µL of DNA to TOP10 cells, gently flick to mix (do not pipet up and down)
    b. Incubate on ice for 15-30 min
    c. Heat shock at 42°C for 30 s
    d. Ice for few min
    e. Recover with 250 µl of room temperature S.O.C. media
    f. Plate 75 µl onto pre-warmed LB+carb or LB +kan plates
10. Prepare overnight cultures from TOPO/TA colonies in 5mL of LB+Kan or LB +Carb
11. Miniprep and send colonies for sequencing (for total of ~8-10 colonies per reaction)

AI.22 Primers for Bisulfite Sequencing of *PHLPP1*

Figure AI.22.1 Primers used to PCR amplify regions of bisulfite converted *PHLPP1* gene and promoter. DNA sequence of bisulfite converted *PHLPP1* gene and promoter (assuming CpG sites are methylated and retained). Boxed sequences indicate the primers used to probe these regions (forward= odd number and reverse=even number primers) and red highlight indicates the ATG start site. Not1 primers are the same with a GCGGCCGC Not1 site added to the 5' end of the forward (odd numbered) primers.

PHLPP Oligo Pairs (in order from promoter region to end of Exon 1):

Odd Number= Forward Primer
Even Number= Reverse Primer

PHLPP-bis-1	5′-gttgggatttgtagtttattatg-3′
PHLPP-bis-2	5′-aatctaaactcattaaatattaatcatac-3′
PHLPP-bis-7	5′-gggatggaatattgagatat-3′
PHLPP-bis-6	5′-cctaaaacctcttccc-3′
PHLPP-bis-9	5′-ggtagtagtagtagtag-3′
PHLPP-bis-8	5′-ctctcctcaacaaaaaaaaattaac-3′
PHLPP-bis-17	5′-gttaatttttttttgttgaggagag-3′
PHLPP-bis-14	5′-ctttataacccaactacacaaac-3′
PHLPP-bis-11	5′-gggtgaggtattagttttag-3′
PHLPP-bis-18	5′-aaaaaacaaaaccccccaac-3′
PHLPP-bis-15	5′-gttgggggttttgtttttt-3′
PHLPP-bis-12	5′-aaaataaactaaaaacctccc-3′
PHLPP-bis-13	5′-gagggttattgatagtt-3′
PHLPP-bis-10	5′-caaaacaaataacttccttacc-3′

AI.23 Western Blot Protocol

MATERIALS:

Ripa buffer

10 mM Tris pH 7.4
150 mM NaCl
1% TritonX-100
0.1% Na-deoxycholate
0.1% SDS
5 mM EDTA

5x sample buffer (10 mL)

1 M Tris/HCl pH 6.8 – 0.6 mL
Glycerol – 5mL
SDS – 1 g
2-Mercaptoethanol – 0.5 mL
Bromophenol blue – 10 mg
To 10 mL with mqH_2O

10x Transfer buffer (1 L)

Tris – 30.3 g
Glycine – 144.1 g
To 1000 mL with mqH_2O
Note: to prepare 1X solution for use, dilute 100 mL into 700 mL mqH_2O + 200 mL methanol

10x running buffer (1 L)

Tris – 30.3 g
Glycine – 144.1 g
SDS – 10 g
To 1000 mL with mqH_2O

10x TBS (1 L) pH 7.6

Tris- 24.2 g
NaCl- 87.7 g
Note: to prepare 1X solution for use, dilute 100 mL into 900 mL mqH_2O + 1 mL Tween (0.1%) (Final is 20 mM Tris pH7.5, 150 m NaCl, 0.1% Tween 20)

Complete protease inhibitor cocktail – Roche 11697498001 (or Sigma P8849)

Halt phosphatase inhibitor – Pierce/Thermo Scientific 78420

Precision Plus Dual Color protein standard- Bio-rad 161-0374

Non-fat dry milk – Apex 20-241

Bovine serum albumin (BSA) – Sigma A7906

Restore Western Blot Stripping Solution – Pierce/Thermo Scientific 21059
IgG Elution buffer – Thermo Scientific 21004
Amersham ECL Plus - GE-Healthcare RPN2132
Super signal west femto sensitivity reagent- Pierce/Thermo Scientific 34096
X-ray films (5”x7”)– Phenix F-BX57
Cell scrapers- Costar 3010 (small, for 6 well/6cm plates) 3011 (large for 10cm plates)
Eppendorf Protein LoBind tubes- Eppendorf 22431091 (1.5 mL), 22431064 (0.5 mL), 22431102 (2mL)
96-well plate (clear bottom)- Fisher 12-565-501 or Corning 3604
Criterion gels (18 well)- Bio-Rad #345-0124
Criterion XT MES buffer system- Bio-Rad #161-0789
Criterion XT 4X sample buffer- Bio-Rad #161-0791

PROTOCOL:

1. Prepare cell lysates for western blot analysis:
    a. Add fresh to Ripa lysis buffer: Protease inhibitor cocktail and Halt phosphatase inhibitor cocktail (can freeze extra complete Ripa buffer in -20°C)
    b. Rinse cells with PBS (can skip this for CLL cells if they are loosely adherent to plate)
    c. Add Ripa lysis buffer to cells in dish (adherent) or spun down in tube (suspension). Depending on number of cells/size of dish, vary the volume of lysis buffer appropriately:
        i. For CLL cells in 24-well or 6-well plate (~1E7-3E7 cells): generally use ~50-75 µL
        ii. For MDAs/HEKs in 6cm dish (~70-80% confluent): use ~100 µL
        iii. For 10 cm dish: can use ~200-250 µL
    d. Let cells lyse on ice in Ripa buffer for ~30 min
    e. Scrape cells with cell scrapers and transfer to 1.5 mL tubes
    f. Clarify by centrifuging at 13,000 rpm for 10 min at 4°C
    g. Transfer supernatant to new, labeled (Lo-Bind) tubes and store lysates in -80°C freezer for storage

2. Perform BCA protein assay on cell lysates to determine total protein concentration (allows equal loading of wells for western blot):
    a. Prepare a working stock of BSA standard at 0.2 mg/mL
    b. Prepare assay in duplicate or triplicate in 96-well plate
    c. Set up BSA standard wells first:
        i. 0 µg – 0 µL
        ii. 1 µg – 5 µL (of the 0.2 mg/mL solution)
        iii. 2 µg – 10 µL
        iv. 3 µg – 15 µL
        v. 4 µg – 20 µL
        vi. 5 µg – 25 µL
    d. For all unknown samples, add 1 µL of sample to each well (if worried about low protein concentration, can use larger volume but remember to take into account at end when calculating the protein concentration
    e. Prepare BCA solution mix: 1:50 ratio of clear:blue solution (so if need 10 mL, add ~9.8 mL of clear solution + 200 µL of blue solution). Mix and solution should turn green
    f. Use multichannel pipetor to distribute 200 µL to each well
    g. Incubate at 37°C for 30 min
    h. Read absorbance using the plate reader at 562 nm
    i. Determine unknown protein concentrations of samples using the BSA standard curve and linear regression.
    j. Calculate volume required for 20 µg of protein lysate and volume for 5 x loading dye
3. Prepare samples for western blot: 20 µg of total protein in 5x sample loading dye. Boil samples for 5-10 min. *Note: if probing for chemokine receptors, do NOT boil because this causes their aggregation and they do not resolve (stay in upper part of gel). Can store at -80°C or -20°C for running later.
4. Prepare SDS-PAGE gels
    a. Clean the glass plates and set-up apparatus with plates
    b. Prepare resolving gel solution and pour:
    For 1x1.5 mm gel, 7.5 ml is sufficient, for 1x1 mm gel, 6 ml is sufficient for resolving gel. Solution for 2x1 mm 10% SDS PAGE gels:

Water	4.75 mL
30% acrylamide	4 mL
1.5 M Tris pH 8.8	3 mL
10% SDS	120 µL
10% APS	120 µL
TEMED	5 µL

*Add TEMED and APS last. Wait until solidifies (~20-30 min).

c. Prepare stacking gel solution and pour:

Allow 2- 2.5 ml of solution for stacking per gel. Solution for 2x1 mm gels:

Water	2.75 mL
30% acrylamide	0.67 mL
1 M Tris pH 6.8	0.5 mL
10% SDS	40 µL
10% APS	40 µL
TEMED	4 µL

Wait until solidifies

5. Load samples onto SDS-PAGE gels with one lane for ~8 µL of Precision Plus protein standard.

6. Run gels at ~100V through stacking gel (~10 min) then can increase to 150-200V through resolving gel (~40 min)

*Time varies between gel thickness, can always run at a slower voltage too and increase the run time

Run gel until the loading dye has reached the bottom of the gel

Remove the upper stacking gel before transfer

7. While gel is running, prepare 1X Transfer buffer from 10X stock and cool on ice or in fridge:

a. 100 ml 10X buffer, 200 ml Methanol, 700 ml mq water
b. Mix well and cool

8. Take out ~5 gel trays for soaking gels, membrane, fiber pads, and filter papers

a. If using PVDF membranes, soak the membranes in 100% methanol (they won't wet in transfer buffer)

b. If using nitrocellulose, soak the membranes in transfer buffer (they dissolve in 100% methanol)
c. Soak the filter papers and fiber pads in transfer buffer
d. Once gels are done running, let them equilibrate for ~5-10 minutes in the transfer buffer

9. Prepare Transfer Sandwich:
a. Mark the membrane on upper right side for orientation and protein side
b. Set up transfer sandwich as follows (add transfer buffer between the different pieces of sandwich so thoroughly wet):
-Black side of plastic sandwich
-1 fiber pad
-2 filter papers
-gel
-membrane
-2 filter papers
-1 fiber pad
-clear plastic side
c. Remove air bubbles from sandwich by squeezing/rolling out
d. Insert sandwich into transfer set-up so black plastic sandwich is towards the black side, clear is towards red. Insert so the notch is at the bottom (flat side is on top).
e. Add the ice pack and a stir bar to the transfer unit
f. Fill completely with transfer buffer

10. Transfer while stirring on ice for ~1.5-2 h (need 3 h for large Criterion transfter unit) at 100 V
a. Arrange apparatus in ice tray to stay cold, place onto stir bar and keep stirring to dissipate heat while transferring
11. Block for >1 h in 5% milk-TBST at room temperature
12. Generally want to incubate in primary antibody O/N at 4°C (check on antibody specs for recommendations for incubation time, solution, and dilution). Most Cell Signaling antibodies: dilute 1:1000 in 5% BSA-TBST and incubate O/N at 4°C.

Keep in covered/sealed container so they do not dry out. For minigels, can use ~5-6 mL/gel, for large Criterion gels need 10-12 mL/gel.

a. Note: can generally reuse antibodies, store in -20°C for later use.

13. Wash blots 3x 10 min with TBST

14. Incubate in secondary antibody >1 h at room temperature (usually dilute the secondary antibody in 5% milk-TBST)

a. Note: for Thermo goat anti-rabbit secondary dilute 1:10,000- 1:20,000 in 5% milk-TBST when using Amersham ECL Plus to develop (stronger antibodies) and dilute ~1:100,000 in 5% milk-TBST when using the Pierce West dura femto sensitivity reagent. (Pierce also has pre-diluted antibody which can be used at 1:1000 instead, but no longer comes in the kit)

15. Wash blots 3x 10 min with TBST

16. Develop with appropriate reagent (Amersham ECL Plus or Pierce West Dura femto) 5 min at room temperature (best to do with lights off)

17. Expose to X-ray films

18. Can strip blots for reprobing or store in fridge or freezer in TBST for later use

a. If re-probing for different protein altogether, use the Pierce Restore stripping solution 10 min at room temperature

b. If re-probing for same protein (e.g p-Akt and then total Akt), better to use the IgG elution buffer to strip off the antibody since it is a more mild solution (had issues with Restore stripping off the protein with the antibody sometimes)

c. If 1st strip, usually don't need to re-block, but otherwise should re-block and then probe with new primary antibody

AI.24 Receptor Internalization Assay

MATERIALS:

CXCL12

PBS – Ice cold

FACS buffer: PBS + 0.5% BSA

Anti-CXCR4-PE (CD184)– BD Pharmingen 551510

IgG2A-PE control– BD Pharmingen 553930

*Note: Antibody clone for CXCR4-PE is 1D9, which should NOT interfere with CXCL12 binding (binds at alternative site), so acid wash is NOT necessary. Our data initially testing with acid wash supports these results, but do NOT need to repeat acid wash steps in future.

If unsure whether antibody binding is the same as ligand binding interface, then need to do an acid wash to remove ligand before staining with antibody:

Acid wash buffer 1: 50 mM glycine +100 mM NaCl pH 3 (w/acetic acid)

Acid wash buffer 2: 150 mM NaCl +150 mM acetic acid, pH 2.7

PROTOCOL:

Analysis of CXCL12-induced CXCR4 internalization by Examining Decrease in Cell Surface Expression of CXCR4

Day 1:

1. Seed 700,000-750,000 cells into 9 ells of 6-well plates for each cell type. For CXCR4 internalization, do not need to set up acid wash wells, but shown for purposes of unknown antibody binding site
2. 9 ells are for:
    a. Unstained control
    b. IgG control
    c. Unstimulated, no acid wash, CXCR4 stain
    d. Unstimulated, Acid wash 1, CXCR4 stain
    e. Unstimulated, Acid wash 2, CXCR4 stain
    f. +200nM CXCL12, no acid wash, CXCR4 stain
    g. +200nM CXCL12, Acid wash 1, CXCR4 stain
    h. +200nM CXCL12, Acid wash 2, CXCR4 stain
    i. Seed extra well of cells to get cell count estimate

Day 2:

3. Stimulate wells with 200 nM CXCL12:
    a. Easiest to prepare stock media solution (RPMI +10% FBS) with 200 nM CXCL12 added.
    b. Aspirate wells
    c. Add fresh media to "- CXCL12 wells" or media +200 nM CXCL12 to stimulated wells
4. Incubate for 45 min at 37°C to allow for internalization.
5. Place on ice and wash with ice cold PBS 2X.
6. Lift cells with 1M EDTA-PBS on ice- 500 µl/well.
    a. Note- next time can use normal 1mM EDTA
    b. Can also try wash with PBS, acid wash in well and then lift.
    c. Could also just have 2x10cm plates (stim and unstim) and then post-EDTA lifting do acid wash or no acid wash after distributing cells to tubes
7. Collect all the cells for staining since <1x10^6 cells per well. Take cell count for estimate with extra well.
8. After lifting cells, spin down at 250 x g for 10 min at 4°C
9. To cells for acid wash (leave non-acid wash tubes sitting on ice):
    a. Add 1 mL Acid Wash buffer (1 or 2) to tubes
    b. Invert several times
    c. Spin at 250 x g for 5 min at 4°C
10. Repeat acid wash step
11. Aspirate and wash with 1 mL FACS buffer to make sure to get out any residual acid buffer (this could interfere with antibody binding)
12. Aspirate all pelleted cell samples and resuspend in 100 uL of FACS buffer for antibody staining and aliquot into 96-well plates
13. Add 1.5 µL of IgG control or anti-CXCR4-PE antibody (BD Pharmingen) to samples. Incubate covered with foil on ice for 20 min to stain.
14. Wash 3 x 5 min with FACS buffer
15. Resuspend in total of 400 µl FACS buffer and analyze by flow cytometry
16. (Optional: can fix with 0.5 mL PBS +1% PFA) to save for analysis at later time

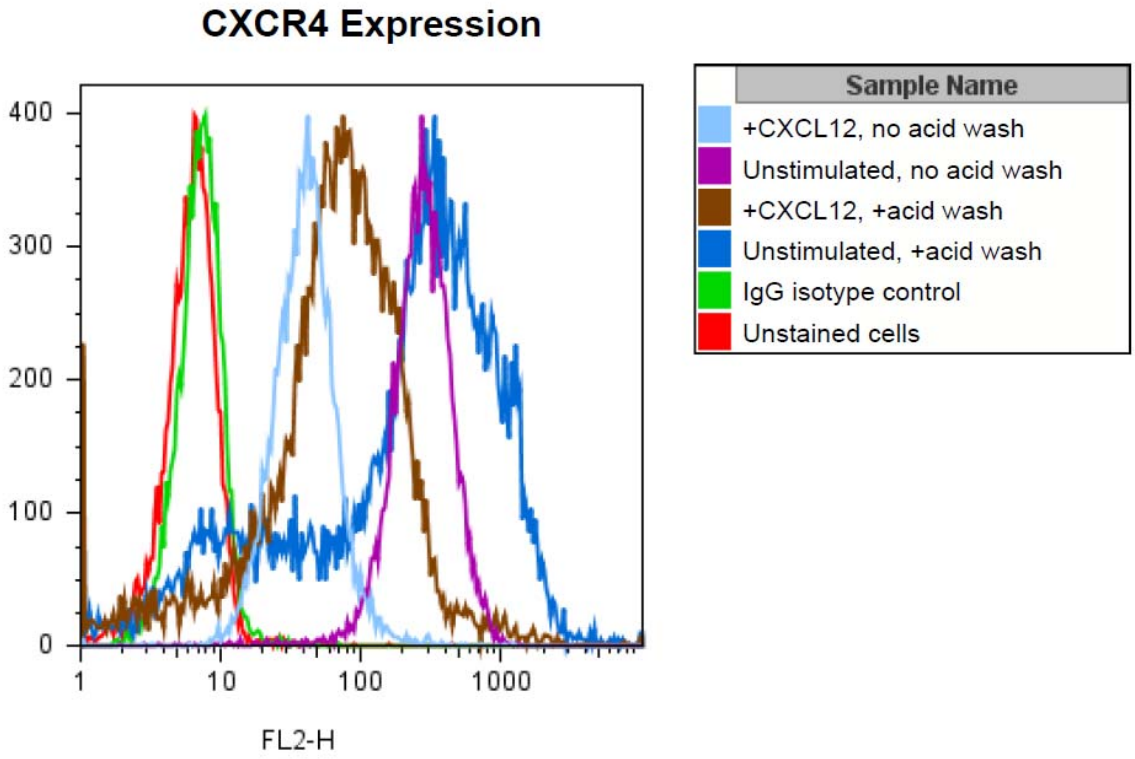

Figure AI.24.1 CXCL12-mediated decrease in CXCR4 surface expression. Ramos cells were left unstimulated or stimulated with CXCL12 (30 nM, for MDAs use 200 nM) for 1 h at 37°C/5% CO_2, treated with (+) or without (no) acid wash, stained for CXCR4 expression and analyzed by flow cytometry.

AI.25 Immunofluorescence Protocol

MATERIALS:

Primary Ab	Catalog #	Stock	Recommended use	To try
Monoclonal Anti-CXCR4 (mouse ∝ hu) IgG2B	R& D MAB172	500 ug/mL	5-15 ug/mL	10 ug/mL
Monoclonal Anti-CXCR7 (mouse ∝ hu) IgG2A	R&D MAB4227	500 ug/mL (10 uL alliqouts)	8-25 ug/mL	10 ug/mL
Monoclonal mouse Anti-IgG2A isotype control	R&D MAB0031	500ug/mL	None	10 ug/mL

Secondary Ab	Catalog #	Stock	Recommended use	To try
Alexa Fluor 488 (goat ∝ mouse IgG)	Invitrogen A11001	2000 ug/mL	None	1:500 or 1:1000

Cover slips- Fisher 12-545-100
Prolong Gold with DAPI– Invitrogen P36935
SeaBlock – Pierce/Thermo Scientific #37527

PROTOCOL:

DAY1:

1. Seed cells onto cover slips in a 6-well plate at 250,000 cells per well
    a. 500,000 seeded previously yielded ~70-80% confluency—a bit much

DAY2:

2. Everything can be done at RT, put coverslips on parafilm for washes and staining in order to conserve reagents
3. Wash 3 x with PBS for 5 min each

4. Fix slides with freshly prepared 3.7% formaldehyde in PBS/4% paraformaldehyde for 15 mins.
5. Wash 3 x with PBS for 5 min each (at this point, can be stored O/N at 4 °C)
6. Permeabilize with ~250 uL/slide of 0.5 % Triton-X 100 in PBS for 10 min (alternatively can use ice cold methanol to permeabilize)
7. Wash 3 x with PBS for 1 min each
8. Block with ~750uL of SeaBlock or 1%BSA/10% goat serum (or whatever species 2° Ab is) for 45m- 1h
9. Wash with 3 x with PBS for 5 min each
10. Incubate with ~250 uL primary antibody for 2 h (or O/N at 4 °C)
11. Prepare antibodies in 20 mg/mL (2%) BSA in PBS
    i. Anti-CXCR4 at 10 ug/mL= 5 uL stock + 245 uL buffer
    ii. Anti-CXCR7 at 10 ug/mL= 5 uL stock + 245 uL buffer
    iii. Anti-IgG2A at 10 ug/mL = 5 uL stock + 245 uL buffer
12. Wash with 3 x with PBS for 5 min each
13. Incubate with ~250 uL of secondary antibody for 30-45 min, covered with foil (Note: spin down secondary before use)

	Volume in 1000uL total (250 uL each)
Alexa Fluor 488 (1:500)	2.0ul
0.5% BSA/PBS	998.0uL

14. Wash 1 x with PBS for 5 min
15. If not using Prolong Gold with DAPI in it, can incubate with 1:1000 DAPI-Hoescht nuclear stain for 20 min
16. Wash 3 x with PBS for 5 min
17. Dip in ddH2O to rinse off PBS
18. Remove excess moisture and allow slide to dry slightly on benchtop before applying mounting solution Prolong Gold
19. Add 1 drop of mounting solution and add coverslip
20. Allow slide to dry O/N at RT
21. Next day, image using the deconvolution microscope

a. Samples can be viewed after 1hr, however for long-term storage dry overnight at room temperature and then store at -20^{o}C.

Using the Deconvolution Microscope at the Cancer Center Core

Contact: Kersi Pestonjamasp kpestonjamasp@*ucsd*.edu

If first user- Turn on UV lamp (Mercury 100W) and blackbox

If last user- Turn off UV lamp (if no one is signed up after you) and blackbox, once UV lamp is off, needs to remain off for 30 min

General system:

2 computers (hardware and software)

- Toggle between the two computers by pressing the switchbox to the left of the monitor

Software for acquisition is SoftWorx- bottom left icon to view programs→ select softworx

Desktop Control

1. Open DV instrument controller box (usually open, if not, will guide you through opening
2. File → Acquire (Acquire series for timelapse experiments)→ Yes (to initialize hardware)
3. Specify/select the following parameters in the toolbar prior to imaging:
4. Size (camera pixels)
    i. Full chip= 1300 x 1024 (larger area)
5. Exposure time (long enough to get adequate signal
    i. Generally ~0.2s-5s; 1s a good starting place
    ii. Find exposure option-will take 3 successive pictures and find the maximum pixels
6. Setup is a 12 bit camera (max range ~1000-1500)
    a. Bin- leave as 1 (only when signal is weak do you try to combine pixels, drawback is that resolution decreases)
    b. Objectives: 10X (dry), 20X (dry), 40X (oil), 60 X 1.4 aperture (oil), 100X 1.4 aperture (oil), 100X-Tirf, 1.49 aperture (oil)

i. Signal brighter under oil
ii. Add drop of oil onto slide and invert onto microscope
iii. We generally use the 60X
iv. Normal numerical aperture is 1.4—tells you how close objective will be to light—higher aperture gives brighter image and better resolution. 100X-Tirf objective lets in more light with slightly higher aperture of 1.49
v. Can't discriminate below ~200nm of points apart

c. Z-spacing
    i. For 60X, 1.4 aperture (smaller depth of field), ideal step size is 0.15
    ii. Spacing dependent on refractive index (RI depends on type of mounting solution, cell dispersion, dry slide); if using coverslip, don't have to worry to much about the depth
    iii. Remove excess mounting medium (could otherwise cause distortions)
d. Camera
    i. CoolsnapHQ is default (standalone is more sensitive, but slower, use only for backup)
    ii. 2 speeds (doesn't matter, so go with higher speed)
    iii. Gain = 2 for all colors
    iv. Blue window in toolbar- changes brightness
    v. Camera settings min and max- max of 1000-1500
    vi. Excitation filter (don't go below 0.5 s; if exp is too long even at ~0.2 s, can add a neutral density filter). Check that excitation and emission filters checked correspond
    vii. When viewing under the microscope and taking pictures, be sure that filter on the microscope matches settings on the computer (FITC and FITC), otherwise can burn eyes with unfiltered fluorescence
e. Automated stage moves in x, y, z
f. Mark and visit (allows you to mark a point, saves the x,y,z coordinates so you can revisit)

g. Lever on right- push back for eye piece, push forward for camera
h. Emission filter (select color on computer)

Microscope

7. Move to objective you designated
8. Add small drop of oil to coverslip (for 100X, need ~1/2 the amount of oil) (ideally, cells are grown on the coverslip)
9. Be sure slide is as dry as possible—press face down on kimwipe while applying pressure
10. Clean coverslip with Chloroform and Q-tip if necessary
11. Add slide oil side down (in contact with objective)
12. Lower the top piece- flip lever up to let light pass
13. Left side of microscope is the button to turn the light on/off
14. To see through eyepiece-- push stick in back position; to connect image to computer—push to forward position
15. Press bottom left hand button on joystick panel to turn on fluorescence, press again to turn off
16. In DAPI (select filter on computer and microscope when looking through eyepiece!), focus on cells with large knob, smaller adjustments with small knob
    a. Towards you—stage up
    b. Away- stage down
17. Turn bright field on for DIC- PHL- DIC analyzer, prism- use blank filter to look through
    a. Open shutter (next to fluorescence)
    b. Trans Ex shutter- exposure low
    c. post processing view blended colors- can collect fluorescent and DIC together
18. Collect series of z-stacks: ~20 sections from each slides
    a. Can start at focus and then move up and down
    b. or start at bottom and go up until through the focused image
19. Click Experiment→design→sectioning setup
    a. optical section 0.2
    b. # of optical: 10-11 (10 -11 above and below)

20. Click first box- color as DAPI, add FITC

21. File→save and exit

22. Deconvolution of Images:

a. Transfer data- DVUser:
    i. Host: 132.239.79.91
    ii. Octane 3 132.239.74.81
    iii. user: worx passwd: ap1dv1 port: 21
    iv. Sign up for time for deconvolution computer
b. Transfer data 1 files from DV computer “scope” to Octane Softworx data folder
c. open softworx and open data
d. Process→deconvolve, OTF=60x
    i. will already add OTF file
    ii. Method- aggressive (little grainy) or conservative based on # of cycles
    iii. 10 cycles of deconvolution is default, if image is dime, use fewer cycles; detailed- use more cycles
e. Try 2 cycles and 10 cycles of deconvolution, for cytosolic proteins, less deconvolution may work better (the 2 cycles)- conservative ratio
f. Drag xxx.r3d file to inbut bar → automatically generates output file
g. Queue multiple files using run options → add to queue
h. Drag other xxx.rd3 files to input bar- should see added to queue
    i. drag/add to input
    ii. click “do it”
    iii. worx- ap1dv1 – run to que
    iv. can take a while, so leave and come back later
i. Viewing/adjusting images:
    i. open xxx.r3d_D3D_Rv file
    ii. Adjust brightness for DAPI and FITC separately:
        1. select sun icon on left hand side toolbar
        2. Drag points on like to adjust brightness/background
    iii. Save as .tiff file
        1. Rename to be more descriptive

2. output size- 24 bit RGB
3. Details: can select z's to save
4. Press "do it", then you're done

iv. on left panel (half filled sun-looking icon)- scale image, copy and paste scale

v. For each image, compare isotype control staining (non-specific staining)

1. Once brightness for DAPI and FITC are adjusted on the sample image, select "copy scale"
2. open IgG image→open brightness icon → select "paste scale"
3. save image as a reference to original image

j. Downloading images

i. Open file transfer program to get remote access to computer

ii. IP address is 132.239.74.81 user: worx pass: ap1dv1

iii. Find folder and transfer to lab computer

AI.26 Detecting Chemokine Receptor Expression by Flow Cytometry

MATERIALS:

0.5% BSA in PBS (FACS buffer)
2% formaldehyde in PBS
0.2% Tween in PBS

anti- hCXCR3-PE mAb, clone 49801 (R&D, #FAB160P)
anti- hCXCR4-PE mAb, clone 1D9 (BD, #551510)
anti- hCXCR7-APC mAb, clone 11G8 (R&D, #FAB4227A)

anti- $IgG2_A$ isotype control-PE (BD, #553930)
anti- IgG_1 isotype control- APC (R&D, IC002A)

Prepare Cells for flow of surface expression:

1. Rinse each plate of cells with 5 mL PBS once (tilt plates and remove any excess PBS)
2. Add 1.5 mL of 1 mM EDTA-PBS to each plate to lift cells, incubate at 37 °C for several minutes (~10-20 min depending on confluency; avoid leaving low density cells incubating with EDTA for too long)
3. Add lifted cells to 2 mL V-bottom centrifuge tube, place on ice
    a. Add 8 mL media back to plate→ Discard if flow is ok, continue to passage if not (or expand if necessary)
4. Count cells on ViCell using 1:5 dilution (110 µL into 440 µL PBS)-
5. Resuspend cells in appropriate volume of FACS buffer to get 5 x 10^6 cells/mL
6. Add 100 µL or 50 µL aliquots of each population for the following samples to V-bottom 96 well plate:

For detection of intracellular receptor expression:

Cell Fixation

7. Aliquot 1 x 10^6 cells (200 µL of 5 x 10^6/mL stock) in FACs buffer to a new tube
8. Bring volume up to 875 µL with cold PBS
9. Add 125 µL of cold 2 % formaldehyde solution, vortex briefly immediately after adding
10. Incubate for 30 min at 4 °C
11. Centrifuge for 5 min at 250xg, remove supe

Cell Permeabilization

12. Resuspend pellet in 1 mL of 0.2% Tween in PBS

13. Incubate for 15 min in a 37 °C waterbath

14. Add 0.9 mL of PBS and spin for 5 min at 250xg

15. Remove supe and continue with staining. Resuspend in 125 uL.

16. Aliquot 50 µL of cells to each well for CXCR7 staining of permeabilized cells and 75µL for IgG controls

For both surface and permeabilized cells, stain as follows:
(Note: for each unique cell type, include an unstained and IgG isotype control)

Unstained

- Keep on ice until other samples are ready
- Transfer to small flow cytometry tubes in 400µL total volume FACS buffer

CXCR7 only (NOTE: CXCR3 staining same procedure)

- Add 10 µL CXCR7-APC 1° Ab
- Incubate on ice, covered for 20 min
- Wash 3 x with 250 µL FACS buffer: spin with MTP rotor 5 min, 250xg, 4 °C
- Resuspend in 400 µL of FACS buffer
- Transfer to small flow cytometry tubes

APC (CXCR7) Isotype control

- Add 10 µL of IgG-APC control
- Incubate on ice, covered for 20 min
- Wash 3 x with 250 µL FACS buffer: spin with MTP rotor, 5 min, 250xg, 4 °C
- Resuspend in 400 µL of FACS buffer
- Transfer to small flow cytometry tubes

CXCR4 only

- Add 1.5 µL CXCR4-PE 1° Ab
- Incubate on ice, covered for 20 min
- Wash 3 x with 250 µL FACS buffer: spin with MTP rotor 5 min, 250xg, 4 °C
- Resuspend in 400 µL of FACS buffer
- Transfer to small flow cytometry tubes

PE (CXCR4) Isotype control

- Add 1.5 µL of IgG-PE control
- Incubate on ice, covered for 20 min
- Wash 3 x with 250 µL FACS buffer: spin with MTP rotor, 5 min, 250xg, 4 °C
- Resuspend in 400 µL of FACS buffer

Transfer to small flow cytometry tubes

AI.27 Compensation on Flow Cytometer

1. Open template (e.g. “GFP and CXCR4 and 7”) or generate new one in BD Cellquest Pro
2. *Example:*
    a. Click icon to make Dot plot, click and drag onto template layout
        i. Should read SSC on y-axis and FSC on x-axis (Normal scale)
    b. Click icon to make Histogram plot, click and drag onto template layout
        i. Select Acquisition
        ii. Select FL-X for x-axis (log scale) and automatically should read counts on y-axis
        iii. Also make plot for Acquisition dot plot with FL-X on x-axis (log scale) and SSC on y-axis
3. Acquire → Connect to cytometer
4. Acquire → Acquisition and storage (To see # of events: Acquire → Counters)
    a. Make new folder for data, and select to collect data to this folder
5. Cytometer → Detectors and Amp (if needed: Cytometer → Compensation)
6. Cytometer → Instrument settings → Open old data point similar to what you’re analyzing now → Set → Done... make adjustments as you see fit using detectors and amps tool bar you already opened
7. Adjust compensation settings according to what you want, e.g. compensation between GFP (FL1) and PE fluorophore (FL2), using various population of cells that are either stained/unstained.
8. *EXAMPLE of populations and associated scatter profiles to adjust to:*
    a. MDA non-GFP unstained (low FL1 and FL2)
    b. MDA-GFP (high FL2, low FL1)
    c. MDA-GFP, CXCR4 stained (high FL1 and FL2)
    d. MDA non GFP, CXCR4 stained (high FL1, low FL2)

AI.28 FACS- Cell Sorting Experiment for Breast Cancer Cells

MATERIALS:
100% FBS for collection
Conditioned media from cells for seeding collected FACS sorted cells
Collection tubes- Falcon #352063
FACS buffer: 2%BSA-PBS
Falcon cell strainers- 352350
Remember to add PI before leave at a 0.5ug/ml final concentration, don't wash out.
CXCR4-PE antibody- BD Pharmingen 551510
3x20ul aliquots of CXCR7 antibody – for future, just use conjugated antibody
Goat anti-mouse APC antibody

NOTES:
Sorting for high receptor expression: CXCR4 (PE) and CXCR7 (APC)
Cell types: MDA MB231 and MCF-7

Time required for cell sorting process: ~3h

Contact:
Dennis Young
UCSD flow cytometry shared resource
djyoung@ucsd.edu
858-822-0407
Second floor of Moore's cancer center: room 2317

Goal: Sort MDA-MB231 and MCF-7 cells for the following populations:
CXCR4+ CXCR7+
CXCR4+CXCR7-
CXCR4-CXCR7+
CXCR4-CXCR7-

CXCR4 antibody is a directly conjugated PE antibody from rat.
CXCR7 antibody staining involves a primary monoclonal Ab from mouse followed by an APC-conjugated goat anti-mouse secondary Ab. *Now have directly conjugated antibody

*Want cells at ~50% confluency for the cell sorting. Day before, split confluent cells 1:4 dilution in order to have ~50% confluency for doing the sorting.

**Collect the top 10% expressing. Want~0.5x10^6 cells collected to culture. Collect into 100%FBS. Bring extra collection tubes.

Want to have at least $1x10^7$ cells of:
Dual stained

Want $5x10^6$ cells of:
Unstained
CXCR4 alone
CXCR7 alone

APC Secondary Control

Resuspend in final volume of 500 µl but bring extra FACS buffer

CXCR4 Ab- need to add 10 µl
Dual stained- use blocking conditions optimized on 7/23/07= 2%BSA-PBS, 1%normal mouse serum
Need to filter cells before sorting

CXCR7 primary staining- add 10 µl of the 500µg/µl stock antibody (normally do 5 µl equivalent, but staining more cells this time)
Secondary staining- 100 µl use 20 µl of secondary since have more cells ($1x10^7$ cells)
CXCR4 staining- need 10 µl in 100 µl with $1x10^7$ cells

Need to keep everything sterile- so do in the hood

PROTOCOL: For both MCF-7s and MDAs

1. Save media that cells grew in O/N. This conditioned media can be used along with 50% of fresh media to plate the cells in after sorting and help recovery. Just make sure to filter the media before use.
    a. Note: Confluency was ~60 % for MDA's and ~30 % for MCF-7s. Next time, seed MCF-7s at a higher density or make another plate.
2. Wash cells with 20 ml PBS.
3. Lift with 5 mL of 1mM EDTA-PBS.
4. Takes awhile for cells to lift even with warming and rocking. MCF-7 cells were especially resistant to lifting. Next time, try using 2 mM EDTA-PBS.
5. Add to 7 mL of PBS to get a total volume of 12 mL for each plate**.**
6. Total volume ~48 mL
7. Pool the 4 plates to a single 50 ml conical tube.
8. Perform cell count- 550 µl.
9. MDA-MB-231:
    a. Count= $0.45x\ 10^6$ cells cells/mL
    b. Total cells= (0.45×10^6 cells cells/mL) x 49 mL = 2.25×10^7 cells
    c. Resuspension volume= 2.25×10^7 cells x (mL/ 10×10^7 cells) = 0.225 mL
10. MCF-7:
    a. Count= 0.2×10^6 cells cells/mL
    b. Total cells= (0.2×10^6 cells cells/mL) x 49 mL = $9.8x\ 10^6$ cells
    c. Resuspension volume= $9.8x\ 10^6$ cells x (mL/ 100×10^6 cells) = 0.098 mL

11. Spin down cells for 5-10 min, 4°C at 250xg using the swinging bucket rotor

12. Resuspend cells so at a concentration of $1x10^8$ cells/ml in FACS buffer (2%BSA-PBS)

13. See above for volumes that cells were resuspended in. However, important to note that volumes end up being larger than what you resuspend in because not all of the supe is aspirated off in order to avoid cell loss. Therefore, cells are slightly more dilute than noted, due to the larger volume. Next time, can aspirate majority of supe and then pipette out the rest.

14. Aliquot cells into 1.5 ml eppe tubes

15. Note: did not have enough cells for all the samples/sample volumes. Decided to not make an APC control sample and to lower the number of cells for the CXCR4 only, CXCR7 only, and unstained samples. Kept the dual stain sample at 1 x 10^7.

a. At least 100 µl ($1x10^7$cells) for dual stain
    i. MDA- 100 µl ($1x10^7$ cells)
    ii. MCF-7- 100 µl (~1-2 $x10^6$ cells)
b. At least 50 µl (5x10^6 cells) for CXCR4 only
    i. MDA- 40 µl ($4x10^6$ cells) plus 40 µL of remaining suspension
    ii. MCF-7- 35 µl (3.5 $x10^6$ cells) plus 20 µl of remaining suspension
c. At least 50 µl ($5x10^6$ cells) for CXCR7 only
    i. MDA- 40 µl ($4x10^6$ cells) plus 40 µL of remaining suspension
    ii. MCF-7- 35 µl (3.5 $x10^6$ cells) plus 20 µl of remaining suspension
d. At least 50 µl of APC secondary control. (?)
    i. None. Not really necessary anyway.
e. At least 50 µl unstained (set aside in flow cytometry tube- add to 400 µl with FACS buffer and filter over cell strainer)
    i. MDA- 40 µl ($4x10^6$ cells) plus 30 µL of remaining suspension
    ii. MCF-7- 30 µl (3 $x10^6$ cells)

16. Start with CXCR7 Antibody staining:

a. To the dual and CXCR7-only tubes:

i. Add 12.5 µl of concentrated stock antibody (500 µg/µl) to the dual tubes (10x more than normal to compensate for the 20x more cells used)
ii. Add 6.25 µl of concentrated stock Antibody (500 µg/µl) to the CXCR7-only tube

b. Incubate on ice for 20 min.
c. Add to 1ml with FACS buffer. Spin at 250xg for 5 min. Wash again with 1 ml FACS buffer. Spin. Resuspend the dual in 75 µl FACS buffer and the single in 80 µl FACS buffer.
d. Add 25 µl of secondary APC antibody to the dual, 20 µl to CXCR7 only, and 20 µl to the secondary control tubes of cells.
e. Incubate on ice for 20min, covered with foil.

17. Serum block and CXCR4 antibody staining:

a. To the dual stain- add 100 µl of 1% normal mouse serum directly to the tubes. Pre-Incubate in serum block for 10 min.
    i. Made 210 µL of 1 % normal mouse serum.
b. To the CXCR7-only and APC control, add 1ml FACS buffer to wash. Centrifuge at 250xg for 5 min and resuspend in 400µl. Filter the cells over the strainers and transfer into the sterile, plastic flow cytometry tubes on ice.
    i. Note- strainers are too big so tilted on an angle over the tube to make sure to collect the filtered cells.
c. To the dual stain- add 15 µl of CXCR4 antibody and inclubate, covered on ice for 15 min.
d. Add 10 µl of CXCR4 antibody to the CXCR4-only stained tubes and incubate, covered on ice for 15 min (keep in TC hood with lights off)
e. Wash 2 x with FACS buffer (1 ml).
f. Filter cells over cell strainers and add to the falcon tubes for cell sorting (used the same tubes as do for collection- 5 ml collection tubes Falcon Cat # 352063).

18. Add PI to all samples just before leaving for the cancer center:

a. Add 0.5 µl of PI (0.5 µg/ml final) to each tube – actually a little higher since 0.5 µg/ml was 0.2 µl, but didn't want to use that small of volume

i. Dennis wants all samples to be PI stained (including “unstained”). Therefore, the unstained, CXCR4, and CXCR7 will technically be dualed stained and the CXCR4/CXCR7 sample will be triple stained.

19. Be sure to take 10 tubes (falcon collection tubes) with FBS to collect the sorted cells. Bring along extra tubes for collection and extra FBS.

20. Keep on ice in dark (foil-lined) container.

FLOW CYTOMETRY- CELL SORTING

Collection took about 3 h. Cells are collected into FBS because pH of media would be too high and would kill cells. Between collections, we brought the MCF-7s back to lab and put them onto plates to recover.

Cell Type	Neg.	CXCR4	CXCR7	Dual	CXCR4 high	CXCR7 high
MDA-MB231	656,452	8,383	725,631	525,628	69,415	104,563
MCF-7	167,670	136,799	115,796	163,239	121,385	93,111

For MCF-7 sorted cells-

- Put cells into sterile 1.5 mL eppis and spun 250xg, 4 °C, 5 min
- Made 50% RPMI-10%FBS conditioned media
- Seeded cells onto 12 well plates in a volume of 2.6 mL

For MDA sorted cells-

- Spun cells down
- CXCR4-only and CXCR4&7 sorted cells were plated onto 96 well plates
    - CXCR4-only were resuspended in 235 µl of conditioned media and seeded into single well
    - CXCR4&7 sorted cells were resuspended in 235 µl of conditioned media and divided into 2 wells (since had more cells) and an additional ~120 µl of fresh media was added to both wells

- Receptor Negative and CXCR7 sorted cells were plated onto 6-well plates. Cells were resuspended in 3 ml of RPMI + 10%FBS (1.5 ml of conditioned media + 1.5 ml of fresh media) and plated into 6-well plate
- CXCR4 high and CXCR7 high sorted cells were plated in 12-well plates in a volume of 2 ml (1ml of conditioned media + 1 ml of fresh media)

Notes-

- phenol red can inhibit single cell growth of some cell types. May want to consider using the RPMI-1640 w/o phenol red after sorting to help cell recovery and growth.
- For MDAs may want to reduce final volume from 400 µL to 200-300 µL. This will speed up the collection process because it's actually the volume that determines how long the sorting will take. However, the MCF-7 may be at their maximal density. If we reduce the final volume anymore, they may begin to aggregate, which is bad for cell sorting.
- For the FACS buffer, Dennis suggests increasing the BSA concentration. Could go as high as 10%. To make 10%, would need to stir O/N. Can store aliquots.

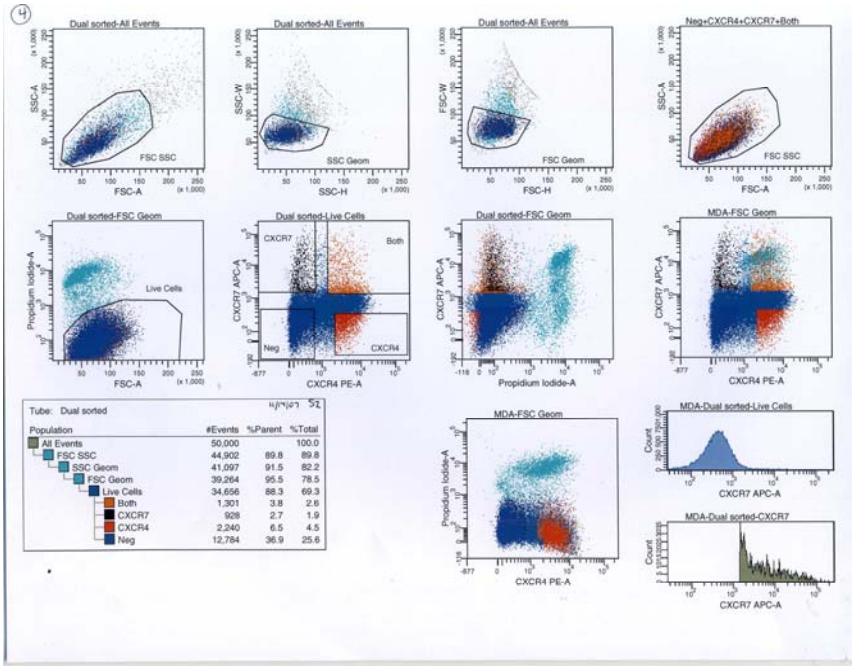

Figure AI.28.1 Representative FACS sort data. FACS of CXCR4 and CXCR7 dual sorted MDA-MB231 cells

AI.29 MTT Assay Protocol

MATERIALS:

RPMI 1640 (NO phenol red) – Sigma R7509

MTT reagent (Thiazolyl Blue Tetrazolium Bromide)– Sigma M5655 – 100 mg

96-well plates – Costar CLS3799

Resolubilization buffer- 0.04M HCl in isopropanol solution:

85 µl concentrated HCl (12.1N) to 25mL isopropanol

PROTOCOL:

DAY 1:

1. Prepare cell suspensions at $1x10^6$ cells per mL for the different cell populations in serum-free RPMI or RPMI+10%FBS (NO PHENOL RED)
2. Try 2 cell densities, $0.5x10^5$ cells/well and $1x10^5$ cells/well
    a. Prepare samples in triplicate and in media + or – 10% FBS media
3. To a 96-well plate:
    a. Add 100 µl of the $1x10^6$ cell/mL suspensions in triplicate to wells for $1x10^5$ cell wells.
    b. Add 50 µl of suspension + 50 µl of media to the $0.5x10^5$cell wells.
4. Incubate overnight at 37°C/5%CO2.

DAY 2:

5. Prepare 5 mg/mL MTT reagent in RPMI w/out phenol red (enough for 10ul per well + little extra):
6. Add 10 µl reagent to each well
7. Let incubate with reagent at 37°C/5%CO_2 for ~2.5 – 3 hours
8. Aspirate the MTT reagent from the wells
9. Add 100 µl of resolubilization buffer (0.04M HCl in isopropanol solution) to each well and pipette up and down to thoroughly mix using a multichannel pipette.
10. Read absorbances at 570nm and 650nm using the plate reader, mix first for 5 seconds.

AI.30 Mammary Fat Pad Injections

Reagents/Supplies:

Hamilton syringe (Hamilton, # 80530)
Kimwipes
Gloves
Styrofoam blocks wrapped in aluminum foil
Lab tape
Aliquoted matrigel (BD, #354234) (on ice)
Aliquoted cells (on ice)
Sterile PBS aliquoted for saline controls
Sterile PBS in 50mL conical (for cleaning hamilton syringe)
70% Ethanol 50mL conical (for cleaning hamilton syringe)
Waste receptacle
Pipettes to mix matrigel and cells (p20, p200) and filter tips
Ear punch
Ear punch code sheet
Shaver
Surgery tools (several pairs of scissors and forceps)
Autoclaved Q-tips (Puritan, #803-WC)
Autoclip kit (BD, #427638), includes autoclip applier, wound clips, and remover
Cauterizer (WPI, #500390) and replacement tips (WPI, #500396)
Spray 70% ethanol
Microwaveable heat pad (provided by vivarium)
Notebook, pen

Surgery Injection Protocol

Cell preparation:

1. Wash cells in 15 cm plates with 5-10 mL PBS
2. Lift with 3 mL of 1 mM EDTA. Add to ~11 mL of PBS in conical and mix.
3. Remove 550 µL for cell count.
4. Spin cells at 250xg for 5-10 minutes to pellet. Aspirate supe and resuspend appropriately as described in step 6.
5. Need to prepare 2 x 10^6 cells/injection for each population and prepare centrifuge tubes with enough for 2 mice + 1 extra injection (2 injections x 2x10^^{6} cells/fatpad x 2 mice + 2x10^^{6} extra cells)= 1x10^^{7} cells needed per tube. Make 3 tubes so have enough for the 5 mice (+1 extra). Resuspend all cells at 1x10^^{7} cells/mL and aliquot 1 mL to each of 2 centrifuge tubes for each population.
6. *Examples:*

a. Mueller-GFP: 98.8% viability
    i. Volume: 10 mL
    ii. Count: 4.7 x 10^6 cells/mL
    iii. Total cells= 4.7x10^7 cells
    iv. Resuspended at 1.6x10^^{7} cells/mL= 2.93 mL and aliquot 1 mL into 2 tubes
    v. Spun down (250xg at 4°C for 10min).
    vi. Aspirate off the supe and resuspend each aliquot in 100µL total volume with PBS (so only added 50 µL PBS since cells take up so much volume)
    vii. Mix with 100 µL Matrigel right before injecting into mice

7. Bring above listed supplies to vivarium

Surgery procedures:

8. Gather a spare cage to put mice in for recovery from surgery.

9. *In the biosafety cabinet located in vivarium surgery room:*
    a. Set up the box for isofluorane aneasthesia
    b. Turn on isoflurane vaporizer— set O_2 levels to 1, isoflurane amount ~3-5.
    c. Place mouse in box for several minutes until no longer moving, then transfer mouse to foil-covered styrofoam rack for surgery; place mask extension immediately on mouse to keep anesthesized.
    d. Once mouse is no longer sensitive to toe pinch, then mouse is ready for surgery

10. Mount mouse, back down, on aluminum foil-covered styrofoam block in the hood and tape the limbs to immobilize (maintain isoflurane flow through mask extension to ensure constant anesthesia is being delivered)

11. Wipe down belly of mouse with EtOH and kimwipe (don't spray ethanol directly on the mouse because it may become too cold)

12. Shave belly to remove fur, wipe away the fur.

13. Make small snip incision in the belly region of mouse, ~ 1.5cm above the anal cavity.

14. Make one ~0.5-0.75cm incision up towards thoracic region. Before making the cut, be sure to keep the scissor tip pointed up and gently prod up to separate the skin from the peritoneal wall. Once tips of scissors inserted to the appropriate distance for the cut, make the incision. Be sure to only make one cut (don't want to do a few small cuts)

15. Make two side incisions, angled toward the hind leg of the mouse between the 4th and 5th fat pads. (About the same size ~0.5-0.75 cm incision is good). Ok to be fairly conservative with incisions (so long as you can locate the fat pad) as it's easier to suture later. The 4th inguinal fat pad will be above the incision line and is used because it is the biggest of the 5 fat pads.

16. Lift skin with forceps and start peeling back skin with the Q-tip (dampen with sterile PBS to make easier). If the mouse starts bleeding- use the cauterizer to stop the bleeding- quick, gentle touch once preheated is all that is needed, then wipe away blood with a Q-tip

17. Peel back skin until you see the cross where 3 veins come together (LN's located here). If you follow the vein leading down into the dorsal side of the mouse, this is where the fat pad is located. While the skin is more of a yellow color, the fat pad is a peach color. (The fat pad placement is deeper then you might think, so keep peeling open until you can see it—it wraps around the side of the mouse)

   a. Prepare Hamilton syringe with 20 µL of 50:50 mi of cells and matrigel (10µL of each, NOTE: This is about the capacity of the fat pad, do not inject more volume than this)- make sure this is really well resuspended; be sure to pipette the suspension up and down to mix each time before injection
   b. Hold the forceps at the top of the fat pad
   c. Inject the cells with the syringe from top down (insert needle in the top of the fat pad and move down to the middle to release the cells). Should see the pouch fill out as the volume goes in. Hold fat pad up for several seconds to wait for the matrigel to start solidifying and then can bring the skin flap back down.
   d. Rinse Hamilton Syringe with PBS between injections in order to remove any residual matrigel that may solidify and make drawing up/injecting cells difficult. Ethanol and PBS the syringe between cell populations

e. Once both fat pads have been injected, suture the incisions with woundclips
    i. Pinch skin together with forceps so the inside of the skin flaps come together. Pinch skin along the entire incision before applying wound clip.
    ii. Be sure to lift up because don't want to catch the clamp on the peritoneal wall, just want to get the skin, so lift up and use forceps to clamp region of incision
    iii. Hold and clamp the wound clip around the incision. Repeat for the other two incisions (total of 3 wounds clips is good for each mouse)
    iv. Subcutaneous injection of diluted Buprenorphine 0.5-1mg/kg, 100 µL per mouse (as per animal protocol). EXAMPLE: For 0.07 mg/kg and ~17g mouse, need ~4µL of the stock Buprenorphine per mouse. Prepare 100µL injections, so dilute 4µL Buprenorphine + 96µL PBS per mouse (prepare 2 x 1mL aliquots).
        1. Stored in locked drawer: Code is 2464

18. Return mouse to cage in which half is placed on a pre warmed heat pad (use microwave to warm pad). Need to keep mice warm, especially in the beginning since they're cold right after surgery. Add some wood chips to cover them to keep them warm. Most mice will awake and move around in a few minutes.

19. Place "post-op" orange sticker on cages of mice that have undergone surgery, write today's date

20. Monitor mice for 5 days post-op and record appearance/health on post-op surgery form

21. Following surgery, check on mice 3 x a week (Measure weight 1/week). Once tumors become apparent, take external caliper measurements and record.

AI.31 Mouse Tumor Harvests for GFP Imaging, Culturing, and Histology

MATERIALS:

70% EtOH

4% PFA (in PBS)

PFA: Sigma, Cat #158127

PBS- Gibco/Invitrogen

Blunt scissors

Suture thread-

20G blunted needle- use HPLC injection needle

Collagenase A- Roche 11088785103

Pen/Strep- Gibco

RPMI 1640- Gibco/invitrogen

PROTOCOL:

Tissue harvest

1. Euthanize mouse with CO_2, mount mouse to styrofoam block
2. Wipe fur with 70% EtOH and kimwipe before making incision
3. Make small incision and cut an inverted Y
4. Separate skin from internal organs to expose mammary fat pads and other organs:
5. Collect various tissues to image GFP fluorescence with microdissection microscope followed by either culture and/or histology. Record Length, Width and mass (g) of tumors and any additional observations.
6. *For fluorescent imaging/ culturing*: Place tissue (e.g. primary tumors, LN tumors, lung, spleen, liver) in sterile 6 well plate filled with sterile PBS, tissues are stable for several hours once in PBS
7. *For histology*: Place tissue in ~10 mL of fresh 4% PFA in glass scintillation vial (see “4% paraformaldehyde preparation” below) (NOTE: lungs require special fixation protocol if preparing for histology; see “Lung fixation protocol” below)

4% Paraformaldehyde (PFA) Preparation

8. NOTES: Use as fixative for tissue samples that you plan to embed in paraffin to carry out histology on. Fix for 24-48 h depending on tissue size. After this time, transfer to 70% EtOH and submit for paraffin embedding/histology.
9. Weigh out 4 g of PFA (Sigma, Cat #158127) (stored at 4 °C)
10. Add to bottle with stir bar
11. Add 100 mL of PBS
12. Loosely screw on lid and place on hot/stirplate in fumehood
13. Place bottle containing 4% PFA in a beaker containing warm water (helps with even heating)
14. Bring temperature up to ~60 °C, while stirring moderately
15. Once solution has turned from cloudy to clear, take off heat and allow to cool (takes awhile)
16. Place at 4 °C (can be used for up to ~1month)

Lung Fixation Protocol

17. NOTES: This protocol describes infusing the lungs with PFA and inflating them for analysis by histology. This protocol also describes how to tie off one of the lobes to preserve for culturing.
18. Cut into ribcage from diaphragm
19. Cut with blunt scissors along both sides of ribcage extending through the thoracic cavity (not through middle), using blunt scissors will help to avoid dulling sharp scissors or accidentally injuring organs within (e.g. lungs, etc.) or major veins/arteries, blood can make difficult to navigate
20. Once ribcage has been cleared enough to probe cavity, identify mouse's left lung lobe (should be single while right side should have 3 lobes)
21. Form a lasso loop with suture (3G) and wedge around top of individual lobe using blunt forcep to position within loop. Tie loop at top where membrane connects lobe and heart and trachea.
22. Cut lobe for culture below suture knot (to prevent formalin flow once applied later on)
23. Place lobe in sterile PBS for GFP imaging and culture
24. Find trachea and infuse fixative:
25. Can remove salivary gland (large gland on top of trachea)

26. Blunt dissect membrane around and under trachea to make accessible for suturing

27. Once trachea has been cleared, place blunt forcep clamp underneath trachea, and pull suture thread through

28. Tie a loose knot

29. Make a perpendicular incision with small scissors to make a hole in the trachea (be sure not to cut all the way through)

30. Using a 20G blunted needle (this is important-- don't want sharp point that can perforate trachea), insert past where knot is loosely tied and lay flat

31. Once in position, tie knot

32. Infuse PFA into lungs (should see lungs visibly inflate to several times their original size).

33. Once inflation levels seem to not change anymore remove needle while firmly tying suture knot to ensure that fixative does not leak out

34. Find thymus (small whitish tissue on top of heart) and remove for culturing

35. Harvest lung lobes for histology:

36. Clear away all the membrane and tissue (includes fat, muscle, skeletal) around trachea

37. Cut trachea above suture knot

38. While holding knot in an upwards fashion, start clearing and separating trachea from body, moving down towards the lung area

39. Make sure ribcage is cleared away or this will hinder your ability to remove trachea and lobes easily

40. Moving from trachea down, continue to cut lungs from membranous tissue until it all comes out in one package

41. Keeping suture knots firmly tied around left lung lobe and on trachea, place everything in fixative (this will prevent deflation)

42. Allow to fix for 24 h at 4 °C

43. After 24 h in fixative, place lung lobes into 70% EtOH O/N at 4 °C

44. Prepare/submit lungs for histology at UCSD histology core:

45. Want to preserve direction of airways. Therefore, cut longitudinally from hyliss (from where it attaches to the airways) to apex (bottom corner)

46. Be consistent when preparing lung histology samples to ensure knowledge of orientation on slide

GFP visualization using microdissection scope

47. To determine if any organs had mets, used Yang Lab (NSB) microdisssection scope

48. Turn on → Switch filter to GFP2 (need to turn mat under scope to black to see)

49. Using tweezers, remove tissue sample from PBS and place on sterile 10cm Petri dish under objective

50. Once satisfied with image, "snap"

51. Stored in RinaMorgan folder with date as subfolder: "Save as" – name "magnification, mouse #, organ"

52. save as .tiff file

53. resolution= 1392 x 1044 FF

Culturing primary tumors and metastases

54. Prepare fresh 1 mg/mL Collagenase A in RPMI-serum free

55. Place tissue in sterile 10 cm dish containing variable amounts of Collagenase A (depending on tissue size)

56. Mince tissue with sterile razor blade (use clamp forceps to hold blade)

57. Place minced tissue into sterile 125mL Erlenmeyer flask with stirbar at 37 °C room. Alternatively, add to 15 or 50 mL conical and rotate end-over-end in 37 °C incubator.

58. Stir or rotate for 1-2 h at 37 °C to allow Collagenase A to digest the ECM

59. Stop Collagenase A digestion by doubling volume with RPMI-10%FBS

60. Pass cells through 70um filter into new conical

61. Spin 250xg for 10 min at 4 °C, all should have visible pellets (LN pellet will be very small)

62. Seed cells depending on amount of cells expected to recover; resuspend pellet with RPMI-10% FBS + Pen-Strep (10 units/mL pen, 10 ug/mL strep) and place into appropriately sized dish or multiwall plate

63. Primary tumors: If digested one whole primary tumor, only need to seed a fraction of the digestion to a 10 cm dish, recovery is usually very good.

64. LN tumors: Seed in smaller dish (e.g. 6 well or 6 cm) depending on size

65. Liver, Lung, Spleen: Depends on extent of metastases evident based on GFP detection and how much contaminating cells are likely present; will require extensive PBS rinsing for several days after plating, recovery typically slower than that of primary and LN tumors b/c mets are less abundant

66. Incubate cells at 37 °C

67. Once cells are confluent, select or split and select into new dish with Blasticidin (RPMI+ 10% FBS + 5 µg/mL Blasticidin). Only GFP+ MDA-MB-231 cells should survive selection.

AI.32 Quantification of lung metastases by monitoring GFP fluorescence

Modified from Dr. Nissi Varki Protocol; Ref: Borsig, L., Wong,R., Hynes,R., Varki,N.M., Varki A. Synergistic effects of L- and P-selectin in facilitating tumor metastasis can involve non-mucin ligands and implicate leukocytes as enhancers of metastasis. PNAS 2002 Vol. 99: no 4. 2193 – 2198

MATERIALS:

Lysis Buffer: 20mM Tris, pH 8

Cell homogenizer

10 mL falcon culture tubes

20% Triton-X 100

PROTOCOL:

1. Transfer lungs to labeled 10 mL falcon culture tubes that have 2ml lysis buffer in them (20mM Tris, pH 8).
2. Homogenize each set of lungs, cleaning the homogenizer probe with 70% EtOH in between lungs and MilliQ water.
    a. Homogenize 20 sec power level 3
    b. Keep on ice
    c. Can use primary tumor as positive control for fluorescence
    d. Use control PBS mouse lungs for negative control and background readings
3. Return tube to ice after homogenization is complete.
4. Add 50 µLof 20% Triton X-100 to each tube (final concentration of 0.5% Triton-X in 20 mM Tris/PBS). Allow to sit on ice for 30 minutes.
5. Transfer homogenate to labeled 2ml Eppendorf tubes.
6. Centrifuge homogenate at maximum speed for 10 minutes at 4°C. Turn on fluorescent lamp so that it can begin warming up (requires ~10-15 minutes).
7. Transfer middle "clear" aqueous layer (under thin oily layer and above larger) to labeled Eppendorf tubes. Put tubes on ice.

8. Obtain the quartz 96-well plate, and create a map for samples. Each sample will be read in a 1:4-1:20 dilution range. 1:4 ratio worked best (50 µLaqueous layer + 150 µL 20 mM Tris)
9. Prepare in triplicate to get average of readings
10. Pipet the appropriate amount of sample (e.g. 50 µL) into the appropriate wells.
11. Pipet the appropriate amount of lysis buffer (e.g 150 µL) into the appropriate wells.
12. Read the fluorescence at gains of 40, 50, and 60 at 485nm (excitation) and 530nm (emission).
13. Normalize to control mouse lung (no GFP mets)

AI.33 Calcium Flux Analysis

Volumes used: 100 µL cells (200,000 cells) + 100 µL calcium 4 dye + 50 µL ligand
(Modified from S. Allen protocol)

MATERIALS:

Calcium 4 assay kit (Molecular Devices #R8142)
Assay buffer: 1x Hanks Balanced salt solution, 20mM HEPES, pH 7.4, 0.1% BSA
Assay plates: Biocoat 96-well plate (BD, #356640)
Compound/ligand plates: 0.3 mL v-bottom 96-well (Costar, #3357)
FACS Buffer (0.5 % BSA in PBS)

PROTOCOL:

Ligand plate

1. Reconstitute ligand at a high concentration in PBS, Tris/HEPES buffer or MQ H_20 and measure concentration.
2. Dilute down to highest starting concentration in PBS and add to 300µL v-bottom assay plate (decreasing concentrations going down the plate). To begin, try 1:4 dilutions, adding 187.5 µL PBS + 62.5 µL of ligand (from above well) to each well. Using these volumes, you will need 1 column of ligand for each set of triplicate experiments.
   a. EXAMPLE: For top lane (A) to get final volume of ligand at 2 uM → A1 gets 50 µL of 10 uM ligand + 200 µL water to get final concentration of 2uM. Remaining wells are diluted as follows: 62.5 µL of ligand + 187.5 µL PBS.

3. NOTE: ligand plate is delivered column by column; so set up ligand and receptor plate accordingly

Receptor plate

4. Lift cells with 5 mL PBS-1mMEDTA, incubate at 37 °C for ~20 min
5. Harvest cells and wash plates with an additional 5 mL of PBS
6. Count cells on ViCell
7. Spin at 250xg, 10min, 4 °C

8. Wash cells twice with FACS buffer
9. Resuspended cells to 2 x 10^6 cells/mL using assay buffer. (About 12 mL of cells is required per 96-well plate or 3 mL of cells for 3 lanes,)
10. Add 100 µL of cells to each well in a 96-well biocoat plate (being careful not to expel completely and create bubbles).
11. Prepare calcium 4 dye (Explorer format) in 10 mL assay buffer. Make sure it all goes into solution by pipetting up and down several times, don't shake! One vial of dye is sufficient for ~ 1 plate.
12. Carefully add 100 µL of dye to cells, trying not to disturb the cells (being careful not to expel completely and create bubbles).
13. Spin plate down for 6 min at 250xg (remember to turn down rates of acceleration/deceleration).
14. Check homogeneity of cells by microscopy and place in 37 °C incubator for 1.5 hr before measuring.
15. Read plate on Flexstation using Ca flux protocol

AI.34 Migration Assay Protocol for Suspension Cells

MATERIALS:

Transwell migration plates- Corning/Costar 0.5 μm pore size, 6.5 mm diameter, polycarbonate treated- 3421

RPMI +10% FBS (or RPMI +1% FBS or RPMI +0.5% BSA)

CXCL12 (or other chemokine)

10 mM Hepes pH 8

PROTOCOLS:

1. Re-suspend a bit of lyophilized CXCL12 (SDF1-alpha) in 500 μl of 10 mM hepes pH 8.0.
2. Determine the concentration by absorbance at 280 nm using the extinction coefficient given by expasy/protparam
   a. $A_{280} = C\varepsilon l$
   b. $C = A_{280}/\varepsilon l$
   c. ε=8730 (oxidized) for CXCL12
3. If you add the correct amount of powdered protein…you should get a concentration in the range of 50 to 100 μM.
4. Adjust the concentration to 50 μM to use that as your stock solution.
5. Test the range of 1nM to 500 nM chemokine for migration. The EC_{50} of SDF1-alpha is around 5-10 nM.
6. So, from the 50 μM stock, prepare: 10 μM, 1 μM, and 100 nM solutions
7. Prepare the dilution in the bottom of the 24 well plates. The total volume of media in the bottom of the wells needs to be 600 μl. So prepare as many wells of each as you want (duplicate or triplicate) of the following:

Dilution in the well	**Volume of SDF1 (conc.)**	**Volume of media**
No chemokine	0	600 μL
500 pM	3 μL (100 nM)	597 μL
1 nM	6 μL (100 nM)	594 μL
5 nM	3 μL (1 μM)	597 μL
10 nM	6 μL (1 μM)	594 μL
50 nM	3 μL (10 μM)	597 μL
100 nM	6 μL (10 μM)	594 μL
500 nM	6 μL (50 μM)	594 μL

8. Note: The 24 well plate packages contain only 12 filters. So it's up to you to use 12 wells per plate or combine two packages to use all 24 wells of one plate. Also, this does not really need to be done in the sterile hood since you are not going to keep the cells after.
9. Move the filters to the well containing media +10%FBS + chemokine.
    a. Note different cells prefer different conditions (e.g. lower serum concentration of 0.5% BSA without serum, so need to optimize for cell type)
10. Do a cell count and prepare a cell suspension of 2.5 X 10^6 cells per mL.
    a. Need 8 conditions in duplicate (x2) +3 just total cell controls and a little extra- so want ~5.0x10^6 total cells
    b. Resuspend the 5x10^6 cells in 2 mL of RPMI+10% FBS so at a concentration of 2.5x10^6 cells/mL
11. Add cell suspension to each filter well: 100 µl of 2.5 X 10^6 cells/ml suspension. Your positive control will be the addition of that same amount of cell directly in the bottom of the wells without filter/without chemokine.
12. Incubate at 37°C/ 5% CO_2 for 2 hours.
13. Pipet up all the 600 µl in the bottom of each well and transfer them to a small flow cytometry tube. Do flow cytometry (count the number of events happening in a given time (30 sec).

AI.35 Migration Assay Protocol for Adherent Cells

From Janine Low-Marchelli in Dr. Jing Yang's lab

MATERIALS:

Transwell inserts - Corning #3422
TC companion plate (24 well plate) Falcon cat no. 3504 (BD#353-504)
Cell culture insert Falcon cat no. 3097 (PET membrane; pore size 8 um; transparent chamber) for the companion 24 well plate (BD # 353-097)
Regular 24 well plate used transiently for inserts (cheaper than using corresponding Falcon brand 24 well dish) and for washing inserts
Flame sterilized forceps
4% Paraformaldehyde (diluted from 16% stock), prepared fresh, 500ul/well for washing
0.1% crystal violet in dH2O, not 10% EtOH, prepared fresh, 500ul/well for washing
Long cotton tipped applicators
PBS-, 500 µl/well for washing
MilliQ ddH2O, 500 µl/well for washing
Fibronectin-Sigma #F2006
10% acetic acid

General Notes:
Use heparin (10 ug/mL final, Calbiochem # 375095) in conditioned medias to facilitate cytokine release.

Remove any air bubbles present on the transwell inserts during all of the steps (ie, during fibronectin coating, incubation during migration, staining), otherwise you may notice circular sections of the membrane with no cells/staining present.

For most steps, use 100 µL on the top of the insert and 600 µL on the bottom chamber.

For washes, fill the top and bottom wells completely.

Use low passage (<12) cells whenever possible.

Label the tops of the transwell inserts to distinguish one group from another.

Be careful to not disturb the migrated cell layer! This can happen if you leave the transwells in their chambers while cleaning the top of the filter with a cotton swab, or if the filter is not completely dry during photographing.

Cell number to use in transwell will vary depending on cell type (~20,000 to 200,000)

Vary time of incubation as well (2 h – 48 h)

PROTOCOL #1:

1. Conditions: Triplicates for each cell line
    i. 250ul media + cells (total) in the upper chamber

ii. 750ul media in the bottom chambers
iii. Wipe top of chamber to assess extent of cell motility
iv. Don't wipe at all to assess total number of cells

2. Assay: Test migration properties of serum starved (14 hours) vs. serum fed MDCK lines (negative control, empty vector and mTwist).
    i. Test migration properties of MDCK (as above) and HMLE lines (high Ras, empty vector and two mTwist clones).
3. Using flame sterilized forceps, place the insert (also called the upper chamber) into a regular 24 well plate.
4. Add 100ul serum free media into the insert. Return to a 37°C TC sincubator for >1hr.
5. Add 750ul media (fully supplemented media or media with no supplements) in the wells (also called the lower chamber) of the Falcon 24 well dish.
6. Using sterile forceps, transfer the insert chambers to the wells containing the media. To avoid air bubbles from being trapped beneath the membrane, tip the insert at an angle as it is lowered into the media.
7. Trypsinize cells. Resuspend in serum free media to count. Seed 5 x 10^4 cells/well in 150 µl media.
8. Immediately add 5 x 10^4 cells/ 150µl serum free media to bring to a final 250 µl media in the upper chamber.
9. After 24-48 hours, aspirate media from the top chamber.
10. Put each chamber in PBS- in another 24 well plates.
11. Add 500 µl PBS- in to the upper chamber and swab with a cotton tipped applicator. Repeat twice. Use fresh applicator per insert?
12. Move chamber to new well with 500ul 4% Paraformaldehyde; fix for 10 min.
13. Move chamber to new well with 500ul MilliQH2O; soak 30 seconds.
14. Move chamber to new well with 500ul 0.1% crystal violet (in H2O); soak for 1 min.
15. Rinse chamber 3X with MilliQH2O.
16. Let dry at room temp; photograph and/or count.
17. To release dye, add 50ul 10% acetic acid; soak 2-5 min.

18. Pipet off acetic acid into a well of a 96 well dish. Quantitate on a spectrophotometer at 540nm.

PROTOCOL #2:

If collecting conditioned media prepare 2 days ahead of time:

Day 1 Plate HMLE or HMLE Twist cells in 24 well plates (20K per well) in MEGM.

Day 2 Change media on HMLE/Twist cells such that the final volume is 600 µL.

Prepare cells for migration:

1. Day 1 serum starve an 80% confluent 10 cm dish of cells overnight (RPMI, no FBS).
2. Day 2 Migration assay:
3. Coat transwell inserts (Corning #3422) with 10 µg/mL Fibronectin (Sigma #F2006), using 100 µL on the top of the insert, 600 µL in the bottom chamber. Place in the 37°C incubator for 2 hours.
4. About 15-20 minutes before fibronectin coating is complete, scrape and count serum starved cells and resuspend in RPMI to a final density of 200K cells/100 µL (100K/100 µL may also work well). *Need to optimize cell number
5. Rinse transwells 1 time with dPBS and place transwells over 600 µL DMEM. Add 100 µL of cell suspension to transwells, being sure to pipette the solution directly onto the filter (do not pipette cell suspension against the wall of the insert, as you may lose these cells). Allow cells to settle/attach to the filter for 2 hrs in the 37°C incubator.
6. After cells have attached, transfer the transwell inserts to the medias of interest (HMLE or Twist containing wells) and let migrate 24 hrs. For negative and positive controls, this will be fresh media +/- recombinant human chemokine.
7. Day 5 Fixation and staining:
    a. Remove media by aspiration, and fix cells with 4% PFA (at least 100 µL on top of insert and 600 µL in the lower chamber) for 30 min at room temperature.
    b. Rinse transwells 1 time with water.
    c. Stain transwells with 0.1% crystal violet stain (at least 100 µL on top of insert and 600 µL in the lower chamber) for 10 min, room temperature.
    d. Rinse transwells 1 time with water.

e. Fill wells with water again and gently and completely swab the top of the filters (unmigrated cells) with a cotton tipped applicator (Fisher 19-063-487). It is important not to press too hard on the filter, because the filter can be dislodged and stretched, making photography more difficult.
f. Rinse and aspirate transwells 2 times with water, completely removing dark purple residue.
g. Let transwells dry completely – a warm room, incubator, hair dryer (be careful not to blow transwells away), or over night at RT work well.
h. Place transwells, migrated cell-side down, on a glass slide to enable observation on an inverted microscope. Photograph 12-15 fields of migrated cells at high magnification (32x objective x 2.5x mag scope = 80x). Count and calculate an average number of migrated cells/field for each experimental group.
i. Alternatively, if have enough cells, can measure absorbance by spectrophotometer:

    i. To release dye, add 50ul 10% acetic acid; soak 2-5 min.
    ii. Pipet off acetic acid into a well of a 96 well dish. Quantitate on a spectrophotometer at 540nm.

Figure AI.35.1 Crystal violet stained transwells.

AI.36 HA-receptor Pull-down Protocol

Protocol modified from John Jones

MATERIALS:

HA-affinity resin- Sigma# E6779

HA-peptide- Sigma# I2149

SilverQuest kit- Invitrogen

All lysis buffers are built upon the same base:

50mM Tris pH 7.4

300mM NaCl

Protease inhibitor cocktail - Sigma #P2714

Phosphotase inhibitor cocktail I and II - Sigma #P5726 and Sigma #P2850

Then, can vary based on detergent:

1) RIPA (**R**adio **I**mmuno**P**recipitation **A**ssay buffer)

1% IPEGAL (NP-40 substitute) (weak nonionic – lyses only cytoplasmic membranes)

0.25% Deoxycholate (mild detergent for the isolation of membrane associated proteins)

0.1% SDS (strong anionic)

10mM BME

Bare in mind…many people use the term RIPA, but it can have 1, 2, or all 3 detergents in it.

2) Ann Richmond's Buffer

0.05% Triton-X 100 (nonionic – for all membranes)

3) CHAPS buffers are typically run at 5-10mM (zwitterionic)

For most signaling/cell bio labs, RIPA is frequently used. Just remember the composition may be different. The one listed above is what my old used exclusively for Co-IPs and lysis of mammalian cells, and it is also the one used by Pascale and Bouvier for the B-arrestin pull downs.

PROTOCOL:

1. Grow cells to ~70-80% confluency in 10 cm dish
2. Wash cells with PBS
3. Serum starve with serum-free RPMI O/N (time may vary depending on the cells)
4. Stimulate w/ 30 nM CXCL12 in serum-free RPMI for 5 min at 37°C

Harvesting non-crosslinked protein lysates

5. Remove stim by aspiration and lyse with 500 µL cold lysis buffer
   a. hand rock and scrape cells off dish
   b. pipette mix and transfer to eppe tube
6. Let cells incubate on rocker at 4°C for 10 min
7. Spin at 10,000 x g for 10 min to clarify
8. Remove clarified supe to a fresh tube

Harvesting crosslinked protein lysates

9. Stop the stim with the addition of 1 ml of 20 mM DSP (2mM final)
   a. Rock with light aggition at RT for 30 min
10. If cells are still adherent, rinse with PBS, and “quench” the DSP with 4 ml of 50 mM Tris, pH 7.4 in PBS for 10min with gentle rocking, then dislodge. If cells are lifting during the crosslinking, remove supe and wash the plate with 4ml of “quench”.
11. Pellet cells (2500 rpm for 5 min) and resuspend in 10 ml of “quench”
12. Pellet once more and aspirate
13. Lyse cells with 500 µL cold lysis buffer
   a. pipette mix and transfer to eppe tube
14. Let cells incubate on rocker at 4°C for 10 min
15. Spin at 10,000 x g for 10 min to clarify
16. Remove clarified supe to a fresh screw-cap tube

Pull-downs

17. 30 µl of HA-affinity resin (Sigma# E6779) is added to 200 µg of the clarified lysates and incubated on a rocker overnight at 4°C

18. Resin is washed 2x with cold lysis buffer

19. Protein is eluted by one of the following methods:

a. Adding 100 µl 2x SDS-PAGE sample buffer
    i. For western blot analysis (not for MS)

b. Adding 100 µl 0.2M Glycine pH 2.0 at RT for 20 min
    i. Quench with 20 µl 1M Tris pH 7.4
    ii. Note- this elution did not work very well in our hands

c. HA peptide
    i. Resuspend HA peptide at 5 mg/mL with mqH_2O
    ii. Use 100 µg/mL peptide at RT or 37°C for 20 min (work equally well at both temperatures)
    iii. This method worked great

20. Take 5 µl samples for Silver stain analysis

Gels

21. Warm sample to 60°C for 5 min (do not boil or receptors with aggregate at the top of the gel)

22. Proteins were resolved by 10% SDS-PAGE and Western blot

a. Silver stains were performed using SilverQuest kit from Invitrogen

b. Western blots were performed by:
    i. α-HA-HRP @ 1:750 for 1.5 h at RT

AI.37 Actin Polymerization Assay

From Jessie F. Fecteau Ref: *Burger et al. Blood. 2005;106:1824-1830*

NOTES:

Reorganization of the actin cytoskeleton is an early event in the migratory response to chemokines. CXCL12 (SDF-1) induces changes in the actin cytoskeleton of CLL cells. Typically, a significant, transient increase in F-actin occurs within 15 seconds of exposure to CXCL12, followed by subsequent depolymerization.

Phalloidin conjugated to FITC will be used to detect by FACS actin polymerization, since this molecule is known to bind only to polymeric and oligomeric forms of actin and not to monomeric actin (Sigma sheet product).

1-α-lysophosphatidylcholine will be used at low concentration to permeabilize the cell surface membranes without complete lysis of the cells (Sigma sheet).

In this assay, the goal is to stain CLL B cells with x-CD19 and x-CD5 before the actual physiologic assay, in which actin polymerisation will be measured after the addition of 30nM of SDF-1 at 15s, 30s, 60s, 120s and 300s.

PROTOCOL:

1. Prepare RPMI-0.5% BSA to pre-incubate the cells and do the assay.
2. Thaw CLL cells, count and resuspend at $1x10^7$ cells/mL in RPMI-0.5% BSA.
3. Seed cells in 24-well plate with 0.75-1mL/well suspension and incubate for 1 hour at 37°C, 5%CO_2 (resting period).
4. Collect the cells and separate them into tubes:
    a. the assay ($1.1x10^7$ cells = 1.1mL)
    b. the isotype ($0.1x10^7$ cells = 0.1mL)
    c. cells only control ($0.1\ x10^7$ cells = 0.1mL)
    d. cells single stained phalloidin-FITC ($0.1x10^7$ cells = 0.1mL)
    e. cells single stained PE ($0.1x10^7$ cells = 0.1mL)
5. Spin down tubes 3000RPM, 3 min 4°C.
6. Resuspend each pellet:
    a. Assay: 1mL FacsWash (FW) + 25µL x-CD19-PE + 25µL x-CD5-APC
    b. Isotype: 100µL FW +2.5µL Mouse IgG1-PE + 2.5uL Mouse IgG1-APC
    c. Cells only control: 100 µL FW
    d. Cells single stained phalloidin-FITC : 100 µL FW
    e. cells single stained PE : 100 µL FW + 2.5uL anti-CD19-PE
7. Incubate 20 min. on ice in the dark.

8. Wash the tubes: add 350µL of FW to the assay tubes and 1.3mL of FW to the isotype and the controls. Spin 3000RPM 3min 4°C.
9. Resuspend the pellets in 1mL FW. Spin 3000RPM 3 min 4°C.
10. Resuspend the pellets at $1.25x10^6$ cell/mL in warm RPMI-0.5% BSA
    f. Assay: 8.8mL
    g. Isotype: 0.8mL
    h. Each control: 0.8mL
11. For the assay, seed 24-well culture plates with 800 µL/well as follow (duplicate is in each well):

1	2	3	4	5	6
No SDF	+ 30nM SDF 15s	+ 30nM SDF 30s	+ 30nM SDF 60s	+ 30nM SDF 120s	+ 30nM SDF 300s

12. Transfer the plates to heat block at 37°C.
13. Add 30nM of SDF (final*) to each well and stop the reaction at the indicated timepoints by adding 200µL of the staining solution** per well.

* Prepare SDF-1 solution in RPMI-0.5%BSA at 1500 nM: 285µL RPMI-BSA + 15µL SDF-1 30 µM and add 16 µL per well to have 30 nM.

** Prepare the staining solution with phalloidin-FITC (adjust the volume according to the number of samples):

- 1.75mL formaldehyde 37%
- 1.75mL PBS
- 30µL 1-α-lysophosphatidylcholine (25mg/mL)
- 3.5µL FITC phalloidin (at 1000X)

***Prepare in parallel a solution <u>without</u> phalloiding-FITC for the controls:

- 0.25mL formaldehyde 37%
- 0.25mL PBS
- 4.3µL 1-α-lysophosphatidylcholine (25mg/mL)

<u>IMPORTANT</u>: the lysophosphatidylcholine stock should be made fresh everytime. Using old solution – even if kept frozen – will affect the results and cause reproducibility issues.

14. Transfer each well into two FACS tubes (500 µL per tube).
15. For the **isotype** : transfer 400 µL in FACS tubes and add 100 µL of staining solution without phalloidin-FITC.
16. For the **controls**: transfer for each 400 µL in FACS tubes. For **cells only and single stained PE**: add 100 µL of staining solution without phalloidin-FITC. For **single stained FITC**: add 100 µL of the complete staining solution.
17. Incubate 15 min. at 37°C.
18. Analyze the fixed cells by FACS within an hour.

Staining solution composition: into 18% formaldehyde in PBS add, $4x10^{-7}$ M FITC-labelled phalloidin and 0.5 mg/mL 1-α-lysophosphatidylcholine.

AI.38 cAMP Radioimmunoassay

From Fiona Murray

MATERIALS:

Buffers

γ-globulin buffer: 100mg human gamma globulins/100ml 50mM NaAc pH 4.75

PEG buffer: 12% polyethylene glycol in 10mM NaAc pH 6.2

Assay buffer: 10mM NaAcetate (950ml H_2O + 50ml 1M NaAc pH 4.75 stock)

PROTOCOL:

Cell Incubation

1. Prepare DMEH: 3.35g (1.34g) DME powder
   1.2g (0.48g) HEPES
   1 pellet NaOH
   250ml (100ml) purified H_2O
   Adjust pH to 7.4
2. Prepare all drug solutions at 10x final concentration in DMEH
3. Aspirate media from cells (generally grown in 24 well plates) and appropriate amount of pre-warmed DMEH so that final assay volume will be 0.5ml. Equilibrate for 30-60min at 37°C
4. OPTIONAL: Add 50µl 2mM IBMX to each well (final concentration 200 µM). Also add antagonists if applicable. Pre-incubate for 20 min
5. Add 50µl agonists of interest to wells and incubate for 10 min
6. Stop reaction by aspiration of media and addition of 250µl ice-cold trichloroacetic acid (7.5%, different depending on number of cells and cell type). If cells are in suspension centrifuge (1,200 rpm 8 min) then aspirate media and add appropriate concentration of 7.5% TCA
7. Store in fridge if necessary

RIA

8. Add 1ml 10mM Sodium Acetate buffer to assay tubes
9. Make standard curve: 12 tubes in duplicate (i.e. 24 tubes).
   a. Set tubes 1,2,13,14 aside (no cAMP addition)
   b. In a new tube add 10µl of 5µM cAMP standard to 5ml Sodium Acetate buffer

c. Take 1ml and add to tube 12 and 24, vortex and take 1ml from each and add to tube 11 and 23
d. Repeat serial dilution until tube 3 and 15. Discard 1ml solution from these.

10. Add appropriate amount of sample to assay tubes (e.g. 30µl for basal, 10µl for stimulated)
11. Acetylate samples in a fume hood by addition of 20µl triethylamine and 10µl acetic anhydride. Vortex immediately
12. Prepare 96 well filter plate – add 50µl Sodium Acetate buffer to each well and vacuum out using Millipore apparatus
13. Add 50µl of diluted, acetylated sample to each well
14. **Do not add antibody to first wells of standard curve (nsb)**. Add 25µl diluted antibody to the remaining wells (dilute 3µl stock in 6ml γ-globulin buffer)
15. Prepare radioactivity - 16µl of ^{125}IcAMP in 3ml γ-globulin buffer. Note actual amount of ^{125}IcAMP added will depend upon date of production (e.g. if old add more – see decay table). Add 25µl diluted radioactivity to each well (should be 5000cpm/sample)
16. Place plate in fridge overnight

Following Day

17. Add 50µl secondary antibody to each well (Biomag Goat anti-Rabbit IgG 8-4300D). Shake at 4°C, 1hr
18. Add 100µl 12% polyethylene glycol to samples and vacuum out using Millipore apparatus. Wash twice more with 100µl polyethylene glycol solution
19. Remove base of plate and fit with punch plate on top. Punch out samples using Millipore device and collect into tubes. Count on γ counter

Data Analysis (assuming samples counted in specific order and using Rik's prism template)

1. STD curve import: Filter - Start at column 1, end at column 24
Placement - By columns. Stack 12 in each row
2. Values import: Filter - Start at column 25, end at last
Placement - By rows. Place 3 values in each row
3. Check that standard curve looks ok, delete outlying points if necessary.

4. To generate fmols cAMP/sample: -Go to Results/standard curve/interpolated x values
-Analyze/transform/user-defined Y Transform/ choose Rik's cAMP antilog*

5. To generate fmols cAMP/well: -Transform the cAMP/sample table using transform/user-defined Y Transform/choose fmols/sample to fmols/well* and put K=volume assayed.

6. Cut and paste respective cAMP/well values into "cAMP (fmols/well)" data table

*user-defined Y equations: Y=(10^Y)*1E+15
Y=Y*(250/K)

AI.39 Detecting Heparin-binding Chemokine from Cell Culture Medium

Protocol from Xin/Mark Fuster

MATERIALS:

Costar transwell insert: 0.4-μm pore size, 6-well format (Corning, 3412)

Heparin Sepharose 6 Fast Flow: GE healthcare, 17-0998-01

2 × protein loading buffer: Bio-Rad 161-0737

PROTOCOL:

1. Grow cells in 6-well plate and treat them accordingly.
2. Place a transwell insert into each well. (For each condition, you may do 2 or 3 replicates so that you can pool them and reduce the variations).
3. Wash the Heparin sepharose twice with PBS and load 100 μL Heparin sepharose in 1 mL of cell growth medium onto the transwell insert. Incubate at 37C, 5% CO2 for 24 h.
4. Transfer the transwell insert into a new 6-well plate. Transfer the Heparin sepharose using P1000 to a clean low-protein binding eppendorf tube. Wash the transwell several times with PBS till no sepharose could be seen and also collect the wash into the same eppendorf tube. If the volume is too high, you may centrifuge (3000 × g, 2 min) in between and discard the supernatant.
5. Wash the sepharose beads with PBS once and carefully remove the supernatant. Add 2 × protein loading buffer to 1 × and beta-mercaptoethanol. Boil the beads and load on SDS-PAGE gel

Notes: Things we should try/test

-Cells in the Transwell system as Xin has outlined with heparin beads on top
-Cells in batch with the heparin beads:
-Acid wash the cells. Spin down cells and debris.
-Collect the media and wash and bring back up to 7.4 pH
-Incubate supernatant with heparin beads in batch, mix
-Elute with acid from heparin beads (for MS) or resuspend in western loading dye
The reason Xin doesn't normally do the batch method is because of cell debris that can interfere/mess up results. Heparin could bind a lot of proteins in cellular debris without the transwell filter to keep that out, so doing this is just something to look for/consider when doing in batch, although the cells and debris should be spun down and pelleted

AI.40 Transendothelial Migration Assay

From Ariane Jansma

Human Umbilical Endothelial Cell (HUVEC) Maintenance

Media: 53% M199 (Cell-gro, 10-060-CV)
25% Endothelial Growth Media, EGM (Cell Applications, 211-500)
20% FBS
1% Sodium pyruvate
1% Glutamax
PenStrep, 1x

NOTE: Always prep T75 plates for HUVECs – add 10 mL of 1% gelatin in PBS, incubate at 37ºC for ~15 minutes, remove gelatin and add media

Defrosting HUVEC Cells: 1 vial defrosted into 1 x T75

1. Thaw at 37ºC for several minutes
2. Add cells to 10 mL Media
3. Centrifuge
4. Remove media and resuspend in 12 mL media
5. Add to T75
6. Incubate at 37ºC, 5% CO_2

Change media 24 hours later to remove any residual DMSO

Splitting HUVEC Cells (split 1:5 every 5-6 days)

1. Coat new T75 with 1% Gelatin in PBS
2. Remove media from old cell plate
3. Add 4 mL Trypsin-EDTA
4. Incubate at 37ºC for ~3 min.
5. Check constantly under microscope
6. Quench as soon as cells come off the bottom of the plate
7. Quench trypsin with 5 mL media
8. Spin cells
9. Remove Gelatin from new T75

10. Resuspend cells in 5 mL media

11. Add 1 mL to new T75

12. Maximum of 10 passages total for cells

Freezing stocks

1. Add Trypsin-EDTA and incubate at 37 for 3 minutes

2. Quench with media and spin cells

3. Resuspend in FBS with 10% DMSO

4. Freeze 1 T25 per cyrovial

Trans Endothelial Migration Assay

1. Assay plates, Transwell Filter plates (5μm filter)

2. Coat transwell inserts with fibronectin (1:40 dilution of 1mg/mL stock in PBS, final: 25 ug/mL, use 60 uL per well). Allow the wells to sit for several hours in the incubator

   a. Remove extra liquid.

   b. Extra plates/wells can be wrapped and kept in the refrigerator.

3. Add media to the wells. Allow them to equilibrate overnight

4. Seed HUVECs (1 x 10^5 cells/well) onto 24-well transwell inserts. Make sure that there is 100uL of media on the top of the transwell.

5. Let the cells grow for 48 hours. Check electrical resistance.

Assay Media, for L1.2 cells:

RPMI

10% FBS

Controls:

3 wells with no filter (maximum possible migration)

3 wells with filters only (no endothelial cells)

Before experiment, remove HUVEC media and carefully wash cells 3x with Assay Media.

1. Add Assay Media + chemokine (total volume, 600 uL) to outside chamber

2. Add 100 µL, containing 250,000 cells in Assay Media to the top chamber
3. Incubate in TC hood, 2 hours, 37ºC, 5% CO_2
4. Remove Filters
5. Count the cells that migrated to the lower chamber by flow cytometry
    a. Count for 30 seconds
    b. Normalize to wells with no filter

Measuring filter-only wells (control):

Evan's Blue - BSA:

Evan's blue – BSA in media

Final concentration: 0.67 mg/mL Evan's blue, 4% BSA

→ Dilute 0.8 g BSA and 13.4 mg Evan's blue in 20 mL media

1. Add 100 uL of Evan's blue – BSA solution to the top chamber (time = 0)
2. At 30, 60, 90, and 120 minutes, transfer filter to new wells
3. Measure the absorbance of 150 uL aliquots of the samples on the plate reader at 630 nm

AI.41 shRNA Design

From Dr. Jing Yang's lab

Note: Used to design shCXCR7 constructs- constructs we got depleted RNA but not protein, but could test on other cells (not MDAs)

1. Designing shRNA constructs

- Before performing RNAi using shRNA, find the coding sequence of your target gene. This information is obtained from on the NCBI website: http://www.ncbi.nlm.nih.gov/.
- The coding sequence is entered into two different shRNA designing programs: Invitrogen's "Block-it" RNAi Designer & MIT Whitehead Institute's RNAi designer. This identifies the best possible sequences that should be targeted for RNA interference. Two different programs are used to get a larger pool of possible shRNA's to choose from.
- The candidate shRNA's produced by the program (usually 20-25) are screened through NCBI's BLAST search to ensure that the shRNA target is unique for the gene of interest.
- Pick at least 5 different shRNA constructs for each target to determine the one with the best restults.
- shRNA constructs are designed as follows:

Coding Oligo (5'-3'): CGAA**(N21)**TTCAAGAGA**( )**TTTTTG

Non-Coding Oligo (5'-3'): GATCCAAAAA**(N21)**TCTCTTGAA**( )**TT

- The sequence of the expressed shRNA should be:

```
                                        U C A
     AA NNNNNNNNNNNNNNNNNNNNN U          A
   UUUU NNNNNNNNNNNNNNNNNNNNN A          G
                                        G  A
```

- There are two restrictions sites on each side of the constructs so that it can be ligated into a transfer vector. The 5' cloning site is BstBI and the 3' cloning site is BamHI.
- The designed constructs are sent out for synthesis.

2. Annealing Constructs

- The constructs arrive single-stranded and lyophilized. They are reconstituted with 1x TE to create a master stock of 200 µM. This is diluted 10x to create a working stock of 20 µM.
    - Volume of TE to add = $\frac{\text{n mol of lyophilized oligo}}{200\ \mu M}$
    - 1x TE recipe: 10mM Tris (Tris(hydroxymethyl)aminomethane)
      1mM EDTA (Ethylenediamine tetraacetic acid)
      pH 7.5 with HCl

- The single-stranded coding and non-coding oligo's need to be annealed to create a functional construct. This is done by mixing equal parts of the coding oligo with the non-coding oligo in buffer.
    - Annealing coding and non-coding oligo's: Combine 1:1 ratio of coding and non-coding oligo's in NEB 2 buffer (New England Biolabs)
    - Annealing Mix:

25 µL	Forward Oligo
25 µL	Reverse Oligo
6 µL	NEB 2 buffer (10x)
4 µL	ddH2O
60 µL	volume

    - Boil samples in 500 mL volume of water at 95ºC for 4 minutes.
    - Allow to cool overnight. This should ideally allow very specific annealing at a temperature drop of 1ºC every minute.
    - For a more sophisticated version, do this with a PCR machine.

3. Cloning into vector (pSP81)

- The pSP81 vector is a pUC19 vector modified with a U6 cassette. The U6 allows expression of the shRNA in mammalian cells to trigger RNAi on the target.
- The pSP81 vector is prepared with BstBI and BamHI. Since the two restriction enzymes do not cut at the same temperatures, a sequential digestion is necessary. BstBI cuts at 65°C while BamHI cuts at 37°C.
    - Digestion mix (1x):

10 µL	DNA
2 µL	NEB buffer (10x)
2 µL	BSA (10x)
1.0 µL	Restriction Enzyme
5.0 µL	ddH2O
20 µL	volume

- BstBI: digest at 65ºC for 3-4 hrs (Use NEB buffer 4)
- BamHI: digest at 37ºC for 3-4 hrs (Use NEB buffer 3)

- After cutting, the vector is isolated by running the digestion mixture through Agarose gel.
  - 1.2% Agarose gel: 0.6g Agarose
    50 mL 1xTAE
    0.5 µL Ethidium Bromide
    ~50 mL volume
  - TAE: 40 mM Tris-Acetate buffer
    1 mM EDTA
  - Weight out Agarose powder and dissolve in 1xTAE.
  - Microwave for 30 seconds-1min to dissolve. Allow to cool.
  - Add EtBr and pour into Geldoc. Choose appropriate comb size.
  - Allow Agarose gel to set.
  - Position gel in chamber and fill with 1xTAE.
  - Add loading dye to samples and pipette into wells. Add a log ladder.
  - Run at 120V for 60 minutes. Visualize with UV light.

- The correct band for the doubly digested vector is cut out and purified using the Wizard® SV Gel and PCR Clean-Up System.
  - Use UV box to cut out desired gel band. Use the lowest wavelength possible and place the gel on the box for the least amount of time possible to avoid nicking of the DNA.
  - Weigh gel piece and add 10 µL of membrane binding solution per 10 mg of Agarose.
  - Incubate @ 50-65ºC for 10 mins until gel is melted.
  - Vortex tube every few mins to dissolve faster.
  - Take out dissolved gel mixture and pipette into SV mini columns with 2mL collecting tube underneath.
  - Centrifuge @ max speed for 1 min.
  - Add 700 µL of membrane wash solution and centrifuge @ max for 1 min.

  - Was again with 500 µL of membrane and centrifuge @ max for 1 min.
  - Discard flow through and centrifuge @ max for 2 min to ensure removal of all ethanol.
  - Place column into new eppendorf tube and add 50 µL of ddH2O.
  - Incubate for 1 min to ensure elution and centrifuge @ max for 2 min.

- After isolation, run 2µL of the cut vector and 2µL of 2log ladder to visualize the approximate amount of vector.

- The double-stranded (annealed) constructs are ligated into the pSP81 vector.
- Dilute the annealed constructs 1:40. Too much input can interfere with ligation.
- Estimate a 1:7 ratio of vector to insert. Adjust ligation mix accordingly.
  - Ligation mix (1x):
    0.6 µL Vector
    2.0 µL Annealed construct (diluted 40x)
    1.0 µL T4 DNA ligase
    2.0 µL Ligation buffer (10x)
    1.0 µL ATP 20 mM
    13.4 µL ddH2O
    20.0 µL volume

  - Ligate overnight at 16ºC.

- The vectors carrying the constructs are transformed into DH5α bacteria.
  - Transformation mix:
    10 µL Ligation mix
    100 µL Competent DH5α cells
    110 µL volume

  - Thaw frozen competent cells on ice.
  - Add DNA and stir.
  - Do not pipette up and down.
  - Heat shock @ 42ºC water bath for 1 min.
  - Chill on ice for 2 min.
  - Add 900 µL of LB media.
  - Allow cells to recover for 1 hr @ 37ºC (230rpm shaker).
  - Warm agar plates to room temp.
  - Plate 100 µL of LB + bacteria on agar plate with drug selection.

  - Plate the rest 900 µL onto second plate.
  - Incubate @ 37ºC overnight.

- After transformation, colonies are picked to grow in liquid LB culture + drug selection.
- With pSP82, Amp selection was used.
- A hand mini prep + digestion verification is done and run on an agarose gel to verify that the right construct is inserted.

  - Mini prep I solution: 50mM glucose
10mM EDTA
25mM Tris/HCl pH8.0
  - Mini prep II solution: 200mM NaOH
1% SDS
  - Mini prep III solution: 3M Potassium Acetate
11.5% Acetic Acid

  - Grow 5mL of bacteria in an overnight culture.
  - Spin down cells @ 5,000 rpm for 1 min @ room temp.
  - Discard supernatant and resuspend in 100 µL of Mini prep I solution.
  - Incubate at 5 min @ room temperature.
  - Add 200 µL of freshly Mini prep II solution.
  - Invert eppendorf tube 3x to mix.
  - Incubate on ice for 5 min.
  - Add 150 µL of ice cold Mini prep III solution.
  - Mix thoroughly, but do no shear genomic DNA.
  - Invert, but do not pipette up and down.
  - Incubate on ice for 5 min.
  - Spin @ 14,000 rpm for 15 minutes @ 4ºC.
  - Transfer supernatant to fresh tube.
  - Add 900 µL of 100% Ethanol. Incubate on ice for 10 minutes.
  - Spin @ 14,000 rpm for 10 minutes @ 4ºC.
  - Discard supernatant and wash pellet with another 200 µL of 70% Ethanol.
  - Spin down, discard supernatant, and allow to air dry.

- Redissolve in 40 µL of 1xTE with RNA-se A (10 µg/ml).

- Digestion verification involves cutting the vector at the same restriction sites used to insert the construct in and then running the digestion products on a gel. But here, we will use BamHI and SalI, since we want to free the construct + U6 cassette.
- The clones with the right insert are grown again on 5mL LB + Amp and the DNA is extracted with a column mini prep.
- Isolated pSP81 vectors + U6 + constructs are sent out for sequencing.
- ApE is used to align the sequencing results and desired construct/cassette sequence to ensure that there are no point mutations during the course of cloning.

4. <u>Subcloning into lenti-viral vector (pSP108)</u>

- The subcloning method must be employed because direct cloning into the lentiviral backbone is known to be very difficult. The lentivirus vector is very large and easy to recombine due to its viral sequences.
- The construct in pSP81 vector is digested with BamHI and SalI to free the construct + U6 cassette. (Digest about 10µg or more of DNA to be able to isolate enough of the construct + U6 later)
- The digested products are run on Agarose gel, the correct band is excised, and purified with Wizard® SV gel and PCR Cleanup system.
- The freed U6 + construct is ligated onto pSP108 vector (already cut with BamHI and SalI.
- DH5□ bacteria are transformed with the vector. Next day, colonies are picked for each sample and cultured in 5mL liquid LB media + Amp.
- Hand mini prep of picked colonies is performed and colonies with the correct insert are identified via digestion verification.
- These colonies with the correct insert are grown in 250 mL of liquid media and column midi prep of the samples performed.

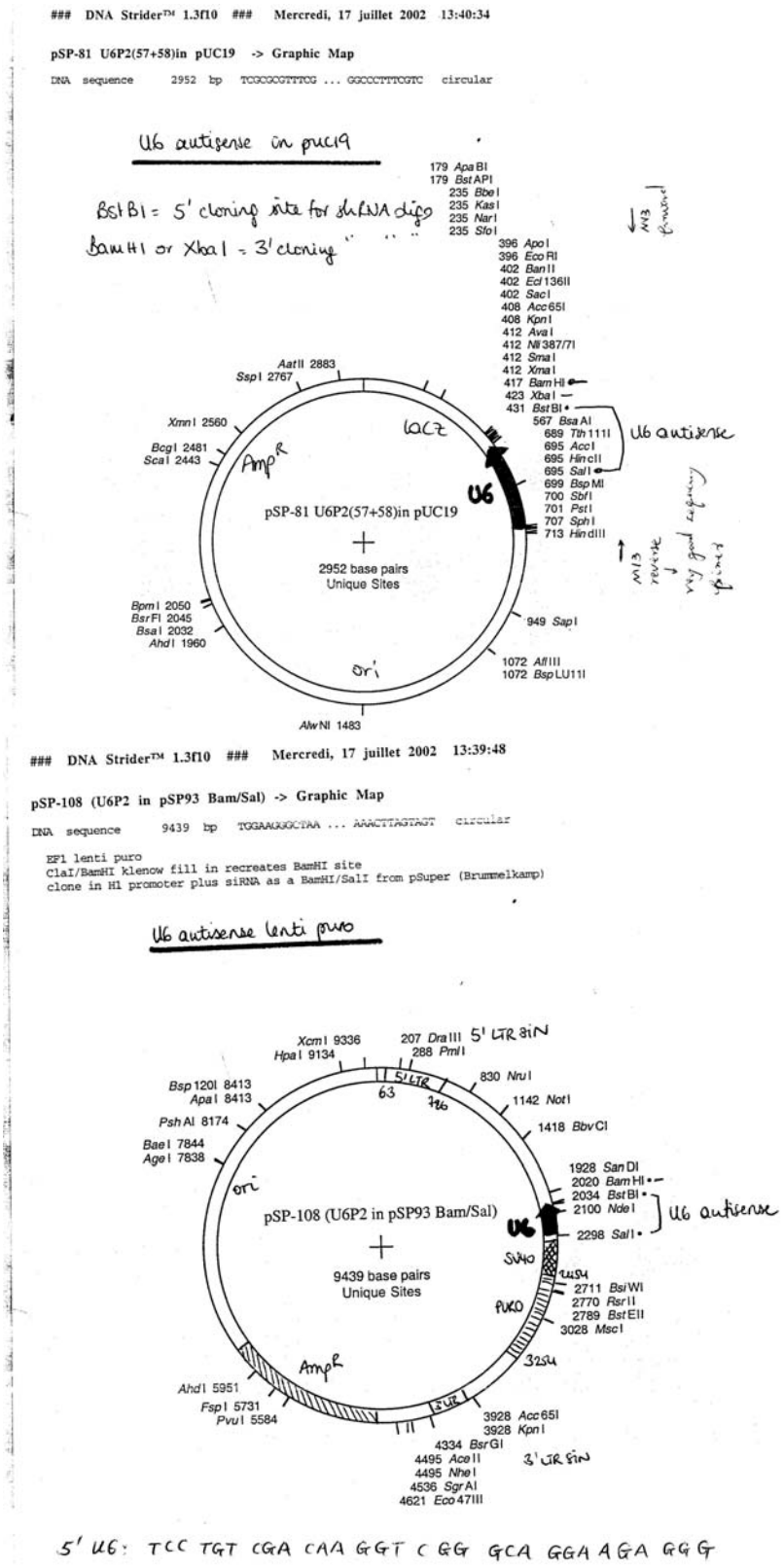

Figure A1.41.1 pSP vector maps – pSP-81 (top) and pSP-108 (bottom).

AI.42 Enterokinase Expression and Purification

From Susan Crown

PROTOCOL:

Note: Instead of purchasing enterokinase from NEB for CXCL12 cleavage, can also prep enterokinase

1. Transform the pEK plasmid into BL21s and plate on LB/CARB.
2. From an overnight culture, inoculate 6 x 1L LB + 100 ug/ml CARB in fernbach flasks. Grow at 37 C.
3. Induce with 0.5 mM IPTG at an OD600 of about 0.4. Grow for about 3 hours.
4. Spin down the cells and resuspend in 10 mM Tris 8, 1 mM MgCl2 with 300 ug DNase. Freeze in a conical tube at –80 C.
5. Thaw the cells. Bring the volume to about 50 ml with cold buffer and lyse cells by sonication (6 x 30s at setting 8, 80% works okay).
6. Add Triton X-100 to 0.1% and incubate for 15 min on gel shaker at RT.
7. Spin lysate either for 30 min in the SS34 Sorvall rotor at 15000 rpm.
8. Resuspend the pellet in 30 ml 10 mM Tris pH 8, 0.25% Deoxycholate. Sonicate (4 x 30s at setting 6, 80% with small tip works). Spin as in step 7.
9. Repeat Step 8 at least once or until the supernatant is pretty clear.
10. Resuspend the pellet in 20 ml of 6 M Guanidine-HCl, 100 mM Tris pH 8, 1 mM EDTA, 15 mM DTT. Spin as in Step 7 to clarify and filter if needed.
11. Dialyze against 1 L of 3 M Guanidine-HCl pH 2.5 in 1 kd MWCO membrane at room temperature. Cut the tubing extra long so that there is room for the additional buffer in step 12. Repeat dialysis with another liter.
12. Add 20 ml 50 mM Tris 9.3, 100 mM GSSG, 6 M GuHCl to the protein.
13. Dialyze against 1.5 L 3M GuHCl pH 8 twice at room temperature.
14. Add the protein dropwise to 500 ml of 700 mM Arginine-HCl pH 8.6, 200 mM GSH, 1 mM EDTA. Stir at 4 C for 4 days.
15. Dialyze against 20 L of 20 mM Tris pH 7.6, 50 mM NaCl. You may want to filter before this dialysis step.
16. Pour a STI-agarose (trypsin inhibitor) column. Use about 5 ml of bead suspension. Wash with 50 ml 20 mM Tris pH 7.6, 50 mM NaCl.
17. Remove the protein from the tubing and add 1:50 molar ratio of trypsin (e = 70870 /M/cm for enterokinase; MW of trypsin is about 30 kd). Stir at room

temperature for about 1-1.5 hours. Stop the reaction by adding ovomucoid. Add 4 fold (molar, but by weight is about the same) of the amount of trypsin added.

18. Load protein to column.

19. Wash with 25 ml 20 mM Tris pH 7.6, 1M NaCl. Then wash with 125 ml 20 mM Tris pH 7.6.

20. Elute with 30 ml 50 mM glycien pH 3 and collect 2 ml fractions. Add 30 ul 1M Tris pH 8 to each fraction and mix to aid neutralization.

21. Re-equilibrate the column with 25 ml Tris pH 7.6. It can be stored by running 25 ml storage buffer of 500 mM NaCl, 0.01 % Na-Azide over it.

22. Check fractions by gel and pool the appropriate elution fractions.

23. Dialyze against the storage buffer, 50% glycerol, 20 mM Tris pH 7.5, 200 mM NaCl, 2 mM CaCl2. This will also concentrate the protein.

24. Check the activity. Store at –20 °C until needed.

AI.43 Detailed IMAC, LTQ tune and MS/MS Protocol

CLL Lysates:
Two similar buffers used:

- Cells were resuspended in FD cytoplasmic lysis buffer containing ("2DLC" buffer)**:**
  20 mM HEPES, pH 7.9
  10 mM KCl
  1.5 mM MgCl2
  0.1 mM EDTA
  protease inhibitor mix (Roche Complete)
  Halt (at 2/3 normal concentration) phosphatase inhibitor.
  - Using 0, 3, 10, 30, and 60 min → 1.5mg

- Cells were resuspended in hypotonic lysis buffer containing ("2DLC" buffer)**:**
  10 mM HEPES, pH 7.9
  10 mM KCl
  1.5 mM $MgCl_2$
  0.5 mM dithiothreitol (DTT)
  protease inhibitor mix (Roche Complete)
  Halt (at 2/3 normal concentration) phosphatase inhibitor.
  - Using 0, 3, 10, 30, and 60 min → 2mg

DAY 1:
Determine protein lysate concentrations. Do prior to the addition of detergent.

- Thaw lysates on ice
- Spin samples at 14,000rpm
- Transferred Ramos and TJK967 memb and nuc pellets to new eppes and stored in -80°C
- Perform BCA protein assay on supe
- Aliquot 1.5-2 mg of protein depending on how much there is for sample prep/IMAC

DENATURE WITH PPS/1%SDS AND IN-SOLUTION DIGEST:
-For consistency, use the 1% SDS method for the TJK24s and as a comparison use the PPS for the TJK967s and Ramos cells

Prepare:

- 10 mL of **25 mM ammonium bicarbonate** (19.7 mg in 10 mL sterile water)
- 0.5 mL of **500 mM DTT** (38.5 mg in 0.5 mL of 25 mM ammonium bicarbonate)
- 5 mL of **100 mM CaCl2** (diluted from a 1M stock)
- (after DTT incubation) 1.5 mL of **1 M Iodoacetamide** (277.5 mg in1.5 mL of 25 mM ammonium bicarbonate) stored in dark
- 50 mL of 50% acetone, 50% Ethanol, 0.1% acetic acid (50uL) → precipitation
- 50 mL of 50 mM Tris pH 8. Diluted 1 M Tris pH8.0 stock 1:20 (2.5mL into 47.5 MQ water). Checked pH=8.0

- 5 mL of 6M urea (prepared with 18.02g in 50mL= 6M) + 0.1 M Tris pH8.0 (550uL of 1 M Tris, pH8.0)

1. BCA assay to determine protein concentration

Sample	**Lysate Concentration**	**Volume for 2mg (1.5mg for TJK24s)**
24- 0’	1.667 mg/ml	0.9 mL
24- 3’	1.434 mg/ml	1.05 mL
24- 10’	1.431 mg/ml	1.05 mL
24- 30’	1.764 mg/ml	0.85 mL
24- 60’	2.206 mg/ml	0.68 mL
967- 0’	4.257 mg/ml	0.47 mL
967- 3’	2.868 mg/ml	0.697 mL
967- 10’	2.697 mg/ml	0.742 mL
967- 30’	2.828 mg/ml	0.707 mL
967- 60’	3.072 mg/ml	0.651 mL
Ramos- 0’ (2mg)	4.938 mg/ml	0.405 mL
Ramos- 3’ (2mg)	5.434 mg/ml	0.369 mL
Ramos- 0’ (5mg)	4.938 mg/ml	1.01 mL
Ramos- 3’ (5mg)	5.434 mg/ml	0.92 mL

2. To TJK24s: Add to 1% SDS to help denature protein before reduction and alkylation. Vortex

- Added ~10 mg SDS to protein, vortexed. Doesn’t dissolve completely—eventually dissolves when heated.
- Check pH with pH paper...impt. to be pH8.0 for reduction/alkylation steps. pH appeared to be at 8.0 for samples from TJK24 and 967

Sample	**SDS for ~1% (w/v)**
24- 0’	10 mg
24- 3’	10.2 mg/ml
24- 10’	10.2 mg/ml
24- 30’	9.9 mg/ml
24- 60’	8.8 mg/ml

3. TO TJK967s and Ramos cells: Add ~0.5 mg PPS to TJK967 and the 2mg Ramos lysates (~0.7-0.1% final), and ~0.75 mg PPS to 5mg Ramos to help denature protein before reduction and alkylation. Vortex

- Resuspended the 1 mg vial of PPS in 20 uL of 25mM ammonium bicarbonate and distributed 10ul each to 2 tubes (e.g. 0’ and 60’). Then rinsed with another 20ul of 25mM ammonium bicarb and distributed 10ul to each tube again. Vortexed. The Ramos 5mg tubes received an extra 5ul PPS and 5ul rinse to each tube.
- Incubate at 60°C for 5 min to denature

- Check pH with pH paper...impt. to be pH8.0 for reduction/alkylation steps.

4. Add DTT (fresh) to final concentration of 10.5 mM. Vortex. Heat at 60-65°C for 20 min. Remove from heat and cool to RT for ~30 min (tried to make faster by cooling on ice for few minutes- cooled a little too long; Let warm back up to RT. Some precipitate in the PPS lysates- especially the Ramos.

- TJK967 and Ramos samples already contain 0.5 mM DTT → Add an additional 10 mM DTT. Add 10.5 mM DTT to TJK24s

Sample	**500 mM DTT to add**
24- 0’	18.9 uL
24- 3’	22.1 uL
24- 10’	22.1 uL
24- 30’	17.9 uL
24- 60’	14.3 uL
967- 0’	9.4 uL
967- 3’	13.94 uL
967- 10’	14.84 uL
967- 30’	14.14 uL
967- 60’	13.02 uL
Ramos- 0’ (2 mg)	8.1 uL
Ramos- 3’ (2 mg)	7.38 uL
Ramos- 0’ (5 mg)	20.2 uL
Ramos- 3’ (5 mg)	18.4 uL

5. Add iodoacetamide (fresh) to a final concentration of 100mM (using 1M stock). Vortex. Incubate at RT for 30 min in dark.

Sample	**Volume**	**1 M Iodoacetamide to add**
24- 0’	~0.90 mL	90 uL
24- 3’	1.05 mL	105 uL
24- 10’	1.05 mL	105 uL
24- 30’	0.85 mL	85.2 uL
24- 60’	0.68 mL	68 uL
967- 0’	0.47 mL	48 uL
967- 3’	0.697 mL	70 uL
967- 10’	0.742 mL	75 uL
967- 30’	0.707 mL	71 uL
967- 60’	0.651 mL	65.5 uL
Ramos- 0’ (2 mg)	0.405 mL	41 uL
Ramos- 3’ (2	0.369 mL	37 uL

mg)		
Ramos- 0' (5 mg)	1.01 mL	101 uL
Ramos- 3' (5 mg)	0.92 mL	92 uL

6. TJK24s: Protein precipitation:

Sample	**Volume**	**Protein (x 3 or 4)**	**Precipitation solvent volume**
24- 0'	~1 mL	~2x0.5 mL	1.5 mL/tube
24- 3'	~1.15 mL	~2x0.58 mL	To top (~1.7mL)
24- 10'	~1.15 mL	~2x0.58 mL	To top (~1.7mL)
24- 30'	~0.95 mL	~2x0.48 mL	1.5 mL/tube
24- 60'	~0.75 mL	~2x0.38 mL	1.2 mL/tube

- Distribute samples into LoBind eppis to account for increase in volume
- Add 3-4 X the starting volume of 50% EtOH/50% Acetone/ 0.1% acetic acid.
- Store in -80 freezer for ~10 min to aid precipitation
- Centrifuge at 4000rpm (1.5xg) for 10 min at 4°C
- Remove supe. Wash one more time with precipitation buffer + 500 uL of MQ water (so, 1/5 water)
    - Used 500 uL MQ water + 1.5 mL precipitation buffer for all samples
- Centrifuge at 4000rpm (1.5xg) for 10 min
- Remove supe completely
- Let air dry O/N, covered with kimwipe (once dry, store at 4 °C until ready for trypsin digest)- put in rack on side to dry.

TJK967 and Ramos: Don't have to do the protein precipitation. Just go straight to the trypsinization rxn

7. Mix 44ul of 25mM ammonium bicarbonate, 6ul of 100 mM CaCl2 (~1.7 mM final conc.) to each 20 ug lyophilized trypsin aliquots. Add trypsin solution to protein samples.
    - Want trypsin:protein ratio to be at 1/50 by weight to sample (e.g. For every 1 mg of protein, add 20 ug of trypsin)
        - Prepare: 2 mg x 10 samples = 20 mg (need 20 trypsin aliquots)
    - $CaCl_2$ recommended to help trypsin reaction
    - pH should be between 7-8 for optimal trypsin activity. pH was ~8.0
    - Didn't have enough trypsin for all of them, so left the 5mg Ramos cell lysates at 4degC until we get more trypsin in. Also, had to use 3x20ug of the aliquots instead of 4 aliquots for the Ramos- 2mg lysates- so distributed the 3 tubes of trypsin evenly between the Ramos lysates. Also, for TJK967s, had 8 instead of 10 aliquots, so distributed evenly between the lysates. So only using ~75-80% of the amount of trypsin we usually use

8. Shake O/N at 37°C.

DAY 2:

TJK24s:
Stored at 4°C until ready to prepare for trypsin digest

9. Resuspend protein pellets in 50 uL of 6 M urea/0.1M Tris, pH8.0, vortexed and incubated for ~1h. Pool the aliquots of each sample timepoint together.
- Rinse the extra tubes with 1 x 100 uL + 2 x 200 ul of 50 mM Tris, pH 8.0, to remove any remaining peptides.

10. Add additional 50 mM Tris, pH 8.0, to the samples so that the urea is diluted 5 fold in the pooled samples.

11. Mix 44ul of 25mM ammonium bicarbonate, 6ul of 100 mM CaCl2 (~1.7 mM final conc.) to each 20 ug lyophilized trypsin aliquots. Add trypsin solution to protein samples.
- Want trypsin:protein ratio to be at 1/50 by weight to sample (e.g. For every 1 mg of protein, add 20 ug of trypsin)
  - Prepare: 2 mg x 10 samples = 20 mg (need 20 trypsin aliquots)
- $CaCl_2$ recommended to help trypsin reaction
- pH should be between 7-8 for optimal trypsin activity. pH was ~8.0

12. Shake O/N at 37°C.

TJK967 and Ramos:

13. Acidification
- Add 10% TFA to final of 0.4% (0.3% to 0.5%) to each sample. pH ~2

Sample	**10%TFA to add**
967- 0’	19.2 ul
967- 3’	28 ul
967- 10’	29.7 ul
967- 30’	28.3 ul
967- 60’	26 ul
Ramos- 0’ (2 mg)	16.2 ul
Ramos- 3’ (2 mg)	14.8 ul

- Acidify and incubate at 37°C for 4hr to hydrolyze the detergent
- Spin for 30min at 14,000rpm to remove the insoluble material
- Save supe into new loBind eppe tube.
- Neutralized solutions with Ammonium hydroxide (10% solution) to pH 7-8

Sample	**10%TFA to add**
967- 0’	70 ul
967- 3’	115 ul
967- 10’	120 ul
967- 30’	115 ul
967- 60’	120 ul
Ramos- 0’ (2 mg)	60 ul
Ramos- 3’ (2 mg)	55 ul

- Dry or save aliquots of Ramos cells for playing with the ITRAQ conditions.

- Speed-vac dry the Ramos 2mg pellets and TJK967s. Stored the Ramos pellets at -80°C (March 2009→ lysates box) and saved the TJK967s at 4°C for running C18 tomorrow. Note: pellets had yellow color to them.

DAY 3:

14. Acidification of TJK24s

- Add 10% TFA to final of 0.4% (0.3% to 0.5%) to each sample. pH ~2

Sample	10%TFA to add
24- 0'	36 ul
24- 3'	42 ul
24- 10'	42 ul
24- 30'	34.5 ul
24- 60'	28 ul

15. Resuspended TJK967 pellets with 500ul of 50mM Tris pH 8.0

16. C18 Cleanup (to remove salt)

- **C18 Prep**(use 50 mg, volume=1.25 mL)
  - Hydrate column w/ methanol (fill to top)
  - Add **80% ACN/1% HAC** (made 35ml) to top of column to clean out column; repeat. Takes ~20-30min for column to drip
  - Wash twice w/ **1 % HAC (prepared ~80ml)** to wash out ACN
  - Add sample to column, and allow to drip down.
    - Collect in LoBind eppi, label "C18-FT", start drying
  - Wash twice w/ **1% HAC**
    - Collect in LoBind eppi, label "C18-Wash1" and "C18-Wash2", start drying
  - Elute w/ 400uL + second 100uL wash at end of **80% ACN/0.1%HAC** (4-5 bed volumes)
    - Collect in LoBind eppi, label "C18-elution", start drying
    - Repeat a second time if you want
    - Speedvac to dry @ 50 °C (set Spector lab speed vac to medium heat)
      - 500 uL take ~2 h to dry.
  - Can later resuspend in 100uL of **1% HAC or water**
  - Stored pellets at 4 °C (at -20°C for longer term)

While doing C18 cleanup, also do bead prep for DAY 4 IMAC columns...

17. Prepared trypsin digest of 5mg Ramos cells with Worthington trypsin borrowed from Steve.

- Only had 100ug of trypsin total (50mg/pellet, so only a 1:100 sample instead of 1:50 trypsin:protein ratio. To compensate, digested in steps. First 4-5 h of with ½ of the trypsin digest, then add the other ½ of the trypsin.
- Resuspended the 100ug of trypsin 250ul total- 220ul of 25mM ammonium bicarb +30ul of 100mM CaCl2. Then added 60ul to each tube of Ramos cells

(0' and 3') for 4-5 h at 37°C shaking. Kept the remaining trypsin on ice and then added remaining (65ul to each tube) for O/N trypsin digest.

18. Bead Prep (~3hr)

Before starting:

Prepare 250 mL of 0.6% HAc for all the solutions (1.5 mL HAC, up to 250 mL with water).

- Add 3 spin columns of NTA-silica resin into 50 mL of **50 mM EDTA, 1 M NaCl** in 50 mL conical tube (e.g. last time, used 4 columns worth for 10 mg of protein, this time had more than enough beads)
  - Can use stock, or add 5 mL 0.5 M EDTA , 10 mL 5 M NaCl, bring volume to 50 mL w/ H_2O
- Shake @ RT for 1 hour, rotate the tube at least once every 15 min. Set-up on the rotator (from TC room)
- Spin down @ 3000-**4000** rpm for 2 min. in swinging bucket rotor (normal acceleration/~6 deceleration), draw up supe with pipette and dump
- Wash with **50 mL of H_2O** to wash; spin down again; dump liquid
- Wash with **50 mL of 0.6% HAC**; spin down; dump liquid
- Add **50 mL of 100 mM $FeCl_3$ in 0.3% HAC (Add iron last when making this solution!!!)**
  - Add 25 mL of 0.6 % HAC, 20 mL of H_2O, then 5 mL of 1 M $FeCl_3$)
  - Always add the iron last; only take the very top of the supernatant, and *do not disturb* precipitate at the bottom
- Shake @ RT for 1 hour, rotate tube at least once every 15 min. Used the rotator (from TC room)
- Spin down @ **4000 rpm** for ~ 2 min., dump liquid
- Wash w/ **50 mL of 0.6% HAC**; spin down; dump liquid
- Add **50 mL of 0.1 M NaCl, 25% ACN, 0.1% HAC**
  - Add 1 mL of 5 M NaCl, 12.5 mL of ACN, and 8.33mL of 0.6% HAC
- Shake @ RT for 10 min.
- Spin down @ 3000-**4000** rpm for ~ 1 min., dump liquid
- Wash twice w/ **50 mL of 0.1% HAC**
  - Prepare 100 mL using 12.66 mL of 0.6% HAC and bringing up to 100 mL with H2O
- Aliquot into an eppi tube, and store @ 4°C (date and do not use after 1 week; fresh is best)... Remove supe to get 50:50 slurry

DAY 4:

IMAC Prep:

19. Make IMAC columns (10 of them) –

- Use gel loading tips to pack columns
- Pinch off a small amount of glass wool and spindle out to a thin string (use water to smooth down)
- Cut ends of spindled wool to make it ~1 inch
- Use a pointy object to push down tip (want it to take up ~1/4 of the actual tip of the gel loading tip)
- Squeeze bottom part with clamp tweezers and cut off bottom part
- Cut off top part of tip to help place on syringe

20. Added 30ul of bead slurry to prepared IMAC columns (=~15ul of beads)**;** just press down gently on the syringe initially and let it flow through on its own (be careful to not apply too much pressure) (use ~20ul for 1mg (so about 10ul of actual IMAC beads))

21. Condition beads w**/ 25% ACN/0.1% HAC**

- prepared 4 mL (plenty): 1 mL ACN, 0.67 mL 0.6%HAC, 2.33 mL H2O

22. Phospho-enrichment

- Resuspend pellets in 100uL of 1 %HAC
  - Note- TJK967s have yellow color to them
- Spun down at 4000 rpm for 2 min
  - Some sample would come up when pipetting to load the columns, so had to re-spin
  - Note- TJK967s had no pellet after spin
- Add supe to column, push through slowly (collect "flowthrough")
  - Collect samples into 0.5 mL LoBind eppis, start drying
- Wash 2x w/ 30 uL **25% ACN/0.1% HAC/0.1 M NaCl** (Add to "wash" tube)
  - 4 mL: 1mL ACN, 0.4 mL 1%HAC, 0.1 mL 4M NaCl
- Wash 2x w/ 15uL of ***0.1%* HAC** *(to remove the salt)* (Combine to "wash")
- Wash 2x w/ H_2O (to remove the acid) (1st wash- 15uL, 2nd wash 30uL) (combine to "wash")
- Elute w/ 50 uL of (20 + 20 + 10 uL) of 1% Phosphoric Acid
  - 10ul phosphoric acid into 990 uL of H2O
  - Divide elutions into two tubes (one to resuspend and run, one to reserve for later) called "elution"
- Speed vac to dry
- Store pellet at -20°C
- Resuspend pellets in 1% acid in order to dissolve the peptides

23. Acidified trypsin digests of the 5mg Ramos samples

- Note- took samples out in afternoon, so they had an extra long digest period.
- Acidified to 0.4% TFA (added ~40ul to each sample).

24. Incubated for 4h at 37°C shaking with the acid to hydrolyze the detergent

25. Spin for 20min at 14,000rpm to remove the insoluble material

26. Save supe into new loBind eppe tube.

27. Neutralized solutions with Ammonium hydroxide (10% solution) to pH 7-8

Sample	**10%TFA to add**
Ramos- 0' (5 mg)	170 ul (only 50ul fresh)
Ramos- 3' (5 mg)	170 ul (only 50ul fresh)

28. Speed-vac dry the Ramos 5mg pellets.

Running Samples on LTQ

Proteomics suite code: 1374
MS room: 46607

Sample assignments:

Loaded samples as stated below:

- 8uL/well for samples (TJK)
- 40uL/well for standards

Added protective film over plate to prevent evaporation. Film (Axygen) has X scored over each well to allow needle to easily draw up sample without getting damaged or clogged.

Equilibrating column:

Equilibrated column as stated below

- *Pathway to direct control*:
  X-Caliber (icon on desktop)
  Instrument setup
  Surveyor pump (left hand side)
  Surveyor MS pump (toolbar)
  Scroll to Direct control and select (direct control box should appear)

- Set conditions at 50% A and B, 200uL/min
  - Monitor pressure. If too high, indicates leak. Stop and readjust/tighten connector pieces.
  - Make sure liquid is coming out of tip...
  - Pressure starting higher ~235bar, but decreases as column packs and becomes equilibrated (normal pressure is ~180bar)
  - After few minutes, started AngII runs (x 2)
  - Look at profile: make sure there's signal (~E5-E6)
  - If both 2nd AngII run looks good, add other samples to Queue (already added to wells)...samples looked fine, started running other samples O/N

Running samples on the LTQ:
Sample assignments: (used plate from 3/26 runs, put same samples in same wells)

SUMMARY OF RESULTS:

BSA digest	**# peptides**	**% coverage**	**# spectra (pvalue cutoff=0.99)**
090419	57	~40%	
090420	47	35.9%	
090421	53	38.4%	135

TJK527 timepoint	**False positives**	**FD rate**	**# peptides**	**P-peptides**	**%phospho-enrichment**	**P-value cutoff**

090419_10	2	1%	198	80	40.4%	0.19
090419_30	4 (3)	2% (1.6%)	197 (186)	75	38.1%	0.6 (0.44)
090419_60	3	2.19%	137	56	40.9%	0.29
090424_0a	6	2.0%	292	103	35.2%	0.27
090424_0b	5	1.2%	405	167	41.1%	0.68
090424_3a	6	2.5%	237	97	40.8	0.20
090424_3b	6	1.6%	372	165	44.4	0.53

TJK24 timepoint	**#FP**	**FD rate**	**# peptides**	**P-peptides**	**%phospho-enrichment**	**P-value cutoff**	**Notes**
090429_30	6	1.57%	318	137	43.1%	0.285	
090419_60	5	1.47%	339	163	48.1%	0.022	
090421_30	3	1.66%	302	171	56.6%	0.07	w/ new Tune file (all next)
090421_0	3	2.3%	130	49	37.7%	0.089	
090422_0b	4	2.2%	178	89	50%	0.12	
090422_0c	5	1.49%	335	165	49.3%	0.28	set mass range to 400-1500m/z (all next)
090422_0d	5	1.75%	285	144	50.5%	0.094	
090421_3	2	1.57%	127	43	33.9%	0.003	
090422_3b	6	1.76%	341	177	51.9%	0.12	
090422_3c	6	1.75%	342	165	48.2%	0.47	
090421_10	6	1.78%	337	167	49.6%	0.0743	
090421_10b	7	1.87%	374	176	47.1%	0.48	
090422_10c	7	1.86%	377	178	42.2%	0.059	
090421_30	3	1.66%	302	171	56.6%	0.07	
090422_30b	6	1.5%	393	229	58.3%	0.265	

090422_30c	5	2.2%	313	174	55.6%	0.16	
090422_60	5	1.8%	272	128	47.1%	0.5	
090422_60b	6	1.9%	323	186	57.6%	0.17	
090422_60c	4	1.38%	290	174	60%	0.13	

TJK967 timepoint	**False positives**	**FD rate**	**# peptides**	**P-peptides**	**%phospho-enrichment**	**P-value cutoff**
090420_0	4	3.5%	114	36	31.6%	0.19
090420_3	4	2.4%	166	89	53.6%	0.28
090420_10	4	2.68%	149	76	51%	0.24
090420_30	3	2.6%	116	73	62.9%	0.29
090420_60	2	0.95%	210	112	53.3%	0.5
090423_0	2	1.59%	125	58	46.4%	0.12
090423_3	3	1.86%	160	99	61.9%	0.28
090423_10	1 (3)	1.36% (3.1%)	72 (96)	39 (56)	54.2% (58.3%)	0.006 (0.05)
090423_30	3	3.1%	95	54	56.8%	0.122
090423_60	3	1.59%	126	77	61.1%	0.37

TJK863 timepoint	**False positives**	**FD rate**	**# peptides**	**P-peptides**	**%phospho-enrichment**	**P-value cutoff**
090424_0a	5	1.3%	352	52	14.8%	0.05
090424_0b	7	1.23%	569	146	25.7%	0.368
090424_0c	8	1.37%	586	159	27.6%	0.29
090424_3a	8	1.43%	559	155	27.7%	0.3
090424_3b	9	1.55%	582	164	28.2%	0.294
090424_3c	8	1.38%	579	172	29.7%	0.171

TJK375 timepoint	**False positives**	**FD rate**	**# peptides**	**P-peptides**	**%phospho-enrichment**	**P-value cutoff**
090425_0a	8	1.67%	478	122	25.5%	0.33
090425_0b	6	1.1%	542	144	26%	0.34
090425_0c	7	1.65%	422	118	26.7%	0.18
090425_3a	7	1.25%	556	150	27%	0.5
090425_3b	11	1.4%	765	226	29.5%	0.29
090425_3c	7	1.38%	507	118	29.6%	0.16

DAY 1: 090419
(Controls and TJK527)

- Removed nanomate and replaced with LC setup
- Attached old column (last used for 12/08 runs with O18/O16 and TJK527 samples)
- Began with running controls:
    - AngII
    - BSA dig
    - AngII
- Verified that BSA digest looked good by Inspect (against cow_protein.trie database): Got 57 peptides and ~40% coverage at a p-value of 0.99
- AngII_2 had a lot of carryover from BSA, no real evident peak, so ran another AngII
- AngII_3 looked good, so started with TJK527_30 to see how well column performs
- Ran TJK527_30 with Inspect, but continued with running additional samples. Started TJK527_60
- Ran AngII_4
- TJK527_30 Inspect run completed—data ok, but could be better (186 peptides, pvalue cutoff 0.44), so decided to start with a new column (never been used)

Sample ID	Position	Method	Time	Folder saved to	Comments
AngII_01	A:A12	Angio or BSA.meth	85	c:\MS\Handel\090418_controlsand527	
BSA dig	A:B12	Angio or BSA.meth	85	c:\MS\Handel\090418_controlsand527	
AngII_02	A:A12	Angio or BSA.meth	85	c:\MS\Handel\090418_controlsand527	lots of BSA carryover, strange
AngII_03	A:A12	Angio or BSA.meth	85	c:\MS\Handel\090418_controlsand527	strong AngII peak
TJK527-30’	A:B9	LTQ_105gradient_090420_105min.meth	105	c:\MS\Handel\090419_TJK527	
TJK527_60	A:B10	LTQ_105gradient_090420_105min.meth	105	c:\MS\Handel\090419_TJK527	
TJK527_10	A:B8	LTQ_105gradient_090420_105min.meth	105	c:\MS\Handel\090419_TJK527	
AngII_04	A:A12	Angio or BSA.meth	85	c:\MS\Handel\090419_TJK527	

DAY 2:
(controls, TJK24, TJK967)

- Controls looked good, AngII had strong peak ~35 min as expected
- BSA digest (4590 spectra),
- Proceeded with TJK24 runs (started with least impt to most impt.)
    - Resuspended pellets in 40 uL of 0.1%HAC; spun down 4000 rpm, 1.5min
    - Only loaded 1-2 samples at one time... cooling unit not working
    - Modified current method settings:
        - m/z range: from 200-2000 → 200-1500
        - Toni Tune file
        - Flow rate in gradient: from 500uL/min → 400 uL/min
        - Dynamic exclusion size: from 200 →100
- Once TJK24_30 min run was completed, ran by Inspect to determine data acquisition quality
    - Took 6 h to analyze
    - 5637 spectra, 0.285 p-value cutoff, 325 total peptides
- Continued with 60, 10, 3, 0
- Ran TJK967 samples (PPS solubilized to compare against TJK24)
    - Resuspended pellets in 40 uL of 0.1%HAC; spun down 4000 rpm, 1.5min

Sample ID	Position	Method	Time	Folder saved to
AngII_1	A:A12	Angio or BSA.meth	85	c:\MS\Handel\090420 newcolumncontrols
BSA dig	A:B12	Angio or BSA.meth	85	c:\MS\Handel\090420 newcolumncontrols
AngII_2	A:A12	Angio or BSA.meth	85	c:\MS\Handel\090420 newcolumncontrols
AngII_3	A:A12	Angio or BSA.meth	85	c:\MS\Handel\090420 newcolumncontrols
090420_TJK24_30	A:A4	LTQ_105gradient_090420_105min.meth	105	c:\MS\Handel\090420 _TJK24
090420_TJK24_60	A:B5	LTQ_105gradient_090420_105min.meth	105	c:\MS\Handel\090420 _TJK24
AngII_4	A:A12	Angio or BSA.meth	85	c:\MS\Handel\090420 _TJK24
090420_TJK24_10	A:B3	LTQ_105gradient_090420_105min.meth	105	c:\MS\Handel\090420 _TJK24
090420_TJK24_3	A:B2	LTQ_105gradient_090420_105min.meth	105	c:\MS\Handel\090420 _TJK24
AngII_5	A:A12	Angio or BSA.meth	85	c:\MS\Handel\090420 _TJK24
090420_TJK2	A:B1	LTQ_105gradient_	105	c:\MS\Handel\090420

4_0		090420_105min.meth		_TJK24
090420_TJK967_0	A:C4	LTQ_105gradient_090420_105min.meth	105	c:\MS\Handel\090420_TJK967
AngII_1	A:A12	Angio or BSA.meth	85	c:\MS\Handel\090420_TJK967
090420_TJK967_3	A:C5	LTQ_105gradient_090420_105min.meth	105	c:\MS\Handel\090420_TJK967
090420_TJK967_10	A:C6	LTQ_105gradient_090420_105min.meth	105	c:\MS\Handel\090420_TJK967
AngII_3	A:A12	Angio or BSA.meth	85	c:\MS\Handel\090420_TJK967
090420_TJK967_30	A:C7	LTQ_105gradient_090420_105min.meth	105	c:\MS\Handel\090420_TJK967
090420_TJK967_60	A:C8	LTQ_105gradient_090420_105min.meth	105	c:\MS\Handel\090420_TJK967
AngII_4	A:A12	Angio or BSA.meth	85	c:\MS\Handel\090420_TJK967

OVERALL: Can compare solubilization techniques (SDS/Urea vs. PPS), although didn't do TJK967 the traditional way to compare with the same sample

-SAME COLUMN
-OLD TUNE FILE (TONI)
-100 LIST SIZE
-M/Z RANGE 200-1500

DAY 3: 090421
(new column controls, Tuning, start of TJK24 triplicates)

- Placed newly packed capillary column on
- Ran normal controls (AngII, BSA, AngII)
- Good website www.rci.rutgers.edu/~layla/AnalMedChem511/LCMS_files/FT_MS.pdf

- **Generated new Tune files:**
  - Removed packed column and replaced with an unpacked column- be sure that the tip is scribed and there is liquid flowing through before using. Be sure to wipe off any droplets before plugging in again (drops can arc and cause problems with the ionization).
  - Changed fittings (unscrewed fitting with filter connected to pump) and attached to fitting connected to syringe
    - Tubing is orange, has clear sleeve that fits over Hamilton syringe needle
  - Filled 250 uL Hamilton syringe, blunt ended, with 250 uL of 2 pmol/uL of AngII (freshly suspended in 0.1%HAc)

    - Placed syringe onto holder—black syringe plunger touching unit that moves (on RH side), needle fully fitted into tubing, plastic tip wedged into filling to secure needle in place while syringe pump is in use
    - In LTQ tune: opened syringe pump control (picture of pump in left side)→ initially set to 10 uL/min, Hamilton 250 uL syringe → apply → make sure ions are detected
    - Then, set to 2 uL/min
    - Start the LTQ-tune (play button)
    - Press Tune icon in toolbar → select automatic → Type in mass → Start
        - Mass Details for Angiotensin II: molecular weight for Sigma AngII-1045
        - So tune to 2+ charge stateis m/z=524, we did 523.75. Might also consider the 3+ state which would be m/z=349.5.
        - Can also tune to AngI 3+ state which would be m/z = 433.2. Accidentally started tune files with this m/z since AngI is good to tune with.
        - We also had a very strong peak at 519, so we did another tune file with the m/z set for 519.
        - Saved all the iterations separately- better ones are the “b” and “c” files
    - Once completed (<1 min), “save as” in folder
    - Continue to tune until % change is low from tune to tune (also can monitor IT- ion time- <1 is good, once tune file has good time, can stop and use that)
    - Once satisfied, switch plumbing back to original settings (watch for leaks at fitting with filter)
    - Replace empty column with packed column
    - Using direct control, test for leaks (be sure column is distanced from vacuum inlet—wick any moisture that forms on tip—can lead to bad problems with instrument if this isn’t done)
    - Start run being sure to adjust method to using newly created tune file
- Changed method to now use Tune method: 090421_Tune_523 file (did for both Angio or BSA and 105 min method)
    - Also adjusted Angio/BSA method to scan m/z 200-1500 to be same as 105 min
- Began AngII run...detected slow leak at filter fitting...clogged
- Stopped run sequence
- Replaced filter with clean one (in tool box in plastic bag that says clean fitting) and put dirty one in 50 mL conical along with other dirty one (NOTE: dark particulates visible in white filter)
    - Be sure to push tubing past the ferrule to get good tight seal
    - Twist new filter fitting onto black fitting
    - Connect beige ferrule to black fitting with filter (twist black fitting with filter before twisting onto beige ferulle because beige part doesn’t twist very well)
- Use Direct control to flow 200uL/min to test fitting
- Started AngII Run again
    - Data looked weird, there were a lot of peaks instead of one strong AngII peak at 35 min (though peaks are at strong intensity E7)...maybe b/c we

stopped the previous AngII run that had already loaded to the column and hadn't eluted off before we loaded another AngII on
    - Rerun AngII (with same tune file) to see if it looks better\
- New AngII Run looked beautiful! Very strong peak (E7) and little to no background
- Proceed with TJK24 0'-60' runs

NEW COLUMN AND NEW TUNE FILE APPLIED...

OVERALL: Have complete TJK24 set with new tune file on a new column to compare to previous run with old tune file and old column
-NEW TUNE FILE
-NEW COLUMN

Figure AI.43.1 LTQ Tune configuration.

DAY 4-7: 090422- 090426
(continuation of TJK24 triplicates, one set of TJK967, triplicates of 0' and 3' for TJK863, TJK375, and duplicates of TJK527)

- AngII controls continue to look good
- Realized after 60 and 0b set that m/z range was at 200-1500. Should be 400-1500.
- Starting with TJK24_0c run, modified both 105 and 85 min control method to have m/z range 400-1500.
- Changed column after TJK24 triplicate and TJK967 runs (all done on one column)
- Ran column controls as usual
- Started to run 0' and 3' triplicates for TJK863, TJK375, and TJK527
    - Had to change column after TJK863, so reduced total time left to run samples ☹
    - Decided to do duplicates of TJK375 and TJK527 for 0' and 3' using the 105 min then the 105 min with a modified dynamic exclusion list with the remaining time
        - Repeat count- 1
        - Repeat duration- 30 s
        - Exclusion list size- 25
        - Exclusion duration- 30s
    - For TJK863 and TJK375, used already resuspended pellets from before
    - For TJK527- confusion about which tube was 0' (label difficult to read and distinguish from 10'), so resuspended other elution pellet in 30 uL of 0.1% HAc; spun at 4k rpm for 2 min before loading onto plate

Sample ID	Position	Method	Time	Folder saved to	Comments
090421_TJK24_10	A:B3	LTQ_105gradient_090422_105min_Tune523	105	c:\MS\Handel\090421_TJK24	
090421_TJK24_30	A:B4	LTQ_105gradient_090422_105min_Tune523	105	c:\MS\Handel\090421_TJK24	
AngII_6	A:A12	Angio or BSA_Tune523	85	c:\MS\Handel\090421_TJK24	excellent
090422_TJK24_60	A:B5	LTQ_105gradient_090422_105min_Tune523	105	c:\MS\Handel\090421_TJK24	
090422_TJK24_0b	A:B1	LTQ_105gradient_090422_105min_Tune523	105	c:\MS\Handel\090421_TJK24	
AngII_7	A:A12	Angio or BSA_Tune523	85	c:\MS\Handel\090421_TJK24	Realized all previous ranges were set to 200 instead of 400 for IT

090422_TJK24_0c	A:B2	LTQ_105gradient_090422_105min_Tune523	105	c:\MS\Handel\090421_TJK24	Modified range to m/z 400-1500
090422_TJK24_3b	A:B3	LTQ_105gradient_090422_105min_Tune523	105	c:\MS\Handel\090421_TJK24	
AngII_8	A:A12	Angio or BSA_Tune523	85	c:\MS\Handel\090421_TJK24	
090422_TJK24_10b	A:B4	LTQ_105gradient_090422_105min_Tune523	105	c:\MS\Handel\090421_TJK24	
090422_TJK24_30b	A:B5	LTQ_105gradient_090422_105min_Tune523	105	c:\MS\Handel\090421_TJK24	
AngII_9	A:A12	Angio or BSA_Tune523	85	c:\MS\Handel\090421_TJK24	

ETC- more runs like this: alternating two samples, then AngII to monitor column performance

General info for loading columns, starting run--

Changed column to put our own column on the MS. First need to remove column on the instrument:

a. Unscrew the column from the fitting
b. Loosen fittings to slide column back from injection port
c. Always remove and load column through the front
d. Loosen column and pull to front. Will need to bend it upwards to get it released.
e. Load on the new column through the front end of the screw so that the narrow part tapers to back end of column and the screw head at the front end, adjusted so the screw is slid up to clear portion of the column tip.
f. Be careful not to hit the tip against anything so that it won't chip or break, and feed the back end through the unit until it comes out
g. Screw the top part of the column in.
h. Screw the back part into the union fittings and make sure this is really tight in order to avoid sample loss. Also, when adjusting into the fitting, be sure to completely unscrew the fittings, slide the screws onto the column end and then screw in tightly, otherwise it can come loose and sample won't load properly.
i. Bring the unit forward towards the injection port by sliding the right portion forward and following by sliding the left part forward until the column tip is ~5mm from the injection port.
j. Use the fine adjustment knobs to adjust the column so the tip is centered with the injection port and ~1mm from the port.

Before starting, test the alignment and the pumps:

k. Check that there are plenty of buffers. Buffer A= 0.1% AcOH in HPLC grade water. Buffer B= 0.1% AcOH in HPLC grade Acetonitrile
l. Also need to have secondary water container for the instrument, even though this isn't part of the buffer system.
m. Open up LTQ Tune to check that the nanospray is working properly
n. Use the direct control to get the pumps going. Run at 95%A, 5% B. Start at 150ul/min flow rate, pressure should be at ~80 bar for this flow rate (it was good ~75-80 bar).
o. Reduce flow rate to 20ul/min in order to test connection. Pressure should increase to ~200 bar. Shouldn't go over 300bar. Emergency shut-off is already set for 400 bar, but make sure below 300 bar because otherwise may have issues. (our pressure was fine, a little on the low side, but still fine at ~180 bar). Wait a few minutes. If something is wrong with the fittings or the connection, then the pressure will quickly drop down to 0. (Pressure maintained though and seemed fine).
p. In order to make sure the nanospray is working, should see noise peaks coming up on the screen. If there is contamination, then will have large peaks, but if clean, then have just background noise, the highest peaks at lowest MW, this is fine.
q. Since we had a brand new column that had only been exposed to MeOH, the first run (first AngII control run) is essentially wasted in setting properties of the column and wetting it with ACN.
r. Another thing to keep in mind are the microfilters that prevent large particles and clogs from going into the instrument (one set before the split flow, one set after the split flow). These don't need changed too often, but they can become clogged and cause increase in pressure, so if there is an issue with pressure, this may be something that needs changed.

Once everything has been checked and seems to be running properly, then you're ready to start the run. Press OK (or start) on the direct control.

s. The LTQ, Surveyor AS and Surveyor MS pump controls should all read "ready to download".

After 1-2 min, should see green light on the instrument switch to injection mode (no split), this should cause the pressure to increase to what we saw before with the 20ul/min flow rate (~200 bar). Injection mode lasts for ~20 min.
After 20 min, the light will switch back to the split flow run, should drop pressure back down to ~80 bar.

AI.44 IMAC with iTRAQ and SCX

IN-SOLUTION DIGEST:
DAY 1: (6/09/09)

Prepare:

- 10 mL of **25 mM ammonium bicarbonate** (19.7 mg in 10 mL sterile water)
- 0.2 mL of **500 mM DTT** (15.4 mg in 0.2 mL of 25 mM ammonium bicarbonate)
- 5 mL of **100 mM CaCl2** (diluted from a 1M stock)
- (after DTT incubation) 0.5 mL of **1 M Iodoacetamide** (92.5 mg in 0.5 mL of 25 mM ammonium bicarbonate) stored in dark
- 75 mL of 50% acetone, 50% Ethanol, 0.1% acetic acid (75uL) → precipitation
- 50 mL of 50 mM Tris pH 8. Diluted 1 M Tris pH8.0 stock 1:20 (2.5mL into 47.5 MQ water). Checked pH=8.0
- 5 mL of 6M urea (prepared with 18.02g in 50mL= 6M) + 0.1 M Tris pH8.0 (550uL of 1 M Tris, pH8.0)

1. Thawed samples (2mg aliquots) at room temperature and performed BCA assay to determine protein concentration

Sample	Concentration (mg/ml)	Volume for 2mg
MJK617- 0’	0.997mg/ml	2.007 mL
MJK617- 3’	1.236 mg/ml	1.618 mL

2. Add to 1% SDS (w/v)to help denature protein before reduction and alkylation. Vortex

- Added 20 mg SDS to MJK617- 0' and 17 mg of SDS to MJK617- 3', vortexed. Doesn’t dissolve completely—eventually dissolves when heated.
- Check pH with pH paper...impt. to be pH8.0 for reduction/alkylation steps. pH appeared to be at 8.0

3. Add DTT (fresh) to final concentration of 10.5 mM. Vortex. Heat at 60-65°C for 20 min. Remove from heat and cool to RT for ~50 min

- Add to 10.5 mM DTT

Sample	500 mM DTT to add
617- 0’	42 uL
617- 3’	35 uL

- SDS dissolved after heating

4. Add iodoacetamide (fresh) to a final concentration of 100mM (using 1M stock). Vortex. Incubate at RT for 30 min in dark.

Sample	Volume	1 M Iodoacetamide to add
617- 0’	2 mL	220 uL
617- 3’	1.65 mL	180 uL

5. Protein precipitation:

- Divided MJK617 0' and 3' into 4 tubes (2ml tubes) each in order to precipitate

Sample	Volume	Protein (x 4)	Precipitation solvent volume
617- 0’	2.2 mL	~0.550 mL	1.5 mL
617- 3’	1.85 mL	~0.470 mL	1.45 mL

- Distribute samples into LoBind eppis to account for increase in volume
  - All were distributed into 4 tubes
- Add 3-4 X the starting volume of 50% EtOH/50% Acetone/ 0.1% acetic acid.
- Store in -80 freezer for ~10 min to aid precipitation
- Centrifuge at 4000rpm (1.5xg) for 10 min at 4°C
- Remove supe. Wash one more time with precipitation buffer + 500 uL of MQ water (so, 1/5 water)
  - Used 500 uL MQ water + 1.5 mL precipitation buffer for all samples
- Centrifuge at 4000rpm (1.5xg) for 10 min
- Remove supe completely
- Let air dry O/N, covered with kimwipe (once dry, store at 4 °C until ready for trypsin digest)- put in rack on side to dry.

DAY 2: (6/10/09)

6. Resuspend protein pellets in 50 uL of 6 M urea/0.1M Tris, pH8.0, vortexed and incubated for ~1h. Pool the aliquots of each sample timepoint together.
  - Rinse the extra tubes with 3 x 100 uL of 50 mM Tris, pH 8.0, to remove any remaining peptides.

7. Add additional 50 mM Tris, pH 8.0, to the samples so that the urea is diluted 5 fold in the pooled samples.

8. Mix 44ul of 25mM ammonium bicarbonate, 6ul of 100 mM CaCl2 (~1.7 mM final conc.) to each 20 ug lyophilized trypsin aliquots. Add trypsin solution to protein samples.
  - Want trypsin:protein ratio to be at 1/50 by weight to sample (e.g. For every 1 mg of protein, add 20 ug of trypsin)
    - Prepare: 2 mg x 2 samples = 80ug (need 4 trypsin aliquots)
  - $CaCl_2$ recommended to help trypsin reaction
  - pH should be between 7-8 for optimal trypsin activity. pH was ~8.0

9. Shake O/N at 37°C.

DAY 3: (6/11/09) C18 cleanup and IMAC beadprep

10. Acidification

- Add 10% TFA to final of 0.4% (0.3% to 0.5%) to each sample

Sample	10%TFA to add
375- 0’	40 uL
375- 3’	40 uL

- Stored at 4 °C until ready to use

11. C18 Cleanup (to remove salt)

- **C18 Prep** (use 50 mg, volume=1.25 mL)
  - Hydrate column w/ methanol (fill to top)

- Add **80% ACN/1% HAC** (made 35ml) to top of column to clean out column; repeat. Takes ~20-30min for column to drip
- Wash twice w/ **1 % HAC (prepared ~80ml)** to wash out ACN
- Add sample to column, and allow to drip down.
    - Collect in LoBind eppi, label "C18-FT", start drying
- Wash twice w/ **1% HAC**
    - Collect in LoBind eppi, label "C18-Wash1" and "C18-Wash2", start drying
- Elute w/ 400uL + second 100uL wash at end of **80% ACN/0.1%HAC** (4-5 bed volumes)
    - Collect in LoBind eppi, label "C18-elution", divided into 5 tubes and started drying
- Lyophilized C18 elutions and washes.
- Can later resuspend in 100uL of **1% HAC or water**
- Stored pellets at -80°C

12. IMAC Bead Prep (~3hr)

Before starting: Prepare 250 mL of 0.6% HAc for all the solutions (1.5 mL HAC, up to 250 mL with water).

- Add 2 spin columns of NTA-silica resin into 50 mL of **50 mM EDTA, 1 M NaCl** in 50 mL conical tube (e.g. last time, used 4 columns worth for 10 mg of protein, this time had more than enough beads)
    - Can use stock, or add 5 mL 0.5 M EDTA , 10 mL 5 M NaCl, bring volume to 50 mL w/ H_2O
- Shake @ RT for 1 hour, rotate the tube at least once every 15 min. Set-up on the rotator (from TC room)
- Spin down @ 3000-**4000** rpm for 2 min. in swinging bucket rotor (normal acceleration/~6 deceleration), draw up supe with pipette and dump
- Wash with **50 mL of H_2O** to wash; spin down again; dump liquid
- Wash with **50 mL of 0.6% HAC**; spin down; dump liquid
- Add **50 mL of 100 mM $FeCl_3$ in 0.3% HAC (Add iron last when making this solution!!!)**
    - Add 25 mL of 0.6 % HAC, 20 mL of H_2O, then 5 mL of 1 M $FeCl_3$)
    - Always add the iron last; only take the very top of the supernatant, and *do not disturb* precipitate at the bottom
- Shake @ RT for 1 hour, rotate tube at least once every 15 min. Used the rotator (from TC room)
- Spin down @ **4000 rpm** for ~ 2 min., dump liquid
- Wash w/ **50 mL of 0.6% HAC**; spin down; dump liquid
- Add **50 mL of 0.1 M NaCl, 25% ACN, 0.1% HAC**
    - Add 1 mL of 5 M NaCl, 12.5 mL of ACN, and 8.33mL of 0.6% HAC
- Shake @ RT for 10 min.
- Spin down @ 3000-**4000** rpm for ~ 1 min., dump liquid
- Wash twice w/ **50 mL of 0.1% HAC**
    - Prepare 100 mL using 12.66 mL of 0.6% HAC and bringing up to 100 mL with H2O
- Aliquot into an eppi tube, and store @ 4°C (date and do not use after 1 week; fresh is best)... Remove supe to get 50:50 slurry

DAY 4: (6/12/09)

IMAC Prep: Make IMAC columns (2) –

- Use gel loading tips to pack columns
- Pinch off a small amount of glass wool and spindle out to a thin string (use water to smooth down)
- Cut ends of spindled wool to make it ~1 inch
- Use a pointy object to push down tip (want it to take up ~1/4 of the actual tip of the gel loading tip)
- Squeeze bottom part with clamp tweezers and cut off bottom part
- Cut off top part of tip to help place on syringe

13. Added 30ul of bead slurry to prepared IMAC columns (=~15ul of beads)**;** just press down gently on the syringe initially and let it flow through on its own (be careful to not apply too much pressure) (use ~20ul for 1mg (so about 10ul of actual IMAC beads))

14. Condition beads w**/ 25% ACN/0.1% HAC (60ul)**

- prepared 2 mL (plenty): 0.5mL ACN, 0.33 mL 0.6%HAC, 1.17 mL H2O

15. Phospho-enrichment

- Resuspend pellets in 100uL of 1 %HAC
- Spun down at 4000 rpm for 2 min
    - Very little/no precipitate
- Add supe to column, push through slowly (collect "flowthrough")
    - Collect samples into 0.5 mL LoBind eppis, start drying
- Wash 2x w/ 30 uL **25% ACN/0.1% HAC/0.1 M NaCl** (Add to "wash" tube)
    - 2 mL: 0.5mL ACN, 0.2 mL 1%HAC, 0.05 mL 4M NaCl
- Wash 2x w/ 15uL of ***0.1%* HAC** *(to remove the salt)* (Combine to "wash")
- Wash 2x w/ H_2O (to remove the acid) (1^{st} wash- 15uL, 2^{nd} wash 30uL) (combine to "wash")
- Elute w/ 50 uL of (20 + 20 + 10 uL) of 1% Phosphoric Acid
    - 10ul phosphoric acid into 990 uL of H2O
- Lyophilized flow through, wash and elute fractions overnight
    - *Note- the elute does not dry completely likely due to the phosphoric acid.

DAY 5: (6/15/09) – iTRAQ labeling

16. iTRAQ labeling

- Removed the 115 (0') and 117 (3') iTRAQ mass tags (1 vial of each) as well as iTRAQ dissolution buffer and ethanol from the -20°C freezer and allowed them to reach room temperature.
- Spin down iTRAQ reagents- short pulse.
- Add 70ul of ethanol (provided) to each vial of iTRAQ reagent.
- Vortexed to mix
- Spun 30s at max speed
- Resuspended the C18 MJK617 pellets in total of 100ul of dissolution buffer. (*Note- should have used 30ul)
    - bubbled when the dissolution buffer was added, but everything appeared to mix fine after that. Vortexed and spun down sample
- After resuspension of the iTRAQ reagent distributed it to the 0' (115) and 3' (117) MJK617 samples

    - Spun down vials of iTRAQ reagent again and added any remaining reagent to samples
- Vortexed and then spun down
- Allow labeling to proceed for1h at room temperature (really ~1h30min)
- Pooled the 0' and 3' fractions together into new eppe tube (so have one tube for IMAC samples and one tube for the C18 samples)
- Stored O/N at 4^{o}C until could do SCX

DAY 6: (6/16/09)- SCX

17. Take over to Maj to do the SCX~ 2hr run, 1ml loop- "iTRAQ SCX slow gradient 1mL loop"

- 1mL injection volume for the SCX column, but want to dilute ~5x with buffer A (250mL ACN, 0.5mL formic acid to 1L H2O). Buffer B= 13.4g NH4Cl, 0.5mL formic acid and 250mL ACN to 1L H2O, Note- using ammonium acetate would be better because with ammonium chloride we'll have to do C18 cleanup prior to IMAC, but ammonium acetate isn't compatible with the polysulfoethylA column.
- So speed vac dried the samples down to ~150-200ul and then diluted up to ~1mL with buffer A and then injected into loop
- Then hit start on the Akta program- ~120 min of sample collection, 30 min wash at the end. Collects ~200ul/fraction (get A1→F12 over sample collection period). Generally don't collect the early fractions (basically all of row A) until you start seeing the conductivity plot increase (only get off non-bound contaminants, etc up until this point). Use A214 and A280 to determine where to collect fractions
- pooled for some good peaks 2 fractions together directly, otherwise pooled many fractions and did the C18 to reduce salts.
- speed vac dry

DAY 7: (6/17/09) – C18

18. C18 cleanup of pools with >2 fractions

- **C18 Prep** (use 50 mg, volume=1.25 mL)
    - Hydrate column w/ methanol (fill to top). Used pipet tip to help out the flow for hydrating and rinsing the column
    - Add **80% ACN/1% HAC** (made 12.5ml) to top of column to clean out column; repeat. Use mixture of gravity and pipet through
    - Wash twice w/ **1 % HAC (used already prepared)** to wash out ACN
    - Add sample to column, and allow **to drip down**.
        - Collect in LoBind eppi, label "C18-FT", start drying
    - Wash twice w/ **1% HAC**
        - Collect in LoBind eppi, label "C18-Wash1" and "C18-Wash2"
    - Elute w/ 400uL + second 100uL wash at end of **80% ACN/0.1%HAC** (4-5 bed volumes). Allow to drip by gravity.
        - Collect in LoBind eppi, label "C18-elution"
    - Lyophilized C18 elutions and washes.

APPENDIX II

Antibody Information

Antibody	Company	Order #	Species	MW	Western dilution	Developing Reagent	Signal Strength/notes
Beta-Actin (13E5)	Cell Signaling	4970	Rabbit mAB	45kDa	1:1000 or 1:2000 in 5%BSA-TBST	GE ECL+	Strong
Akt	Cell Signaling	9272	Rabbit	60kDa	1:1000 in 5%BSA-TBST	GE ECL+	Strong
phospho-Akt (Ser473)	Cell Signaling	4058 (also 9271)	Rabbit mAB	60kDa	1:1000 in 5%BSA-TBST	Pierce femto	Weak *Do this 1st before other Abs
phospho-Akt (Ser473)-mouse	Cell Signaling	4051	Mouse mAB	60kDa	1:1000 in 5%BSA-TBST	Pierce femto	Weak *Rabbit mAB is better in general
phospho-Akt (Thr308)	Cell Signaling	9275	Rabbit	60kDa	1:1000 in 5%BSA-TBST	Pierce femto	Haven't probed
phospho-ATF-2	Cell Signaling	5112	Rabbit	70kDa	1:1000 in 5%BSA-TBST	Pierce femto	good
β-galactosidase/LacZ-Peroxidase (*directly conjugated to HRP)	Rockland	200-4336	Rabbit	116 kDa	1:2000-1:5000 in 5%BSA-TBST	GE-ECL+	
BAD	Cell Signaling	9292	Rabbit	23kDa	1:1000 in 5%BSA-TBST	GE ECL+	good
phospho-BAD (S112)	Cell Signaling	9296	Mouse mAB	23kDa	1:1000-1:2000 in 5%BSA-TBST	Pierce femto	high
phospho-BAD (S136)	Cell Signaling	9295	Rabbit	23kDa	1:500-1:1000 in 5%BSA-TBST	Pierce femto	good signal with femto
Cap1 (M-30) (Deli case)	Santa Cruz	100917	Mouse mAB	52kDa	1:200 in 5%BSA-TBST	Pierce?	Haven't probed
CXCR7 (GPCR RDC1)	Abcam	Ab38089	Rabbit	~60kDa	1:250-1:500	GE ECL+	sample b/c aggregates at
EGFR	Cell Signaling	2232	Rabbit	175kDa	1:1000 in 5%BSA-TBST	used GE- no	B cells, try pierce
ERK1/2	Upstate	06-182	Rabbit	42/44kDa	1:3000 in 5%milk-TBST	GE ECL+	Strong, aliquot Ab
phospho-ERK1/2	Upstate	07-467	Rabbit	42/44kDa	1:1000 in 5%milk-TBST	Pierce femto	Ok (stronger than p-AKT, but not great)
FOXO3A	Cell Signaling	2497	Rabbit	82-97	1:1000 in 5%BSA-TBST	GE ECL+	good
phospho-FOXO3A (S318/32	Cell Signaling	9465	Rabbit	97 kDa	1:1000 in 5%BSA-TBST	Pierce femto	Weak
FOXO4	Cell Signaling	9472	Rabbit	65 kDa	1:1000 in 5%BSA-TBST	GE ECL+	good
GFP (Taylor Deli)	Abcam	ab290	Rabbit	~38kDa	1:5000 in 5% BSA-TBST	GE ECL+	VERY strong
phospho-GSK3a (Ser21)	Cell Signaling	9316	Rabbit	51 kDa	1:5000 in 5% BSA-TBST	GE ECL+	good
phospho-GSK3b (Ser9)	Cell Signaling	9336	Rabbit	46kDa	1:1000 in 5%milk-TBST	GE ECL+/Pie	GE
Growth Hormone Receptor (MAB263)	Abcam	ab11380	Mouse mAB				unsuitable for WB, flow
HA-peroxidase (3F10) (*directly conjugated to HRP)	Roche	2013819	Rat mAb		1:750 in 5% BSA-TBST	GE ECL+	Good
hnRNP A1 (4B10) (Deli case)	Santa Cruz	32301	Mouse mAB	36 kDa	1:200 in 5%BSA-TBST	Pierce	Haven't probed
hnRNP D0 (T10) (Deli case)	Santa Cruz	22368	Goat poly	82 Kda	1:200 in 5%BSA-TBST	Pierce?	pretty good-used with 2DE
hnRNPU (C-15) (Deli case)	Santa Cruz	13663	Goat poly	142kDa	1:200 in 5%BSA-TBST	Pierce?	Haven't probed
phospho-HSP27 (Ser82)	Cell Signaling	2401S	Rabbit	27kDa	1:1000 in 5%BSA-TBST	Pierce femto	Decent signal if used 1st
phospho-SAPK/JNK (T183/Y185)	Cell Signaling	4671	Rabbit mAB	46,54kDa	1:1000 in 5%BSA-TBST	Pierce	Weak
LAP2 (Y-20)(Deli case)	Santa Cruz	19783	Goat	50 kDa	1:200 in 5%BSA-TBST	Pierce	Haven't probed
Phospho-LSP (S252) (Deli case)	AnaSpec	28161-025	Rabbit Ab	52kDa	1:500 in (5%BSA-TBST) recommended	Pierce	Very good
Phospho-Lyn (Tyr507)	Cell Signaling	2731	Rabbit	53, 56kDa	1:1000 in 5%BSA-TBST	Pierce	good signal
phospho-MAPKAPK2 (T334)	Cell Signaling	3007	Rabbit	49-50kDa	1:1000 in 5%BSA-TBST	Pierce	stripping
Phospho-MCM2 (S40/S41)	Bethyl	A300-788A	Rabbit	~117 kDa	1:1000 in 5%BSA-TBST (or more dilu	Pierce	Haven't probed
MCM2	Bethyl	A300-191A	Rabbit	~117 kDa	1:1000 in 5%BSA-TBST (or more dilu	Pierce	Haven't probed
phospho-MDM2 (Ser166)	Cell Signaling	3521	Rabbit	90kDa	1:1000 in 5%BSA-TBST	GE ECL+	good signal
mTOR	Cell Signaling	2972	Rabbit	289kDa	1:1000 in 5%BSA-TBST	GE ECL+ ?	Haven't probed
phospho-mTOR (Ser2448)	Cell Signaling	2971	Rabbit	289kDa	1:1000 in 5%BSA-TBST	Pierce femto	gradient gel
phospho-PAK2 (Ser20)	Cell Signaling	2607	Rabbit	61-67kDa	1:1000 in 5%BSA-TBST	GE ECL+	good
phospho-pdcd4 (pS457)	Rockland	600-401-964	Rabbit	52kDa	1:2000 (or more dilute..) in 5%BSA-TE	GE ECL+	very strong, *Aliquot in -20
phospho-pdcd4 (p67)	Sigma	P0072	Rabbit	51kDa	1:1000 in 5%BSA-TBST	Pierce/GE EC	strong and multiple bands with Pierce, *Aliquot in -20
Pdcd4	Rockland	600-401-965	Rabbit	52kDa	1:2000-1:10,000 in 5%BSATBST	GE ECL+ ?	Haven't probed
PDGFR-beta	Santa Cruz	432	Rabbit	180-190 kDa	1:200 in 5%BSA-TBST	Pierce femot	not great
p27-Kip1	Cell Signaling	2552	Rabbit	27kDa	1:1000 in 5%BSA-TBST	GE ECL+ ?	Haven't probed
phospho-p27/Kip1 (T157)	R&D systems	AF1555	Rabbit	27kDa	1:2000 in 5%milk-TBST	GE ECL+	strong
phospho-p38 (T180/Y182)	Cell Signaling	9215	Rabbit	42kDa	1:1000 in 5%BSA-TBST	Pierce	ok signal
p53 (FL-393) (Deli case)	Santa Cruz- 4°C	6243	Rabbit	53kDa	1:1000 in 5%BSA-TBST	GE ECL+	ok- some background- only see in irradiated

p53 *Ab is bad- don't use	Cell Signaling	2524	Mouse mAB	53kDa	1:2000 in 5%BSA-TBST	GE ECL+	antibody not good
PHLPP1 (Deli case)	Bethyl- 4°C	A300-660A	Rabbit	150, 180*, 250kDa	1:1000-1:2000 in 5%BSA-TBST	GE ECL+	Ok signal- Probe PHLPP1 1st
PHLPP2 (Deli case)	Bethyl- 4°C	A300-661A	Rabbit	150kDa, 250kDa	1:1000-1:2000 in 5%BSA-TBST	GE ECL+	good signal- Probe PHLPP1 1st
PKCalpha (C-20) (Deli case)	Santa Cruz- 4°C	SC-208	Rabbit	~80kDa	1:2000-1:5000* in 5%BSA-TBST	GE-ECL+	very strong
PKCbetaII (c-18) (Deli case)	Santa Cruz- 4°C	SC-210	Rabbit	~80kDa	1:2000-1:5000 in 5%BSA-TBST	GE-ECL+	very strong
PKC epsillon (Deli case)	Santa Cruz- 4°C	sc-214	Rabbit	~80kDa		GE-ECL+	Haven't probed
PKCzeta (Deli case)	Santa Cruz- 4°C	sc-216	Rabbit	~80kDa		GE-ECL+	Haven't probed
PKCdelta (Deli case)	Santa Cruz- 4°C	sc-937	Rabbit	~80kDa		GE-ECL+	Haven't probed
Prolactin Receptor U5	Abcam	ab2772	Mouse mAB	40, 100kDa	1:1000 Need to optimize		poor quality, high back
Prolactin Receptor ECD clon	Zymed	359200	Mouse mAB	85-90kDa	1:500 in 5%BSA-TBST		
Prostaglandin E Receptor (E	Abcam	ab21227	Rabbit	55kDa	1:500, need to optimize		poor quality, high back
PTEN	Cell Signaling	9552	Rabbit	54kDa	1:1000 in 5%BSA-TBST	GE ECL+	good signal
RAD23A (HR23A)	Rockland	600-101-291	Goat	~60kDa (few banc	1:2000 in 5%BSA-TBST	GE ECL+	strong signal
phospho-p70 S6K (Thr389)	Cell Signaling	9206	Mouse mAB	70, 85 kDa	1:1000 in 5%BSA-TBST	Pierce femto	rinse
SCOP (PHLPP)	Santa Cruz	sc-46452	Goat	135-140kDa	1:100-1:1000		
TCL1	Cell Signaling	4016	Mouse mAB	14kDa	1:1000 in 5%BSA-TBST	GE ECL+	strong
alpha-Tubulin	Sigma	T 6074	Mouse mAB	50kDa	1:10,000 or so, in 5%BSA-TBST	GE ECL+	very strong
XIAP	Cell Signaling	2045	Rabbit mAB	53kDa	1:1000 in 5%BSA-TBST	GE ECL+ ?	Haven't probed
Secondaries							
Pierce goat anti-Rabbit HRP	Pierce	with femto kit	goat		1:2000-1:5000 in 5%Milk-TBST	Pierce femtos	Strong (Ab pre-diluted, can't use withGE)
Pierce goat anti-Mouse HRP	Pierce	with femto kit	goat		1:2000-1:5000 in 5%Milk-TBST	Pierce femtos	Strong (Ab pre-diluted, can't use withGE)
Stock goat anti-Rabbit HRP	?	lab -20	goat		1:10,000 in 5%Milk-TBST	GE ECL+	Strong
Stock goat anti-Mouse HRP	?	lab -20			1:10,000-1:20,000 in 5%Milk-TBST	GE ECL+	Strong
Rabbit anti-Goat HRP	Calbiochem	401515	rabbit	my Deli case	1:10,000 in 5%Milk-TBST	GE ECL+	Strong
Goat anti-Rabbit HRP	Thermo		goat	laab and my -20	1:10,000 for GE, 1:100,000 for femto		
LY294002 Inhibitor	Cell Signaling	9901					
Piceattanol							
AMD3100	Sigma						
Pertussis Toxin	List Biologicals	180					

Antibody Name	Vendor	Catalog Number	Container Size	Unit of Measure	Location
Alpha-Adaptin (1/2)	Santa Cruz	SC-10701	1.5	ul	John's Delicase
Anti DARC (pAb Goat)	abcam	ab40821	1.5 mL	50 uL	-20 (AJ)
Anti-goat-PE	abcam	ab7004	1.5 mL	50 uL	-20 (AJ)
Anti-Flag-PE	Prozyme	PJ315	1	mL	Damon's Delicase
Anti-hCCR1	R&D	MAB145	30 uL	EA	20 (common)
Anti-hCCR10-PE	R&D	FAB3478P	10 mL	EA	Delicase (AJ)
Anti-hCCR3	R&D	FAB155P	10 mL	EA	Delicase (AJ)
Anti-hD6-PE	R&D	FAB1364P	10 mL	EA	Delicase (AJ)
mouse IgG2B (isotype control)	R & D	MAB0042	25	uL	3131
Anti-Rabbit IgG-PE	R&D	F0110	vial	mL	Morgan's delicase
Anti-Rabbit IgG-APC	R&D	F0101B	vial	mL	Morgan's delicase
Anti-mouse IgG-PE	R&D	F0102B	vial	mL	Morgan's delicase
Alexa-Fluor 488	Invitrogen	A11001	0.5	mL	Morgan's delicase
Rat Anti-Human CD184 (CXCR4)-PE	BD Pharmingen	551510	1	mL	Morgan's delicase
Rat anti-IgG2A-PE	BD Pharmingen	553930	1	mL	Morgan's delicase
anti-hCCR1_PE	R&D	fab145p			Damon 4C delicase
anti-hCCR2_PE	R&D	fab151p			Damon 4C delicase
anti-hCCR3_PE	R&D	fab155p			Damon 4C delicase
anti-hCCR5_PE	R&D	fab1802p			Damon 4C delicase
anti-hD6_PE	R&D	fab1364p			Damon 4C delicase
anti-hCCL7/MCP3_PE	R&D	ic282p			Damon 4C delicase
Ubiquitin	Santa Cruz	SC-9133	1.5	ul	John's Delicase
hCXCR7-APC	R&D	FAB4227A			Morgan's Delicase
alpha EEA1	BD	610457			John Delicase
alpha 205 plotcosome	Calbiochem	ST1049			John Delicase
alpha beta adaptin	Santa Cruz	SC-10762			John Delicase
Mouse IgGaB isotype control	R&D	MAB004			Rina -80C
Mouse Anti-g3p (pIII) Antibody	Mo Bi Tec	PSKAN3			Common use -20C
goat anti-mouse IgG, DyLight488					
mouse anti-human CCR1	R&D	MAB145	25	uL	common -20C
rabbit anti-human/mouse CCR1	Affinity BioReagen	PA1-41062	50	uL	common -20C
rabbit anti-FLAG	Sigma	F7425-.2MG	50	uL	common -20C
mouse IgG2B isotype control	R&D	MAB0042	25	uL	common -20C
rabbit anti-CXCR1	Affinity BioReagen	PA1-41096		mL	common -20C
rat anti-HA high affinity	Roche	11802600	50	mg	Taylor's delicase
rabbit anti-GFP, whole antisesum	Abcam	ab290	50	uL	Taylor's delicase

goat anti-mouse - MRP	Abcam	ab6789	1	mg	John's Delicase
mouse anti-SNX1	BD	611482	50	ug	John's Delicase
NSF antibody	Cell Signaling	2145	100	uL	John's Delicase
anti-20s Proteosome	Cal biochem	ST1049	100	uL	John's Delicase
rabbit anti-Barrestin 1	Abcam	ab32099	100	uL	John's Delicase
mouse anti-Barrestin 2	Abcam	ab77208-100	100	uL	John's Delicase
anti-sp64 antibody	ebioscience	14-6991-85	1	mL	John's Delishelf
anti-human CCR2	R&D	Fab151P	1	mL	John's Delicase
anti-Barrestin 1	Santa Cruz	sc-6388	1	mL	John's Delicase
anti-Barrestin 2	Santa Cruz	sc-13140	1	mL	John's Delicase
anti-Barestin 1/2	Santa Cruz	sc-53781	1	mL	John's Delicase
anti-Ubiquitin	Santa Cruz	sc-9133	1	mL	John's Delicase
anti-Adaptin 1/2	Santa Cruz	sc-10761	1	mL	John's Delicase
anti-Beta Adaptin	Santa Cruz	sc-10762	1	mL	John's Delicase
anti-EEA1	BD	610457	1	mL	John's Delicase
anti-G alpha i1	Santa Cruz	sc-56536	1	mL	John's Delicase
anti-G p1	Santa Cruz	sc-25016	1	mL	John's Delicase
anti-G gamma2/3/4/7	Santa Cruz	sc-28589	1	mL	John's Delicase
anti-NA - NRP	Roche	2013819	1	mL	John's Delicase
anti-NA - affinity matrix	Roche	11-815-016-001	1	mL	John's Delicase
Goat anti-mouse 554	unKnown		25	uL	John's Delicase
Goat anti-rabbit 488	unKnown		25	uL	John's Delicase
Goat anti-rabbit 594	unKnown		25	uL	John's Delicase
Chicken anti-Goat 594	unKnown		25	uL	John's Delicase
CXCR7/RDC-1	R&D	MAB42273	100	ug	Common -20C
IgG1	R&D	MAB002	500	ug	Common -20C
CXCR4 (fusin)			20	uL	Morgan's -80C
Mouse IgG2A Isotype control	R&D	MAB003	1	aliquot	Morgan's -80C
Protein A/G Plus Agarose	Santa Cruz	SC-2003	2	mL	Taylor's delicase
Briostatin- PKC inhibitor/partial agonist	R&D	MAB172			Morgan's -20C

APPENDIX III

Q-PCR primers

Primers used for Q-PCR (most primer designs are from the Harvard Primer Bank):

Human GAPDH

Forward 5’- GAGAGACCCTCACTGCTG 3’

Reverse 5’- GATGGTACATGACAAGGTGC -3’

Human PHLPP1

Forward 5’- ACTGGGATTTGGGGAGCTG -3’

Reverse 5’- CGTCTTGTCCATCGGTTCACT -3’

Human PHLPP2

Forward 5’- ATGGAGCAGACACTACCACTG -3’

Reverse 5’- GCAAAGGACGAGATGTAAGTCA -3’

Human CXCR4

Forward 5’- TACACCGAGGAAATGGGCTCA -3’

Reverse 5’- TTCTTCACGGAAACAGGGTTC -3’

Human CXCR7

Forward 5’- TGCATCTCTTCGACTACTCAGA -3’

Reverse 5’- GGCATGTTGGGACACATCAC -3’

Human RPL30 (alternative housekeeping gene for leukemia cells)

Forward 5'-TCCAGGTGACTCTGACATCATT-3'

Reverse 5'-TTGCAGGTTTAAGGTTTGCAG-3'

Human Lamin B1 (alternative housekeeping gene for leukemia cells)

Forward 5’- GCATGAGAATTGAGAGCCTTTCA -3’

Reverse 5’- TGCGACGAGAGTTGTCTTTTTC -3’

Human PKG-1 (alternative housekeeping gene for leukemia cells)

Forward 5'-TTAAAGGGAAGCGGGTCGTTA -3'

Reverse 5'-TCCATTGTCCAAGCAGAATTTGA -3'

Human Growth Hormone Receptor (may not be the best)- used to try to validate Tracy's microarray data from her sabbatical

Forward 5'- GCTGCTGTTGACCTTGGC -3'

Reverse 5'- ACCTCATCTGTCCAGTGG -3'

Alternative:

Forward 5'- CGTTCACCTGAGCGAGAGA -3'

Reverse 5'- TGAGTCCATTCTTGAGTGTTCC -3'

Human Prolactin Receptor PRLR- used to try to validate Tracy's microarray data from her sabbatical

Forward 5'- CAGCACAACCCCAGATCCTC -3'

Reverse 5'- GGCGTATCCTGGTCAGTCTC -3'

Human Prostaglandin E3 (PTGER3) (may not be the best)- used to try to validate Tracy's microarray data from her sabbatical

Forward 5'- GTGCTGTCGGTCTGCTG -3'

Reverse 5'- CTTTCTGCTTCTCCGTGTG -3'

Alternative:

Forward 5'- ATCATGTGCGTGCTGTCG -3'

Reverse 5'- GAAGATCATTTTCAACATCATTATCAG -3'